Synthesis and Characterization of Amino Acid Ionic liquids and Low Symmetry Ionic liquids based on the triaminocyclopropenium cation

Ruhamah Yunis

A Thesis Submitted in the Partial Fulfillment of the Requirements for the Degree of Philosophy in Chemistry

Department of Chemistry

University of Canterbury

2015

Table of Contents

Table of Contents

Acknowledgements

First, I would like to convey my deepest thanks to my supervisor Prof. Owen J Curnow for the continuous support of my Ph.D study and research, for his patience, motivation, enthusiasm, and immense knowledge. I attribute the level of my PhD degree to his encouragement and without him this thesis would have not been completed or written. His guidance helped me throughout my research. I could not have imagined having a better advisor and mentor for my Ph.D study.

Besides my mentor, I would like to thank the rest of my thesis committee: Prof. Greg Russel, Prof. Peter Steel, and Prof. Paul Kruger, and Prof Andy Pratt for their comments, and checking of my progress reports.

I would like to thank all the technical staff of chemistry department, who, for four years, helped in ensure that my research ran smoothly. My special gratitude goes to Dr Mark Staiger from mechanical Engineering Department for the usage and training of DSC. The support I gained at the start of my Phd, from the University of Waikato, for accomodating me as a refugee after the February 2011 Earthquake was amazing.

I thank my fellow lab-mates in the Ionic Liquid group: Dr Kelvin J Walst, James Shields, Michael Holmes, Patrick Dronk, William Kerr, and Chaminda Jayasinghe, for the cheerful group discussions, and for all the fun we had over the last four years. Also I thank my friends from other research groups, who were a part of our communal office.

Last but not the least, I would like to thank my lovely husband Shahzad Sarwar, my parents and my sisters for supporting me always throughout my study.

Special thanks to the University of Canterbury for UC Doctoral Scholarship. I thoroughly enjoyed my life in New Zealand during my PhD research and write-up

Abstract

This thesis involves the synthesis of two main classes of triaminocyclopropenium (tac) Ionic Liquids (ILs) (i) Amino Acid Ionic Liquids (AAILs) and (ii) reduced-symmetry cations.

$[C_3(NEt_2)_2(NRR')]X$ (X = TFSA and $MeSO_4$) were prepared, whereby NHR is derived from amino acids. Optically pure AAILs, $[E_4AminoAcid]X$ (X = TFSA and $MeSO_4$) were obtained as a mixture of the IL and its zwitterion. The ratios of these mixtures were determined by *p*H titration and microanalysis. The AAILs specific rotations and *p*Ka values were determined. AAILs can be used for chiral discrimination and form diasterreomeric salts with the entioenriched sodium salt of Mosher's acid. The AAILs were also successfully used as a solvent and/or catalyst in an aldol reaction and a Diels-Alder reaction.

The low-molecular weight series, $[C_3(NMe_2)_2(NRR')]X$ and $[C_3(NMe_2)_2(NR'_2)]X$ was synthesized and characterized: protic ILs NRR', where R = ethyl, propyl, allyl, butyl, $-CH_2CH_2OCH_3$ and pentyl, R' = H and X = TFSA: and aprotic ILs NRR', where R = Me, R' = ethyl, allyl, propyl, butyl, $-CH_2CH_2OCH_3$ and hexyl and X = TFSA and DCA.

ILs with C_{2v} symmetry $[C_3(NEt_2)_2(NH_2)]X$ (X = TFSA and $MeSO_4$), $[C_3(NEt_2)_2(NBu_2)]I$, $[C_3(NEt_2)_2(NHex_2)]I$ and $[C_3(NEt_2)_2(NHex_2)]OTf$ were also synthesized and characterized. The C_{3h} cations, $[C_3(NMeR)_3]X$ (R = ethyl, allyl, $-CH_2CH_2OCH_3$ and phenyl, X = TFSA and DCA) were successfully prepared as well.

The D_{3h} cation salts $[C_3(NEt_2)_3]X$ (X = $MeC_6H_4SO_3$, OTf, I and F_5C_6O) and $[C_3(NBu_2)_3]X$ (X = $B(CN)_4$ and FAP) were also prepared.

The tac-based ILs $[C_3(NEt_2)_3]^+$ and $[C_3(NBu_2)_3]^+$ were also complexed with metal halides forming salts with $FeCl_4^-$, $SnCl_3^-$, $CuCl_4^{2-}$ and $ZnCl_4^{2-}$.

Reaction of pentachlorocyclopropane (C_3Cl_5H) with $BuNH_2$ gave the open ring allylium product $[H_2C_3(NBuH)_4]^{2+}$. This was characterized as Cl^- and $TFSA^-$ salt. During the synthesis of $[C_3(NMe_2)_3]Cl$, the open ring cation $[HC_3(NMe_2)_4]^+$ was also isolated and was characterized as the $TFSA^-$ salt.

The TGA, DSC, density, viscosity, conductivity, and molar conductivity properties for the ILs were measured where possible. The viscosity and conductivity data was fitted for the Arrhenius and Vogel-Fulcher Tamman equations. The entire tac-based ILs lie below the KCl ideal line in Walden plot. A fragility plot was obtained by fitting the viscosity data and all the tac-based ILs were fragile.

The crystal structures of $[C_3(NPhH)_3]TFSA$, $[C_3(NEt_2)_3]FeCl_4$ and $[HC_3(NMe_2)_4]Cl.2CH_3Cl$ were determined.

Abbreviations/Glossary

tac	Triaminocyclopropenium
ILs	Ionic Liquids
AAILs	Amino Acid Ionic Liquids
CILs	Chiral Ionic Liquids
TFSA	Bis(trifluoromethanesulfonyl)amide
DCA	Dicyanamide
OTf	Trifluoromethanesulfonate
OTs	Toluenesulfonate
FAP	Tris(pentafluoroethyl)trifluorophosphate
Me	Methyl
Et	Ethyl
Pr	Propyl
Bu	Butyl
Pe	Pentyl
Hex	Hexyl

Introduction

Introduction

Over the last two decades, ionic liquids (ILs) have opened up a new face of chemistry to scientists. More than 1500 ILs have been reported in the literature with over a million possible in theory.[1] The number of publications and papers about ILs has increased dramatically in recent years. The research presented here is a study on the synthesis and characterization of chiral ionic liquids (CILs) derived from amino acids and some low-symmetry ionic liquids derived from the triaminocyclopropenium (tac) cation. Applications of CILs have also been successfully studied in asymmetric synthesis.

1.1 Ionic Liquids

Gabriel reports the first protic IL (PIL) ethanolammonium nitrate with melting point of 52-55 °C.[2] Later in 1914, the preparation of a room temperature IL (RTIL) ethylammonium nitrate was reported.[3] The term 'ionic liquid' refers to ionic materials that are liquids having melting points below 100 °C. They consist exclusively of ions. Those which are liquid at or around the room temperature are 'RTILs'. They are often considered to be green solvents and have attracted increasing international interest during the past years.

1.1.1 Commonly used Cations and Anions

ILs are commonly composed of a bulky organic cation and an organic or inorganic anion. They are notable because they consist of negatively and positively charged ions (fig 1.1) but melt at a relatively low temperatures. Ionic systems with higher melting points are termed as molten salts, whereas ionic liquids remain liquids at lower temperatures because they do not pack well in the solid state. Thus, blending of bulky and asymmetric cations and unevenly-shaped anions make them liquids[4] as melting points[5] are lowered.

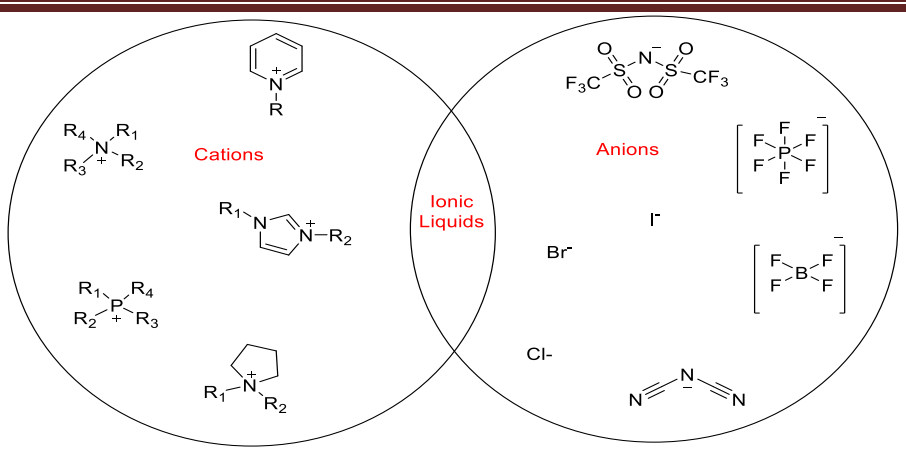

Figure 1.1-Common cations and anions used to make ILs.

ILs have two main classes: aprotic and protic. Most of the ILs contain aprotic cations in which the parent base molecule is ionized (cation) by accepting any group other than a proton. Protic ILs (PILs), on the other hand, are formed by proton transfer from a Brønsted acid (HA) to a Brønsted base (B) (fig.1.2). Most PILs have a small amount of the molecular species (HA and B) in them if the proton transfer is incomplete. In some cases, PILs can be distilled *via* the neutral acid and base. PILs can be used as solvents in organic synthesis and are also suitable as electrolytes in fuel cells.

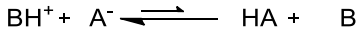

Figure 1.2-Equilibrium between protonated and ionized form in PIL.

Another class of ILs includes binary mixtures of organic and inorganic salts. Deep eutectic ILs are characterized by a depression in the melting points when two different ILs are mixed together.

Some of the ILs are designed for specific properties via functionalized cations and anions. For example, CILs can have a chiral cation, chiral anion or both. By modifying the structure, their properties can be altered to influence the outcome in asymmetric synthesis. However, most of this work is focused on the synthesis of chiral cations derived from amino acids. They are potentially useful in asymmetric synthesis as chiral solvents or chiral catalysts.

1.1.2 Properties

The interest in ILs comes from the ability to tune the properties of the ILs by variation of the structure of the cation and the anion as indicated in fig 1.1. The tunability of physical properties (density,

viscosity, conductivity, solvent properties, water miscibility, melting point and decomposition temperature) is one of the most important characteristics and advantages of ILs.

ILs are generally non-flammable and have negligible vapor pressure.[6] The lack of vapor pressure arises from the strong Coulombic interactions between the ions. They do not evaporate at room temperature and are generally non-volatile. It is only possible to distill certain ILs at high temperatures and low pressures. ILs show little or no evidence of distillation below their thermal decomposition temperatures at atmospheric pressure.

ILs also have a wide liquid range which makes them attractive as solvents. This range is much greater than the common molecular solvents. ILs thus offer opportunities for control in reactivity. The melting points of an IL defines the lower end of its liquidus range.[7] However, most ILs have super cooling properties that allow to form glasses. This can also make it difficult to measure their melting points; instead, their glass transition temperatures (around -70 °C) are reported. The charge distribution of ions, H-bonding, symmetry of ions and van der Waals forces can affect the melting points. In contrast to molecular solvents, the upper limit for the liquid range for ionic liquids is the decomposition temperature rather than a boiling point. The thermal decomposition is dependent on both the cation and the anion. ILs containing weakly nucleophilic anions (more basic) are stable at higher temperatures than weakly basic anions.[8]

ILs are generally denser than organic solvents, with typical densities ranging from 0.9 to 1.7 g cm^{-3} with little sensitivity to temperature changes.[9] The density is affected both by the cation and anion, with the latter having significant control. The density is also related to temperature, relative molecular mass, and the interaction between the molecules and molecular structure.

Most ILs are moderately viscous liquids. They are much more viscous than most molecular solvents. Viscosity ranges from 21 ([emim]DCA) to >1000 cP at room temperature. The viscosity can be lowered by increasing temperature or by dilution with molecular solvents.[10] Viscosity decreases as the temperature increases, but its dependence is more complicated than the molecular solvents, as they do not follow ordinary Arrhenius behavior (equation 1.1) but follows Vogel-Fulcher-Tammann behavior (equation 1.2).

Arrhenius equation $\eta = A\, exp\left(\frac{E_a}{RT}\right)$ **equation 1.1**

Vogel-Fulcher-Tammann (VFT) equation $\eta = \eta_o\, exp\left(\frac{B}{T-T_o}\right)$ **equation 1.2**

In equation 1.1, η is viscosity, A is the pre-exponential factor, E_a is activation energy, R is the gas constant and T is the temperature. While in equation 1.2 η_o, B and T_o are fitting parameters.

The choice of solvent can have a dramatic effect on a chemical reaction. Solvent effects depend mostly on the concept of solvent polarity. The polarity is the sum of all (specific and non-specific) intermolecular interactions between the solvent and solute, excluding the interactions that lead to chemical reactions, and thus constitute the combined strength of solute-solvent interactions. Kamlet Taft parameters (polarity-sensitive dyes) and miscibility studies are used to investigate polarity. Most commonly, chemists measure the dielectric constant to measure the polarity of molecular liquids. Unfortunately, this method requires a non-conducting medium and is not applicable to ionic liquids. Most ILs have a strong effective polarity and may dissolve many organic and inorganic compounds.[11] Increasing the alkyl chain length in the IL makes them lipophilic (less polar) which increases their solubility in organic solvents.

Knowledge of the electrochemical stability of a solvent is required before utilizing it in electrochemical studies. ILs have wide electrochemical windows and possess reasonably good electrical conductivity. The electrochemical window is the range of voltages over which the solvent is electrochemically inert. This is dependent on the anion's resistance to oxidation and the cation's resistance to reduction. Ionic liquids have found use in applications like battery electrolytes and electrochemical processing of metal surfaces.

The conductivity of a solvent is of critical importance in its selection for electrochemical applications. Conductivity is a measure of available charge carriers and their mobility. The ionic conductivities of ILs are good and are comparable to the non-aqueous solvent/electrolyte systems ($\sim$ 10 mS/cm)[12] but are less conductive than concentrated aqueous electrolytes.

A straightforward way to prepare CILs is to attach chiral molecules to the IL. Amino acids are effective and excellent starting materials for preparing functionalized ILs due to their biodegradability,[13] lower toxicity,[14] and possibility of chirality.[15] Amino acids bring their own properties to ILs. We first report CILs composed of tac cations tethered to amino acids. Amino acids also provide functional groups (amino and carboxylate) that can be candidates to act for functional ILs.

1.2 The Triaminocyclopropenium cation

The triaminocyclopropenium (tac) cation has been reviewed by Walst.[16] This is a summary of his review and subsequent research into tac cation.

1.2.1 Structure

The triphenylcyclopropenium cation was the first reported cyclopropenium cation but it is not stable to nucleophiles when compared to the tris(isopropyl)cyclopropenium cation due to the weaker π-conjugative effect of the phenyl groups, as shown by HMO and INDO calculations.[17,18] However, the tris(dimethylamino)cyclopropenium[19] cation has a higher stability due to amino substituents having an electron donating π-conjugative effect.[17,18] Thus, tac cations have more electron density on the ring carbon atoms and a lower bond order between ring carbons. The nitrogen atoms are the areas of highest electron density whereas the least electron density is found on the alkyl substituents (and specifically on the hydrogens).[17]

The measured barriers of the exocyclic C-N bond rotation for monoaminocyclopropeniums[20] $[C_3X_2NR_2]^+$, diaminocyclopropeniums[21] $[C_3X(NR_2)_2]^+$ and triaminocyclcopropeniums[21] $[C_3(NR_2)_3]^+$ were determined by variable temperature NMR and were reported as ΔG = 95-105 kJ mol^{-1}, ΔG = 75 kJ mol^{-1} and ΔG = 48.1 kJ mol^{-1} respectively. In the case of $[C_3X_2NR_2]^+$, a single amino group in conjugation with the ring should reflect high rotational barrier (fig 1.3). The lowest barrier should be expected for $[C_3(NR_2)_3]^+$ due to the presence three amino substituents in conjugation with the ring. The electron-donating π-conjugation effect of amino groups is larger than Cl and CH_3 and is responsible for reducing the C-C π bond order while providing stability to the cation by disturbing the charge.[22]

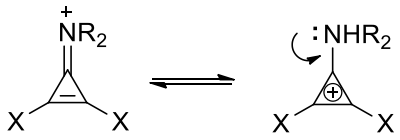

Figure 1.3-Conjugation of an amino group with the cyclopropenium ring.[21]

The canonical structures of the triaminocyclopropenium ring are in analogy with the guanidinium cation (fig 1.4).[23] A significant amount of positive charge movement from the C_3^+ ring to the amino groups gives a large amount of charge delocalization (proposed by INDO type calculations) which is responsible for stabilization of cyclopropenium ion. The nitrogen are the sites of highest electron charge density, whereas the least electron density is found on the alkyl substituents (and specifically on

the hydrogens). There is an empirical correlation between the stability of cyclopropenium ring (pK_{R+}) and the IR frequencies of the cyclopropenium ring.[23]

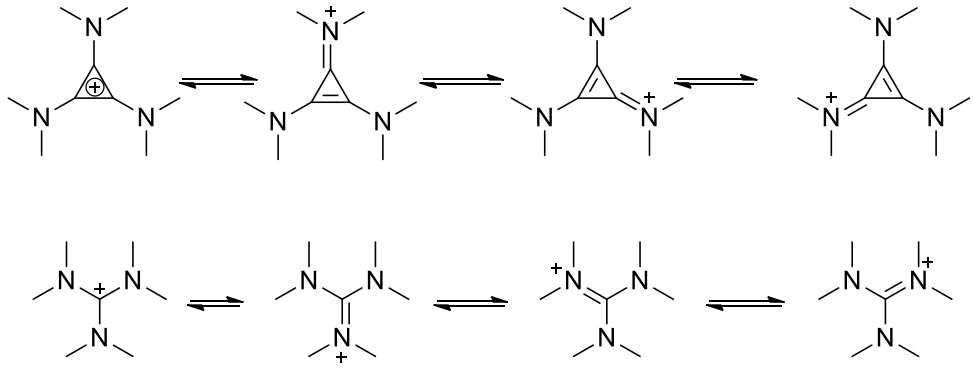

Figure 1.4-Canonical forms of the triaminocyclopropenium and guanidinium cation.[23]

Crystal structures have been reported for the tris(dimethylamino)cyclopropenium cation with various anions; ClO_4^-, $[Pd_2Cl_6]^{2-}$, tetracyanoquinodimethanide, 2,3-dichloro-5,6-dicyanobenzoquinonid, $[NbOCl_4.H_2O]^-$, $[NbCl_6]^-$, $[TaCl_6]^-$, $[SbCl_6]^-$ and I^{3-}.[24] Additionally, the crystal structures for $[C_3(NC_5H_{10})_3]ClO_4$, $[C_3(N^iPr_2)_3]ClO_4$ and $[C_3(N^iPr_2)_2NMe_2]ClO_4$ have also been reported. [21, 24h, i] The tris(dimethylamino)cyclopropenium[24a] ring has bent sigma bonds due to shorter C-C (1.363 Å) bonds than benzene (1.398 Å). The cation is not quite planar but its structure can be approximated to D_{3h} symmetry. The only exception to having all the nitrogen substituent planar is found in the tris(diisopropylamino)cyclopropenium cation[21h, i] and dicylcohexylamino-substituted cations[25] due to steric hindrance of the bulky diisopropyl and dicyclohexyl groups.

The cyclopropenium ring is highly-strained causing increased p character in the ring sigma bonds compared to exocyclic C-N bond and is sp^3 hybridized rather than sp^2.[26] This reduced the angle from 120 to 109° for the sigma bond. The exocylic C-N bonds are sp hybridized (fig 1.5). The MO diagram (fig 1.6) is a combination of cyclopropenium a and e π-orbitals and the nitrogen p-orbitals. The HOMO is of high energy as it is C_3 bonding but C-N antibonding.[27]

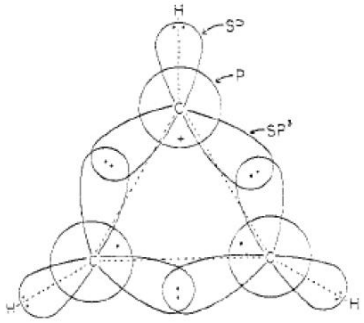

Figure 1.5–Hybridization in cyclopropenium orbitals.[26]

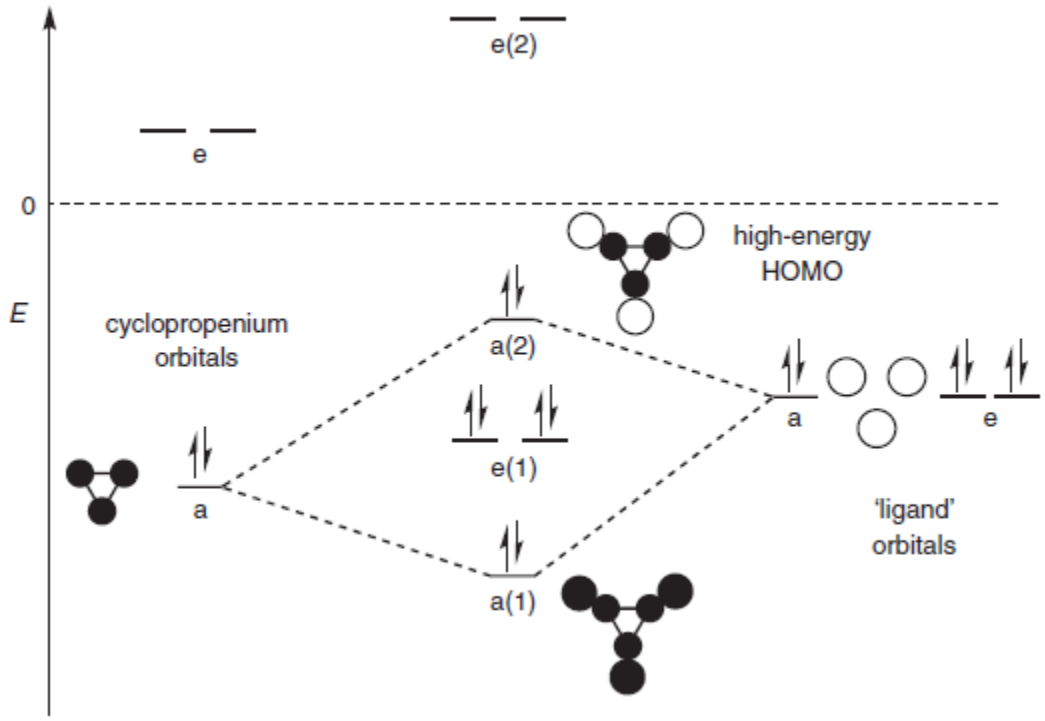

Figure 1.6-MO diagram of triaminocyclopropenium direct reproduction from review article by Lambert.[27a, 28]

1.2.2 Properties

Compared to trichloro- and triphenylcyclopropenium salts, triaminocyclopropenium salts[17, 19, 22-23, 27b, 29] are more stable and are more soluble in polar organic solvents. UV-Vis spectrometry shows that all triaminocyclopropeniums have a peak in the range of 206-312 nm and INDO calculations determined this to be due to charge transfer from the amino groups to the cyclopropenium ring.[21, 23]

Dipropylcyclopropenium and tripropylcyclopropenium cations were synthesized and their stability was compared with diphenylcyclopropenium cations by comparing the pK_{R+}'s.[30] The pK_{R+} is the pH necessary to establish 1:1 equilibrium between the diphenylcyclopropenium and the derived alcohol or in other words it is the pH for 50% ionization of carbinol to cation.

$$R^+ \underset{}{\overset{K}{\rightleftharpoons}} ROH$$

$$pK_{R+} = -\log K$$

Thus the more stable the cation is, the more it resists the hydroxide attack, and the higher the pH gets to establish 1:1 ratio. These values suggest that alkyl groups have largely inductive effects rather than hyperconjugation, by the order alkyl> phenyl> hydrogen. Relative influence of different alkyl substituents on cyclopropenyl cations were carried out by comparing pK_{R+} and the order was found to be Me> n-Pr> i-Pr> t-Bu.[31] This order follows the steric hinderance of solvation which parallels with the hyperconjugation. However, this order gave no distinction between these two effects.

The pK_{R+} values showed the thermodynamic stability of cyclopropenium cations and interrelated the stability of the cation with hydroxide attack.[32] Thus, cyclopropenium cations with dialkylamino substituents are much more stable than those with carbon, oxygen, sulfur or hydrogen substituents. Yoshida attempted to calculate pK_{R+} of triaminocyclopropenium salts, however, the potentiometric titration was not successful. They reported an empirical correlation between known pK_{R+} values and the position of an infrared peak of tac (C_3^+ ring) and calculated pK_{R+} was approximately 13 for triaminocyclopropenium.[22-23]

The electrochemistry of $[C_3(NMe_2)_3]^+$ was investigated by Johnson and it was found to oxidize easily to a dication and then to a trication.[27b, 33] Its oxidation potential is relatively low and similar to the oxidation of Cl^- because of a high-lying HOMO. Interestingly, the cation could not be reduced. Since the LUMO is relatively high it is hard to reduce, while the HOMO is relatively high so it is easily oxidized. Weiss[34] isolated and Surman[35] *et al.* generated (using pulse radiolysis) stable tac radical dications.

The tac is electron rich which was seen when H/D^+ was exchanged (electrophilic substitution) on bis(dialkylamino)cyclopropenium (fig 1.7).[36] Weiss suggested that the electron-rich nature of the cation and the electron-rich nature of the anion of tris(dimethylamino)cyclopropenium halide creates

ion-pair strain through closed-shell repulsion (fig 1.8).[27a] It induces strain within the ion-pair which could be increased or reduced by coordination of the electron-rich anions to suitable acceptor systems.

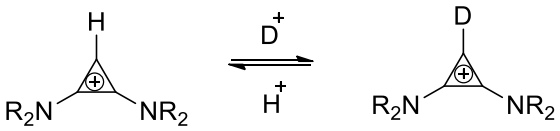

Figure 1.7-H/D exchange of diaminocyclopropenium.[36]

An X-ray structure of the benzoic acid adduct of $[C_3(NMe_2)_3]Cl$ suggested strong hydrogen bonding between chloride and acid due to ion-pair strain (hard-hard interaction).[37,38] Such chloride-acid adducts had never been isolated before.

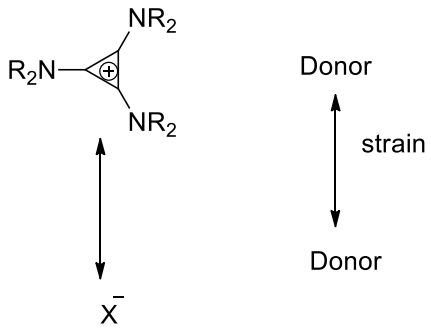

Figure 1.8-Ion pair strain between cation and anion.[37]

The iodide adducts were also formed by ion-pair strain through soft-soft interactions. Later, it was thought that ion-pair strain was responsible for a rare discrete dichloride[39] cluster in the crystal structure of $[C_3(N^iPr_2)_3]Cl.3H_2O$, that was reported by Curnow's group (fig 1.9).[24h]

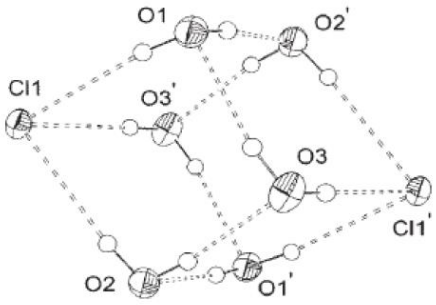

Figure 1.9–Dichloride hexahydrate cluster in $[C_3(N^iPr_2)_3]Cl.3H_2O$.[39]

1.2.3 Synthesis

Yoshida reported the synthesis of tac salts from the reaction of tetrachlorocyclopropene (tccp) with an excess of amine.[19] A reaction mechanism was proposed by Yoshida which suggests that a nucleophile (amine) can attack the vinylic carbon, liberating a chloride ion (fig 1.10).[17] The chloride is removed twice by repeating the same process until triaminochlorocyclopropene ionizes to form the cyclopropenium ring. However, another mechanism has also been proposed by Clark in which the cyclopropene ionizes after addition of a second amine.[21]

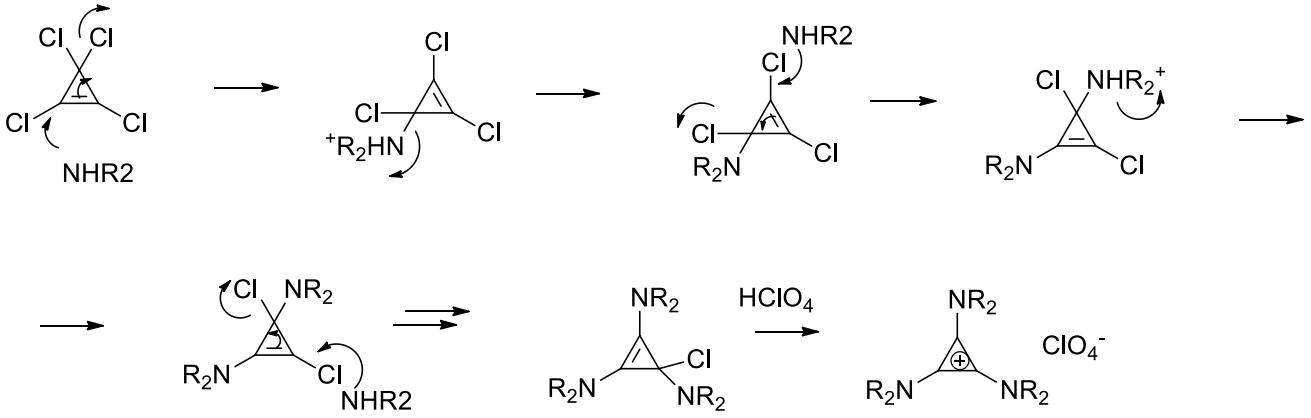

Figure 1.10–Reaction mechanism proposed by Yoshida.[17]

One route[17] to less symmetric cations was achieved via the easily accessible bis(diisopropylamino)chlorocyclopropenium[19] (fig 1.11). Another route involves starting with bis(dialkylamino)cyclopropenone which can react with thionyl chloride or an alkylating agent (e.g. triethyloxoniumtetrafluoroborate) to form a bis(dialkylamino)chlorocyclopropenium or bis(dialkylamino)alkoxycyclopropenium salt respectively (fig 1.11).[40] This can then be further reacted with a primary or secondary amine to generate less symmetric cations.

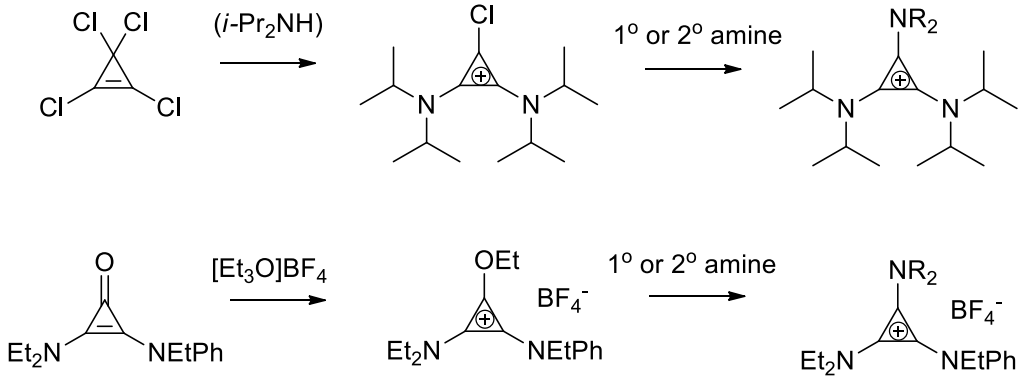

Figure 1.11-Reaction schemes for less symmetric tac salts.[17]

Kreb reacted arylisocyanides with bis(dialkylamino)acetylenes in a [1+2] cycloaddition to form bis(dialkylamino)cyclopropenimine in low to moderate yields (fig 1.12).[40b] The imines could be easily protonated to generate a less symmetric protic tac cation.

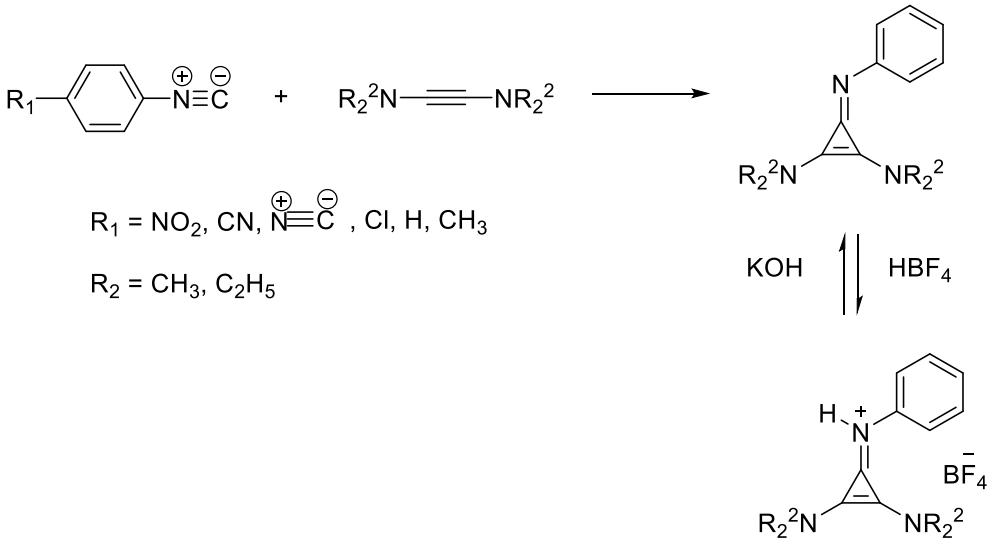

Figure 1.12-Reaction scheme for less symmetric tac salts by Krebs.[40b]

Weiss synthesized tac salts by reacting silylamines with tccp. Later, he reported the same reaction using an anion-dependent substitution for generating mono-amino $[(C_3(NMe_2)Cl_2)]^+$, bis-amino $[(C_3(NMe_2)_2Cl)]^+$, and tris(dimethylamino)cyclopropeniums, by reaction of $[C_3Cl_3]SbCl_6$ with trimethylsilyldimethylamine (fig 1.13).[41] This reaction was not possible when attempted with $[C_3Cl_3]BF_4$ or $[C_3Cl_3]OTf$ and the tris-substituted product was formed directly. Weiss also reported tris(phenylamino)cyclopropenium in which tccp reacted with trimethylsilylphenylamine.[41]

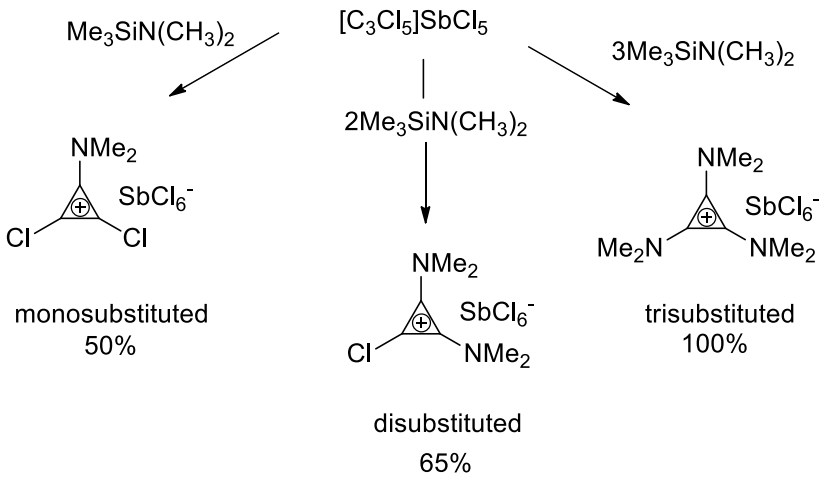

Figure 1.13-Reaction scheme for tac salt with anion dependent substitution.[41]

Taylor *et al.* simplified the overall synthesis by reacting pentachlorocyclopropane (pccp) with excess of amine to generate tac salts.[42] Previously, tccp was synthesized from pccp. The Curnow group used the same approach and formed tris(diisopropylamino)cyclopropenium, bis(diisopropyl)dimethylaminocyclopropenium.[24h, i] and other tac cations.[43] In the syntheses described herein, we use pccp to synthesize all the tacs.

1.2.4 Reactions

A wide range of nucleophiles have been found to react with tac salts. They can react with hydroxide, activated methylene compounds,[29f, 44] iminopyridinium ylides,[45] sodium sulfide[29d] or sodium selenide[29e] to form cyclopropenone,[17, 29a, d] diaminofulvene, bis(dialkylamino)cyclopropenimine, bis(dialkylamino)cyclopropenethione, or bis(dialkylamino)cyclopropeneselenone, respectively.

Protic tac salts such as $[C_3(NR_2)_2(NHR)]$ can be easily deprotonated with a strong base[40b, 46] (KOH, Hunig's base or *n*-BuLi) (fig 1.14) to give bis(dialkylamino)cyclopropenimine, which can easily be alkylated or reprotonated with an acid. Deprotonated trisaminocyclopropenium ions are used as Brønsted base catalysts.[25]

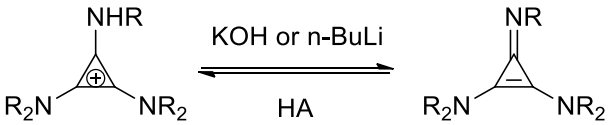

Figure 1.14-Reaction scheme for synthesis of bis(dialkyamino)cyclopropenimine.[25]

1.2 Amino Acid Ionic liquids (AAILs)

Some AAILs are constructed without modification of the amino acid residue. The side chain of the amino acid moiety remain largely preserved, with alteration of acidity or basicity or polyfunctional modification of both the amine and carboxylic group. The amino acids can be directly used to prepare CILs as a cation or anion by protonation or deprotontion of the carboxylic group or amino group with an acid or base, respectively. The chirality is preserved in the CIL, but various properties can be tuned by variation of the organic or inorganic acid or base.

1.2.1 Amino Acid as the Cation or Anion without Modification

Amino acids are a biodegradable, easily available, and cheap chiral source for the construction of CILs. Plenty of work has been done to utilize unmodified amino acids as cations in combination with various anions. Amino acid-derived CILs, [amino acid][HSO_4]/[1/2SO_4] have been synthesized by reaction of

alanine, valine, leucine, glycine, tyrosine, glutamic acid, proline, lysine, histidine or arginine with 98% H_2SO_4.[47]

Tao and coworkers reported 22 chiral ionic liquids,[48] in which the cations were derived directly from α-amino acids (L-proline)[49] by a one-step acidification of amino acids with HCl, HNO_3, HBF_4, HPF_6, CF_3COOH or H_2SO_4 or by anion metathesis of an α-amino acid ester[50,51] chloride (e.g. *tert*-butyl ester chloride[52]) with metal NO_3^-, BF_4^-, PF_6^-, NTf_2^-, CH_3COO^- or lactate (fig 1.15). The procedure involved is atom-economic without any generation of toxic by-products. Among the obtained CILs, half were white solids while the other half had melting points below 100 °C. They were viscous liquids due to strong hydrogen bonding. This was minimized by introducing an amino acid ester group. Esterification provided a tool for adjusting the properties of the resulting ILs. The thermal stabilities ranged from 150-263 °C, lower than imidazolium ILs, but much higher than described by Wasserscheid[15] for ephedrine-type CIL. DSC results showed that RTILs ([IleC_1]NO_3 and [AlaC_1]NO_3) have different characteristics giving solid-solid transitions at lower temperatures and solid-liquid transitions at higher temperatures. The chirality was maintained in the resulting ILs.

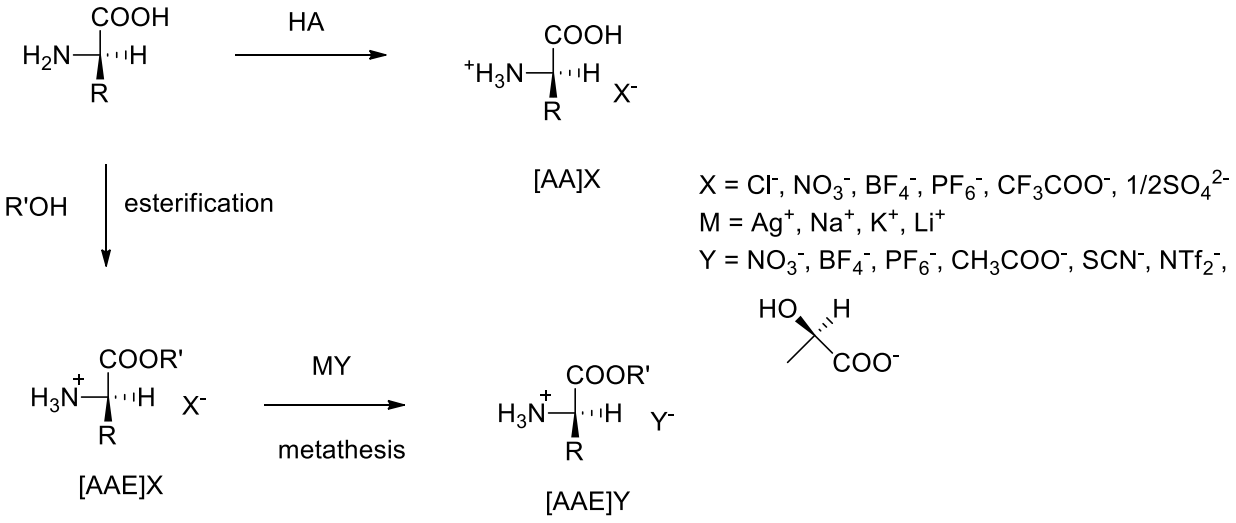

Figure 1.15-Reaction scheme.

Tao also reported 'fully green' ILs derived from natural α-amino acid ester salts as "fully green" ionic liquids with nitrate (**1.1** and **1.2**) (a low toxicity anion) and saccharinate (**1.3**) (sac) (a well known food additive) as the anion.[53] Their characteristics were similar to conventional ionic liquids. Esterification of the acidic functionality proved to increase the biodegradability of the CILs.[54] Their thermal stabilities ranged from 150-230 °C and all had solid-solid transition temperatures. Half of them had

melting points below 0 °C. [AAE][sac] (Amino Acid Ester = AAE) is a liquid at ambient temperature with a melting point below 8 °C.

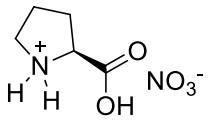

1.1

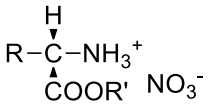

1.2

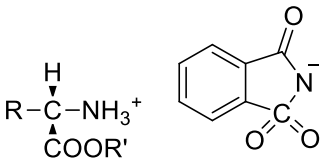

1.3

Meiyan patented the synthesis of CILs via the reaction of imidazolium, *N*-alkyl pyridines, quaternary ammonium salts and quaternary phosphonium chloride salts with the sodium salt of L-valine or D-valine in acetone with stirring for 3 days, followed by centrifugation to remove NaCl.[55]

1.2.2 Metal CILs (MCILs)

The formation of MCILs by the reaction of a halide salt with Lewis acids ($AlCl_3$ or $FeCl_3$) has been an important area in IL. Salts containing main group (Zn, Al) and transition metal (Fe) element, with an amino acid moiety as the cation, were synthesized by reacting the amino acid ester hydrochloride with aluminum chloride, ferric chloride or zinc chloride (fig 1.16).[50,56] The MIL having $FeCl_4^-$ as an anion is regarded as a novel new material which combines the properties of a CIL with a catalyst, and magnetic properties originating from the metal. Warner and coworkers determined the enantiomeric purity of [AA][$FeCl_4$] by circular dichroism.[56] This was also characterized by UV-Vis, ^1H and ^{13}C NMR, FT-IR, and elemental analysis. The thermal decomposition temperature (195-216 °C), glass transition temperature (−30 to −48 °C), and magnetic properties (molar magnetic susceptibility and effective magnetic moment) were also determined.[56]

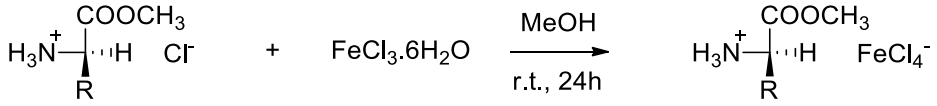

Figure 1.16-Synthesis of magnetic chiral ionic liquid from natural amino acids.[56]

Qian and coworkers reported novel chiral salts containing natural amino acid anions and crown ether-chelated alkali metal cation (K^+).[57] The synthesis of [18-C-6K][L-AA] (**1.4**) involved reaction of L-AA, KOH and 18-C-6 in 1.1:1:1 molar ratio. The thermal decomposition temperatures (150-230 °C), optical rotation, and melting points (most were above 100 °C) were measured.

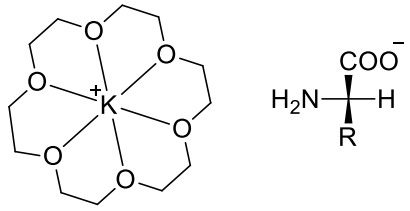

1.4

1.2.3 Modification of Amino Acid Functional Groups

Although, the direct reaction of amino acids with an acid or base is the simplest and fastest way to produce an IL, it suffers from sensitivity to pH changes. Thus, better structures involve non-protonated cations and non-coordinating anions, whilst also retaining the integrity of the amino acid.

(*S*)-Histidine was utilized as a chiral source by the modification of its side chain for the preparation of imidazolium-based CILs, with the amine and carboxylate unprotected, *N*- (PG_2) or *O*-protected (PG_1) or both protected (fig 1.17).[58] (*S*)-Histidine has an imidazole ring, upon selective alkylation of both imidazole nitrogens while leaving behind the amino and the carboxyl groups. The anions could be exchanged to alter the physical properties.

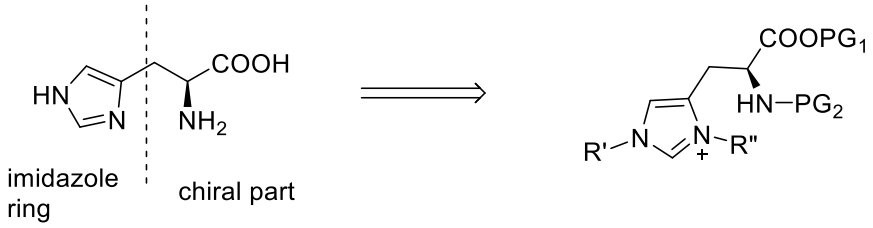

Figure 1.17-Chiral bifunctional histidine as an ionic liquid.[58a]

Guillen[58a] was astonished to obtain a cyclic urea by heating a mixture of carbonyldiimidazole with histidine methyl ester dihydrochloride at 80 °C without using DMF (as solvent).[59] The cyclic urea (viscous liquid) was alkylated with methyl iodide and formed crystalline solid with a high melting point. The cyclic urea was opened by *tert*-butanol in the presence of diisopropylethylamine, and then alkylated to form chiral hygroscopic imidazolium salts (fig 1.18). This methodology inverted the substitution pattern of the imidazolium ring simply by inverting the alkylating steps. The amino and carboxyl groups can undergo further reduction and peptide coupling. Finally, anion metathesis with PF_6^-, BF_4^- or NTf_2^- generated low viscosity CILs. In order to increase the hydrophobicity the same group later prepared histidinium bearing longer alkyl chains (*n*-octyl and *n*-dodectyl).[60] The resulting

hydrophobic CILs were soluble under acidic and basic aqueous solutions but could be precipitated when shifting the pH near 7 as the solubility decreases when the amino acid exists in zwitterionic form. The DSC (glass transition temperature) and optical rotation were measured.

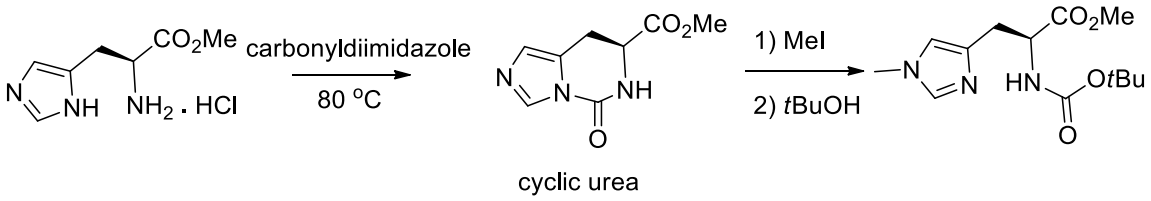

Figure 1.18-Reaction scheme for the formation and ring opening of a cyclic urea.[58a]

(*S*)-Histidine was alkylated with *n*-propyl bromide after *O*-protection (OMe) by ester formation and *N*-protection with *N-tert*-butoxycarbonyl (Boc). The alkylation of bis-protected PG-His-OMe (PG = Bz or Boc) formed a "symmetrical" imidazolium bromide (fig 1.19).[61] The melting points ranged from 40-55 °C.

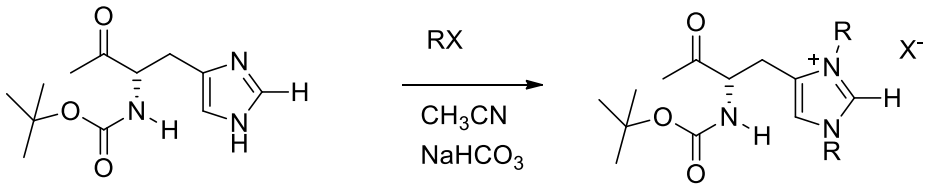

Figure 1.19- Reaction scheme.[61]

Mono- and polymeric forms of CILs are synthesized upon alkylation of L-leucinol or L-prolinol with undecenoxycarbonyl bromide to generate an undecenoxy-L-amino alcohol bromide (fig 1.20).[62] The undeceneoxycarbonyl-L-leucinol bromide is a RTIL, whereas undecenoxycarbonyl-L-pyrrolidinol bromide melts at 30-35 °C. This material was characterized to determine the critical micelle concentration, polarity, optical rotation, and partial specific volume.

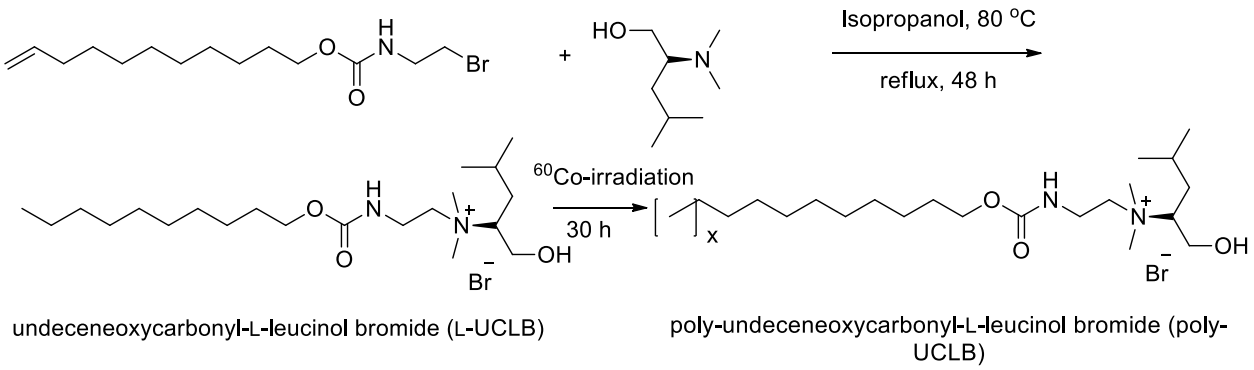

Figure 1.20-Reaction scheme.[62]

N-alkylation of L-proline[63] or the L-proline[64] ester with alkyl iodide or alkyl bromide yielded *N*,*N*-dialkyl-L-proline alkyl ester iodide. The physical properties were determined after the anion metathesis with NO_3^-, BF_4^- or PF_6^-. Most of them had melting points below 100 °C. Thermal decomposition temperatures ranged from 185-340 °C, and their optical rotation was measured. The $[\alpha]_D^{20}$ values were affected by the alkyl chain length of L-proline.[63] The ^{19}F NMR spectra showed that these CILs had different chiral recognition abilities towards racemic Mosher's acid, which was related directly to the alkyl chain length. It was also seen that as the $[\alpha]_D^{20}$ increases (with the decrease of alkyl chain length), Δδ (it is the signal splitting for the two diastreomeric -CF_3 groups of racemic Mosher's acid in CIL) values in Hz also increased (fig 1.21), which in turn tune the chiral recognition abilities of the CILs in racemic Mosher's acid.

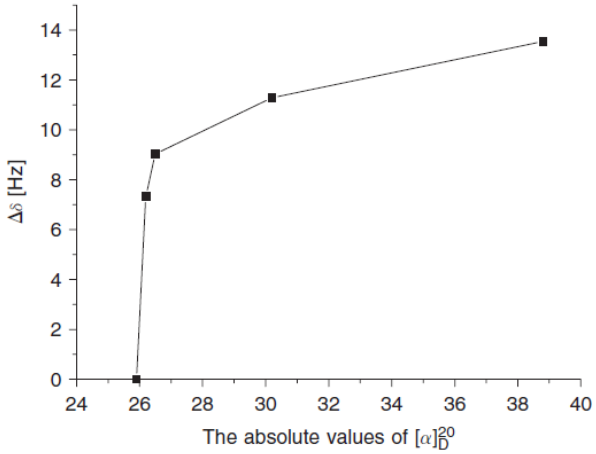

Figure 1.21-$[\alpha]_D^{20}$ versus Δδ (Hz) values of the –CF_3 signal of racemic Mosher's acid.[63]

1.2.4 Ammonium

A lot of work has been done on ammonium-based CILs where chirality is derived from an amino acid anion. The neutralization of choline,[65] tetrabutylammonium,[66] triethylhexylammonium,[67]

tetraalkylammonium (R = 1-12 carbon chain),[68,69,70] didecyldimethylammonium, benzylalkonium, and *N*,*N*-dimethyl-*N*-(2-phenoxyethyl)-1-dodecanaminium[71] hydroxide with amino acids, form the corresponding salts without any by-products other than water. The bulky nature of the tetrabutylammonium cation ([TBA]) reduces the intermolecular attraction and increases the probability of the resulting salt to be a liquid. The color of the ionic liquids ranged from colorless to orange. A clear upfield shift was seen by comparing the chemical shift of the starting acid and subsequent CIL on the ^{1}H NMR spectrum. The magnitude of the specific rotation $[\alpha]_D^{20}$, was smaller than for the free amino acid, which was previously observed due to a small amount of acid or base.[72]

Wood studied the changes in the optical activity of several amino acids (leucine, aspartic acid, and glutamic acid) in the presence of varying amounts of acids and alkali. The solutions of amino acids used had a concentration of 1 to 2% but in case of aspartic acid dilute solutions were used due to sparing solubility. The dilute solutions can give inaccurate values of specific rotation and the salts present may be taken as their completely ionized form. In case of free leucine, the value of $[\alpha]_D^{25}$ is $-9.84°$ in an aqueous solution. However, upon addition of HCl (fig 1.22) or alkali (fig 1.23) to an aqueous solution of leucine a marked change in the optical activity of the solution is observed. The effect of alkali on the specific rotation of leucine is of similar nature to the influence of the HCl. The irregularity in the values of specific rotation is thought to be due to racemization but unfortunately, no evidence was obtained. There was no appreciable variation in optical activity of leucine, in the presence of excess NaOH. Similar effect was noticed by the added acid or alkali to the solution of aspartic acid and glutamic acid. However, strength of added acid influenced the specific rotation of aspartic acid. The weak nature of acetic acid didn't produce much change in the specific rotation compared to HCl. When the ratio of added acid or base to amino acid is greater than unity, the break in the curve is reached which indicates the specific activity of the completion of salt-formation of the amino acid (fig 1.24).

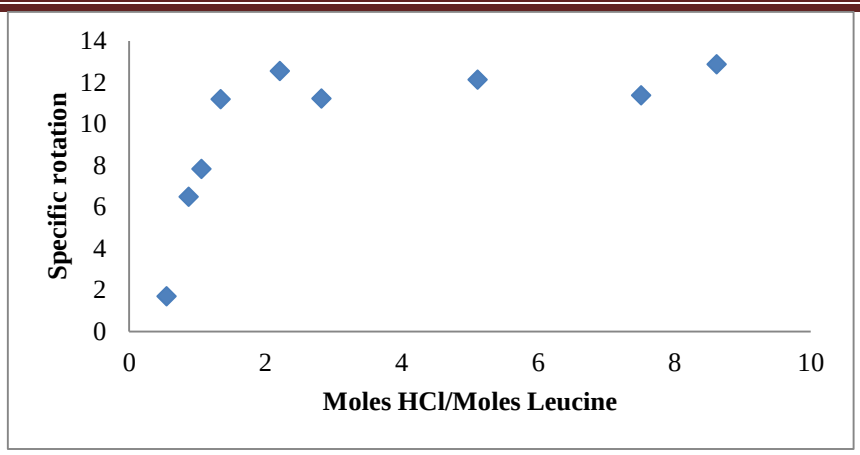

Figure 1.22-Graphical representation between specific rotation and Moles HCl/Moles Leucine.[72]

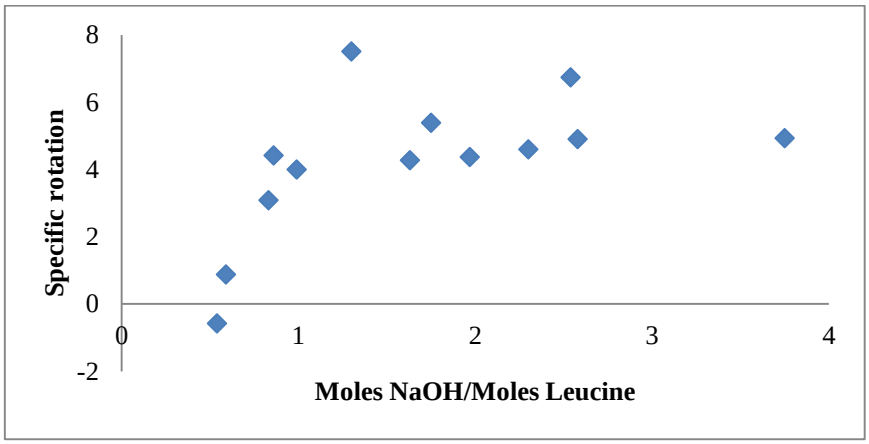

Figure 1.23-Graphical representation between specific rotation and Moles NaOH/Moles Leucine.[72]

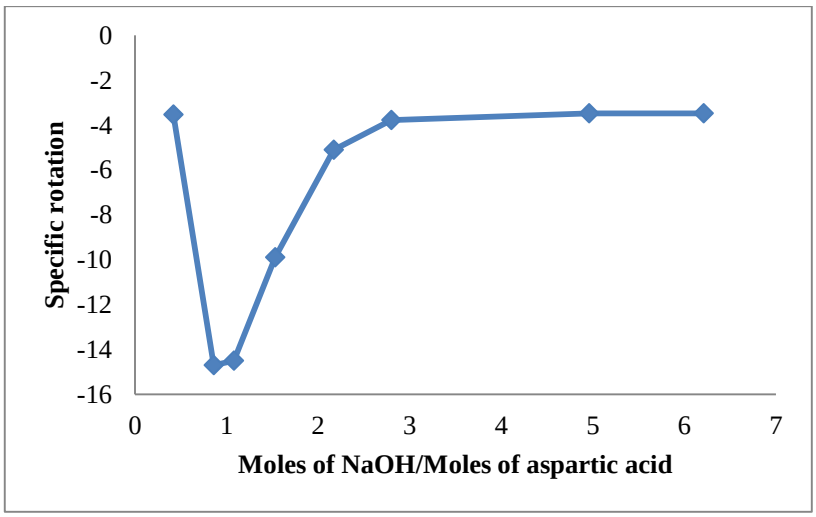

Figure 1.24-Graphical representation between specific rotation and Moles NaOH/Moles aspartic acid.[72]

During the formation of [TBA][L-Hglu] and [TBA][L-Glu], no racemization was observed, which was further indicated by comparing the solutions of both with free amino acids in 5 M HCl. All of the synthesized CILs were insoluble in diethyl ether, hexane and toluene, but were soluble in water, acetonitrile, acetone, dichloromethane and chloroform. Thermal stabilities (150-170 °C) of these CILs were low and showed significant darkening when heated to temperatures of 110 °C. DSC measurements showed that the symmetric ammonium salt was solid whilst the asymmetric salt was liquid (-40 °C). Thus, CILs with low viscosity and high thermal decomposition temperatures could not be obtained with the ammonium cation. The viscosity and ionic conductivity of [tetraethylammonium][AA] was improved compared to similar AAILs.[73] Didecyldimethylammonium[71] L-prolinate was found to be a very effective anti-microbial and anti-fungal compared to other CILs.

Amino acid ionic liquid-supported Schiff bases were synthesized by the condensation of an amino acid moiety (L-threonine, L-valine, L-leucine, L-isoleucine and L-histidine) of [tetrabutylammonium][AA] with salicylaldehyde (fig 1.26).[74] These were then characterized by NMR, UV-Vis, IR and mass spectrometry. The imidazole ring in L-histidine weakened the interactions between the carboxylate and amine groups, and stabilized the OH-form as illustrated in fig 1.25. While in other amino acid IL-supported Schiff bases, a proton transfer equilibrium existed where the carboxylate group stabilized the proton transferred amine form.

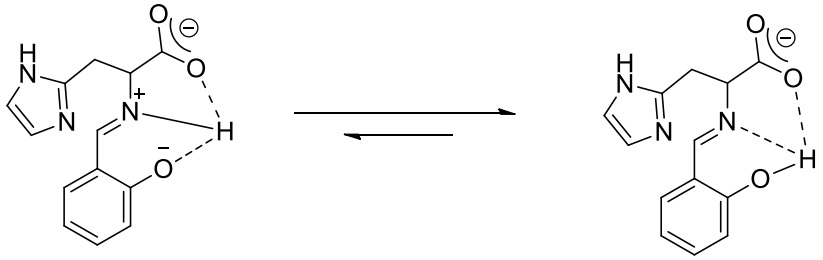

Figure 1.25-Influence of imidazolium ring on the proton transfer.[74]

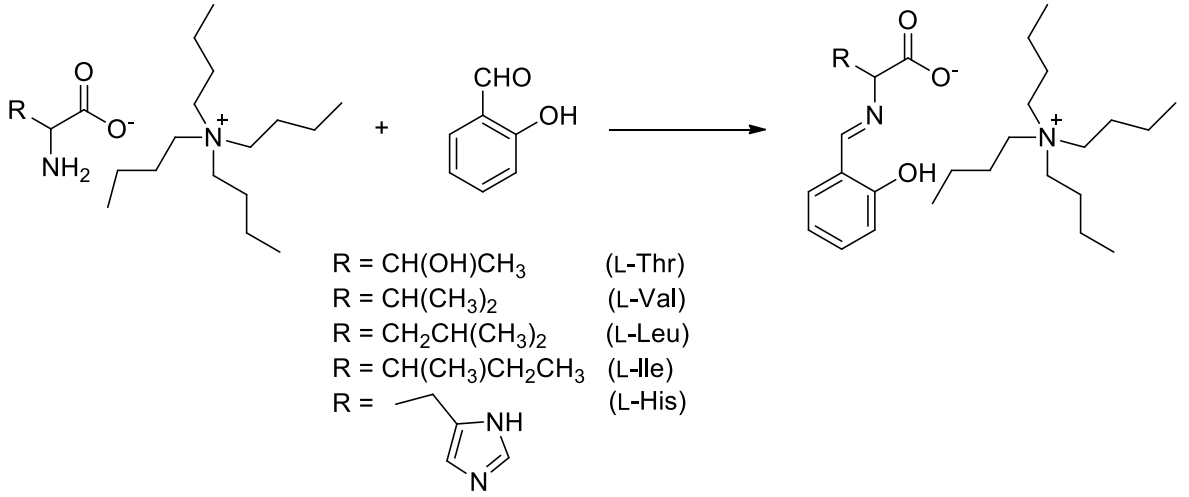

Figure 1.26-Synthesis of amino acid ionic liquid supported Schiff bases.[74]

Two pyrrolidine-type CILs were synthesized by activating (+)-*cis*-2-benzamidocyclohexane-carboxylic acid with ethyl chloroformate followed by reaction with dimethylamine. *cis*-Diamide was reduced and debenzylated to form *cis*-1,3-diamine.[75] The *N*-Cbz-L-proline was coupled with the *cis*-1,3-diamine followed by alkylation and metathesis to generate the ammonium salts (fig 1.27). Both of the CILs were viscous liquids at room temperature. They were soluble in polar solvents such as alcohols, dichloromethane and THF, but immiscible in non-polar solvents, such as diethyl ether and *n*-hexane.

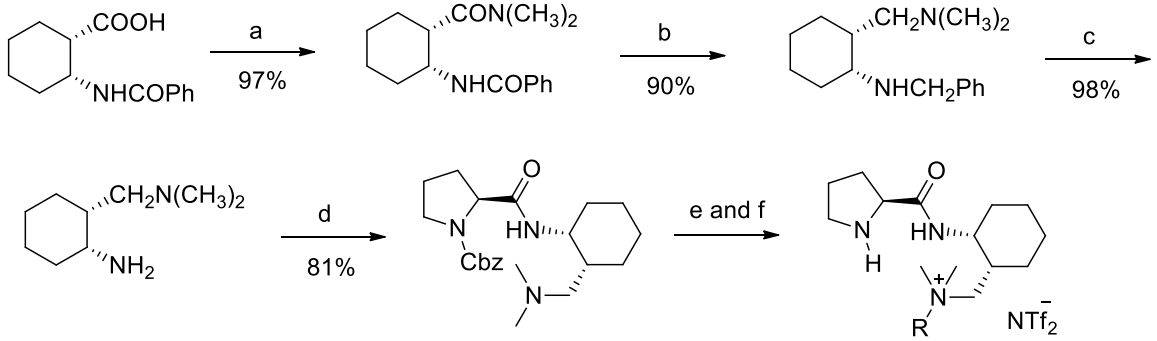

Figure 1.27-Reaction scheme a) Ethyl chloroformate ($ClCO_2Et$), Et_3N, 50% Me_2NH solution b) $LiAlH_4$ c) Pd/C, H_2 d) *N*-Cbz-L-proline e) RI, $LiNTf_2$ f) Pd/C, H_2.[75]

Liu and coworkers patented the synthesis of CILs based on the cheap and easily-available L-cysteine hydrochloride; a series was prepared having a morpholine cation with (*R*)-thiazolidine-2-thione-4-carboxylic acid as the anion.[76]

1.2.5 Phosphonium

Ohno's group synthesized and characterized 20 CILs by neutralizing *N*-tetrabutylphosphonium hydroxide with amino acids.[67] These had better thermal properties, lower viscosities, and lower toxicities than imidazolium, ammonium, pyridinium, and pyrolidinium CILs. The better thermal stability and lower viscosity was attributed to the cation structure. Interestingly, phosphonium salts with $TFSA^-$ and BF_4^- as the anion, have higher viscosities. Their melting points were below 100 °C and they retained their chirality even after heating for 10 h at 100 °C, as determined by optical rotation and ^1H NMR.[77]

Later, the same group coupled a stable aqueous solution of tetrabutylphosphonium ($[P_{4444}]$) hydroxide with hydrophobic derivatives of amino acids (L-alanine, L-valine, L-leucine, L-isoleucine and L-phenylalanine) by introducing both the trifluoromethane sulfonyl group and methyl ester group [Tf-Leu] (fig 1.28).[78,79] $[P_{4448}]$[Tf-Leu] was prepared by coupling $[P_{4448}]$[OH] with Tf-Leu. Thermal properties, melting points, and glass transition temperatures gave superior ILs when $[P_{4444}]^+$ was coupled with an imide anion derived from an amino acid. This was due to poor packing of ions and disordering of the amino acid derivative compared to NTf_2^- anion. Viscosity increases with longer alkyl side chains of the amino acid derivative. Introduction of an imide structure in the amino acid increased the viscosity compared with NTf_2 and dicyanamide salts. Melting point, viscosity and hydrophobicity were not improved over hydrophobic ILs such as [bmim][Tf_2N]. Optical rotation confirmed the chirality remained unaffected even when heated up to 100 °C for few hours. Phosphonium ($[P_{4444}]$) ILs showed a two-phase separation when dissolved in water due to the presence of the hydrophobic butyl chains but this was controllable by changing the side chains of the amino acids.[80] A three-phase system was constructed by mixing of the above two-phase system with hexane. Low critical solution temperature (LCST) studies were done by mixing an equimolar ratio of $[P_{4444}]$[Tf-Leu] and water. The mixture of $[P_{4444}]$[Tf-Leu] and water was cooled and heated gradually by stirring with a penetrating temperature sensor, after coloring the IL phase with Nile Red. Upon cooling (22 °C), water dissolved in the IL phase, however phase separation occurred as the temperature was increased to 25 °C and a cloudy suspension was generated due to emulsion formation. All the ILs synthesized exhibited LCST-type behavior, however for $[P_{4448}]$[Tf-Leu], the phase-separation temperature reached the freezing point of water. The phase-separation could be controlled by varying the side-chain length of the cation and the water/IL ratio.

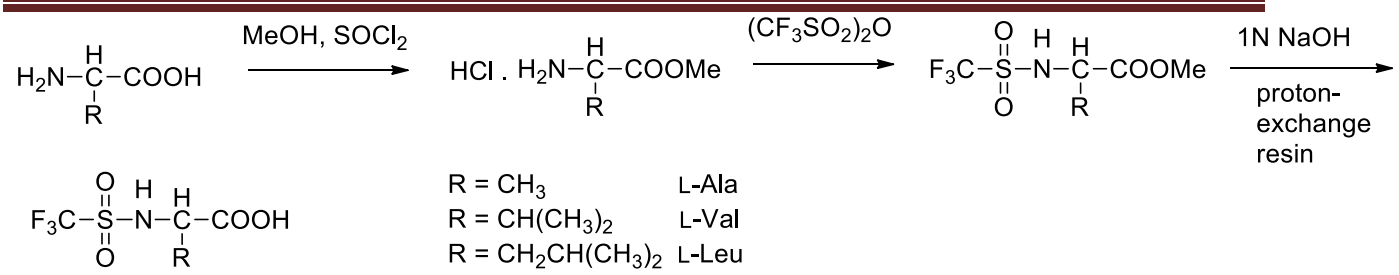

Figure 1.28-Reaction scheme.[80]

The glass transition temperature, melting points and optical rotations of phosphonium-type CIL were measured (Table 1.1).[79] Melting points ranged from 51 °C to 64 °C, while $[P_{4448}][Tf\text{-}Leu]$ (**1.5**) gave a T_g at −50 °C. The melting point of $[P_{4444}][Tf_2N]$ was 86 °C, which was very high compared with the amino-acid type. Chirality was also maintained even after heating to temperatures of 150 °C.

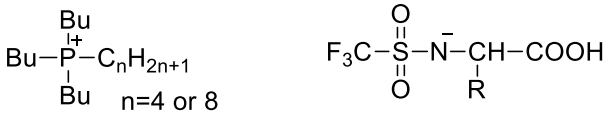

1.5

Table 1.1-Physical properties of phosphonium CILs.[79]

entry	cation	R	T_m /°C	$[\alpha]_D^{20}$
1	$[P_{4444}]$	$CH(CH_3)_2$	51	4.5
2	$[P_{4444}]$	$CH_2CH(CH_3)_2$	64	9.8
3	$[P_{4448}]$	$CH_2CH(CH_3)_2$	−50*	7.0
4	$[P_{4444}]$	$CH(CH_3)C_2H_5$	51	3.6
5	$[P_{4444}]$	$CH_2(C_6H_5)$	64	1.5

*Tg (°C)

Other quaternary phosphonium salt cations such as $[R_4P]^+$, where alkyl chain length ranged from C_1-C_{12}, were reported.[68] The chirality was derived from anions having L-glutamate ions, chiral pyroglutamate,[68] tyrosine,[69] leucine and isoleucine.[70]

1.2.6 Imidazolium

CILs were synthesized from imidazolium by modifying the cation or by functionalization at the 1, 2 or 3 position of the ring.

1.2.6.1 Without Modification of the Imidazolium cation

Fukumoto and coworkers prepared novel RTILs by the neutralization of 1-ethyl-3-methylimidazolium hydroxide [emim][OH] with 20 naturally-occurring amino acids utilizing an anion-exchange resin.[81] Wang patented his synthesis of the imidazolium salts[68] where chirality was derived from L-glutamate or chiral pyroglutamate[68], tyrosine[69], leucine and isoleucine[70]. [emim][AA] are colorless liquids at room temperature. Miscibility studies, differential scanning calorimetric measurements (T_g ranging from −65 to 6 °C), thermal decomposition (stable up to 200 °C), and ionic conductivity (10^{-9} to 10^{-4} S/cm at 25 °C) were measured. However, the ILs with anions derived from Arg, His, Try, Asn, Gln, and Glu had low ionic conductivities. Physico-chemical properties were strongly affected by the structure of the side chain of the amino acid moiety. These findings were thought to be useful for designing ionic liquids for specific applications. However, due to the hydrogen bonding at the C-2 position of the imidazolium cation ring with its amino acid anion, relatively high viscosities for the AAILs was observed.

1-Butyl-3-methylimidazolium hydroxide was neutralized with *N*-trifluoromethane sulfonyl amino acid (L-alanine, L-valine and L-leucine) methyl ester (fig 1.28) resulting in hydrophilic chiral anion ionic liquids and did not require special purification procedures.[78] Melting points, glass transition temperatures, thermal decomposition temperature, viscosities, and optical rotation measurements were obtained. Decomposition temperatures were around 250 °C, lower than [bmim]TFSA. This should be attributed to the presence of methyl ester bond. These chiral imidazolium salts were totally miscible with water. Therefore, chiral and hydrophilic ionic liquids were prepared by introducing trifluoromethane sulfonyl and methyl ester groups in the anion. However, their physico-chemical properties were not improved compared to [bmim][Tf_2N].

1.2.6.2 Imidazolium Rings Obtained from Amino Acids

There are two ways of obtaining imidazolium rings from amino acids as proposed by Bao. Firstly, by reducing the amino acids to amino alcohols and then condensing them with an aldehyde to form an

imidazole ring. Secondly, the hydroxyl group may interfere with the condensation of amino group with aldehydes. Bao utilized the second route by allowing the amino acids to condense with aldehydes to form imidazole ring under basic conditions. Imidazolium rings were synthesized in four steps by condensation of amino acids with aldehydes under basic conditions in 30-33% overall yield (fig 1.29).[82] Esterification, reduction and alkylation formed the corresponding salts by already known procedures. Their melting points (5-16 °C), thermal stabilities (up to 180 °C), chemical stability (vs. water) and viscosities were compared with the reported values by Wasserscheid (melting point 80 °C; thermal stability up to 100 °C; good chemical stability vs water and common organic substrates and relatively low viscosity) and were found to be very similar to the imidazolium cations.[15] Later Xie and coworkers, used a similar reaction procedure to synthesize chiral di-imidazolium molecular tweezers from (*S*)-alanine and (*S*)-phenylalanine (fig 1.29).[83]

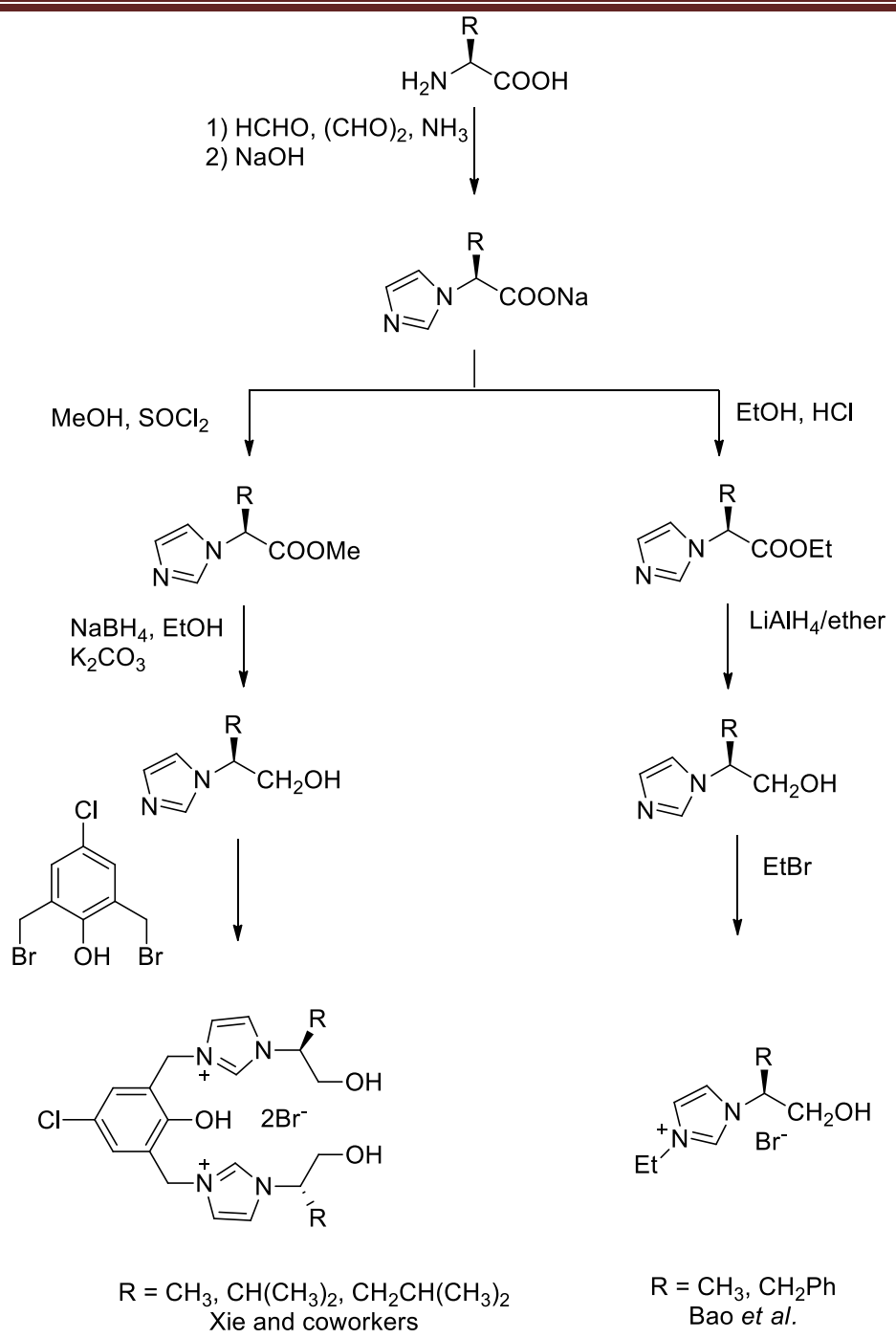

Figure 1.29-Reaction scheme.[82,83]

Armstrong[84] patented isoleucine-based imidazolium salts (either as an alcohol or as an ester) (**1.6** and **1.7**) by using the reaction scheme of Bao.[82]

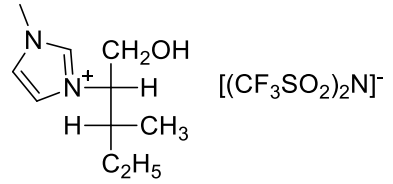

1.6

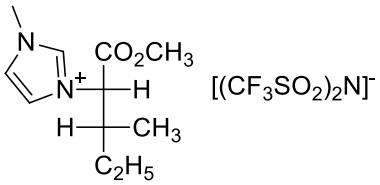

1.7

The long chain surface-active CIL, *S*-3-hexadecyl-1-(1-hydroxy-propan-2-yl)-imidazolium[85] bromide (**1.8**) was derived from L-alanine by using the same reaction scheme used by Bao[82] but altering the alkylating agent ($C_{16}H_{33}Br$). Its adsorption and aggregation behaviors were studied in aqueous solution. The critical micelle concentration of this surface-active CIL has a superior capacity compared to traditional ionic surfactants. These long chain CILs may find applications in chiral separation. The *S*-3-hexadecyl-1-(1-hydroxy-propan-2-yl)-imidazolium-$AuCl_4$ complex was also synthesized by exchanging the bromide anion with $AuCl_4$. These gold nanoparticle aggregated structures may find potential applications in electronics, photonics, biological labeling, chemical sensing and imaging.[86]

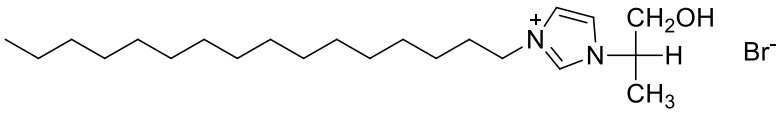

1.8

Ishida and coworkers reported imidazolium-based enantiopure CILs with cyclophane-type planar chiraity derived from (*S*)-valinol (fig 1.30).[87] These were liquid at room temperature and had thermal stabilities up to 270 °C.

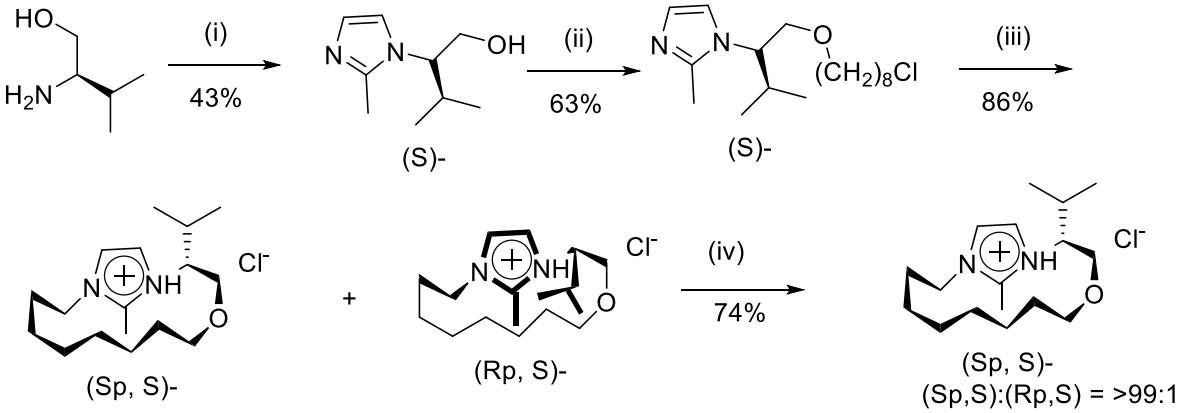

Figure 1.30-Reaction scheme i) CH_3CHO (5.0 equiv), glyoxal (1.0 equiv), NH_4OAc (1.0 equiv), MeOH, rt; ii) NaH (1.2 equiv), 1,8-dichlorooctane (3.0 equiv), DMF, 0 °C then 50 °C; iii) dimethylacetamide (DMAc), 150 °C; iv) recrystallization from CH_2Cl_2/AcOEt.[87]

Luis and coworkers synthesized an imidazole ring by reacting formaldehyde, ammonium acetate, glyoxal and chiral α-amino amides (L-valine, L-phenylalanine and L-leucine were starting materials) and obtained imidazolium cations.[88] Subsequent alkylation and anion exchange formed the CILs (fig 1.31). The DSC (m.p. ranged from −49 to 61 °C) and TGA (280 to 400 °C) analyses were done on the CILs.

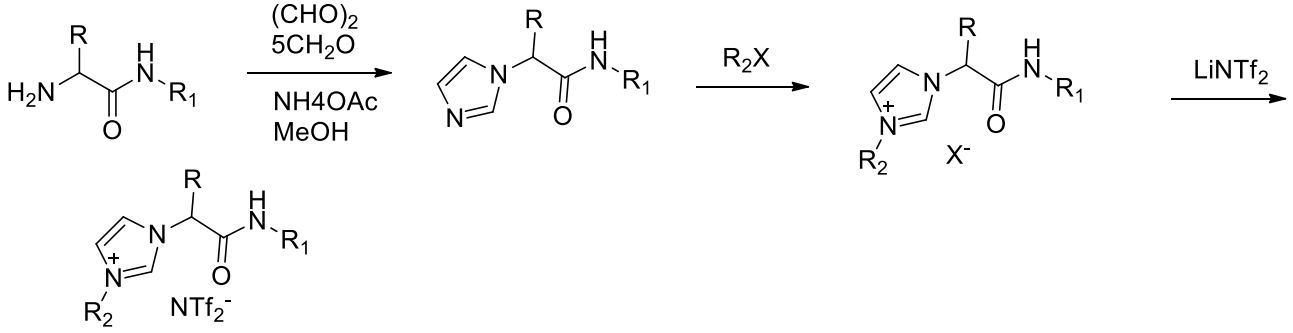

Figure 1.31-Reaction scheme.[88]

1.2.6.3 Modification *via* Substitution at 1/3 position of imidazolium

Chiral imidazolium ionic liquids were derived from naturally-occurring amino acids (L-alanine, L-valine and L-leucine) by substitution on the 1/3 position of imidazolium by modification of the amino group.

Most of the work done was by reduction of the amino acid to an amino alcohol by $LiAlH_4$ or $NaBH_4/I_2$ followed by substitution on the imidazole ring directly or by further modification using route I to V (fig 1.32).

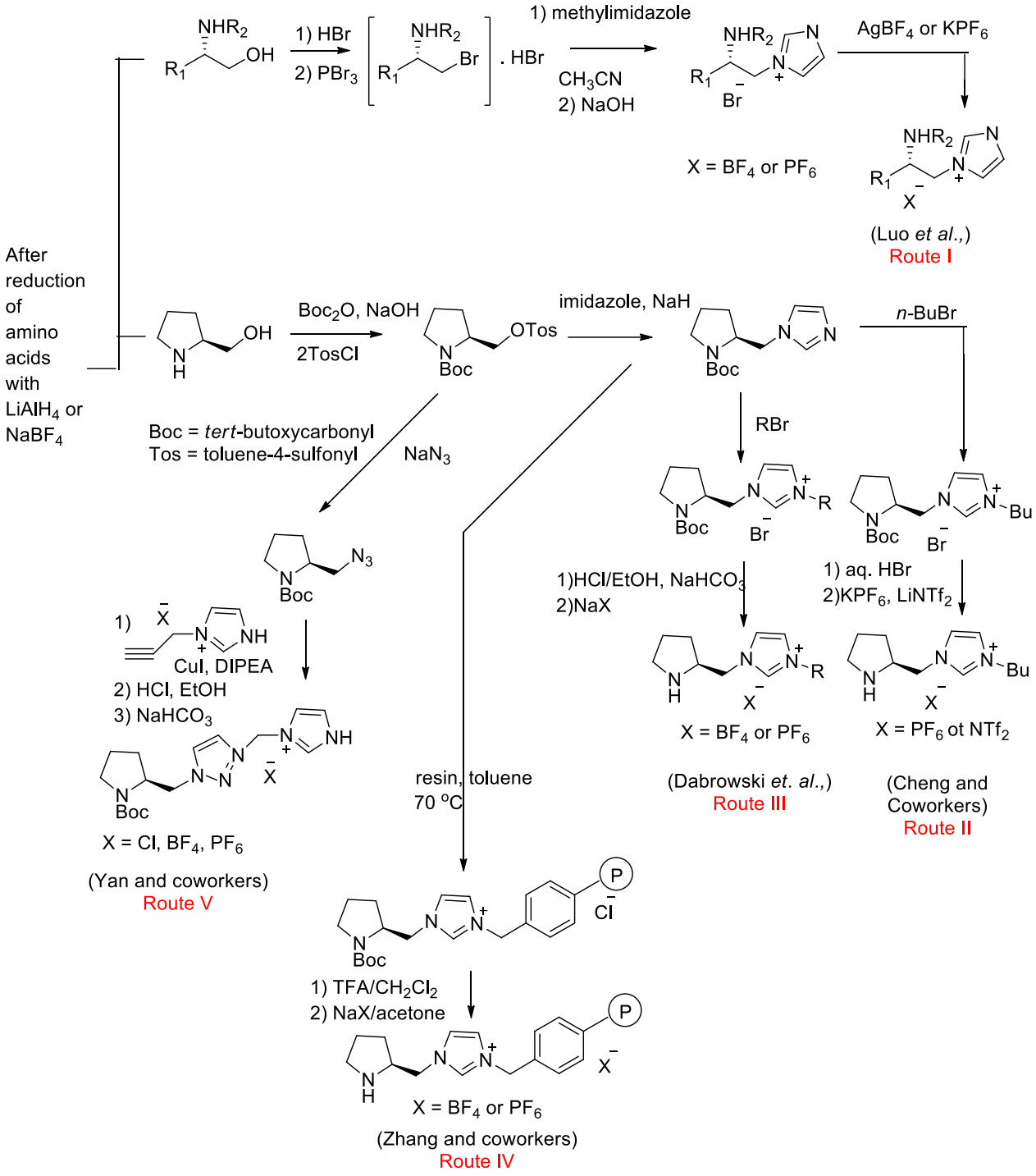

Figure 1.32-Reaction scheme.[89,90,91,92]

In route I an amino alcohol (L-alaninol, L-valinol, L-leucinol, L-isoleucinol and L-prolinol) was brominated with PBr_3 and led to chiral compounds in up to 76% yield.[89a] This was followed by alkylation of methylimidazole and then neutralization with NaOH to give the bromide salts (fig 1.32). The anions were exchanged to form RTILs. DSC studies were carried out to determine melting points and glass transition temperatures, which ranged from −49 to 145 °C, differences primarily due to the anion. They were thermally stable up to at least 210 °C. Later, CILs derived from L-prolinol were synthesized by similar synthetic procedure in good yields (up to 70%).[93] These were viscous liquids and were soluble in most of the polar solvents but insoluble in non-polar solvents.

In route II, (fig 1.32) (*S*)-prolinol was protected by *N*-Boc and tosylation in pyridine led to the tosyl intermediate in 68% yield.[89b] This was followed by substitution of the imidazole, leading to the pyrrolidine imidazole in 83% yield. Finally, alkylation and anion metathesis formed the new pyrrolidine imidazolium ionic liquid (fig 1.33). All the synthesized CILs were soluble in chloroform, dichloromethane, and methanol, but insoluble in diethyl ether, ethyl acetate, and hexane.

Imidazolium-based CILs, where chirality was derived from (*S*)-proline[90] (fig 1.32) and hydroxyproline[94] (**1.9**) followed route III. These CILs were characterized by ^{1}H, ^{13}C and ^{19}F NMR.

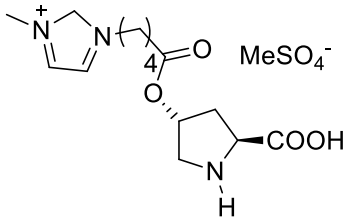

1.9[94]

Li and coworkers synthesized three polymer-immobilized pyrrolidine-based CILs, which were prepared by attaching the protected L-prolinol at *N*-1 position of imidazole in route IV (fig 1.32).[92]

Efficient "click chemistry" was utilized to develop an imidazolium-anchored pyrrolidine-type organocatalyst in route V.[91b] This CIL derives its chirality from L-proline and has triazolinium and an imidazolium functionalities as well (fig 1.32). The chloride anion was exchanged for tetrafluoroborate and hexafluorophosphate to study them as catalysts in a Michael addition.

Ou and Huang erroneously reported that when an amino alcohol was substituted to the imidazolium ring by refluxing the L-amino alcohols with 1-(2,4-dinitrophenyl)-3-methylimidazolium chloride using a reaction similar to Zincke reaction to give the chiral imidazolium salts (fig 1.33).[95] The chloride was

exchanged with other anions in 70-80% yield. The melting points and specific rotation were measured. Later, it was shown this study was wrong and treatment of 1-(2,4-dinitrophenyl)-3-methylimidazolium chloride with L-alaninol completely decomposed the starting material by an S_NAr route instead of the expected Zincke process.[96]

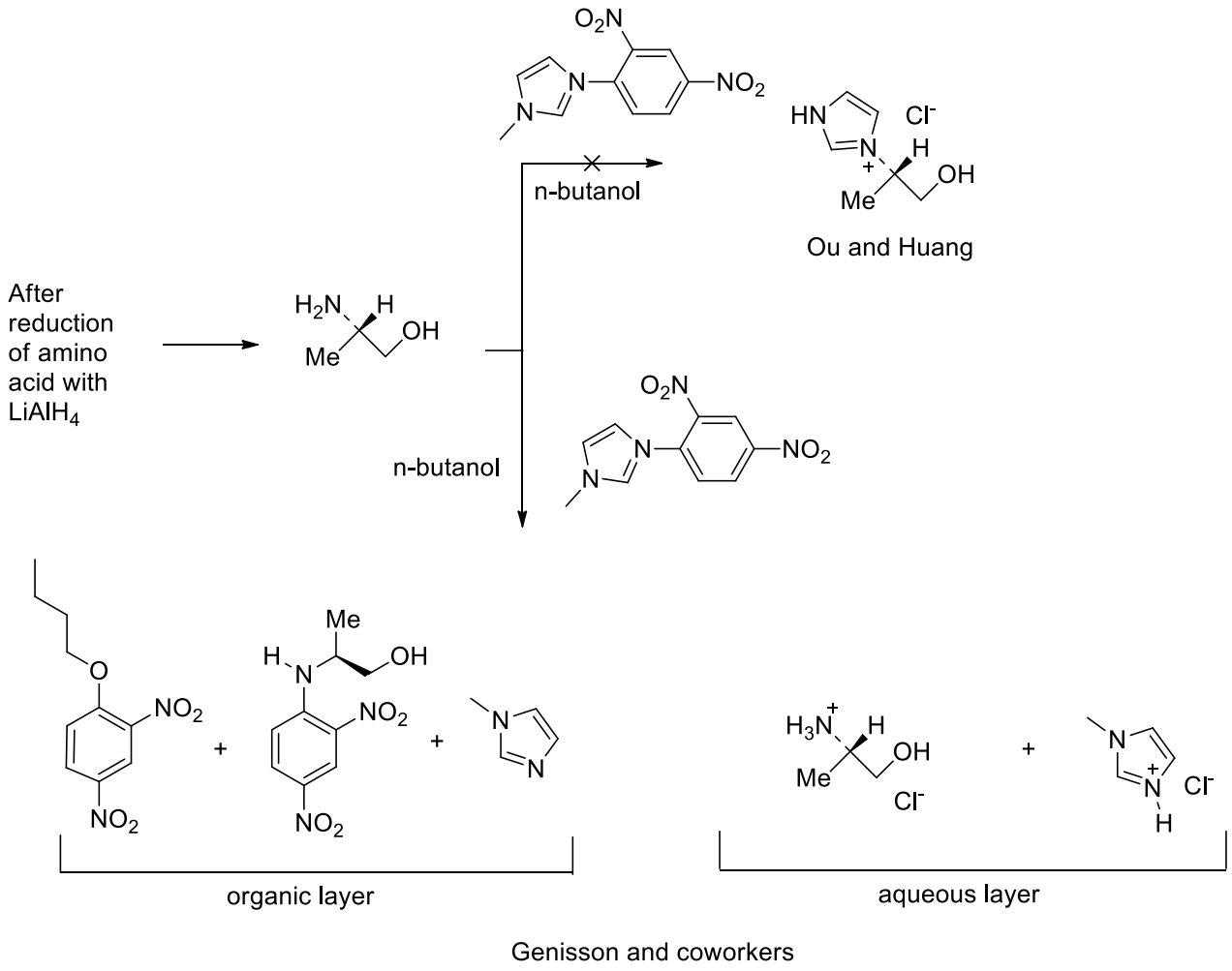

Figure 1.33-Reaction scheme.[95,96]

Silica gel supported CIL-based catalysts were derived from (*S*)-Boc-L-prolinol. The imidazole is substituted with protected L-prolinol followed by attachment to the silica support (fig 1.34).[97]

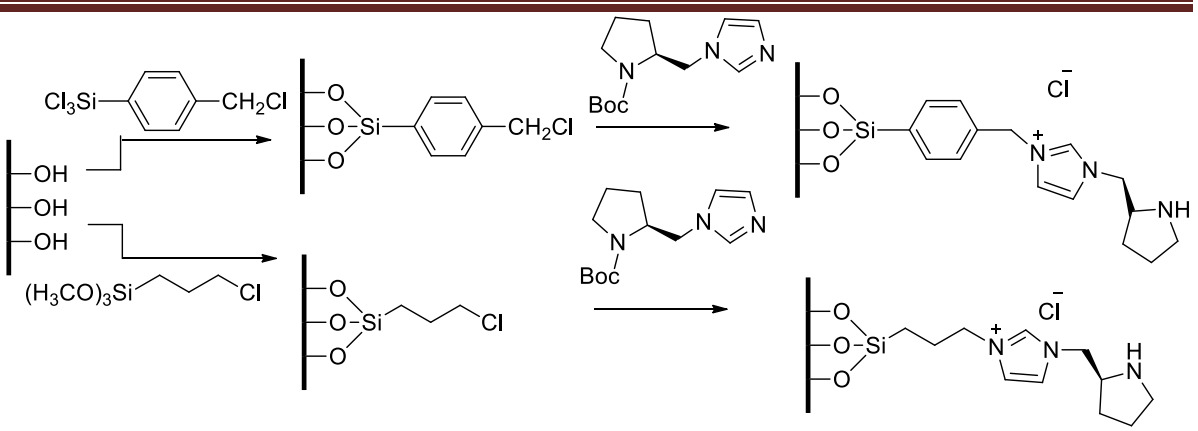

Figure 1.34-Reaction scheme for silica-gel supported pyrrolidine-based CILs.[97]

Ni and coworkers designed, synthesized and characterized pyrrolidine-based imidazolium CILs derived from L-proline.[98] The reaction of 3-chloropropanesulfonyl chloride with (*S*)-2-amino-1-*N*-Boc-pyrrolidine followed by alkylation to form the imidazolium salt. This functionalized salt not only contains a pyrrolidine moiety attached to an imidazolium, but also had an acidic (NH next to sulfonyl group) functionality on it as well (fig 1.35). Later, the same group synthesized more acidic CILs, in which the electron withdrawing group, the imidazolium cation, is separated from the sulfonyl group by a methylene unit (**1.10**).[99] The acidic hydrogen is essential for the activity and selectivity as a catalyst to form hydrogen bonds with reactants and intermediates in asymmetric synthesis.

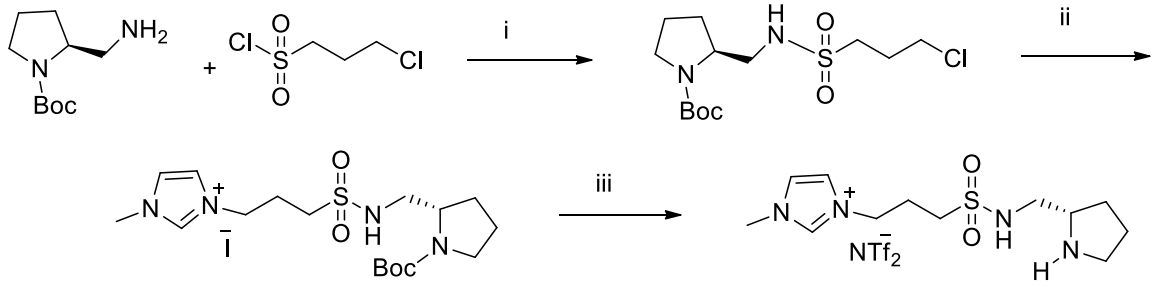

Figure 1.35-Reaction scheme i) Et_3N, CH_2Cl_2, 72%; ii) 1)NaI, acetone, 96%; 2) 1-methylimidazole, CH_3CN; 86% for 2 steps; iii) 1) CF_3COOH, CH_2Cl_2; 2) $LiNTf_2$, H_2O.[98]

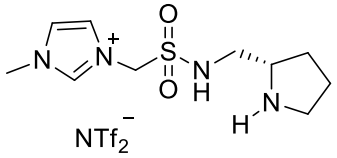

1.10[99]

Another way of substituting at the *N*-3 of imidazole was found by coupling a protected 4-hydroxyproline to the imidazolium cation *via* an ether function.[100] The synthesis involved cheap commercially-available starting materials and a straight-forward 3-step procedure (fig 1.36).

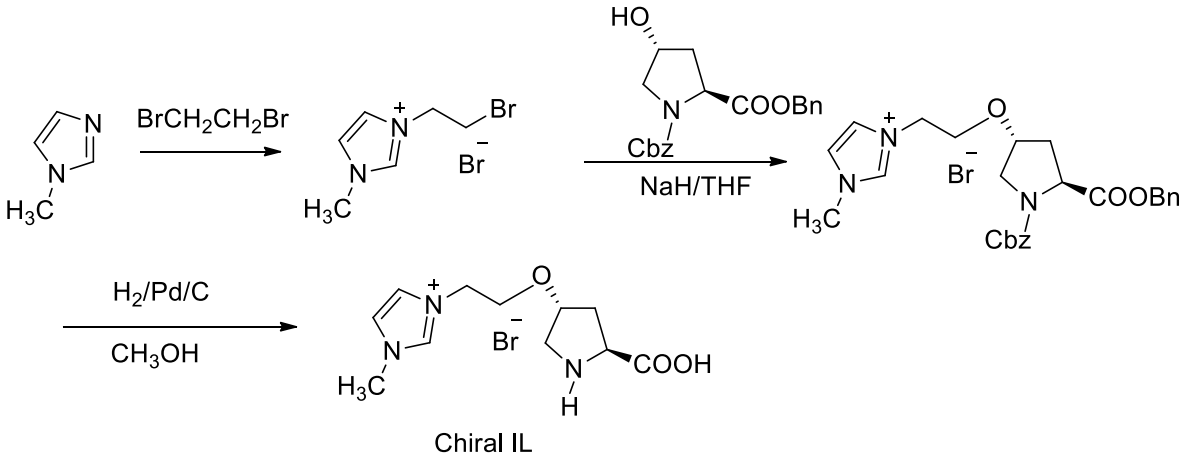

Figure 1.36-Reaction scheme.[100]

A new family of chiral imidazolium salts were reported from isocyanate derivatives of amino acids by reaction of aminopropylimidazole with isocyanates to form urea derivatives, followed by alkylation and anion exchange to form ionic liquids (fig 1.37).[101]

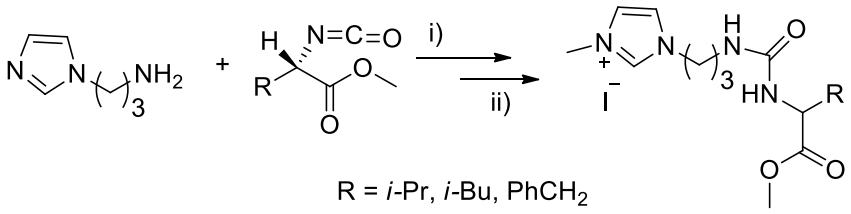

Figure-1.37-Reaction scheme; i) CH_2Cl_2, r.t., 24 h; ii) MeI, 40 °C, 20h.[101]

Zlotin and coworkers synthesized two CIL-immobilized catalysts bearing a (*S*)-diphenylvalinol moiety (fig 1.38).[102] These CILs have melting points of 103-105 °C and 98-100 °C and their solubility in water was dependent on the anion.

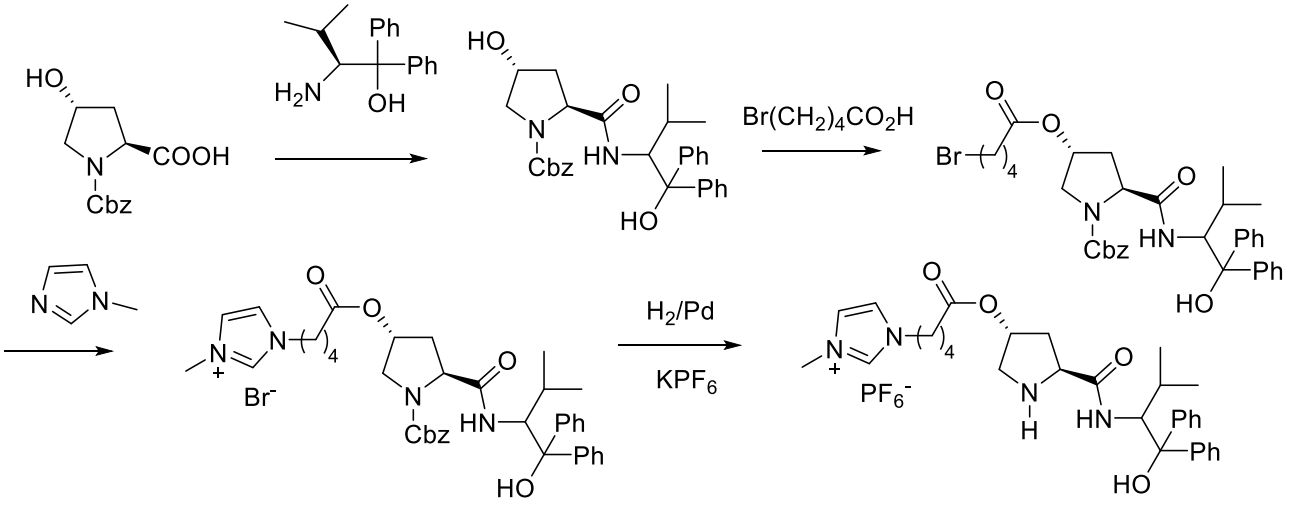

Figure 1.38-Reaction scheme.[102]

CILs were derived from L-tyrosine by incorporation of both imidazolium and triazolium rings by the following reaction scheme (fig 1.39).[103]

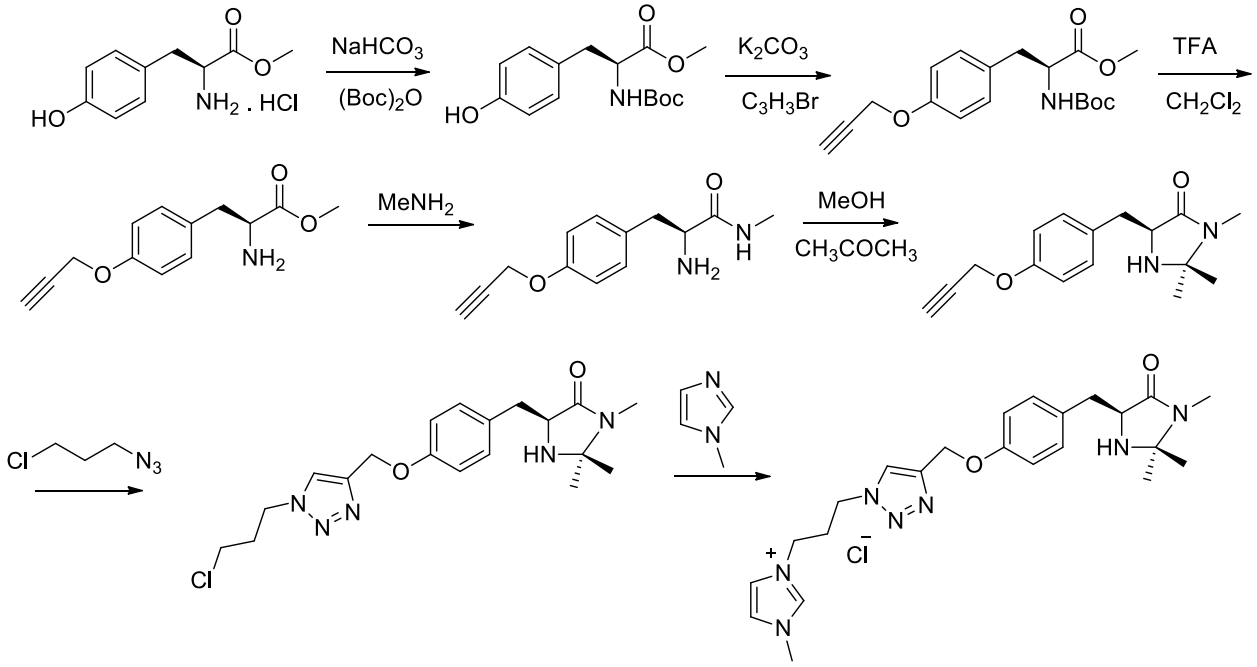

Figure 1.39-Reaction scheme.[103]

Bifunctional CILs were synthesized with amino acid esters and dipeptidyl functionalities (fig 1.40) in the cation side chain.[104] Antimicrobial toxicity against bacterial and fungal strains allowed for screening of toxicity in the environment and for medicinal properties. The presence of an amide and ester moiety in the CIL's side chain provides the possibility for enzymatic cleavage. The presence of

the lipophilic, aromatic phenylalanine moiety in the dipeptide side chain resulted in active antibacterial, although it had low antifungal toxicities.

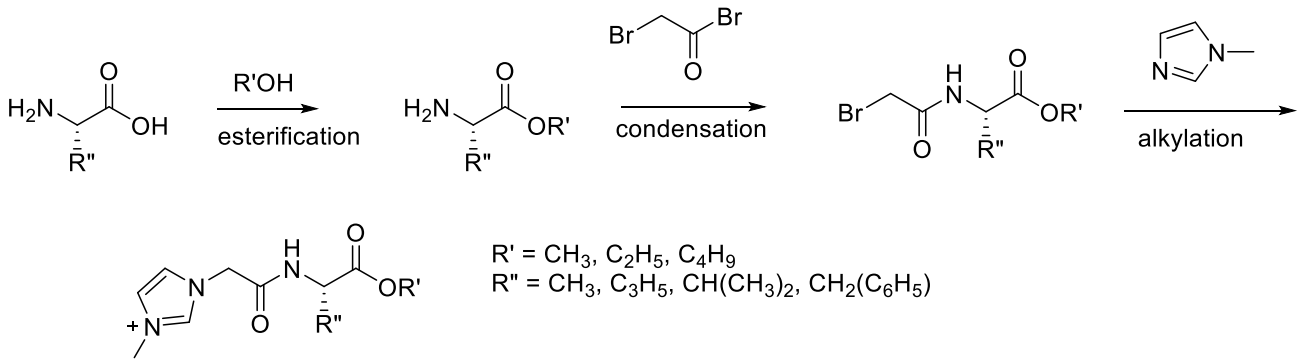

Figure 1.40-Reaction scheme.[104]

Liu and coworkers synthesized imidazolium-type CILs having (*R*)-thiazolidine-2-thione-4-carboxylic acid as the anion, where chirality was derived from L-cysteine hydrochloride (**1.11**).[76]

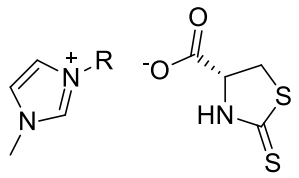

1.11

Taokai patented the preparation of amido imidazolium bromide ionic liquids derived from natural amino acids by the reaction scheme in fig 1.41.[105]

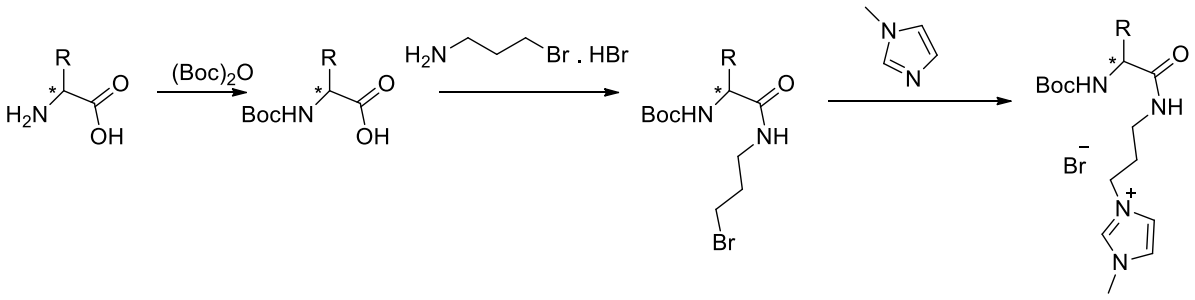

Figure 1.41-Reaction scheme.[105]

1.2.6.4 Functionalization at the 2 position of an imidazolium cation

The acidic hydrogen at the C-2 position of the imidazolium ring can be avoided by alkylating the C-2 position or by attaching the amino derivative at the C-2 position.

Ni *et al*. synthesized 15 chiral RTILs by incorporation of an amino alcohol at the C-2 position of the imidazolium ring (fig 1.41).[106] Condensation of a chiral amino alcohol with 1-methyl-2-imidazolecarboxaldehyde formed the corresponding Schiff base precursor. Which was followed by reduction and alkylation formed the imidazolium salts. Upon anion metathesis, these were transformed into ionic liquids. Most of them were solids or viscous oils, but no DSC data was reported. These ILs could be utilized as solvents under basic conditions which was not previously possible with butylmethylimidazolium chloride, as it deprotonates at the C-2 position (Baylis-Hillman reaction).[107] Later, the same group synthesized six imidazolium salts by the condensation of 1-methyl-2-imidazolecarboxylate with (*R*)-alaninol, (*R*)-leucinol and (*S*)-phenylalaninol at the C-2 position of the imidazole ring.[108] The imidazole derivatives were tosylated with *p*-toluenesulfonyl chloride. Finally, the double-tosylated salts were subjected to ring closure in toluene and finally OTs^- anions were exchanged with PF_6^- and NTf_2^- (fig 1.42). Salts that contain PF_6^- (m.p. >168 °C) were solids but NTf_2^- salts were liquids.

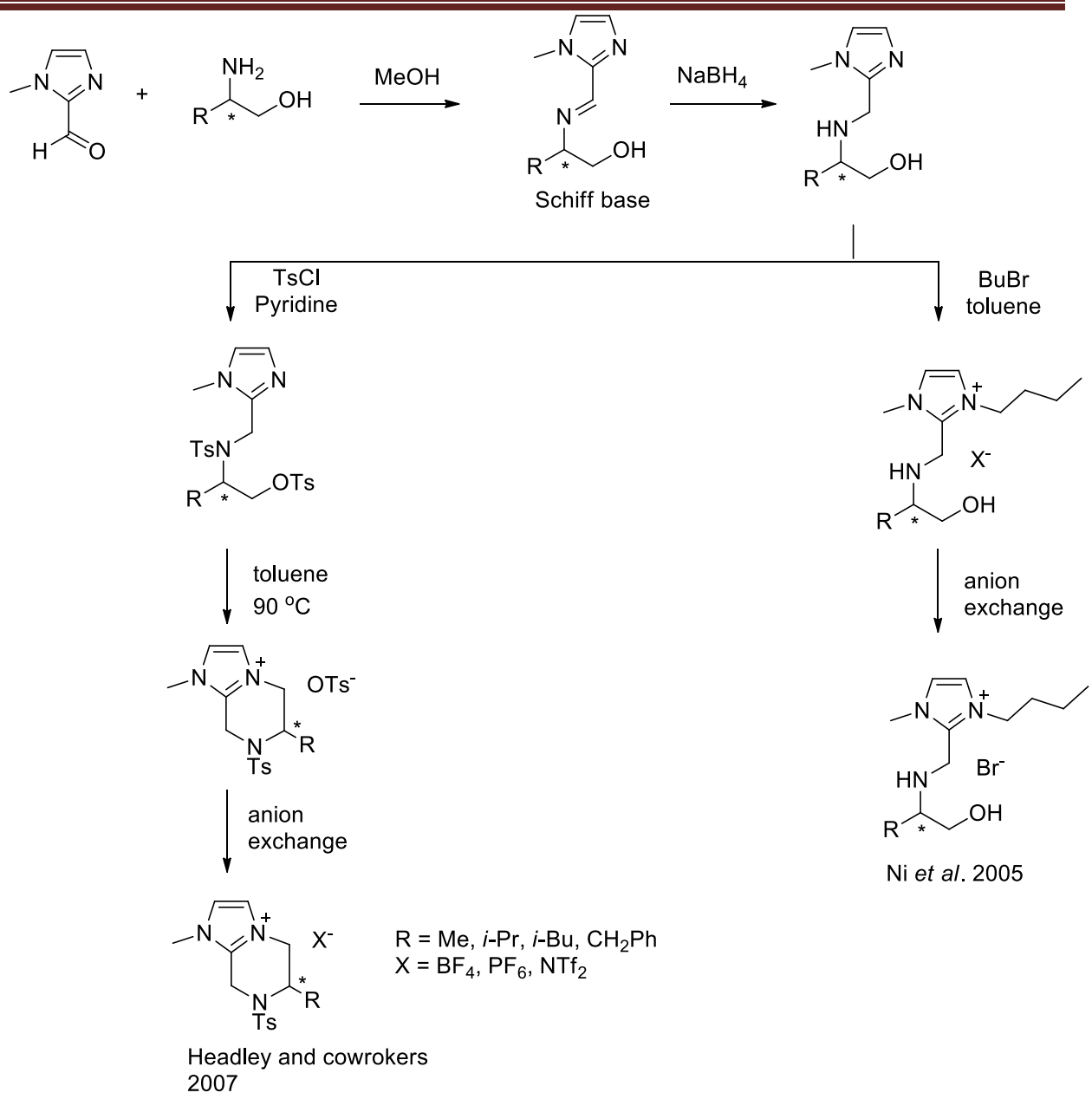

Figure 1.42-Reaction scheme. [106,108]

Another route attached an amino acid-derived halogenated fatty amine haloid at the *N*-1 position of imidazole, followed by anion exchange (fig 1.43).[109]

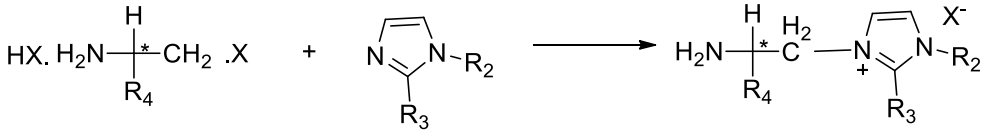

Figure 1.43-Reaction scheme.[109]

Alkyl imidazole L-proline chiral salt is synthesized by stirring alkyl imidazole bromide with base and then neutralizing with L-proline.[110] The optical rotation and optical purity were determined. An advantage of this method is that it is environmentally friendly and no secondary pollution is generated in the preparative method (fig 1.44).

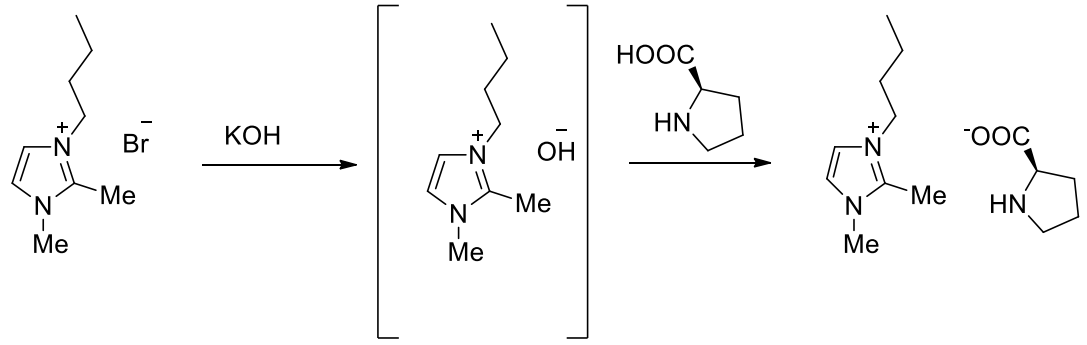

Figure 1.44-Reaction scheme.[110]

1.2.7 Imidazolinium

Clavier and coworkers reported five imidazolinium salts synthesized from *N*-Boc-*S*-valine in 3-steps (fig 1.45).[111] Upon reaction of the protected amino acid and ^{t}Bu-aniline, the amide was formed. Deprotection, followed by reduction gave the corresponding diamine. The imidazole ring was formed after formation of the hydrochloride derivative followed by condensation with triethylorthoformate. Finally, alkylation and anion metathesis gave the imidazolium salts. The PF_6^- anion gave solid salts while the NTf_2^- anion gave liquid salts.

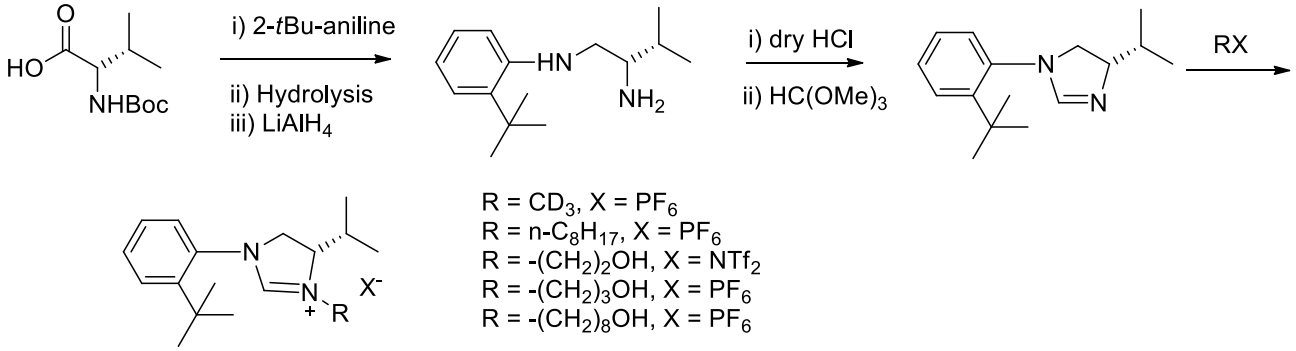

Figure 1.45-Reaction scheme.[111]

1.2.8 Thiazolium

Gaumont and coworkers prepared thiazolium salts by polyfunctional modification of amino acids.[58b] The thiazoline was synthesized via a thioacylation/cyclization sequence of 2-amino alcohol and easily-accessible dithioesters (sulphur source). Dithioesters were synthesized by known procedures.[112] Twelve chiral thiazolinium salts were obtained by alkylation of thiazoline followed by anion exchange (fig 1.46). Their melting points (42-175 °C), solubility studies, thermal and chemical stability were measured. Their properties could be varied by varying the substituent on the imidazolium ring or by varying the anions.

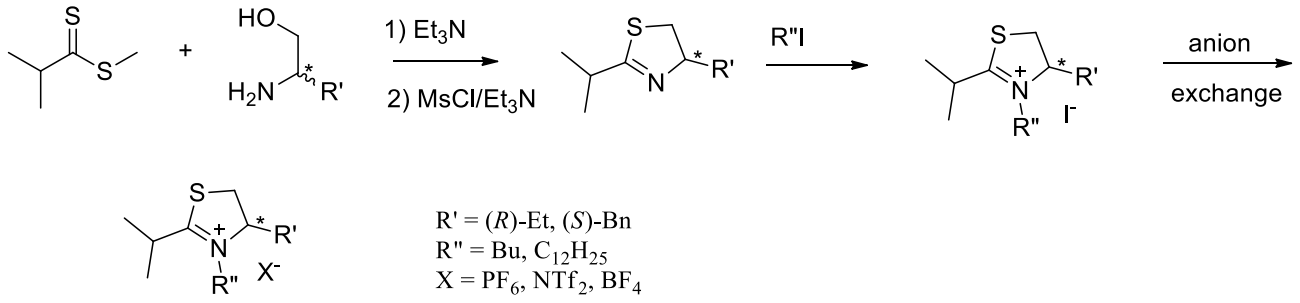

Figure 1.46-Reaction scheme.[58b]

1.2.9 Oxazoline

Ionic liquids having chiral cations were synthesized by Wasserscheid *et al*.[15] These were derived from an oxazoline, (synthesized from (*S*)-valinol) on a multi-gram scale, by condensation of propionic acid in xylene. After alkylation of the oxazoline using an alkyl bromide, followed by metathesis with HPF_6, the new oxazolinium salts were obtained (**1.12**). Their melting points ranged from 63-79 °C. The overall yield was low and they were not stable in acidic media, leading to ring opening. After basic hydrolysis of (*S*)-2-ethyl-3-pentyl-4-isopropyloxazolinium hexafluorophosphate, followed by reaction with (*S*)-Mosher's acid chloride, enantiopurity was determined by ^{19}F NMR.

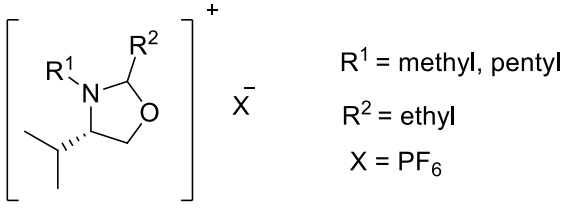

1.12

1.2.10 Pyridinium

Amino acid derived CILs have been reported with pyridinium. Several routes have been developed. One of the routes involves the amino acid or derivative of the anion without modification of the cation.

Ohno and coworkers synthesized[67] CILs by neutralizing pyrrolidinium and pyridinium hydroxide with L-alanine, tyrosine,[69] leucine and isoleucine.[70]

Liu and coworkers synthesized pyridine-type CILs containing (*R*)-thiazolidine-2-thione-4-carboxylic acid as the anion, where chirality was derived from L-cysteine hydrochloride.[76]

CILs having pyrrolidine, triazole and pyridinium rings were derived from L-proline by a multi-step reaction (fig 1.47).[91a] The derivative of L-proline was synthesized by the procedure described above in fig 1.32 (route V)[91b]. It was characterized by NMR and elemental analyses.

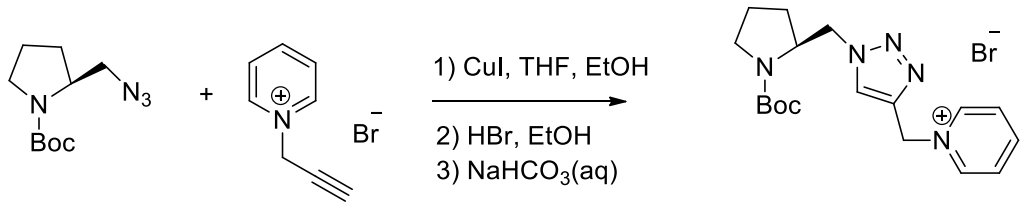

Figure 1.47-Reaction scheme.[91a]

Three CILs were synthesized by reacting 2-(aminomethyl)pyridine with *N*-Boc-L-proline, *N*-Boc-L-hydroxyproline and *N*-Boc-L-acetoxyproline (fig 1.48), followed by alkylation with butyl iodide and anion exchange to form the desired CILs.[113]

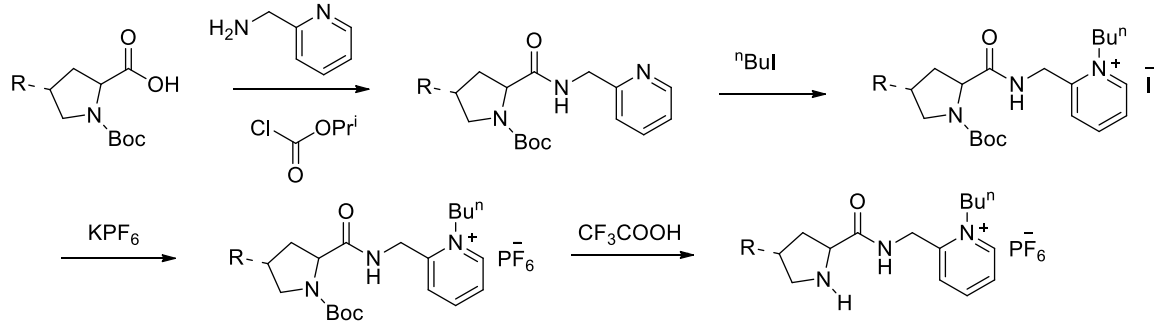

Figure 1.48-Reaction scheme.[113]

1.2.11 Guanidinium

Guanidinium salts were prepared by combining *N*-protected alanine and hydroxyproline (**1.13**) with the guanidinium cation.[114] After anion exchange, RTILs were formed which were stable up to 220 °C. The physical properties were determined, including viscosity and DSC measurements.

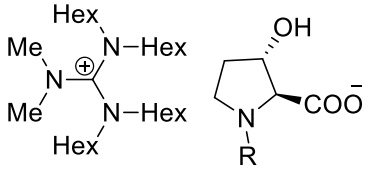

1.13

Pentasubstituted guanidines (fig 1.49) were synthesized in which tetrasubstituted-urea-derived chloroamidinium salts reacted with amino acid methyl ester (L-alanine, L-valine and L-leucine) in the presence of triethylamine in acetonitrile.[115] These resulting strongly basic guanidines were treated with sodium methoxide and were isolated by Kugelrohr distillation. Following simple refluxing with methyl iodide, hexasubstituted guanidines were generated. The hexasubstituted guanidines with aliphatic substituents have an expectation of lower melting points and are chiral RTILs. These are more bulky, more electron-rich and are stable in strongly basic solutions than trisubstituted guanidines. This methodology was further applied to cyclic chloroamidinium salts and chiral imidazolidinimines generated were liquids at room temperature (fig 1.50). After anion metathesis[116] with tetrafluoroborate and dicyanamide, salts were obtained with melting points below 100 °C.

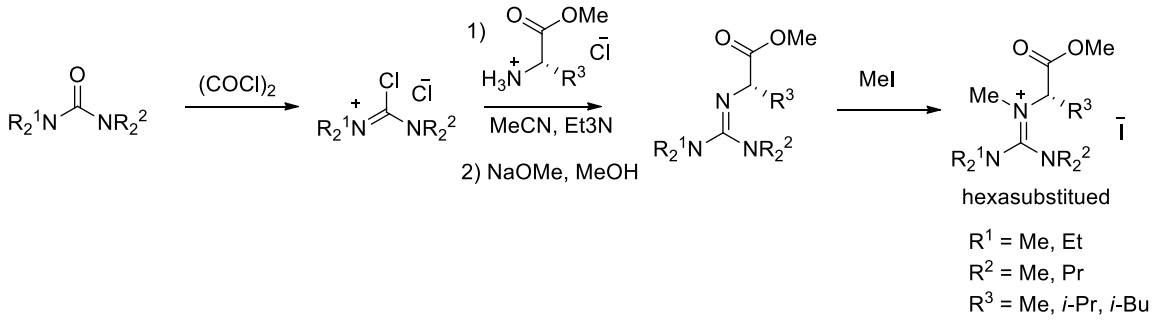

Figure 1.49-Reaction scheme.[116]

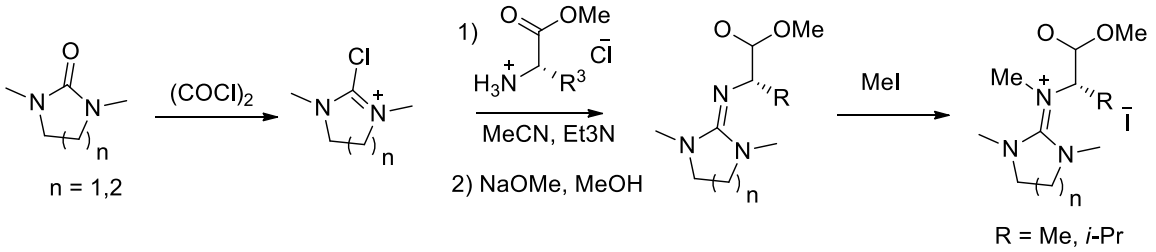

Figure 1.50-Reaction scheme.[116]

1.2.12 Cyclopropenium

Bandar and Lambert synthesized the first chiral tac-based crystalline solid by attaching phenylalaninol to the tac cation. This synthetic route is very similar to this present study of thesis,[25] where I have attached amino acids with the tac cation. Yoshida's preparative methods were used by reacting tetrachlorocyclopropene with an excess of dicyclohexylamine for 4 hours, followed by addition of phenylalaninol. The obtained CIL was isolated as the HCl solid salt. This tac-salt was deprotonated with a base (NaOH) to form cyclopropenimine. Cyclopropenimine was used as a Brønsted base catalyst in Michael addition reaction.

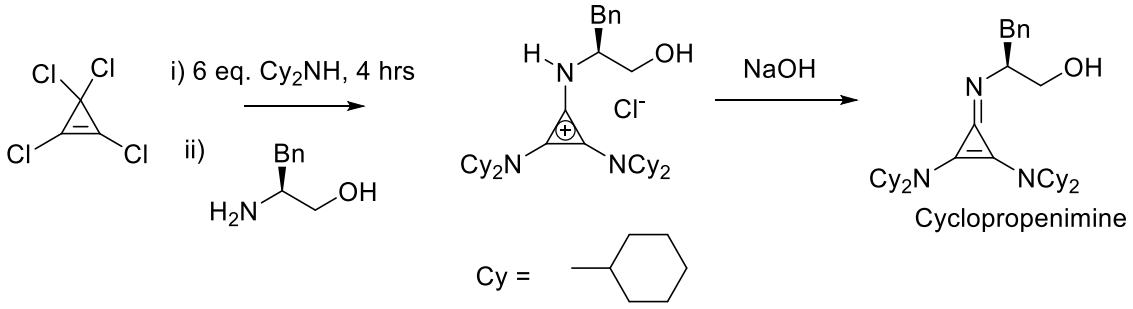

Figure 1.51-Reaction scheme.

1.2.13 Carbamates

Wang synthesized carbamate-based CILs which could be transformed reversibly to their non-ionic liquid states (fig 1.52). They were transformed to amidinium carbamates by exposing CO_2 to a 1:1 mixture of an amidine (*N'*-alkyL-*N*,*N*-dimethylacetamidine) and an alkyl ester[117] of an amino acid (L-leucine, L-isoleucine, L-valine and L-phenylalanine) or an amino alcohol[118] (L-valinol, L-leucinol, L-isoleucinol, L-methioninol, L-phenylalaninol and L-prolinol). Forty chiral RTILs were obtained with amino alcohols and were stable under CO_2 atmosphere and all remain liquids to −20 °C. Ionic liquids obtained from amino esters remained liquids in a CO_2 atmosphere except the methyl ester of tyrosine which was immiscible with amidine even when heated to 80 °C. The non-ionic state could be returned by passing nitrogen gas through these RTILs or when they were heated to 50 °C in air. They remained RTILs under a CO_2 atmosphere and their stability was low compared to other ionic liquids. Except for tyrosine derivatives all other RTILs were liquid at room temperature. Thermal and spectroscopic properties (IR, NMR) of ionic and non-ionic phases were also reported. The polarity of one reversible amidine/amino acid ester was determined using a solvatochromic dye (1-(*p*-dimethylaminophenyl)-2-methylene) (DAPNE) as a probe.[117] Before CO_2 exposure it showed a maximum absorbance at 425 nm

which indicates an environment similar to toluene (λ_{max}= 425 nm). After CO_2 exposure, it showed a maximum absorbance at 443 nm (slightly less polar than *N*,*N*-dimethylformamide, λ_{max}= 446 nm).

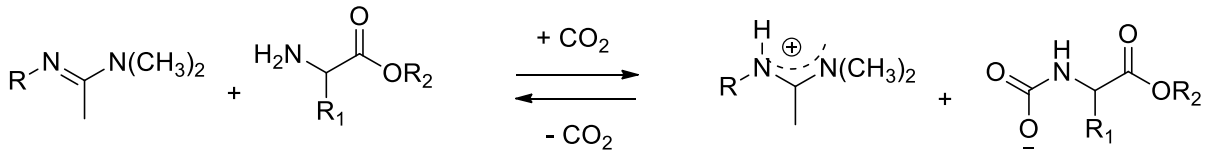

Figure 1.52-Reversible carbamate formation.[117]

1.4 Applications and Uses of AAILs

In recent years, CILs have become an exciting area of research because they can be used as recyclable reaction media instead of conventional molecular solvents. When amino acid-derived CILs are used as catalysts or solvents in asymmetric reactions, it can result in enhancement of yields, enantiomeric excesses (*ee)* and diastereoselectivities. However, it must be noted that use of CILs is not necessarily an environmentally-friendly alternative. CILs provide a local ordering that result in enhancements in reactivity.

1.2.1 Asymmetric Synthesis

Asymmetric synthesis is an important process in modern pharmaceutical chemistry where the formation of a compound as a single enantiomer or diastereomer can be critical as the different enantiomers or diastereomers of a compound can have different biological activity. The applications of the AAILs are based mainly on imidazolium, ammonium, and pyridinium salts, however, unavailability of CILs from commercial sources limits its use. Problems also arise with high viscosity, and low chemical stability of CILs, which depends on both the cation and anion utilized.

1.2.6.1 Diels-Alder Reaction

The Diels-Alder reaction is a very useful reaction in organic chemistry which requires very little energy to create a cyclohexene ring upon cycloaddition between a conjugated diene and an alkene.

Amino acid ester-based CILs are used as catalysts and as "fully green" solvents in the Diels-Alder reaction between cyclopentadiene and methyl acrylate (fig 1.53).[53] A high loading of catalyst from 30 mol% to 100 mol% is required for small enhancements of the *endo/exo* ratios. [Amino acid ester]saccaride ([AAE]Sac) gives better stereoselectivity than [AAE]NO_3. The ee of *endo* and *exo*

products were found to be less than 3%. The greater degree of hydrogen-bonding interactions in [AAE]Sac and small steric requirements of methyl acrylate are thought to give low ee.[119]

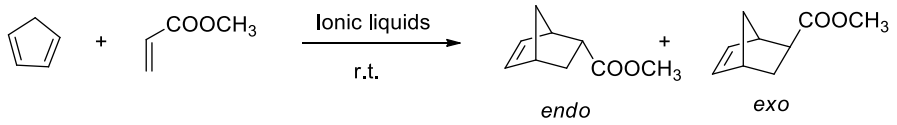

Figure 1.53-Diels-Alder reaction.[53]

Doherty *et al.* used imidazolium-tagged bis(oxazoline) (derived from L-valinol) (**1.14**) CILs as a chiral ligand in the copper (II)-catalyzed reaction of *N*-acryloyl- and *N*-crotonoyloxazolidinones with cyclopentadiene and 1,2-cyclohexadiene in [emim]NTf_2 or CH_2Cl_2 at room temperature.[120] Regardless of the solvent ([emim]NTf_2 or CH_2Cl_2), *tert*-butyl-substituted bis(oxazolines) gave higher ee (95%) than their corresponding isopropyl-substituted counterparts. A significantly high reaction rate (up to 100%) and high ee (95%) were observed in [emim]NTf_2 compared to organic solvents. The performance of chiral catalysts based on bromide salts are poor compared to NTf_2 salts. Another advantage is the shorter metal-ligand complexation times of copper catalyst which produce high selectivities in ILs (5 minutes) compared to dichloromethane (3 hours or longer). The introduction of bis(oxazolines) onto the imidazolium ring improved the recycling of the catalyst ten times without loss of activity or ee.

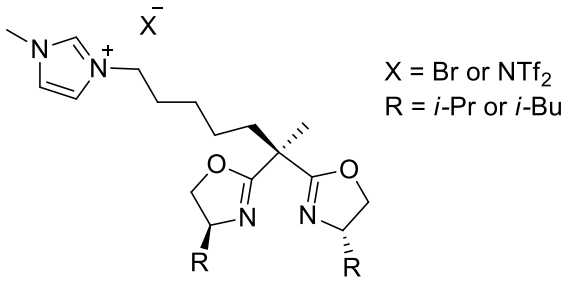

1.14

[EMIm][Pro][81] was employed by Zheng[121] as a catalyst for the first direct asymmetric aza Diels-Alder reaction between 2-cyclohexen-1-one, aqueous formaldehyde and *p*-anisidine (fig 1.54). The reaction proceeded efficiently to provide exclusively the *endo* product in 40-93% yield, 92 to >99% ee and 84/16 to >99/1 diastereomeric ratios (*dr*). Reducing the catalyst loading from 20 mol% to 10 mol% resulted in sharply decreasing *dr* and ee values. The catalyst can be recycled up to six times without significant loss of activity.

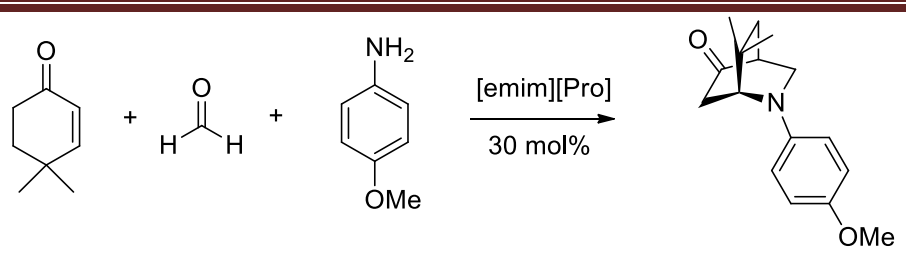

Figure 1.54-Asymmetric aza Diels Alder reaction.[121]

1.2.6.2 Aldol Reaction

The Aldol reaction combines two carbonyl compounds to form a C-C bond generating a β-hydroxy carbonyl compound. Asymmetric aldol reactions are very important for the introduction of chirality in organic synthesis. Scientists have developed catalysts to mimic the features of natural aldolases. For the reaction to be carried out in aqueous media synthetic organocatalysts require hydrophilic[122] as well as hydrophobic regions[123]. Chiral ionic liquids have been known for years as an alternative chiral solvent and are potentially suitable for inducing stereoselectivity in the aldol reaction.

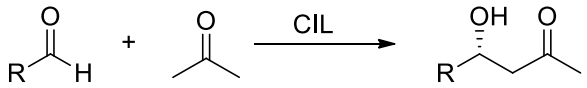

Figure 1.55-Aldol reaction between aldehyde and ketone.

Proline is a five-member cyclic secondary amine which has been previously recognized as an organocatalyst under mild conditions. Many examples of functionalized imidazolium cations as catalysts have been reported. The aldol reaction between a variety of aldehydes and acetone was catalyzed by a L-proline-based CIL (10 mol%) (fig 1.53) (derived from imidazolium) in the presence of [Bmim][BF_4].[100] It gave better results than from the use of acetone, DMSO or [Bmim][PF_6] as the solvent. An aromatic aldehyde bearing electron-withdrawing groups (chloro, bromo, cyano, trifluoromethyl, and nitro) runs reaction smoothly with acetone giving good yields (53-94%) and good enantioselectivities (64-93%) while aldehydes with electron-donating groups (methyl) undergo aldol condensation with acetone to give low yields (53%) and good enantioselectivities (77%). The catalyst and IL were recycled up to six times with minor decreases in yields while the ee was maintained.

When imidazolium-tagged catalysts were coupled with proline with BF_4^- as an anion (**1.15**) in the presence of DMSO or acetone as a co-solvent, the catalytic loading was very high (30 mol%) and resulted in poor TONs (Turn Over Number) (fig 1.52).[124] However, when this catalyst having Tf_2N

anion was used, it resulted in higher efficiency and TONs of up to 17 were achieved.[125] In biphasic conditions, these catalysts also gave higher dr and ee.[126]

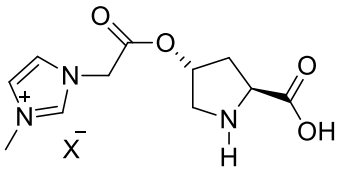

1.15

X=BF_4 or Tf_2N[124]

A pyrrolidine-containing L-proline (20 mol%) (**1.16**) effectively catalyzed the aldol reaction between acetone and various aldehydes.[93] Acetic acid and water facilitated the desired aldol reaction and suppressed the formation of any aldol condensation by-products.[127] It was recycled and reused up to six times with a slight reduction in activity. Even a lower loading of 0.1 mol% of *cis*-4-hydroxy-L-proline produced TONs of up to 930 and ee of up to >99%.[128]

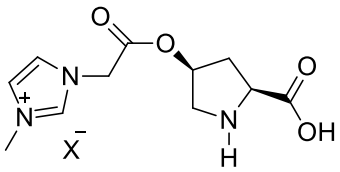

1.16[128]

The aldol reaction could be performed by using (*S*)-proline-modified[129,130], proline, serine or threonine moieties[130,131], imidazolium or pyridinium cations, and prolinamide derivatives[102] as catalysts between cycloalkanones and aromatic aldehydes in the presence of water. The aldols were generated in high yields with good selectivity (*dr* and ee) and could be easily recycled.

The aldol reaction between cyclohexanone and 4-nitrobenzaldehyde in the presence of L-proline as a catalyst, with or without CIL (**1.17**), in DMSO/H_2O was performed. The yields (up to 88%), stereoselectivities (> 99:1) and ee (up to 98%) were enhanced significantly for *syn*-selective aldol reaction by utilizing a proline-type CIL in comparison to without CIL.[132]

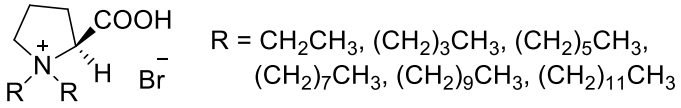

1.17

Despite being readily accessible and inexpensive, chiral amino acids and their derivatives suffer from a few drawbacks; high catalyst loading (5-30 mol%), low reaction rates and selectivity, addition of strong acidic additives, and utilizing highly polar solvents, made catalyst recovery and recycling difficult. Asymmetric aldol reaction of 4-nitrobenzenealdehyde and acetone catalyzed by an organocatalyst based on a basic CIL (prepared from (*S*)-pyrogluthaminic acid or from (*S*)-proline) gave excellent yield and good ee (80%).[133] This CIL replaced the toxic and corrosive trifluoroacetic acid, which was based on permanent charge. Although catalyst recycling remained below the authors' expectations, it could replace active protic intermediates.

So far, only a few examples of an aldol reaction catalyzed by a chiral cation have been reported. Some examples where aldol reaction is catalyzed by CIL with a chiral anion will be discussed. The first example reported a RTIL (2-hydroxyethyl)-triethyl-ammonium (*S*)-2-pyrrolidinecarboxylic acid salt and resulted in ee of less than 10% (fig 1.56).[134] When [emim][Pro] was used as a catalyst, it gave good yields and excellent selectivities.[135] Later, excellent yields (up to 99%) were obtained with *trans*-L-hydroxyproline.[136]

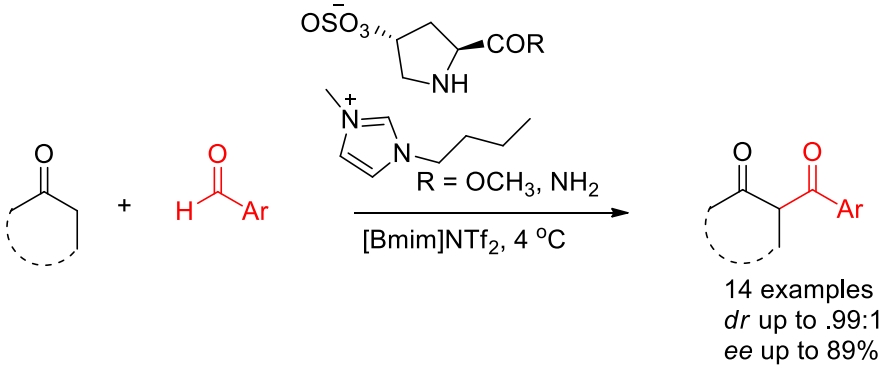

Figure 1.5-Aldol reaction catalyzed by CIL.[136]

1.2.6.3 Michael Addition Reaction

The asymmetric Michael addition reaction is widely studied as one of the most powerful C-C single bond formation reactions in which a nucleophilic carbanion (Michael donor) undergoes conjugate addition to an α,β-unsaturated carbonyl compound (Michael acceptor).[6]

Michael addition of 1,3-diphenylprop-2-en-1-one with ethylmalonate was catalyzed by an L-amino alcohol derived imidazolium CIL and formed diethyl 2-(3-oxo-1,3-diphenylpropyl) malonate in low ee (15%) (figure 1.57).[95]

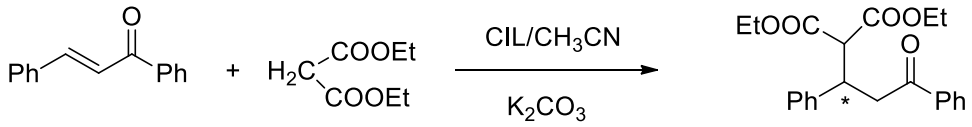

Figure 1.57-Michael addition reaction between 1,3-diphenylprop-2-en-1-one with ethyl malonate in CIL.[95]

Previous studies have shown that chiral catalyst with an imidazolium core (having L-proline) (15 mol%) in the presence of trifluoroacetic acid (TFA) (5 mol%) was superior to their 2-methyl counterparts in activities and ee.[89b, 90]

The first successful asymmetric intermolecular desymmetrization *via* organocatalytic Michael addition was reported by Luo *et al*.[137] The side chains of the functionalized CIL cation having protic groups or longer alkyl chains resulted in a decrease in both the catalytic activity and enantioselectivity. Pyrrolidine-CIL demonstrated good catalytic activity compared with thiazolidine, which was totally inactive. The optimal results in terms of both activity and stereoselectivity were seen in the presence of an acid additive. The BF_4^- anion enhanced activities more than Br^- and PF_6^-. The catalyst could be recycled up to four times maintaining similar stereoselectivities. Loss of activity was obtained in the third and fourth reuse.

It was thought that the acidic hydrogen of the amine played an important role in the reaction by forming a hydrogen bond to stabilize the transition state (fig. 1.58).[98] The great advantage of this organocatalyst was its ability to be recycled without the loss of activity. Moderate yields (29-64%), good ee (64-82%), and high *dr* were obtained when diethyl ether was used as the solvent.

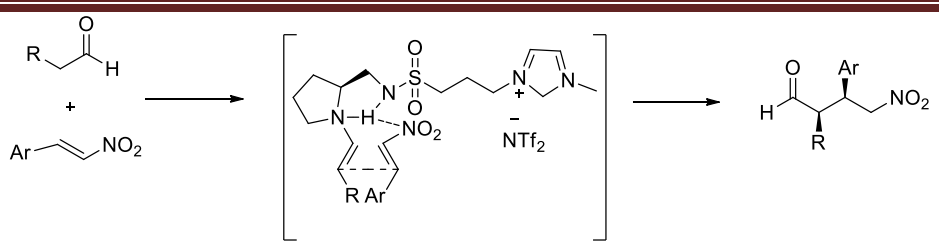

Figure 1.58-Mechanism for the Michael addition reaction.[98]

Polymer[92] and silica[97] gel-supported pyrrolidine-type CILs are employed by Li as catalysts in solvent-free reaction conditions. However, the reactions carried out on a silica gel-support gave higher yields and selectivities than the polymer-based catalyst. Later, the same group developed a CIL with a more acidic NH group by the introduction of a methylene unit between the imidazolium cation and the sulfonyl group (**10**).[99] It enhanced the yields (99%), ee (85%), and diastereoselectivities (syn/anti 97:3) and could be recycled at least five times. Some of the organocatalyst containing a pyrrolidine[91b,92] moiety could be recycled up to eight times without loss of activity.

Ni demonstrated the effect of the anion of a CIL derived from pyrrolidine-based pyridinium on catalysis in a Michael addition.[138] The catalyst with Cl^- and BF_4^- as the anion resulted in comparable selectivity with enhanced reaction activity. When TFA (trifluoroacetic acid) was added, it gave the best performances with high yields, high diastereo- and enantioselectivity. However, PF_6^- and NTf_2^- resulted in slightly lower selectivities.

Maltsev found that an α,α-diphenylprolinol with an IL moiety catalyzed the addition of dialkyl malonates to α,β-enals.[139] This catalyst and the majority of all other pyrrolidine-based recoverable organocatalysts have the (*S*)-configuration that allowed the synthesis of the same configuration to be synthesized in a Michael reaction. In regards to the curing of central nervous system disorders, (*S*)-enantiomers of the γ-amino acid derivatives formed in the presence of (*S*)-catalysts are less active than (*R*)-enantiomers. Later, the same group reported that (*R*)- and (*S*) adducts were obtained for the asymmetric Michael addition of nitroalkanes to α,β-enals bearing silylated recoverable (*S*)- or (*R*)-prolinol units tagged to the imidazolium moiety.[140]

Compared to the extensive work on the proline-derived chiral imidazolium, pyrrolidinium and pyridinum ILs, ammonium ILs have been explored relatively less in the Michael addition reaction.[75] These catalysts proved to be very efficient but, unfortunately, the catalyst recycling was difficult.

Proline-amide-based organocatalysts were employed by Zlotin and showed minimum activation of the reactants, which was not achieved earlier by other catalysts.[141] The same group showed a deactivation pathway of CILs in an asymmetric Michael reaction of α,β-unsaturated carbonyl compounds with C- and N-nucleophiles that involved an iminium-ion formation step (fig 1.59).[142] The deactivation of catalyst was not due to leaching but was caused due to side reactions that poisoned the catalyst. The ESI-MS method was a powerful tool used for the analysis of organocatalytic reactions to study the deactivation pathways. They treated the catalyst with AcOH to reactivate it. The author claimed that this study was useful for the catalyst development and processing for large-scale industrial applications.

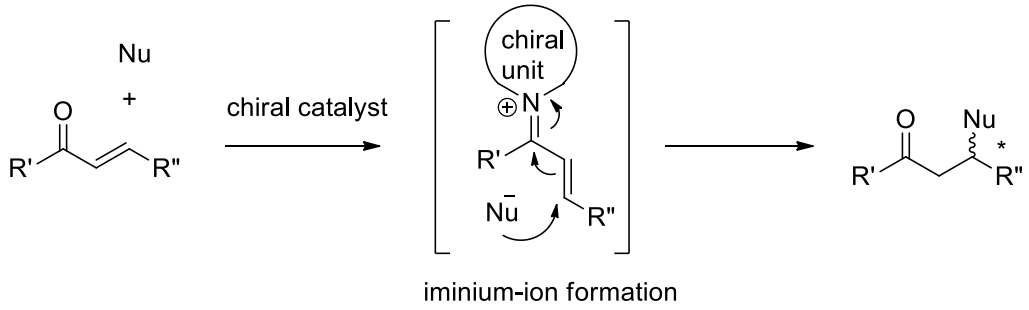

Figure 1.59-Iminium-ion formation in Michael addition.[142]

Anion-modified 1-methyl-3-ethylimidazolium-(*S*)-2-pyrrolidine carboxylic acid salt was employed as a catalyst by Qian.[143] Although, a high loading amount was required (200 mol%), the products were obtained in excellent yields (85-98%), in less time, and with moderate to good enantioselectivities (16-94%). The solvent had a significant effect on the rate and stereoselectivity of reaction. When the reaction was performed in toluene (selectivity = 27%), THF (selectivity = 41%) or DCM (selectivity = 6%) moderate yields were obtained. Good selectivities were obtained with methanol (86%) and ethanol (69%). However, DMSO (−78%) gave inversion of configuration in comparison to methanol and ethanol. Later, ammonium-type CILs having L-prolinate[71] as the anion was used as an organocatalyst in the presence of CH_2Cl_2, however, they were less efficient than the previously-reported imidazolium ones.

1.4.1.4 Heck Reaction

Heck cross-coupling is a palladium-catalyzed reaction for the formation of C-C bonds leading to arylated olefins as the reaction products. It can be used to perform arylation of olefins bearing electron-withdrawing (-COOR, -CN) or electron-donating (-OR) olefinic groups. One of the problems of the

Heck reaction is recovery of the palladium catalyst at the end of the reaction.[6] [Bu_4N][L-Pro] was used as a chiral agent for the palladium catalyzed ($Pd(OAc)_2$) Heck arylation of 2,3-dihydrofuran with aryl iodides (figure 1.60).[144] The stereoselectivity observed by this amino acid-based CIL was exceptionally high. The effect of non-chiral bulky cation turned out to be very important and gave higher ee (>99%) values than the less bulky ammonium cation. It was thought that the Pd(0) nanoparticles were stabilized by CILs due to electrostatic interactions. The cationic part of CIL played an important part in determining the nucleophilicity of the chiral anion and its reactivity in the catalytic pathway.

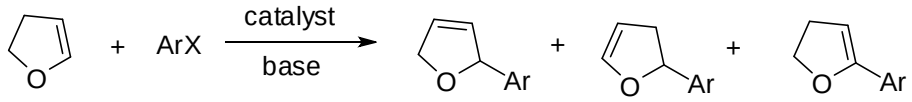

Figure 1.60-Heck cross-coupling of 2,3-dihydrofuran with iodobenzene in the presence of CIL.[144]

1.4.1.5 Hydrogenation

Asymmetric hydrogenation reactions are catalyzed by chiral metal complexes having chiral ligands such as atropoisomeric (*atropos*) binaphthyls and biphenyls. Atropisomerism describes compounds with a chiral axis where the chirality is maintained due to the lack of free rotation about a single covalent bond. Francio and coworkers used a rhodium complex-type containing pro-tropoisomeric or *tropos* ligand (chirally flexible) as a catalyst in the presence of AAIL ([ProMe]NTf_2) as only source of fixed chirality and obtained enantio-enriched (69%) hydrogenation products (fig 1.61).[145] The phenyl rings (biphenylphoshine) in these ligands rotate rapidly and, therefore, are not chiral. When this CIL-catalyst system is used for the hydrogenation of methyl 2-acetamidoacrylate and dimethyl itaconate ($CH_3O_2CCH_2C(=CH_2)COOCH_3$) significant enantioselectivities were obtained. The products were obtained by flushing supercritical CO_2 allowing the CIL-catalyst system to be reused. s

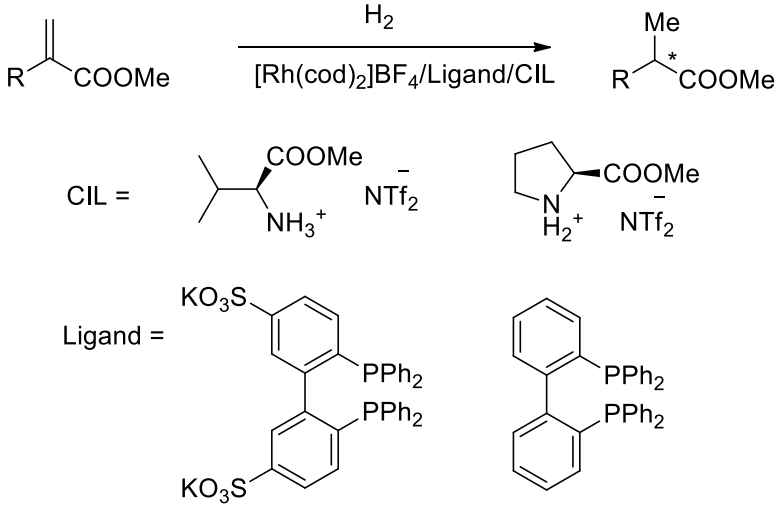

Figure 1.61- Hydrogenation catalyzed by *tropos* ligands.[145]

Later, the same team showed that this CIL induced high levels of enantioselectivity for the hydrogenation of the same two substrates (dimethyl itaconate and methyl *N*-acetamido acrylate) with rhodium catalyst having racemic *atropos* binap (2,2'-bis(diphenylphosphanyl)-1,1'-binaphthyl) ligands (**1.18**). The AAIL poisoned the catalytic cycle for one of the two enantiomers of the transition metal catalyst.[146] However, the enantioselectivities obtained from racemic catalyst and enantiopure catalyst were identical.

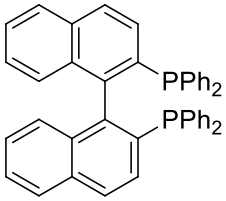

binap

1.18[146]

Chiral pyrrolidinodiphosphine-bearing amino acid tethered to imidazolium were applied to Rh-catalyzed asymmetric hydrogenation of α-enamide esters in [bmim]BF_4 and [bmim]BF_4/co-solvent.[147] The position of the stereogenic centre in the amino acid ligand has a very important impact on the catalytic activity and decreased the activity as the stereogenic centre moved towards the pyrrolidine ring. The interaction between the stereogenic centre and Rh was also thought to be involved in catalytic activity. After several cycles, there was no significant loss in activity and enantioselectivity. The imidazolium-tagged CIL showed excellent ee (95%) with TOF of 24,054 h^{-1}.

1.4.1.6 A tandem Knoevenagel, Michael and ring transformation

Mercaptopyranothiazoles have high potential pharmacologically and agrochemically but none of the known synthetic procedures could be used for its synthesis. 6-Mercaptopyranothiazole[148] was synthesized in the presence of CIL ($[Pro_2]SO_4$)[48] (as reaction medium and catalyst) by reacting 3-arylrhodanines, aromatic aldehydes, and a mercaptoacetyl transfer agent (2-methyl-2-phenyl-1,3-oxathiolan-5-one) (fig 1.62). It involved tandem Knoevenagel, Michael and ring transformations. This method was fast and efficient for enantio- and diastereoselective pyranthiazoles.

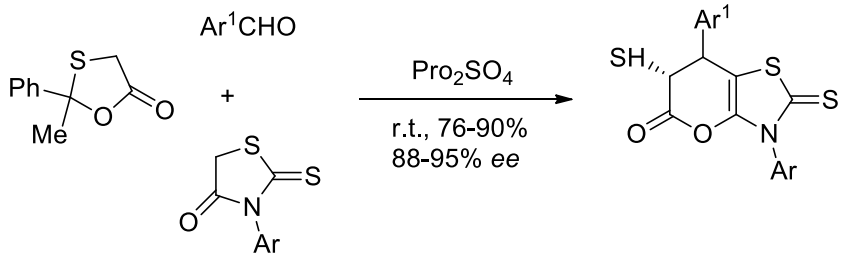

Figure 1.62-Synthesis of 6-Mercaptopyranothiazole.[148]

1.4.1.7 Biginelli reaction

The Biginelli reaction is a fundamental one-pot three-component cyclocondensation reaction for the synthesis of dihydropyrimidine derivatives. These derivatives are superior in potency and duration for antihypertensive activity to known classical drugs. An unprecedented Biginelli reaction (fig 1.63) was catalyzed by using either L-prolinium sulfate, L-alaninium hexafluorophosphate, or L-threonium nitrate between urea/thiourea and active methylene components for enantio- and diastereoselective synthesis of polyfunctionalized perhydroimidines.[149] The L-prolinium sulfate gave the best enhancements in enantio- and diastereoselectivities among all other CILs.

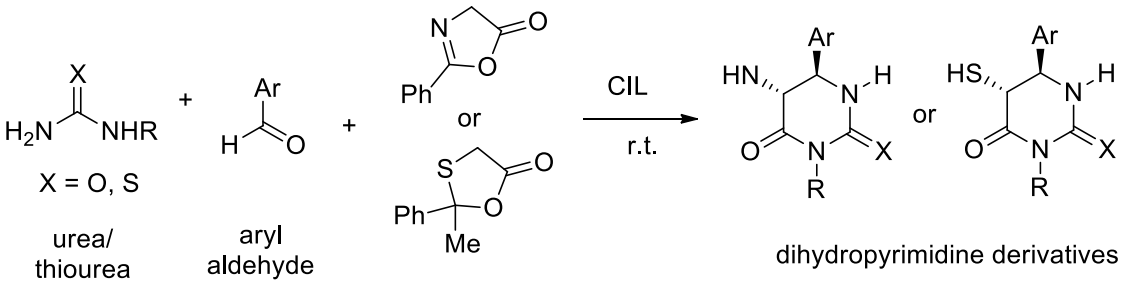

Figure 1.63-Biginelli reaction catalyzed by CIL.[149]

1.4.1.8 Cycloaddition of CO_2 and epoxide

Some AAILs can be used as catalysts in the cycloaddition of CO_2 and propylene oxide (epoxide) to form propylene carbonate. Propylene carbonate is used as an aprotic polar solvent in organic synthesis and find uses in a range of pharmaceutical, agrochemical and other industries.[6] Tetrabutylammonium-type CILs having anions derived from amino acids are used as catalysts along with (Salen)Co(OAc) for the asymmetric cycloaddition of CO_2 to epoxide.[150] The (Salen)Co(OAc) and chiral co-catalyst worked together in an additive or a synergistic manner. Catalyst was recycled three times without loss of activity. Later, the same group synthesized chiral cyclic carbonates by using an efficient catalytic system of alkali metal containing CILs having crown ether-chelated (co-catalyst) and (Salen)Co($OOCCCl_3$) (fig 1.64) for the enantioselective cycloaddition of epoxides and CO_2.[57] The cyclic carbonates obtained from epoxides like epichlorohydrin (4%), 1,2-epoxy-3-phenoxy propane (3%) and styrene oxide (2%) gave lower ee values due to larger substituted groups in comparison to 1,2-epoxybutane (50.8%). The catalyst was recycled five times.

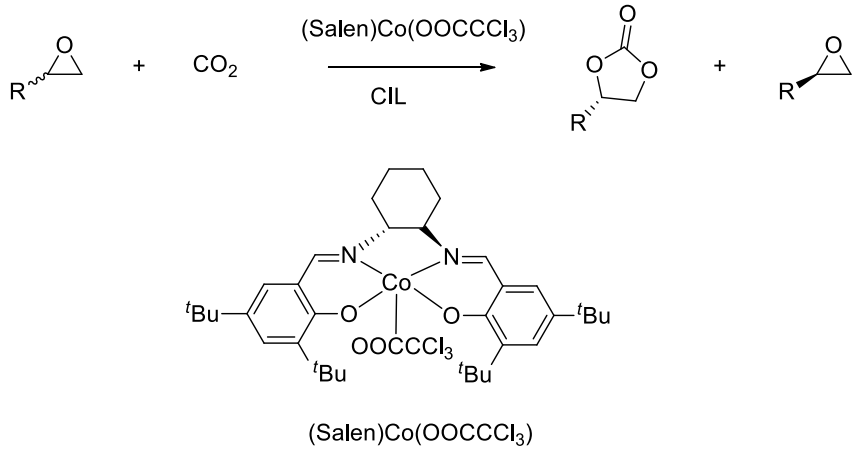

Figure 1.64-Cycloaddition of epoxides and CO_2.[57]

1.4.1.9 Dihydroxylation of Olefins

For the asymmetric dihydroxylation of olefins, a methodology was proposed by Branco *et al.,* to recycle the catalytic system (osmium + chiral ligand) by extraction with an organic solvent or supercritical CO_2. However, when *N*-methylmorpholine was used as co-oxidant in a Sharpless asymmetric dihydroxylation reaction, a slow addition of olefin was required to decrease the secondary catalytic effect cycle which leads to erosion of the enantioselectivity. This slow addition of olefin was avoided by utilizing a functionalized ionic liquid. Later, guanidium-type CILs were used as an alternative chiral promoter to replace the Sharpless chiral ligand.[114] The use of CILs offered an alternative reaction media for asymmetric dihydroxylation previously optimized by Sharpless with

chiral ligands (Cinchona alkaloids). The combined utilization of guadinium-type CILs as chirality-inducing media and super critical CO_2 as extracting media was carried out (fig 1.65).[151] The yields and ee were higher than the conventional systems (Sharpless chiral ligands). This method offered the advantage of the performing reaction without the slow addition of olefins. Secondly, the CILs were used in combination with non-chiral imidazolium ionic liquids. The reaction media and the catalytic system were successfully recycled at least five times without significant decrease in yield or enantioselectivity.

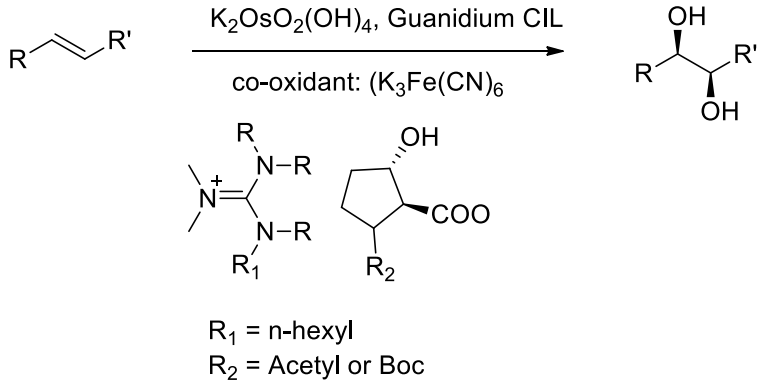

Figure 1.65-Asymmetric dihydroxylation of olefins.[151]

1.4.1.10 Synthesis of (*S*)-Hajos dione

Hajos dione is an important intermediate in the synthesis of Vitamin D and other pharmaceutical products. Imidazolium-based CIL was used as a catalyst for the reaction of 2-methyl-1,3-cyclopentadione and methyl vinyl ketone at 80 °C in the presence of water for 13 hours and gave (*S*)-Hajos dione in 84% yield (fig 1.66).[94]

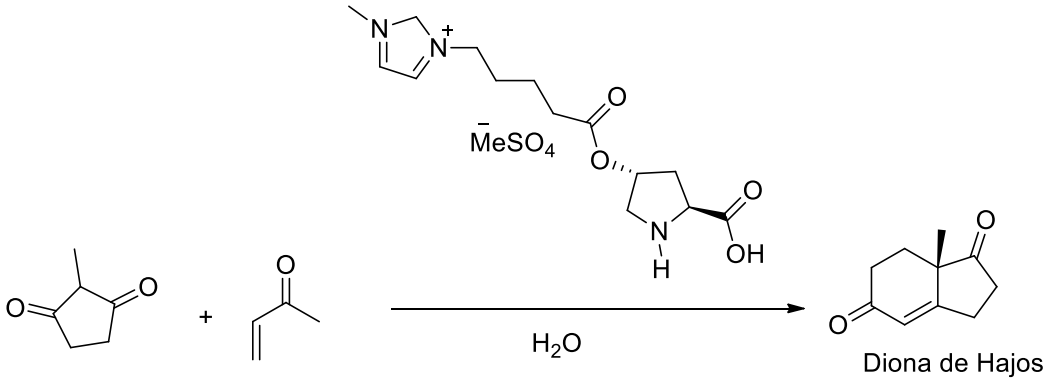

Figure 1.66-Synthesis of (*S*)-Hajos dione catalyzed by CIL.[94]

1.2.2 Chromatography

The negligible vapor pressure, high thermal stability, good polarity and versatile solubility of ILs, makes them attractive to be used in chromatography. Enantioseparation techniques include high performance liquid chromatography (HPLC), gas chromatography (GC), and liquid chromatography (LC). The basic principle involved in a chiral separation is an enantioselective interaction between the analyte and the chiral separator. The mobile phase (either liquid or gas) which carries the analyte (substance to be analyzed) is passed through a stationary phase that retains and separates the analyte.[6]

ILs exhibit ionic conductivity as well and this makes them useful as electrolytes for capillary electrophoresis (CE). This technique rely on the migration of charged analyte under the influence of an externally-applied electric field through a capillary tube (made of fused silica).[6] UV/Vis, or some other techniques is used to determine the separated analyte.

[1-alkyl-3-methylimidazolium][L-proline],[152] $[Cu(L\text{-}Pro)_2][C_nmim]_2$[153] and $[Pro][CH_3COO]$[49] were coordinated to Cu(II) for the enantio-separation of racemic pairs of DL-amino acids by HPLC or CE. The cation structure, copper ion concentration, amino acid concentration, and buffer *p*H were thought to be the key factors responsible for separation. Heckman, in her thesis,[154] tested the synthesized amino acid-type CILs for discrimination ability using $Eu(dpa)_3^{3-}$ (dpa=dipicolinato) and cobalt complexes with luminescence quenching. [BMIm][L-ornithine][155] and [C_6mim][L-Lysine][156] were coordinated[155] to Zn(II) for the enantioseparation of dansyl amino acids. This method was also utilized for screening enzyme inhibitors and in drug discovery.

The use of *N*-undecenoxycarbonyl-L-leucinol bromide (L-UCLB) and *N*-undecenoxycarbonyl-L-pyrrolidinolol bromide (L-UCPB) as a pseudo-phase in micellar CE for separation of acid analytes was reported by Shamsi and Rizvi.[62] The separation was strongly dependent on the presence of opposite charges and the interaction between the chiral selector and analyte. Wang and coworkers combined *N*-undecenoxycarbonyl-L-leucinol bromide (L-UCLB) with 2,3,6-tri-*O*-methyl-β-cyclodextrin (TM-β-CD) for the enantioseparation of five anionic profen drugs by CE (fig 1.66). The enantioseparation of these drugs was achieved with the addition of L-UCLB with buffer containing TM-β-CD. CILs act as an inhibitor by reducing the interactions between L-UCLB and TM-β-CD. The *R*- and *S*-profens have different binding constants thus resulting in enantioseparation. Decrease in the migration times was observed but, unfortunately, no effect on enantiomeric separation was observed with the decrease of the length of hydrocarbon chain on the cation of CIL. The bonding constants between L-UCLB and

TM-β-CD were determined which were similar to the binding constants between imidazole-type ILs and TM-β-CD.[157,158]

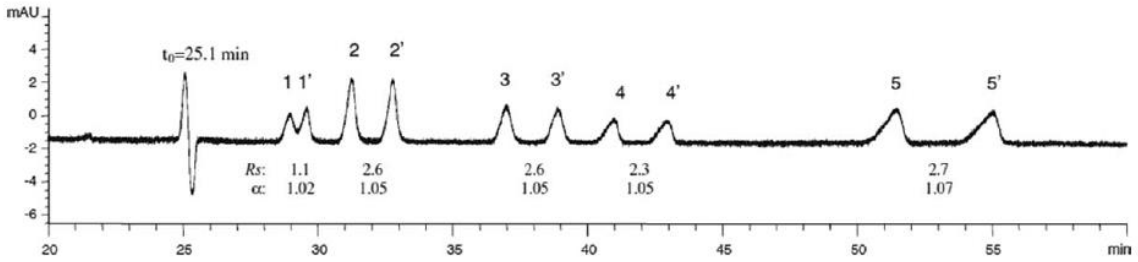

Figure 1.67-Simulataneous enantioseparation of five profen drugs using CIL by CE.[157]

Recently, amino acid ester-based CILs were used as chiral selectors in capillary electrophoresis and successfully separated 1,1'-binaphthyl-2,2-dihydrogen phosphate enantiomers.[159] The important factors involved in the enantiomeric separation were the presence of a *tert*-butyl ester group, the configuration of the CIL and *p*H. It was also seen that steric hindrance (of the *tert* butyl group), electrostatic interaction (between cation of CIL and negatively charged analyte), and the hydrogen-bonding ability (of phosphate groups) are key factors required for the achievement of chiral separation. Later, D-alanine *tert*-butyl ester lactate was used as a background electrolyte additive for the enantiomeric separation of clinically-important compounds (fucose and pipecolic acid).[160] It gave increased resolution from 1.41 to 1.87, but, unfortunately, prolonged the migration times due to increased viscosity of the CIL or/and wall adsorption.

1.2.3 Circularly-Polarized Luminescence (CPL) Spectroscopy

CPL spectroscopy is a recently designed and developed technique which is used by a limited number of research groups to give information about chiral compounds in their excited state. This spectroscopy is the emission analog to circular dichronism (CD) spectroscopy. Many of the techniques (NMR or fluorescence spectroscopy) utilized for the chiral dischrimination requires addition of co-solvents. The chiral discrimination ability of five CILs including L- and D-alanine methyl ester bis(trifluoromethanesulfonyl)amide, L-leucine methyl bis(trifluoromethanesulfonyl)amide, L-proline bis(trifluoromethanesulfonyl)amide and tetrabutylammonium L-alanate were studied by dissolving these in a racemic mixture of dissymmetric tris(2,6-pyridinedicarboxylate) europium complexes and measuring the CPL spectra.[161] Thus chiral discrimination was determined in one step without the

addition of co-solvent. The spectroscopic results suggested that the chiral discrimination is due to enthalpic interactions between the cation of CIL ($[L\text{-}AlaC_1]^+$, $([D\text{-}AlaC_1]^+$, and $([L\text{-}ProC_1]^+$) and the anionic europium complex. However, $[L\text{-}LeuC_1]^+$ differ from the rest of CILs due to largest side chain showed entirely entropic discrimination.

1.2.4 Chiral Discrimination Studies by NMR

The usefulness of amino acid-derived CILs for chiral discrimination was investigated. The potential of L-proline[64] derived CIL and L- and D-alanine[52] *tert*-butyl ester bis(trifluoromethane) sulfonamide was investigated by forming the diastereomeric salts with the racemic salt of Mosher's acid and examining the diastereomeric interactions with ^1H or ^{19}F NMR (fig 1.68). The extent of signal splitting of $-OCH_3$ or $-CF_3$ is attributed to a diastereomeric interaction. Enantiomeric excesses are calculated by simply integrating the signal peaks. The structure[162] of the cation plays an important part in chiral recognition abilities.[162] Ion-pair, hydrogen bonding, π-π stacking, dipole stacking, and steric interactions are thought to be responsible for chiral discrimination.

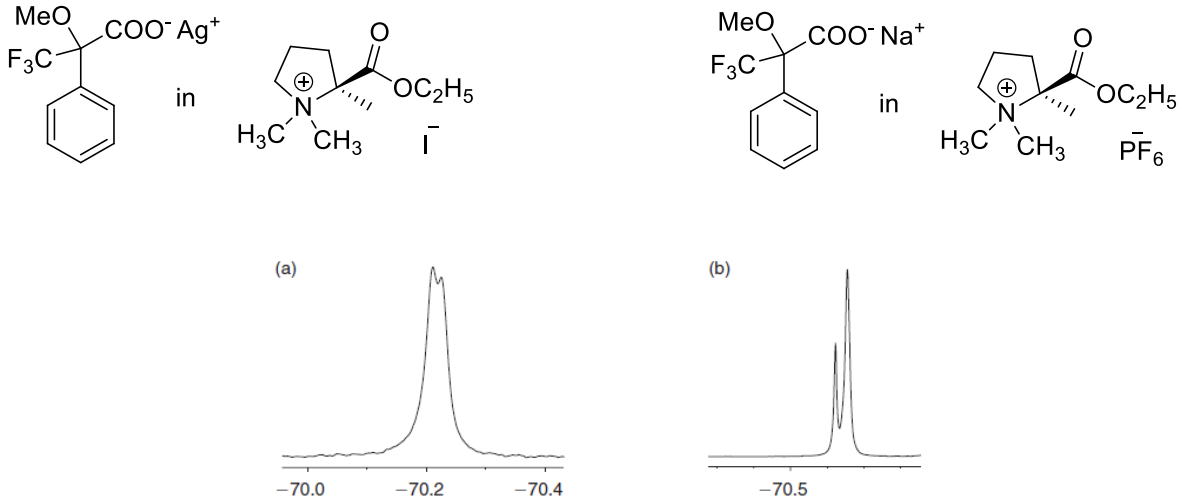

Figure 1.68-^{19}F NMR of Mosher's acid of salt in CIL with a) iodide anion b) PF_6 anion.[64]

N-heterocyclic-type zwitterions having imidazolium and alkyl sulfonate or sulfamate groups were utilized as chiral solvating agents for a racemic mixtures of Mosher's acid, alcohols, cyanohydrins, amino alcohols, nitro alcohols, thiols, and carboxylic acids by using ^1H and ^{19}F NMR (figure 1.69).[163]

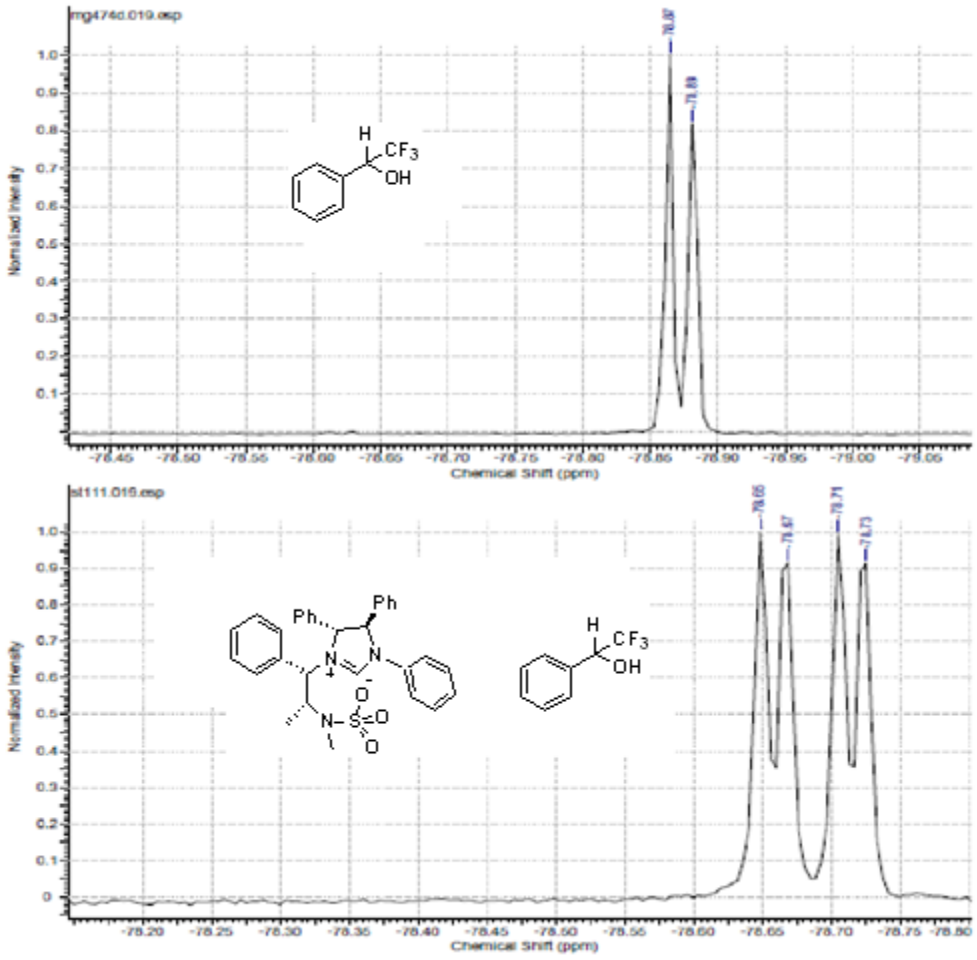

Figure 1.69-^{19}F NMR of racemic compound in the presence of chiral zwitterions.[163]

Imidazolium-type CILs having an amino acid as a chiral moiety were explored as chiral shift reagents for the racemic triethylamine mandelate salt by ^{1}H NMR.[88] A greater diastereomeric interaction between the CIL and the racemic guest gives a greater degree of chiral recognition.

1.2.5 Fluorescence Spectroscopy

Bwambok *et al*. studied alanine-based CILs as chiral selectors for the enantioseparation of drugs. The difference in the emission intensity was attributed to the different enantiomeric compositions as a result of diastereomeric interactions (figure 1.70).[52] The same group later used phenylalanine ester bis(trifluoromethanesulfonyl)amide as a solvent, chiral selector, and a fluorescent reporter for enantiomeric recognition of fluorescent and nonfluorescent analytes. This CIL provided both enantio- and chemoselectivity for multiple analytes.[164]

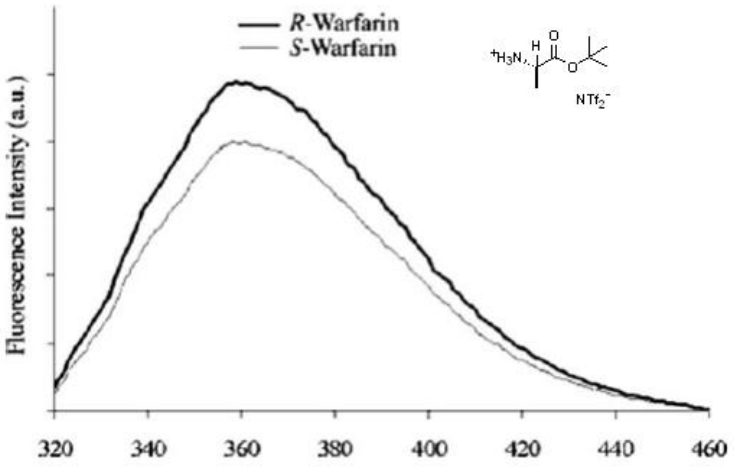

Figure 1.70-Fluorescence emission spectra of (*R*) and (*S*)-warfarin in CIL.[52]

1.2.6 Biotechnology (Activating Agent)

Lipase is an enzyme that catalyzes cleavage of fats and oils in nature.[6] They are a widely used enzyme for various substrates, but enantioselectivity depends on both substrate and the reaction medium. It is highly desirable to improve lipase performance. Four types of pyrrolidine-type imidazolium CIL (**1.19-1.20**) coated lipase were prepared and their activities were evaluated. The transesterification of (±)-1-phenylethanol with two kinds of acyl donors (vinyl acetate and 2,2,2-trifluoroethyl acetate) in the presence of commercial lipase and CIL (lipase coated imidazole salts) was carried out (fig 1.70). A D-pyrrolidine (D-ProMe) (**1.20**) substituted imidazolium CIL derived from unnatural D-proline worked as the best activating agent for the lipase protein and catalyzed the reaction 58 times faster than commercial lipase.[165] It was noteworthy that the (D)-isomer of the imidazolium worked better than the (L)-isomer. Both L- and D-ProMe gave better results than those of corresponding L- (**1.21**) and D-ProH (**1.19)** salts. Thus, the imidazolium cation interacts directly with the enzyme protein and caused modification of the reactivity. The origin of activation was thought to be unaffected by the acylating agents.

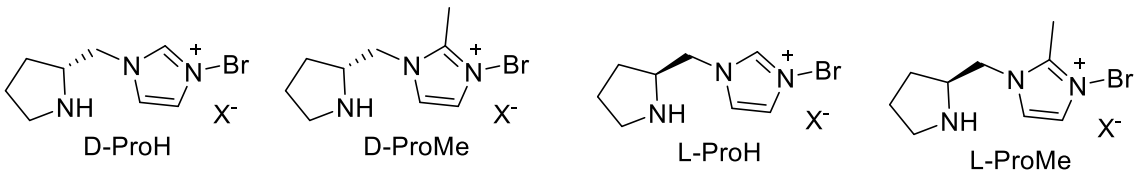

1.19 **1.20** **1.21** **1.22**

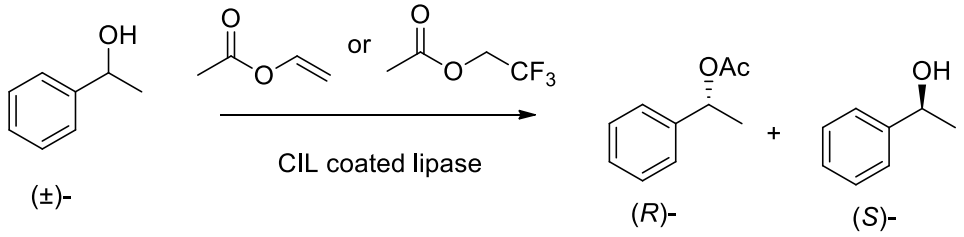

Figure 1.71-Transesterification of (±)-1-phenylethanol with acyl donors in the presence of a lipase-coated CIL.[165]

1.2.7 Absorption of CO_2

From the green chemistry point of view, absorption of CO_2 from the combustion of fossil fuels is very important for environmental issues such as reduction of the greenhouse effect. ILs are composed of ions and, due to negligible volatility, makes them attractive for absorption of gases. The CILs [Bu_4P][AA] (L-alanine, L-β-alanine, L-serine, and L-lysine) were supported on silica gel and effected fast and reversible absorption of CO_2.[166] The rates of absorption of silica-supported CILs were higher as compared to the viscous neat IL. The absorption capacity is $1CO_2/2$[Bu_4P][AA]. However, in the presence of water (1 wt %), the ILs absorbed equimolar amounts of CO_2. The proposed first mechanism suggested that a CO_2 molecule attacks the free electron pair of the N atom on the NH_2 (of amino acid) group forming a carbamate ($–NHCO_2^–$), during which forms hydrogen bond O--H--N with the NH_2 group of another amino acid (route A). However, one of the H atoms in the NH_2 group is taken by $CO_2^–$ and formed a new COOH group (route B) (fig 1.72).

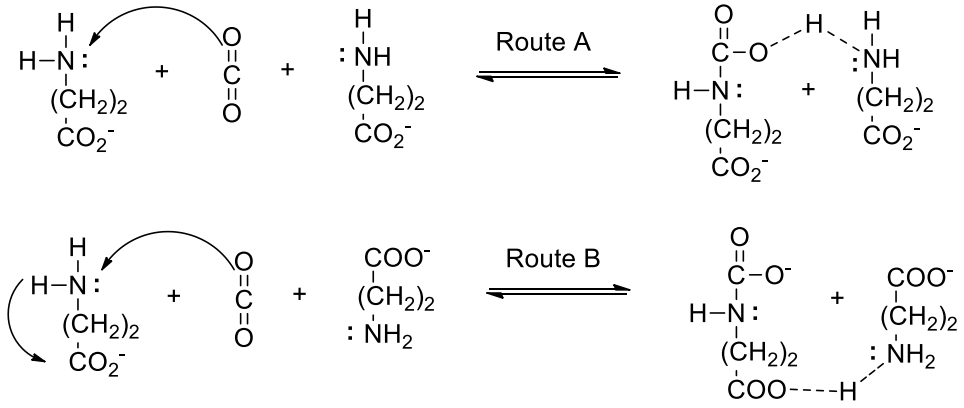

Figure 1.72-Proposed mechanism for absorption of CO_2.[166]

References

1. Luis, P.; Ortiz, I.; Aldaco, R.; Irabien, A. *Exotoxicology and Environmental Safety* **2007,** *67*, 423.
2. Gabriel, S. *Ber.* **1888,** *21*, 2669.
3. Walden, P., Bull Acad Imper Sci: 1914; p 1800.
4. Renner, R., *Ionic Liquids: an industrial cleanup solution*. Environ. Sci. Technol.: 2001; Vol. 35, p 410A.
5. Yang, Q.; Dionysiou, D. D. *J Photochem. Photobiol. A:Chem* **2004,** *165*, 229.
6. Freemantle, M., *An Introduction to Ionic Liquids*. Royal Society of Chemistry: 2010.
7. Cao, Y.; Yao, s.; Wang, X.; Peng, Q.; Song, H., *Handbook of Ionic Liquids*. Nova Science Publishers, Inc.: New York, 2012; p 145.
8. Wasserceid, P.; Gerhard, D.; Himmler, S.; Hormann, S.; Schulz, P. S., *New Ionic Liquids Based on Anion Fucntionalization*. American Chemical Society: Washington, DC, 2005; p 259.
9. Mantz, R. A.; Trulove, P. C., *Viscosity and density of ionic liquids, in:*. Wiley-VCH Verlag GmbH and Co: Germany, 2002.
10. Poolea, C. F.; Pooleb, S. K. *Journal of Chromatographic A* **2010,** *1217*, 2268.
11. Reichardt, C., *Solevnt Effetcs in Organic Chemistry*. Chemical Industry Press: Beijing, 1987.
12. Trulove, P. C.; Mantz, R. A., *Ionic Liquids in Synthesis*. WILEY-VCH Verlag GmbH & Co. kGaA, Weinheim: 2008; Vol. 1.
13. (a) Gathergood, N.; Scammells, O.; Garcia, M. *Green Chemistry* **2006,** *8*, 156; (b) Garcia, M.; Gathergood, N.; Scammells, P. *Green Chemistry* **2005,** *7*, 9.
14. Pretti, C.; Chiappe, C.; Pieraccini, D.; Gregori, M.; Abramo, F.; Monni, G.; Intorre, L. *Green Chemistry* **2006,** *8*, ASAP.
15. Wasserscheid, P.; Bösmanna, A.; Bolmb, C. *Chem. Commun.* **2002**, 200.
16. Walst, K. J. Synthesis and Characterization of Triaminocyclopropenium as a New Class of Ionic Liquids. PhD Thesis, University of Canterbury, Christchurch, 2013.
17. Yoshida, Z. *Top. Curr. Chem.* **1973,** *40*, 47.
18. Pittman, C. U.; Kress, A.; Patterson, T. B.; Walton, P.; Kispert, L. D. *J. Org. Chem.* **1974,** *39* (3), 373.

19. Yoshida, Z. i.; Tawara, Y. *J. Am. Chem. Soc.* **1971**, 2573.
20. Krebs, A.; Breckwoldt, J. *Tetrahedron Lett.* **1969,** *10*, 3797.
21. Clark, G. R.; Surman, P. W. J.; Taylor, M. J. *J. Chem. Soc. Faraday Trans.* **1995,** *91* (10), 1523.
22. Yoshida, Z.; Ogoshi, H.; Hirota, S. *Tetr. Lett.* **1973,** *11*, 869.
23. Yoshida, Z.-i.; Tawara, Y.; Hirota, S.; Ogoshi, H. *Bull. Chem. Soc. Jpn.* **1974,** *47* (4), 797.
24. (a) Ku, A. T.; Sundaralingam, M. *J. Am. Chem. Soc.* **1972,** *94*, 1688; (b) Cowman, C. D.; Thibeault, J. C.; Ziolo, R. F.; Gray, H. B. *J. Am. Chem. Soc.* **1976,** *98* (11), 3209; (c) Thibeault, C. J.; Ziolo, F. R.; Gray, B. H. *Crystal Structure Communication* **1974,** *3*, 473; (d) Radhakrishna, P. T.; Engen, V. D.; Soos, G. Z. *Mol. Cryst. Liq. Cryst.* **1987,** *150b*; (e) Radhakrishna, P. T.; Eugen, V. D.; Soos, G. Z. *J. Phys. Chem.* **1987,** *91*, 3273; (f) Schafer, H. N.; Burzlaff, H.; Grimmeiss, A. M. H.; Weiss, R. *Acta Cryst.* **1992,** *C48*, 912; (g) Weiss, R.; Rechinger, M.; F, H. *Zeitschrift Fuer Kristallographie* **1995,** *210*, 71; (h) Butchard, J. R.; Curnow, O. J.; Garrett, D. J.; Maclagan, R. G. A. R. *Angew. Chem. Int. Ed.* **2006,** *45*, 7550; (i) Butchard, J. R.; Curnow, O. J.; Pipal, R. J.; Robinson, W. T.; Shang, R. *J. Phys. Org. Chem.* **2008,** *21*, 127.
25. Bandar, J. S.; Lambert, T. H. *J. Am. Chem. Soc.* **2012,** *134*, 5552.
26. Breslow, R.; Groved, J. T. *J. Am. Chem. Soc.* **1970,** *92* (4), 984.
27. (a) Weiss, R.; Schwab, O.; Hampel, F. *Chem. Eur. J.* **1999,** *5* (3), 968; (b) Gerson, F.; Plattner, G. *Mol. Phys.* **1971,** *21* (6), 1027.
28. Bandar, J. S.; Lambert, T. H. *Synthesis* **2013,** *45*, 2485.
29. (a) Yoshida, Z.; Komishi, H.; Tawara, Y.; Ogoshi, H. *J. Am. Chem. Soc.* **1973,** *95* (9), 3043; (b) Yoshida, Z.; Konishi, H.; Ogoshi, H. *Isr. J. Chem.* **1981,** *21*, 139; (c) Yoshida, Z.-i.; Hirota, S.; Ogoshi, H. *Spectrochim. Acta* **1974,** *30A*, 1105; (d) Yoshida, Z.; Konishi, H.; Tawara, Y.; Nishikawa, K.; Ogoshi, H. *Tetra. Lett.* **1973,** (28), 2619; (e) Yoshida, Z.-i.; Konishi, H.; Ogoshi, H. *J. Chem. Soc. Chem. Commun.* **1975**, 359; (f) Yoshida, Z.-i.; Tawara, Y. *Tetrahedron Lett.* **1971,** (39), 3603.
30. Breslow, R.; Hover, H.; Chang, H. W. **1962,** *84*, 3168.
31. Ciabattoni, J.; Nathan., E. C. *Tetrahedron Lett.* **1969,** (57), 4997.
32. Kerber, R. C. *J. Am. Chem. Soc.* **1973,** *95* (10), 3239.
33. Johnson, R. W. *Tetrahedron Lett.* **1976,** *8*, 589.
34. Weiss, R.; Sohloter, K. *Tetrahedron Lett.* **1975,** *40*, 3491.

35. Surman, P. W. J.; Anderson, R. F.; Packer, J. E.; Taylor, M. J. *J. Phys. Chem. A* **1997,** *101*, 2732.
36. Clark, T.; Weiss, R. *J. Org. Chem.* **1980,** *45*, 1790.
37. Weiss, R.; Brenner, T.; Hampel, F.; Wolski, A. *Angew. Chem. Int. Ed.* **1994,** *34* (4), 439.
38. Weiss, R.; Brenner, T.; Hampel, F.; Wolski, A. *Angew. Chem. Int. Ed.* **1995,** *34* (4), 439.
39. Butchard, J. R.; Curnow, O. J.; Garrett, D. J.; Maclagan, R. G. A. R.; Libowitzky, E.; Piccoli, P. M. B.; Schultz, A. J. *Dalton Trans.* **2012,** *41* (38), 11765.
40. (a) Schulenberg, W. J. Ed. US. Patent U, 1974; (b) Krebs, A.; Gtintner, A.; Versteylen, S.; Schulz, S. *Tetr. Lett.* **1984,** *25* (22), 2333.
41. Weiss, R.; Hertel, M. *J.C.S. Chem. Comm.* **1980**, 223.
42. Taylor, M. J.; Surman, P. W. J.; Clark, G. R. *J. Chem. Soc., Chem. Commun.* **1994**, 2517.
43. Curnow, O. J.; MacFarlane, D. R.; Walst, K. J. *ChemComm* **2011,** *47*, 10248.
44. Weber, H.-M.; Maas, G. *Chem. Ber.* **1988,** *121*, 1791.
45. Inoue, S.; Yasuda, G.; Hori, T. *Chem. Lett.* **1976**, 1215.
46. Eicher, T.; Graf, R.; Konzmann, H.; Pick, R. *Synthesis* **1987**, 887.
47. Shan, Y.; Dai, L.; Ye, S.; He, M. Method for preparation of CIL of L-amino acid sulfate. 2002.
48. Tao, G.-h.; He, L.; Sun, N.; Kou, Y. *Chem. Communications (Cambridge, England)* **2005,** (28), 3562.
49. Mu, X.; Qi, L.; Zhang, H.; Shen, Y.; Qiao, J.; Ma, H. *Talanta* **2012,** *97*, 349.
50. Yuan, K.; Guohong, T.; Ling, H.; Sun, N. Method for producing ionic liquid of amino acid ester cation. 2005.
51. Marwani, H. M. *Centr. Eur. J. Chem.* **2010,** *8* (4), 946.
52. Bwambok, D. K.; Marwani, H. M.; Fernand, V. E.; Fakayode, S. O.; Lowry, M.; Negulescun, I.; Strongin, R. M.; Warner, I. M. *Chirality* **2008,** *20* (2), 151.
53. Tao, G.-h.; He, L.; Liu, W.-s.; Xu, L.; Xiong, W.; Yuan, T. W. a. *Green Chemistry* **2006,** *8*, 639.
54. Gathergood, N.; Garica, M. T.; Scammells, P. J. *Green Chem.* **2004,** *6*, 166.
55. Meiyan, M. Process for preparation of ionic liquid with chiral valine counter ions. 2012.
56. Li, M.; Rooy, S. L. D.; Bwambok, D. K.; El-Zahab, B.; DiTusab, J. F.; Warner, I. M. *Chem. Commun.* **2009,** *45*, 6922.

57. Ying, S. Y.; QianRu, J.; SuLing, Z.; HuanWang, J.; QianQian, Z. *Sci. China Chem.* **2011,** *54* (7), 1044.
58. (a) Guillen, F.; Bregeon, D.; Plaquevent, J.-C. *Tetrahedron Lett.* **2006,** *47*, 1245; (b) Bregeon, D.; Levillain, J.; Guillen, F.; Plaquevent, J.-C.; Gaumont, A.-C. *Amino Acids* **2008,** *35* (1), 175.
59. Jain, R.; Cohen, L. *Tetrahedron* **1996,** *52*, 5363.
60. Zgonnik, V.; Gonella, S.; Mazieres, M.-R.; Guillen, F.; Coquerel, G.; Saffon, N.; Plaquevent, J.-C. *Org. Process Res. Dev.* **2012,** *16*, 277.
61. Hannig, F.; Kehr, G.; Frohlich, R.; Erker, G. *J. Organomet. Chem.* **2005,** *690* (5959-5972).
62. Rizvi, S. A. A.; Shamsi, S. A. *J. Anal. Chem.* **2006,** *78* (19), 7061.
63. Yu, W.; Zhang, H.; Zhang, L.; Zhou, X. *Aust. J. Chem.* **2010,** *63*, 299.
64. Gao, H.-S.; Hu, Z.-G.; Wang, J.-J.; Qiu, Z.-F.; Fan, F.-Q. *Aust. J. Chem.* **2008,** *61*, 521.
65. (a) Brennecke, J. F.; ROgers, R. D.; Seddon, K. R., *Ionic Liquids IV Not Just Solvents Anymore*. ACS: 2007; p 351; (b) Tao, D.-J.; Cheng, Z.; Chen, F.-F.; Li, Z.-M.; Hu, N.; Chen, X.-S. *J. Chem. Eng. Data* **2013,** *58*, 1542.
66. Allen, C. R.; Richard, P. L.; Ward, A. J.; Water, L. G. A. v. d.; Masters, A. F.; Maschmeyer, T. *Tetr. Lett.* **2006,** *47*, 7367.
67. Kagimoto, J.; Fukumoto, K.; Ohno, H. *Chem. Commun.* **2006**, 2254.
68. Wang, Z.; Li, D. Chiral glutamate ionic liquid. 2009.
69. Wang, Z. Chiral Tyrosine radical ionic liquid. 2011.
70. Wang, Z. Process for preparation of chiral leucine or isoleucine anion containing ionic liquids. 2011.
71. Cybulski, J.; Wisniewska, A.; Kulig-Adamiak, A.; Da˛browski, Z.; Praczyk, T.; Michalczyk, A.; Walkiewicz, F.; Materna, K.; Pernak, J. *Tetrahedron Lett.* **2011,** *52*, 1325.
72. Wood, J. K. *J. Chem. Soc.* **1914,** *105*, 1988.
73. Rahman, M. B. A.; Jumbri, K.; Basri, M.; Abdulmalek, E.; Sirat, K.; Salleh, A. B. *Molecules* **2010,** *15*, 2388.
74. Ossowicz, P.; Janus, E.; Schroeder, G.; Rozwadowski, Z. *Molecules* **2013,** *18*, 4986.
75. Wang, W.-H.; Wang, X.-B.; Kodama, K.; Hirose, T.; Zhang, G.-Y. *Tetrahedron* **2010,** *66*, 4970.

76. Liu, C.; Zhu, L.; Luo, H.; Liu, X. Process for preparation of chiral ionic liquid containing 2-thioxo-4-thiazolidinecarboxylic acid. 2012.
77. Fukumoto, K.; Kohno, Y.; Ohno, H. *Chem. Lett.* **2006,** *35* (11), 1252.
78. Fukumoto, K.; Ohno, H. *Chem. Commun.* **2006,** *29*, 3081.
79. Ohno, H.; Fukumoto, K. *Acc. Chem. Res.* **2007,** *40* (11), 1122.
80. Fukumoto, K.; Ohno, H. *Angew. Chem. Int. Ed.* **2007,** *46*, 1852.
81. Fukumoto, K.; Yoshizawa, M.; Ohno, H. *J. Am. Chem. Soc.* **2005,** *127*, 2398.
82. Bao, W.; Wang, Z.; Li, Y. *J. Org. Chem.* **2003,** *68* (2), 591.
83. Luo, K.; Jiang, H.-y.; You, J.-s.; Xiang, Q.-x.; Guo, S.-j.; Lan, J.-b.; Xie, R.-g. *Lett. Org. Chem.* **2006,** *3*, 363.
84. Armstrong, D. W.; Ding, J. Optically enhanced chiral ionic liquids. 2006.
85. Li, X.-W.; Gao, Y.-A.; Liu, J.; Zheng, L.-Q.; Chen, B.; Wu, L.-Z.; Tung, C.-H. *J. Colloid Interface Sci.* **2010,** *343*, 94.
86. Bai, X.; Li, X.; Zheng, L. *Langmuir* **2010,** *26* (14), 12209.
87. Ishida, Y.; Sasaki, D.; Miyauchi, H.; Saigo, K. *Tetrahedron Lett.* **2006,** *47*, 7973.
88. Gonzalez, L.; Altava, B.; Bolte, M.; Burguete, M. I.; García-Verdugo, E.; Luis, S. V. *Eur J Org Chem* **2012**, 4996.
89. (a) Luo, S.-P.; Xu, D.-Q.; Yue, H.-D.; Wang, L.-P.; Yang, W.-L.; Xu, Z.-Y. *Tetrahedron: Asymmetry* **2006,** *17*, 2028; (b) Luo, S.; Mi, X.; Zhang, L.; Liu, S.; Xu, H.; Cheng, J.-P. *Angew. Chem. Int. Ed.* **2006,** *45*, 3093.
90. Dabrowki, Z.; Wisniewska, A.; Kulig-Adamiak, A.; Kaminski, J.; Cybulski, J. *Polymery* **2012,** *57* (5), 375.
91. (a) Yaqin, Y. *Journal of Tianjin Normal University (Natural Science Edition)* **2009,** *29* (4), 47; (b) Miao, T.; Wang, L.; Li, P.; Yan, J. *Synthesis* **2008,** (23), 3828.
92. Li, P.; Wang, L.; Wang, M.; Zhang, Y. *Eur J Org Chem* **2008**, 1157.
93. Luo, S.; Mi, X.; Zhang, L.; Liu, S.; Xu, H.; Cheng, J.-P. *Tetrahedron* **2007,** *63*, 1923.
94. Yagamare, F. D.; Generosa, G. P.; Emilia, T. S.; Lamine, G. M.; Ousmane, D.; Massene, S.; Alioune, F. E. H. Preparation of an imidazolium chiral ionic liquid derived from proline and its use as catalyst in the one-pot synthesis of the (S)-Hajos dione. 2012.
95. Ou, W.-H.; Huang, Z.-Z. *Green Chem* **2006,** *8*, 731.
96. Pastre, J. C.; Correia, C. R. D.; Genisson, Y. *Green Chem* **2008,** *10*, 885.
97. Li, P.; Wang, L.; Zhang, Y.; Wang, G. *Tetrahedron* **2008,** *64*, 7633.

98. Ni, B.; Zhang, Q.; Headley, A. D. *Green Chem.* **2007,** *9*, 737.

99. Zhang, Q.; Ni, B.; Headley, A. D. *Tetrahedron* **2008,** *64*, 5091.

100. Zhou, L.; Wang, L. *Chem. Lett.* **2007,** *36* (5), 628.

101. Ni, B.; Headley, A. D. *Tetrahedron Lett.* **2006,** *47*, 7331.

102. Siyutkin, D. E.; Kucherenko, A. S.; Zlotin, S. G. *Tetrahedron* **2010,** *66*, 513.

103. Huan, Z.; Haigang, L.; Haihong, W. *Chinese Journal of Organic Chemistry* **2011,** *31* (9), 1433.

104. Coleman, D.; Spulak, M.; Garcia, M. T.; Gathergood, N. *Green Chemistry* **2012,** *14*, 1350.

105. Taokai, Y.; Qiaojian, W.; Ye, Y.; Ningting, Z.; Zhuowei, J.; Xianyi, C.; Jiajia, L. Process for preparation of chiral amido imidazolium bromide ionic liquid from natural amino acid. 2012.

106. Ni, B.; Headley, A. D.; Li, G. *J. Org. Chem.* **2005,** *70* (25), 10600.

107. Aggarwal, V. K.; Emme, I.; Mereu, A. *Chem. Commun.* **2002**, 1612.

108. Ni, B.; Garre, S.; Headley, A. D. *Tetrahedron Lett.* **2007,** *48*, 1999.

109. Xu, D.; Luo, S.; Xu, Z.; Shen, Y. Process for preparation of amino-containing chiral ionic liquids. 2006.

110. (a) Liu, H.; Xu, Q.; Dai, J. Alkyl imidazole-L-proline salt chiral ionic liquid and preparation method thereof 2010; (b) Hong-xia, L.; Jian-fei, D.; Qun, X. *Chinese language* **2012**, 108.

111. Clavier, H.; Boulanger, L.; Audic, N.; Toupet, L.; Mauduit, M.; Jean-Claud *Chem. Commun.* **2004**, 1224.

112. Abrunhosa, I.; Gulea, M.; Levillain, J.; Masson, S. *Tetrahedron Asymmetry* **2001,** *12*, 2851.

113. Zhao-zhao, L.; Yue-cheng, Z.; Ji-quan, Z. *Chinese Journal of Synthetic Chemistry* **2012,** *20* (5), 568.

114. Branco, L. C.; Gois, P. M. P.; Lourenco, N. M. T.; Kurteva, V. B.; Afonso, C. A. M. *Chem. Commununications (Cambridge, England)* **2006,** (22), 2371.

115. Shah, J.; Liebscher, J. *Syn.* **2008,** (6), 917.

116. Liebscher, J.; Shah, J.; Yacob, Z.; Sadiq, S.; Hanelt, S.; Blumenthal, H. *Processes in Isotopes and Molecules Journal of Physics: Conference Series* **2009,** *182*, 1.

117. Yamada, T.; Lukac, P. J.; Yu, T.; Weiss, R. G. *Chem. Mater.* **2007,** *19*, 4761.

118. Yu, T.; Yamada, T.; Gaviola, G. C.; Weiss, R. G. *Chem. Mater.* **2008,** *20*, 5337.
119. Earle, M. J.; McCormac, P. B.; Seddon, K. R. *Green Chem.* **1999,** *1*, 23.
120. Doherty, S.; Goodrich, P.; Hardacre, C.; Knight, J. G.; Nguyen, M. T.; Parvulescu, V. I.; Paun, C. *Adv. Synth. Catal.* **2007,** *349*, 951.
121. Zheng, X.; Qian, Y.; Wang, Y. *Catal. Commun.* **2010,** *11*, 567.
122. Font, D.; Sayalero, S.; Bastero, A.; Jimeno, C.; Pericas, M. A. *Org. Lett.* **2008,** *10* (2), 337.
123. Huang, J.; Zhang, X.; Armstrong, D. W. *Angew. Chem. Int. Ed.* **2007,** *46*, 9073.
124. Miao, W.; Chan, T. H. *Adv. Synth. Catal.* **2006,** *348*, 1711.
125. Lombardo, M.; Pasi, F.; Easwar, S.; Trombini, C. *Adv. Synth. Catal.* **2007,** *349*, 2061.
126. Lombardo, M.; Pasi, F.; Easwar, S.; Trombini, C. *Synlett* **2008**, 2471.
127. Nakadai, M.; Saito, S.; Yamamoto, H. *Tetrahedron* **2002,** *58*, 8167.
128. Lombardo, M.; Easwar, S.; Pasi, F.; Trombini, C. *Adv. Synth. Catal.* **2009,** *351*, 276.
129. Siyutkin, D. E.; Kucherenko, A. S.; Struchkova, M. I.; Zlotin, S. G. *Tetrahedron Lett.* **2008,** *49*, 1212.
130. Larionova, N. A.; Kucherenko, A. S.; Siyutkin, D. E.; Zlotin, S. G. *Tetrahedron* **2011,** *67*, 1948.
131. Siyutkin, D. E.; Kucherenko, A. S.; Zlotin, S. G. *Tetrahedron* **2009,** *65*, 1366.
132. Zhang, L.; Zhang, H.; Luo, H.; Zhou, X.; Cheng, G. *J. Braz. Chem. Soc.* **2011,** *22* (9), 1736.
133. Vasiloiu, M.; Rainer, D.; Gaertner, P.; Reichel, C.; Schroder, C.; Bica, K. *Catal. Today* **2013,** *200*, 80.
134. Ho, S.; Jiang, T.; Zhang, Z.; Zhu, A.; Han, B.; Song, J.; Xie, Y.; Li, W. *Tetrahedron Lett.* **2007,** *48* (32), 5613.
135. Qian, Y.; Zheng, X.; Wang, Y. *J. Org. Chem.* **2010,** *19*, 3672.
136. Gauchot, V.; Schmitzer, A. R. *Journal Organic Chemistry* **2012,** *77*, 4917.
137. Luo, S.; Zhang, L.; Mi, X.; Qiao, Y.; Cheng, J.-P. *J. Org. Chem.* **2007,** *72*, 9350.
138. Ni, B.; Zhang, Q.; Headley, A. D. *Tetrahedron Lett.* **2008,** *49*, 1249.
139. Maltsev, O. V.; Kucherenko, A. S.; Zlotin, S. G. *Eur. J. Org. Chem.* **2009**, 5134.
140. Maltsev, O. V.; Kucherenko, A. S.; Beletskaya, I. P.; Tartakovsky, V. A.; Zlotin, S. G. *Eur. J. Org. Chem.* **2010**, 2927.

141. Kucherenko, A. S.; Siyutkin, D. E.; Maltsev, O. V.; Kochetkov, S. V.; Zlotin, S. G. *Russian Chemical Bulletin, Internaternational Edition* **2012,** *61*, 1313.
142. Zlotin, S. G.; Kuherenko, A. S.; Maltsev, O. V.; Chizhov, A. O. *Top. Catal.* **2013**.
143. Qian, Y.; Xiao, S.; Liu, L.; Wang, Y. *Tetrahedron Asymmetry* **2008,** *19*, 1515.
144. Morel, A.; Silarska, E.; Trzeciak, A. M.; Pernak, J. *Dal. Trans.* **2013,** *42*, 1215.
145. Schmitkamp, M.; Chen, D.; Leitner, W.; Klankermayer, J.; Francio, G. *Chem. Commun.* **2007**, 4012.
146. Chen, D.; Schmitkamp, M.; Francio, G.; Klankermayer, J.; Leitner, W. *Angew. Chem. Int. Ed.* **2008,** *47*, 7339.
147. Jin, X.; Xu, X.-f.; Zhao, K. *Tetrahedron Asymmetry* **2012,** *23*, 1058.
148. Yadav, L. D. S.; Yadav, B. S.; Rai, V. K. *J. Heterocyclic Chem.* **2008,** *45*, 1315.
149. Yadav, L. D. S.; Rai, A.; Rai, V. K.; Awasthi, C. *Tetrahedron* **2008,** *64*, 1420.
150. Zhang, S.; Huang, Y.; Jing, H.; Yao, W.; Yan, P. *Green Chem.* **2009,** *11*, 935.
151. Branco, L. C.; Serbanovic, A.; Ponte, M. N. d.; Afonso, C. A. M. *ACS Catal.* **2011,** *1*, 1408.
152. Liu, Q.; Wu, K.; Tang, F.; Yao, L.; Yang, F.; Nie, Z.; Yao, S. *Chem. Eur. J.* **2009,** *15* (38), 9889.
153. Tang, F.; Zhang, Q.; Ren, D.; Nie, Z.; Liu, Q.; Yao, S. *Journal of Chromatographic A* **2010,** *1217*, 4669.
154. Heckman, L. M. Chiral Recognition Study of a Bimolecular Process in Amino Acid Chiral Ionic Liquids. Butler University, Indianapolis, IN, 2011.
155. Mu, X.; Qi, L.; Shen, Y.; Zhang, H.; Qiao, J.; Ma, H. *Analyst* **2012,** *137*, 4235.
156. Zhang, H.; Qi, L.; Shen, Y.; Qiao, J.; Mao, L. *Electrophoresis* **2013,** *34*, 846.
157. Wang, B.; He, J.; Bianchi, V.; Shamsi, S. A. *Electrophoresis* **2009,** *30*, 2812.
158. Wang, B.; He, J.; Bianchi, V.; Shamsi, S. A. *Electrophoresis* **2009,** *30*, 2820.
159. Stavrou, I. J.; P., C.; Kapnissi-Christodoulou *Electrophoresis* **2013,** *34*, 524.
160. Hadjistasi, C. A.; Stavrou, I. J.; Staden, R.-I. S.-V.; Aboul-enein, H. Y.; Kapnissi-Christodoulou, C. P. *Chirality* **2013**.
161. Kroupa, D. M.; Brown, C. J.; Heckman, L. M.; Hopkins, T. A. *J. Phys. Chem. B* **2012,** *116*, 4952.
162. Li, M.; Gardella, J.; Bwambok, D. K.; El-Zahab, B.; Rooy, S. d.; Cole, M.; Lowry, M.; Warner, I. M. *J. Comb. Chem.* **2009,** *11*, 1105.

163. Tabassum, S.; Gilani, M. A.; Wilhelm, R. *Tetrahedron Asymmetry* **2011,** *22*, 1632.

164. Bwambok, D. K.; Challa, S. K.; Lowry, M.; Warner, I. M. *Anal Chem* **2010,** *82*, 5028.

165. Malhotra, S. V., *Ionic Liquid Applications: Pharmaceuticals, Therapeutics, and Biotechnology*. Oxford University Press, 2010.

166. Zhang, J.; Zhang, S.; Dong, K.; Zhang, Y.; Shen, Y.; Lv, X. *Chem. Eur. J.* **2006,** *12*, 4021.

Experimental

Experimental

2.1 Analytical techniques

2.1.1 NMR

^{1}H and ^{13}C {H} NMR spectra were recorded in $CDCl_3$ or CD_3OD on a Varian Unity300 instrument at 300 and 75 MHz respectively, Agilent MR400 NMR Spectrophotometer (running at $J_{3.2}$ Software) at 400 and 100 MHz respectively or on a Varian INOVA500 Spectrophotometer (running at $J_{3.2}$ Software) at 500 and 126 MHz respectively with tetramethylsilane (TMS) as an internal standard. ^{19}F NMR was recorded in 20% DMSO-$CDCl_3$ on a Agilent MR400 NMR Spectrophotometer (running $J_{3.2}$ Software) at 376 MHz.

2.1.2 Mass Spectrometry

Electrospray mass spectrometry was measured on a maXis 3G UHR-Qq-TOF Mass Spectrophotometer running Compass, Hystar and DataAnalysis Sofware (Bruker Dalronik Gm,bH, Bremen, Germany) couples to a Dionex Ultimate 3000 LC System (ThermoFisher) after dissolving samples in methanol or acetonitrile.

2.1.3 Microanalysis

Microanalysis was performed by Campbell Microanalytical Laboratory, Dunedin. For some of the ILs, water was added to the calculated microanalysis to match the experimental result.

2.1.4 Water Content

The water content of the samples was measured by using 831 Karl Fischer Coulometer. The weighted sample is inserted into the methanolic solution of iodine, sulphur dioxide and a base as a buffer.[1] The I_2 reacts quantitatively with water and hence determines the water content. The liquid samples were inserted directly, however in the case of highly viscous or solid samples solutions were made in dry DCM.

2.1.5 Chloride Content

The chloride content of all the samples was measured by Orion 9617 ionplus® Sure Flow® Combination Chloride Electrodes. This measures free chloride ions in aqueous solution or

ethanolic aqueous solution. The electrode was calibrated always before use and the slope should be between 54-60 mV/decade. The electrodes are immersed in the sample solution and an aliquot of the standard 0.1 M KCl is added to the sample. The change in potential before and after addition each addition gives the original sample concentration. The level of chloride ions corresponding to the measured potential is described by Nerst equation:

$$E = E_o - S\ log\ X$$

where, E = measured electrode potential, E_o= reference potential (constant), S = slope and X = level of chloride ions in solution.

2.1.6 Viscosity

The viscosities for all the samples were measured from 20 °C (or above if solid) to 90 °C on a Brookfield DV-II+ Pro cone and plate sealed viscometer under inert atmosphere. The non-Newtonian behavior was also recorded over a limited shear rate range.

2.1.7 Conductivity

The conductivity was measured using a Schott LF4100+ probe, an impedance bridge conductivity meter, after calibrating with 0.01 M KCl solution. The probe contained two platinum wires. The Nyquist Plot was used to determine resistance and conductivity was calculated by $\kappa = \frac{l}{AR}$ where $\frac{l}{A}$ is a cell constant, determined by 0.01 M KCl solution at 25 °C. The conductivity was measured from 20 °C to 90 °C under an inert atmosphere.

2.1.8 Thermal Gravimetric Analysis

Thermal Gravimetric Analysis (TGA) was determined with a thermal analysis instrument TA Q600 SDT (DSC-TGA) by utilizing platinium pans with 5 to 10 mg of the dry sample. The heating rate for TGA was 1 °C min^{-1} and 10 °C min^{-1} under nitrogen from 25 to 600 °C. The instrument was calibrated with temperature using zinc (419.6 °C) and heat flow with sapphire standard. The pans were heated up to 600 °C in an air atmosphere to clean them.

2.1.9 Differential Scanning Calorimetry

Differential scanning calorimetry (DSC) was carried out on a Perkin Elmer DSC 8000. The DSC 8000 was calibrated using indium (156.60 °C) and cyclohexane (−87.0 and 6.5 °C). Three heating and colling cylces were carried out from −100 to 100 °C or −100 to 150 °C using a scan rate of 10 °C/ min, using a sample size of 2-10 mg and data was taken from the second run.

2.1.10 Density

The density was measured on an Anton Parr DMA 5000 instrument having an isolating U-tube density meter, ranging from 20 °C to 90 °C in 10 °C steps.

2.1.11 Polarimetery

Specific rotation was measured on a Perkin Elmer Polarimeter 341 after dissolving the sample in $CHCl_3$ or CH_3CN. The optical rotation (∝) was measured of known concentration (c) of the sample and then the specific rotation, $[\propto]_D^{25}$ was calculated by using the following formula;

$$[\propto]_D^{25} = \frac{\propto \times l}{c}$$

2.1.12 Magnetic Susceptibility Balance

The magnetic susceptibility was measured with a Magway MSB MK1. The constant characteristic ($C_{Bal\ New}$) was calibrated with the sealed tube of $MnCl_2.2H_2O$. The sample (solid or liquid) was packed in the clean dry tube and the sample mass (m) and sample length Ami(l) was noted. Magnetic susceptibility (χ_g) is calculated by the following formula;

$$\chi_g = \frac{C_{Bal\ New} \times l\ (R - R_0)}{10^9 \times m}$$

Similarly, molar magnetic susceptibility (χ_m) and effective magnetic moment (μ_{eff}) are calculated as follows:

$$\chi_m = \chi_g \times \text{Molecular weight}$$

$$\mu_{eff} = 2.828\sqrt{T \times \chi_m}$$

2.1.13 Miscibility and Solubility

Miscibility studies were carried out on the liquid and solubility on the solid samples at 25 °C using a water bath. For solid samples, 0.1 g of the sample was taken and 1.5 mL of the dry solvent was added. If the solid dissolves then it was soluble, if it formed a separate layer then it was immiscible and if it remained as a solid then its insoluble. But in case of liquid samples, 0.5 mL of the sample was taken and 0.05 mL of dry solvent was added four times, 0.1 mL was added three times, 0.25 mL was added twice, 0.5 mL was added twice followed by 1 mL and 1.5 mL once. If the layers are homogeneous they are miscible and if remained as separate layers they were immiscible.

2.2 Synthetic details

The syntheses requiring dry conditions were done under an inert atmosphere using standard Schlenk lines. Most of the chemicals were purchased from either Sigma Aldrich or Merck. The dried solvents were obtained from "in-house built Grubbs solvent delivery system" whenever required. The solvents are degassed with nitrogen before introduction to the system, and move through activated alumina and are dispensed immediately in nitrogen.[2]

2.2.1 Pentachlorocyclopropane[3]

Sodium trichloroacetate (501 g, 2.70 mol) was added to trichloroethene (1.65 L, 18.3 mol) and brought to reflux. The trichloroethene-water azeotrope was removed by continuous reflux for three hours. Dried dimethoxyethane (260 mL, 2.51 mol) was added to the trichloroethene solution and refluxed for 7 days. The solution was washed with water (3×1L), HCl (0.1 mol/L, 3×1 L), and water (3×1L). Excess trichloroethene was removed *in vacuo* from the crude mixture. The pentachlorocyclopropane (125 mL, 37% yield) was distilled from the crude mixture.

2.2.2 *N*-Ethylmethylamine (HNEtMe)

Prepared by a modification of methods described by Lucire and Wawzonek.[4] Sodium hydroxide (19 g, 481 mmol) solution in 50 mL water was added slowly to a stirred solution of ethylammonium chloride (30 g, 370 mmol) in 50 mL water. Ethylamine was obtained as a colorless liquid (15 g, 90%) after distillation at 40 °C *in vacuo* into a receiving flask immersed in a dry-ice bath. Ethylamine (14.5 mL, 222 mmol) was added dropwise for an hour to the stirred ice-cold solution of benzaldehyde (23 mL, 222 mmol), at a rate such that solution temperature remains below 15 °C.[4a] Water was separated from the *N*-benzylideneethylamine using a

separating funnel. Dimethyl sulphate (28 g, 370 mmol) solution in benzene (25 mL) was added dropwise to the stirred ice-cold solution of N-benzylideneethylamine in benzene (50 mL) and the solution was left stirring overnight at ambient temperature.[4b] The reaction mixture was heated to reflux for 30 minutes. Water (80 mL) was added to the solution and heated to reflux for another 30 minutes. Residue was cooled down and diethyl ether (3×50 mL) washes were done to remove benzaldehyde. Ammonium salts were concerntrated *in vacuo.* Distillation was performed at 50 °C by adding sodium hydroxide (13.3g, 555 mmol) solution (in water 30 mL) drop by drop to the stirred solution of ammonium salt *in vacuo*. Ethylmethylamine was collected in receiving flask immersed in dry-ice bath (−78 °C). ^{1}H NMR suggested presence of ethylamine and ethylmethylamine in the ratio 1:4. Benzaldehyde was added to the mixture to react with the ethylamine leaving behind ethylmethylamine. Pure *N*-ethylmethylamine was obtained after distillation at 50 °C (10.5 mL, 54%).

2.2.3 *N*-Allylmethylamine (HNAllylMe)

N-Allylamine was synthesized by the procedure described in literature from allyl isothiocyanate.[5] Allylamine (101 mL, 1.35 mol) was added drop by drop for an hour to the stirred ice-cold solution of benzaldehyde (137 mL, 1.35 mol), in an inert atmosphere.[4] Water was separated from the *N*-benzylideneallylamine with the help of separating funnel. Dimethyl sulphate (127 mL, 1.35 mol) solution in benzene (100 mL) was added drop by drop to the stirred ice-cold solution of *N*-benzylidenallylamine in benzene (100 mL) and solution was left on stirring overnight at ambient temperature.[4] The reaction mixture was heated under reflux for 30 minutes. Water (200 mL) was added to the above reaction mixture and reflux for another 30 minutes. Residue was cooled down and diethyl ether (3×50 mL) washes were done to remove benzaldehyde. The solution was concentrated *in vacuo.* Distillation was performed at 60 °C by adding sodium hydroxide (135 g, 1.82 mol) solution (in water 200 mL) drop by drop to the stirred solution of ammonium salt *in vacuo*. Allylmethylamine was collected in receiving flask immersed in dry-ice bath (−78 °C). ^{1}H NMR suggested presence of allylamine and allylmethylamine in the ratio 1:4. Benzaldehyde was added to the mixture to react with the allylamine and pure *N*-allylmethylamine was obtained after distillation at 60 °C (30.21 mL, 37%).

2.2.4 *N*-(2-Methoxyethyl)methylamine (HNErMe)[4]

2-Methoxyethylamine (70 mL, 801 mmol) was added drop by drop for an hour to the stirred ice-cold solution of benzaldehyde (90 mL, 801 mmol), in an inert atmosphere.[4a] Water was separated from the *N*-benzylidene-2-methoxyethylamine with the help of separating funnel. Dimethyl sulphate (99 mL, 801 mmol) solution in benzene (100 mL) was added drop by drop to the stirred ice-cold solution of *N*-benzyliden-2-methoxyethylamine in benzene (100 mL) and solution was left on stirring overnight at ambient temperature.[4b] The reaction mixture was heated under reflux for 30 minutes. The water (150 mL) was added to the above mixture and was refluxed for another 30 minutes. Residue was cooled down and diethyl ether (3×50 mL) washes were done to remove benzaldehyde. The mixture was concerntrated *in vacuo.* Distillation was performed at 60 °C by adding sodium hydroxide (80 g, 2 mol) solution (in water) to the stirred solution of ammonium salt *in vacuo*. *N*-(methylamine-2-methoxyethyl)amine was collected in receiving flask immersed in dry-ice bath (−78 °C). ^{1}H NMR suggested presence of 2-methoxyethylamine and *N*-(2-methoxyethyl)methylamine in the ratio 1:4. Benzaldehyde was added to the mixture to react with the *N*-(2-methoxyethyl)amine and pure *N*-(2-methoxyethyl)methylamine was obtained after distillation at 60 °C (50 mL, 70%).

2.2.5 Tris(dimethylamino)cyclopropenium chloride, $[C_3(NMe_2)_3)]Cl$, $[M_6]Cl$

Pentachlorocyclopropane (6.91 mL, 49 mmol) was added dropwise to a stirred solution of Me_2NH (40% solution in water) (44 g, 392 mmol) at 0 °C for an hour.[6] The solution was left stirring overnight at ambient temperature. The product mixture contained the open ring product (**2.1**) along with $[C_3(NMe_2)_3)]Cl$ and $[Me_2NH_2]Cl$. The peak ratio of $[C_3(NMe_2)_3]Cl$:$[HC_3(NMe_2)_4]^+$ in the mass spectrometer was 4:1 respectively The remaining mixture was dissolved in acetonitrile:toluene (2:1) and kept in freezer overnight to crystallize out ammonium salts. The mixture was dissolved in water (50 mL) and acidified with conc. HCl to pH = 1-2. $[C_3(NMe_2)_3)]Cl$ was then extracted with $CHCl_3$ (3×50 mL) while leaving behind the dication of the open ring product $[H_2C_3(NMe_2)_4]^{2+}$ in the water layer.[7] ^{1}H NMR (500 MHz, $CDCl_3$): δ 3.2 (s, 18H, NC*H*$_3$). ^{13}C {^{1}H} NMR (126 MHz, $CDCl_3$): δ 118.29 (ring C), 42.76 (N*C*H$_3$). EI MS: Found m/z 168.1499 (M^+); Calcd: 168.1495 (M^+).

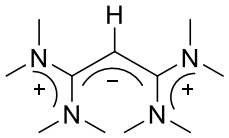

2.1

2.2.6 Bis(dimethylamino)cyclopropenone, $(Me_2N)_2C_3O$, M_4O

NaOH (15%) was dissolved into water (150 mL). Tris(dimethylamino)cyclopropenium chloride[6] (60 g, 0.295 mol) was added to the solution, and heated to 70 °C for 2 h in an open mouth beaker to allow escape of Me_2NH. The solution was acidified to pH = 2 and the organic compound was extracted from aqueous solution using $CHCl_3$ (3 ×250 mL) leaving behind the open ring product (**2.1**). $CHCl_3$ was removed *in vacuo*, yielding a yellow solid (24 g, 56%). ^{1}H NMR (500 MHz, $CDCl_3$): δ 2.92 (s, 12H, NC*H*$_3$). ^{13}C {^{1}H} NMR (126 MHz, $CDCl_3$): δ 134.03 (*C*O), 121.37 (ring C), 42.76 (N*C*H$_3$). EI MS: Found m/z 141.1023 (M+H); Calcd: 141.1022 (M+H). NMR consistant with literature.[8]

2.2.7 Bis(dimethylamino)methoxycyclopropenium methylsulphate, $[(Me_2N)_2C_3OMe]MeSO_4$, $[M_4OMe]MeSO_4$

Dry bis(dimethylamino)cyclopropenone (2.69 g, 19.2 mmol) was stirred with Me_2SO_4 (2.36 mL, 25 mmol) for 2 hours in an inert atmosphere. The mixture was washed with dry diethyl ether several times to remove methanol and excess dimethylsulfate. This gave an orange viscous oil (4.57 g, 90%). ^{1}H NMR (500 MHz, $CDCl_3$): δ 4.15 (s, 3H, OC*H*$_3$), 3.63 (s, 3H, C*H*$_3$SO$_4$), 3.16 (s, 12H, NC*H*$_3$). ^{13}C{^{1}H} NMR (126 MHz, $CDCl_3$) δ 122.76 (equivalent ring C), 119.89 (unique ring C), 63.87 (O*C*H$_3$), 54.17 (*C*H$_3$SO$_4$), 41.13 (N*C*H$_3$). EI MS: Found m/z 155.1177 (M^+); Calcd: 155.1179 (M^+). Anal. calcd for $C_9H_{18}N_2O_5S.1.5.H_2O$: C, 38.62; H, 7.02; N, 10.01. Found: C, 38.33; H, 6.93; N, 9.76.

2.2.8 Bis(diethylamino)cyclopropenone, $(Et_2N)_2C_3O$, E_4O[8]

NaOH (250 g) was dissolved into water (4 L). Tris(diethylamino)cyclopropenium chloride[6a] (42 g, 0.15 mol) was added to the solution, and heated to 70 °C for 18 h in an open mouth beaker to allow escape of Et_2NH. The solution was neutralized and acetone (100 mL) was added to allow filtering to remove NaCl, followed by removing acetone *in vacuo*. The organic compound was

extracted from aqueous solution using $CHCl_3$ (3×250 mL). $CHCl_3$ was removed *in vacuo*, yielding a yellow solid (22 g, 77%). ^{1}H NMR (300 MHz, $CDCl_3$): δ 3.21 (q, $^3J_{HH}$ = 7.2 Hz, 8H, NCH_2CH_3). 1.20 (t, $^3J_{HH}$ = 7.2 Hz, 12H, NCH_2CH_3). ^{13}C {^{1}H} NMR (75 MHz, $CDCl_3$): δ 134.03 (*C*O), 121.37 (ring C), 46.01 (NCH_2CH_3), 14.18 (NCH_2CH_3). EI MS: Found m/z 196.1049 (M+); Calcd: 197.1648 (M+H)

2.2.9 Bis(diethylamino)methoxycyclopropenium tetrafluoroborate, $[C_3(NEt_2)_2(OMe)]BF_4$, $[E_4OMe]BF_4$

Dry bis(diethylamino)cyclopropenone (1.03 g, 5 mmol) was stirred with $[Me_3O]BF_4$ (1.01 mL, 6.5 mmol) for 4 h in an inert atmosphere to give $[C_3(NEt_2)_2(OMe)]BF_4$ as a yellow oil (1.3 g, 83%). ^{1}H NMR (500 MHz, $CDCl_3$): δ 4.19 (q, 3H, OCH_3), 3.43 (q, $^3J_{HH}$ = 7.3 Hz, 8H, NCH_2CH_3), 1.3 (t, $^3J_{HH}$ = 7.25 Hz, 12H, NCH_2CH_3). EI MS: Found m/z 211.1805 (M^+); Calcd: 211.1838 (M^+). Microanalysis was not carried out due to its instability.

2.2.10 Bis(diethylamino)methoxycyclopropenium trifluoromethylsulfonate, $[C_3(NEt_2)_2OMe]OTf$, $[E_4OMe]OTf$

Dried bis(diethylamino)cyclopropenone (1.14 g, 6 mmol) was stirred with $MeCF_3SO_3$ (0.8 mL, 8 mmol) in dry dichloromethane for 2 h in an inert atmosphere. Solvent was removed *in vacuo.* The mixture was washed with dry diethyl ether several times to remove excess $MeCF_3SO_3$ and cyclopropenone. This gave an orange viscous oil of $[C_3(NEt_2)(OMe)]CF_3SO_3$ (1.46 g, 70%). ^{1}H NMR (500 MHz, $CDCl_3$): δ 4.19 (q, 3H, OCH_3), 3.43 (q, $^3J_{HH}$ = 7.3 Hz, 8H, NCH_2CH_3), 1.3 (t, $^3J_{HH}$ = 7.25 Hz, 12H, NCH_2CH_3). Microanalysis was not carried out due to its instability.

2.2.11 Bis(diethylamino)ethoxycyclopropenium iodide, $[C_3(NEt_2)_2OEt]I$, $[E_4OEt]I$

Dried bis(diethylamino)cyclopropenone (4.19 g, 21 mmol) was refluxed with ethyl iodide (43 mL, 534 mmol) for 20 h in an inert atmosphere. Excess ethyl iodide was recycled by distillation. The mixture was washed with dry diethyl ether several times to remove cyclopropenone. This gave a yellow solid of $[C_3(NEt_2)(OEt)]I$ (3.44 g, 46%). ^{1}H NMR (500 MHz, $CDCl_3$): δ 4.59 (q, $^3J_{HH}$ = 7 Hz, 2H, OCH_2), 3.48 (q, $^3J_{HH}$ = 7.3 Hz, 8H, NCH_2CH_3), 1.47 (t, $^3J_{HH}$ = 7Hz, OCH_2CH_3), 1.32 (t, $^3J_{HH}$ = 7.5 Hz, 12H, NCH_2CH_3). EI MS: Found m/z 225.1968 (M^+); Calcd: 225.1961 (M^+). Microanalysis was not carried out due to its instability.

2.2.12 Bis(diethylamino)methoxycyclopropenium methylsulphate, $[C_3(NEt_2)_2OMe]$ $MeSO_4$, $[E_4OMe]MeSO_4$

Dried bis(diethylamino)cyclopropenone (1.14 g, 6 mmol) was stirred with Me_2SO_4 (0.98 mL, 8 mmol) for 2 h in an inert atmosphere. Solvent was removed *in vacuo.* The mixture was washed with dry diethyl ether several times to remove excess Me_2SO_4 and cyclopropenone. This gave an orange viscous oil of $[C_3(NEt_2)(OMe)]MeSO_4$ (1.46 g, 70%). ^{1}H NMR (500 MHz, $CDCl_3$): δ 4.19 (s, 3H, OC*H*$_3$), 3.5 (s, 3H, CH_3SO_4), 3.43 (q, $^3J_{HH}$ = 7.3 Hz, 8H, NC*H*$_2$CH$_3$), 1.3 (t, $^3J_{HH}$ = 7.25 Hz, 12H, NCH$_2$C*H*$_3$). Microanalysis was not carried out due to its instability.

2.3 Synthesis of Bis(dimethylamino)alkylaminocyclopropenium salts

2.3.1 Bis(dimethylamino)ethylaminocyclopropenium bis(trifluoromethanesulfonyl)amide, $[C_3(NMe_2)_2(NEtH]TFSA$, $[M_4EH]TFSA$

$[C_3(NMe_2)_2(OMe)]MeSO_4$ (8.82 g, 33 mmol) was stirred with $EtNH_2$ (3.25 mL, 43 mmol) in dry dichloromethane (20 mL) for 30 minutes in an inert atmosphere. Dichloromethane was removed *in vacuo*. The mixture was washed with dry diethyl ether several times to remove excess amine. The mixture was dissolved in water, and the product was extracted with chloroform (3 ×30 mL). The solvent was removed *in vacuo* to give $[C_3(NMe_2)_2(NEtH)]MeSO_4$ as a light brown oil, which was then stirred with LiTFSA (18.94 g, 66 mmol) in H_2O (20 mL) and the product was extracted with $CHCl_3$ (3×30 mL) and the solvent was removed *in vacuo* to give a light brown oil (8.5 g, 86%). ^{1}H NMR (400 MHz, $CDCl_3$): δ 6.29 (br, 1H, N*H*), 3.33 (q, $^3J_{HH}$ = 8 Hz, 2H, NC*H*$_2$), 3.11 (s, 12H, NC*H*$_3$), 1.28 (t, $^3J_{HH}$ = 8 Hz, 3H, NCH$_2$C*H*$_3$). ^{13}C{^{1}H} NMR (100 MHz, $CDCl_3$): δ 119.84 (q, $^1J_{CF}$ = 321 Hz, CF_3), 117.08 (equivalent ring C), 115.48 (unique ring C), 42.40 (N*C*H$_2$), 41.72 (N*C*H$_3$), 15.04 (NCH$_2$*C*H$_3$). EI MS: Found m/z 168.1495 (M^+); Calcd: 168.1495 (M^+). Anal. calcd for $C_{11}H_{18}N_4O_4S_2F_6$: C, 29.47; H, 4.04; N, 12.49. Found: C, 30.09; H, 4.13; N, 12.26. With water content of 1040 ppm.

2.3.2 Bis(dimethylamino)allylaminocyclopropenium bis(trifluoromethanesulfonyl)amide, $[C_3(NMe_2)_2(HN(CH_2CHCH_2))]TFSA$, $[M_4AH]TFSA$

$[C_3(NMe_2)_2(OMe)]MeSO_4$ (4.51 g, 28 mmol) was stirred with $CH_2CHCH_2NH_2$ (4.24 mL, 36 mmol) in dry dichloromethane (10 mL) for 1 h in an inert atmosphere. Dichloromethane was removed *in vacuo.* The mixture was washed with dry diethyl ether several times to remove excess

amine. The mixture was dissolved in acetone and kept in a freezer to precipitate out ammonium salts which were removed by filteration. The mixture was dissolved in ice cold water and the product was extracted with $CHCl_3$:ethanol 2:1 (3 ×30 mL). The solvent was removed *in vacuo* to give $[C_3(NMe_2)_2(NH(CH_2CHCH_2))]MeSO_4$ as a light yellow oil, which was then stirred with LiTFSA (7.51 g, 27 mmol) in H_2O (20 mL). The product was extracted with chloroform (3×30 mL). The solvent was removed in *in vacuo* to give a light yellow oil (4.04 g, 97%). ^{1}H NMR (400 MHz, $CDCl_3$): δ ^{1}H NMR ($CDCl_3$, 400 MHz): δ 6.5 (br, 1H, N*H*), 5.85 (ddt, $^3J_{HH}$ = 4.7 Hz, $^3J_{HH}$ = 10.56 Hz, $^3J_{HH}$ = 22.3 Hz, 1H, NCH_2CH=CH_2), 5.27 (d, $^3J_{HH(cis)}$ = 7.04 Hz, 2H, NCH_2CH=CH_2), 5.25 (d, $^3J_{HH(trans)}$ = 14.1 Hz, 2H, NCH_2CH=CH_2), 3.90 (t, $^3J_{HH}$ = 5.29 Hz, 2HH, NCH_2CH=CH_2), 3.1 (s, 12H, NCH_3). ^{13}C{^{1}H} NMR (100 MHz, $CDCl_3$): δ 132.88 (NCH_2CH), 119.82 (q, $^1J_{CF}$ = 321 Hz, CF_3), 117.35 (NCH_2CHCH_2), 117.26 (equivalent ring C), 115.27 (unique ring C), 48.67 (NCH_2), 41.74 (NCH_3). EI MS: Found m/z 180.1498 (M^+); Calcd: 180.1495 (M^+). Anal. calcd for 0.97($C_{13}H_{20}N_4O_4S_2F_6$):0.03($C_{13}H_{25}N_5O_4S_2F_6$): C, 31.60; H, 4.02; N, 12.35. Found: C, 32.04; H, 4.27; N, 12.26. Microanalysis suggested presence of 3% of open ring (**2.1**). With water content of 1137 ppm.

2.3.3 Bis(dimethylamino)propylaminocyclopropenium bis(trifluoromethanesulfonyl)amide, $[C_3(NMe_2)_2(N(CH_2CH_2CH_3)H)]$TFSA, $[M_4PrH]$TFSA

$[C_3(NMe_2)_2(OMe)]MeSO_4$ (3.96 g, 15 mmol) was stirred with $H_2N(CH_2CH_2CH_3)$ (1.59 mL, 20 mmol) in dry dichloromethane (5 mL) for 1 h in an inert atmosphere. Dichloromethane was removed *in vacuo*. The mixture was washed with dry diethyl ether several times to remove excess amine. The mixture was dissolved in water and the product was extracted with chloroform (3 ×50 mL). The solvent was removed *in vacuo* to give $[C_3(NMe_2)_2(N(CH_2CH_2CH_3)H)]MeSO_4$ as a light yellow oil, which was then stirred with LiTFSA (7.51 g, 27 mmol) in H_2O (20 mL). The product was extracted with chloroform (3×30 mL). The solvent was removed *in vacuo* to give a yellow oil (4.05 g, 92%). ^{1}H NMR ($CDCl_3$, 400 MHz): δ 6.29 (br t, 1H, N*H*), 3.23 (t, $^3J_{HH}$ = 8 Hz, 2H, NCH_2), 3.11 (s, 12H, NCH_3), 1.66 (m, 2H, NCH_2CH_2), 0.96 (t, $^3J_{HH}$ = 8 Hz, 3H, $NCH_2CH_2CH_3$). ^{13}C{^{1}H} NMR ($CDCl_3$, 100 MHz): δ 119.92 (q, $^1J_{CF}$ = 320 Hz, CF_3), 117.69 (equivalent ring C), 117.47 (unique ring C), 49.30 (NCH_2), 41.79 ($N(CH_3)_2$), 23.19 (NCH_2CH_2), 10.90 ($NCH_2CH_2CH_3$). EI MS: Found m/z 182.1653 (M^+); Calcd: 182.1652 (M^+). Anal. calcd for $C_{12}H_{20}N_4O_4S_2F_6$: C, 31.17; H, 4.36; N, 12.11. Found: C, 31.34; H, 4.47; N, 11.91. With water content of 843 ppm.

2.3.4 Bis(dimethylamino)-N-(methoxyethyl)aminocyclopropenium bis(trifluoromethanesulfonyl)amide, $[C_3(NMe_2)_2(N(CH_2CH_2OCH_3)H)]TFSA$, $[M_4ErH]TFSA$

$[C_3(NMe_2)_2(OMe)]MeSO_4$ (4.1 g, 15 mmol) was stirred with $H_2NCH_2CH_2OCH_3$ (1.75 mL, 20 mmol) in dry dichloromethane (5 mL) for 1 h in an inert atmosphere. Dichloromethane was removed *in vacuo.* The mixture was washed with dry diethyl ether several times to remove excess of amine. The mixture was dissolved in water and acidified to pH = 2 with HCl and the product was extracted with chloroform (3×50 mL). The solvent was removed *in vacuo* to give $[C_3(NMe_2)_2(N(CH_2CH_2OCH_3)H)]MeSO_4$ (2.6g, 55%) as a light yellow oil, which was then stirred with LiTFSA (10.4 g, 36 mmol) in H_2O (20 mL). The product was extracted with chloroform (3×30 mL). The solvent was removed *in vacuo* to give a yellow oil (6.53 g, 96%). ^{1}H NMR ($CDCl_3$, 400 MHz): δ 6.34 (br, 1H, N*H*), 3.53 (t, $^3J_{HH}$ = 4.8 Hz, 2H, NCH_2CH_2), 3.42 (t, $^3J_{HH}$ = 5.3 Hz, 2H, NCH_2CH_2), 3.33 (s, 3H, $NCH_2CH_2OCH_3$), 3.11 (s, 12H, NCH_3). ^{13}C {^{1}H} NMR ($CDCl_3$, 100 MHz): δ 119.93 (q, $^1J_{CF}$ = 320 Hz, CF_3), 116.79 (equivalent ring C), 116.12 (unique ring C), 71.98 (NCH_2CH_2), 58.92 (NCH_2CH_2), 47.161 (OCH_3), 41.79 ($N(CH_3)_2$). EI MS: Found m/z 198.1602 (M^+); Calcd: 198.1601 (M^+). Anal. calcd for $0.95(C_{12}H_{20}N_4O_5S_2F_6)$:$0.05(C_{13}H_{25}N_5O_4S_2F_6)$: C, 30.67; H, 4.33; N, 12.05. Found: C, 31.1; H, 4.33; N, 11.78. Microanalysis suggested 5% of open ring product (**2.1**). With water content of 308 ppm.

2.3.5 Bis(dimethylamino)butylaminocyclopropenium bis(trifluoromethanesulfonyl)amide, $[C_3(NMe_2)_2(NBuH)]TFSA$, $[M_4BH]TFSA$

$[C_3(NMe_2)_2(OMe)]MeSO_4$ (5 g, 19 mmol) was stirred with $BuNH_2$ (2.4 mL, 25 mmol) in dry dichloromethane (5 mL) for 2 h in an inert atmosphere. Dichloromethane was removed *in vacuo.* The mixture was washed with dry diethyl ether several times to remove excess amine. The mixture was dissolved in water and the pH lowered to 1 with HClaq (37%) and the product was extracted with dichloromethane (3×30 mL). The solvent was removed *in vacuo* to give $[C_3(NMe_2)_2(NBuH)]MeSO_4$ as a brown viscous oil which was then stirred with LiTFSA (6.4 g, 24 mmol) in H_2O (20 mL). The product was extracted with chloroform:ethanol 2:1 (3×30 mL) and the solvent was removed *in vacuo* to give a brown oil (3.26 g, 89%). ^{1}H NMR (400 MHz, $CDCl_3$): δ 6.23 (br, 1H, N*H*), 3.25 (q, 2H, $^3J_{HH}$ = 6.8 Hz, NCH_2), 3.1 (s, 12H, NCH_3), 1.59 (m,

2H, NCH_2CH_2), 1.36 (m, 2H, $NCH_2CH_2CH_2$), 0.92 (t, $^3J_{HH}$ = 7.2 Hz, 3H, $CH_2CH_2CH_3$). ^{13}C {^1H} NMR (100 MHz, CDCl3): δ 119.14 (q, $^1J_{CF}$ = 322 Hz, CF_3), 118.20 (unique ring C), 115.55 (equivalent ring C), 47.38 (NCH_2), 41.77 (NCH_3), 31.90 (NCH_2CH_2), 19.65 ($NCH_2CH_2CH_2$), 13.55 ($NCH_2CH_2CH_2CH_3$). EI MS: Found m/z 196.1812 (M^+); Calcd: 196.1808 (M^+). Anal. calcd for $C_{13}H_{22}N_4O_4S_2F_6$: C, 32.77; H, 4.65; N, 11.76. Found: C, 33.16; H, 4.74; N, 11.87. With water content of 374 ppm.

2.3.6 Bis(dimethylamino)pentylaminocyclopropenium bis(trifluoromethanesulfonyl)amide, $[C_3(NMe_2)_2(NPeH)]TFSA$, $[M_4PeH]TFSA$

$[C_3(NMe_2)_2(OMe)]MeSO_4$ (6.59 g, 25 mmol) was stirred with $PeNH_2$ (3.73 mL, 33 mmol) in dry dichloromethane (5 mL) for 2 h in an inert atmosphere. Dichloromethane was removed *in vacuo*. The mixture was dissolved in chloroform (50 mL) and washed with ice-cold water (4 ×30 mL). The solvent was removed *in vacuo* to give $[C_3(NMe_2)_2(NPeH)]MeSO_4$ as a brown oil which was then stirred with LiTFSA (11.78 g, 42 mmol) in H_2O (20 mL). The product was extracted with chloroform (3× 30 mL) and the solvent was the removed *in vacuo* to give a brown oil (5.57 g, 84%). ^1H NMR (400 MHz, $CDCl_3$): δ 6.35 (br t, 1H, N*H*), 3.25 (dt, $^3J_{HH}$ = 7 Hz, 2H, NCH_2), 3.12 (s, 12H, NCH_3), 1.61 (m, 2H, NCH_2CH_2), 1.32 (m, 4H, $NCH_2CH_2CH_2CH_2$), 0.90 (t, $^3J_{HH}$ = 7 Hz, 3H, $NCH_2CH_2CH_2CH_2CH_3$). $^{13}C\{^1H\}$ NMR (100 MHz, $CDCl_3$): δ 119.82 (q, $^1J_{CF}$ = 321 Hz, CF_3), 117.00 (equivalent ring C), 115.75 (unique ring C), 47.72 (NCH_2), 41.79 (NCH_3), 29.61 (NCH_2CH_2), 28.60 ($NCH_2CH_2CH_2$), 22.19 ($NCH_2CH_2CH_2CH_2$), 13.80 ($NCH_2CH_2CH_2CH_2CH_2CH_3$). EI MS: Found m/z 210.1968 (M^+); Calcd: 210.1965 (M^+). Anal. calcd for $C_{14}H_{24}N_4O_4S_2F_6$: C, 34.28; H, 4.93; N, 11.42. Found: C, 34.92; H, 5.06; N, 11.10. With water content of 1212 ppm.

2.4 Synthesis of Bis(dimethylamino)dialkylaminocyclopropenium salts

2.4.1 Bis(dimethylamino)ethylmethylaminocyclopropenium bis(trifluoromethanesulfonyl)amide, $[C_3(NMe_2)_2(NEtMe]TFSA$, $[M_5E]TFSA$

$[C_3(NMe_2)_2N(EtH)]TFSA$ was dried under vacuum overnight. $[C_3(NMe_2)_2N(EtH)]TFSA$ (3.51 g, 8 mmol) was stirred with dry THF at -78 °C and n-BuLi (5.38 mL of 1.6 M, 8.8 mmol) was added drop wise in an inert atmosphere. The reaction mixture was stirred for 30 minutes and then allowed to warm to room temperature for another 30 minutes. Me_2SO_4 (0.98 mL, 10 mmol) was

then added and the solution was stirred for another 30 minutes. THF was then removed *in vacuo*. The mixture was dissolved in $CHCl_3$ (50 mL) and $LiMeSO_4$ was filtered off. Then the $CHCl_3$ layer was washed with water (3×50 ML). The solvent was removed *in vacuo* to give a yellow oil (2.22 g, 77%). ^{1}H NMR (400 MHz, $CDCl_3$): δ 3.39 (q, $^3J_{HH}$ = 7 Hz, 2H, NC*H*$_2$), 3.12 (s, 12H, NC*H*$_3$), 3.09 (s, 3H, C*H*$_3$), 1.26 (t, $^3J_{HH}$ = 7 Hz, 6H, NCH_2CH_3). $^{13}C\{^1H\}$ NMR (100 MHz, $CDCl_3$): δ 119.91 (q, $^1J_{CF}$ = 322 Hz, CF_3), 117.88 (equivalent ring C), 115.48 (unique ring C), 50.09 (N*C*H$_2$), 42.21 (N*C*H$_3$), 39.24 (N*C*H$_3$), 15.04 (NCH_2CH_3). ESI MS: Found m/z 182.1652 (M^+): Calcd. 182.1652 (M^+). Anal. calcd for $C_{12}H_{20}N_4O_4S_2F_6$: C, 31.17; H, 4.36; N, 12.11. Found: C, 31.56; H, 4.37; N, 12.05. With water content of 878 ppm.

2.4.2 Bis(dimethylamino)diethylaminocyclopropenium bis(trifluoromethanesulfonyl)amide, $[C_3(NMe_2)_2(NEt_2)]TFSA$, $[M_4E_2]TFSA$

$[C_3(NMe_2)_2(OMe)]MeSO_4$ (4.6 g, 17.4 mmol) was stirred with Et_2NH (2.34 mL, 23 mmol) in dry dichloromethane (5 mL) for 2 h in an inert atmosphere. Dichloromethane was removed *in vacuo*. The mixture was washed with dry diethyl ether several times to remove excess amine. The mixture was dissolved in ice cold water, and the product was extracted with chloroform:ethanol (2:1) (3 ×30 mL). The solvent was removed *in vacuo* to give $[C_3(NMe_2)_2(NEt_2)]MeSO_4$ as a light yellow oil, which was then stirred with LiTFSA (14.98 g, 52 mmol) in H_2O (20 mL) and the product is extracted with $CHCl_3$ (3×30 mL) and the solvent was removed *in vacuo*, the mixture was dissolved in ethanol and kept in freezer for overnight and filtered off to give white crystals (3.0 g, 36%). ^{1}H NMR (400 MHz, $CDCl_3$): δ 3.39 (q, $^3J_{HH}$ = 7 Hz, 4H, NC*H*$_2$), 3.12 (s, 12H, NC*H*$_3$), 1.26 (t, $^3J_{HH}$ = 7 Hz, 6H, NCH_2CH_3). $^{13}C\{^1H\}$ NMR (100 MHz, CDCl3): δ 119.91 (q, $^1J_{CF}$ = 322 Hz, CF_3), 117.74 (equivalent ring C), 116.41 (unique ring C), 47.45 (N*C*H$_2$), 42.11 (N*C*H$_3$), 13.74 (NCH_2CH_3). EI MS: Found m/z 196.1810 (M^+); Calcd: 196.1808 (M^+). Anal. calcd for $C_{13}H_{22}N_4O_4S_2F_6$: C, 32.78; H, 4.65; N, 11.76. Found: C, 33.01; H, 4.64; N, 11.89. With water content of 117 ppm.

2.4.3 Bis(dimethylamino)allylmethylaminocyclopropenium bis(trifluoromethanesulfonyl)amide, $[C_3(NMe_2)_2(N(CH_2CHCH_2)Me)]TFSA$, $[M_5A]TFSA$

$[C_3(NMe_2)_2(OMe)]MeSO_4$ (4.26 g, 16 mmol) was stirred with CH_2CHCH_2NMe (2 mL, 21 mmol) in dry dichloromethane (10 mL) for 1 h in an inert atmosphere. Dichloromethane was removed *in vacuo*. The mixture was washed with dry diethyl ether several times to remove excess amine. The

mixture was dissolved in water and the product was extracted with $CHCl_3$:ethanol 2:1 (3 ×30 mL). The solvent was removed *in vacuo* to give $[C_3(NMe_2)_2(N(CH_2CHCH_2)Me)]MeSO_4$ as a light yellow oil, which was then stirred with LiTFSA (5.89 g, 21 mmol) in H_2O (20 mL). The product was extracted with chloroform (3×30 mL). The solvent was removed *in vacuo* to give a light yellow oil (3.19 g, 95%). ^{1}H NMR (400 MHz, $CDCl_3$): δ ^{1}H NMR ($CDCl_3$, 400 MHz): δ 5.82 (ddt, $^3J_{HH}$ = 5.48 Hz, $^3J_{HH}$ = 10.56 Hz, $^3J_{HH}$ = 22.3 Hz 1H, NCH_2CH=CH_2), 5.32 (d, $^3J_{HH(cis)}$ = 10.7 Hz, 1H, NCH_2CH=CH_2), 5.26 (d, $^3J_{HH(trans)}$ = 17.6 Hz, 1H, NCH_2CH=CH_2), 3.90 (d, $^3J_{HH}$ = 4.7 Hz, 2H, NCH_2CH=CH_2), 3.12 (s, 3H, NCH_3), 3.10 (s, 12H, $N(CH_3)_2$). ^{13}C{^{1}H} NMR (126 MHz, $CDCl_3$) δ 130.88 (NCH_2CH), 119.92 (q, $^1J_{CF}$ = 321 Hz, CF_3), 118.62 (NCH_2CHCH_2), 117.99 (equivalent ring C), 117.32 (unique ring C), 57.25 (NCH_2), 42.21 (NCH_3), 39.96 (NCH_3). EI MS: Found m/z 194.1654 (M^+); Calcd: 194.1652 (M^+). Anal. calcd for $0.92(C_{13}H_{20}N_4O_4S_2F_6)$:$0.08(C_{13}H_{25}N_5O_4S_2F_6)$: C, 33.57; H, 4.44; N, 12.34. Found: C, 34.02; H, 4.86; N, 12.00. Microanalysis suggested 8% of open ring product (**2.1**). With water content of 885 ppm.

2.4.4 Bis(dimethylamino)allylmethylaminocyclopropenium dicyanamide, $[C_3(NMe_2)_2(N(CH_2CHCH_2)Me)]DCA$, $[M_5A]DCA$

$[C_3(NMe_2)_2(OMe)]MeSO_4$ (4.17 g, 16 mmol) was stirred with $(CH_2CHCH_2)NMe$ (1.95 mL, 21 mmol) in dry dichloromethane (5 mL) for 30 minutes in an inert atmosphere. Dichloromethane was removed *in vacuo.* The mixture was washed with dry diethyl ether several times to remove excess amine. The mixture was dissolved in water and the product was extracted with $CHCl_3$:ethanol 2:1 (3×30 mL). The solvent was removed *in vacuo* to give $[C_3(NMe_2)_2(N(CH_2CHCH_2)Me)]MeSO_4$ as a light yellow oil (4 g, 80%), which was then stirred with NaDCA (3.3 g, 36 mmol) in H_2O (50 mL). The product was extracted with chloroform (3×30 mL). The solvent was removed in *in vacuo* to give a light yellow oil (3 g, 87%). ^{1}H NMR (400 MHz, $CDCl_3$): δ 5.83 (ddt, $^3J_{HH}$ = 5.48 Hz, $^3J_{HH}$ = 10.17 Hz, $^3J_{HH}$ = 22.3 Hz 1H, NCH_2CH=CH_2), 5.34 (d, $^3J_{HH(cis)}$ = 12 Hz, 2H, NCH_2CH=CH_2), 5.27 (d, $^3J_{HH(trans)}$ = 20 Hz, 2H, NCH_2CH=CH_2), 3.98 (m, 2H, NCH_2CH=CH_2), 3.17 (s, 12H, NCH_3). ^{13}C {^{1}H} NMR (126 MHz, $CDCl_3$) δ 130.75 (NCH_2CH), 119.89 (CN), 118.75 (NCH_2CHCH_2), 118.01 (equivalent ring C), 117.35 (unique ring C), 57.35 (NCH_2), 42.44 (NCH_3), 40.25 (NCH_3). EI MS: Found m/z 194.1652 (M^+); Calcd: 194.1652 (M^+). Anal. calcd for $C_{13}H_{20}N_6.0.9H_2O$: C, 56.46; H, 7.95; N, 30.38. Found: C, 56.93; H, 8.31; N, 29.75.

2.4.5 Bis(dimethylamino)diallylaminocyclopropenium bis(trifluoromethanesulfonyl)amide, $[C_3(NMe_2)_2(N(CH_2CHCH_2)_2)]TFSA$, $[M_4A_2]TFSA$

$[C_3(NMe_2)_2(OMe)]MeSO_4$ (5.0 g, 19 mmol) was stirred with $(CH_2CHCH_2)_2NH$ (3.0 mL, 25 mmol) in dry dichloromethane (5 mL) for 2 h in an inert atmosphere. Dichloromethane was removed *in vacuo.* The mixture was washed with dry diethyl ether several times to remove excess amine. The mixture was dissolved in water and the product was extracted with dichloromethane (3 ×30 mL). The solvent was removed *in vacuo* to give $[C_3(NMe_2)_2(N(CH_2CHCH_2)_2)]MeSO_4$ as a light yellow oil, which was then stirred with LiTFSA (11 g, 39 mmol) in H_2O (20 mL). The product was extracted with chloroform (3×30 mL). The solvent was removed *in vacuo* and was dissolved in ethanol (10 mL) and kept in freezer for overnight to give white crystals (5.68 g, 89%). ^{1}H NMR (400 MHz, $CDCl_3$): δ 5.81 (m, 2H, $NCH_2C\mathit{H}=CH_2$), 5.31 (d, $^3J_{HH}$ = 10.8 Hz, 2H, $NCH_2CH=C\mathit{H}_2$), 5.25 (d, $^3J_{HH}$ = 17 Hz, 2H, $NCH_2CH=C\mathit{H}_2$), 3.95 (d, $^3J_{HH}$ = 5.2 Hz,4H, $NC\mathit{H}_2CH=CH_2$), 3.68 (s, 3H, $C\mathit{H}_3SO_4$), 3.1 (s, 12H, $NC\mathit{H}_3$). ^{13}C {H} NMR (100 MHz, CDCl3): δ 131.07 ($NCH_2\mathit{C}H$), 120.10 (q, $^1J_{CF}$ = 322 Hz, CF_3), 118.64 ($NCH_2CH\mathit{C}H_2$), 118.04 (equivalent ring C), 116.53 (unique ring C), 54.71 ($N\mathit{C}H_2$), 42.10 (NCH_3). EI MS: Found m/z 220.1811 (M^+); Calcd: 220.1808 (M^+). Anal. calcd for $C_{15}H_{22}N_4O_4S_2F_6$: C, 36.00; H, 4.43; N, 11.19. Found: C, 36.23; H, 4.36; N, 11.19. With water content of 81 ppm.

2.4.6 Bis(dimethylamino)propylmethylaminocyclopropenium bis(trifluoromethanesulfonyl)amide, $[C_3(NMe_2)_2(N(CH_2CH_2CH_3)Me)]TFSA$, $[M_5Pr]TFSA$

$[C_3(NMe_2)_2(OMe)]MeSO_4$ (5.00 g, 19 mmol) was stirred with $H_2N(CH_2CH_2CH_3)$ (2.0 mL, 25 mmol) in dry dichloromethane (5 mL) for 2 h in an inert atmosphere. Dichloromethane was removed *in vacuo.* The mixture was washed with dry diethyl ether several times to remove excess amine. The mixture was in dissolved water and the product was extracted with chloroform (3 ×50 mL). The solvent was removed *in vacuo* to give $[C_3(NMe_2)_2(N(CH_2CH_2CH_3)H)]MeSO_4$ as a light yellow oil, which was then stirred with LiTFSA (13.60 g, 47 mmol) in H_2O (20 mL). The product was extracted with chloroform (3×30 mL). The solvent was removed *in vacuo* to give a yellow oil (6.5 g, 89%) of $[C_3(NMe_2)_2(N(CH_2CH_2CH_3)H)]TFSA$. This was dried under vacuum overnight. $[C_3(NMe_2)_2(N(CH_2CH_2CH_3)H)]TFSA$ (6.5g, 14.06 mmol) was stirred with dry THF at -78 °C and n-BuLi (9.66 mL of 1.6 M, 15.5 mmol) was added drop wise in an inert atmosphere. Reaction mixture was stirred for 3 hours and then allowed to warm to room temperature. Me_2SO_4

(1.73 mL, 18.27 mmol) was then added and the solution was stirred for another 30 minutes. THF was then removed *in vacuo*. Mixture was dissolved in $CHCl_3$ (50 mL) and $LiMeSO_4$ was filtered off and then wash the $CHCl_3$ layer with water (3× 50 ML). The solvent was removed *in vacuo* to give a yellow oil (6 g, 90%). ^{1}H NMR ($CDCl_3$, 400 MHz): δ 3.27 (t, $^3J_{HH}$ = 7.4 Hz, 2H, NC*H*$_2$), 3.11 (s, 12H, NC*H*$_3$), 3.10 (s, 3H, NC*H*$_3$), 1.67 (m, 2H, NCH_2CH_2), 0.933 (t, $^3J_{HH}$ = 7.4 Hz, 3H, $NCH_2CH_2CH_3$). ^{13}C {^{1}H} NMR ($CDCl_3$, 100 MHz): δ 119.92 (q, $^1J_{CF}$ = 320 Hz, CF_3), 117.69 (equivalent ring C), 117.47 (unique ring C), 57.02 (NCH_2), 42.25 ($N(CH_3)_2$), 40.07 (NCH_3), 20.94 (NCH_2CH_2), 10.84 ($NCH_2CH_2CH_3$). EI MS: Found m/z 196.1813 (M^+); Calcd: 196.1808 (M^+). Anal. calcd for $C_{13}H_{22}N_4O_4S_2F_6$: C, 32.77; H, 4.65; N, 11.76. Found: C, 33.07; H, 4.64; N, 11.71. With water content of 543 ppm.

2.4.7 Bis(dimethylamino)propylmethylaminocyclopropenium dicyanamide, [C$_3$(NMe$_2$)$_2$(N(CH$_2$CH$_2$CH$_3$)Me)]DCA, [M$_5$Pr]DCA

$[C_3(NMe_2)_2(OMe)]MeSO_4$ (4.7 g, 18 mmol) was stirred with $H_2N(CH_2CH_2CH_3)$ (18 mL, 23 mmol) in dry dichloromethane (5 mL) for 2 h in an inert atmosphere. Dichloromethane was removed *in vacuo.* The mixture was in dissolved water and the product was extracted with chloroform:ethanol 2:1 (3×30 mL). The solvent was removed *in vacuo* to give $[C_3(NMe_2)_2(N(CH_2CH_2CH_3)H)]MeSO_4$ (3.51 g, 59%) as a light yellow oil, which was then stirred with NaDCA (2.79 g, 14 mmol) in H_2O (20 mL). The product was extracted with chloroform (3×30 mL). The solvent was removed *in vacuo* to give a yellow oil (3 g, 98%) of $[C_3(NMe_2)_2(N(CH_2CH_2CH_3)H)]DCA$. This was dried under vacuum overnight. $[C_3(NMe_2)_2(N(CH_2CH_2CH_3)H)]DCA$ (3 g, 10 mmol) was stirred with dry THF at −78 °C and n-BuLi (6.87 mL of 1.6 M, 11 mmol) was added drop wise in an inert atmosphere. Reaction mixture was stirred for 30 minutes and then allowed to warm to room temperature for another 30 minutes. Me_2SO_4 (1.66 mL, 13 mmol) was then added and the solution was stirred for another 30 minutes. $LiMeSO_4$ was removed by filteration. THF was then removed *in vacuo*. The mixture was dissolved in water (50 mL) with NaDCA (1 g, 11 mmol) and the product was extracted with $CHCl_3$ (3×50 mL). The solvent was removed *in vacuo* to give a yellow oil (3 g, 96%). ^{1}H NMR ($CDCl_3$, 400 MHz): δ 3.32 (t, $^3J_{HH}$ = 8 Hz, 2H, NC*H*$_2$), 3.17 (s, 12H, NC*H*$_3$), 3.15 (s, 3H, NC*H*$_3$), 1.69 (m, 2H, NCH_2CH_2), 0.94 (t, $^3J_{HH}$ = 8 Hz, 3H, $NCH_2CH_2CH_3$). ^{13}C {^{1}H} NMR ($CDCl_3$, 100 MHz): δ 118.88 (CN), 117.71 (equivalent ring C), 117.51 (unique ring C), 57.15 (NCH_2), 42.49 ($N(CH_3)_2$), 40.30 (NCH_3), 21.06 (NCH_2CH_2), 10.95 ($NCH_2CH_2CH_3$). EI MS: Found m/z

196.1808 (M^+); Calcd: 196.1808 (M^+). Anal. calcd for $C_{13}H_{22}N_6.0.75H_2O$: C, 56.60; H, 8.58; N, 30.46. Found: C, 56.96; H, 8.07; N, 30.33. With water content of 793 ppm.

2.4.8 Bis(dimethylamino)dipropylaminocyclopropenium bis(trifluoromethanesulfonyl)amide, $[C_3(NMe_2)_2(NPr_2)]TFSA$, $[M_4Pr_2]TFSA$

$[C_3(NMe_2)_2(OMe)]MeSO_4$ (5.43 g, 20 mmol) was stirred with Pr_2NH (3.6 mL, 26 mmol) in dichloromethane (5 mL) for 2 h in an inert atmosphere. Dichloromethane was removed *in vacuo.* The mixture was washed with dry diethyl ether several times to remove excess amine. The mixture was dissolved in ice cold water and the product was extracted with chloroform:ethanol (2:1) (3×30 mL). The solvent was removed *in vacuo* to give $[C_3(NMe_2)_2(NPr_2)]MeSO_4$ as a brown solid which was then stirred with LiTFSA (9.0 g, 32 mmol) in H_2O (20 mL). The product was extracted with chloroform (3×50 mL) and the solvent was then removed *in vacuo* to give a brown solid (5.0 g, 94%). ^1H NMR ($CDCl_3$, 400 MHz): δ 3.26 (t, 3JHH = 7.6 Hz, 4H, NC*H*$_2$CH$_2$), 3.12 (s, 12H, NC*H*$_3$), 1.66 (m, 4H, NCH2C*H*$_2$), 0.93 (t, $^3J_{HH}$ = 7 Hz, 6H, NCH$_2$CH$_2$C*H*$_3$). $^{13}C\{^1H\}$ NMR ($CDCl_3$, 100 MHz): δ 120.10 (q, $^1J_{CF}$ = 322 Hz, CF_3), 117.65 (equivalent ring C), 116.76 (unique ring C), 55.05 (N*C*H$_2$), 42.22 (N*C*H$_3$), 21.86 (NCH$_2$*C*H$_2$), 10.81 (NCH$_2$CH$_2$*C*H$_3$). EI MS: Found m/z 224.2125 (M^+); Calcd: 2242121 (M^+). Anal. calcd for $C_{15}H_{26}N_4O_4S_2F_6$: C, 35.71; H, 5.19; N, 11.10. Found: C, 35.92; H, 5.2; N, 11.22. With water content of 757 ppm.

2.4.9 Bis(dimethylamino)-N-(methoxyethyl)methylaminocyclopropenium bis(trifluoromethanesulfonyl)amide, $[C_3(NMe_2)_2(N(CH_2CH_2OCH_3)Me)]TFSA$, $[M_5Er]TFSA$

$[C_3(NMe_2)_2(OMe)]MeSO_4$ (5.4 g, 20 mmol) was stirred with $H_2NCH_2CH_2OCH_3$ (2.3 mL, 26 mmol) in dry dichloromethane (5 mL) for 2 h in an inert atmosphere. Dichloromethane was removed *in vacuo.* The mixture was washed with dry diethyl ether several times to remove excess amine. The mixture was dissolved in water and the pH was lowered to 1 with HClaq (37%). The product was then extracted with chloroform:ethanol 2:1 (3×30 mL). The solvent was removed *in vacuo* to give $[C_3(NMe_2)_2(N(CH_2CH_2OCH_3)H)]MeSO_4$ as a light yellow oil, which was then stirred with LiTFSA (15 g, 54 mmol) in H_2O (20 mL). The product was extracted with chloroform (3×30 mL). The solvent was removed *in vacuo* to give a yellow oil (7.68 g, 92%) of $[C_3(NMe_2)_2(N(CH_2CH_2OCH_3)H)]TFSA$ which was dried under vacuum overnight.

$[C_3(NMe_2)_2(N(CH_2CH_2OCH_3)H)]$TFSA (6.78 g, 14.2 mmol) was stirred with dry THF at -78 °C and n-BuLi (9.74 mL of 1.6 M, 15.6 mmol) was added drop wise. The reaction mixture was stirred for 3 hours and then allowed to warm to room temperature. Then Me_2SO_4 (1.74 mL, 18.46 mmol) was added and the solution was stirred for another 30 minutes. The solvent was removed *in vacuo*. The mixture was dissolved in $CHCl_3$ (50 mL) and $LiMeSO_4$ was filtered off and then washed with water (3×50 mL). The solvent was removed *in vacuo* to give a yellow oil (6.32 g, 91%). ^{1}H NMR ($CDCl_3$, 400 MHz): δ 3.56 (t, $^3J_{HH}$ = 4.8 Hz, 2H, NCH_2CH_2), 3.49 (t, $^3J_{HH}$ = 4.4 Hz, 2H, NCH_2CH_2), 3.35 (s, 3H, $NCH_2CH_2OCH_3$), 3.14 (s, 3H, NCH_3), 3.12 (s, 12H, NCH_3). EI MS: Found m/z 212.1759 (M^+); Calcd: 212.1757 (M^+). ^{13}C {^{1}H} NMR ($CDCl_3$, 100 MHz): δ 119.93 (q, $^1J_{CF}$ = 320 Hz, CF_3), 117.92 (unique ring C), 117.58 (equivalent ring C), 69.42 (NCH_2CH_2), 59.09 (NCH_2CH_2), 55.14 (OCH_3), 42.28 ($N(CH_3)_2$), 40.31 (NCH_3). Anal. calcd for $C_{13}H_{22}N_4O_4S_2F_6$: C, 31.71; H, 4.5; N, 11.37. Found: C, 32.24; H, 4.5; N, 11.40. With water content of 681 ppm.

2.4.10 Bis(dimethylamino)-N-(methoxyethyl)methylaminocyclopropenium dicyanamide, $[C_3(NMe_2)_2(N(CH_2CH_2OCH_3)Me)]$DCA, $[M_5E_r]$DCA

$[C_3(NMe_2)_2(OMe)]MeSO_4$ (5.14 g, 19 mmol) was stirred with $HNMe(CH_2CH_2OCH_3)$ (3.11 mL, 29 mmol) in dry dichloromethane (5 mL) for 1 h in an inert atmosphere. Dichloromethane was removed *in vacuo.* The mixture was washed with benzene several times to remove excess amine. The mixture was dissolved in water and the product was extracted with chloroform:ethanol 2:1 (3×30 mL). The solvent was removed *in vacuo* to give $[C_3(NMe_2)_2(N(CH_2CH_2OCH_3)Me)]MeSO_4$ (24.21g, 67%) as a light yellow oil, which was then stirred with NaDCA (3.48 g,39 mmol) in H_2O (20 mL). The product was extracted with chloroform (3×30 mL). The solvent was removed *in vacuo* to give a yellow oil (3.3 g, 91%). ^{1}H NMR ($CDCl_3$, 400 MHz): δ 3.58 (t, $^3J_{HH}$ = 6 Hz, 2H, NCH_2CH_2), 3.54 (t, $^3J_{HH}$ = 6 Hz, 2H, NCH_2CH_2), 3.36 (s, 3H, $NCH_2CH_2OCH_3$), 3.19 (s, 3H, NCH_3), 3.17 (s, 12H, $N(CH_3)_2$). ^{13}C {^{1}H} NMR ($CDCl_3$, 100 MHz): δ 119.87 (CN), 117.94 (unique ring C), 117.58 (equivalent ring C), 69.38 (NCH_2CH_2), 59.19 (NCH_2CH_2), 55.28 (OCH_3), 42.50 ($N(CH_3)_2$), 40.47 (NCH_3). EI MS: Found m/z 212.1757 (M^+); Calcd: 212.1757 (M^+). Anal. calcd for $C_{13}H_{22}N_6.1.8H_2O$: C, 53.33; H, 8.12; N, 28.70. Found: C, 53.15; H, 7.73; N, 29.57. With water content of 1301 ppm.

2.4.11 Bis(dimethylamino)-N-(dimethoxyethyl)aminocyclopropenium bis(trifluoromethanesulfonyl)amide, $[C_3(NMe_2)_2(N(CH_2CH_2OCH_3)_2)]TFSA$, $[M_4Er_2]TFSA$

$[C_3(NMe_2)_2(OMe)]MeSO_4$ (5.09 g, 19 mmol) was stirred with $HN(CH_2CH_2OCH_3)_2$ (3.67 mL, 25 mmol) in dry dichloromethane (5 mL) for 2 h in an inert atmosphere. Dichloromethane was removed *in vacuo.* The mixture was washed with dry diethyl ether several times to remove excess amine. The mixture was dissolved in water and the product was extracted with chloroform:ethanol 2:1 (3×30 mL). The solvent was removed *in vacuo* to give $[C_3(NMe_2)_2(N(CH_2CH_2OCH_3)H)]MeSO_4$ as a light yellow oil, which was then stirred with LiTFSA (12 g, 42 mmol) in H_2O (20 mL). The product was extracted with chloroform (3×30 mL). The solvent was removed *in vacuo* to give a yellow oil (7.32 g, 94%). ^{1}H NMR ($CDCl_3$, 400 MHz): δ 3.56 (t, $^3J_{HH}$ = 4.8 Hz, 2H, NCH_2CH_2), 3.49 (t, $^3J_{HH}$ = 4.4 Hz, 2H, NCH_2CH_2), 3.35 (s, 3H, $NCH_2CH_2OCH_3$), 3.14 (s, 3H, NCH_3), 3.12 (s, 12H, NCH_3). ^{13}C {^{1}H} NMR ($CDCl_3$, 100 MHz): δ 119.94 (q, $^1J_{CF}$ = 320 Hz, CF_3), 117.86 (unique ring C), 117.38 (equivalent ring C), 70.19 (NCH_2CH_2), 59.04 (NCH_2CH_2), 53.32 (OCH_3), 42.33 ($N(CH_3)_2$). EI MS: Found m/z 256.2023 (M^+); Calcd: 256.2020 (M^+). Anal. calcd for $C_{13}H_{22}N_4O_4S_2F_6$: C, 33.58; H, 4.88; N, 10.44. Found: C, 33.82; H, 4.87; N, 10.54. With water content of 1092 ppm.

2.4.12 Bis(dimethylamino)butylmethylaminocyclopropenium bis(trifluoromethanesulfonyl)amide, $[C_3(NMe_2)_2(NBuMe)]TFSA$, $[M_5B]TFSA$

$[C_3(NMe_2)_2(OMe)]MeSO_4$ (4.5 g, 17 mmol) was stirred with BuMeNH (2.6 mL, 22 mmol) in dry dichloromethane (5 mL) for 2 h in an inert atmosphere. Dichloromethane was removed *in vacuo.* The mixture was washed with dry diethyl ether several times to remove excess amine. The mixture was dissolved in water and the pH lowered to 1 with HCl(aq) (37%) and the product was extracted with dichloromethane (3 ×30 mL). The solvent was removed *in vacuo* to give $[C_3(NMe_2)_2(NBuH)]MeSO_4$ as a brown oil which was then stirred with LiTFSA (5 g, 18 mmol) in H_2O (20 mL). The product was extracted with dichloromethane (3×30 mL) and the solvent was the removed *in vacuo* to give a brown oil (2.8 g, 98%). ^{1}H NMR (400 MHz, $CDCl_3$): δ 3.33 (t, 2H, $^3J_{HH}$ = 7.4 Hz, NCH_2), 3.12 (s, 12H, NCH_3), 3.1 s, 3H, NCH_3), 1.62 (m, 2H, NCH_2CH_2), 1.33 (m, 2H, $NCH_2CH_2CH_2$), 0.93 (t, $^3J_{HH}$ = 7.4 Hz, 3H, $CH_2CH_2CH_3$). ^{13}C {^{1}H} NMR (100 MHz, CDCl3): δ 119.92 (q, $^1J_{CF}$ = 322 Hz, CF_3), 117.73 (equivalent ring C), 117.47 (unique ring C), 55.29 (NCH_2), 42.27 ($N(CH_3)_2$), 40.07 (NCH_3), 29.78 (NCH_2CH_2), 19.78 ($NCH_2CH_2CH_2$),

13.63 ($NCH_2CH_2CH_2\mathit{C}H_3$). EI MS: Found m/z 210.1968 (M^+); Calcd: 210.1965 (M^+). Anal. calcd for $C_{14}H_{24}N_4O_4S_2F_6$: C, 34.28; H, 4.93; N, 11.42. Found: C, 35.22; H, 5.11; N, 11.23. With water content of 490 ppm.

2.4.13 Bis(dimethylamino)butylmethylaminocyclopropenium dicyanamide, [$C_3(NMe_2)_2(NBuMe)$]DCA, [M_5B]DCA

[$C_3(NMe_2)_2(OMe)$]$MeSO_4$ (3.3 g, 13 mmol) was stirred with BuMeNH (1.9 mL, 17 mmol) in dry dichloromethane (5 mL) for 30 minutes in an inert atmosphere. Dichloromethane was removed *in vacuo.* The mixture was washed with dry diethyl ether several times to remove excess amine. The mixture was dissolved in water and the product was extracted with dichloromethane (3 ×30 mL). The solvent was removed *in vacuo* to give [$C_3(NMe_2)_2(NBuMe)$]$MeSO_4$ (3.27 g, 80%) as a brown oil which was then stirred with NaDCA (2.7 g, 123 mmol) in H_2O (20 mL). The product was extracted with chloroform (3×30 mL) and the solvent was then removed *in vacuo* to give a brown oil (2.66 g, 95%). ^{1}H NMR (400 MHz, $CDCl_3$): δ 3.33 (t, 2H, $^3J_{HH}$ = 8 Hz, $NC\mathit{H}_2$), 3.16 (s, 12H, $NC\mathit{H}_3$), 3.14 s, 3H, $NC\mathit{H}_3$), 1.63 (m, 2H, $NCH_2C\mathit{H}_2$), 1.33 (m, 2H, $NCH_2CH_2C\mathit{H}_2$), 0.93 (t, $^3J_{HH}$ = 8 Hz, 3H, $CH_2CH_2C\mathit{H}_3$). ^{13}C {^{1}H} NMR (100 MHz, CDCl3): δ 119.88 (CN), 117.79 (equivalent ring C), 117.52 (unique ring C), 55.44 ($NC\mathit{H}_2$), 42.51 ($N(\mathit{C}H_3)_2$), 40.31 ($NC\mathit{H}_3$), 29.80 ($NCH_2\mathit{C}H_2$), 19.83 ($NCH_2CH_2\mathit{C}H_2$), 13.72 ($NCH_2CH_2CH_2\mathit{C}H_3$). EI MS: Found m/z 210.1964 (M^+); Calcd: 210.1965 (M^+). Anal. calcd for $C_{14}H_{24}N_6.0.4H_2O$: C, 59.29; H, 8.81; N, 29.64. Found: C, 58.94; H, 8.99; N, 29.13. With water content of 1482 ppm.

2.4.14 Bis(dimethylamino)dibutylaminocyclopropenium bis(trifluoromethanesulfonyl)amide, [$C_3(NMe_2)_2(NBu_2)$]TFSA, [M_4B_2]TFSA

[$C_3(NMe_2)_2(OMe)$]$MeSO_4$ (2.4 g, 9 mmol) was stirred with Bu_2NH (1.97 mL, 12 mmol) in dry dichloromethane (5 mL) for 2 h in an inert atmosphere. Dichloromethane was removed *in vacuo* and excess amine was removed by washing several times with dry diethylether to give [$C_3(NMe_2)_2(NBu_2)$]$MeSO_4$ as a light yellow oil, which was then stirred with LiTFSA (6.92 g, 24 mmol) in H_2O (10 mL). The solvent was removed *in vacuo*, the mixture was dissolved in chloroform:ethanol (2:1) (30 mL), and the product was washed with ice cold water (3 ×30 mL) to remove ammonium salts. The solvent was then removed *in vacuo* to give a light yellow oil (3.4 g, 80%). ^{1}H NMR (400 MHz, $CDCl_3$): δ 3.28 (t, $^3J_{HH}$ = 7.6Hz, 4H, NCH_2), 3.11 (s, 12H, NCH_3), 1.60 (m, 4H, NCH_2CH_2), 1.32 (m, 4H, $NCH_2CH_2CH_2$), 0.94 (t, $^3J_{HH}$ = 7.6Hz, 6H, NCH_2

$CH_2CH_2CH_3$). ^{13}C {^1H} NMR (100 MHz, $CDCl_3$): δ 119.89 (q, $^1J_{CF}$ = 322 Hz, CF3), 117.59 (equivalent ring C), 116.66 (unique ring C), 53.22 (NCH_2), 42.17 (NCH_3), 30.56 (NCH_2CH_2), 19.79 (NCH_2 CH_2CH_2), 13.65 ($NCH_2CH_2CH_2CH_3$). EI MS: Found m/z 252.2435 (M^+); Calcd: 252.4255 (M^+). Anal. calcd for $C_{17}H_{30}N_4O_4S_2F_6$: C, 38.35; H, 5.68; N, 10.52. Found: C, 39.3; H, 5.87; N, 10.71. With water content of 758 ppm.

2.4.15 Bis(dimethylamino)pentylmethylaminocyclopropenium bis(trifluoromethanesulfonyl)amide, [$C_3(NMe_2)_2$(NPeMe)]TFSA, [M_5Pe]TFSA

[$C_3(NMe_2)_2$(NPeH)]TFSA was dried under vacuum overnight. [$C_3(NMe_2)_2$(NPeH)]TFSA (2.58 g, 5 mmol) was stirred with dry THF at -78 °C and n-BuLi (3.62 mL of 1.6 M, 6 mmol) was added drop wise in an inert atmosphere. The reaction mixture was stirred for 3 hours and then allowed to warm to room temperature. Then Me_2SO_4 (0.65 mL, 7 mmol) was added and the solution was stirred for another 30 minutes. The solvent was removed *in vacuo*. The mixture was dissolved in $CHCl_3$ (50 mL) and $LiMeSO_4$ was filtered off. Then the $CHCl_3$ layer was washed with water (3×50 mL) and the solvent was removed *in vacuo* to give a yellow oil (2.42 g, 91%). ^1H NMR (400 MHz, $CDCl_3$): δ 3.31 (t, $^3J_{HH}$ = 8 Hz, 2H, NC*H*$_2$), 3.13 (s, 12H, NC*H*$_3$), 3.11 (s, 3H, NC*H*$_3$), 1.64 (m, 2H, NCH_2CH_2), 1.35 (m, 2H, $NCH_2CH_2CH_2$), 1.29 (m, 2H, $NCH_2CH_2CH_2CH_2$), 0.88 (t, $^3J_{HH}$ = 6.8 Hz, 3H, $NCH_2CH_2CH_2CH_2CH_3$). $^{13}C\{^1H\}$ NMR (100 MHz, $CDCl_3$): δ 119.90 (q, $^1J_{CF}$ = 320 Hz, CF_3), 117.82 (equivalent ring C), 117.57 (unique ring C), 55.55 (NCH_2), 42.29 (NCH_3), 40.06 (NCH_3), 28.68 (NCH_2CH_2), 27.39 ($NCH_2CH_2CH_2$), 22.29 ($NCH_2CH_2CH_2CH_2$), 13.85 ($NCH_2CH_2CH_2CH_2CH_2CH_3$). EI MS: Found m/z 224.2122 (M^+); Calcd: 224.2121 (M^+). Anal. calcd for 0.89($C_{15}H_{26}N_4O_4S_2F_6$):0.11($C_{13}H_{25}N_5O_4S_2F_6$): C, 35.71; H, 5.19; N, 11.10. Found: C, 36.11; H, 5.35; N, 11.91. Micoanalysis suggested presence of 11% of open ring (**2.1**). With water content of 499 ppm.

2.4.16 Bis(dimethylamino)hexylmethylaminocyclopropenium bis(trifluoromethanesulfonyl)amide, [$C_3(NMe_2)_2$(NHexMe)]TFSA, [M_5Hex]TFSA

[$C_3(NMe_2)_2$(OMe)]$MeSO_4$ (4.11 g, 15 mmol) was stirred with HexMeNH (2.88 mL, 19 mmol) in dry dichloromethane (10 mL) for 2 h in an inert atmosphere. Dichloromethane was removed *in vacuo*. The mixture was dissolved in ice cold water and the product was extracted with chloroform:ethanol (2:1) (3 ×30 mL). The solvent was removed *in vacuo* to give [$C_3(NMe_2)_2$(NHexMe)]$MeSO_4$ as a light yellow oil, which was stirred with LiTFSA (9.85g, 34

mmol) in H_2O (50 mL) for 30 mins. The solvent was then removed *in vacuo*. The mixture was dissolved in chloroform:ethanol (2:1) (30 mL) and the product was washed with ice cold water (3×30 mL) to remove ammonium salts. Solvent was removed *in vacuo* and the product was dissolved in $CHCl_3$ (50 mL) and washed with water (3×50 mL). The solvent was removed *in vacuo* to give a light yellow oil (5.62 g, 95%). ^{1}H NMR (400 MHz, $CDCl_3$): δ 3.29 (t, $^3J_{HH}$ = 7.6 Hz, 2H, NCH_2), 3.12 (s, 12H, NCH_3), 3.10 (s, 3H, NCH_3), 1.63 (m, 2H, NCH_2CH_2), 1.29 (m, 6H, $NCH_2CH_2CH_2CH_2CH_2CH_2$), 0.88 (t, $^3J_{HH}$ = 6.8Hz, 6H, $NCH_2CH_2CH_2CH_2CH_2CH_3$). ^{13}C {^{1}H} NMR (100 MHz, $CDCl_3$): δ 119.91 (q, $^1J_{CF}$ = 347 Hz, CF_3), 117.73 (equivalent ring C), 117.45 (unique ring C), 55.55 (NCH_2), 42.25 (NCH_3), 40.07 (NCH_3), 31.33 (NCH_2CH_2), 27.64 ($NCH_2CH_2CH_2$), 26.21 ($NCH_2CH_2CH_2CH_2$), 22.42($NCH_2CH_2CH_2CH_2CH_2$), 13.88 ($NCH_2CH_2CH_2CH_2CH_2CH_3$). EI MS: Found m/z 238.2279 (M^+); Calcd: 238.2278 (M^+). Anal. calcd for $C_{16}H_{28}N_4O_4S_2F_6$: C, 37.06; H, 5.44; N, 10.80. Found: C, 37.28; H, 5.57; N, 10.94. With water content of 460 ppm.

2.4.17 Bis(dimethylamino)dihexylaminocyclopropenium bis(trifluoromethanesulfonyl)amide, $[C_3(NMe_2)_2(NHex_2)]TFSA$, $[M_4Hex_2]TFSA$

$[C_3(NMe_2)_2(OMe)]MeSO_4$ (2 g, 8 mmol) was stirred with Hex_2NH (2.3 mL, 10 mmol) in dry dichloromethane (5 mL) for 2 h in an inert atmosphere. Dichloromethane was removed *in vacuo*, the mixture was dissolved in ice cold water, and the product was extracted with chloroform:ethanol (2:1) (3×30 mL). The solvent was removed *in vacuo* to give $[C_3(NMe_2)_2(NHex_2)]MeSO_4$ as a light yellow oil, which was then stirred with LiTFSA (5.22g, 18 mmol) in H_2O (10 mL). The solvent was removed *in vacuo*, the mixture was dissolved in chloroform:ethanol (2:1) (30 mL), and the product was washed with ice cold water (3×30 mL) to remove ammonium salts. The solvent was removed *in vacuo* to give a light yellow oil (3 g, 80%). ^{1}H NMR (400 MHz, $CDCl_3$): δ 3.28 (t, $^3J_{HH}$ = 8Hz, 4H, NCH_2), 3.11 (s, 12H, NCH_3), 1.61 (m, 4H, NCH_2CH_2), 1.29 (m, 12H, $NCH_2CH_2CH_2CH_2CH_2CH_2$), 0.88 (t, $^3J_{HH}$ = 6.8Hz, 6H, $NCH_2CH_2CH_2CH_2CH_2CH_3$). ^{13}C NMR (100 MHz, $CDCl_3$): δ 120.06 (q, $^1J_{CF}$ = 347 Hz, CF_3), 117.69 (equivalent ring C), 116.73 (unique ring C), 53.52 (NCH_2), 42.18 (NCH_3), 31.32 (NCH_2CH_2), 28.55 ($NCH_2CH_2CH_2$), 26.23 ($NCH_2CH_2CH_2CH_2$), 26.23 ($NCH_2CH_2CH_2CH_2CH_2$), 26.23 ($NCH_2CH_2CH_2CH_2CH_2CH_3$). EI MS: Found m/z 308.3064 (M^+); Calcd: 308.3060 (M^+). Anal. calcd for $C_{21}H_{38}N_4O_4S_2F_6$: C, 42.85; H, 6.50; N, 9.51. Found: C, 43.3; H, 6.69; N, 9.35. With water content of 520 ppm.

2.5 Synthesis of tris(alkylmethylamino)cyclopropenium salts

2.5.1 Tris(ethylmethylamino)cyclopropenium bis(trifluoromethanesulfonyl)amide, $[C_3(NEtMe_2)_3]TFSA$, $[(ME)_3]TFSA$

Pentachlorocyclopropane (4.27 mL, 33 mmol) was added dropwise to a stirred solution of MeEtNH (10 mL, 116 mmol) and Et_3N (18.55 mL, 132 mmol) in dichloromethane (20 mL) at 0 °C for an hour. The solution was left on stirring overnight at ambient temperature. The product was a mixture of the open ring product (**2**) with $[C_3(NMeEt)_3]Cl$ and $[MeEtNH_2]Cl$. The peak ratio of $[C_3(NMeEt)_3]Cl$:$[HC_3(NMeEt)_4]^+$ in the mass spectrometer was 23:1 respectively. The mixture was dissolved in water (50 mL) and acidified with conc. HCl to pH = 1-2. $[C_3(NMeEt)_3]Cl$ was then extracted with $CHCl_3$ (3×50 mL) while leaving behind the dication of the open ring product, $[H_2C_3(NMeEt)_4]^{2+}$ in the water layer. $[C_3(NMeEt)_3]Cl$ was then stirred with LiTFSA (8.09 g, 27 mmol) in H_2O (10 mL). The solvent was removed *in vacuo*, the mixture was dissolved in chloroform (30 mL), and the product was washed with conc. HCl (3×30 mL) to remove the open ring product, followed by washing the organic layer with water (3×30 mL). The solvent was removed *in vacuo* to give a light brown oil (3.70 g, 80%). ^1H NMR (400 MHz, $CDCl_3$): δ 3.38 (q, $^3J_{HH}$ = 6.8Hz, 6H, NC*H*$_2$), 3.09 (s, 9H, NC*H*$_3$), 1.27 (t, $^3J_{HH}$ = 6.8Hz, 6H, NCH$_2$C*H*$_3$). ^{13}C {^1H} NMR (100 MHz, $CDCl_3$): δ 119.92 (q, $^1J_{CF}$ = 324 Hz, CF_3), 118.96 (ring C), 50.05 (N*C*H$_2$), 39.00 (N*C*H$_3$), 12.81 (NCH$_2$*C*H$_3$). EI MS: Found m/z 210.1967 (M^+); Calcd: 210.1965 (M^+). Anal. calcd for $C_{14}H_{24}N_4O_4S_2F_6$: C, 34.28; H, 4.93; N, 11.42. Found: C, 34.84; H, 5.18; N, 11.58. With water content of 993 ppm.

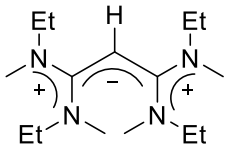

2.2

2.5.2 Tris(allylmethylamino)cyclopropenium dicyanamide, $[C_3(NAllylMe)_3]DCA$, $[(MA)_3]DCA$

Pentachlorocyclopropane (9.1 mL, 71 mmol) was added dropwise to a stirred solution of MeAllylNH (24 mL, 249 mmol) and Et_3N (39 mL, 284 mmol) in dichloromethane (100 mL) at 0 °C for an hour. The solution was left stirring overnight at ambient temperature. The product was

a mixture of the open ring product (**2.3**) with $[C_3(NMeAllyl)_3]Cl$ and $[Et_3NH]Cl$. The peak ratio of $[C_3(NMeAllyl)_3]Cl$:$[HC_3(NMeAllyl)_4]^+$ in the mass spectrometer was 3:2 respectively. The mixture was dissolved in water (50 mL) and acidified with conc. HCl to pH = 1-2. $[C_3(NMeEt)_3]Cl$ was then extracted with CH_2Cl_2 (3×50 mL) while leaving behind the dication of the open ring $[H_2C_3(NMeAllyl)_4]^{2+}$ in the water layer. Dichloromethane was removed *in vacuo* to give a light yellow oil (2.93g, 15%). $[C_3(NMeEt)_3)]Cl$ was then stirred with NaDCA (2.78g, 30 mmol) in H_2O (50 mL). The product was extracted with chloroform (3×50 mL). The solvent was removed *in vacuo* to give a light brown oil (2.5 g, 75%). ^1H NMR ($CDCl_3$, 400 MHz): δ 5.84 (ddt, $^3J_{HH}$ = 5.09 Hz, $^3J_{HH}$ = 10.56 Hz, $^3J_{HH}$ = 22.3 Hz 1H, $NCH_2C\mathit{H}{=}CH_2$), 5.33 (d, $^3J_{HH(cis)}$ = 10.4 Hz, 2H, $NCH_2CH{=}C\mathit{H}_2$), 5.27 (d, $^3J_{HH(trans)}$ = 17.2 Hz, 2H, $NCH_2CH{=}C\mathit{H}_2$), 3.99 (d, 2H, $^3J_{HH}$ = 4 Hz $NC\mathit{H}_2CH{=}CH_2$), 3.14 (s, 12H, $NC\mathit{H}_3$). ^{13}C {^1H} NMR (100 MHz, $CDCl_3$) δ 130.91 ($NCH_2\mathit{C}H$), 119.91 (CN), 118.87 ($NCH_2CH\mathit{C}H_2$), 117.44 (ring C), 57.31 ($N\mathit{C}H_2$), 39.95 (NCH_3). EI MS: Found m/z 246.1966 (M^+); Calcd: 246.1965 (M^+). Anal. calcd for $C_{17}H_{24}N_6.0.6H_20$; C, 63.17; H, 7.85; N, 26.00. Found: C, 63.11; H, 7.84; N, 25.42. With water content of 1531 ppm.

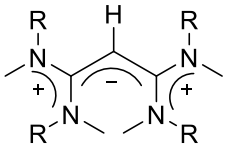

R = allyl-

2.3

2.5.3 Tris(allylmethylamino)cyclopropenium bis(trifluoromethanesulfonyl)amide, $[C_3(NAllylMe_2)_3]TFSA$, $[(MA)_3]TFSA$

The mixture containing $[H_2C_3(NMeAllyl)_4]^+$ and $[C_3(NMeAllyl)_3)]Cl$ was stirred with LiTFSA (14.29g, 50 mmol) in H_2O (50 mL) for 30 minutes. The solvent was removed *in vacuo*, the mixture was dissolved in chloroform (30 mL), and the product was washed with conc. HCl (3×30 mL) to remove open ring products, followed by washing of the organic layer with water (3×30 mL). The solvent was removed *in* vacuo to give a colourless oil (3.76 g, 43%). ^1H NMR ($CDCl_3$, 400 MHz): δ 5.80 (ddt, $^3J_{HH}$ = 5.09 Hz, $^3J_{HH}$ = 5.09 Hz, $^3J_{HH}$ = 10.56 Hz, 1H, $NCH_2C\mathit{H}{=}CH_2$), 5.32 (d, $^3J_{HH(cis)}$ = 10 Hz, 2H, $NCH_2CH{=}C\mathit{H}_2$), 5.26 (d, $^3J_{HH(trans)}$ = 17.2 Hz, 2H, $NCH_2CH{=}C\mathit{H}_2$), 3.93 (d, 2H, $^3J_{HH}$ = 3.2 Hz $NC\mathit{H}_2CH{=}CH_2$), 3.1 (s, 12H, $NC\mathit{H}_3$). ^{13}C {^1H} NMR (100 MHz, $CDCl_3$): δ 130.94 ($NCH_2\mathit{C}H$), 119.93 (q, $^1J_{CF}$ = 320 Hz, CF_3), 118.76 ($NCH_2CH\mathit{C}H_2$), 117.38

(ring C), 57.20 (N*C*H_2), 39.68 (NCH_3). EI MS: Found m/z 246.1967 (M^+); Calcd: 246.1965 (M^+). Anal. calcd for $C_{17}H_{24}N_4O_4S_2F_6$: C, 38.78; H, 4.59; N, 10.64. Found: C, 39.22; H, 4.58; N, 10.57. With water content of 272 ppm.

2.5.4 Tris-(*N*-(methoxyethyl)methyl)cyclopropenium bis(trifluoromethanesulfonyl)amide, $[C_3(NMeCH_2CH_2OCH_3)_3]$TFSA, $[(MEr)_3]$TFSA

Pentachlorocyclopropane (7.65 mL, 60 mmol) was added dropwise to a stirred solution of $Me(CH_3OCH_2CH_2)NH$ (32 mL, 300 mmol) and Et_3N (33 mL, 240 mmol) in dichloromethane (100 mL) at 0 °C for an hour. The solution was left on stirring overnight at ambient temperature. The reaction mixture was then heated to reflux for 5 hours. The product mixture contained open ring product (**2.4**) with $[C_3(NMe(CH_2CH_2OCH_3)_3)]Cl$ and $[Et_3NH]Cl$. The peak ratio of $[C_3(NMe\ CH_2CH_2OCH_3)_3]Cl$:$[HC_3(NMe\ CH_2CH_2OCH_3)_4]^+$ in the mass spectrometer was 16:1 respectively The mixture was kept in a freezer for an hour and ammonium salts were filtered off. The mixture having open ring product (**2.4**) with $[C_3(NMeEt)_3)]Cl$ was then stirred with LiTFSA (12.81 g, 45 mmol) in H_2O (50 mL). The solvent was removed *in vacuo*, the mixture was dissolved in chloroform (30 mL), and the product was washed with conc. HCl (3×30 mL) to remove the open ring product, followed by washing of the organic layer with water (3×30 mL). The solvent was removed *in vacuo* to give a light yellow oil (5.8 g, 67%). ^{1}H NMR ($CDCl_3$, 400 MHz): δ 3.56 (t, $^3J_{HH}$ = 4.3 Hz, 2H, NCH_2C*H*$_2$), 3.52 (t, $^3J_{HH}$ = 4.3 Hz, 2H, NC*H*$_2$CH$_2$), 3.35 (s, 3H, NCH$_2$CH$_2$OC*H*$_3$), 3.15 (s, 3H, NC*H*$_3$), 3.12 (s, 12H, NC*H*$_3$). ^{13}C {^{1}H} NMR ($CDCl_3$, 100 MHz): δ 119.93 (q, $^1J_{CF}$ = 320 Hz, CF_3), 117.33 (ring C), 69.48 (NCH$_2$*C*H$_2$), 59.08 (N*C*H$_2$CH$_2$), 54.99 (O*C*H$_3$), 40.29 (N*C*H$_3$). EI MS: Found m/z 300.2284 (M^+); Calcd: 300.2282 (M^+). Anal. calcd for $C_{17}H_{30}N_4O_7S_2F_6$: C, 35.17; H, 5.21; N, 9.65. Found: C, 35.45; H, 5.27; N, 9.7. With water content of 61 ppm.

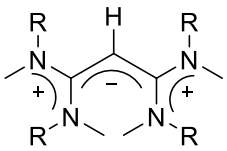

R = $CH_3CH_2OCH_2$-

2.4

2.5.5 Trisanilinocyclopropenium bis(trifluoromethanesulfonyl)amide, $[C_3(NPhH)_3]TFSA$

$[C_3(NPhH)_3]Cl$ was prepared by a reported[37] method. $[C_3(NPhH)_3]Cl$ (2.0 g, 6 mmol) was stirred with LiTFSA (4.95 g, 18 mmol) in water (10 mL) for 1 h. The product was extracted with dichloromethane (3 ×10 mL) and solvent is removed *in vacuo* to give yellow crystals (3 g, 88%). ^1H NMR (500 MHz, $CDCN_3$): δ 8.8 (br, 1H, NH), 7.52 (dt, $^3J_{HH}$ = 8 Hz, 2H, Ph), 7.32 (t, $^3J_{HH}$ = 8 Hz, 1H, Ph), 7.28 (dd, $^3J_{HH}$ = 8 Hz, 2H, Ph). $^{13}C\{^1H\}$ NMR (126 MHz, CD_3CN): δ 138.44 (*ipso*-Ph), 130.32 (*m*-Ph), 125.30 (*p*-Ph), 118.45 (*o*-Ph), 113.05 (C_3). EI MS: Found m/z 312.1499 (M^+); Calcd: 312.1495 (M^+). Anal. calcd for $C_{23}H_{18}N_4O_4F_6S_2$: C, 46.66; H, 3.21; N, 9.35. Found: C, 46.62; H, 3.06; N, 9.45.

2.6 Synthesis of bis(diethylamino)aminocyclopropenium salt

2.6.1 1,2-Bis(diethylamino)-3-aminocyclopropenium methylsulphate, $[(Et_2N)_2C_3(NH_2)]MeSO_4$, $[E_4H_2]MeSO_4$

Through rapidly stirred $[C_3(NEt_2)_2(OMe)]MeSO_4$ (3 g, 9 mmol) was passed NH_3(g) (excess) for 2 hours in an inert atmosphere. Excess NH_3 was removed *in vacuo* to give an orange viscous oil of $[(Et_2N)_2C_3(NH_2)]MeSO_4$ (2.86 g, 100%). ^1H NMR (500 MHz, D_2O): δ 3.60 (s, 3H, $MeSO_4$), 3.24 (q, $^3J_{HH}$ = 7.3 Hz, 8H, $NC\mathit{H}_2CH_3$), 1.08 (t, $^3J_{HH}$ = 7.3 Hz, 12H, $NCH_2C\mathit{H}_3$). ^{13}C $\{^1H\}$NMR (126 MHz, D_2O) δ 116.57 (equivalent ring C), 113.97 (unique ring C), 55.55 ($MeSO_4$), 46.42 (NCH_2CH_3), 13.80 (NCH_2CH_3). EI MS: Found m/z 1196.1811 (M^+); Calcd: 196.1808 (M^+). Anal. calcd for $C_{12}H_{25}N_3O_4S$: C, 43.10; H, 8.43; N, 12.56. Found: C, 42.78; H, 8.29; N, 12.84. With water content of $[E_4H_2]MeSO_4.1.5H_2O$.

2.7 Syntheses of Bis(diethylamino)alkylaminocyclopropenium

2.7.1 Bis(diethylamino)butylaminocyclopropenium methylsulfate, $[C_3(NEt_2)_2(NHBu)]MeSO_4$, $[E_4BH]MeSO_4$

H_2N^nBu (5.9 mL, 60 mmol) was added to a stirred solution of $[C_3(NEt_2)_2OMe]MeSO_4$ (14.78 g, 60 mmol) at room temperature in an inert atmosphere for 2 hours. The product was washed several times with diethyl ether to remove unreacted amine. The mixture was dissolved in water and the product was extracted with $CHCl_3$ (3×30 mL). The solvent was removed *in vacuo* to give an orange liquid (10.46 g, 71%). ^1H NMR (500 MHz, $CDCl_3$): δ 8.14 (br, 1H, NH), 3.67 (s, 3H, CH_3SO_4), 3.35 (q, $^3J_{HH}$ = 7.2 Hz, 2H, $NC\mathit{H}_2CH_3$), 3.20 (t, $^3J_{HH}$ = 6.8 Hz, 2H, $NC\mathit{H}_2CH_2$), 1.61

(m, 2H, NCH_2CH_2), 1.33 (m, 2H, $NCH_2CH_2CH_2$), 1.21 (t, $^3J_{HH}$ = 7.3 Hz, 3H, NCH_2CH_3), 0.87 (t, $^3J_{HH}$ = 7.3 Hz, 3H, $CH_2CH_2CH_3$). ^{13}C {^1H} NMR (126 MHz, $CDCl_3$): δ 115.94 (equivalent C_3 atoms), 114.65 (br, unique C_3 atom), 53.92 (CH_3SO_4), 46.79 (NCH_2CH_2), 46.27 (NCH_2CH_3), 32.044 (NCH_2CH_2), 19.46 ($NCH_2CH_2CH_2$), 13.95 (NCH_2CH_3), 13.34 ($CH_2CH_2CH_3$). EI MS: Found m/z 252.2437 (M^+); Calcd: 252.2434 (M^+). Anal. calcd for $C_{16}H_{33}N_3O_4S$: C, 52.86; H, 9.14; N, 11.55. Found: C, 52.27; H, 9.25; N, 11.49. With water content of 365 ppm.

2.7.2 Bis(diethylamino)butylaminocyclopropenium bis(trifluoromethanesulfonyl)amide, [$C_3(NEt_2)_2(NHBu)$]TFSA, [E_4BH]TFSA

[$C_3(NEt_2)_2(NHBu)$]$MeSO_4$ (3.40 g, 9 mmol) was stirred with LiTFSA (8.10 g, 28 mmol) in H_2O (150 mL). The product was extracted with chloroform (150 mL), washed with H_2O (2×100 mL) and dried *in vacuo* to yield an orange liquid (3.67 g, 73.7%). ^1H and ^{13}C {^1H} NMR similar to [$C_3(NEt_2)_2(NHBu)$]$MeSO_4$ with some differences: ^1H NMR NH resonance at 6.22 ppm. ^{13}C NMR resonance for TFSA at 119.79 ppm (q, $^1J_{CF}$ = 322 Hz, CF_3), C_3 ring resonances at 115.40 (equivalent C_3 atoms) and 115.37 (unique C_3 atom) ppm. EI MS: Found m/z 252.2441 (M^+); Calcd: 252.2434 (M^+). Anal. calcd for $C_{17}H_{30}N_6$: C, 63.22; H, 9.51; N, 26.02. Found: C, 63.91; H, 9.93; N, 25.96. With water content of 216 ppm.

2.7.3 Bis(diethylamino)butylaminocyclopropenium dicyanoamide, [$C_3(NEt_2)_2(NHBu)$]DCA, [E_4BH]DCA

[$C_3(NEt_2)_2(NHBu)$]$MeSO_4$ (5.92 g, 16 mmol) was stirred with NaDCA (4.37 g, 49 mmol) in H_2O (150 mL). The product was extracted with chloroform (2×100 mL), washed with H_2O (4×100 mL) and dried *in vacuo* to yield an orange liquid (3.36 g, 65%). ^1H and ^{13}C NMR similar to [$C_3(NEt_2)_2(NHBu)$]$MeSO_4$ with some differences: ^1H NMR resonance for NH at 7.92 ppm. ^{13}C {^1H} NMR resonance for DCA at 119.39 ppm, C_3 ring resonances at 115.54 (equivalent C_3 atoms) and 114.81 (slightly br, unique C_3 atom) ppm. EI MS: Found m/z 252.2441 (M^+); Calcd: 252.2434 (M^+). Anal. calcd for $C_{17}H_{30}N_4O_4S_2F_6.0.25H_2O$: C, 38.34; H, 5.67; N, 10.52. Found: C, 38.81; H, 5.97; N, 10.56. With water content of 2238 ppm.

2.7.4 Bis(diethylamino)butylaminocyclopropenium tetrafluoroborate, $[C_3(NEt_2)_2(NBuH)]BF_4$, $[E_4BH]BF_4$

Butylamine (0.56 mL, 5.67 mmol) was added to a stirred $[C_3(NEt_2)_2(OMe)]BF_4$ (1.3 g, 4.36 mmol) under an inert atmosphere for 2 h. The product was washed several times with diethyl ether to remove unreacted amine. This yielded a yellow oil (1.2 g, 82%). ^{1}H NMR (500 MHz, $CDCl_3$): δ 6.18 (br, 1H, NH), 3.37 (q, 8H, $^3J_{HH}$ = 7 Hz, NCH_2), 3.23 (m, 2H, NCH_2), 1.63 (m, 2H, NCH_2CH_2), 1.36 (m, 2H, $NCH_2CH_2CH_2$), 1.26 (t, $^3J_{HH}$ = 7 Hz, 3H, NCH_2CH_3), 0.92 (t, $^3J_{HH}$ = 8 Hz, 3H, $CH_2CH_2CH_3$). ^{13}C {^{1}H} NMR (126 MHz, $CDCl_3$): δ 119.79 (q, $^1J_{CF}$ = 322 Hz, CF_3), 116.16 (Equivalent ring C), 115.19 (unique ring C), 47.31(NCH_2), 46.66 (NCH_2CH_3), 32.23 (NCH_2CH_2), 19.74 ($NCH_2CH_2CH_2$), 14.23 (NCH_2CH_3), 13.62 ($NCH_2CH_2CH_2CH_3$). EI MS: Found m/z 252.2433 (M^+); Calcd: 252.2434 (M^+). Anal. calcd for $C_{15}H_{29}N_3F_4B$: C, 52.31; H, 9.23; N, 12.22. Found: C, 52.41; H, 8.94; N, 12.22. With water content of 906 ppm.

2.8 Synthesis of bis(diethylamino)dialkylaminocyclopropenium salts

2.8.1 Bis(diethylamino)dihexylaminocyclopropenium iodide, $[C_3(NEt_2)_2(NBu_2)]I$, $[E_4B_2]I$

Dibutylamine (2.1 mL, 14 mmol) was added to a solution of $[C_3(NEt_2)_2(OEt)]I$ (3.44 g, 10 mmol) in dichloromethane and stirred for 2 h. Dichloromethane was removed *in vacuo*. The product was washed several times with diethyl ether to remove unreacted amine. This gave a yellow liquid (3 g, 71%). ^{1}H NMR (500 MHz, $CDCl_3$): δ 3.44 (q, $^3J_{HH}$ = 98 Hz, 8 H, NCH_2), 3.32 (t, $^3J_{HH}$ = 8Hz, 4H, NCH_2), 1.63 (m, 4H, NCH_2CH_2), 1.335 (m, 4H, $NCH_2CH_2CH_2$), 1.31 (t, $^3J_{HH}$ = 7 Hz, 12H, NCH_2CH_3), 0.95 (t, $^3J_{HH}$ = 7 Hz, 6H, NCH_2 $CH_2CH_2CH_3$). ^{13}C {^{1}H} NMR (126 MHz, $CDCl_3$): δ 116.28 (unique ring C), 115.19 (equivalent ring C), 52.81 (NCH_2), 47.06 (NCH_2CH_3), 30.79 (NCH_2CH_2), 19.57 ($NCH_2CH_2CH_2$), 14.23 (NCH_2CH_3), 13.46 ($NCH_2CH_2CH_2CH_3$). EI MS: Found m/z 308.3071 (M^+); Calcd: 308.3060 (M^+). Anal. calcd for $C_{19}H_{38}N_3I$: C, 52.87; H, 8.95; N, 9.61. Found: C, 52.41; H, 8.79; N, 9.65.

2.8.2 Bis(diethylamino)dihexylaminocyclopropenium iodide, $[C_3(NEt_2)_2(NHex_2)]I$, $[E_4Hex_2]I$

Dihexylamine (1.72 mL, 7 mmol) was added to a solution of $[C_3(NEt_2)_2(OEt)]I$ (2.0 g, 5.6 mmol) (prepared as described above for $[C_3(NEt_2)_2(NBu_2)]I$) in dichloromethane (10 mL) and stirred for

2 h. Dichloromethane was removed *in vacuo*. The product was washed several times with diethyl ether to remove unreacted amine. This gave a yellow liquid (2.5 g, 87%). ^{1}H and ^{13}C {^{1}H}NMR as for $[C_3(NEt_2)_2(NHex_2)]MeSO_4$ with no peaks due to $MeSO_4$. ^{1}H NMR (400 MHz, $CDCl_3$): δ 3.42 (q, $^{3}J_{HH}$ = 7 Hz, NC*H*$_2$), 3.29 (t, $^{3}J_{HH}$ = 8 Hz, 4H, NC*H*$_2$), 1.62 (quintet, 4H, NCH$_2$C*H*$_2$), 1.28 (t, $^{3}J_{HH}$ = 7 Hz, 12H, NCH$_2$C*H*$_3$), 1.27 (br s, 12 H, NCH$_2$CH$_2$C*H*$_2$C*H*$_2$C*H*$_2$CH$_3$), 0.86 (t, $^{3}J_{HH}$ = 6.75Hz, 6H, NCH$_2$CH$_2$CH$_2$CH$_2$CH$_2$C*H*$_3$). ^{13}C{^{1}H} NMR (126 MHz, $CDCl_3$): δ 116.43 (unique ring C), 116.25 (equivalent ring C), 53.24 (N*C*H$_2$), 47.25 (NCH$_2$*C*H$_3$), 31.28 (NCH$_2$*C*H$_2$), 28.97 (NCH$_2$CH$_2$*C*H$_2$), 26.16 (NCH$_2$ CH$_2$CH$_2$*C*H$_2$), 22.36 (NCH$_2$CH$_2$CH$_2$CH$_2$*C*H$_2$), 14.39 (NCH$_2$*C*H$_3$), 13.81 (NCH$_2$CH$_2$CH$_2$CH$_2$CH$_2$*C*H$_3$). EI MS: Found m/z 364.3701 (M^+); Calcd: 364.3686 (M^+). Anal. calcd for $C_{23}H_{46}N_3I.0.25H_2O$: C, 55.62; H, 9.53; N, 8.52. Found: C, 55.69; H, 9.44; N, 8.47. With water content of 1279 ppm.

2.8.3 Bis(diethylamino)dihexylaminocyclopropenium trifluoromethylsulfonate, $[C_3(NEt_2)_2(NHex_2)]OTf$, $[E_4Hex_2]OTf$

$[C_3(NEt_2)(OMe)]CF_3SO_3$ (1.46 g, 4 mmol) was stirred with Hex_2NH (1.23 mL, 5.2 mmol) for 2 h. The mixture was dissolved in chloroform:ethanol (2:1) (30 mL) and the product was washed with water (3x30 mL) to remove ammonium salts. Solvent was removed *in vacuo* to give a brown oil (1.6 g, 77%). ^{1}H NMR (400 MHz, $CDCl_3$): δ 3.38 (q, $^{3}J_{HH}$ = 7 Hz, NC*H*$_2$), 3.27 (t, $^{3}J_{HH}$ = 8 Hz, 4H, NC*H*$_2$), 1.61 (quintet, 4H, NCH$_2$C*H*$_2$), 1.28 (t, 12H, NCH$_2$C*H*$_3$), 1.27 (br s, 12 H, NCH$_2$CH$_2$C*H*$_2$C*H*$_2$C*H*$_2$CH$_3$), 0.88 (t, $^{3}J_{HH}$ = 6.4Hz, 6H, NCH$_2$CH$_2$CH$_2$CH$_2$CH$_2$C*H*$_3$). ^{13}C {^{1}H} NMR (126 MHz, $CDCl_3$): δ 116.43 (unique ring C), 116.25 (equivalent ring C), 53.14 (N*C*H$_2$), 47.00 (NCH$_2$*C*H$_3$), 31.34 (NCH$_2$*C*H$_2$), 28.94 (NCH$_2$CH$_2$*C*H$_2$), 26.23 (NCH$_2$ CH$_2$CH$_2$*C*H$_2$), 22.46 (NCH$_2$CH$_2$CH$_2$CH$_2$*C*H$_2$), 14.14 (NCH$_2$*C*H$_3$), 13.89 (NCH$_2$CH$_2$CH$_2$CH$_2$CH$_2$*C*H$_3$). EI MS: Found m/z 364.6951 (M^+); Calcd: 364.3686 (M^+). Anal. calcd for $C_{24}H_{46}N_3O_3SF_3$: C, 55.95; H, 9.23; N, 7.96. Found: C, 56.11; H, 9.02; N, 8.18. With water content of 720 ppm.

2.9 Synthesis of Chiral Ionic Liquids from Amino Acids

2.9.1 Bis(diethylamino)-S-(1-carboxyethylamino)cyclopropenium methylsulfate, $[C_3(NEt_2)_2(NH(CHMeCOOH))]MeSO_4$, $[E_4Ala]MeSO_4$

$[C_3(NEt_2)_2(OMe)]MeSO_4$ (10 g, 31 mmol) was stirred with L-alanine (3.59 g, 40 mmol) and NEt_3 (6.44 mL, 40 mmol) in water (50 mL) overnight. Water was removed *in vacuo* and the product

was dissolved in acetone (20 mL) and filtered to remove unreacted L-alanine. The mixture was dissolved in ice cold water and the product was extracted with chloroform:ethanol (2:1) (3×30 mL). The solvent was removed *in vacuo* to give an orange viscous oil of $[C_3(NEt_2)_2(NH(CHMeCOOH))]MeSO_4$ (9.03 g, 77%). ^{1}H NMR (500 MHz, $CDCl_3$): δ 8.36 (m, 1H, NH), 5.65 (br, 1H, COOH), 4.01 (m, 1H, CH), 3.71 (s, 1.7H, $MeSO_4$), 3.38 (m, 8H, NCH_2CH_3), 1.58 (d, $^3J_{HH}$ = 7Hz, 3H, Me), 1.24 (t, $^3J_{HH}$ = 6.6 Hz, 12H, NCH_2CH_3). ^{13}C {^{1}H}NMR (126 MHz, $CDCl_3$) δ 175.37 (COOH), 115.75 (unique ring C), 115.18 (equivalent ring C), 56.54 (*C*HMe), 54.74 ($MeSO_4$), 46.54 (NCH_2CH_3), 18.34 ($CHCH_3$), 14.22 (NCH_2CH_3). EI MS: Found m/z 268.2023 (M^+); Calcd: 268.2020 (M^+). Anal. calcd for $0.62(C_{15}H_{29}N_3O_6S)$:$0.48(C_{14}H_{25}N_3O_2)$: C, 51.04; H, 8.47; N, 12.28. Found: C, 51.70; H, 8.34; N, 11.82 (IL:Zwitterion 0.62:0.38). With water content of 4.3%.

2.9.2 Bis(diethylamino)- S-(1-carboxyethylamino)cyclopropenium TFSA, $[C_3(NEt_2)_2(NH(CHMeCOOH))]TFSA$, $[E_4Ala]TFSA$

[E4Ala]$MeSO_4$ (2.1 g, 5 mmol) was stirred with LiTFSA (4.77 g, 15 mmol) in 10 mL of water. The product was extracted with chloroform (3×10 mL) to give $[E_4Ala]TFSA$ (2.57 g, 81%). ^{1}H NMR (500 MHz, $CDCl_3$): δ 9.18 (br, 1H, COO*H*), 6.99 (d, $^3J_{HH}$ = 7.0 Hz, 1H, N*H*), 4.03 (m, 1H, C*H*), 3.35 (q, $^3J_{HH}$ = 7.5 Hz, 8H, NCH_2CH_3), 1.51 (d, $^3J_{HH}$ = 7.0Hz, 3H, CH_3), 1.22 (t, $^3J_{HH}$ = 7.2 Hz, 12H, NCH_2CH_3). ^{13}C {^{1}H} NMR (126 MHz, $CDCl_3$) δ 175.36 (*C*OOH), 119.82 (q, $^1J_{CF}$ = 320 Hz, CF_3), 116.04 (equivalent ring C), 114.01 (unique ring C), 56.05 (*C*HMe), 46.65 (NCH_2CH_3), 18.65 (CH_3), 14.1 (NCH_2CH_3). EI MS: Found m/z 268.2021 (M^+); Calcd: 268.2020 (M^+). Anal. calcd for $0.93(C_{16}H_{26}N_4O_6S_2F_6)$:$0.07(C_{14}H_{25}N_3O_2)$: C, 36.61; H, 5.16; N, 10.49. Found: C, 36.14; H, 5.31; N, 10.40 (IL:Zwitterion 0.93:0.07). With water content of 0.99%.

2.9.3 Bis(diethylamino)-S-(2-carboxypyrrolidino)cyclopropenium methylsulfate, $[C_3(NEt_2)_2(N(C_4H_7COOH))]MeSO_4$, $[E_4Pro]MeSO_4$

$[C_3(NEt_2)_2(OMe)]MeSO_4$ (5.65 g, 18 mmol) was stirred with L-proline (2.62 g, 23 mmol) and NEt_3 (3.64 mL, 23 mmol) in water (20 mL) overnight. Water was removed *in vacuo* and the product was dissolved in acetone (20 mL) and filtered to remove unreacted L-proline. The mixture was dissolved in ice cold water and the product was extracted with chloroform:ethanol (2:1) (3×30 mL). The solvent was removed *in vacuo* to give an orange oil of $[C_3(NEt_2)_2(N(C_4H_7COOH))]MeSO_4$ (5.53 g, 78%). ^{1}H NMR (400 MHz, $CDCl_3$): δ 7.37 (br, 1H,

COOH), 4.42 (dd, $^{3}J_{HH}$ = 3.6Hz, $^{3}J_{HH}$ = 8Hz, 1H, CH), 3.72 (m, 1H, NC*H*$_2$), 3.68 (s, 1.4H, $CH_3SO_4^-$), 3.60 (ddd, $^{3}J_{HH}$ = 7.9Hz, 1H, NC*H*$_2$), 3.34 (m, 8H, NC*H*$_2$CH$_3$), 2.31 (m, 2H, NCH$_2$CH$_2$C*H*$_2$), 2.01 (m, 2H, NCH$_2$C*H*$_2$), 1.21 (t, $^{3}J_{HH}$ = 6.6 Hz, 12H, NCH$_2$C*H*$_3$).^{13}C {^{1}H} NMR (100 MHz, $CDCl_3$) δ 174.09 (*C*OOH), 116.08 (equivalent ring C), 114.80 (unique ring C), 64.60 (N*C*H), 54.26 ($MeSO_4$), 51.89 (N*C*H$_2$), 46.77 (N*C*H$_2$CH$_3$), 31.13 (NCH*C*H$_2$), 24.32 (NCH$_2$*C*H$_2$CH$_2$), 13.94 (NCH$_2$*C*H$_3$). EI MS: Found m/z 294.2179 (M^+); Calcd: 294.2176 (M^+). Anal. calcd for 0.65($C_{17}H_{31}N_3O_6S$):0.35($C_{16}H_{27}N_3O_2$): C, 54.03; H, 8.33; N, 11.40. Found: C, 54.57; H, 8.89; N, 11.59 (IL:Zwitterion 0.65:0.35). With water content of 2.91%.

2.9.4 Bis(diethylamino)-S-(2-carboxypyrrolidino)cyclopropenium TFSA, [C$_3$(NEt$_2$)$_2$(N(C$_4$H$_7$COOH))]TFSA, [E$_4$Pro]TFSA

[E$_4$Pro]$MeSO_4$ (2.0 g, 5 mmol) was stirred with LiTFSA (4.2 g, 15 mmol) in 10 mL of water. Then the product was extracted with chloroform (3×10 mL) to give a [E$_4$Pro]TFSA (1.0 g, 36%). ^{1}H NMR (500 MHz, $CDCl_3$): δ 7.55 (br, 1H, COO*H*), 4.44 (dd, $^{3}J_{HH}$ = 3.5Hz, $^{3}J_{H}$ = 8.5Hz, 1H, NC*H*COOH), 3.70 (dt, $^{3}J_{HH}$ = 6.5Hz, $^{3}J_{HH}$ = 8.3Hz 1H, NC*H*), 3.64 (q, $^{3}J_{HH}$ = 7.5Hz, 1H, NC*H*), 3.34 (m, 8H, NC*H*$_2$CH$_3$), 2.38 (m, 1H, NCHCOOHC*H*), 2.23 (m, 1H, NCHCOOHC*H*), 2.05 (m, 2H, NCH$_2$C*H*$_2$), 1.25 (t, $^{3}J_{HH}$ = 7.25 Hz, 12H, NCH$_2$C*H*$_3$). ^{13}C {^{1}H} NMR (126 MHz, $CDCl_3$) δ 173.80 (*C*OOH), 119.61 (q, $^{1}J_{CF}$ = 322 Hz, CF_3), 116.08 (equivalent ring C), 113.74 (unique ring C), 63.33 (N*C*H), 51.54 (N*C*H$_2$), 46.74 (N*C*H$_2$CH$_3$), 30.51 (NCH*C*H$_2$), 23.90 (NCH$_2$*C*H$_2$CH$_2$), 13.70 (NCH$_2$*C*H$_3$). EI MS: Found m/z 294.2170 (M^+); Calcd: 294.2176 (M^+). Anal. calcd for 0.85($C_{18}H_{28}N_4O_6S_2F_6$):0.15($C_{16}H_{27}N_3O_2$): C, 40.59; H, 5.73; N, 10.13. Found: C, 40.41; H, 5.69; N, 10.24 (IL:Zwitterion 0.85:0.15). With water content of 2.91%.

2.9.5 Bis(diethylamino)-S-(1-carboxy-2-methylpropylamino)cyclopropenium methylsulfate, [C$_3$(NEt$_2$)$_2$(NH(C$_4$H$_8$COOH))]MeSO$_4$, [E$_4$Val]MeSO$_4$

[C$_3$(NEt$_2$)$_2$(OMe)]$MeSO_4$ (15 g, 47 mmol) was stirred with L-valine (7.09 g, 61 mmol) and NEt_3 (9.67 mL, 61 mmol) in water (50 mL) overnight. Water was removed *in vacuo* and the product was dissolved in acetone (20 mL) and filtered to remove unreacted L-valine. The mixture was dissolved in ice cold water and product was extracted with chloroform:ethanol (2:1) (3×30 mL). The solvent was removed *in vacuo* to give a yellow solid of [C$_3$(NEt$_2$)$_2$(N(C$_4$H$_8$COOH))]$MeSO_4$ (10.00 g, 55%). ^{1}H NMR (400MHz, $CDCl_3$): δ 8.44 (br, 1H, N*H*), 3.67 (s, 0.9H, $CH_3SO_4^-$), 3.62

(d, $^3J_{HH}$ = 6.4Hz, 1H, C*H*), 3.38 (m, 8H, NC*H*$_2$CH$_3$), 2.23 (m, 1H, C*H*), 1.22 (t, $^3J_{HH}$ = 7.2 Hz, 12H, NCH$_2$C*H*$_3$), 1.03 (d, $^3J_{HH}$ = 6.8 Hz, 3H, C*H*$_3$), 0.98 (d, $^3J_{HH}$ = 6.8 Hz, 3H, C*H*$_3$). ^{13}C {^{1}H} NMR (100 MHz, $CDCl_3$) δ 174.25 (*C*OOH), 115.87 (equivalent ring C), 115.46 (unique ring C), 68.82 (*C*HNH), 54.27 ($MeSO_4$), 46.62 (N*C*H$_2$CH$_3$), 31.00 (*C*H(CH$_3$)$_2$), 19.28 (*C*H$_3$), 18.80 (*C*H$_3$), 14.27 (NCH$_2$*C*H$_3$). EI MS: Found m/z 296.2335 (M^+); Calcd: 296.2333 (M^+). Anal. calcd for 0.45($C_{17}H_{33}N_3O_6S$):0.55($C_{16}H_{29}N_3O_2$): C, 57.74; H, 9.13; N, 12.34. Found: C, 57.10; H, 9.01; N, 12.08 (IL:Zwitterion 0.45:0.55). With water content of 0.99%.

2.9.6 Bis(diethylamino)-S-(1-carboxy-2-methylpropylamino)cyclopropenium TFSA, [C$_3$(NEt$_2$)$_2$(NH(C$_4$H$_8$COOH))]TFSA, [E$_4$Val]TFSA

[E$_4$Val]$MeSO_4$ (2.0 g, 5 mmol) was stirred with LiTFSA (4.2g, 15 mmol) in 10 mL of water. The product was extracted with chloroform (3×10 mL) to give [E$_4$Val]TFSA (1.7 g, 60%). ^{1}H NMR (500 MHz, $CDCl_3$): δ 7.13 (d, $^3J_{HH}$ = 8.5 Hz 1H, N*H*), 3.66 (t, $^3J_{HH}$ = 7.8 Hz, 1H, C*H*), 3.38 (q, $^3J_{HH}$ = 7.16 Hz, 8H, NC*H*$_2$CH$_3$), 2.18 (m, 1H, C*H*), 1.23 (t, $^3J_{HH}$ = 7.25 Hz, 12H, NCH$_2$C*H*$_3$), 1.02 (d, $^3J_{HH}$ = 6.5 Hz, 3H, C*H*$_3$), 0.99 (d, $^3J_{HH}$ = 7.0 Hz, 3H, C*H*$_3$).^{13}C {^{1}H} NMR (126 MHz, $CDCl_3$) δ 173.93 (*C*OOH), 119.80 (q, $^1J_{CF}$ = 322 Hz, CF_3), 115.96 (equivalent ring C), 114.24 (unique ring C), 67.36 (*C*HNH), 46.73 (N*C*H$_2$CH$_3$), 31.07 (*C*H(CH$_3$)$_2$), 18.73 (*C*H$_3$), 18.36 (*C*H$_3$), 14.11 (NCH$_2$*C*H$_3$). EI MS: Found m/z 296.2331 (M^+); Calcd: 296.2333 (M^+). Anal. calcd for 0.80($C_{18}H_{30}N_4O_6S_2F_6$):0.20($C_{16}H_{29}N_3O_2$): C, 41.75; H, 6.31; N, 10.31. Found: C, 41.38; H, 6.46; N, 10.56 (IL:Zwitterion 0.80:0.20). With water content of 2.91%.

2.9.7 Bis(diethylamino)-S-(1-carboxy-2-hyroxylpropylamino)cyclopropenium methylsulfate, [C$_3$(NEt$_2$)$_2$(NH(C$_3$H$_6$OCOOH))]MeSO$_4$, [E$_4$Thr]MeSO$_4$

[C$_3$(NEt$_2$)$_2$(OMe)]$MeSO_4$ (10 g, 31 mmol) was stirred with L-threonine (4.8 g, 40 mmol) and NEt_3 (6.45 mL, 40 mmol) in water (50 mL) overnight. Water was removed *in vacuo* and the product was dissolved in acetone (20 mL) and filtered to remove unreacted L-threonine. The mixture was dissolved in ice cold water and the product was extracted with chloroform:ethanol (2:1) (3×30 mL). The solvent was removed *in vacuo* to give a yellow solid of [C$_3$(NEt$_2$)$_2$(N(C$_3$H$_6$OCOOH))]$MeSO_4$ (9.30 g, 76%). ^{1}H NMR (500 MHz, $CDCl_3$): δ 8.04 (br, 1H, N*H*), 5.27 (br, 2H, O*H*+H_20), 4.08 (m,1H, NC*H*), 3.69 (m, 1H, C*H*OH), 3.67 (s, 0.6H, $CH_3SO_4^-$), 3.37 (q, $^3J_{HH}$ = 7.16 Hz, 8H, NC*H*$_2$CH$_3$), 1.23 (d, $^3J_{HH}$ = 7.5 Hz, 3H, C*H*$_3$), 1.21 (t, $^3J_{HH}$

= 7.25 Hz, 12H, NCH_2CH_3).^{13}C {^{1}H} NMR (126 MHz, $CDCl_3$) δ 173.37 (*C*OOH), 115.98 (equivalent ring C), 115.35 (unique ring C), 67.78 (*C*HCH_3), 67.20 (*C*HNH), 54.31 ($MeSO_4$), 46.49 (NCH_2CH_3), 19.42 (*C*H_3), 14.20 (NCH_2CH_3). EI MS: Found m/z 298.2125 (M^+); Calcd: 298.2125 (M^+). Anal. calcd for 0.45($C_{16}H_{31}N_3O_7S$):0.55($C_{15}H_{27}N_3O_3$): C, 54.31; H, 8.78; N, 12.23. Found: C, 54.43; H, 8.461; N, 12.38 (IL:Zwitterion 0.45:0.55).

2.9.8 Bis(diethylamino)-S-(1-carboxy-2-hyroxylpropylamino))cyclopropenium TFSA, [$C_3(NEt_2)_2(NH(C_3H_6OCOOH))$]TFSA, [E_4Thr]TFSA

[E_4Thr]$MeSO_4$ (2.0 g, 5 mmol) was stirred with LiTFSA (4.2 g, 15 mmol) in 10 mL of water. The product was extracted with chloroform (3×10 mL) to give [E_4Thr]TFSA (1.4 g, 49%). ^{1}H NMR (500 MHz, $CDCl_3$): δ 7.18 (br, 1H, COO*H*), 6.75 (d, $^3J_{HH}$ = 9.0 Hz, 1H, NH), 5.26 (br, 2H, O*H*+*H*$_2$O), 4.39 (dq,1H, NC*H*), 3.76 (dd, $^3J_{HH}$ = 2.5 Hz, $^3J_{HH}$ = 6.5 Hz, 1H, C*H*OH), 3.36 (q, $^3J_{HH}$ = 7.2 Hz, 8H, NC*H*$_2$CH$_3$), 1.29 (d, $^3J_{HH}$ = 6.5 Hz, 3H, C*H*$_3$), 1.24 (t, $^3J_{HH}$ = 7.3 Hz, 12H, NCH_2CH_3).^{13}C {^{1}H} NMR (126 MHz, $CDCl_3$) δ 170.40 (*C*OO), 117.38 (q, $^1J_{CF}$ = 291 Hz, CF_3), 116.28 (equivalent ring C), 114.74 (unique ring C), 72.64 (*C*HNH), 67.80 (*C*HCH3), 46.78(NCH_2CH_3), 19.50 (*C*H_3), 14.02 (NCH_2CH_3). EI MS: Found m/z 298.2130 (M^+); Calcd: 298.2125 (M^+). Anal. calcd for 0.85($C_{17}H_{28}N_4O_7S_2F_6$):0.15($C_{15}H_{27}N_3O_3$): C, 38.32; H, 5.74; N, 10.35. Found: C, 38.57; H, 5.51; N, 10.52 (IL:Zwitterion 0.85:0.15). With water content of 1.96%.

2.9.9 Bis(diethylamino)-S-(1-carboxy-4-guanidinobutylamino)cyclopropenium bis(trifluoromethanesulfonyl)amide, [$C_3(NEt_2)_2(NH(C_5H_{11}N_3COOH))$]TFSA, [$E_4$Arg]TFSA

[$C_3(NEt_2)_2$(OMe)]$MeSO_4$ (5 g, 16 mmol) was stirred with L-arginine (3.51 g, 21 mmol) and NEt_3 (3.22 mL, 21 mmol) in water (50 mL) for an hour. A cold solution of NaOH (8 g in 10 mL water) was added to the aqueous mixture and Et_3N was extracted with diethyl ether (6×50 mL). The solution was acidified to pH =1-2 with HCl and stirred with LiTFSA (9.65 g, 34 mmol) in 50 mL of water for 30 minutes. Ethanol (1 mL) was added to induce the formation of a separate layer, which was then washed with water (3×10 mL). The product was dried *in vacuo* to give a light yellow viscous liquid of [E_4Arg]TFSA (2.19 g, 73%). ^{1}H NMR (400 MHz, CD_3OD): δ 3.88 (dd, $^3J_{HH}$ = 5 Hz, $^3J_{HH}$ = 7 Hz, 1H, NC*H*), 3.42 (q, $^3J_{HH}$ = 7 Hz, 8H, NC*H*$_2$CH$_3$), 3.23 (dd, $^3J_{HH}$ = 4 Hz, 2H, $NHCHCH_2CH_2CH_2$), 1.98 (m, 1H, $NHCHCH_2CH_2$), 1.82 (m, 1H, $NHCHCH_2CH_2$), 1.78 (m, 2H, $NHCHCH_2$), 1.25 (t, $^3J_{HH}$ = 7 Hz, 12H, NCH_2CH_3). ^{13}C {H} NMR (100 MHz, CD_3OD) δ

175.65 (*C*OOH), 157.25 (guanidinium C), 119.93 (q, $^{1}J_{CF}$ = 320 Hz, CF_3), 116.07 (equivalent ring C), 115.02 (unique ring C), 60.73 (NH*C*H), 46.21 (N*C*H_2CH_3), 40.61 (CH_2CH_2*C*H_2), 29.38 (NHCH*C*H_2), 25.21 (NHCHCH_2*C*H_2), 13.18 (NCH_2*C*H_3). EI MS: Found m/z 177.1366 (M^{2+}), 353.2660 (M^{+}); Calcd: 177.1366 (M^{2+}), 353.2660 (M^{+}). Anal. calcd for 0.73($C_{21}H_{34}N_8O_{14}S_4F_{12}$):0.27($C_{19}H_{33}N_7O_6S_2F_6$); C, 30.81; H, 4.22; N, 13.81. Found: C, 30.67; H, 4.28; N, 13.45 (M^{2+}:M^{+} 0.73:0.27).

2.9.10 Bis(diethylamino)-S-(1,3-dicarboxy-ethylamino)cyclopropenium bis(trifluoromethanesulfonyl)amide, [$C_3(NEt_2)_2$($NHCOOHC_2H_3COOH$))]TFSA, [E_4Asp]TFSA

[$C_3(NEt_2)_2$(OMe)]$MeSO_4$ (5 g, 16 mmol) was stirred with L-aspartic acid (2.68 g, 21 mmol) and NEt_3 (6.4 mL, 42 mmol) in water (50 mL) for an hour. A cold solution of NaOH (8g in 10 mL water) was added to the aqueous mixture and Et_3N was extracted with diethyl ether (6×50 mL). The solution was acidified with HCl to pH = 1-2 and water was removed *in vacuo*. The mixture was dissolved in ethanol and filtered to remove NaCl and L-asparatic acid. The solvent was removed *in vacuo* to give a yellow viscous oil of [E_4Asp]$MeSO_4$ (5.77 g, 88%). [E_4Asp]$MeSO_4$ was stirred with LiTFSA (11.9 g, 41 mmol) in 50 mL of water for 30 minutes. Ethanol (1 mL) was added to induce a separate layer, which was washed with water (3×10 mL). Ethanol results in a mixture of IL with ethyl esters. Esters are hydrolyzed by refluxing with conc. HCl overnight (100 mL). The solution was dissolved in $CHCN_3$ (50 mL) followed by water washes (3×50 mL). The $CHCN_3$ was dried *in vacuo* to give a light yellow viscous oil of [E_4Asp]TFSA (3 g, 37%). ^{1}H NMR (400 MHz, CD_3OD): δ 3.44 (q, $^{3}J_{HH}$ = 7.2 Hz, 8H, NC*H*$_2$$CH_3$), 1.27 (t, $^{3}J_{HH}$ = 7.2 Hz, 12H, NCH_2C*H*$_3$). We were not able to see the peaks of amino acid chain after hydrolysis probably due to rapid exchange of protons with CD_3OD. EI MS: Found m/z 312.1923 (M^{+}); Calcd: 312.1918 (M^{+}). Anal. calcd for 0.90($C_{17}H_{26}N_4O_8S_2F_6$):0.10($C_{15}H_{25}N_3O_4$): C, 36.80; H, 4.78; N, 9.86. Found: C, 37.27; H, 5.03; N, 9.66 (IL:Zwitterion 0.90:0.10).

2.9.11 Bis(diethylamino)-S-(1-carboxy-2-imidazolethylamino)cyclopropenium bis(trifluoromethanesulfonyl)amide, [$C_3(NEt_2)_2$($NHCOOHC_2H_3C_3H_2N_2H$))]TFSA, [E_4His]TFSA

[$C_3(NEt_2)_2$(OMe)]$MeSO_4$ (5 g, 16 mmol) was stirred with L-histidine (3.13 g, 21 mmol) and NEt_3 (3.2 mL, 21 mmol) in water (50 mL) for an hour. A cold solution of NaOH (8 g in 10 mL water)

was added to the aqueous mixture and Et_3N was extracted with diethyl ether (6×50 mL). The solution was acidified with HCl to pH = 1-2 and water was removed *in vacuo*. The mixture was dissolved in ethanol and filtered to remove NaCl and L-histidine. The solvent was removed *in vacuo* to give a yellow viscous oil of $[E_4His]MeSO_4$ (5.84 g, 85%). $[E_4His]MeSO_4$ was stirred with LiTFSA (11.29g, 39 mmol) in 50 mL of water for 30 minutes. Ethanol (1 mL) was added to induce a separate layer. The product is washed with water (3×10 mL) and dried *in vacuo* to give a mixture of $[E_4His]TFSA$ with its methyl and ethyl esters. The mixture was refluxed overnight with conc. HCl (60 mL) to hydrolyze the esters and dried *in vacuo*. The product was washed with water (3×50 mL) and dried *in vacuo* to give a light yellow viscous oil of $[E_4His]TFSA$ (7 g, 87%). ^1H NMR (400 MHz, CD_3OD): δ 8.74 (s, 1H, NC*H*NH), 7.41 (s, 1H, NCHNHC*H*), 4.29 (dd,1H, $^3J_{HH}$ = 4 Hz, $^3J_{HH}$ = 10 Hz, NC*H*), 3.42 (q, $^3J_{HH}$ = 7 Hz, 9H, NCH_2CH_3/CH_2), 3.22 (dd, = 8 Hz, $^3J_{HH}$ = 12 Hz, 1H, CH_2), 1.24 (t, $^3J_{HH}$ = 7 Hz, 12H, NCH_2CH_3). ^{13}C {H} NMR (100 MHz, CD_3OD) δ 171.91 (*C*OOH), 133.73 (imidazolium ring C), 129.24 (imidazolium ring C), 119.78 (q, $^1J_{CF}$ = 319 Hz, CF_3), 117.31 (symmetric ring C), 116.79 (unique ring C), 113.86 (imidazolium ring C), 58.45 (NH*C*H), 46.67 (NCH_2CH_3), 26.72 ($NHCHCH_2$**),** 13.02 (NCH_2CH_3). EI MS: Found m/z 167.6167 (M^{2+}), 334.2243 (M^+); Calcd: 167.6155 (M^{2+}), 334.2238 (M^+). Anal. calcd for $0.91(C_{21}H_{29}N_7O_{10}S_4F_{12})$:$0.09(C_{19}H_{28}N_6O_6S_2F_6)$; C, 29.73; H, 3.47; N, 11.47. Found: C, 29.28; H, 3.51; N, 10.90 (Dication:Monocation (zwiterion) 0.91:0.09).

2.9.12 Bis(diethylamino)-S-(1-carboxy-3-methylthioproylamino)cyclopropenium bis(trifluoromethanesulfonyl)amide, $[C_3(NEt_2)_2(NHCOOHC_3H_5SCH_3))]TFSA$, $[E_4Met]TFSA$

$[C_3(NEt_2)_2(OMe)]MeSO_4$ (5 g, 16 mmol) was stirred with L-methionine (3 g, 21 mmol) and NEt_3 (3.2 mL, 21 mmol) in water (50 mL) for an hour. A cold solution of NaOH (8 g in 10 mL water) was added to the aqueous mixture and Et_3N was extracted with diethyl ether (6×50 mL). The solution was acidified with HCl to pH = 1-2 and water was removed *in vacuo*. The mixture was dissolved in ethanol and filter to remove NaCl and L-methionine. The solvent was removed *in vacuo* to give a yellow viscous oil of $[E_4Met]MeSO_4$ (5 g, 71%). $[E_4Met]MeSO_4$ was stirred with LiTFSA (13.78 g, 48 mmol) in 50 mL of water for 30 minutes. Ethanol (1 mL) was added to induce formation of a separate layer. The product was washed with water (3×10 mL) and dried *in vacuo* to give a light yellow viscous oil of $[E_4Met]TFSA$ (2.93 g, 72%). ^1H NMR (400 MHz, CD_3OD): δ 3.97 (dd, $^3J_{HH}$ = 8 Hz, $^3J_{HH}$ = 12 Hz, 1H, NC*H*), 3.43 (q, $^3J_{HH}$ = 7.2 Hz, 8H,

NC*H*$_2$CH$_3$), 2.67 (m, 1H, CH$_3$SC*H*$_2$), 2.62 (m, 1H, CH$_3$SC*H*$_2$), 2.26 (m, 1H, CH$_3$SCH$_2$C*H*$_2$), 2.1 (s, 3H, C*H*$_3$S), 1.96 (m, 1H, CH$_3$SCH$_2$C*H*$_2$), 1.26 (t, $^3J_{HH}$ = 7.2 Hz, 12H, NCH$_2$C*H*$_3$). ^{13}C {H} NMR (100 MHz, CD$_3$OD) δ 176.74 (*C*OOH), 119.81 (q, $^1J_{CF}$ = 319 Hz, CF$_3$), 115.79 (symmetric ring C), 115.75 (unique ring C), 60.75 (NH*C*H), 46.21 (N*C*H$_2$CH$_3$), 31.56 (S*C*H$_2$**),** 30.29 (SCH$_2$*C*H$_2$), 13.19 (*C*H$_3$S), 13.02 (NCH$_2$*C*H$_3$). EI MS: Found m/z 328.2067 (M^+); Calcd: 328.2053 (M^+). Anal. calcd for 0.72($C_{18}H_{30}N_4O_6S_3F_6$):0.28($C_{16}H_{29}N_3O_2S_1$); C, 41.82; H, 5.96; N, 9.99. Found: C, 42.00; H, 6.07; N, 10.22 (IL:Zwitterion 0.72:0.28).

2.9.13 Bis(diethylamino)-S-(1-carboxy-3,3-dimethylethylamino)cyclopropenium bis(trifluoromethanesulfonyl)amide, [C$_3$(NEt$_2$)$_2$(NHCOOHC$_3$H$_4$(CH$_3$)$_2$))]TFSA, [E$_4$Leu]TFSA

[C$_3$(NEt$_2$)$_2$(OMe)]MeSO$_4$ (5 g, 19 mmol) was stirred with L-leucine (2.4 g, 25 mmol) and NEt$_3$ (3.87 mL, 25 mmol) in water (50 mL) for an hour. A cold solution of NaOH (8g in 10 mL water) was added to the aqueous mixture and Et$_3$N was extracted with diethyl ether (6×50 mL). The solution was acidified with HCl to pH = 1-2 and water was removed *in vacuo*. The mixture was dissolved in ethanol and filter to remove NaCl and L-leucine and solvent was removed *in vacuo* to give a yellow viscous oil of [E$_4$Leu]MeSO$_4$ (4.22 g, 54%). [E$_4$Leu]MeSO$_4$ was stirred with LiTFSA (11.29 g, 39 mmol) in 50 mL of water for 30 minutes. The product was extracted with CHCl$_3$ (3×50 mL), washed with water (3×50 mL), and dried *in vacuo* to give a light yellow viscous oil of [E$_4$Leu]TFSA (2.5 g, 85%). ^{1}H NMR (400 MHz, CDCl$_3$): δ 6.92 (d, $^3J_{HH}$ = 9 Hz, 1H, N*H*), 3.95 (m, 1H, NHC*H*), 3.41 (m, $^3J_{HH}$ = 8 Hz, 4H, NC*H*$_2$CH$_3$), 3.38 (q, $^3J_{HH}$ = 7 Hz, 4H, NC*H*$_2$CH$_3$),3.37 q, $^3J_{HH}$ = 7 Hz, 4H, NC*H*$_2$CH$_3$), 1.81 (m, 1H, C*H*(CH$_3$)$_2$), 1.74 (m, 2H, C*H*$_2$CH(CH$_3$)$_2$), 1.26 (t, $^3J_{HH}$ = 7 Hz, 12H, NCH$_2$C*H*$_3$), 1.00 (d, $^3J_{HH}$ = 6 Hz, 3H, CH(C*H*$_3$)), 0.96 (d, $^3J_{HH}$ = 6 Hz, 3H, CH(C*H*$_3$)). ^{13}C {H} NMR (100 MHz, CDCl$_3$) δ 175.07 (*C*OOH), 119.79 (q, $^1J_{CF}$ = 319 Hz, CF$_3$), 116.17 (symmetric ring C), 114.81 (unique ring C), 58.49 (N*C*H), 46.29 (N*C*H$_2$CH$_3$), 40.63 (*C*H(CH$_3$)$_2$**),** 24.66 (*C*H$_2$CH), 21.89 (CH(*C*H$_3$)**),** 20.35 (CH(*C*H$_3$)), 13.13 (NCH$_2$*C*H$_3$). EI MS: Found m/z 311.2528 (M+1); Calcd: 310.2489 (M^+). Anal. calcd for 0.85($C_{19}H_{32}N_4O_6S_2F_6$):0.15($C_{17}H_{31}N_3O_2$); C, 42.74; H, 6.15; N, 10.10. Found: C, 42.35; H, 6.09; N, 9.79 (IL:Zwitterion 0.85:0.15).

2.9.14 Bis(diethylamino)-S-(1-carboxy-2-methylbutylamino)cyclopropenium bis(trifluoromethanesulfonyl)amide, $[C_3(NEt_2)_2(NHCOOHC_2H_2(CH_3)CH_2CH_3COOH))]TFSA$, $[E_4Ile]TFSA$

$[C_3(NEt_2)_2(OMe)]MeSO_4$ (5 g, 16 mmol) was stirred with L-isoleucine (2.64 g, 21 mmol) and NEt_3 (3.23 mL, 21 mmol) in water (50 mL) for an hour. A cold solution of NaOH (8 g in 10 mL water) was added to the aqueous mixture and Et_3N was extracted with diethyl ether (6×50 mL). The solution was acidified with HCl to pH = 1-2 and water was removed *in vacuo*. The mixture was dissolved in ethanol and filter to remove NaCl and L-isoleucine and solvent was removed *in vacuo* to give a yellow viscous oil of $[E_4Ile]MeSO_4$ (5.55 g, 85%). $[E_4Ile]MeSO_4$ was stirred with LiTFSA (11.25g, 39 mmol) in 50 mL of water for 30 minutes. The product was extracted with $CHCl_3$ (3×50 mL), washed with water (3×50 mL) and dried *in vacuo* to give a light yellow viscous oil of $[E_4Ile]TFSA$ (6.59 g, 95%). ^{1}H NMR (400 MHz, $CDCl_3$): δ 6.64 (d, $^3J_{HH}$ = 8 Hz, 1H, N*H*), 3.79 (dd, $^3J_{HH}$ = 4 Hz, $^3J_{HH}$ = 8 Hz, 1H, NHC*H*), 3.39 (q, $^3J_{HH}$ = 8 Hz, 8H, NCH_2CH$_3$), 1.95 (m, 1H, NHCHC*H*), 1.59 (m, 1H, NHCHCHCH_2), 1.29 (m, 1H, NHCHCHCH_2), 1.25 (t, $^3J_{HH}$ = 7 Hz, 12H, NCH$_2$CH_3), 0.99 (d, $^3J_{HH}$ = 8 Hz, 12H, CHCH_3), 0.93 (t, $^3J_{HH}$ = 6 Hz, 12H, CH$_2$CH_3). ^{13}C {H} NMR (100 MHz, $CDCl_3$) δ 173.93 (*C*OOH), 119.82 (q, $^1J_{CF}$ = 319 Hz, CF_3), 116.34 (symmetric ring C), 113.87 (unique ring C), 65.56 (NH*C*H), 46.81 (N*C*H$_2$CH$_3$), 37.55 (NHCH*C*H), 25.14 (CHCH*C*H$_2$), 15.05 (CH$_2$(*C*H$_3$))**,** 14.07 (NCH$_2$*C*H$_3$), 11.21 (CH(*C*H$_3$)). EI MS: Found m/z 310.2493 (M^+); Calcd: 310.2489 (M^+). Anal. calcd for 0.9($C_{19}H_{32}N_4O_6S_2F_6$):0.1($C_{17}H_{31}N_3O_2$); C, 41.37; H, 5.92; N, 9.89. Found: C, 41.01; H, 5.88; N, 9.6 (IL:Zwitterion 0.9:0.1).

2.9.15 Bis(diethylamino)-S-(1-carboxy-2-(1H-indol-3-yl)ethylamino)cyclopropenium bis(trifluoromethanesulfonyl)amide, $[C_3(NEt_2)_2(NHCOOHC_2H_3C_8H_6N))]TFSA$, $[E_4Try]TFSA$

$[C_3(NEt_2)_2(OMe)]MeSO_4$ (5 g, 16 mmol) was stirred with L-tryptophan (4.12 g, 21 mmol) and NEt_3 (3.23 mL, 21 mmol) in water (50 mL) for an hour. A cold solution of NaOH (8g in 10 mL water) was added to the aqueous mixture and Et_3N was extracted with diethyl ether (6×50 mL). The solution was acidified with HCl to pH =1-2 and water was removed *in vacuo*. The mixture was dissolved in ethanol and filter to remove NaCl and L-tryptophan and solvent was removed *in vacuo* to give a yellow viscous oil of $[E_4Try]MeSO_4$ (4 g, 52%). $[E_4Try]MeSO_4$ was stirred with

LiTFSA (6.96 g, 24 mmol) in 50 mL of water for 30 minutes. The product was extracted with $CHCl_3$ (3×50 mL), washed with water (3×50 mL) and dried *in vacuo* to give a light yellow viscous oil of [E_4Try]TFSA (3.55 g, 79%). ^{1}H NMR (400 MHz, $CDCl_3$): δ 10.42 (br, 1/2H, COO*H*), 7.61 (d, $^3J_{HH}$ = 8 Hz, 1H, indol ring(**2.5**)), 7.34 (d, 1H, $^3J_{HH}$ = 8 Hz, 1H, indol ring), 7.15 (s, 1H, indol ring), 7.10 (dd, $^3J_{HH}$ = 7 Hz, 1H, indol ring), 7.03 (dd, $^3J_{HH}$ = 7 Hz, 1H, indol ring), 4.10 (dd, $^3J_{HH}$ = 4 Hz, $^3J_{HH}$ = 10.6 Hz, 1H, NHC*H*), 3.51 (dd, $^3J_{HH}$ = 4 Hz, $^3J_{HH}$ = 14.5 Hz, 1H, NHCHCH_2), 3.18 (q, $^3J_{HH}$ = 7 Hz, 8H, NCH_2CH$_3$), 3.08 (dd, $^3J_{HH}$ = 10.17 Hz, $^3J_{HH}$ = 14.5 Hz, 1H, NHCHCH_2), 1.08 (t, $^3J_{HH}$ = 7 Hz, 12H, NCH$_2$CH_3). ^{13}C {H} NMR (100 MHz, $CDCl_3$): δ 173.94 (*C*OOH), 136.70 (indol ring C9), 127.19 (indol ring C8), 123.58 (indol ring C2), 121.28 (indol ring C4), 119.82 (q, $^1J_{CF}$ = 319 Hz, CF_3), 118.73 (indol ring C5), 117.79 (indol ring C6), 115.07 (symmetric ring C), 114.93 (unique ring C), 111.23 (indol ring C7), 110.12 (indol ring C1), 62.82 (NH*C*H), 45.99 (N*C*H$_2$CH$_3$), 29.32 (NHCH*C*H$_2$), 13.01 (NCH$_2$*C*H$_3$). EIMS (*m/z*): EI MS: Found m/z 383.2445 (M^+); Calcd: 383.2442 (M^+) (M^+). Anal. calcd for 0.79($C_{24}H_{31}N_5O_6S_2F_6$):0.21($C_{22}H_{30}N_4O_2$); C, 48.82; H, 5.37; N, 11.41. Found: C, 49.25; H, 5.44; N, 11.33 (IL:Zwitterion 0.79:0.21).

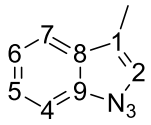

2.5

2.9.16 Bis(diethylamino)-S-(1-carboxy-2-hydroxyphenylethylamino)cyclopropenium bis(trifluoromethanesulfonyl)amide, [C_3(NEt_2)$_2$(NHCOOHC$_2$H$_3$C$_6$H$_5$O))]TFSA, [E_4Tyr]TFSA

[C_3(NEt_2)$_2$(OMe)]$MeSO_4$ (5 g, 16 mmol) was stirred with L-tyrosine (3.65 g, 21 mmol) and NEt_3 (3.23 mL, 21 mmol) in water (50 mL) for an hour. A cold solution of NaOH (8 g in 10 mL water) was added to the aqueous mixture and Et_3N was extracted with diethyl ether (6×50 mL). The solution was acidified with HCl to pH =1-2 and water was removed *in vacuo*. The mixture was dissolved in ethanol and filter to remove NaCl and L-tryptophan and solvent was removed *in vacuo* to give a yellow viscous oil of [E_4Tyr]$MeSO_4$ (5.1 g, 70%). [E_4Tyr]$MeSO_4$ was stirred with LiTFSA (9.14 g, 33 mmol) in 50 mL of water for 30 minutes. The product was extracted with $CHCl_3$ (3×50 mL), washed with water (3×50 mL) and dried *in vacuo* to give a mixture of

[E_4Tyr]TFSA with its methyl and ethyl esters. The mixture was refluxed overnight with conc. HCl (60 mL) to hydrolyze esters and dried *in vacuo*. The product was washed with water (3×50 mL) and dried *in vacuo* to give a light yellow viscous oil of [E_4Tyr]TFSA (6.21 g, 91%). ^{1}H NMR (400 MHz, CD_3OD): δ 7.09 (d, $^3J_{HH}$ = 8.4 Hz, 2H, benzyl ring), 6.72 (d, $^3J_{HH}$ = 8.4 Hz, 2H, benzyl ring), 4.05 (dd, $^3J_{HH}$ = 4 Hz, $^3J_{HH}$ = 10 Hz, 1H, NHC*H*), 3.37 (q, $^3J_{HH}$ = 7 Hz, 1H, NHC*H*$_2$), 3.25 (dd, $^3J_{HH}$ = 4 Hz, $^3J_{HH}$ = 14 Hz, 1H, NHCHC*H*$_2$), 2.83 (dd, $^3J_{HH}$ = 4 Hz, $^3J_{HH}$ = 14 Hz, 1H, NHCHC*H*$_2$), 1.19 (t, $^3J_{HH}$ = 7 Hz, 1H, $NHCH_2CH_3$). ^{13}C {H} NMR (100 MHz, $(CD_3)_3SO_2$): δ 172.91 (*C*OOH), 156.66 (benzyl ring *C* with OH), 130.77 (benzyl ring *C*), 127.51 (benzyl ring *C*), 119.82 (q, $^1J_{CF}$ = 319 Hz, CF_3), 115.55 (symmetric ring *C*), 114.88 (asymmetric ring *C*), 62.61 (NH*C*H), 46.33 ($NHCH_2CH_3$), 37.67 (NHCH*C*H$_2$), 14.39 (NCH_2CH_3). EI MS: Found m/z 360.2290 (M^+); Calcd: 360.2282 (M^+). Anal. calcd for 0.91($C_{22}H_{30}N_4O_7S_2F_6$):0.09($C_{20}H_{29}N_3O_3$); C, 48.82; H, 5.37; N, 11.41. Found: C, 49.25; H, 5.44; N, 11.33 (IL:Zwitterion 0.91:0.09).

2.9.17 Bis(diethylamino)-S-(1-carboxy-2-phenylethylamino)cyclopropenium bis(trifluoromethanesulfonyl)amide, [$C_3(NEt_2)_2(NHCOOHC_2H_3C_6H_5)$]TFSA, [$E_4$Phe]TFSA

[$C_3(NEt_2)_2$(OMe)]$MeSO_4$ (4 g, 12 mmol) was stirred with L-phenylalanine (2.67 g, 16 mmol) and NEt_3 (2.6 mL, 16 mmol) in water (50 mL) for an hour. A cold solution of NaOH (8g in 10 mL water) was added to the aqueous mixture and Et_3N was extracted with diethyl ether (6×50 mL). The solution was acidified with HCl to pH =1-2 and water was removed *in vacuo*. The mixture was dissolved in acetone and filter to remove NaCl and L-phenylalanine and solvent was removed *in vacuo* to give a yellow viscous oil of [E_4Phe]$MeSO_4$ (3 g, 51%). [E_4Phe]$MeSO_4$ was stirred with LiTFSA (6.51 g, 24 mmol) in 50 mL of water for 30 minutes. The product was extracted with $CHCl_3$ (3×50 mL), washed with water (3×50 mL) and dried *in vacuo* to give a light yellow viscous oil of [E_4Phe]TFSA (4.13 g, 85%). ^{1}H NMR (400 MHz, $CDCl_3$): δ 7.96 (br, 1H, COO*H*), 7.29 (m, 5H, phenyl ring), 6.66 (d, $^3J_{HH}$ = 9.2 Hz, 1H, N*H*), 4.1 (ddd, $^3J_{HH}$ = 4 Hz, $^3J_{HH}$ = 9.6 Hz, 1H, NHC*H*), 3.33 (dd, $^3J_{HH}$ = 4 Hz, $^3J_{HH}$ = 14 Hz, 1H, NHCHC*H*$_2$), 3.27 (q, $^3J_{HH}$ = 7 Hz, 8H, NC*H*$_2$), 3.09 (dd, $^3J_{HH}$ = 9.6 Hz, $^3J_{HH}$ = 14 Hz, 1H, NHCHC*H*$_2$), 1.17 (t, $^3J_{HH}$ = 7 Hz, 12H, NCH_2CH_3).^{13}C {H} NMR (100 MHz, $CDCl_3$): δ 173.86 (*C*OOH), 136.32 (phenyl ring), 129.44 (phenyl ring), 128.76 (phenyl ring), 127.26 (phenyl ring), 119.82 (q, $^1J_{CF}$ = 319 Hz, CF_3), 116.15 (symmetric ring *C*), 113.93 (asymmetric ring *C*), 62.37 (NH*C*H), 46.75 (NCH_2), 38.28 (NHCH*C*H$_2$), 13.99 ($NHCH_2CH_3$). EI MS: Found m/z 344.2344 (M^+); Calcd: 344.2333 (M^+).

Anal. calcd for 0.90($C_{21}H_{28}N_4O_6S_2F_6$):0.10($C_{19}H_{28}N_3O_2$); C, 48.82; H, 5.37; N, 11.41. Found: C, 49.25; H, 5.44; N, 11.33 (IL:Zwitterion 0.90:0.10).

2.9.18 Bis(diethylamino)-S-(1-carboxy-2-hydroxyethylamino)cyclopropenium bis(trifluoromethanesulfonyl)amide, [$C_3(NEt_2)_2(NHCOOHC_2H_3CH_2OH)$]TFSA, [$E_4$Ser]TFSA

[$C_3(NEt_2)_2$(OMe)]$MeSO_4$ (4 g, 12 mmol) was stirred with L-serine (1.69 g, 16 mmol) and NEt_3 (2.6 mL, 16 mmol) in water (50 mL) for an hour. A cold solution of NaOH (8g in 10 mL water) was added to the aqueous mixture and Et_3N was extracted with diethyl ether (6×50 mL). The solution was acidified with HCl to pH =1-2 and water was removed *in vacuo*. The mixture was dissolved in acetone and filter to remove NaCl and L-serine and solvent was removed *in vacuo* to give a yellow viscous oil of [E_4Ser]$MeSO_4$ (4.7 g, 92%). [E_4Ser]$MeSO_4$ was stirred with LiTFSA (9.84 g, 33 mmol) in 50 mL of water for 30 minutes. The product was extracted with $CHCl_3$ (3×50 mL), washed with water (3×50 mL) and dried *in vacuo* to give a light yellow viscous oil of [E_4Ser]TFSA (4.13 g, 68%). ^{1}H NMR (400 MHz, $(CD_3)_3SO_2$): δ 8.41 (d, $^3J_{HH}$ = 8 Hz, 1H, NH), 4.027 (m, $^3J_{HH}$ = 8 Hz, NHCH), 3.78 (dd, $^3J_{HH}$ = 4 Hz, $^3J_{HH}$ = 8 Hz, 1H, NHCHC*H*$_2$), 3.78 (dd, $^3J_{HH}$ = 4 Hz, $^3J_{HH}$ = 11 Hz, 1H, NHCHC*H*$_2$), 3.73 (dd, $^3J_{HH}$ = 4 Hz, $^3J_{HH}$ = 11 Hz, 1H, NHCHC*H*$_2$), 3.37 (q, $^3J_{HH}$ = 7 Hz, 8H, NC*H*$_2$), 1.16 (t, $^3J_{HH}$ = 7 Hz, 8H, NCH_2CH_3). ^{13}C {H} NMR (100 MHz, $(CD_3)_3SO_2$): δ 171.94 (*C*OOH)), 119.82 (q, $^1J_{CF}$ = 319 Hz, CF_3), 115.84 (symmetric ring *C*), 115.47 (asymmetric ring *C*), 62.31 (NH*C*H), 62.13 (NHCH*C*H$_2$), 46.29 (N*C*H$_2$), 14.43 ($NHCH_2CH_3$). EI MS: Found m/z 284.1973 (M^+); Calcd: 284.1969 (M^+). Anal. calcd for 0.94($C_{16}H_{26}N_4O_7S_2F_6$):0.06($C_{14}H_{25}N_3O_3$); C, 35.56; H, 4.89; N, 10.21. Found: C, 35.95; H, 4.95; N, 10.11 (IL:Zwitterion 0.94:0.06).

2.9.19 Bis(diethylamino)-S-(1-carboxy-3-carbamoylpropylamino)cyclopropenium bis(trifluoromethanesulfonyl)amide, [$C_3(NEt_2)_2(NH_2COC_2H_3NHCOOH)$]$TFSA_2$, [$E_4$Asn]TFSA

[$C_3(NEt_2)_2$(OMe)]$MeSO_4$ (5 g, 16 mmol) was stirred with L-glutamine (2.26 g, 21 mmol) and NEt_3 (3.23 mL, 21 mmol) in water (50 mL) for an hour. A cold solution of NaOH (8g in 10 mL water) was added to the aqueous mixture and Et_3N was extracted with diethyl ether (6×50 mL). The mixture was dissolved in acetone and filtered to remove NaCl and L-glutamine. The solvent was removed *in vacuo* to give a yellow viscous oil of [E_4Asn]$MeSO_4$ (5.1 g, 78%).

$[E_4Gln]MeSO_4$ was stirred with LiTFSA (10.40 g, 36 mmol) in 50 mL of water and $CHCl_3$ (30 mL) mixture for 30 minutes. The organic layer was washed with water (3×10 mL). The product was dried *in vacuo* to give a light yellow viscous oil of $[E_4Asn]TFSA$ (5.54 g, 78%). ^1H NMR (400 MHz, CD_3OD): δ 4.45 (dd, $^3J_{HH}$ = 9.2 Hz, $^3J_{HH}$ = 4.4 Hz, NHC*H*), 3.44 (q, $^3J_{HH}$ = 7.2 Hz, 8H, NC*H*$_2$), 2.94 (dd, $^3J_{HH}$ = 16 Hz, $^3J_{HH}$ = 4.4 Hz, NHC*H*$_2$), 2.71 (dd, $^3J_{HH}$ = 16 Hz, $^3J_{HH}$ = 8.8 Hz, NHC*H*$_2$), 1.29 (t, $^3J_{HH}$ = 7.2 Hz, 8H, NCH_2CH_3). ^{13}C {H} NMR (100 MHz, CD_3OD): δ 172.59 (*C*OOH), 172.54 (*C*ONH_2), 119.79 (q, $^1J_{CF}$ = 319 Hz, CF_3), 116.11 (symmetric ring *C*), 114.67 (asymmetric ring *C*), 56.29 (NH*C*H), 46.56 (N*C*H_2CH_3), 36.71 (NCH*C*H_2), 13.09 ($NHCH_2CH_3$). EI MS: Found m/z 311.2084 (M^+); Calcd: 311.2078 (M^+). Anal. calcd for $C_{17}H_{27}N_5O_7S_2F_6.1.85H_2O$: C, 32.67; H, 4.95; N, 11.20. Found: C, 33.19; H, 4.48; N, 10.66.

2.9.20 Bis(diethylamino)-S-(1-carboxy-4-carbamoylbutylamino)cyclopropenium bis(trifluoromethanesulfonyl)amide, $[C_3(NEt_2)_2(NH_2COC_3H_5NHCOOH))]TFSA_2$, $[E_4Gln]TFSA$

$[C_3(NEt_2)_2(OMe)]MeSO_4$ (5 g, 16 mmol) was stirred with L-glutamine (2.26 g, 21 mmol) and NEt_3 (3.23 mL, 21 mmol) in water (50 mL) for an hour. A cold solution of NaOH (8g in 10 mL water) was added to the aqueous mixture and Et_3N was extracted with diethyl ether (6×50 mL). The solution was acidified with HCl to pH = 1-2 and water was removed *in vacuo*. The mixture was dissolved in ethanol and filtered to remove NaCl and L-glutamine. The solvent was removed *in vacuo* to give a yellow viscous oil of $[E_4Gln]MeSO_4$ (5.27g, 80%). $[E_4Gln]MeSO_4$ was stirred with LiTFSA (10.33 g, 36 mmol) in 50 mL of water and $CHCl_3$:CH_3CN 3:1 (30 mL) mixture for 30 minutes. The organic layer was washed with water (3×10 mL). The product was dried *in vacuo* to give a light yellow viscous oil of $[E_4Gln]TFSA_2$ (3 g, 62%). EI MS: Found m/z 325.2240 (M^+); Calcd: 325.2234 (M^+). Anal. calcd for $0.95(C_{31}H_{48}N_8O_{11}S_4F_{14})$:$0.05(C_{29}H_{47}N_7O_7S_2F_6)$: C, 35.81; H, 4.66; N, 10.72. Found: C, 35.67; H, 4.84; N, 10.3 (IL (2 tac):Zwitterion 0.95:0.05) or (IL(1tac):Zwitterion 0.95:.05).

2.9.21 Tetrakis(diethylamino)-bis(bis(diethylamino)cyclopropenium)-S-(1-carboxy-5-aminopentylamine)cyclopropenium bis(trifluoromethanesulfonyl)amide, $[C_3(NEt_2)_2(NHCOOHC_5H_9NH)\ C_3(NEt_2)_2]TFSA_2$, $[E_8Lys]TFSA_2$

$[C_3(NEt_2)_2(OMe)]MeSO_4$ (5 g, 16 mmol) was stirred with L-lysine (1.12 g, 8 mmol) and NEt_3 (3.87 mL, 25 mmol) in water (50 mL) for an hour. A cold solution of NaOH (8 g in 10 mL water)

was added to the aqueous mixture and the Et_3N was extracted with diethyl ether (6×50 mL). The solution was acidified with HCl to pH = 1-2 and water was removed *in vacuo*. The mixture was dissolved in ethanol and filtered to remove NaCl and L-lysine and the solvent was removed *in vacuo* to give a yellow viscous oil of mixture of $[E_4Lys]MeSO_4$ (**2.7**) and $[E_8Lys](MeSO_4)_2$ (**2.6**) (3.86g). The mixture containing $[E_4Lys]MeSO_4$ (**2.7**) and $[E_8Lys](MeSO_4)_2$ (**2.6**) was stirred with LiTFSA (4.36 g, 15 mmol) in 50 mL of water for 30 minutes. The water was then removed *in vacuo* and the reaction mixture was dissolved in $CHCl_3$:CH_3CN 2:1 (50 mL) and washed with conc. HCl (3×50 mL) and dried *in vacuo* to give a light yellow viscous oil of $[E_8Lys]TFSA_2$ (1.32 g, 95%). ^{1}H NMR (400 MHz, CD_3CN): δ 6.41 (d, $^3J_{HH}$ = 8 Hz, 1H, N*H*), 6.17 (t, $^3J_{HH}$ = 8 Hz, 1H, N*H*), 4.00 (ddd, 1H, NHC*H*), 3.39 (m, $^3J_{HH}$ = 8 Hz, 16H, NC$H_2$$CH_3$), 3.28 (q, $^3J_{HH}$ = 8 Hz, 2H, NCHCH_2), 1.96 (m, 1H, CH_2), 1.82 (m, 1H, CH_2), 1.65 (m, 2H, CH_2), 1.52 (m, 2H, CH_2), 1.22 (t, $^3J_{HH}$ = 8 Hz, 24H, CH_2CH_3). ^{13}C {H} NMR (100 MHz, CD_3CN) δ 1752.84 (*C*OOH), 120.82 (q, $^1J_{CF}$ = 319 Hz, CF_3), 117.62 (symmetric ring C), 116.85 (symmetric ring C), 115.84 (unique ring C), 114.485 (unique ring C), 60.13 (N*C*H), 47.44 (N*C*$H_2$$CH_3$), 47.36 (N*C*$H_2$$CH_3$), 46.92 (N*C*$H_2$**),** 32.29 (NCH*C*$H_2$), 30.39 (N$CH_2$*C*$H_2$**),** 23.21 (*C*$H_2$), 14.42 (N$CH_2$*C*$H_3$), 14.36 (N$CH_2$*C*$H_3$). EI MS: Found m/z 252.2080 (M^{2+}); Calcd: 252.2070 (M^{2+}). Anal. calcd for $C_{32}H_{52}N_8O_{10}S_4F_{12}$; C, 36.09; H, 4.92; N, 10.52. Found: C, 36.36; H, 5.05; N, 10.45.

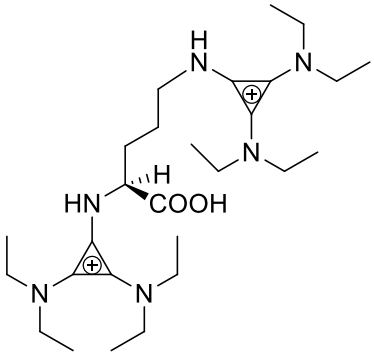

2.6

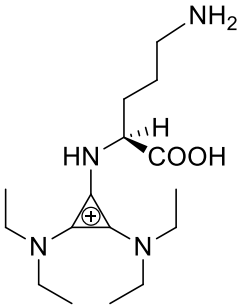

2.7

2.10 Synthesis of Tris(diethylamino)cyclopropenium salts

2.10.1 Tris(diethylamino)cyclopropenium *p*-toluenesulfonate, $[C_3(NEt_2)_3][MeC_6H_4SO_3]$, $[E_6]OTs$

$[C_3(NEt_2)_3]Cl$ (4.99 g, 17 mmol) was stirred with *para*-toluenesulfonic acid (29.88 g, 173 mmol) in H_2O (200 mL). The product was extracted with chloroform (100 mL), washed with H_2O (3 ×100 mL) and dried *in vacuo* to yield an orange liquid (6.59 g, 90%). ^1H NMR ($CDCl_3$, 500 MHz): δ 7.70 (d, $^3J_{HH}$ = 1.5 Hz, 2H, CH), 6.98 (d, $^3J_{HH}$ = 8.5 Hz, 2H, CH), 3.407 (q, $^3J_{HH}$ = 7.16 Hz, 12H, NCH_2), 2.20 (s, 3H, $C_6H_4CH_3$), 1.264 (t, $^3J_{HH}$ = 7.0 Hz, 18H, NCH_2CH_3). ^{13}C NMR ($CDCl_3$, 126 MHz): δ 144.46 (CSO_3), 137.38 (CH), 127.39 (CH), 125.52 (CCH_3). 116.128 (C_3), 47.172 (CH_2), 14.423 (CH_3). EI MS: Found m/z 252.2434 (M^+); Calcd: 252.2434 (M^+). Anal. calcd for $C_{22}H_{37}N_3O_3S$: C, 61.72; H, 8.83; N, 9.81. Found: C, 61.73; H, 9.23; N, 9.83. With water content of $[E_6]OTs.0.25H_2O$.

2.10.2 Tris(diethylamino)cyclopropenium trifluoromethanesulfonate, $[C_3(NEt_2)_3]OTf$, $[E_6]OTf$

$[C_3(NEt_2)_3]Cl$ (3.58 g, 13 mmol) was stirred with LiOTf (5.83 g, 37 mmol) in H_2O (200 mL). The product was extracted with dichloromethane (100 mL), washed with H_2O (3 ×100 mL) and dried *in vacuo* to yield a yellow solid (4.51 g, 90%). ^1H NMR ($CDCl_3$, 300 MHz): δ 3.22 (q, $^3J_{HH}$ = 7.2 Hz, 12H, NCH_2), 1.10 (t, $^3J_{HH}$ = 4.9 Hz, 18H, NCH_2CH_3). ^{13}C NMR ($CDCl_3$, 126 MHz): δ 120.39 (q, $^1J_{CF}$ = 322 Hz, CF_3). δ 115.57 (C3), 46.40 (CH_2), 13.57 (CH_3). Anal. calcd for $C_{16}H_{30}N_3O_3SF_3$: C, 47.86; H, 7.53; N, 10.47. Found: C, 48.03; H, 7.65; N, 10.44. MS^+ as for $[C_3(NEt_2)_3]Cl$.

2.10.3 Tris(diethylamino)cyclopropenium iodide, $[C_3(NEt_2)_3]I$, $[E_6]I$

$[C_3(NEt_2)_3]Cl$ (1.15 g, 4 mmol) was heated to reflux with ethyl iodide (6.43 mL, 80 mmol) for 20 h in an inert atmosphere. Unreacted ethyl iodide was distilled out and the residue was dissolved in dichloromethane (20 mL) and washed with water (3 ×10 mL). Dichloromethane was removed *in vacuo* to give orange crystals (1.2 g, 79%). ^1H NMR (500 MHz, $CDCl_3$): δ 3.44 (q, $^3J_{HH}$ = 7 Hz, 12H, NCH_2), 1.30 (t, $^3J_{HH}$ = 7 Hz, 18H, NCH_2CH_3). $^{13}C\{^1H\}$ NMR (126 MHz, CD_3CN): δ 116.13 (ring C), 47.17 (NCH_2CH_3), 14.42 (NCH_2CH_3). Anal. calcd for $C_{15}H_{30}N_3I$: I, 33.45. Found (ion chromatography): I, 32.35. Chloride content was determined by ion chromatography

to be 14 ppm. Anal. calcd for $C_{15}H_{30}N_3I$: C, 47.49; H, 8.35; N, 10.72. Found: C, 48.44; H, 7.97; N, 11.07. MS^+ as for $[C_3(NEt_2)_3]Cl$.

2.10.4 Tris(diethylamino)cyclopropenium pentafluorophenoxide, $[C_3(NEt_2)_3]F_5C_6O$, $[E_6]F_5C_6O$

Sodium pentafluorophenoxide was prepared from pentafluorophenol by a known method[9]. $[C_3(NEt_2)_3]Cl$ (5.37 g, 19 mmol) was refluxed overnight with sodium pentafluorophenoxide (12 g, 57 mmol) in water (50 mL). The product was extracted with $CHCl_3$ (3×50 mL), and the organic phase was washed with water (3×50 mL). The product was dried *in vacuo* to yield a brown solid (8 g, 98%). ^1H, ^{13}C NMR and MS^+ as for $[C_3(NEt_2)_3]Cl$ with no additional peak in ^{13}C NMR due to anion. Anal. calcd for $C_{21}H_{30}N_3F_5O.1.5H_2O$: C, 54.53; H, 7.19; N, 9.08, F, 20.53 Found: C, 55.00; H, 6.66; N, 8.67, F, 22.44.

2.10.5 Tris(diethylamino)cyclopropenium tetrachloroferrate(III), $[C_3(NEt_2)_3]FeCl_4$, $[E_6]FeCl_4$

Dried $[C_3(NEt_2)_3]Cl$ (3 g, 15 mmol) was stirred overnight with anhydrous $FeCl_3$ (1.7 g, 15 mmol) in MeOH (50 mL). The product was dried *in vacuo* to yield a dark brown solid (4.36 g, 67%). MS^+ as for $[C_3(NEt_2)_3]Cl$. Anal. calcd for $C_{15}H_{31}N_3FeCl_4O_{0.5}$: C, 39.24; H, 6.8; N, 9.15, Cl, 30.89 Found: C, 39.27; H, 6.65; N, 8.98, Cl, 31.3.

2.10.6 Tris(diethylamino)cyclopropenium trichlorostannate(II), $[C_3(NEt_2)_3]SnCl_3$, $[E_6]SnCl_3$

Dried $[C_3(NEt_2)_3]Cl$ (3 g, 15 mmol) was stirred overnight with $SnCl_2.2H_2O$ (2.35 g, 10 mmol) in MeOH (50 mL). The product was dried *in vacuo* to yield a light yellow solid (4.9 g, 96%). MS^+ as for $[C_3(NEt_2)_3]Cl$. Anal. calcd for $C_{15}H_{32}N_3SnCl_3O$: C, 36.36; H, 6.50; N, 8.48, Cl, 21.46 Found: C, 36.77; H, 6.27; N, 8.49, Cl, 22.37.

2.10.7 Tris(diethylamino)cyclopropenium tetrachlorozincate(II), $[C_3(NEt_2)_3]_2ZnCl_4$, $[E_6]_2ZnCl_4$

Dried $[C_3(NEt_2)_3]Cl$ (5 g, 17 mmol) was stirred overnight with anhydrous $ZnCl_2$ (1.18 g, 8.5 mmol) in MeOH (50 mL). The product was dried *in vacuo* to yield a light brown solid (4.36 g,

81%). MS^+ as for $[C_3(NEt_2)_3]Cl$. Anal. calcd for $C_{30}H_{61}N_6ZnCl_4O_{0.5}$: C, 49.97; H, 8.52; N, 11.65, Cl, 19.66 Found: C, 49.83; H, 8.72; N, 11.59, Cl, 20.51.

2.10.8 Tris(diethylamino)cyclopropenium tetrachlorocuprate(II), $[C_3(NEt_2)_3]_2CuCl_4$, $[E_6]_2CuCl_4$

Dried $[C_3(NEt_2)_3]Cl$ (3 g, 10 mmol) was stirred overnight with anhydrous $CuCl_2$ (0.7 g, 5 mmol) in MeOH (50 mL). The product was dried *in vacuo* to yield a orange solid (3.2 g, 90%). MS^+ as for $[C_3(NEt_2)_3]Cl$. Anal. calcd for $C_{30}H_{60}N_6CuCl_4$: C, 50.73; H, 8.51; N, 11.83, Cl, 19.96 Found: C, 50.84; H, 8.78; N, 11.97, Cl, 18.66.

2.11 Synthesis of Tris(dibutylamino)cyclopropenium salts

2.11.1 Tris(dibutylamino)cyclopropenium tetracyanoborate, $[C_3(NBu_2)_3]B(CN)_4$, $[B_6]B(CN)_4$

1-Ethyl-3-methylimidazolium tetracyanoborate (2.43 g, 11 mmol) was stirred with $[C_3(NBu_2)_3]Cl$ (5.62 g, 12 mmol) in water (50 mL) at 60 °C overnight. The product was extracted with diethyl ether (3 ×10 mL) and then washed with water. The solvent was removed *in vacuo* to give a yellow liquid (4.86 g, 81%). ^1H NMR (500 MHz, $CDCl_3$): δ 3.28 (t, $^3J_{HH}$ = 8 Hz, 12H, NCH_2), 1.62 (m, 12H, NCH_2CH_2), 1.34 (m, 12H, $NCH_2CH_2CH_2$), 0.98 (t, $^3J_{HH}$ = 8 Hz, 18H, $NCH_2CH_2CH_2CH_3$). ^{13}C {^1H} NMR (126 MHz, $CDCl_3$): δ 122.66 (q, $^1J_{CB}$ = 71.6 Hz, $[B(CN)4]^-$), 116.28 (ring C), 52.81 (NCH_2), 30.79 (NCH_2CH_2), 19.57 ($NCH_2CH_2CH_2$), 13.46 ($NCH_2CH_2CH_2CH_3$). EI MS: Found m/z 420.4324 (M^+); Calcd: 420.4312 (M^+). Anal. calcd for $C_{31}H_{54}N_7B$: C, 69.51; H, 10.16; N, 18.30. Found: C, 69.75; H, 10.30; N, 18.48. With water content of 315 ppm.

2.11.2 Tris(dibutylamino)cyclopropenium tris(pentafluoroethyl)trifluorophosphate, $[C_3(NBu_2)_3]FAP$, $[B_6]FAP$

1-Ethyl-3-methylimidazolium tris(pentafluoroethyl)trifluorophosphate (3.85 g, 7 mmol) was stirred with $[C_3(NBu_2)_3]Cl$ (3.48 g, 8 mmol) in 50 mL of water at 60 °C overnight. The product was extracted with diethyl ether (3 ×10 mL) and then washed with water. The solvent was removed *in vacuo* to give a yellow liquid (5.26 g, 88%). ^1H NMR (500 MHz, $CDCl_3$): δ 3.23 (t, $^3J_{HH}$ = 8 Hz, 12H, NCH_2), 1.58 (m, 12H, NCH_2CH_2), 1.31 (m, 12H, $NCH_2CH_2CH_2$), 0.95 (t, $^3J_{HH}$

= 8 Hz, 18H, NCH_2 $CH_2CH_2CH_3$). ^{13}C NMR (126 MHz, $CDCl_3$): δ 116.35 (ring C), 52.72 (NCH_2), 30.71 (NCH_2CH_2), 19.80 ($NCH_2CH_2CH_2$), 13.6 ($NCH_2CH_2CH_2CH_3$). ^1H, $^{13}C\{^1H\}$ NMR and MS^+ as for $[C_3(NBu_2)_3]^+$. Anal. calcd for $C_{33}H_{54}N_3PF_{18}$: C, 45.79; H, 6.28; N, 4.85. Found: C, 46.72; H, 6.48; N, 4.77. With water content of 347 ppm.

2.11.3 Tris(dibutylamino)cyclopropenium tetrachloroferrate(III), $[C_3(NBu_2)_3]FeCl_4$, $[B_6]FeCl_4$

Dried $[C_3(NBu_2)_3]Cl$ (3 g, 7 mmol) was stirred overnight with anhydrous $FeCl_3$ (1.48 g, 7 mmol) in MeOH (50 mL). The product was dried *in vacuo* to yield a dark brown liquid (4.36 g, 77%). MS^+ as for $[C_3(NBu_2)_3]Cl$. Anal. calcd for $C_{27}H_{55}N_3FeCl_4O_{0.5}$: C, 51.68; H, 8.83; N, 6.69, Cl, 22.60 Found: C, 51.58; H, 8.90; N, 6.69, Cl, 23.50.

2.11.4 Tris(dibutylamino)cyclopropenium trichlorostannate(II), $[C_3(NBu_2)_3]SnCl_3$, $[B_6]SnCl_3$

Dried $[C_3(NBu_2)_3]Cl$ (3 g, 7 mmol) was stirred overnight with $SnCl_2.2H_2O$ (1.48 g, 7 mmol) in MeOH (50 mL). The product was dried *in vacuo* to yield a light yellow liquid (3.74 g, 83%). MS^+ as for $[C_3(NBu_2)_3]Cl$. Anal. calcd for $C_{15}H_{32}N_3SnCl_3O$: C, 36.36; H, 6.5; N, 8.48, Cl, 21.46 Found: C, 36.77; H, 6.27; N, 8.49, Cl, 22.37.

2.11.5 Tris(dibutylamino)cyclopropenium tetrachlorozincate(II), $[C_3(NBu_2)_3]_2ZnCl_4$, $[B_6]_2ZnCl_4$

Dried $[C_3(NBu_2)_3]Cl$ (3 g, 7 mmol) was stirred overnight with anhydrous $ZnCl_2$ (0.45 g, 3 mmol) in MeOH (50 mL). The product was dried *in vacuo* to yield a light brown liquid (3.29 g, 85%). MS^+ as for $[C_3(NBu_2)_3]Cl$. Anal. calcd for $C_{30}H_{61}N_6ZnCl_4O_{0.5}$: C, 49.97; H, 8.52; N, 11.65, Cl, 19.66 Found: C, 49.83; H, 8.72; N, 11.59, Cl, 20.51.

2.11.6 Tris(dibutylamino)cyclopropenium tetrachlorozincate(II), $[C_3(NBu_2)_3]_2CuCl_4$, $[B_6]_2CuCl_4$

Dried $[C_3(NBu_2)_3]Cl$ (3 g, 7 mmol) was stirred overnight with anhydrous $CuCl_2$ (0.44 g, 3 mmol) in MeOH (50 mL). The product was dried *in vacuo* to yield a orange liquid (3.09 g, 80%). MS^+ as

for $[C_3(NBu_2)_3]Cl$: Anal. calcd for $C_{54}H_{110}N_6CuCl_4O_1$: C, 60.91; H, 10.41; N, 7.89, Cl, 13.31 Found: C, 60.72; H, 10.63; N, 7.93, Cl, 13.29.

2.12 Synthesis of 1,1,3,3-Tetrakis(dialkylamino)allyl salts

2.12.1 Purification of bis(dimethylamino)cyclopropenone, $C_3(NMe_2)_2O$, M_4O

During the synthesis of bis(dimethylamino)cyclopropenone one of the challenges encountered was the removal of the open-ring side product. Initially, the solution was acidified to give the more water-soluble dication of the open ring (**2.1**); however, the cycopropenone was also protonated.

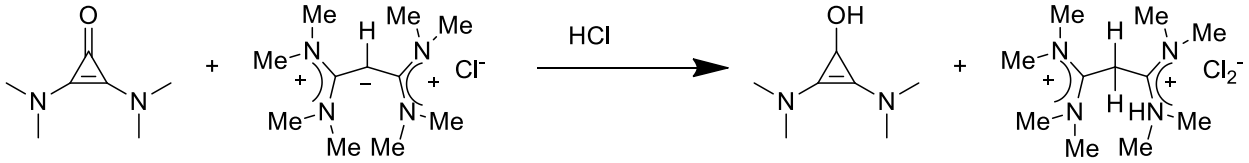

I found that the protonated cyclopropenone was not soluble in acetone and this made possible its separation from the open ring. Protonated cyclopropenone can be easily deprotonated with a base.

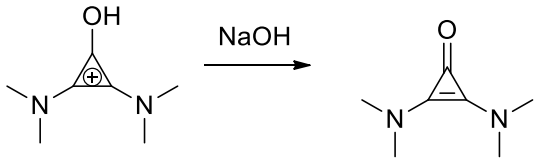

2.12.2 1,1,3,3-Tetrakis(dimethylamino)allyl chloride, $[(Me_2HN)CCH_2C(NHMe_2)]Cl_2$, $[M_8]Cl_2$[6]

Pentachlorocyclopropane (6.91 mL, 49 mmol) was added dropwise to a stirred solution of Me_2NH (40% solution in water) (44 g, 392 mmol) at 0 °C for an hour. Solution was left on stirring overnight at ambient temperature. Product mixture resulted in open ring[7] product (**1**) with $[C_3(NMe_2)_3)]Cl$ and $[Me_2NH_2]Cl$. The mixture was acidified and was kept in freezer after dissolving in acetone and kept in freezer to crystallize out white crystals of $[(Me_2HN)_2CCHC(NHMe_2)_2]Cl_2.2CHCl_3$.[6] The $[(Me_2HN)_2CCHC(NHMe_2)_2]Cl_2.2CHCl_3$ was characterized by x-ray. EI MS: Found m/z 213.2075 (M^+); Calcd: 213.2074 (M^+).

2.12.3 1,1,3,3-Tetrakis(butylamino)allyl chloride, $[(BuHN)_2CCH_2C(NHBu)_2]Cl_2$, $[B_8]Cl_2$

H_2N^nBu (55.00 mL, 56 mmol) was added dropwise to a stirred solution of Cl_5C_3H (8.90 mL, 69 mmol), in CH_2Cl_2 (150 mL) at 0 °C in an inert atmosphere and then the mixture was stirred overnight followed by reflux for 5 hours. After rotavaping the CH_2Cl_2 off, the mixture was dissolved in $CHCl_3$ (50 mL) and ammonium salts were extracted with water (3×50 mL), then the $CHCl_3$ layer was taken and extract product with water (3×50 mL) to get light brown viscous oil (13 g, 47%). ^{1}H NMR (500 MHz, D_2O): δ 4.03 (s, < 2H, CC*H*$_2$C), 3.30 (t, $^3J_{HH}$ = 7.5 Hz, 4H, NC*H*$_2$), 3.25 (t, $^3J_{HH}$ = 7.0 Hz, 4H, NC*H*$_2$), 1.53 (m, 8H, NCH_2CH_2), 1.27 (m, 8H, $NCH_2CH_2CH_2$), 0.82 (two triplets overlapping, 12H, NCH_2 CH_2 CH_2CH_3). ^{13}C {^{1}H} NMR (126 MHz, D_2O): δ 158.15 (equivalent allyl atoms), 44.48 (NCH_2), 42.83 (NCH_2), 31.03 (NCH_2CH_2), 28.69 (NCH_2CH_2), 19.64 ($NCH_2CH_2CH_2$), 19.40 ($NCH_2CH_2CH_2$), 13.05 ($NCH_2CH_2CH_2CH_3$), 12.98 ($NCH_2CH_2CH_2CH_3$). EIMS (*m/z*): found 163.1701 (M^{2+}), 325.3327 (M^+): Calcd. 163.1699 (M^{2+}), 325.3326 (M^+). Mass spec suggested the ratio of M^+:M^{2+} is 3:1. Anal. calcd for $C_{19}H_{43}N_4O_{0.5}Cl_2$: C, 56.12; H, 10.65; N, 13.78. Found: C, 55.65; H, 10.72; N, 13.82. With water content of 241 ppm.

2.12.4 1,1,3,3-Tetrakis(butylamino)allyl bis(trifluoromethanesulfonyl)amide, $[(BuHN)_2CCH_2C(NHBu)_2]TFSA$, $[B_8]TFSA_2$

$[(BuHN)_2CCH_2C(NHBu)_2]Cl_2$ (2.0 g, 5 mmol) was stirred with LiTFSA (4.33 g, 15 mmol) in water (10 mL) for 1 h. The product was extracted with $CHCl_3$ (3 ×10 mL) and solvent is removed *in vacuo* to give viscous liquid (3 g, 67%). ^{1}H, ^{13}C {^{1}H} NMR and MS similar to $[(BuHN)_2CCH_2C(NHBu)_2]^+$ cation however additional peaks for TFSA anion were seen in ^{13}C {^{1}H} NMR. Mass spec suggested the ratio of M^+:M^{2+} is 1:1.Anal. calcd for $C_{23}H_{42}N_6O_8F_{12}S_4$: C, 31.15; H, 4.77; N, 9.47. Found: C, 31.86; H, 4.91; N, 9.26.

References

1. Dietrich, A. *Am. Lab*. **1994,** *36*.
2. Pangborn, A. B.; Giardello, M. A.; Grubbs, R. H.; Rosen, R. K.; Timmers, F. J. *Organometallics* **1996,** *15*, 1518.
3. Tobey, S. W.; West, R. *J. Am. Chem. Soc.* **1965**, 2478.

4. (a) Lucier, J. J.; Harris, D. A.; Korosec, S. P. **1964,** *44*, 72; (b) Wawzonek, S.; Mckillip, W.; Peterson, C. **1964,** *44*, 75.
5. Leffler, M. T. *Organic Synthesis* **1938,** *18*, 5.
6. (a) Yoshida, Z. i.; Tawara, Y. *J. Am. Chem. Soc.* **1971**, 2573; (b) Taylor, M. J.; Surman, P. W. J.; Clark, G. R. *J. Chem. Soc., Chem. Commun.* **1994**, 2517.
7. Yoshida, Z.; Konishi, H.; Tawara, Y.; Nishikawa, K.; Ogoshi, H. *Tetra. Lett.* **1973,** (28), 2619.
8. Wilcox, C.; Breslow, R. *Tetrahedron Lett.* **1980,** *21*, 3241.
9. Pasquale, R. J. D.; Tamborski, C. **1967,** *32*, 3163.

Physical Properties

Results

The discovery of a new IL is easy but to determine its usefulness as a solvent requires knowledge of the physical and chemical properties-if a new material needs to be accepted as a useful material. Chemists must present reliable data on the physico-chemical properties needed by engineers to design processes and devices.

*M=soluble or miscible, N= insoluble or immiscible

The units of the tabulated physic-chemical properties are stated here;

Physical Property	**Abbreviation**	**Units**
Glass transition temperature	T_g	°C
Solid-solid transition	$T_{s\text{-}s}$	°C
Melting point	T_m	°C
Enthalpy Change	ΔH	kJ/mol
Decomposition Temperature	$T_d(1)$	1 °C/min
Decomposition Temperature	$T_d(10)$	10 °C/min
Chloride Content	Chloride	ppm
Temperature	T	°C
Viscosity	η	mPa s
Conductivity	σ	mS cm^{-1}
Density	ρ	g mL^{-1}
Specific Rotation	$[\alpha]_D^{20}$	°
Molecular weight	M_w	g/mol
Molar Magnetic Susceptibility	χ_M	emu mol^{-1}
Molar Magnetic Susceptibility measured at 300 K	χ_T	emu K mol^{-1}
Effective magnetic moment	μ_{eff}	μ_B

3.2 C_s Cations

3.1.1 Bis(dimethylamino)ethylaminocyclopropenium bis(trifluoromethanesulfonyl)amide, [$C_3(NMe_2)_2(NEtH)$]TFSA, [M_4EH]TFSA

Physical State	T_g	T_{s-s}	**ΔH**	T_m	**ΔH**	T_d**(1)**	T_d**(10)**	***Chloride***
Viscous Liquid	−71.7	---	---	---	---	276	335	343

T	**20**	**30**	**40**	**50**	**60**	**70**	**80**	**90**
η	143.5	79.7	47.8	31.9	21.7	15.5	12	9.09
σ	1.37	2.29	3.59	5.22	7.17	9.46	12.07	14.99
ρ	1.401	1.391	1.382	1.373	1.363	1.354	1.343	1.335

Miscibility	**H_2O**	**MeOH**	**Et_2O**	**Toluene**	**Hexane**
	N	M	M ≥ 50% IL	M ≥ 50% IL	M ≥ 50% IL

3.1.2 Bis(dimethylamino)ethylmethylaminocyclopropenium bis(trifluoromethanesulfonyl)amide, [$C_3(NMe_2)_2(NEtMe]$TFSA, [M_5E]TFSA

Physical State	T_g	T_{s-s}	**ΔH**	T_m	**ΔH**	T_d**(1)**	T_d**(10)**	***Chloride***
Solid	---	−6.0	4.5	63.2	46.5	211	315	125
	---	32.2	6.2	---	---			

T	**70**	**75**	**80**	**85**	**90**
η	13.6	12	10.6	9.71	8.58

Miscibility	**H_2O**	**MeOH**	**Et_2O**	**Toluene**	**Hexane**
	N	M	N	N	N

3.1.3 Bis(dimethylamino)allylaminocyclopropenium bis(trifluoromethanesulfonyl)amide, $[C_3(NMe_2)_2(HN(CH_2CHCH_2))]TFSA$, $[M_4AH]TFSA$

Physical State	T_g	$T_{s\text{-}s}$	**ΔH**	T_m	**ΔH**	T_d**(1)**	T_d**(10)**	***Chloride***
Viscous Liquid	−71.3	---	---	---	---	284	326	297

T	**20**	**30**	**40**	**50**	**60**	**70**	**80**	**90**
η	153.2	84.8	51.3	33.3	22.5	16.1	12.1	9.35
σ	1.20	2.02	3.18	4.64	6.42	8.51	10.91	13.52
ρ	1.393	1.384	1.374	1.365	1.356	1.346	1.337	1.328

Miscibility	**H_2O**	**MeOH**	**Et_2O**	**Toluene**	**Hexane**
	N	M	M ≥ 50% IL	M ≥ 40% IL	N

3.1.4 Bis(dimethylamino)allylmethylaminocyclopropenium bis(trifluoromethanesulfonyl)amide, $[C_3(NMe_2)_2(N(CH_2CHCH_2)Me)]TFSA$, $[M_5A]TFSA$

Physical State	T_g	$T_{s\text{-}s}$	**ΔH**	T_m	**ΔH**	T_d**(1)**	T_d**(10)**	***Chloride***
Viscous Liquid	---	---	---	14.8	109.7	241	344	332

T	**20**	**30**	**40**	**50**	**60**	**70**	**80**	**90**
η	69.0	43.5	28.6	19.7	14.3	10.9	8.38	6.69
σ	2.96	4.47	6.49	8.83	11.52	14.54	17.84	21.80
ρ	1.372	1.362	1.353	1.343	1.334	1.325	1.316	1.307

Miscibility	**H_2O**	**MeOH**	**Et_2O**	**Toluene**	**Hexane**
	N	M	M ≥ 50% IL	M ≥ 50% IL	N

3.1.5 Bis(dimethylamino)allylmethylaminocyclopropenium dicyanamide, $[C_3(NMe_2)_2(N(CH_2CHCH_2)Me)]DCA$, $[M_5A]DCA$

Physical State	T_g	$T_{s\text{-}s}$	ΔH	T_m	ΔH	T_d(1)	T_d(10)	*Chloride*
Viscous Liquid	−61.8					233	258	5351

T	20	30	40	50	60	70	80	90
σ	4.10	6.85	10.54	15.37	21.0	27.4	34.5	42.1

Miscibility	H_2O	MeOH	Et_2O	Toluene	Hexane
	M	M	M ≥ 50% IL	M ≥ 50% IL	N

3.1.6 Bis(dimethylamino)propylaminocyclopropeniumbis(trifluoromethanesulfonyl)amide, $[C_3(NMe_2)_2(N(CH_2CH_2CH_3)H)]TFSA$, $[M_4PrH]TFSA$

Physical State	T_g	$T_{s\text{-}s}$	ΔH	T_m	ΔH	T_d(1)	T_d(10)	*Chloride*
Viscous Liquid	−71.5	---	---	---	---	236	293	168

T	20	30	40	50	60	70	80	90
η	156.8	86.8	52.1	34.1	23.5	16.7	12.1	9.55
σ	1.08	1.85	2.88	4.22	5.90	7.92	10.20	12.80
ρ	1.373	1.364	1.354	1.345	1.336	1.327	1.317	1.308

Miscibility	H_2O	MeOH	Et_2O	Toluene	Hexane
	N	M	M ≥ 40% IL	M ≥ 50% IL	N

3.1.7 Bis(dimethylamino)propylmethylaminocyclopropenium bis(trifluoromethanesulfonyl)amide, [$C_3(NMe_2)_2(N(CH_2CH_2CH_3)Me)$]TFSA, [$M_5Pr$]TFSA

Physical State	T_g	$T_{s\text{-}s}$	**ΔH**	T_m	**ΔH**	T_d**(1)**	T_d**(10)**	***Chloride***
Viscous Liquid	---	---	---	19.7	105.9	247	291	20
T	**20**	**30**	**40**	**50**	**60**	**70**	**80**	**90**
η	72.5	45.2	29.6	20.0	14.6	11.2	8.68	6.90
σ	2.71	4.17	6.07	8.30	10.83	13.76	16.95	20.6
ρ	1.356	1.346	1.337	1.328	1.319	1.309	1.301	1.292

Miscibility	**H_2O**	**MeOH**	**Et_2O**	**Toluene**	**Hexane**
	N	M	M ≥ 50% IL	M ≥ 50% IL	N

3.1.8 Bis(dimethylamino)propylmethylaminocyclopropenium dicyanamide, [$C_3(NMe_2)_2(N(CH_2CH_2CH_3)Me)$]DCA, [$M_5Pr$]DCA

Physical State	T_g	$T_{s\text{-}s}$	**ΔH**	T_m	**ΔH**	T_d	T_d	***Chloride***
Viscous Liquid	−73.6	---	---	---	---	233	257	2089
T	**20**	**30**	**40**	**50**	**60**	**70**	**80**	**90**
η	107.3	61.3	38.2	25.1	17.5	12.8	10.1	8.02
σ	3.17	5.42	8.44	12.38	16.90	22.50	28.30	35.0
ρ	1.045	1.039	1.032	1.025	1.019	1.013	1.007	1.001

Miscibility	**H_2O**	**MeOH**	**Et_2O**	**Toluene**	**Hexane**
	M	M	N	M ≥ 83% IL	N

3.1.9 Bis(dimethylamino)-N-(methoxyethyl)aminocyclopropenium bis(trifluoromethanesulfonyl)amide, $[C_3(NMe_2)_2(N(CH_2CH_2OCH_3)H)]TFSA$, $[M_4ErH]TFSA$

Physical State	T_g	T_{s-s}	**ΔH**	T_m	**ΔH**	T_d**(1)**	T_d**(10)**	***Chloride***
Viscous Liquid	−64.3	---	---	---	---	283	336	633
T	**20**	**30**	**40**	**50**	**60**	**70**	**80**	**90**
η	214.5	112.4	62.8	37.6	26.6	18.7	13.3	10.2
σ	0.813	1.46	2.45	3.71	5.28	7.17	9.35	11.83
ρ	1.392	1.383	1.373	1.363	1.354	1.345	1.336	1.327

Miscibility	**H_2O**	**MeOH**	**Et_2O**	**Toluene**	**Hexane**
	N	M	M ≥ 40% IL	M ≥ 40% IL	N

3.1.10 Bis(dimethylamino)-N-(methoxyethyl)methylaminocyclopropenium bis(trifluoromethanesulfonyl)amide, $[C_3(NMe_2)_2(N(CH_2CH_2OCH_3)Me)]TFSA$, $[M_5Er]TFSA$

Physical State	T_g	T_{s-s}	**ΔH**	T_m	**ΔH**	T_d**(1)**	T_d**(10)**	***Chloride***
Viscous Liquid	−73.5	---	---	---	---	289	326	79
T	**20**	**30**	**40**	**50**	**60**	**70**	**80**	**90**
η	92.5	55.6	36.2	24.3	17.5	12.6	9.71	7.66
σ	1.98	3.20	4.74	6.73	8.98	11.50	14.41	17.45
ρ	1.378	1.368	1.356	1.349	1.339	1.330	1.321	1.312

Miscibility	H_2O	MeOH	Et_2O	Toluene	Hexane
	N	M	M ≥ 50% IL	M ≥ 50% IL	N

3.1.11 Bis(dimethylamino)-N-(methoxyethyl)methylaminocyclopropenium dicyanamide, $[C_3(NMe_2)_2(N(CH_2CH_2OCH_3)Me)]DCA$, $[M_5Er]DCA$

Physical State	T_g	T_{s-s}	ΔH	T_m	ΔH	T_d(1)	T_d(10)	*Chloride*
Viscous Liquid	−69.3	---	---	29.1	236.1	244	310	1158
T	**20**	**30**	**40**	**50**	**60**	**70**	**80**	**90**
η	127.7	67.9	39.0	24.5	16.6	12.1	9.25	7.15
σ	2.42	4.33	6.96	10.47	14.57	19.32	25.00	31.00
ρ	1.077	1.069	1.061	1.053	1.045	1.038	1.031	1.026

Miscibility	H_2O	MeOH	Et_2O	Toluene	Hexane
	M	M	N	M ≥ 50% IL	N

3.1.12 Bis(dimethylamino)butylaminocyclopropenium bis(trifluoromethanesulfonyl)amide, $[C_3(NMe_2)_2(NBuH)]TFSA$, $[M_4BH]TFSA$

Physical State	T_g	T_{s-s}	ΔH	T_m	ΔH	T_d(1)	T_d(10)	*Chloride*
Viscous Liquid	−73.2	---	---	---	---	256	312	293
T	**20**	**30**	**40**	**50**	**60**	**70**	**80**	**90**
η	170.6	91.9	57.2	36.8	25.3	18.0	13.6	10.3

σ	0.89	1.56	2.48	3.69	5.15	6.93	8.96	11.32
ρ	1.347	1.337	1.328	1.319	1.310	1.301	1.292	1.283

Miscibility	**H_2O**	**MeOH**	**Et_2O**	**Toluene**	**Hexane**
	N	M	M ≥ 33% IL	M ≥ 50% IL	N

3.1.13 Bis(dimethylamino)butylmethylaminocyclopropenium bis(trifluoromethanesulfonyl)amide, [$C_3(NMe_2)_2$(NBuMe)]TFSA, [M_5B]TFSA

Physical State	T_g	T_{s-s}	**ΔH**	T_m	**ΔH**	T_d**(1)**	T_d**(10)**	***Chloride***
Viscous Liquid	−82.6	---	---	5.6	25.6	274	321	31

T	**20**	**30**	**40**	**50**	**60**	**70**	**80**	**90**
η	76.1	47.4	31.1	21.9	15.4	12.2	9.3	7.41
σ	2.36	3.61	5.23	7.23	9.46	12.01	14.85	17.94
ρ	1.331	1.321	1.313	1.303	1.294	1.285	1.276	1.266

Miscibility	**H_2O**	**MeOH**	**Et_2O**	**Toluene**	**Hexane**
	N	M	M ≥ 40% IL	M ≥ 50% IL	N

3.1.14 Bis(dimethylamino)butylmethylaminocyclopropenium dicyanamide, [C3(NMe2)2(NBuMe)]DCA, [M5B]DCA

Physical State	T_g	T_{s-s}	ΔH	T_m	ΔH	T_d(1)	T_d(10)	*Chloride*
Viscous Liquid	−72.6	---	---	---	---	259	287	1795
T	**20**	**30**	**40**	**50**	**60**	**70**	**80**	**90**
η	67.4	40.3	25.3	17.2	12.1	9.14	7.05	5.57
σ	4.38	7.13	10.69	15.09	20.5	26.3	32.7	39.6
ρ	1.032	1.026	1.020	1.014	1.007	1.002	0.995	0.989

Miscibility	H_2O	MeOH	Et_2O	Toluene	Hexane
	M	M	N	M ≥ 50% IL	N

3.1.15 Bis(dimethylamino)pentylaminocyclopropenium bis(trifluoromethanesulfonyl)amide, [C3(NMe2)2(NPeH)]TFSA, [M4PeH]TFSA

Physical State	T_g	T_{s-s}	ΔH	T_m	ΔH	T_d(1)	T_d(10)	*Chloride*
Viscous Liquid	---	---	---	---	---	263	322	143
T	**20**	**30**	**40**	**50**	**60**	**70**	**80**	**90**
η	201.3	110.3	65.9	42.3	28.0	19.8	14.6	10.7
σ	0.64	1.10	1.76	2.65	3.77	5.16	6.77	8.50
ρ	1.318	1.309	1.300	1.291	1.282	1.274	1.265	1.256

Miscibility	H_2O	MeOH	Et_2O	Toluene	Hexane
	N	M	M ≥ 33% IL	M ≥ 50% IL	N

3.1.16 Bis(dimethylamino)pentylmethylaminocyclopropenium bis(trifluoromethanesulfonyl)amide, [$C_3(NMe_2)_2(NPeMe)$]TFSA, [M_5Pe]TFSA

Physical State	T_g	$T_{s\text{-}s}$	**ΔH**	T_m	**ΔH**	T_d**(1)**	T_d**(10)**	***Chloride***
Viscous Liquid	---	---	---	---	---	263	325	730

T	**20**	**30**	**40**	**50**	**60**	**70**	**80**	**90**
η	112.9	67.4	43.1	28.6	20.8	15.4	11.5	8.89

Miscibility	**H_2O**	**MeOH**	**Et_2O**	**Toluene**	**Hexane**
	N	M	M ≥ 40% IL	M ≥ 40% IL	N

3.1.17 Bis(dimethylamino)hexylmethylaminocyclopropenium bis(trifluoromethanesulfonyl)amide, [$C_3(NMe_2)_2(NHexMe)$]TFSA, [M_5Hex]TFSA

Physical State	T_g	$T_{s\text{-}s}$	**ΔH**	T_m	**ΔH**	T_d**(1)**	T_d**(10)**	***Chloride***
Viscous Liquid	---	---	---	−13.7	16.0	264	295	78

T	**20**	**30**	**40**	**50**	**60**	**70**	**80**	**90**
η	94.0	56.4	36.4	24.7	18.0	13.4	10.3	8.07
σ	1.31	2.17	3.34	4.83	6.63	8.73	11.09	13.74
ρ	1.292	1.283	1.274	1.266	1.256	1.248	1.239	1.231

Miscibility	**H_2O**	**MeOH**	**Et_2O**	**Toluene**	**Hexane**
	N	M	M ≥ 25% IL	M ≥ 40% IL	N

3.1.18 Bis(diethylamino)butylaminocyclopropenium methylsulfate, $[C_3(NEt_2)_2(NHBu)]MeSO_4$, $[E_4BH]MeSO_4$

Physical State	T_g	$T_{s\text{-}s}$	**ΔH**	T_m	**ΔH**	T_d**(1)**	T_d**(10)**	***Chloride***
Viscous Liquid	−77.1	---	---	---	---	193	233	1063

T	**20**	**30**	**40**	**50**	**60**	**70**	**80**	**90**
η	344.3	188.0	106.3	67.4	45	31.7	22.7	16.8

Miscibility	**H_2O**	**MeOH**	**Et_2O**	**Toluene**	**Hexane**
	M	M	M ≥ 33% IL	M ≥ 40% IL	N

3.1.19 Bis(diethylamino)butylaminocyclopropenium bis(trifluoromethanesulfonyl)amide, $[C_3(NEt_2)_2(NHBu)]$TFSA, $[E_4BH]$TFSA

Physical State	T_g	$T_{s\text{-}s}$	**ΔH**	T_m	**ΔH**	T_d**(1)**	T_d**(10)**	***Chloride***
Viscous Liquid	−85.7	---	---	---	---	296	324	1437

T	**20**	**30**	**40**	**50**	**60**	**70**	**80**	**90**
η	175.7	96.0	54.5	36.5	25.5	18.4	13.8	10.8
σ	0.69	1.14	1.75	2.55	3.52	4.70	6.07	7.64
ρ	1.266	1.257	1.249	1.240	1.232	1.223	1.214	1.206

Miscibility	**H_2O**	**MeOH**	**Et_2O**	**Toluene**	**Hexane**
	N	M	M ≥ 50% IL	M ≥ 40% IL	N

3.1.20 Bis(diethylamino)butylaminocyclopropenium dicyanoamide, [C3(NEt2)2(NHBu)]DCA, [E4BH]DCA

Physical State	T_g	$T_{s\text{-}s}$	ΔH	T_m	ΔH	T_d(1)	T_d(10)	*Chloride*
Viscous Liquid	−71.9	---	---	---	---	198	233	2033
T	**20**	**30**	**40**	**50**	**60**	**70**	**80**	**90**
η	251.3	126.2	75.6	47.0	31.6	23.0	17.0	12.9
σ	1.28	2.16	3.43	5.13	7.30	9.98	13.20	16.97
ρ	0.995	0.989	0.983	0.977	0.971	0.965	0.959	0.953

Miscibility	H2O	MeOH	Et2O	Toluene	Hexane
	N	M	N	M ≥ 33% IL	N

3.1.21 Bis(diethylamino)butylaminocyclopropenium tetrafluoroborate, [C3(NEt2)2(NHBu)]BF4, [E4BH]BF4

Physical State	T_g	$T_{s\text{-}s}$	ΔH	T_m	ΔH	T_d(1)	T_d(10)	*Chloride*
Viscous Liquid	−76.3	---	---	---	---	197	267	25
T	**20**	**30**	**40**	**50**	**60**	**70**	**80**	**90**
η	521.0	271.8	153.2	89.4	56.2	38.2	26.6	19.1
σ	0.318	0.595	1.02	1.66	2.54	3.66	5.10	6.82
ρ	1.079	1.072	1.062	1.059	1.052	1.045	1.039	1.032

Miscibility	H2O	MeOH	Et2O	Toluene	Hexane

N	M	N	M	N	

3.1.22 Bis(diethylamino)-*S*-(1-carboxyethylamino)cyclopropenium methylsulfate, $[C_3(NEt_2)_2(NH(CHMeCOOH))]MeSO_4$, $[E_4Ala]MeSO_4$

Mixture of IL:Zwitt 0.533:0.466

Physical State	T_g	$T_{s\text{-}s}$	**ΔH**	T_m	**ΔH**	T_d**(1)**	T_d**(10)**	***Chloride***
Very Viscous Liquid	−36.5	---	---	---	---	188	215	2289

T	**65**	**70**	**75**	**80**	**85**	**90**
η	1006.0	741.7	561.9	437.3	362.7	348.9

Miscibility	H_2O	CH_3CN	MeOH	CH_2Cl_2	$CHCl_3$	Et_2O	Toluene	Hexane
	M	M	M	M	M	N	N	N

pKa	$[\alpha]_D^{20}$
3.15	−26.46° (c 3.4, EtOH)

3.1.23 Bis(diethylamino)-*S*-(−)-(1-carboxyethylamino)cyclopropenium TFSA, $[C_3(NEt_2)_2(NH(CHMeCOOH))]TFSA$, $[E_4Ala]TFSA$

Mixture of IL:Zwitt 0.91:0.09

Physical State	T_g	$T_{s\text{-}s}$	**ΔH**	T_m	**ΔH**	T_d**(1)**	T_d**(10)**	***Chloride***
Very	−26.0	---	---	---	---	210	245	435

Viscous Liquid							
T	**60**	**65**	**70.1**	**75**	**80**	**85**	**90**
η	820.4	589.5	435.2	329.0	244.7	196.7	156.3

Miscibility	**H_2O**	**CH_3CN**	**MeOH**	**CH_2Cl_2**	**$CHCl_3$**	**Et_2O**	**Toluene**	**Hexane**
	N	M	M	M	M ≥ 50% IL	N	N	N

pKa	$[\alpha]_D^{20}$
3.2	−31.18° (c 2.0, EtOH)

3.1.24 Bis(diethylamino)-*S*-(−)-(2-carboxypyrrolidino)cyclopropenium methylsulfate, $[C_3(NEt_2)_2(N(C_4H_7COOH))]MeSO_4$, $[E_4Pro]MeSO_4$

Mixture of IL:Zwitt 0.71:0.28

Physical State	T_g	$T_{s\text{-}s}$	**ΔH**	T_m	**ΔH**	T_d**(1)**	T_d**(10)**	***Chloride***
Visocus Liquid	−15.7	---	---	−7.3	0.8	200	231	9706

T	**75**	**79.9**	**85**	**90.1**
η	837.7	614.1	459.7	411.7

Miscibility	**H_2O**	**CH_3CN**	**MeOH**	**CH_2Cl_2**	**$CHCl_3$**	**Et_2O**	**Toluene**	**Hexane**
	M	M	M	M	M	N	N	N

pKa	$[\alpha]_D^{20}$
2.90	−88.26° (c 0.6, H_2O)

3.1.25 Bis(diethylamino)-*S*-(−)-(2-carboxypyrrolidino)cyclopropenium TFSA, $[C_3(NEt_2)_2(N(C_4H_7COOH))]TFSA$, $[E_4Pro]TFSA$

Mixture of IL:Zwitt 0.93:0.07

Physical State	T_g	$T_{s\text{-}s}$	ΔH	T_m	ΔH	T_d(1)	T_d(10)	*Chloride*
Viscous Liquid	−40.9	---	---	---	---	230	272	174

T	**60**	**64.9**	**70.2**	**75**	**79.9**	**84.9**
η	564.0	405.6	302.9	230.4	178.8	138.9

Miscibility	H_2O	CH_3CN	MeOH	CH_2Cl_2	$CHCl_3$	Et_2O	Toluene	Hexane
	N	M	M	M	M	N	N	N

pKa	$[\alpha]_D^{20}$
4.44	−42.47° (c 2.2, EtOH)

3.1.26 Bis(diethylamino)-*S*-(−)-(1-carboxy-2-methylpropylamino)cyclopropenium methylsulfate, $[C_3(NEt_2)_2(NH(C_4H_8COOH))]MeSO_4$, $[E_4Val]MeSO_4$

Mixture of IL:Zwitt 0.36:0.63

Physical State	T_g	$T_{s\text{-}s}$	ΔH	T_m	ΔH	T_d(1)	T_d(10)	*Chloride*
Solid	−50.9	---	---	---	---	190	215	41369

Miscibility	H_2O	CH_3CN	MeOH	CH_2Cl_2	$CHCl_3$	Et_2O	Toluene	Hexane
	M	M	M	M	M	N	N	N

pKa	$[\alpha]_D^{20}$
3.55	−0.57° (c 1.7, H_2O)

3.1.27 Bis(diethylamino)-*S*-(−)-(1-carboxy-2-methylpropylamino)cyclopropenium TFSA, [$C_3(NEt_2)_2(NH(C_4H_8COOH))$]TFSA, [$E_4$Val]TFSA

Mixture of IL:Zwitt 0.98:0.01

Physical State	T_g	T_{s-s}	ΔH	T_m	ΔH	T_d(1)	T_d(10)	*Chloride*
Viscous Liquid	---	---	---	---	---	209	245	185

T	**70.4**	**75**	**80**	**84.9**	**89.6**
η	790.8	574.2	417.9	310.1	233.4

Miscibility	H_2O	CH_3CN	MeOH	CH_2Cl_2	$CHCl_3$	Et_2O	Toluene	Hexane
	N	M	M	M	M	N	N	N

pKa	$[\alpha]_D^{20}$
2.97	−16.54° (c 1.3, EtOH)

3.1.28 Bis(diethylamino)-*S*-(−)-(1-carboxy-2-hyroxylpropylamino)cyclopropenium methylsulfate, [$C_3(NEt_2)_2(NH(C_3H_6OCOOH))$]$MeSO_4$, [E_4Thr]$MeSO_4$

Mixture of IL:Zwitt 0.64:0.36

Physical State	T_g	T_{s-s}	ΔH	T_m	ΔH	T_d(1)	T_d(10)	*Chloride*
Solid	---	---	---	40.4	---	151	188	3229

Miscibility	H_2O	CH_3CN	MeOH	CH_2Cl_2	$CHCl_3$	Et_2O	Toluene	Hexane
	M	M	M	M	M	N	N	N

pKa	$[\alpha]_D^{20}$
3.97	−5.49° (c 2.7, H_2O)

3.1.29 Bis(diethylamino)-*S*-(−)-(1-carboxy-2-hyroxylpropylamino))cyclopropenium TFSA, [$C_3(NEt_2)_2(NH(C_3H_6OCOOH))$]TFSA, [E_4Thr]TFSA

Mixture of IL:Zwitt 0.97:0.03

Physical State	T_g	$T_{s\text{-}s}$	ΔH	T_m	ΔH	T_d(1)	T_d(10)	*Chloride*
Viscous Liquid	−15.8	---	---	---	---	145	178	38

T	**75**	**80.2**	**84.8**	**90**
η	883.7	617.1	455.7	329.0

Miscibility	H_2O	CH_3CN	MeOH	CH_2Cl_2	$CHCl_3$	Et_2O	Toluene	Hexane
	N	M	M	M	M	N	N	N

pKa	$[\alpha]_D^{20}$
4.79	−18.1° (c 8.2, EtOH)

3.1.30 Bis(diethylamino)-*S*-(+)-(1-carboxy-4-guanidinobutylamino)cyclopropenium bis(trifluoromethanesulfonyl)amide, [$C_3(NEt_2)_2(NH(C_5H_{11}N_3COOH))$]TFSA , [$E_4$Arg]TFSA

Mixture of IL:Zwitt 0.951:0.04

Physical State	T_g	$T_{s\text{-}s}$	ΔH	T_m	ΔH	T_d(1)	T_d(10)	*Chloride*
Solid	---	---	---	---	---	220	254	475

Miscibility	H_2O	CH_3CN	CH_2Cl_2	$CHCl_3$	Et_2O	Toluene	Hexane
	N	M	N	N	N	N	N

pKa	$[\alpha]_D^{20}$

3.5	+9.7° (c 1.9, CH_3CN)

3.1.31 Bis(diethylamino)-*S*-(1,3-dicarboxy-ethylamino)cyclopropenium bis(trifluoromethanesulfonyl)amide, [$C_3(NEt_2)_2(NHCOOHC_2H_3COOH)$)]TFSA , [$E_4$Asp]TFSA

Mixture of IL:Zwitt 0.91:0.086

Physical State	T_g	$T_{s\text{-}s}$	**ΔH**	T_m	**ΔH**	T_d**(1)**	T_d**(10)**	***Chloride***
	---	---	---	---	---	161	195	---

Miscibility	H_2O	CH_3CN	CH_2Cl_2	$CHCl_3$	Et_2O	**Toluene**	**Hexane**
	N	M	N	N	N	N	N

pKa
3.22

3.1.32 Bis(diethylamino)-*S*-(−)-(1-carboxy-2-imidazolethylamino)cyclopropenium bis(trifluoromethanesulfonyl)amide, [$C_3(NEt_2)_2(NHCOOHC_2H_3C_3H_2N_2H)$)]TFSA , [$E_4$His]TFSA

Mixture of IL:Zwitt 0.7:0.3

Physical State	T_g	$T_{s\text{-}s}$	**ΔH**	T_m	**ΔH**	T_d**(1)**	T_d**(10)**	***Chloride***
Viscous Liquid	−17.6	---	---	---	---	215	244	161

Miscibility	H_2O	CH_3CN	CH_2Cl_2	$CHCl_3$	Et_2O	**Toluene**	**Hexane**
	N	M	N	N	N	N	N

pKa	$[\alpha]_D^{20}$
3.31	−1.39° (c 1.9, CH_3CN)

3.1.33 Bis(diethylamino)-*S*-(−)-(1-carboxy-3-methylthioproylamino)cyclopropenium bis(trifluoromethanesulfonyl)amide, $[C_3(NEt_2)_2(NHCOOHC_3H_5SCH_3))]$TFSA, $[E_4Met]$TFSA

Mixture of IL:Zwitt 0.539:0.4609

Physical State	T_g	$T_{s\text{-}s}$	ΔH	T_m	ΔH	T_d(1)	T_d(10)	*Chloride*
Viscous Liquid	---	---	---	---	---	218	238	968

Miscibility	H_2O	CH_3CN	CH_2Cl_2	$CHCl_3$	Et_2O	Toluene	Hexane
	M	M	M	M	N	N	N

pKa	$[\alpha]_D^{20}$
3.02	−28.63° (c 2.2, CH_3CN)

3.1.34 Bis(diethylamino)-*S*-(−)-(1-carboxy-3,3-dimethylethylamino)cyclopropenium bis(trifluoromethanesulfonyl)amide, $[C_3(NEt_2)_2(NHCOOHC_3H_4(CH_3)_2))]$TFSA , $[E_4Leu]$TFSA

Mixture of IL:Zwitt 0.805:0.194

Physical State	T_g	$T_{s\text{-}s}$	ΔH	T_m	ΔH	T_d(1)	T_d(10)	*Chloride*
Viscous Liquid	---	---	---	---	---	214	244	93

Miscibility	H_2O	CH_3CN	CH_2Cl_2	$CHCl_3$	Et_2O	Toluene	Hexane
	N	M	M	M	N	N	N

pKa	$[\alpha]_D^{20}$
3.41	−36.36°(c 1.4, CH_3CN)

3.1.35 Bis(diethylamino)-*S*-(−)-(1-carboxy-2-methylbutylamino)cyclopropenium bis(trifluoromethanesulfonyl)amide, [$C_3(NEt_2)_2(NHCOOHC_2H_2(CH_3)CH_2CH_3COOH))$]TFSA , [$E_4$Ile]TFSA

Mixture of IL:Zwitt 0.95:0.05

Physical State	T_g	$T_{s\text{-}s}$	**ΔH**	T_m	**ΔH**	T_d**(1)**	T_d**(10)**	***Chloride***
Viscous Liquid	−37.2	---	---	---	---	227	260	109

Miscibility	H_2O	CH_3CN	CH_2Cl_2	$CHCl_3$	Et_2O	**Toluene**	**Hexane**
	N	M	M	M	N	N	N

pKa	$[\alpha]_D^{20}$
3.47	−20.95°(c 2.0, CH_3CN)

3.1.36 Bis(diethylamino)-*S*-(−)-(1-carboxy-2-(1H-indol-3-yl)ethylamino)cyclopropenium bis(trifluoromethanesulfonyl)amide, [$C_3(NEt_2)_2(NHCOOHC_2H_3C_8H_6N))$]TFSA , [$E_4$Try]TFSA

Mixture of IL:Zwitt 0.54:0.45

Physical State	T_g	$T_{s\text{-}s}$	**ΔH**	T_m	**ΔH**	T_d**(1)**	T_d**(10)**	***Chloride***
Solid	---	---	---	---	---	227	263	89

Miscibility	H_2O	CH_3CN	CH_2Cl_2	$CHCl_3$	Et_2O	**Toluene**	**Hexane**
	N	M	M	N	N	N	N

pKa	$[\alpha]_D^{20}$
3.62	−29.9° (c 1.0, CH_3CN)

3.1.37 Bis(diethylamino)-*S*-(−)-(1-carboxy-2-hydroxyphenylethylamino)cyclopropenium bis(trifluoromethanesulfonyl)amide, $[C_3(NEt_2)_2(NHCOOHC_2H_3C_6H_5O))]TFSA$, [E4Tyr]TFSA

Mixture of IL:Zwitt 0.716:0.28

Physical State	T_g	T_{s-s}	ΔH	T_m	ΔH	T_d(1)	T_d(10)	*Chloride*
Viscous Liquid	0.3	---	---	---	1.289	238	268	474

Miscibility	H_2O	CH_3CN	CH_2Cl_2	$CHCl_3$	Et_2O	Toluene	Hexane
	N	M	M	N	N	N	N

pKa	$[\alpha]_D^{20}$
3.30	−11.5°(c 1.0, CH_3CN)

3.1.38 Bis(diethylamino)-*S*-(−)-(1-carboxy-2-phenylethylamino)cyclopropenium bis(trifluoromethanesulfonyl)amide, $[C_3(NEt_2)_2(NHCOOHC_2H_3C_6H_5)]TFSA$, [E4Phe]TFSA

Mixture of IL:Zwitt 0.69:0.31

Physical State	T_g	T_{s-s}	ΔH	T_m	ΔH	T_d(1)	T_d(10)	*Chloride*
Viscous Liquid	---	---	---	---	---	213	259	112

Miscibility	H_2O	CH_3CN	CH_2Cl_2	$CHCl_3$	Et_2O	Toluene	Hexane
	N	M	M	M	N	N	N

pKa	$[\alpha]_D^{20}$

3.35	−14.28°(c 1.5, CH_3CN)

3.1.39 Bis(diethylamino)-*S*-(−)-(1-carboxy-2-hydroxyethylamino)cyclopropenium bis(trifluoromethanesulfonyl)amide, $[C_3(NEt_2)_2(NHCOOHC_2H_3CH_2OH)]TFSA$, $[E_4Ser]TFSA$

Mixture of IL:Zwit 0.94:0.06

Physical State	T_g	$T_{s\text{-}s}$	**ΔH**	T_m	**ΔH**	T_d**(1)**	T_d**(10)**	***Chloride***
Viscous Liquid	−20.9	---	---	---	---	131	161	100

Miscibility	H_2O	CH_3CN	CH_2Cl_2	$CHCl_3$	Et_2O	**Toluene**	**Hexane**
	N	M	M	N	N	N	N

pKa	$[\alpha]_D^{20}$
3.9	−6.89° (c 2.03, CH_3CN)

3.1.40 Tetrakis(diethylamino)-*S*-(−)-(1-carboxy-4-carbamoylethtylamino)cyclopropenium bis(trifluoromethanesulfonyl)amide, $[C_3(NEt_2)_2(NH_2COC_3H_5COOH)\ C_3(NEt_2)_2)]TFSA_2$, $[E_8Gln]TFSA_2$

Mixture of IL:Zwitt 0.72:0.276

Physical State	T_g	$T_{s\text{-}s}$	**ΔH**	T_m	**ΔH**	T_d**(1)**	T_d**(10)**	***Chloride***
Viscous Liquid	---	---	---	---	---	132	166	36

Miscibility	H_2O	CH_3CN	CH_2Cl_2	$CHCl_3$	Et_2O	**Toluene**	**Hexane**
	N	M	M	N	N	N	N

pKa	$[\alpha]_D^{20}$
3.37	−20.26°(c 1.53, CH_3CN)

3.1.41 Tetrakis(diethylamino)-*S*-(−)-(1-carboxy-5-aminopentylamine)cyclopropenium bis(trifluoromethanesulfonyl)amide, [$C_3(NEt_2)_2(NHCOOHC_5H_9NH)$ $C_3(NEt_2)_2$]TFSA, [E_8Lys]$TFSA_2$

Mixture of IL:Zwitt 0.9:0.1

Physical State	T_g	$T_{s\text{-}s}$	ΔH	T_m	ΔH	T_d(1)	T_d(10)	*Chloride*
Viscous Liquid	−48.3	---	---	---	---	223	252	182

Miscibility	H_2O	CH_3CN	CH_2Cl_2	$CHCl_3$	Et_2O	Toluene	Hexane
	N	M	M	M	N	N	N

pKa	$[\alpha]_D^{20}$
3.89	−4.31° (c 2.32, CH_3CN)

3.2 C_{2v}Cations

3.2.1 Bis(dimethylamino)diethylaminocyclopropenium bis(trifluoromethanesulfonyl)amide, [$C_3(NMe_2)_2(NEt_2)$]TFSA, [M_4E_2]TFSA

Physical State	T_g	$T_{s\text{-}s}$	ΔH	T_m	ΔH	T_d(1)	T_d(10)	*Chloride*
Solid	---	27.2	57.1	43.5	50.8	232	334	345

T	50	60	70	80	90
η	25.1	18.2	13.5	10.5	8.17
σ	5.15	7.13	9.43	12.21	15.40

Miscibility	H_2O	MeOH	Et_2O	Toluene	Hexane
	N	M	immiscible layer	N	N

3.2.2 Bis(dimethylamino)diallylaminocyclopropenium bis(trifluoromethanesulfonyl)amide, $[C_3(NMe_2)_2(N(CH_2CHCH_2)_2)]TFSA$, $[M_4A_2]TFSA$

Physical State	T_g	T_{s-s}	ΔH	T_m	ΔH	T_d(1)	T_d(10)	*Chloride*
Viscous Liquid	---	---	---	15.6	59.3	235	335	60

T	20	30	40	50	60	70	80	90
η	95.5	58.4	37.6	24.7	17.7	12.9	10.1	7.71
σ	2.07	3.26	4.80	6.67	8.85	11.30	14.07	17.06
ρ	1.343	1.332	1.323	1.314	1.305	1.296	1.287	1.278

Miscibility	H_2O	MeOH	Et_2O	Toluene	Hexane
	N	M	M ≥ 40% IL	M ≥ 40% IL	N

3.2.3 Bis(dimethylamino)dipropylaminocyclopropenium bis(trifluoromethanesulfonyl)amide, $[C_3(NMe_2)_2(NPr_2)]TFSA$, $[M_4Pr_2]TFSA$

Physical State	T_g	T_{s-s}	ΔH	T_m	ΔH	T_d(1)	T_d(10)	*Chloride*
Solid	---	---	---	51.6	24.8	243	317	757

T	40	50	60	70	80	90
η	---	28.9	19.8	14.7	11.0	8.63
σ	3.44	5.09	7.01	9.20	11.64	14.53
ρ	---	1.287	1.279	1.271	1.262	1.254

Miscibility	H_2O	MeOH	Et_2O	Toluene	Hexane
	N	M	M ≥ 71% IL	immiscible layer	N

3.2.4 Bis(dimethylamino)-N-(dimethoxyethyl)aminocyclopropenium bis(trifluoromethanesulfonyl)amide, $[C_3(NMe_2)_2(N(CH_2CH_2OCH_3)_2)]TFSA$, $[M_4Er_2]TFSA$

Physical State	T_g	$T_{s\text{-}s}$	ΔH	T_m	ΔH	T_d(1)	T_d(10)	*Chloride*
Viscous Liquid	−70.4	---	---	---	---	262	363	9.4

T	20	30	40	50	60	70	80	90
η	141.0	78.7	54.7	31.1	20.9	15.2	11.2	8.58
σ	1.06	1.83	2.88	4.21	5.82	7.7	9.87	12.28
ρ	1.355	1.346	1.336	1.327	1.318	1.309	1.299	1.290

Miscibility	H_2O	MeOH	Et_2O	Toluene	Hexane
	N	M	M ≥ 40% IL	M ≥ 40% IL	N

3.2.5 Bis(dimethylamino)dibutylaminocyclopropenium bis(trifluoromethanesulfonyl)amide, $[C_3(NMe_2)_2(NBu_2)]TFSA$, $[M_4B_2]TFSA$

Physical State	T_g	$T_{s\text{-}s}$	ΔH	T_m	ΔH	T_d(1)	T_d(10)	*Chloride*
Viscous Liquid	−42.1	---	---	36.3	22.9	250	314	487

T	20	30	40	50	60	70	80	90
η	117.5	69	43.3	28.6	19.8	14.6	11.2	8.68
σ	1.23	2.03	3.12	4.50	6.16	8.10	10.29	12.80

ρ	1.272	1.261	1.253	1.244	1.236	1.228	1.219	1.210

Miscibility	**H_2O**	**MeOH**	**Et_2O**	**Toluene**	**Hexane**
	N	M	M ≥ 33% IL	M ≥ 50% IL	N

3.2.6 Bis(dimethylamino)dihexylaminocyclopropenium bis(trifluoromethanesulfonyl)amide, $[C_3(NMe_2)_2(NHex_2)]TFSA$, $[M_4Hex_2]TFSA$

Physical State	T_g	T_{s-s}	**ΔH**	T_m	**ΔH**	T_d**(1)**	T_d**(10)**	***Chloride***
Viscous Liquid	−48.4	---	---	20.8	24.7	295	348	158

T	**20**	**30**	**40**	**50**	**60**	**70**	**80**	**90**
η	---	110.3	65.4	42.3	29.0	21.3	16.1	13.2
σ	0.29	0.53	0.89	1.41	2.12	3.03	4.15	5.52
ρ	1.209	1.200	1.192	1.184	1.176	1.168	1.159	1.151

Miscibility	**H_2O**	**MeOH**	**Et_2O**	**Toluene**	**Hexane**
	N	M	M	M ≥ 40% IL	N

3.2.7 1,2-Bis(diethylamino)-3-aminocyclopropenium methylsulphate, $[(Et_2N)_2C_3(NH_2)]MeSO_4$, $[E_4H_2]MeSO_4$

Physical State	T_g	T_{s-s}	**ΔH**	T_m	**ΔH**	T_d**(1)**	T_d**(10)**	***Chloride***
Solid	−47.7	---	---	---	---	146	181	199

Miscibility	**H_2O**	**MeOH**	**Et_2O**	**Toluene**	**Hexane**
	Not stable	M	N	N	N

3.2.8 1,2-Bis(diethylamino)-3-aminocyclopropenium bis(trifluoromethanesulfonyl)amide, $[(Et_2N)_2C_3(NH_2)]TFSA$, $[E_4H_2]TFSA$

Physical State	T_g	$T_{s\text{-}s}$	ΔH	T_m	ΔH	T_d(1)	T_d(10)	*Chloride*
Solid	−59.5	---	---	94.2	17.4	275	309	523

Miscibility	H_2O	MeOH	Et_2O	Toluene	Hexane
	Not stable	M	Immiscible Layer	Immiscible Layer	N

3.2.9 Bis(diethylamino)dihexylaminocyclopropenium iodide, $[C_3(NEt_2)_2(NBu_2)]I$, $[E_4B_2]I$

Physical State	T_g	$T_{s\text{-}s}$	ΔH	T_m	ΔH	T_d(1)	T_d(10)	*Chloride*
Solid	---	---	---	75.1	150.5	296	328	---

Miscibility	H_2O	MeOH	Et_2O	Toluene	Hexane
	N	M	N	Immiscible layer	N

3.2.10 Bis(diethylamino)dihexylaminocyclopropenium iodide, $[C_3(NEt_2)_2(NHex_2)]I$, $[E_4Hex_2]I$

Physical State	T_g	$T_{s\text{-}s}$	ΔH	T_m	ΔH	T_d(1)	T_d(10)	*Chloride*
Viscous Liquid	−45.6	---	---	---	---	281	326	---

T	20	30	40	50	60	70	80	90
η	---	---	544.6	283.0	122.6	75.1	36.4	24.9

σ	0.0137	0.0386	0.0948	0.206	0.396	0.711	1.192	1.885
ρ	1.130	1.123	1.17	1.09	1.102	1.096	1.095	1.083

Miscibility	**H_2O**	**MeOH**	**Et_2O**	**Toluene**	**Hexane**
	N	M	M ≥ 33% IL	M	N

3.2.11 Bis(diethylamino)dihexylaminocyclopropenium trifluoromethylsulfonate, $[C_3(NEt_2)_2(NHex_2)]OTf$, $[E_4Hex_2]OTf$

Physical State	T_g	$T_{s\text{-}s}$	**ΔH**	T_m	**ΔH**	T_d**(1)**	T_d**(10)**	***Chloride***
Viscous Liquid	−68.9	---	---	---	---	284	326	125

T	**20**	**30**	**40**	**50**	**60**	**70**	**80**	**90**
η	444.4	240.1	137.9	82.8	54.7	38.8	26.2	20.5
σ	0.0936	0.186	0.344	0.586	0.946	1.44	2.09	2.95
ρ	1.077	1.070	1.063	1.056	1.049	1.042	1.035	1.029

Miscibility	**H_2O**	**MeOH**	**Et_2O**	**Toluene**	**Hexane**
	N	M	M	M	N

3.3 C_{3h} Cations

3.3.1 Tris(ethylmethylamino)cyclopropenium bis(trifluoromethanesulfonyl)amide, $[C_3(NEtMe_2)_3]TFSA$, $[M_3E_3]TFSA$

Physical State	T_g	$T_{s\text{-}s}$	**ΔH**	T_m	**ΔH**	T_d**(1)**	T_d**(10)**	***Chloride***
Viscous Liquid	---	1.7	23.9	7.3	5.9	275	366	129

T	**20**	**30**	**40**	**50**	**60**	**70**	**80**	**90**
η	72.5	45.8	31.3	22.0	16.2	12.2	9.45	7.46
σ	2.42	3.62	5.19	7.05	9.18	11.57	14.26	17.19
ρ	1.333	1.324	1.315	1.306	1.297	1.288	1.279	1.270

Miscibility	**H_2O**	**MeOH**	**Et_2O**	**Toluene**	**Hexane**
	N	M	M ≥ 50% IL	M ≥ 40% IL	N

3.3.2 Tris(allylmethylamino)cyclopropenium bis(trifluoromethanesulfonyl)amide, $[C_3(NAllylMe_2)_3]TFSA$, $[M_3A_3]TFSA$

Physical State	***T_g***	***T_{s-s}***	**ΔH**	***T_m***	**ΔH**	***T_d*(1)**	***T_d*(10)**	***Chloride***
Viscous Liquid	−82.8	---	---	---	---	247	329	116

T	**20**	**30**	**40**	**50**	**60**	**70**	**80**	**90**
η	76.1	45.4	29.4	20.6	14.3	11.0	8.33	6.54
σ	1.83	2.87	4.25	5.99	7.99	10.24	12.77	15.54
ρ	1.315	1.306	1.297	1.288	1.279	1.270	1.261	1.252

Miscibility	**H_2O**	**MeOH**	**Et_2O**	**Toluene**	**Hexane**
	N	M	M ≥ 33% IL	M ≥ 40% IL	N

3.3.3 Tris(allylmethylamino)cyclopropenium dicyanamide, $[C_3(NAllylMe)_3]DCA$, $[(MA)_3]DCA$

Physical State	T_g	T_{s-s}	**ΔH**	T_m	**ΔH**	T_d**(1)**	T_d**(10)**	***Chloride***
Viscous Liquid	−72.6	---	---	---	---	250	276	2684

T	**20**	**30**	**40**	**50**	**60**	**70**	**80**	**90**
η	146.1	72	40.5	25.5	17.4	12.7	9.09	6.95
σ	2.21	3.83	6.14	9.17	12.81	16.97	22.0	27.4
ρ	1.044	1.037	1.030	1.024	1.018	1.012	1.006	0.999

Miscibility	**H_2O**	**MeOH**	**Et_2O**	**Toluene**	**Hexane**
	N	M	N	M ≥ 56% IL	N

3.3.4 Tris(*N*-(methoxyethyl)methyl)cyclopropenium bis(trifluoromethanesulfonyl)amide, $[C_3(NMeCH_2CH_2OCH_3)_3]TFSA$, $[(MEr)_3]TFSA$

Physical State	T_g	T_{s-s}	**ΔH**	T_m	**ΔH**	T_d**(1)**	T_d**(10)**	***Chloride***
Viscous Liquid	−65.3	---	---	---	---	286	347	117

T	**20**	**30**	**40**	**50**	**60**	**70**	**80**	**90**
η	183.9	96	55.7	34.1	23.3	16.4	12.1	9.04
σ	0.703	1.26	2.12	3.21	4.55	6.15	7.96	10.11
ρ	1.329	1.321	1.311	1.302	1.293	1.284	1.275	1.266

Miscibility	**H_2O**	**MeOH**	**Et_2O**	**Toluene**	**Hexane**
	N	M	M ≥ 40% IL	M ≥ 40% IL	N

3.3.5 Trisanilinocyclopropenium bis(trifluoromethanesulfonyl)amide, $[C_3(NPhH)_3]TFSA$

Physical State	T_g	$T_{s\text{-}s}$	ΔH	T_m	ΔH	T_d(1)	T_d(10)
Solid	---	---	---	16.7	0.5	273	308

3.4 D_{3h} Cations

3.4.1 Tris(diethylamino)cyclopropenium *p*-toluenesulfonate, $[C_3(NEt_2)_3][MeC_6H_4SO_3]$, $[E_6]OTs$

Physical State	T_g	$T_{s\text{-}s}$	ΔH	T_m	ΔH	T_d(1)	T_d(10)	*Chloride*
Viscous Liquid	−50.4	---	---	---	---	145	201	1402

T	20	30	40	50	60	70	80	90
η	764.2	338.2	171.6	97.1	57.4	37.2	25.2	-
σ	0.089	0.217	0.446	0.828	1.394	2.180	3.220	4.51
ρ	1.103	1.097	1.090	1.084	1.077	1.071	1.065	1.058

Miscibility	H_2O	MeOH	Et_2O	Toluene	Hexane
	M	M	M ≥ 50% IL	N	N

3.4.2 Tris(diethylamino)cyclopropenium trifluoromethanesulfonate, $[C_3(NEt_2)_3]OTf$, $[E_6]OTf$

Physical State	T_g	T_{s-s}	ΔH	T_m	ΔH	T_d(1)	T_d(10)	*Chloride*
Solid	---	−0.3 50.3	1.1 11.8	77.5	5.7	288	335	217

Miscibility	H_2O	MeOH	Et_2O	Toluene	Hexane
	M	M	M ≥ 25% IL	N	N

3.4.3 Tris(diethylamino)cyclopropenium iodide, $[C_3(NEt_2)_3]I$, $[E_6]I$

Physical State	T_g	T_{s-s}	ΔH	T_m	ΔH	T_d(1)	T_d(10)	*Chloride*
Solid	---	---	---	48.3	13.9	268	294	14*

Miscibility	H_2O	MeOH	Et_2O	Toluene	Hexane
	N	M	N	N	N

*determined by ion chromatography

3.4.4 Tris(diethylamino)cyclopropenium pentafluorophenoxide, $[C_3(NEt_2)_3]F_5C_6O^-$, $[E_6]F_5C_6O$

Physical State	T_g	T_{s-s}	ΔH	T_m	ΔH	T_d(1)	T_d(10)	*Chloride*
Solid	−49.3	---	---	71*	---	159	198	562

Miscibility	H_2O	MeOH	CH_2Cl_2	$CHCl_3$	Et_2O	Toluene	Hexane

N	M	M	M	immiscible layer	immiscible layer	N

*determined by TGA

3.4.5 Tris(diethylamino)cyclopropenium tetrachloroferrate(III), $[C_3(NEt_2)_3]FeCl_4$, $[E_6]FeCl_4$

Physical State	T_g	$T_{s\text{-}s}$	**ΔH**	T_m	**ΔH**	T_d**(1)**	T_d**(10)**
Solid	---	−4.4 50.1	4.9 3.4	148.7	8.0	260	320

Miscibility	**H_2O**	**MeOH**	**CH_2Cl_2**	**$CHCl_3$**	**Et_2O**	**Toluene**	**Hexane**
	partially soluble	M	M	M	N	immiscible layer	N

M_w	χ_M	χ_T	μ_{eff}
459.05	0.014835	4.34	5.89

3.4.6 Tris(diethylamino)cyclopropenium trichlorostannate(II), $[C_3(NEt_2)_3]SnCl_3$, $[E_6]SnCl_3$

Physical State	T_g	$T_{s\text{-}s}$	**ΔH**	T_m	**ΔH**	T_d**(1)**	T_d**(10)**
Solid	---	---	---	58.2	1.5	277	305

Miscibility	**H_2O**	**MeOH**	**CH_2Cl_2**	**$CHCl_3$**	**Et_2O**	**Toluene**	**Hexane**
	N	N	Immiscible Layer	Immiscible Layer	N	N	N

3.4.7 Tetrakis(diethylamino)cyclopropenium tetrachlorozincate(II), $[C_3(NEt_2)_3]_2ZnCl_4$, $[E_6]_2ZnCl_4$

Physical State	T_g	T_{s-s}	ΔH	T_m	ΔH	T_d(1)	T_d(10)
Solid	---	---	---	80.9	40.4	280	314

Miscibility	H_2O	MeOH	CH_2Cl_2	$CHCl_3$	Et_2O	Toluene	Hexane
	M	M	M	M	N	N	N

3.4.8 Tetrakis(diethylamino)cyclopropenium tetrachlorocuprate(II), $[C_3(NEt_2)_3]_2CuCl_4$, $[E_6]_2CuCl_4$

Physical State	T_g	T_{s-s}	ΔH	T_m	ΔH	T_d(1)	T_d(10)
Solid	---	---	---	26.5	35.8	146	182
						261[a]	293[a]

Miscibility	H_2O	MeOH	CH_2Cl_2	$CHCl_3$	Et_2O	Toluene	Hexane
	M	M	M	M	N	N	N

[a]second-decomposition temperature due to two-step decomposition.

3.4.9 Tris(dibutylamino)cyclopropenium tetracyanoborate, $[C_3(NBu_2)_3]B(CN)_4$, $[B_6]B(CN)_4$

Physical State	T_g	T_{s-s}	ΔH	T_m	ΔH	T_d(1)	T_d(10)	*Chloride*
Viscous Liquid	---	---	---	29.3	26.2	251	281	373

T	20	30	40	50	60	70	80	90
η	263.6	148.1	85.8	54.7	35.8	24.7	17.5	13.1
σ	0.423	0.746	1.227	1.881	2.72	3.77	5.02	6.46
ρ	0.928	0.922	0.915	0.909	0.896	0.890	0.883	---

Miscibility	H_2O	MeOH	Et_2O	Toluene	Hexane
	N	M	M	M ≥ 50% IL	N

3.4.10 Tris(dibutylamino)cyclopropenium tris(pentafluoroethyl)trifluorophosphate, $[C_3(NBu_2)_3]FAP$, $[B_6]FAP$

Physical State	T_g	T_{s-s}	ΔH	T_m	ΔH	T_d(1)	T_d(10)	*Chloride*
Viscous Liquid	−72.6	---	---	---	---	232	259	134

T	20	30	40	50	60	70	80	90
η	391.3	212.5	120.6	79.6	48.4	33.1	22.9	16.9
σ	0.145	0.278	0.493	0.809	1.256	1.85	2.59	3.54
ρ	1.246	1.237	1.229	1.220	1.211	1.202	1.193	1.184

Miscibility	H_2O	MeOH	Et_2O	Toluene	Hexane
	N	M	M	M ≥ 50% IL	N

3.4.11 Tris(dibutylamino)cyclopropenium tetrachloroferrate(II), $[C_3(NBu_2)_3]FeCl_4$, $[B_6]FeCl_4$

Physical State	T_g	T_{s-s}	ΔH	T_m	ΔH	T_d(1)	T_d(10)
Viscous Liquid	−65.9	---	---	8.8	0.2	244	306

Miscibility	H_2O	MeOH	CH_2Cl_2	$CHCl_3$	Et_2O	Toluene	Hexane
	N	M	M	M	N	N	N

M_w	χ_M	χ_T	μ_{eff}
589.195	0.01179846	3.456	5.25

3.4.12 Tris(dibutylamino)cyclopropenium trichlorostannate(II), $[C_3(NBu_2)_3]SnCl_3$, $[B_6]SnCl_3$

Physical State	T_g	T_{s-s}	ΔH	T_m	ΔH	T_d(1)	T_d(10)
Viscous Liquid	−31.6	---	---	---	---	144	223
						290[a]	350[a]

Miscibility	H_2O	MeOH	CH_2Cl_2	$CHCl_3$	Et_2O	Toluene	Hexane
	N	M	M	M	N	N	N

[a]second-decomposition temperature due to two-step decomposition.

3.4.13 Tetrakis(dibutylamino)cyclopropenium tetrachlorozincate(II), $[C_3(NBu_2)_3]_2ZnCl_4$, $[B_6]_2ZnCl_4$

Physical State	T_g	T_{s-s}	ΔH	T_m	ΔH	T_d(1)	T_d(10)
Viscous Liquid	−34.3	---	---	---	---	146	188
						293[a]	318[a]

Miscibility	H_2O	MeOH	CH_2Cl_2	$CHCl_3$	Et_2O	Toluene	Hexane
	N	M	M	M	N	N	N

[a]second-decomposition temperature due to two-step decomposition.

3.4.14 Tetrakis(dibutylamino)cyclopropenium tetrachlorocuprate(II), $[C_3(NBu_2)_3]_2CuCl_4$, $[B_6]_2CuCl_4$

Physical State	T_g	T_{s-s}	ΔH	T_m	ΔH	T_d(1)	T_d(10)
Viscous Liquid	−54.1	---	---	---	---	163	199
						256[a]	298[a]

Miscibility	H_2O	MeOH	CH_2Cl_2	$CHCl_3$	Et_2O	Toluene	Hexane
	N	M	M	M	M	M	N

[a]second-decomposition temperature due to two-step decomposition.

3.5. Open ring Cations

3.5.1 1,1,3,3-Tetrakis(dimethylamino)allyl chloride, $[(Me_2N)_2CCH_2C(NMe_2)_2]Cl_2$, $[M_8]Cl_2$

Physical State	T_g	$T_{s\text{-}s}$	ΔH	T_m	ΔH	T_d(1)	T_d(10)
Solid	---	---	---	201*	---	239	268

Miscibility	H_2O	MeOH	Et_2O	Toluene	Hexane
	M	M	N	N	N

*determined by TGA

3.5.2 1,1,3,3-Tetrakis(butylamino)allyl chloride, $[(BuHN)_2CCH_2C(NHBu)_2]Cl_2$, $[B_8]Cl_2$

Physical State	T_g	$T_{s\text{-}s}$	ΔH	T_m	ΔH	T_d(1)	T_d(10)
Viscous Liquid	---	---	---	49.5	0.6	188	255

Miscibility	H_2O	MeOH	Et_2O	Toluene	Hexane
	M	M	N	N	N

3.5.3 1,1,3,3-Tetrakis(butylamino)allyl bis(trifluoromethanesulfonyl)amide, $[(BuHN)_2CCH_2C(NHBu)_2]TFSA_2$, $[B_8]TFSA_2$

Physical State	T_g	$T_{s\text{-}s}$	ΔH	T_m	ΔH	T_d(1)	T_d(10)
Viscous Liquid	---	---	---	−43.8	0.3	244	318

Miscibility	H_2O	MeOH	Et_2O	Toluene	Hexane
	N	M	N	N	N

Discussion of Synthesis

Synthesis

This chapter will discuss the preparation of chiral and low symmetry tac salts. Yoshida[1] and Taylor[2] synthetic routes were used to synthesize highly symmetric (D_{3h} and C_{3h}) cyclopropenium salts. While, less symmetric (C_{2v} and C_s) triaminocyclopropenium salts were synthesized by using Krebs procedure.[3]

4.1 Pentachlorocyclopropane, C_3Cl_5H

C_3Cl_5H was prepared regularly in our laboratory by the reaction of sodium trichloroacetate with trichloroethene in the presence of 1,2-dimethoxyethane (fig. 4.1).[4] Sodium trichloroacetate undergoes a thermal decarboxylation to generate a dichlorocarbene. It reacts with trichloroethene in a [1+2] cycloaddition to form C_3Cl_5H in the presence of the aprotic solvent, 1,2-dimethoxyethane.[5,6,7]

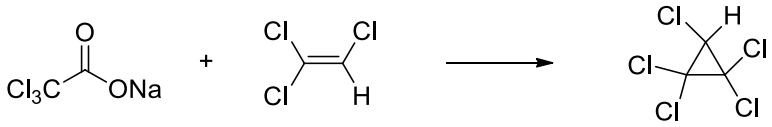

Figure-4.1 Synthesis of pentachlorocyclopropane.[4]

4.2 Synthesis of Amines

N-ethylmethylamine, *N*-Allylmethylamine and *N*-(2-methoxyethyl)methylamine were synthesized from *N*-ethylamine, *N*-allylamine and *N*-(2-methoxyethyl)amine respectively. They were prepared by a modification of methods described by Lucire and Wawzonek.[8]

Benzaldehyde (1 equivalent) reacts with an ice-cold solution of primary amine (RNH_2) (1 equivalent) to form *N*-benzylidenealkylamine and water. In the literature, this product is purified by distillation *in vacuo*. But the mixture proved to be difficult to separate by distillation. This adduct was then methylated with dimethyl sulphate (Me_2SO_4), followed by hydrolysis to give the methylated ammonium salts (fig. 4.2). The distillation is performed after the addition of aqueous NaOH to the ammonium salt solution to give a mixture of primary (RNH_2) and secondary amines (RMeNH) at a ratio of 1:4 as determined by mass spectrometry. Trialkylamine was present in the mixture because some of the RNH_2 did not react with benzaldehyde and subsequently reacted with Me_2SO_4.

The reaction procedure was altered by adding 1.1 equivalents, instead of 1 equivalent, of Me_2SO_4 but again the mixture of amines was obtained. Possibly, the high water content in the *N*-benzylidenealkylamine adduct hydrolyzes the Me_2SO_4 to methanol and methyl sulphuric acid, which protonates rather than methylates the adduct. However, Lucier and coworkers have reported the product as RMeNH. Erroneously, they also reported that during the hydrolysis of *N*-benzylidenealkylammonium methyl sulphate, alkylmethylammonium hydrogen sulphate is formed. A lot of present research involved the study of ILs with a methyl sulphate anion and show it is very stable, even in boiling water.

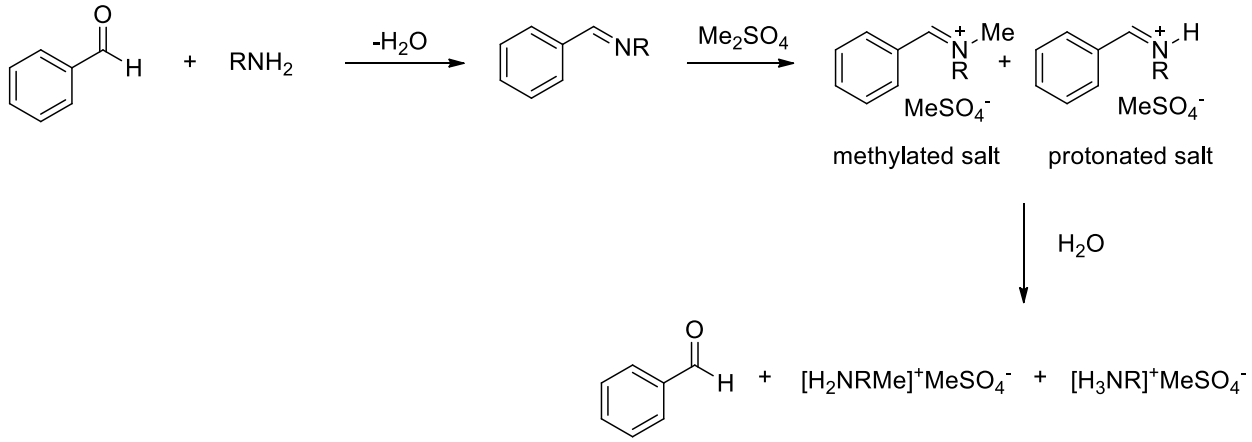

Figure 4.2-Reaction scheme for the synthesis of secondary amines.

Recently, Jacquemin described the hydrolysis of ILs with alkyl sulphate anions. The nature of the cation (imidazolium, ammonium or pyrrolidinium) played a minimal role towards the hydrolysis of the anion. The degradation of methyl- and ethyl sulphate anions to hydrogen sulphate in water was observed above 423 K.[9]

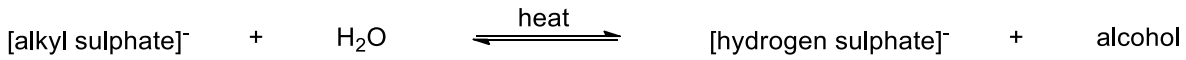

Figure 4.3-Hydrolysis of alkyl sulphate anions.[9]

To separate the mixtures of primary and secondary amines, benzaldehyde was again added. The primary amine reacts with benzaldehyde forming *N*-benzylidenealkylamine leaving behind the secondary amine. This mixture was distilled again *in vacuo* and the pure secondary amine was obtained. NaOH pellets were added to the secondary amines to reduce the water content.

4.3 Synthesis and purification of tris(dimethylamino)cyclopropenium chloride, $[C_3(NMe_2)_3]Cl$

$[C_3(NMe_2)_3]Cl$ was synthesized by using known procedures[1,2] by reacting C_3Cl_5H with Me_2NH. The procedure was altered by utilizing a 40% aqueous solution of Me_2NH, which is much easier to handle compared to anhydrous Me_2NH with a b.p. of 7 °C. Initially, the product was thought to be $C_3(NMe_2)_2O$, as previously Surman had obtained $C_3(N^iPr_2)_2O$ along with a small amount of $[C_3(N^iPr_2)_4H]Cl$, when he refluxed $[C_3(N^iPr_2)_2Cl]Cl$ with an excess of $^iPr_2NH$ for an extended period in air.[10] Instead the product mixture was found to contain the open ring product ($[HC_3(NMe_2)_4]^+$), along with $[C_3(NMe_2)_3)]Cl$ and $[Me_2NH_2]Cl$. The ratio of $[C_3(NMe_2)_3]^+$:$[HC_3(NMe_2)_4]^+$ in the mass spectrometer was 4:1. Initially, it was thought that water was causing the opening of the ring but it was later found to be due to the less bulky nature of Me_2NH, that the mixture of $[C_3(NMe_2)_3]Cl$ and $[HC_3(NMe_2)_4]^+$ was obtained.[11] Previously, it was known that primary and secondary amines are of similar basicity and both will deprotonate C_3Cl_5H and less sterically-hindered amines will react faster than more bulky ones. Rapid substitution will favor the ring to open up while slow rates will produce tac salts.[10] The mixture was dissolved in acetonitrile:toluene (2:1) and kept in the freezer overnight to crystallize out the ammonium salts. The next challenge was to remove $[HC_3(NMe_2)_4]^+$.[12] Upon acidification with HCl, $[HC_3(NMe_2)_4]^+$ is converted to the dication $[H_2C_3(NMe_2)_4]^{2+}$. $[H_2C_3(NMe_2)_4]^{2+}$ is more water soluble than $[HC_3(NMe_2)_4]^+$ due to its high charge, so $[C_3(NMe_2)_3]Cl$ was easily separated into an organic solvent (fig. 4.4).

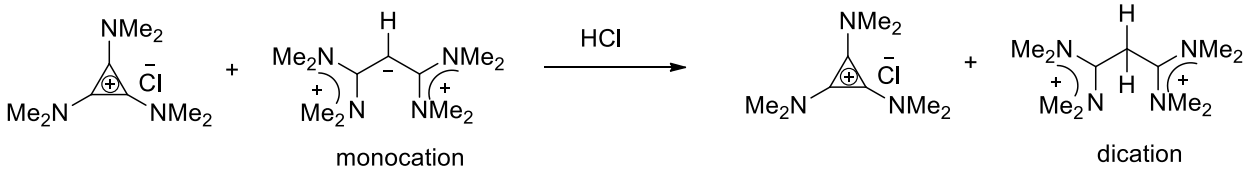

Figure 4.4-Reaction scheme for the conversion of $[HC_3(NMe_2)_4]^+$ to $[HC_3(NMe_2)_4]^{2+}$ by altering *p*H.

It was thought that the mixture of open ring and closed ring products were obtained by first forming the closed ring product by Yoshida's mechanism.[13] The methyl group is small the closed ring is attacked further by Me_2NH and ring is opened up:

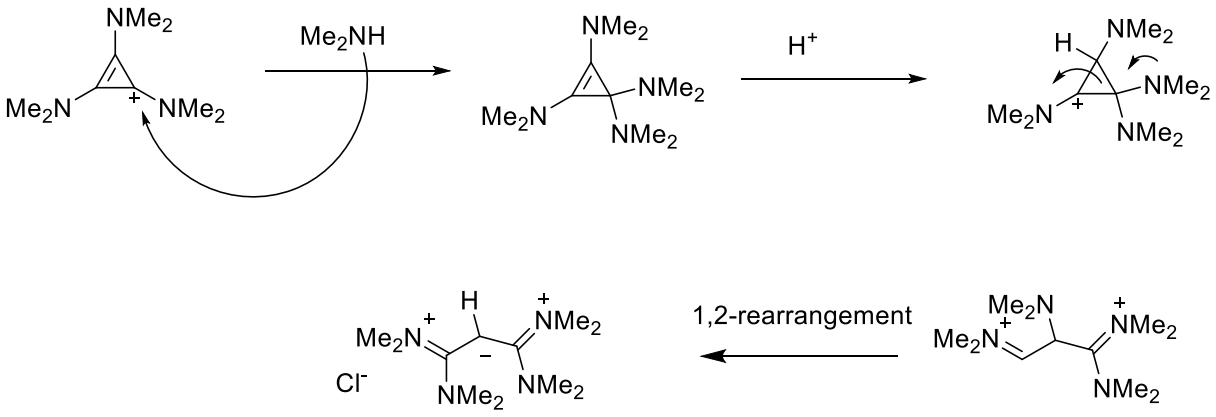

Figure 4.5-Mechanism for the open ring products.[14]

4.4 Synthesis of C_{3h} cations

Upon reaction of C_3Cl_5H with MeRNH (R = ethyl, allyl or $–CH_2CH_2OCH_3$), a mixture of $[HC_3(NMeR)_4]^+$ with $[C_3(NMeR)_3]Cl$ and $[MeRNH_2]Cl$ are formed. The peak ratio in the mass spectra suggested a greater amount of $[C_3(NMeR)_3]Cl$ than $[HC_3(NMeR)_4]^+$. The mixtures were dissolved in water and acidified with conc. HCl to *p*H = 1-2. $[C_3(NMeR)_3]Cl$ was then extracted with $CHCl_3$ (3×50 mL), leaving behind ($[H_2C_3(NMeR)_4]^{2+}$) and $[MeRNH_2]Cl$ in the aqueous layer. A small amount of $[H_2C_3(NMeR)_4]^{2+}$ remained with $[C_3(NMeR)_3]Cl$.

In order to remove the remaining open ring product, chloride anion was exchanged with TFSA and this allowed the separation of $[C_3(NMeR)_3]$TFSA from $[HC_3(NMeR)_4]$TFSA. The mixture was dissolved in $CHCl_3$ and the open ring form was extracted with conc. HCl followed by washing of the organic layer with water until the *p*H was neutral. This separation was possible because $[HC_3(NMeR)_4]$TFSA was converted to $[H_2C_3(NMeR)_4]Cl_2$, thus making separation easy due to a presence of a hydrophilic anion. The closed ring remained with the TFSA anion.

4.5 Bis(dimethylamino)cyclopropenium based ILs

4.5.1 Synthesis of bis(dimethylamino)cyclopropenone, $C_3(NMe_2)_2O$

For the synthesis of low symmetry (C_{2v} and C_s) tac salts, $C_3(NMe_2)_2O$ was required. $C_3(NMe_2)_2O$ was prepared by the procedure already published by Wilcox.[15] However, we used a mixture of $[C_3(NMe_2)_3]Cl$, $[HC_3(NMe_2)_4]^+$, and $[Me_2NH_2]^+$. This was dissolved in an aqueous 15% KOH solution and stirred at 70 °C in an open mouth beaker for 2 hours to allow the escape of Me_2NH. Reaction times of less than 2 hours were found to have unreacted $[C_3(NMe_2)_3]Cl$, as shown by

mass spectra. Yoshida obtained a mixture of $C_3(NMe_2)_2O$ and $[HC_3(NMe_2)_4]^+$ (9%) after alkaline hydrolysis of $[C_3(NMe_2)_3]Cl$.[12]

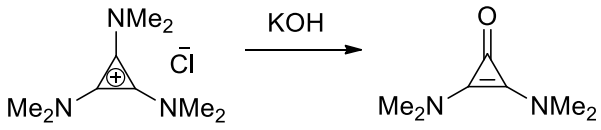

Figure 4.6-Reaction scheme for the formation of $C_3(NMe_2)_2O$.

The most difficult challenge was to separate $C_3(NMe_2)_2O$ from $[HC_3(NMe_2)_4]^+$. $C_3(NMe_2)_2O$ has a zwitterionic nature (fig. 4.7) and its polarity is very similar to $[HC_3(NMe_2)_4]^+$.

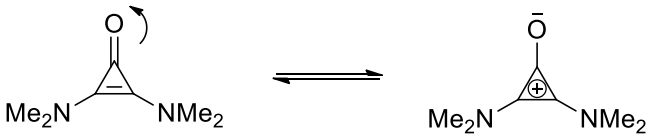

Figure 4.7-Zwitterionic nature of $C_3(NMe_2)_2O$.

The mixture was acidified with HCl to convert $[HC_3(NMe_2)_4]^+$ to $[H_2C_3(NMe_2)_4]^{2+}$. $[H_2C_3(NMe_2)_4]^{2+}$is more water soluble than the monocation and $C_3(NMe_2)_2O$ was easily extracted out with $CHCl_3$.

Sometimes during the purification process, the $C_3(NMe_2)_2O$ was protonated by HCl. The protonated cyclopropenone cannot be alkylated. It was easily deprotonated back to cyclopropenone by the addition of NaOH (fig. 4.8).

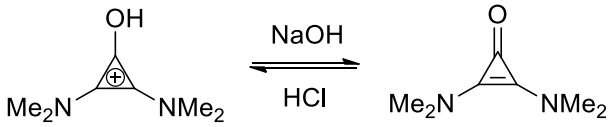

Figure 4.8-Deprotonation of cyclopropenone.

4.5.2 Alkylation of bis(dimethylamino)cyclopropenone

It is known, by the previous studies by the Curnow group, that Me_2SO_4 is the most useful alkylating agent for cyclopropenones since it is efficient and cheap.[16] In addition, $MeSO_4^-$ can easily be exchanged with other anions. By using 1.3 equivalents of Me_2SO_4,

methoxybis(dimethylamino)cyclopropenium $[C_3(NEt_2)_2OMe]MeSO_4$ salts are formed in good yields, and without heating (fig. 4.9).

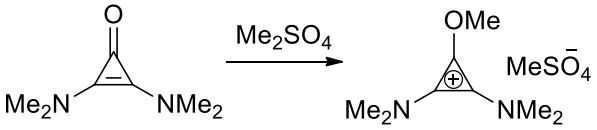

Figure 4.9-Methylation of cyclopropenone.

Me_2SO_4 reacts with moisture rapidly forming methanol and methyl sulphuric acid, which protonates cyclopropenone (fig. 4.10) and prevents it from reacting with Me_2SO_4.[16] Samples are dried before alkylation using isopropanol azeotropic drying to prevent the hydrolysis of Me_2SO_4.

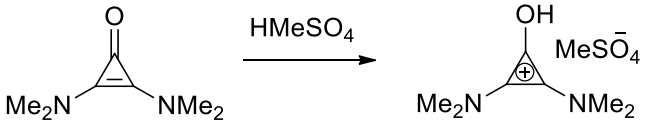

Figure 4.10-Protonation of cyclopropenone from methyl sulphuric acid.

Unreacted Me_2SO_4 was easily removed by washes with diethyl ether, otherwise, in the next step, the amine may be methylated. After the addition of a primary or secondary amine, the $[C_3(NMe_2)_2OMe]MeSO_4$ reacts to form $[C_3(NMe_2)_2NR'R"]^+$ in less than 5 minutes without heating. ^1H NMR and mass spectra suggested the formation of $C_3(NMe_2)_2O$ along with $[C_3(NMe_2)_2NR'R"]^+$. This cyclopropenone is formed due to a side reaction in which the amine attacks the methyl group instead of the C_3 ring.[16]

4.5.3 Synthesis of C_{2v} and C_s cations from $[C_3(NMe_2)_2OMe]MeSO_4$

Upon reaction of $[C_3(NMe_2)_2OMe]MeSO_4$ with an amine, low symmetry (C_{2v} and C_s) tac salts were formed. The methyl sulphate anion was easily exchanged with the hydrophobic anion bis(trifluoromethanesulfonyl)amide (TFSA). The hydrophobic nature helped in the removal of the residual $C_3(NMe_2)_2O$ and $[HC_3(NMe_2)_4]^+$: The product mixture was dissolved in $CHCl_3$ and, by repeated washing with conc. HCl, $C_3(NMe_2)_2O$ and $[HC_3(NMe_2)_4]^+$ were washed out.

It is known that protic ILs can be deprotonated easily by using *n*-BuLi in THF at −78 °C. This route will be discussed in detail later in the chapter. This route was applied in an attempt to synthesize $[C_3(NMe_2)_2(NMe(CH_2CH_3))]MeSO_4$ from $[C_3(NMe_2)_2NH(CH_2CH_3))]MeSO_4$.

However, $[C_3(NMe_2)_2NHEt]MeSO_4$ is not soluble in THF and the reaction did not happen. The anions were exchanged with TFSA to increase the solubility in THF, however, the synthesis of $[C_3(NMe_2)_2(NMe(CH_2CH_3))]TFSA$ from $[C_3(NMe_2)_2(NH(CH_2CH_3))]TFSA$ still proved to be difficult (fig. 4.11).

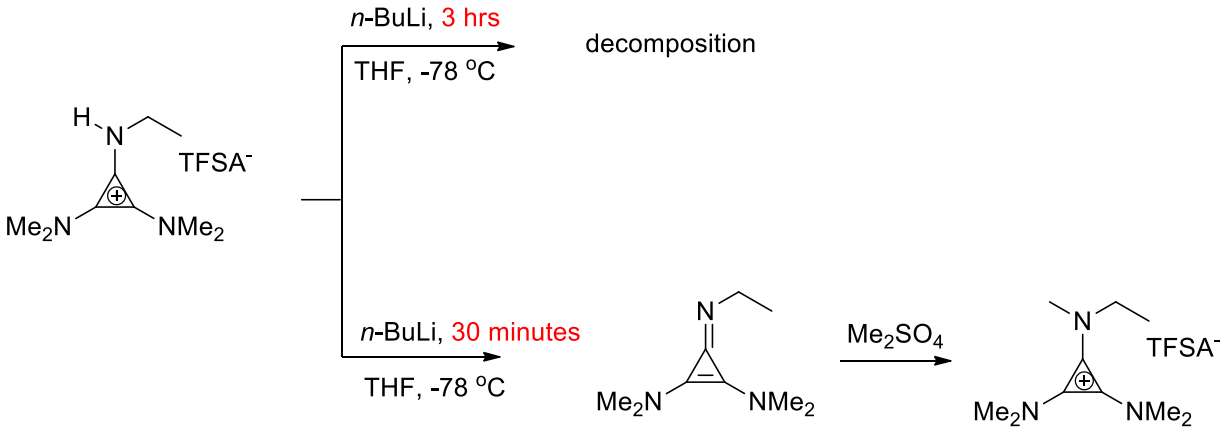

Figure 4.11-Failed synthesis of $[M_5E]TFSA$ form $[M_4EH]TFSA$ using n-BuLi.

Reduction of the reaction time from 3 hours to 30 minutes gave 100% conversion to $[C_3(NMe_2)_2(NMe(CH_2CH_3))]TFSA$, although the final product turned into a dark color probably due to some side products which did not show up on the NMR, mass spectrometry or micro analysis.

Attempts were also made to synthesize $[C_3(NMe_2)_2(NMe(CH_2CHCH_2))]TFSA$ from $[C_3(NMe_2)_2(NH(CH_2CHCH_2))]TFSA$ by stirring with *n*-BuLi for 30 minutes. However, due to acidic protons in the allyl chain, side reactions occurred and the desired product could not be obtained by this route. Weaker bases were also tried, such as NaOH and KH, but the product remained as a mixture of $[C_3(NMe_2)_2(NH(CH_2CHCH_2))]^+$ and $[C_3(NMe_2)_2(NMe(CH_2CHCH_2))]^+$. It was instead prepared via reaction of $[C_3(NMe_2)_2OMe]MeSO_4$ with $HN(CH_2CHCH_2)Me$.

$[C_3(NMe_2)_2(NMe(CH_2CH_2CH_3))]TFSA$, $[C_3(NMe_2)_2(NMe(CH_2CH_2OCH_3))]TFSA$ and $[C_3(NMe_2)_2(NMePentyl)]TFSA$ were similarly synthesized from $[C_3(NMe_2)_2(NH(CH_2CH_2CH_3))]TFSA$, $[C_3(NMe_2)_2(NH(CH_2CH_2OCH_3))]TFSA$ and $[C_3(NMe_2)_2(NHPentyl)]TFSA$, respectively, using *n*-BuLi in THF for 3 hours. It was thought that propyl, $-CH_2CH_2OCH_3$ and pentyl chains, provide more steric protection. Ethyl and allyl chains

have less steric protection and acidic protons and tend to react with *n*-BuLi to give undesirable side products.

AAILs, $[C_3(NMe_2)_2(Aminoacid)]MeSO_4$ were prepared by stirring bis(dimethylamino)-methoxycyclopropenium, Et_3N and amino acid in water at room temperature. Detailed syntheses of CILs will be discussed later in this chapter. During the synthesis of $[C_3(NMe_2)_2(Aminoacid)]MeSO_4$, the most difficult aspect encountered was the purification of the AAIL. When Et_3N is used in the reaction, it forms Et_3NH^+ salts. The polarity of the CIL and the ammonium salt is very similar. Several methods were tried to separate them, but all were unsuccessful.

A cold solution of NaOH (8%) was added to the mixture to convert the triethylammonium salt to the Et_3N and diethyl ether (5×10 mL) washes were done to remove the amine. Instead, the cyclopropenones were formed (fig. 4.12), as confirmed by ^1H NMR and mass spectrometry.

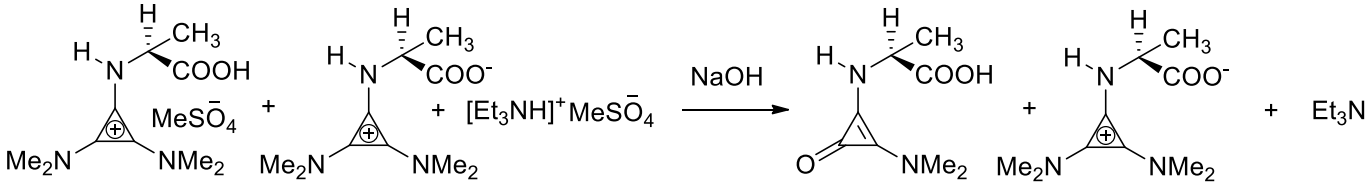

Figure 4.12-Reaction scheme for the purification of $[M_4AA]MeSO_4$.

This occurs due to reduced steric protection compared to the analogous NEt_2 system.

The nucleophilic base NaOH was utilized during the synthesis instead of Et_3N to avoid any formation of ammonium salts, but unfortunately NaOH converted some $[M_4OMe]MeSO_4$ to $C_3(NMe_2)_2O$ (fig. 4.12). The product was therefore a mixture of CIL and $C_3(NMe_2)_2O$. Due to the zwitterionic nature of $C_3(NMe_2)_2O$, its polarity is very similar to the cyclopropenium salt and it proved difficult to separate from this mixture. The hydrophilic $MeSO_4^-$ was exchanged with hydrophobic TFSA, but still it proved difficult to obtain pure CIL.

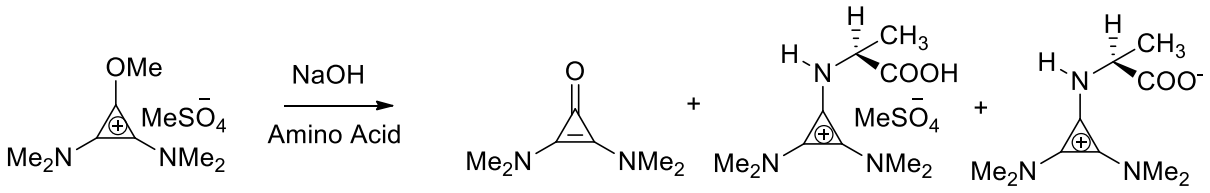

Figure 4.13-Reaction scheme for the synthesis of $[M_4AA]MeSO_4$ using NaOH as a base.

Later, other non-nucleophilic bases, Me_3N (hydrophilic), and Bu_3N (hydrophobic), were used instead of Et_3N. It was initially thought that the separation of the salts could be achieved, but, in the case of Me_3N, the separation was very difficult due to the more hydrophilic nature of Me_3N compared to Et_3N. With Bu_3N, the reaction did not occur due to its hydrophobic nature-it remained as a separate layer even upon stirring overnight.

Attachment of an amino acid moiety to $[C_3(NMe_2)_2OMe]MeSO_4$ was abandoned due to the difficulty in its separation from the ammonium salts.

4.6 Bis(diethylamino)cyclopropenium-based ILs

4.6.1 Alkylation of bis(diethylamino)cyclopropenone, $C_3(NEt_2)_2O$

$C_3(NEt_2)_2O$ was required for the synthesis of low symmetry cations. It was alkylated with dimethyl sulphate similarly to $C_3(NMe_2)_2O$. Other alkylating agents, such as ethyl iodide, trimethyloxonium tetrafluoroborate, and methyl trifluoromethanesulfonate, were also used. Dimethyl sulphate, trimethyloxonium tetrafluoroborate and methyl trifluoromethanesulfonate are strong alkylating agents and form the $[C_3(NEt_2)_2OMe]X$ (X = methyl sulphate, tetrafluoroborate or trifluoromethanesulfonate) salts in less than 5 minutes in excellent yields (70-83%). Unfortunately, there were difficulties encountered during the handling of trimethyloxonium tetrafluoroborate (also called "Meerwein salt"). Trimethyloxonium reacts with moisture immediately forming dimethyl ether, methanol and tetrafluoroboric acid, which protonates the cyclopropenone (fig. 4.14). Trimethyloxonium tetrafluoroborate was always handled in a dry glove box but even then it resulted in a mixture of protonated and alkylated cyclopropenone (in a ratio of 1:5) as seen by mass spectrometry. The dimethyl ether formed as a by-product volatilized off easily *in vacuo*. The amine was added to the mixture in the next step, and this reacted with alkylated cyclopropenone to form $[C_3(NEt_2)_2NR_2]BF_4$ while leaving unreacted protonated

cyclopropenone. The mixture was dissolved in water and $[C_3(NEt_2)_2NR_2]BF_4$ was extracted with $CHCl_3$.

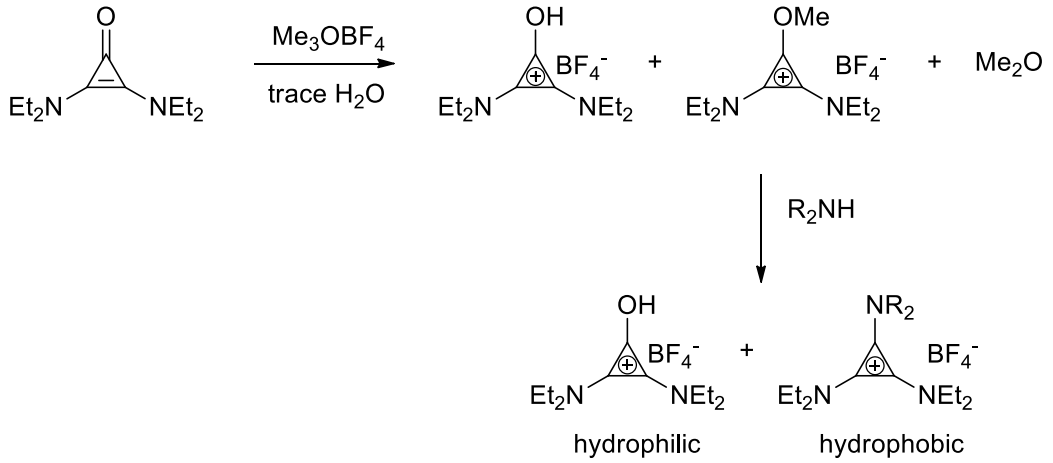

Figure 4.14-Methylation of cyclopropenone using trimethyloxonium tetrafluoroborate.

4.6.2 Synthesis of C_{2v} ILs from bis(diethylamino)methoxycyclopropenium

Diprotic tac cations were synthesized by reaction of an alkoxycyclopropenium salt with dry ammonia gas for an hour, but when the anion exchange was carried out in water, a mixture of $[C_3(NEt_2)_2NH_2]$TFSA and $C_3(NEt_2)_2O$ in a ratio of 0.96:0.04 was observed, as confirmed by ^{1}H NMR and microanalysis (fig. 4.15), probably due to hydrolysis (fig. 4.16);

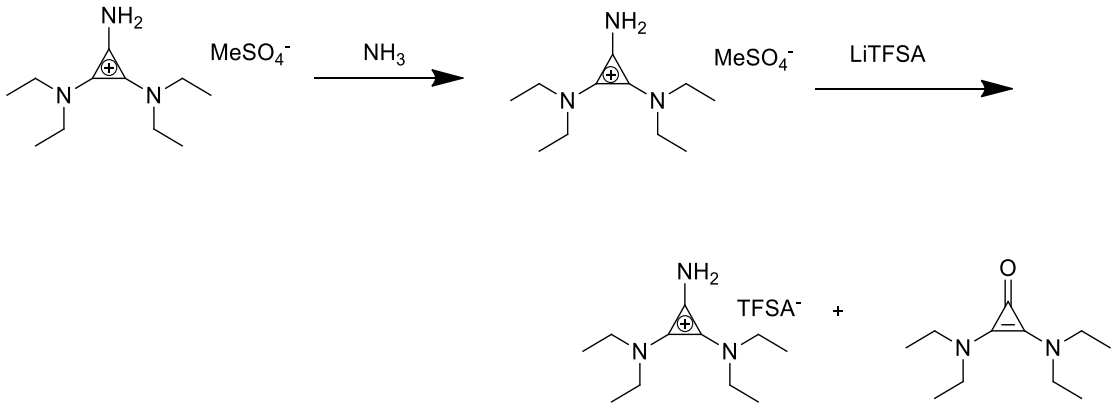

Figure 4.15-Reaction scheme for the synthesis of $[C_3(NEt_2)_2NH_2]$TFSA.

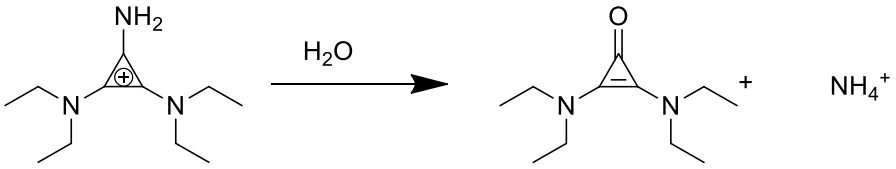

Figure 4.16-Hydrolysis of $[C_3(NEt_2)_2NH_2]^+$.

Diethyl ether washes to get rid of $C_3(NEt_2)_2O$ did not work well due to the high polarity of the IL and greater solubility of cyclopropenone in the IL.

4.6.3 Synthesis of C_s tac cations

4.6.3.1 Deprotonation of Protic ILs $[C_3(NEt_2)_2NBuH]^+$

$[C_3(NEt_2)_2NBuH]^+$ cannot be directly alkylated with dimethyl sulphate to $[C_3(NEt_2)_2NBuMe]^+$:$[C_3(NEt_2)_2NBuH]^+$ was stirred with 1.5 equivalents of dimethyl sulphate overnight; ^{1}H NMR and mass spectra showed that no reaction had taken place.

Deprotonation of $[C_3(NEt_2)_2NBuH]^+$ with *n*-BuLi in THF forms an imine which can then be alkylated with Me_2SO_4 in 100% conversion to give $[C_3(NEt_2)_2NBuMe]MeSO_4$ (fig. 4.17).[3]

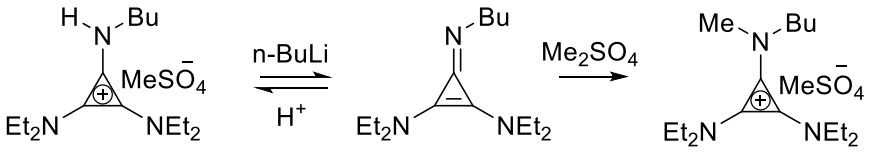

Figure 4.17- Deprotonation of $[C_3(NEt_2)_2NBuH]^+$ with *n*-BuLi.

The solutions turned from light yellow to dark brown indicating the presence of some side products.

4.6.3.2 Synthesis of CILs from bis(diethylamino)methoxycyclopropenium

The main part of the project was to synthesize CILs by attaching a chiral amine to $[C_3(NEt_2)_2OMe]MeSO_4$. Amino acids are utilized as a cheap, chiral, and biodegradable source. Although, resulting AAILs might not be biodegradable.

Initially $[C_3(NEt_2)_2OMe]MeSO_4$ was stirred with L-alanine in dry THF at 50 °C overnight., however, NMR and mass spectrometry showed that no reaction had taken place. This was

probably due to the zwitterionic nature of the amino acid in THF giving an ammonium centre. Therefore the amino acid was converted to the amino acid anion with a tertiary amine (Et_3N). The dissolution of L-alanine in water and addition of Et_3N, gave the negatively charged carboxylate with a neutral α-amino group (fig. 4.18).

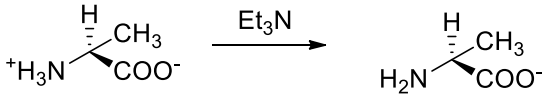

Figure 4.18-Conversion of zwitterionic form of L-alanine to negatively charged carboxylate.

$[C_3(NEt_2)_2OMe]MeSO_4$ was added to the above mixture of amino acid, Et_3N and water (fig. 4.19). The solution was stirred for an hour at room temperature and the AAIL was then formed.

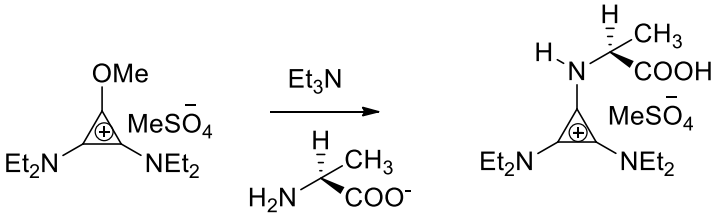

Figure 4.19-Reaction scheme for the formation of $[E_4AA]MeSO_4$.

The water was removed *in vacuo* and the product mixture was dissolved in acetone and the excess of amino acid was filtered off. One thing needs to be noted that Et_3N was used instead of NaOH because $[C_3(NEt_2)_2OMe]MeSO_4$ starts converting back to $C_3(NEt_2)_2O$ in the presence of hydroxide (as explained above). The most difficult challenge was to remove $[Et_3NH]MeSO_4$ from the CIL due to their similar solubility. One technique utilized to remove ammonium salts involved dissolving the mixture in ice-cold water followed by extraction of the product with $CHCl_3$/EtOH (2:1). Pure IL was obtained, but the yield was low. This purification technique was, however, used to synthesize CILs with the $MeSO_4^-$ anion.

The easiest purification technique was to dissolve the mixture in cold dilute NaOH solution (8%), extracting the Et_3N with repeated diethyl ether washes, and to then immediately neutralize the *p*H with HCl. In this way, pure CIL was obtained with excellent yields, although some of $MeSO_4^-$ anions were exchanged with chloride. Upon anion metathesis with TFSA, hydrophobic CILs were obtained.

The above reaction route for the synthesis of tac-based AAILs is very similar to that used to prepare optically-active guanidinium salts derived from α-chiral amino esters as potential organocatalysts and ionic liquids (fig. 4.20).[17] The reaction of a chloroamidinium salt with an amino acid ester hydrochloride was carried out in acetonitrile in the presence of Et_3N. The hexalkylguanidinium cation is similar to the tac cation: a central cation is stabilized by three surrounding nitrogen substituents.

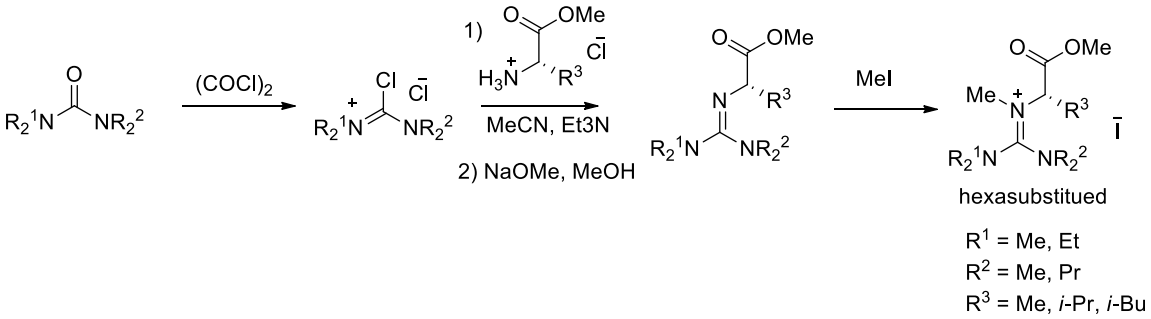

Figure 4.20-Reaction scheme for the synthesis of guanidinium-type AAILs.[17]

4.6.3.2.1 Calculation of AAIL and zwitterion ratios

After the synthesis of the AAIL, it was extracted with the organic solvent from an aqueous layer and was obtained as a mixture of IL and its zwitterion.

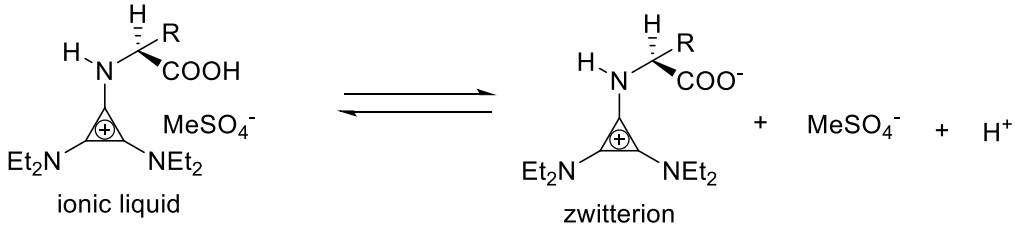

Figure 4.21-Equilibrium between IL and zwitterion.

^{1}H NMR and microanalysis indicated an equilibrium mixture of the desired IL and its zwitterion (fig. 4.21). The integral for the $MeSO_4^-$ was always low in ^{1}H NMR.

Attempts were made to calculate the IL:zwitterion ratio of water soluble AAILs (with $MeSO_4^-$) by polarimetry. The specific rotation of an optically-active substance varies with the nature of solvent.[18] Optical rotation was measured by making aqueous solutions of the mixture, IL (in HCl) and zwitterion (in NaOH). However, ratios obtained in this way did not agree with either ^{1}H

NMR or microanalysis. Wood has shown previously that the addition of acid or base to an amino acid solution produces a marked and unpredictable change in the specific rotation.[19] This may be due to formation of salt/zwitterion hydrogen-bonded aggregates with different optical rotations due to varying conformations at intermediate *p*Hs.[20]

Then, *p*H titrations were performed to determine the amount of IL and zwitterion in the IL/zwitterion mixture. After plotting the graph between the *p*H and volume of NaOH added, the amount of acid (IL) in the mixture is calculated from the equivalence point. Ultimately *p*H titrations compared more favorably to the microanalysis results (table 4.1).

Table 4.1-Comparison of IL and zwitterion ratios from microanalysis and *p*H titrations

	AAIL	IL:Zwitterion (from microanalysis)	IL:Zwitterion (from *p*H titrations)	IL:Zwitterion (from ^{1}H NMR)*
1	$[E_4Ala]MeSO_4$	0.62:0.38	0.53:0.47	0.56:0.44
2	$[E_4Ala]TFSA$	0.93:0.07	0.91:0.09	
3	$[E_4Pro]MeSO_4$	0.65:0.35	0.71:0.28	0.47:0.53
4	$[E_4Pro]TFSA$	0.85:0.15	0.93:0.07	
5	$[E_4Val]MeSO_4$	0.45:0.55	0.36:0.63	0.32:0.68
6	$[E_4Val]TFSA$	0.80:0.20	0.98:0.01	
7	$[E_4Thr]MeSO_4$	0.45:0.55	0.64:0.36	0.21:0.80
8	$[E_4Thr]TFSA$	0.85:0.15	0.97:0.03	
9	$[E_4Arg]TFSA_2$	0.73:0.27 (M^{2+}:M^+)	0.951:0.04	
10	$[E_4Asp]TFSA$	0.90:0.10	0.91:0.09	
11	$[E_4His]TFSA_2$	0.91:0.09 (M^{2+}:M^+)	0.70:0.30	
12	$[E_4Met]TFSA$	0.72:0.28	0.54:0.46	
13	$[E_4Leu]TFSA$	0.85:0.15	0.81:0.20	
14	$[E_4Ile]TFSA$	0.90:0.10	0.95:0.05	
15	$[E_4Try]TFSA$	0.79:0.21	0.54:0.45	
16	$[E_4Tyr]TFSA$	0.91:0.09	0.72:0.28	
17	$[E_4Phe]TFSA$	0.90:0.10	0.69:0.31	
18	$[E_4Ser]TFSA$	0.94:0.06	0.94:0.06	
19	$[E_8Gln]TFSA_2$	(IL (2 tac):IL(1tac) 0.95:0.05)	(IL (2 tac):IL(1 tac)	

		or (IL(2tac):Zwitterion 0.95:0.05)	0.78:0.22) or (IL(2tac):Zwitterion 0.72:0.28) or (IL (1 tac): IL (2tac) 0.72:0.28)
20	[E_4Asn]TFSA	no zwitterions	0.88:0.12
21	[E_8Lys]$TFSA_2$	no zwitterions	0.90:0.10

*upon integrating the methyl sulphate peak

4.6.3.2.2 Optical purity of AAILs

To check the optical purity of these CILs, the *S*-CIL was dissolved with the sodium salt of *S*-Mosher's acid. ^1H and ^{19}F NMR was run in $CDCl_3$. There was no splitting of the –OMe and $–CF_3$ signal of Mosher's acid, suggesting the CIL was enantiopure.

4.6.3.2.3 Failed separation of AAIL and zwitterion by *p*H alteration

Altering the *p*H of the aqueous solution of the AAIL has no effect on the IL:zwitterion ratio in the organic layer (fig. 4.22).

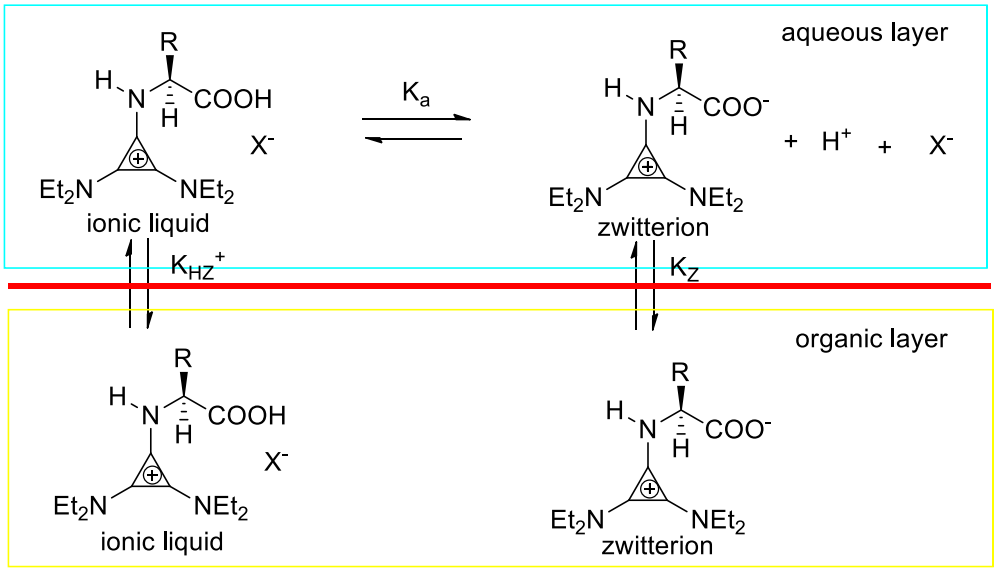

Figure 4.22–Equilibrium of IL/zwitterion in aqueous and organic layer.

As the *p*H is decreased with HCl, the upper equilibrium (fig. 4.23) is shifted backwards and results in the formation of more AAIL:

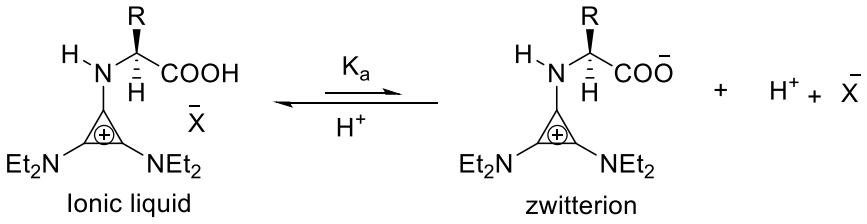

Figure 4.23–Effect on equilibrium with the decrease of *p*H.

Upon extraction of AAIL with organic solvent from the aqueous layer, more of the ionic liquid moves into the organic layer. Ionic liquids, being polar, increase the polarity of the organic layer. So K_Z does not remain constant. As K_Z changes, more zwitterion from the aqueous layer moves into the organic layer, thus, the IL/zwitterion ratio remains almost constant with a change in *p*H.

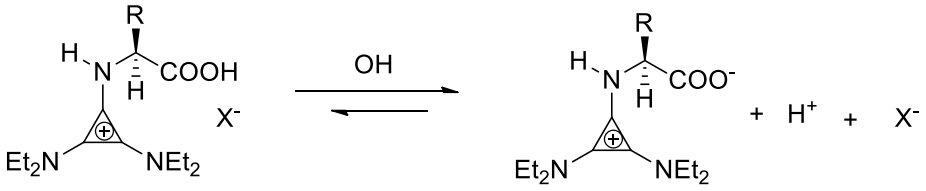

Figure 4.24–Effect on equilibrium with the increase of *p*H.

AAILs with TFSA as an anion are more soluble in organic solvents. These hydrophobic AAILs, [E_4AA]TFSA do not change the polarity of the organic layer as much as it changed for the hydrophilic AAILs, thus, [E_4AA]TFSA gives a lower amount of zwitterion (5 to 28%) compared to [E_4AA]$MeSO_4$ (35-55% zwitterion) in the isolated product.

4.6.3.2.4 Comparison of tac-based AAIL/zwitterion with other classes of AAILs

We obtained IL/zwitterion mixtures of tac-based AAILs. Now we will compare our tac-based AAIL mixtures with other classes of AAILs. Our tac-based IL/zwitterion mixtures were identified by ^{1}H NMR and microanalysis: AAILs with $MeSO_4^-$ as anion give a low integral for the methyl sulphate peak in the ^{1}H NMR, while in the microanalysis, IL/zwitterion mixtures give an increase in percentage of C, H and N. *p*H titrations were also used to determine the IL: zwitterion ratios and ratios agreed with the microanalysis results (table 4.1).

Remarkably none of the paper on AAILs have discussed the formation of a mixture of IL and zwitterion. Importantly, these papers do not have microanalyses quoted at all or have skipped microanalyses for particular AAILs.[17, 21]

Tao et al. reported the AAILs [AA]NO_3, [AA]Saccharinate, [AAE]NO_3 and [AAE]Saccharinate (AA = Gly, L-Ala, L-Val, L-IIe, L-Thr, L-Leu, L-Pro, L-Phe and L-Ser), and characterized them by ^{1}H, ^{13}C NMR and mass spectrometry. Microanalysis results were not reported for any of these AAILs.[21b, g] It was thought that probably the authors were getting mixtures of AAILs with zwitterion.

Later, Mike et al. syntheszied [L-ValMe]TFSA and [L-ProMe]TFSA using Tao's procedure. [L-ValMe]TFSA and [L-ProMe]TFSA were characterized by ^{1}H, ^{13}C NMR and mass spectrometry, but microanalysis results were again not given.[21h] Probably, esters undergo hydrolysis, resulting in AAIL and zwitterion mixture, which could be the reason for not mentioning microanalysis.

Shah and Liebscher synthesized hexasubstituted guanidinium (**4.1**) and cyclic chloroamidinium (**4.2**) salts as AAILs from α-amino acids. The hexasubstituted guanidinium and cyclic chloroamidinium salts were characterized by ^{1}H, ^{13}C NMR and mass spectrometry. But microanalysis results were not reported. The guanidinium cation is analogous to triaminocyclopropenium cation, thus there is certainty about the IL and zwitterion mixtures for these guanidimium (**4.1**) AAILs.[17] Possibly, the hydrolysis of methyl esters (guanidinium cation)

might have resulted in the formation of AAIL and zwitterion mixtures and micro results were not reported.

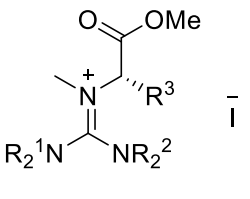

R^1 = Me or Et
R^2 = Me or Pr
R^3 = Me, *i*-Pr, or *i*-Bu

4.1[17]

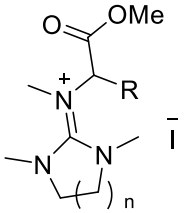

R = Me or *i*-Pr

4.2[17]

4.6.3.2.5 Significance of mixtures of ILs with zwitterion

Zwitterions can be considered as a sub-class of ionic liquids. For example, Yoshizawa and Ohno synthesized imidazolium cations (**4.3** and **4.4**) containing covalently-bound anionic sites (sulfonate or sulfonamide groups).[22]

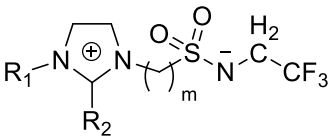

R_1 = ethyl or methyl
R_2 = H or methyl

4.3[22]

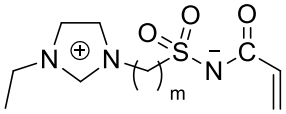

4.4[22]

These zwitterions (**4.3** and **4.4**) have low conductivities but, upon addition of an equimolar amount of LiTFSA, show high conductivities of 10^{-4} S cm^{-1} at 50 °C,[22] thus providing better properties as a binary mixture.

Combination of imidazolium-based zwitterions (**4.5**) and HTFSA formed a thermally-stable couple.[23] This zwitterion/acid mixture is known to act as an acid catalyst for the esterification of alcohols and acetate derivatives.[24]

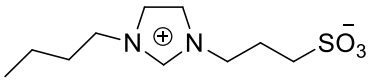

4.5[23]

4.6.3.2.6 Failed synthesis of [E4Asp]TFSA and [E4Glu]TFSA

During the synthesis of [E4Asp]TFSA and [E4Glu]TFSA, each containing two carboxylic acid groups, the removal of ammonium salts was found to be very difficult due to the product's higher affinity to water.

Mass spectra and microanalysis (IL:Zwi in 0.9:0.1) confirmed the formation of the [E4Glu]TFSA, however, messy NMR spectra showed the presence of unknown side products.

4.6.3.2.7 Esterification of [E4tyrosine]TFSA

In the case of [E4tyrosine]TFSA, ^{1}H NMR and mass spectra suggested that mixtures of IL, methyl ester and ethyl ester were formed (fig. 4.25). The esters were probably formed upon addition of alcohols during washings.

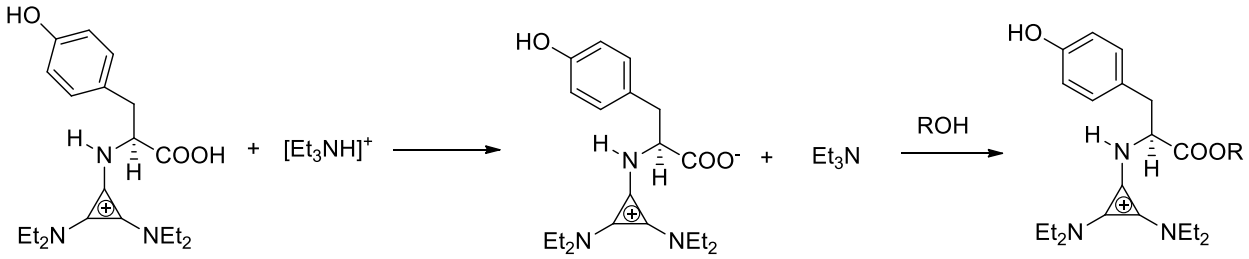

Figure 4.25-Formation and hydrolysis of esters during the synthesis of [E4tyrosine]TFSA.

The esters were hydrolyzed with HCl under reflux. It was found that the methyl esters are easier to hydrolyze than the ethyl esters. Basic hydrolysis was avoided because OH^- starts to attack the cyclopropenium ring.

4.6.3.2.8 Synthesis of AAILs from L-lysine

During the synthesis of [E4Lysine]TFSA, a mixture of $[E_4Lysine]^+$ (**4.6**) and the dicyclopropenium dication $[E_8Lysine]^{2+}$ (**4.7**) was obtained in which the ratio was dependent upon the ratio of $[E_4OMe]^+$ to L-Lysine. When 1:1 of $[E_4OMe]^+$:L-Lysine was utilized, it resulted in a 2:1 ratio of $[E_8Lysine]^{2+}$:$[E_4Lysine]^+$ as observed by mass spectra, but when a 2:1 ratio of

$[E_4OMe]^+$:L-Lysine was utilized, it resulted in a 2.6:1 ratio of $[E_8Lysine]^{2+}$:$[E_4Lysine]^+$ by mass spectrometry. A reaction was carried out with a 2:1 ratio of $[E_4OMe]^+$:L-Lysine followed by anion metathesis to $TFSA^-$. Conc. HCl washes were carried out to remove the monocation and to obtain the dication $[E_8Lysine]^{2+}$ in pure form. It was thought that $[E_8Lysine]TFSA_2$ is more hydrophobic than $[E_4Lysine]TFSA$, due to the two TFSA anions and two cyclopropenium groups, and this made the separation easy.

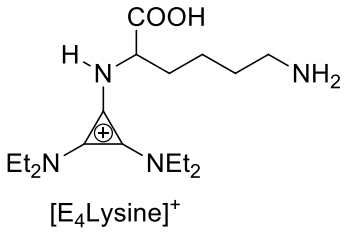

$[E_4Lysine]^+$

4.6

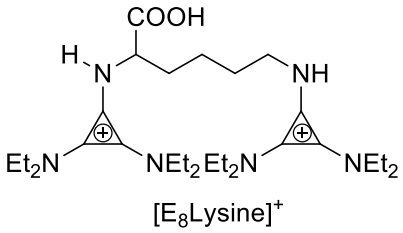

$[E_8Lysine]^+$

4.7

4.6.3.2.9 Failed synthesis of [E4Cysteine]TFSA

Similarly, in the case of L-Cysteine, when a 1:1 ratio of $[E_4OMe]^+$:L-Cysteine was used, it formed $[E_8Cysteine]^{2+}$ and $[E_4Cysteine]^+$. It is known that amino substituents on cyclopropenium rings are much more stable than thiol substituents.[25] Unfortunately, the separation of monocation (**4.8**) and dication (**4.9**) proved to be difficult and was not completely achieved.

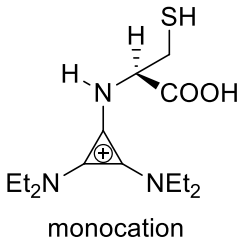

monocation

4.8

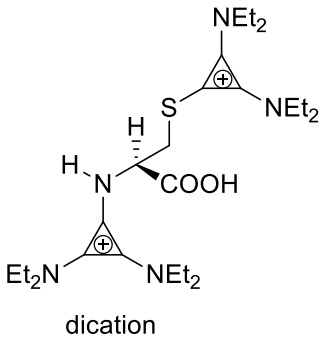

dication

4.9

4.6.3.2.10 Synthesis of AAILs for L-glutamine and L-asparagine

Glutamine and asparagine have an amide linkage in the amino acid side chain.

Mass spectrometry indicated the formation of $[E_4Asn]^+$ (**4.10**) and microanalysis suggested formation of $[E_4Asn]TFSA$ with no zwitterion.

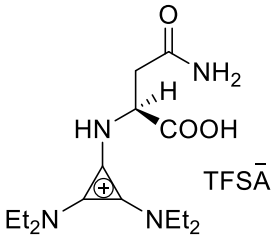

4.10

In $[E_4Gln]TFSA$, mass spectrometry suggested the formation of the desired monocation (**4.11**).

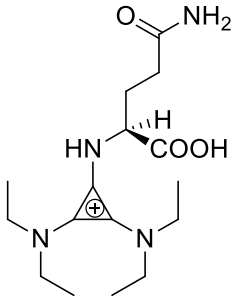

4.11

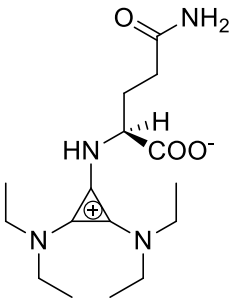

4.12

In the ^1H (fig 4.26) and ^{13}C NMR (fig. 4.27) spectra of the product we are able to see two sets of peaks. The ^1H NMR integrals are consistent with the monocation (**4.11**) and its zwitterion (**4.12**). However, we have never seen separate peaks for any other IL/zwitterion pair due to rapid proton exchange. The addition of either DCl or NaOH to a solution of $[E_4Gln]TFSA$ in D_2O did not significantly affect the ratios.

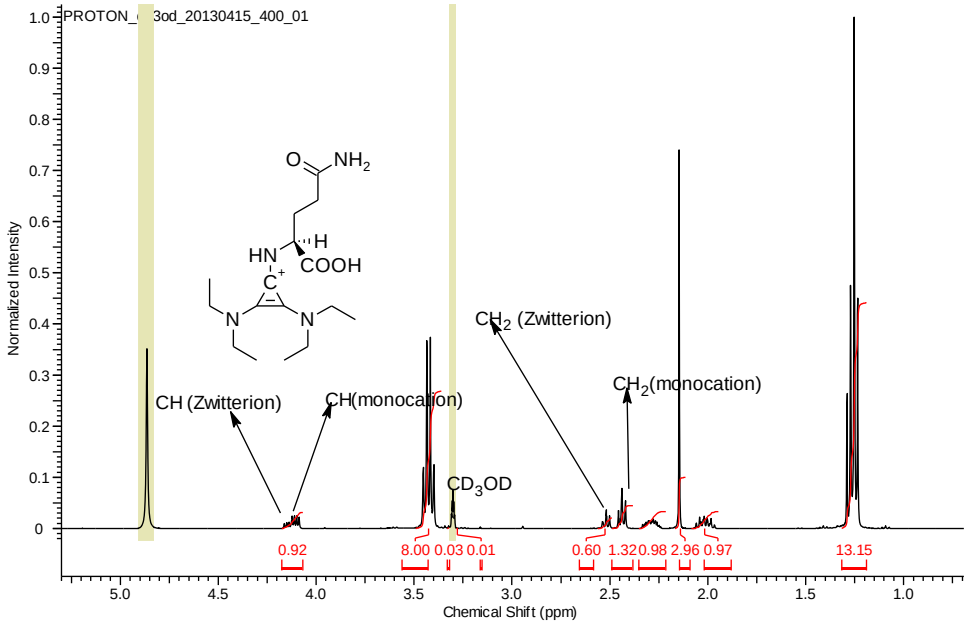

Figure 4.26- ^{1}H NMR of [E$_4$Gln]TFSA in CD$_3$OD.

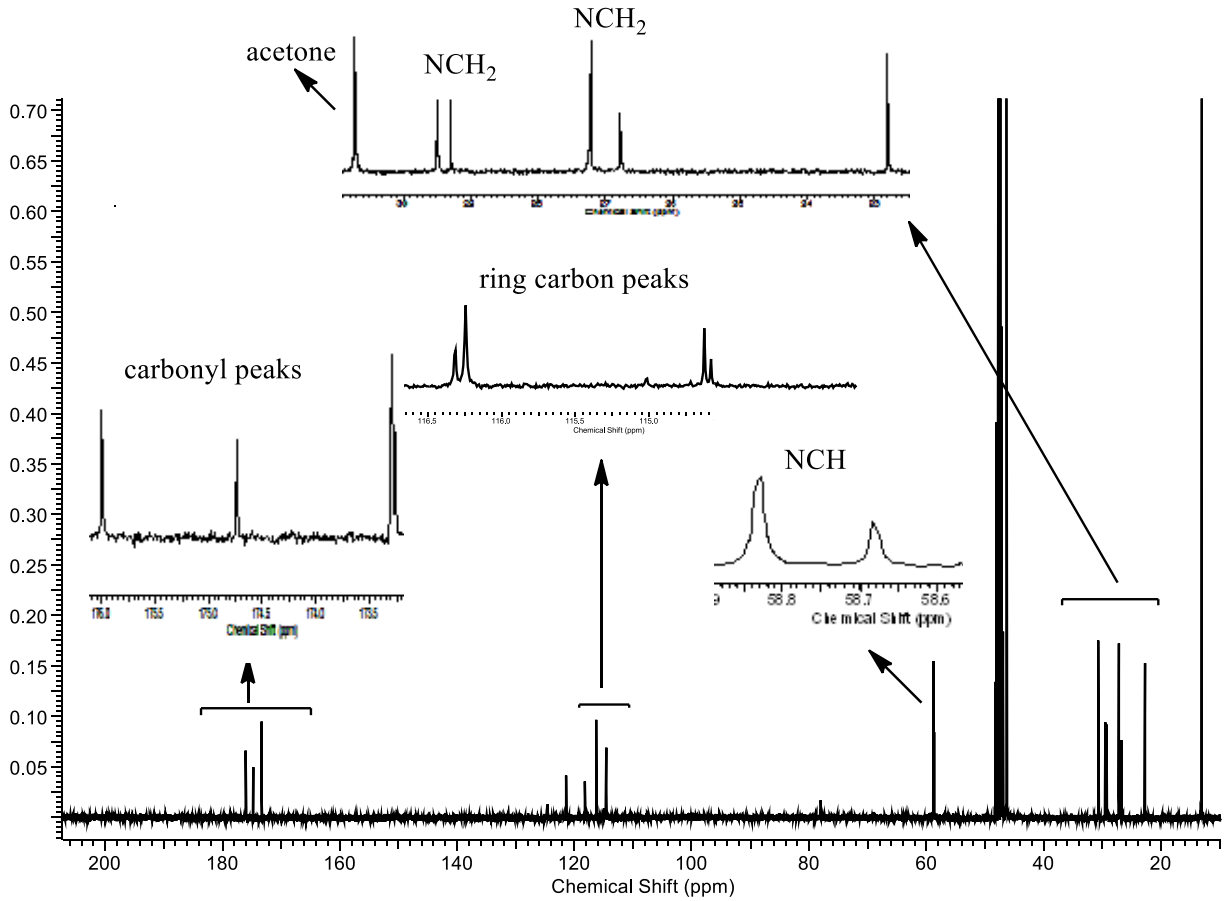

Figure 4.27- ^{13}C ^{26}NMR of [E$_4$Gln]TFSA in CD$_3$OD.

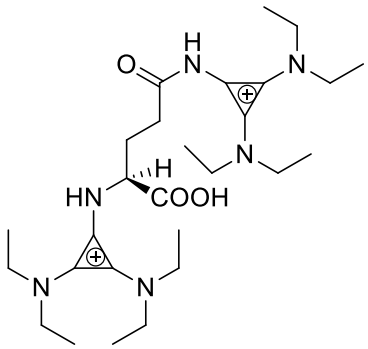

4.13

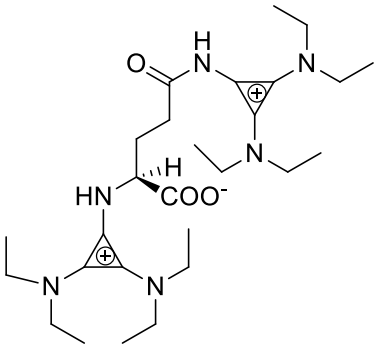

4.14

Microanalysis suggests either a 0.95:0.05 ratio of dication (**4.13**) and its zwitterion (**4.14**) or a 0.95:0.05 dication (**4.13**) and monocation (**4.11**). However, these would not be consistent with the observed ^{1}H NMR integrals a particularly-stable hydrogen-bonded cluster (**4.15**) with a 2:1 ratio is a possible explanation.

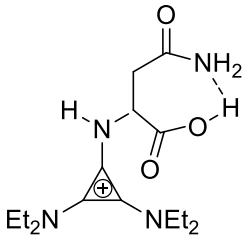

4.15

4.7 Formation of CIL Esters

The CILs were obtained as mixtures (IL and zwitterions) and were very viscous due to inter- and intramolecular hydrogen bonding (**4.16**).

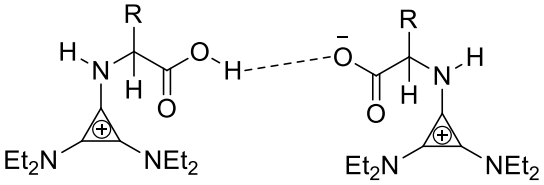

4.16

It was thought to convert the carboxylic/carboxylate groups to a esters in order to reduce the viscosity, but the pure esters were unobtainable (fig. 4.28). A mixture of the ester and zwitterion was always obtained. The alkylation was repeated three times, but 100% conversion was never achieved. The esters were found to rapidly hydrolyze under acid, base and neutral aqueous conditions.

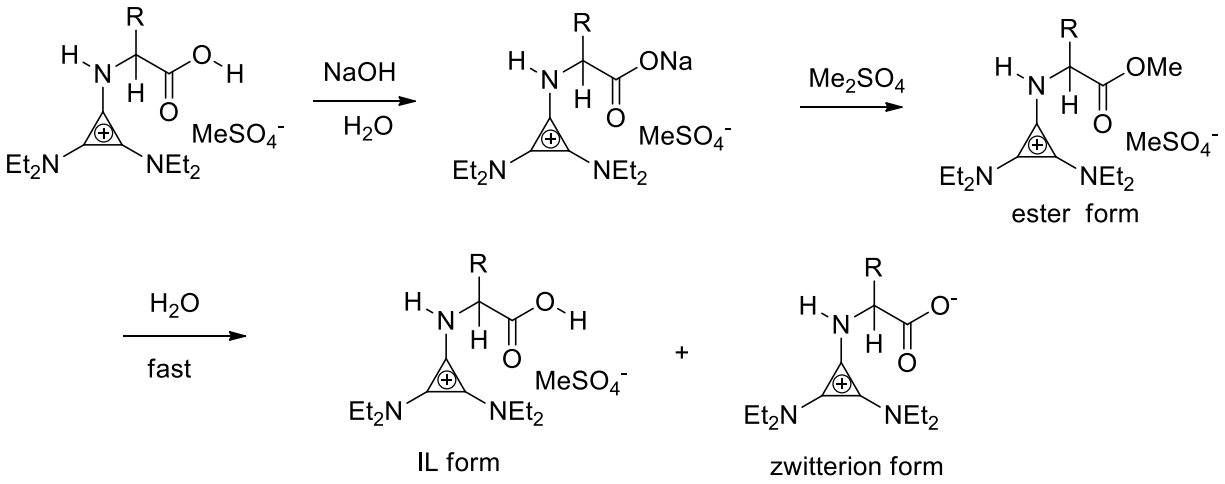

Figure 4.28-Failed reaction scheme for the esterification of AAILs using aqueous NaOH.

An attempt to make the ester by avoiding water via deprotonation with NaOH in isopropanol was made this gave a mixture of the desired ester and a dimethylated IL (in which the amino acid N atom has also been methylated) (fig. 4.29). This mixture was difficult to separate as aqueous solutions rapidly hydrolyze the esters:

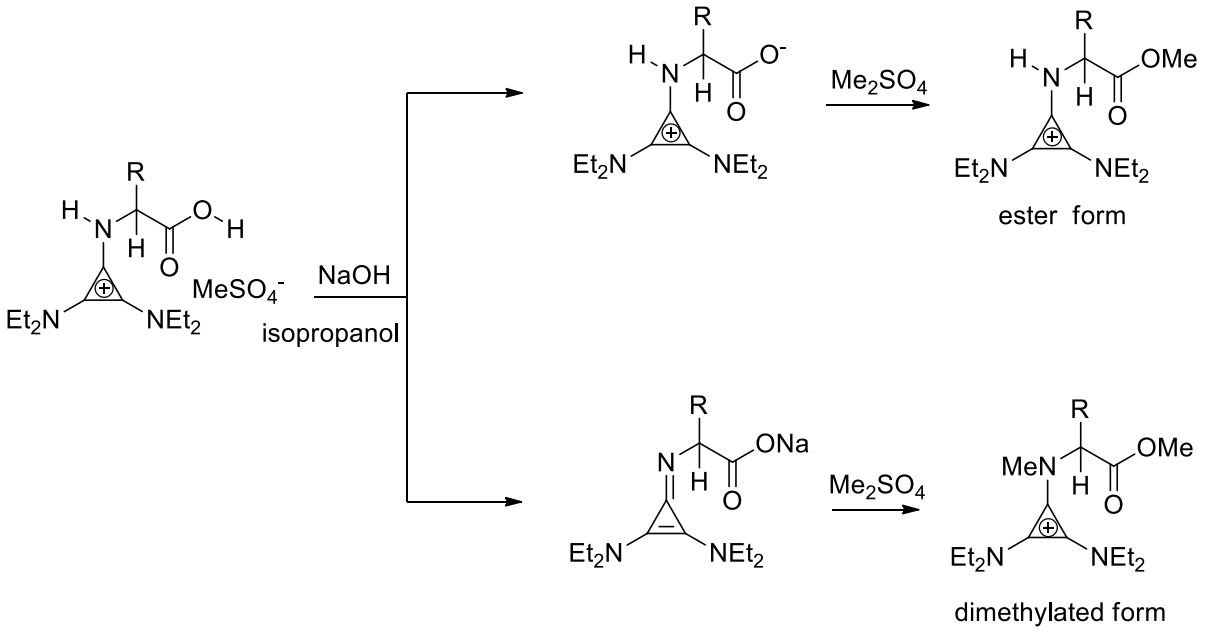

Figure 4.29Failed reaction scheme for the esterification of group of AAILs using NaOH in isopropanol.

Attempts to prepare the pure dimethylated product were not successful. *n*-BuLi was also used as a base, but the same mixture was formed along with additional side products.

4.8 Failed synthesis of tris(toluidino)cyclopropenium chloride

Stephen and co-workers, reported the synthesis of $[C_3(NHPh)_3]^+$ by reaction of $PhNHSiMe_3$ with C_3Cl_4. I converted $[C_3(NPhH)_3]Cl$ to the TFSA salt and DSC data and thermal decomposition temperatures were measured.

In an attempt to prepare methyl-substituted derivatives, C_3Cl_5H was reacted with *o*-toluidine or *p*-toluidine but no reaction took place. *o*-Toluidine or *p*-toluidine were then converted to trimethylsilyltoluidine and treated with C_3Cl_5H, but again no reaction took place (fig. 4.30).[27]

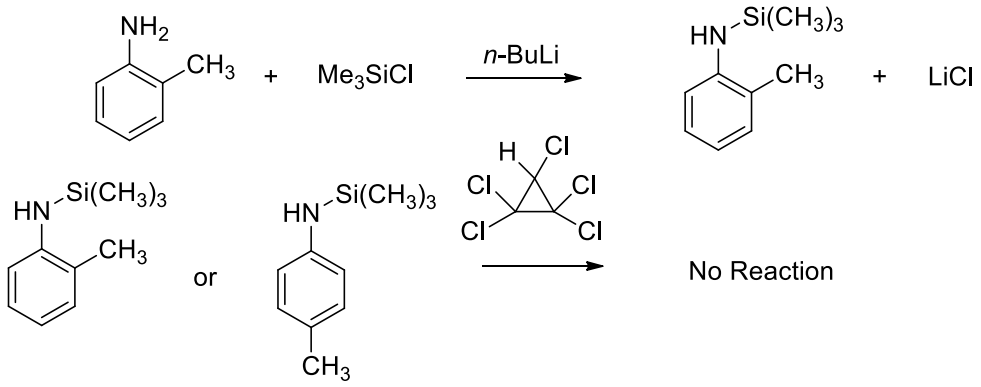

Figure 4.30-Failed reaction scheme for the synthesis of [C_3(NH(toluidine))$_3$]Cl.

The procedure was altered by adding NEt_3 to a mixture of *o*-toluidine, and C_3Cl_5H. Ammonium salts and trimethylsilylamine were obtained along with C_3Cl_4 (fig. 4.31).

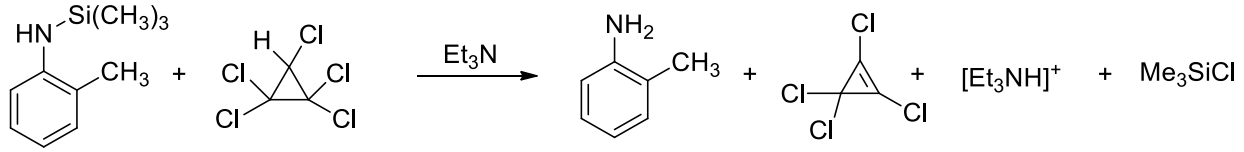

Figure 4.31-Failed reaction scheme for the synthesis of [C_3(NH(toluidine))$_3$]Cl using Et_3N.

No reaction occurred between tetrachlorocyclopropene and trimethylsilyltoluidine, probably due to steric effects (fig. 4.32).[28]

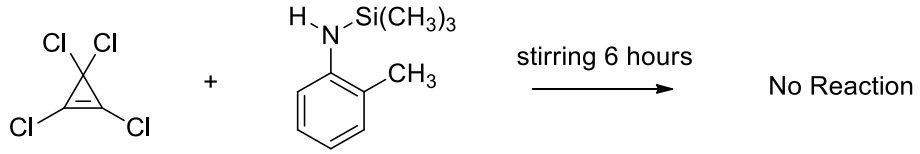

Figure 4.32-Failed reaction scheme for the synthesis of [C_3(NH(*o*-toluidine)$_3$)]Cl using tetrachlorocyclopropene.

4.9 Failed synthesis of tris(butylamino)cyclopropenium chloride

An attempt to synthesise triprotic $[(C_3(NHBu)_3]^+$ was made by reacting C_3Cl_5H and $BuNH_2$ at 0 °C followed by heating to reflux (fig. 4.33).

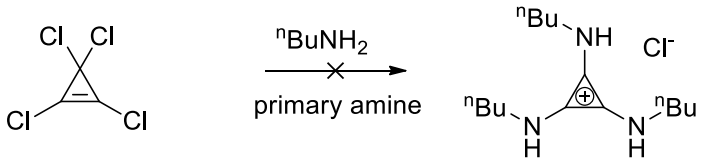

Figure 4.33-Failed reaction scheme for the synthesis of $[(C_3(NHBu)_3]^+$.

Instead, the open ring diamidinium dication, $[C_3H_2(NBuH)_4]^{2+}$, was formed (fig.4.34);

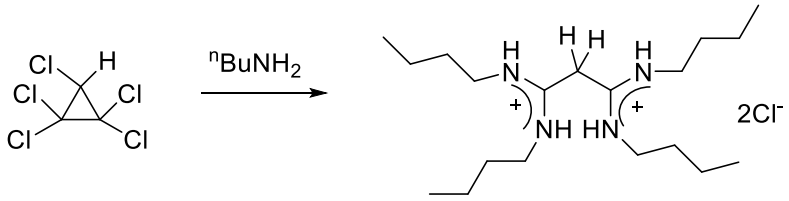

Figure 4.34-Reaction scheme for the preparation of $[C_3H_2(NBuH)_4]^{2+}$ using $^nBuNH_2$.

The reaction was repeated without heating to reflux, but the same open ring product was obtained.[2]

Another route was tried by reacting C_3Cl_5H with trimethylsilylbutylamine, but again the open ring product was obtained (fig. 4.35).[2, 27]

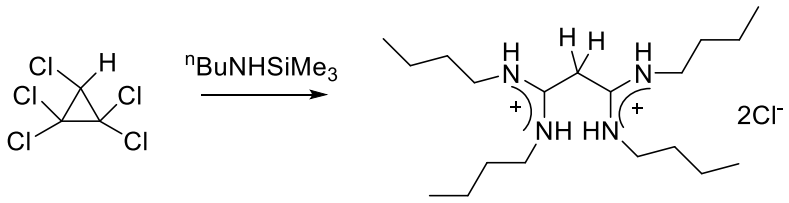

Figure 4.35-Reaction scheme for the synthesis of $[C_3H_2(NBuH)_4]^{2+}$ using $^nBuNHSiMe_3$.

Exchange of the chloride anion to TFSA was successful and this $[C_3H_2(NBuH)_4]TFSA_2$ was fully characterized (fig. 4.36). Thermal decomposition temperature, melting point and miscibility/solubility studies were carried out.

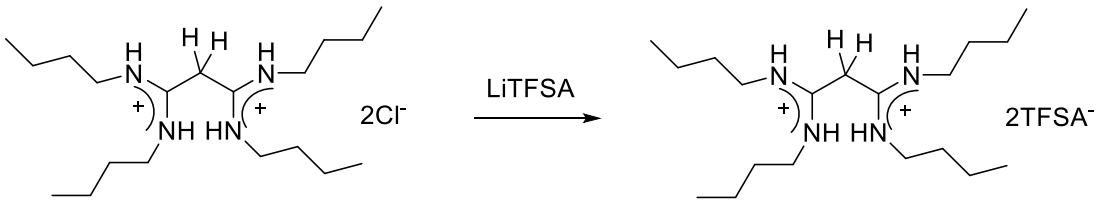

Figure 4.36-Formation of $[C_3H_2(NBuH)_4]TFSA_2$.

It was deduced that whenever a primary alkyl amine reacts with C_3Cl_5H or C_3Cl_4 it always opens the ring, probably due to reduced steric hindrance.

It is known that less bulky secondary amines form monocations while primary amines ($^nBuNH_2$) react with C_3Cl_5H to form exclusively the dication (fig. 4.37).[10]

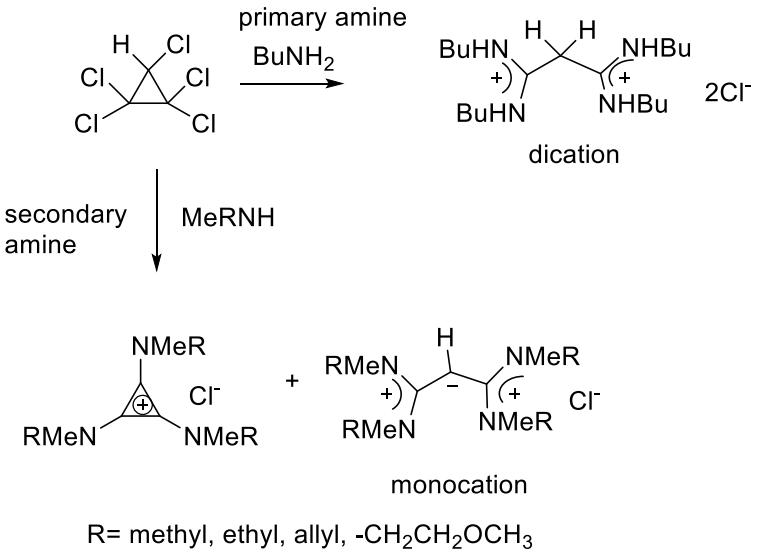

Figure 4.37-Reaction scheme for monocation and dication formation.[10]

The monocation contains tertiary bridging carbons which, upon protonation, convert to a dication. Often, both species are present in an acid/base equilibrium (fig. 4.38):[10]

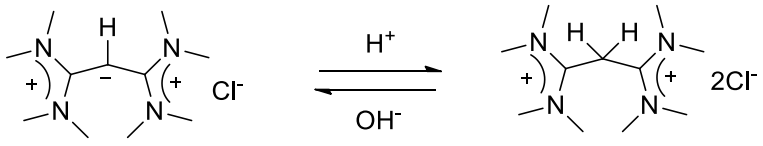

Figure 4.38-Equilibrium between monocation and dication by altering *p*H.[10]

4.10 Anion-exchange Reactions

Anion-exchange reactions are subdivided into the following four main classes; anion metathesis, direct reaction of halide salts with Lewis acids, halide-free anion metathesis, and cross-metathesis.

4.10.1 Anion Metathesis

The synthesis of an IL usually consists of the formation of cations, and then anion exchange through anion metathesis. Generally, ion metathesis involves the exchange of halide salts with metal salts. In this work, an excess of group (I) metal or ammonium/silver salts (TFSA, DCA, SCN or pentafluorophenoxide) were mixed with tac chloride or methyl sulphate salts in an aqueous solution. The hydrophobic anions usually generate a separate layer with the tac cation, while group (I) metals or ammonium cations form a hydrophilic layer with chloride or methyl sulphate in the aqueous layer. The IL is then extracted with an organic solvent, followed by repeated washes of the organic layer with water. The ILs are formed normally in good yields (80-90%).

This method has limitations and is not applied on an industrial scale due to metal or halide contamination and the high cost of organic solvents, thus there is a need for new methods.

4.10.2 Lewis acid-based Ionic Liquids

Upon reaction of a tac chloride salt with a Lewis acid MX_n, a metal IL (MIL) is formed. Reaction involves simple mixing of the Lewis acid with the halide salt (fig. 4.39). The water-sensitive nature of some metal chlorides requires the reaction to be carried out under an inert atmosphere.[29]

$$[C_3(NR_2)_3]Cl + FeCl_3 \longrightarrow [C_3(NR_2)_3]FeCl_4$$

$$[C_3(NR_2)_3]Cl + SnCl_2.2H_2O \longrightarrow [C_3(NR_2)_3]SnCl_3$$

$$2[C_3(NR_2)_3]Cl + CuCl_2 \longrightarrow [C_3(NR_2)_3]_2CuCl_4$$

$$2[C_3(NR_2)_3]Cl + ZnCl_2 \longrightarrow [C_3(NR_2)_3]_2ZnCl_4$$

R = Ethyl or Butyl

Figure 4.39-Reaction scheme for the synthesis of MILs.

It is previously seen that by mixing 1-octyl-3-methylimidazolium chloride with various molar ratios of zinc(II) chloride formed chlorozincate(II) ionic liquids, which were characterized by Raman spectroscopy and differential scanning calorimetry. Electrospray mass spectrometry for the chlorozincate(II) ionic liquid systems is an unreliable technique to study liquid-phase speciation.[30]

Similarly, Raman spectroscopic studies were examined for chloroferrate(III) systems which confirmed the presence of $[FeCl_4]^-$ in all the compositions but for X_{FeCl3} (molar ratio) > 0.50, $[Fe_2Cl_7]^-$ species were also detected.[31] While, for chlorocuprate(II) systems mainly have $[CuCl_4]^{2-}$ anion species.[32–33] While for higher molar ratios of $CuCl_2$, $[Cu_2Cl_6]^{2-}$ is found in equilibrium with $[CuCl_4]^{2-}$ species.[33]

MILs find applications as liquid electrolytes for electrochemistry and battery applications. They can also be used as Lewis acid catalysts in organic synthesis.[34]

4.10.3 Anion metathesis with alkylating agent

$[C_3(NEt_2)_3]I$ was prepared by an alkylation methodology. A similar method has been used previously by Bielawski to synthesize a range of ionic liquids bearing non-nucleophilic and non-coordinating anions.[35] They treated a range of halide salts with alkylating agents (Me_2SO_4, MeOTs, Me_3PO_4, Me_3OBF_4, Et_3OBF_4 and Et_3OPF_6). to generate an alkyl halide and an IL with the corresponding anion ($MeSO_4^-$, OTs^-, $Me_2PO_4^-$, BF_4^- and PF_6^-, respectively). We applied this practical and environmentally-friendly alkylation methodology with EtI to prepare $[C_3(NEt_2)_3]I$ from $[C_3(NEt_2)_3]Cl$ (fig. 4.40). This is the first example of the conversion of a tris(diethylamino)cyclopropenium chloride to an iodide salt using an alkylating agent. Previously, Sinyashin and coworkers have synthesized tris(diethylamino)cyclopropenium iodide from chloride salt by anion exchange with KI.[36] The iodide salts are of particular interest for the synthesis of iodide ILs for dye-sensitized solar cells. This method minimized metal waste by-products and purification techniques. $[E_6]Cl$ was heated to reflux with ethyl iodide for 20 hours under an inert atmosphere. The chloride was removed as gaseous ethyl chloride during the reaction. The chloride content was only 14 ppm, as determined by ion chromatography. There is a certainty about the higher chloride content in $[E_6]I$ synthesized by anion exchange rather than present alkylating agent method.[36]

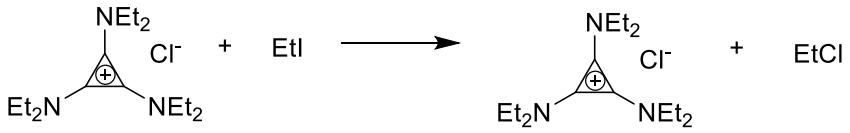

Figure 4.40-Synthesis of [E6]I from [E6]Cl.

4.10.4 Ionic liquid ion cross-metathesis

Previously, Zgonnik synthesized two new ILs by mixing two ILs in a mutual ion exchange.[37] The driving force responsible for cross metathesis makes the hydrophobic ions combine in the hydrophobic layer, while the hydrophilic ions unite in the water layer. This technique is known as "ionic liquid ion cross-metathesis".

This technique was utilized to synthesize [B_6][$B(CN)_4$] and [B_6]FAP. [B_6]Cl is a hydrophilic ionic liquid, which when dissolved in hydrophobic ionic liquids [1-ethyl-3-methylimidazolium][$B(CN)_4$] or [1-ethyl-3-methylimidazolium]FAP, undergoes ion cross-metathesis. The more hydrophilic ions (imidazolium and chloride) can be extracted into a water layer while hydrophobic ions (tris(dibutylamino)cyclopropenium and $B(CN)_4$/FAP) separate in the IL layer.[38] This procedure offered a metal and chloride reduced content synthesis of these ILs.

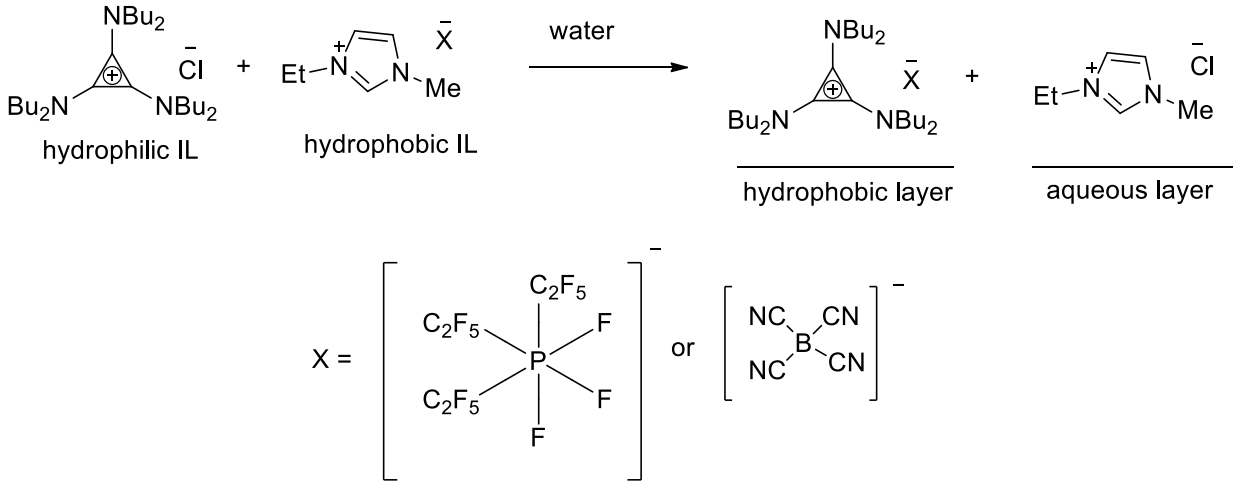

Figure 4.41-Reaction scheme for ionic liquids ion-cross metathesis.

Most efficient ion-cross metathesis was achieved when a small excess, 1.1 equivalents, of [B_6]Cl was added to 1 equivalent of [1-ethyl-3-methylimidazolium]X. This made possible for [B_6]X to

separate as the hydrophobic layer and the excess of $[B_6]Cl$ along with [1-ethyl-3-methylimidazolium]Cl stayed in the water layer. The anion purity of the resulting ILs ($[B_6][B(CN)_4]$ and $[B_6]$FAP) was determined by measuring the chloride content, which was around 300 ppm. ^{1}H NMR was used to check the purity of $[B_6][B(CN)_4]$ and $[B_6]$FAP and no peaks for imidazolium were found.

Conclusions

A total of 74 ILs are successfully synthesized with a range of symmetry, C_s, ($[C_3(NMe_2)_2(NRH)]$TFSA, $[C_3(NMe_2)_2(NMeR")]$TFSA, $[C_3(NMe_2)_2(NMeR")]$DCA, $[C_3(NEt_2)_2(NHBu)]X$ (X = $MeSO_4^-$, $TFSA^-$, DCA^-, and BF_4^-), $[C_3(NEt_2)_2$(Aminoacids)]X (X = $MeSO_4^-$ and TFSA)), C_{2v} ($[(C_3(NMe_2)_2(NR_2)]$TFSA, $[(Et_2N)_2C_3(NR_2)]X$ (X = $TFSA^-$, I^-, and OTf^-)), C_{3h} ($[C_3(NRMe)_3]X$ ($TFSA^-$ and DCA^-), $[C_3(NPhH)_3]$TFSA), D_{3h} ($[C_3(NR_2)_3]X$ (X = $MeC_6H_4SO_3^-$, I^-, OTf^-, $F_5C_6O^-$, $B(CN)_4^-$, and FAP^-)), open ring compounds ($[(BuHN)_2CCH_2C(NHBu)_2]X_2$ (X = $TFSA^-$ and Cl^-) and $[(Me_2N)_2CCH_2C(NMe_2)_2]Cl_2$) and metal ILs.

$C_3(NMe_2)_2O$ and $C_3(NEt_2)_2O$ is methylated with dimethyl sulphate to form $[C_3(NMe_2)_2OMe]MeSO_4$ and $[C_3(NEt_2)_2OMe]MeSO_4$ respectively, for the synthesis of reduced symmetry cations (C_s and C_{2v}).

Optically pure AAILs are obtained as a mixture of IL and zwitterion. The ratios of IL and zwitterion determined from *p*H titrations and microanalysis agreed well. Unfortunately, these mixtures failed to separate by the changes in *p*H. $[E_4$Asp]TFSA, $[E_4$Glu]TFSA, $[E_4$Asn]TFSA, and $[E_4$Gln]TFSA were not obtained in pure forms due to ambiguity in their mass spectra, NMR and microanalysis. $[E_4$Cysteine]TFSA was synthesized but failed to be separated in pure form, from the product mixture.

An attempt was made to reduce the viscosity of AAILs by converting the carboxylic group of amino acid side chain to esters but it failed.

The synthesis of tris(toluidino)cyclopropenium chloride and tris(butylamino)cyclopropenium chloride was unsuccessful.

Lewis acid-based ILs were successfully synthesized, $[C_3(NEt_2)_3]X$ and $[C_3(NBu_2)_3]X$ (X = $FeCl_4^-$, $CuCl_4^{2-}$, $ZnCl_4^{2-}$ and $SnCl_3^-$). $[C_3(NEt_2)_3]I$ was synthesized using halide-free anion metathesis methodology. Ion cross-metathesis was utilized to prepare $[C_3(NBu_2)_3]B(CN)_4$ and $[C_3(NBu_2)_3]FAP$.

References

1. Yoshida, Z. i.; Tawara, Y. *J. Am. Chem. Soc.* **1971**, 2573.
2. Taylor, M. J.; Surman, P. W. J.; Clark, G. R. *J. Chem. Soc., Chem. Commun.* **1994**, 2517.
3. Krebs, A.; Gtintner, A.; Versteylen, S.; Schulz, S. *Tetr. Lett.* **1984,** *25* (22), 2333.
4. Tobey, S. W.; West, R. *J. Am. Chem. Soc.* **1965**, 2478.
5. Wagner, W. M. *Proc. Chem. Soc.* **1952**, 229.
6. Wagne, W. M.; Kloosterziel, H.; Ven, S. V. D. *Recl. Trav. Chim. Pays-Bas* **1961,** *80*, 740.
7. Wagner, W. M.; Kloosterziel, H.; Ven, S. V. D. *Recueil* **1961,** *80*, 740.
8. (a) Lucier, J. J.; Harris, D. A.; Korosec, S. P. **1964,** *44*, 72; (b) Wawzonek, S.; Mckillip, W.; Peterson, C. **1964,** *44*, 75.
9. Jacquemin, J.; Goodrich, P.; Jiang, W.; Rooney, D. W.; Hardacre, C. *J. Phys. Chem. B* **2013,** *117*, 1938.
10. Surman, P. W. J. Novel Products from Pentachlorocyclopropane: A Synthetic and Structural Investigation. PhD Thesis, University of Auckland, Auckland, 1996.
11. Jayasinghe, C. *Persn. Commun.* **2013**.
12. Yoshida, Z.; Konishi, H.; Tawara, Y.; Nishikawa, K.; Ogoshi, H. *Tetra. Lett.* **1973,** (28), 2619.
13. Yoshida, Z. *Top. Curr. Chem.* **1973,** *40*, 47.
14. Bandar, J. S.; Lambert, T. H. *Synthesis* **2013,** *45*, 2485.
15. Wilcox, C.; Breslow, R. *Tetrahedron Lett.* **1980,** *21*, 3241.
16. Walst, K. J. Synthesis and Characterization of Triaminocyclopropenium as a New Class of Ionic Liquids. PhD Thesis, University of Canterbury, Christchurch, 2013.
17. Shah, J.; Liebscher, J. *Syn.* **2008,** (6), 917.
18. Kumata, Y.; Furukawa, J.; Fueno, T. *Bull. Chem. Soc. Jpn.* **1970,** *43*, 3920.
19. Wood, J. K. *J. Chem. Soc.* **1914,** *105*, 1988.
20. (a) Pecul, M. *Chem. Phys. Lett.* **2006,** *418*, 1; (b) Pecul, M.; Ruud, K.; Rizzo, A.; Helgaker, T. *J. Phys. Chem. A* **2004,** *108*, 4269.
21. (a) Fukumoto, K.; Yoshizawa, M.; Ohno, H. *J. Am. Chem. Soc.* **2005,** *127*, 2398; (b) Tao, G.-h.; He, L.; Sun, N.; Kou, Y. *Chem. Communications (Cambridge, England)* **2005,** (28), 3562; (c)

Fukumoto, K.; Ohno, H. *Chem. Commun.* **2006,** *29*, 3081; (d) Guillen, F.; Bregeon, D.; Plaquevent, J.-C. *Tetrahedron Lett.* **2006,** *47*, 1245; (e) Luo, K.; Jiang, H.-y.; You, J.-s.; Xiang, Q.-x.; Guo, S.-j.; Lan, J.-b.; Xie, R.-g. *Lett. Org. Chem.* **2006,** *3*, 363; (f) Luo, S.-P.; Xu, D.-Q.; Yue, H.-D.; Wang, L.-P.; Yang, W.-L.; Xu, Z.-Y. *Tetrahedron: Asymmetry* **2006,** *17*, 2028; (g) Tao, G.-h.; He, L.; Liu, W.-s.; Xu, L.; Xiong, W.; Yuan, T. W. a. *Green Chemistry* **2006,** *8*, 639; (h) Schmitkamp, M.; Chen, D.; Leitner, W.; Klankermayer, J.; Francio, G. *Chem. Commun.* **2007**, 4012; (i) Yamada, T.; Lukac, P. J.; Yu, T.; Weiss, R. G. *Chem. Mater.* **2007,** *19*, 4761; (j) Bregeon, D.; Levillain, J.; Guillen, F.; Plaquevent, J.-C.; Gaumont, A.-C. *Amino Acids* **2008,** *35* (1), 175; (k) Jin, X.; Xu, X.-f.; Zhao, K. *Tetrahedron Asymmetry* **2012,** *23*, 1058.

22. Yoshizawa, M.; Hirao, M.; Ito-Akita, K.; Ohno, H. *J. Mater. Chem.* **2001,** *11*, 1057.
23. Yoshizawa, M.; Ohno, H. *Chem. Commun.* **2004**, 1828.
24. Cole, A. C.; Jensen, J. L.; Ntai, I.; Tran, K. L. T.; Weaver, K. J.; Forbes, D. C.; Davis, J. H. *J. Am. Chem. Soc.* **2002,** *124*, 5962.
25. Yoshida, Z.; Ogoshi, H.; Hirota, S. *Tetr. Lett.* **1973,** *11*, 869.
26. Cyclopropenylidene-stabilized phosphenium cations. 30 august 2012.
27. Stephen, L. T.; William, C. *J. Chem. Soc., Dalton Trans.*, **2001**, 402.
28. Weiss, R.; Hertel, M. *J.C.S. Chem. Comm.* **1980**, 223.
29. Gordon, C. M.; Muldoon, M. J., *Synthesis and Purfication*. WILEY-VCH Verlag GmbH & Co. KGaA: 2008; Vol. 2, p 57.
30. Estager, J.; Nockemann, P.; Seddon, K. R.; Swadzba-Kwasny, M.; Tyrrell, S. *Inorg. Chem.* **2011,** *50*, 5258.
31. Sitze, M. S.; Schreiter, E. R.; Patterson, E. V.; Freeman, R. G. *Inorg. Chem.* **2001,** *40*, 2298.
32. Leesakul, N.; Runrueng, W.; Saithong, S.; Pakawatchai, C. *Acta Cryst.* **2012,** *E68*, m837.
33. Golubeva, E. N.; Kokorin, A. I.; Kochubei, D. I.; Pergudhov, V. I.; Kriventsov, V. V. *Kinet. Kalal.* **2002,** *43*, 408.
34. Cocalia, V. A.; Visser, A. E.; Rogers, R. D.; Holbrey, J. D., *Ionic Liquid in Synthesis*. WILEY-VCH: 2008; Vol. 1.
35. Vu, P. D.; Boydston, A. J.; Bielawski, C. W. *Green Chem.* **2007,** *9*, 1158.
36. Milyukov, V. A.; Shakirova, L. R.; Bezkishko, I. A.; Krivolapov, D. B.; Sinyashin, O. G. *Russian Chemical Bulletin, International Edition* **2012,** *61* (7), 1483.
37. Zgonnik, V.; Zedde, C.; Genisson, Y.; Mazieres, M.-R.; Plaquevent, J.-C. *Chem. Commun.* **2012,** *48*, 3185.
38. Ignatev, N. V.; Welz-Biermann, U.; Kucheryna, A.; Bissky, G.; Willner, H. *J. Fluorine Chem.* **2005,** *126*, 1150.

Discussion of Properties

For some of properties such as vapor pressure, it is possible to make generalizations that apply to all classes of ILs. Unfortunately for other properties, including decomposition temperatures, glass transition temperatures, melting points, viscosity, conductivity, density, ionicity, fragility, pK_a, optical rotation, and solubility/miscibility studies, generalizations cannot be made. One of the most unique features of ILs is wide variations in their properties.

This chapter will discuss the physical properties of ionic liquids with regards to their structure.

5.1 Halide and water impurities

Impurities such as residual halide and water can have a large impact on the physico-chemical properties of an IL. Chloride is a common impurity in tac ILs because the tac salts were synthesized from C_3Cl_5H, additionally, although asymmetric salts were synthesized from cyclopropenones, during clean-up, either neutralization or washes with HCl were required. The chloride concentration was determined using a chloride-selective electrode.[1] Sometimes, the counterions (SCN^- and I^-) interfere with the ion-selective electrode, due to the insolubility of the silver salt. Thus, ion chromatography was used to determine the chloride content in $[E_6]I$.

For most of the samples, the chloride content was lower than 500 ppm. In the case of ILs with DCA and $MeSO_4^-$, anions, high chloride contents were observed. The highest chloride content was found for CILs having methyl sulphate as the anion. In $[E_4Val]MeSO_4$, this was found to be 41,396 ppm. This was probably due to hydrogen bonding from the cation incorporating chloride ions.

A high chloride content increases viscosity, decreases conductivity, and decreases thermal decomposition temperature, thus, chloride content is always given with any physical property.

Water is another major impurity in most samples. It enters in the sample through the atmosphere or during washings with water. High water content decreases viscosity and increases conductivity. If water is not zero ppm, it is always written with the sample. Samples are usually dried under vacuum with stirring and heating for at least 72 hours before the measurement of any property. Karl-Fischer Coulometry is used to determine water content.[2] Liquid samples are inserted directly in Karl-Fischer Coulometer for water determination. For viscous and solid samples, after dissolving in a suitable dried solvent, water content was estimated. Hydrophilic anions (Cl^-, DCA and $MeSO_4^-$) usually have higher water content than those of hydrophobic ones (TFSA and BF_4^-).

5.2 Thermal Stability

Thermogravimetric measurements were conducted on a TA Q600 SDT thermo-gravimetry/differential scanning calorimetry (TGA-DSC) from room temperature to 600 °C at a heating rate of 1 °C min^{-1} and 10 °C min^{-1}, under a nitrogen atmosphere (100 mL min^{-1}) using open platinum pans. The instrument used gave a simultaneous TGA-DSC, although heat flow information obtained was less accurate than the DSC data discussed later in this chapter.

Thermal decomposition temperature (T_d) is affected by the chloride and water content in the IL. These impurities can significantly reduce the T_d. The nature of the pans (aluminium or platinium), time and heating rate can also affect the T_d. These factors need to be considered for an accurate determination of T_d for high-temperature applications.[3] A fast heating rate (10 °C/min) will increase the onset decomposition temperature than a slow heating rate (1 °C/min). The onset temperature is an overestimate and is inexact because it is a function of the evaporation and decomposition processes which are highly dependent upon the heating rate. Note that all T_d tabulated in the table 5.1 are onset temperatures as determined from step tangents. In other words, the onset T_d is the cross between the tangent straight lines to the TGA curve before and after the decomposition.[4]

Table 5.1-TGA data for ILs

	C_s Cations	Mol wt cation	T_d 1 °C/min	T_d 10 °C/min
1	$[C_3(NMe_2)_2(NEtH)]$TFSA	168.26	276	335
2	$[C_3(NMe_2)_2(NEtMe]$TFSA	182.29	211	315
3	$[C_3(NMe_2)_2(HN(CH_2CHCH_2))]$TFSA	180.27	284	326
4	$[C_3(NMe_2)_2(N(CH_2CHCH_2)Me)]$TFSA	194.30	241	344
5	$[C_3(NMe_2)_2(N(CH_2CHCH_2)Me)]$DCA	194.30	233	258
6	$[C_3(NMe_2)_2(N(CH_2CH_2CH_3)H)]$TFSA	182.29	236	293
7	$[C_3(NMe_2)_2(N(CH_2CH_2CH_3)Me)]$TFSA	196.31	247	291
8	$[C_3(NMe_2)_2(N(CH_2CH_2CH_3)Me)]$DCA	196.31	233	257
9	$[C_3(NMe_2)_2(N(CH_2CH_2OCH_3)H)]$TFSA	198.29	283	336
10	$[C_3(NMe_2)_2(N(CH_2CH_2OCH_3)Me)]$TFSA	212.31	289	326
11	$[C_3(NMe_2)_2(N(CH_2CH_2OCH_3)Me)]$DCA	212.31	244	310
12	$[C_3(NMe_2)_2(NBuH)]$TFSA	196.31	256	312
13	$[C_3(NMe_2)_2(NBuMe)]$TFSA	210.34	274	321
14	$[C_3(NMe_2)_2(NBuMe)]$DCA	210.34	259	287
15	$[C_3(NMe_2)_2(NPeH)]$TFSA	210.34	263	322
16	$[C_3(NMe_2)_2(NPeMe)]$TFSA	224.37	263	325
17	$[C_3(NMe_2)_2(NHexMe)]$TFSA	238.39	264	295
18	$[C_3(NEt_2)_2(NHBu)]MeSO_4$	252.42	193	233
19	$[C_3(NEt_2)_2(NHBu)]$TFSA	252.42	296	324
20	$[C_3(NEt_2)_2(NHBu)]$DCA	252.42	198	234
21	$[C_3(NEt_2)_2(NHBu)]BF_4$	252.42	197	267
22	$[E_4Ala]MeSO_4$	268.37	188	215
23	$[E_4Ala]$TFSA	268.37	210	245
39	$[E_4Ser]$TFSA	284.37	131	161

24	$[E_4Pro]MeSO_4$	294.41	200	231
25	$[E_4Pro]TFSA$	294.41	230	272
26	$[E_4Val]MeSO_4$	296.43	190	215
27	$[E_4Val]TFSA$	296.43	209	245
28	$[E_4Thr]MeSO_4$	298.40	151	188
29	$[E_4Thr]TFSA$	298.40	145	178
34	$[E_4Leu]TFSA$	310.45	214	244
35	$[E_4Ile]TFSA$	310.45	227	260
31	$[E_4Asp]TFSA$	312.38	161	195
40	$[E_8Gln]TFSA_2$	325.42	132	166
41	$[E_8Lys]TFSA_2$	325.47	223	252
33	$[E_4Met]TFSA$	328.49	218	238
32	$[E_4His]TFSA_2$	335.34	215	244
38	$[E_4Phe]TFSA$	344.47	213	259
30	$[E_4Arg]TFSA$	353.48	220	254
37	$[E_4Tyr]TFSA$	360.47	238	268
36	$[E_4Try]TFSA$	383.51	227	263
	C_{2v} Cations			
42	$[C_3(NMe_2)_2(NEt_2)]TFSA$	196.31	232	334
43	$[C_3(NMe_2)_2(N(CH_2CHCH_2)_2)]TFSA$	220.33	235	335
44	$[C_3(NMe_2)_2(NPr_2)]TFSA$	224.37	243	317
45	$[C_3(NMe_2)_2(N(CH_2CH_2OCH_3)_2)]TFSA$	256.35	262	363
46	$[C_3(NMe_2)_2(NBu_2)]TFSA$	252.42	250	314
47	$[C_3(NMe_2)_2(NHex_2)]TFSA$	308.52	295	348
48	$[(Et_2N)_2C_3(NH_2)]MeSO_4$	196.31	146	181
49	$[C_3(NEt_2)_2(NBu_2)]I$	308.55	296	328
50	$[C_3(NEt_2)_2(NHex_2)]I$	364.63	281	326
51	$[C_3(NEt_2)_2(NHex_2)]OTf$	364.63	284	326
	C_{3h} Cations			
52	$[C_3(NEtMe_2)_3]TFSA$	210.34	275	366
53	$[C_3(NAllylMe_2)_3]TFSA$	246.37	247	329

54	$[C_3(NAllylMe)_3]DCA$	246.37	250	276
55	$[C_3(NMeCH_2CH_2OCH_3)_3]TFSA$	300.39	286	347
56	$[C_3(NPhH)_3]TFSA$	312.39	273	308
	D_{3h} Cations			
57	$[C_3(NEt_2)_3][MeC_6H_4SO_3]$	252.42	145	201
58	$[C_3(NEt_2)_3]OTf$	252.42	288	335
59	$[C_3(NEt_2)_3]I$	252.42	268	294
60	$[C_3(NEt_2)_3]F_5C_6O$	252.42	159	198
61	$[C_3(NBu_2)_3]B(CN)_4$	420.59	251	281
62	$[C_3(NBu_2)_3]FAP$	420.59	232	259
	Open ring Cations			
63	$[(Me_2N)_2CCH_2C(NMe_2)_2]Cl_2$	214.35	239	268
64	$[(BuHN)_2CCH_2C(NHBu)_2]Cl_2$	326.56	188	255
65	$[(BuHN)_2CCH_2C(NHBu)_2]TFSA_2$	326.56	244	318

Thermal decomposition is usually the upper limit of the liquidus range for ionic liquids rather than vaporization.[5] T_ds are very high among common classes of ILs,[5] some of them having thermal stabilities of up to 400 °C.[6] This doesn't mean that these ILs can be used up to their T_d. Most ILs start to decompose well below their T_d, thus thermal behavior needs to be analyzed at constant temperature when considering a high temperature application.

Decomposition usually occurs with volatilization of the fragments. ILs with organic anions undergo exothermic decomposition as compared to endothermic decomposition for inorganic anions.[6] The highest T_d observed in the present study is 366 °C for $[C_3(NMeEt)_3]TFSA$ at a heating rate of 10 °C min^{-1}. The TGA curve for $[C_3(NMeEt)_3]TFSA$ is shown in fig. 5.1. TFSA is a "neutral" or "weakly basic" anion, exhibiting weak electrostatic interactions with the cation resulting in a high T_d.[7] Up to 220 °C no significant weight loss is seen (weight being > 99%). When the decomposition starts, it is completed in one step. In $[(C_3(NEtMe)_3]TFSA$ (fig. 5.1), 9% of weight remains in the pan as residual charred material, which is removed by heating under an oxidizing atmosphere.[8] A high inorganic character of the anion is related to a high T_d.[4]

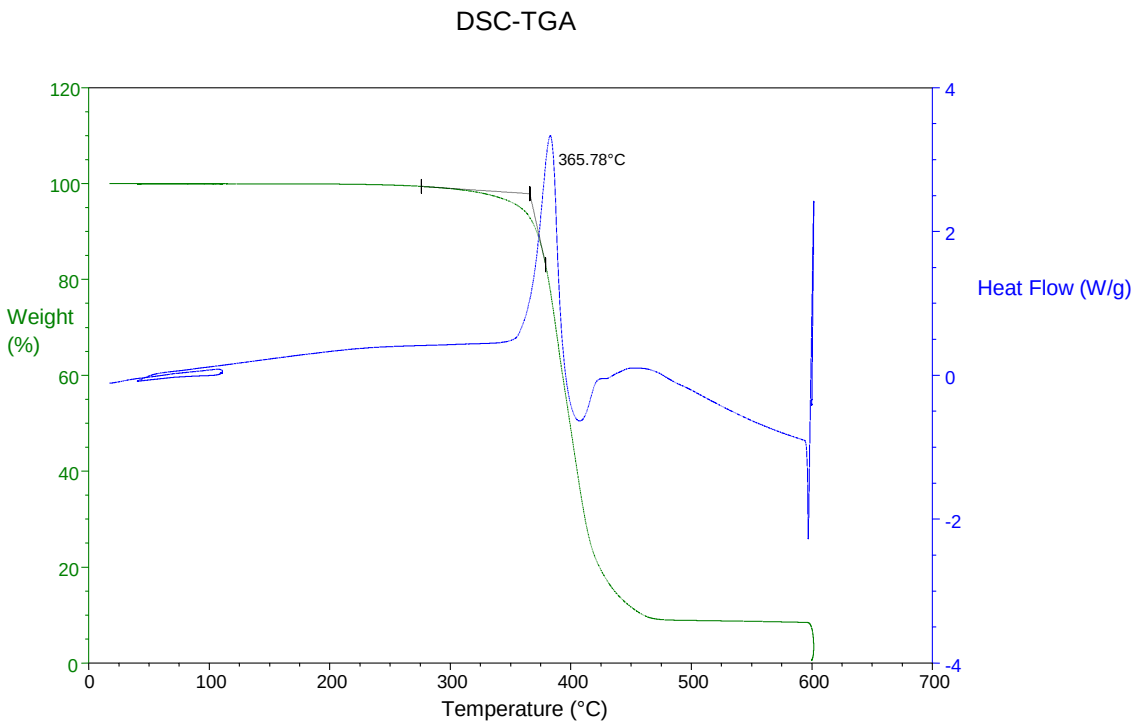

Figure 5.1–TGA curve for $[C_3(NMeEt)_3]$TFSA at heating rate of 10 °C min^{-1}.

Generally, T_d depends slightly on the alkyl chain length of the cation.[3] But in tac salts, upon extension of the alkyl chain, T_d was hardly affected. Because this thesis involves work mainly with tac cation having reduced symmetry.

There is no regular trend observed for T_d with the increase in size of cation among $[C_3(NMe_2)_2(NRH)]$TFSA (R = ethyl, allyl, propyl, $-CH_2CH_2OCH_3$, butyl, and pentyl) and $[C_3(NMe_2)_2(NMeR)]$TFSA (R = ethyl, allyl, propyl, $-CH_2CH_2OCH_3$, butyl and hexyl) series, all the T_d lie almost in the same range (290 to 330 °C). However, in contrast of $[C_3(NMe_2)_2(NMeR)]$DCA (allyl, propyl, $-CH_2CH_2OCH_3$ and butyl) with $[C_3(NMe_2)_2(NMeR)]$TFSA (allyl, propyl, $-CH_2CH_2OCH_3$ and butyl), the DCA salts have lower T_d (250 to 310 °C) compared to the TFSA ones (290 to 350 °C). T_d is seen to be more affected by anion rather than cation size.

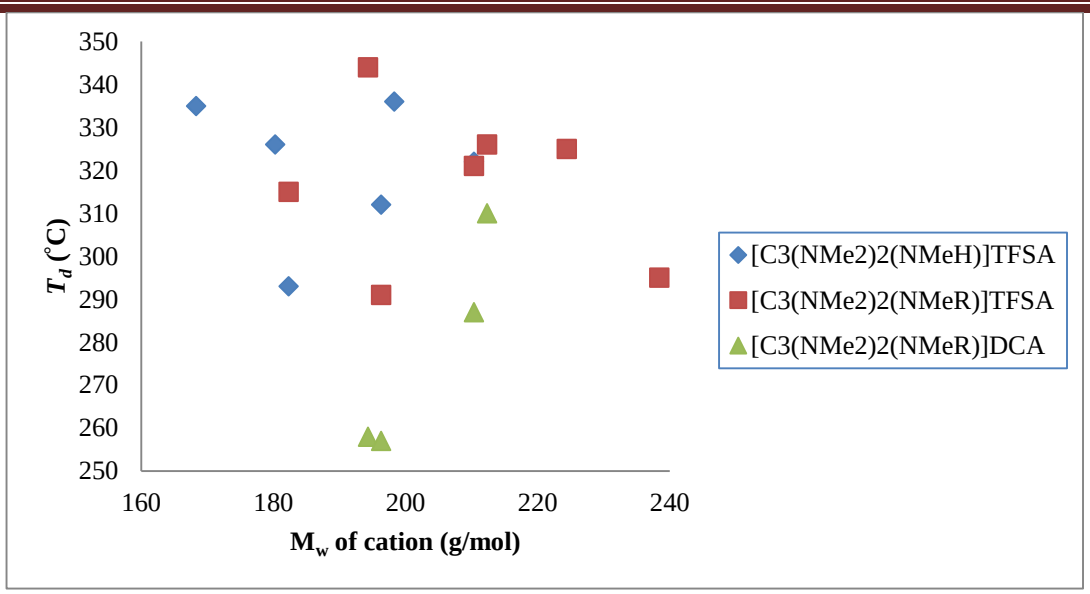

Figure 5.2–T_d (10 °C/min) *vs* molecular weight of C_s cations.

Similarly, among $[C_3(NMe_2)_2(NR_2)]$TFSA (ethyl, allyl propyl, butyl, -$CH_2CH_2OCH_3$, butyl and hexyl) and $[C_3(NMeR)_3]$TFSA (ethyl, allyl, -$CH_2CH_2OCH_3$ and aniline) series, no regular trend was observed for T_d with the increasing size of cation and all the T_d were above 300 °C. Again, the T_d observed for $[C_3(NMeAllyl)_3]$TFSA (329 °C at 10 °C/min) was higher than $[C_3(NMeAllyl)_3]$DCA (276 °C at 10 °C/min).

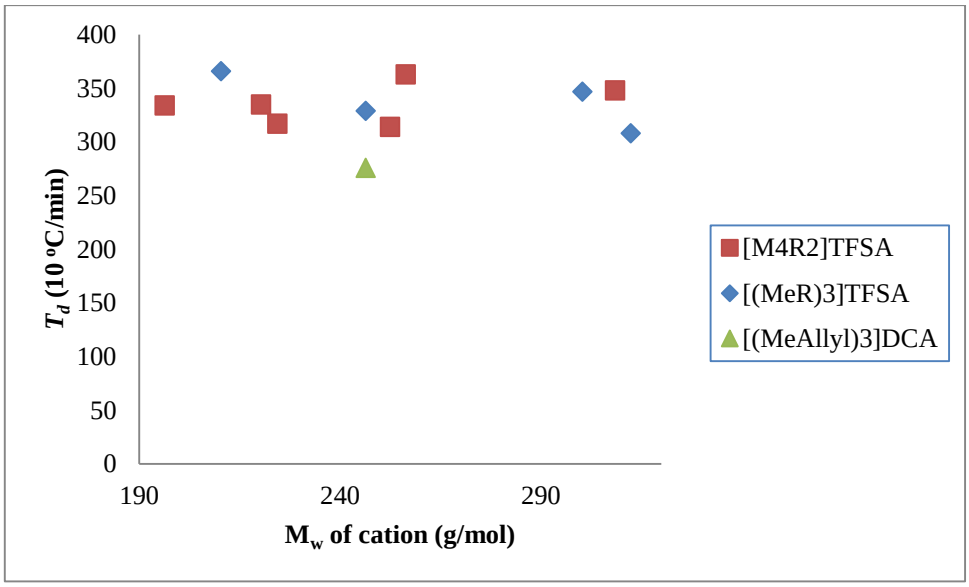

Figure 5.3–T_d (10 °C/min) *vs* molecular weight of C_{2v} and C_{3h} cations.

In protic ILs (PILs), T_d are usually low due to the transfer of protons between acid/base pairs. This increases their volatility and allows them to recombine upon condensation, leading to their ability to be distilled.[9] Among the PILs synthesized, the decomposition temperatures ranged from 193 ($[C_3(NEt_2)_2NBuH]MeSO_4$) to 296 °C ($[C_3(NEt_2)_2NBuH]$TFSA) and 233

([$C_3(NEt_2)_2$NBuH]$MeSO_4$) to 336 °C ([$C_3(NMe_2)_2$NErH]TFSA) at 1 °C min^{-1} and 10 °C min^{-1}, respectively. The thermal stability of PILs depends more on the coordinating ability of the anion. Thus ILs containing weakly nucleophilic anions are most stable. The anion trend for [$C_3(NEt_2)_2$(NBuH)]X with decreasing T_d (at 10 °C/min) follows the pattern $TFSA^-$ (280 g/mol) > BF_4^- (86 g/mol) > DCA^- (66 g/mol) > $MeSO_4^-$ (111 g/mol) Except [$C_3(NEt_2)_2$(NBuH)]$MeSO_4$, the T_d increases proportionally with the increasing molecular weight of the anion (fig. 5.4). The behavior of IL's during thermal decomposition is dependent on the nucleophilicity of the anion.[4] ILs containing weakly nucleophilic anions are highly stable. The more stable anion forms weakly stable R-X species. Weakly nucleophilic anions restricts the tight ion-pair formation, which lowers the vapor pressure due to less Columbic interactions. The weakly nucleophilic anions result in an increase of the upper limit.

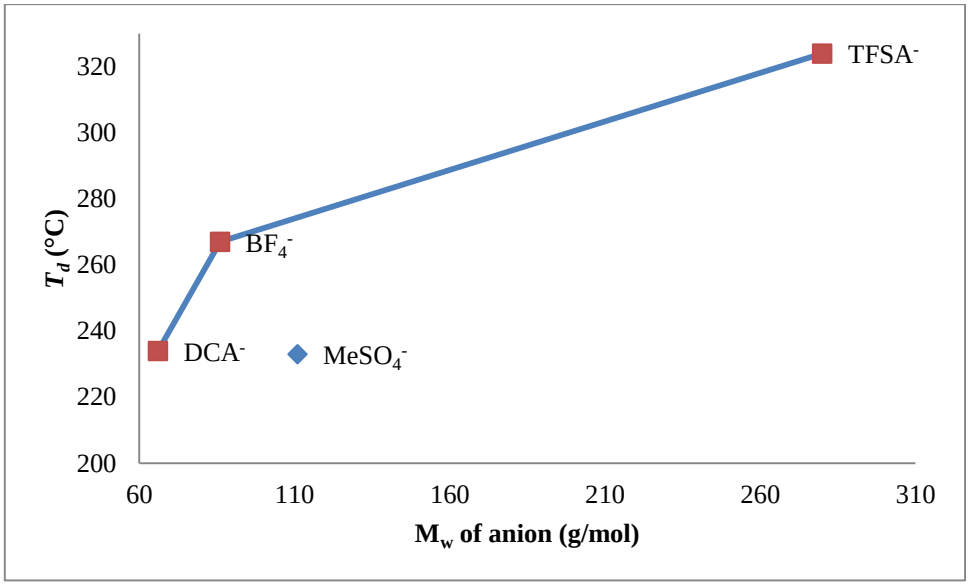

Figure 5.4-T_d (10 °C min^{-1}) *vs* molecular weight of anions for [$C_3(NEt_2)_2$(NBuH)]X

Among the AAILs, the T_d's were lower compared to other ILs prepared and ranged from 131 ([E_4Ser]TFSA) to 238 °C ([E_4Tyr]TFSA) and 161 ([E_4Ser]TFSA) to 272 °C ([E_4Pro]TFSA) at 1°C min^{-1} and 10 °C min^{-1}, respectively. The different functional groups of the amino acid side chain affect T_d. The lowest T_d was observed for [E_4Ser]TFSA at 131 °C (1°C $min^{-1)}$. An important feature was that AAILs having $MeSO_4^-$ as the anion showed lower T_d compared to the corresponding $TFSA^-$ anions, due to the large size of latter anion. In contrast, imidazolium-based AAILs ([emim]AA) are stable at temperatures up to 250 °C, except for [emim][Cys] which has a T_d of 173 °C.[10] These results are similar to our tac-based AAILs.

The T_d of phosphonium-based AAILs was similar to the pure amino acids and ranged from 200 to 300 °C. This suggests that the amino acid anion in phosphonium-based AAILs starts to decompose before the phosphonium cation.[10]

Now we will consider the T_d of $[C_3(NMeAllyl)_3]DCA$. Dicyanamide is a basic anion and is responsible for providing advantageous properties to ILs such as lower viscosity and decrease of melting point.[7] The T_d for $[C_3(NMeAllyl)_3]DCA$ is 276 °C at 10 °C min^{-1} (fig. 5.5).

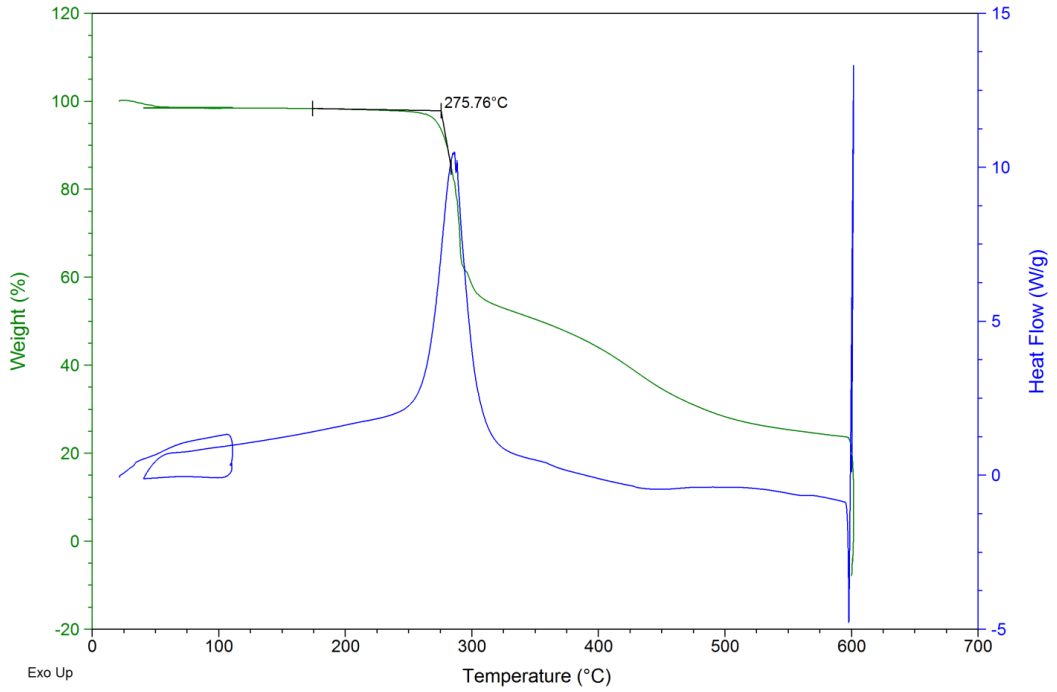

Figure 5.5-TGA curve for $[C_3(NMeAllyl)_3]DCA$ showing onset T_d (10 °C min^{-1}).

ILs with the dicyanamide anion exhibited lower T_d compared to the corresponding TFSA salts.[8] ILs having *N*-based cations and CN containing anions are thought to undergo polymerization during decomposition.[8] Trimerization of dicyanamide anions at elevated temperatures are thought to occur.

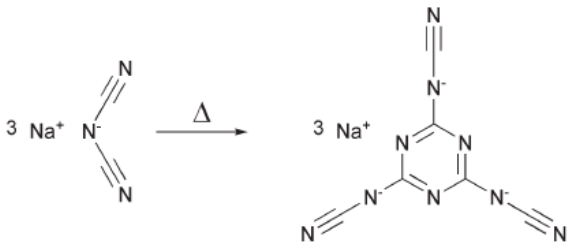

Figure 5.6-Reaction showing the trimerization of dicyanamide anion.

This trimerization is thought to be responsible for evolution of heat during decomposition.

Among the open ring cations, the T_d observed for $[(NMe_2)_2CCH_2C(NMe_2)_2]Cl_2$ is 239 °C and 268 °C at 1 °C min^{-1} and 10 °C min^{-1}, respectively. Upon increasing the size of cation to $[(NBuH)_2CCH_2C(NBuH)_2]Cl_2$, the T_d decreased to 188 °C and 255 °C at 1 °C min^{-1} and 10 °C min^{-1}, respectively. It was thought that the protons present in the $[(NBuH)_2CCH_2C(NBuH)_2]^{2+}$ provide less steric protection and cause the T_d to decrease. While in $[(NBuH)_2CCH_2C(NBuH)_2]TFSA_2$, due to the weaker nucleophilic nature of the TFSA anion as compared to chloride anion, the thermal stability increases to 244 °C and 318 °C at 1 °C min^{-1} and 10 °C min^{-1}, respectively.

The T_d of tac-based ILs synthesized in this thesis are around 300 °C at 10 °C min^{-1} due to less steric protection of cyclopropenium ring. This is less than the imidazolium-based ILs, which usually have T_d > 400 °C at 10 °C min^{-1}.[11] However, the tac-based ILs previously synthesized by Curnow group have T_ds (10 °C/min) over 400 °C as observed for $[C_3(NPr_2)_3]TFSA$ (413 °C), $[C_3(NBu_2)_3]TFSA$ (403 °C), $[C_3(NHex_2)_3]TFSA$ (406 °C), $[C_3(NDec_2)_3]TFSA$ (401 °C) and $[C_3(NEt_2)_2NBu_2]TFSA$ (403 °C).[12]

Table 5.2-Decomposition temperatures of imidazolium-type ILs.

	IL[11]	T_d 10 °C min^{-1}
1	[mmim]TFSA	444
2	[emim]TFSA	439
3	[bmim]TFSA	427
4	$[C_6mim]TFSA$	428
5	$[C_8mim]TFSA$	425

Now I will compare the T_d of my tac-based ILs with previously[12] synthesized tac-based ILs by Curnow group. In contrast of the T_d (10 °C/min) of $[C_3(NMe_2)_2NBuMe]TFSA$ (M_w cation = 210 g/mol, T_d = 321 °C) and $[C_3(NMe_2)_2NMeHex]TFSA$ (M_w cation = 238 g/mol, T_d = 295 °C) with $[C_3(NEt_2)_2NMeBu]TFSA$[12] (M_w cation = 266 g/mol, T_d = 371 °C) and $[C_3(NEt_2)_2NMeHex]TFSA$[12] (M_w cation = 294 g/mol, T_d = 398 °C) (fig. 5.7) respectively. It is seen that the T_ds for larger cations, $[C_3(NEt_2)_2NBu_2]^+$ and $[C_3(NEt_2)_2NHex_2]^+$ are high over 50 °C in contrast to the smaller cations, $[C_3(NMe_2)_2NBu_2]^+$ and $[C_3(NMe_2)_2NHex_2]^+$, respectively.

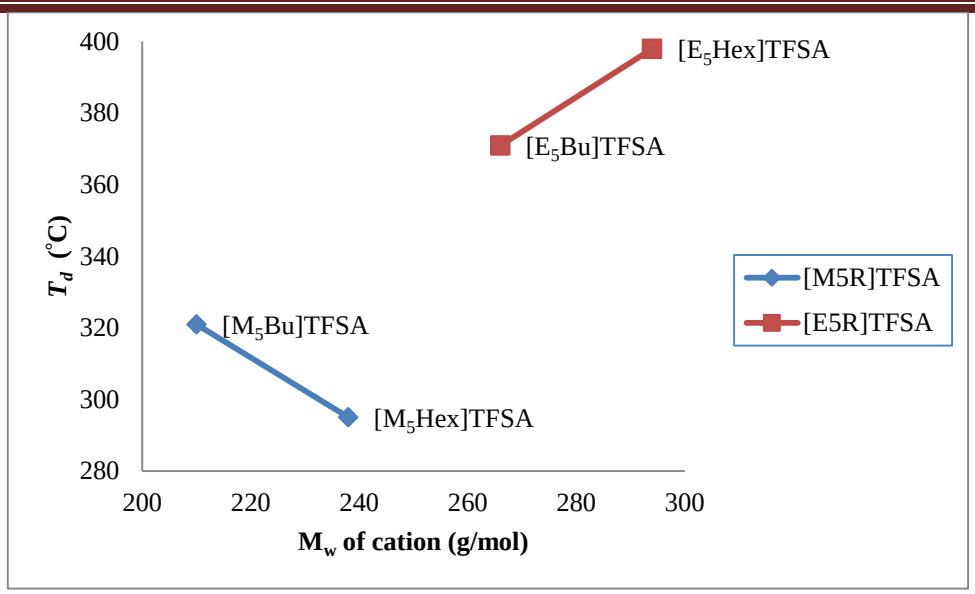

Figure 5.7-T_d (10 °C min^{-1}) *vs* molecular weight of C_s cation [C_3(NR'$_2$)$_2$NR'R"]TFSA (R' =Me or Et, R" = Bu or Hex)

In contrast of T_ds (10 °C/min) of C_{2v} cations, [C_2(NMe_2)$_2$N(Allyl)$_2$]TFSA (M_w cation = 220 g/mol, T_d = 335 °C), [C_2(NMe_2)$_2$NBu_2]TFSA (M_w cation = 252 g/mol, T_d = 314 °C), and C_2(NMe_2)$_2$NHex_2]TFSA (M_w cation = 309 g/mol, T_d = 348 °C), with [C_2(NEt_2)$_2$N(Allyl)$_2$]TFSA (M_w cation = 276 g/mol, T_d = 358 °C),[12] [C_2(NEt_2)$_2$NBu_2]TFSA (M_w cation = 308 g/mol, T_d = 403 °C),[12] and [C_2(NEt_2)$_2$NHex_2]TFSA (M_w cation = 364 g/mol, T_d = 396 °C),[12] respectively. The NEt_2 analogue shows higher T_ds than NMe_2, due to largerer size of the former cation providing more steric protection.

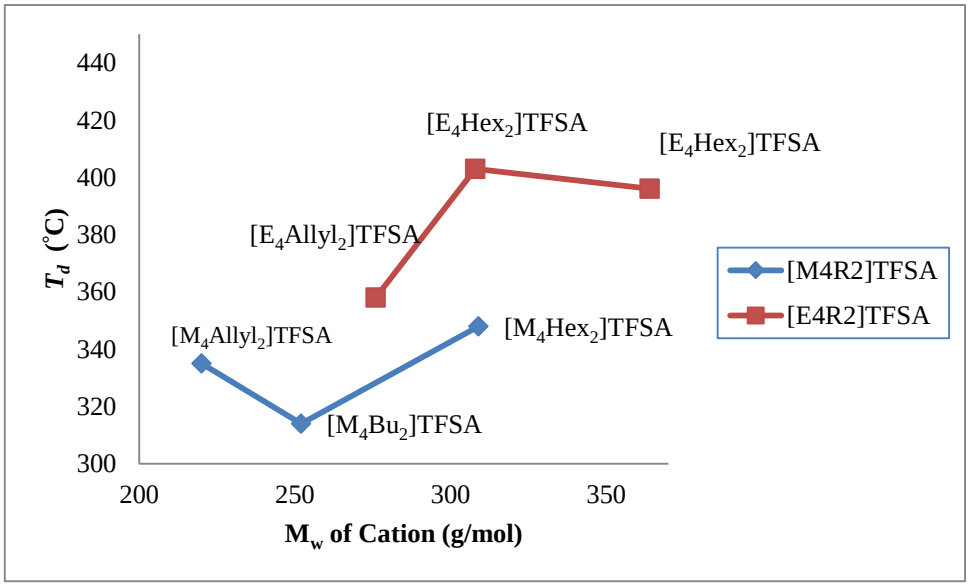

Figure 5.8-T_d (10 °C min^{-1}) *vs* molecular weight of cation of C_{2v} cation [C_3(NR'_2)$_2$NR''_2]TFSA (R' =Me or Et, R" = Allyl, Bu or Hex)

As the size of anion increased for $[C_3(NEt_2)_3]^+$ cation, from Cl^- (34g/mol) < DCA^- (66 g/mol) < I^- (126 g/mol) < OTf^- 149 g/mol) < $MeC_6H_4SO_3^-$ (171 g/mol) < $F_5C_6O^-$ (183 g/mol) < $TFSA^-$ (280 g/mol), the decomposition temperatures (10 °C/min) increases from $[C_3(NEt_2)_3]Cl$ (T_d = 306 °C),[12] $[C_3(NEt_2)_3]DCA$ (T_d = 330 °C),[12] $[C_3(NEt_2)_3]OTf$ (T_d = 335 °C), and $[C_3(NEt_2)_3]TFSA$ (T_d = 393 °C).[12] However, for $[C_3(NEt_2)_3]I$ (T_d = 294 °C), $[C_3(NEt_2)_3]OTs$ (T_d = 201 °C) and $[C_3(NEt_2)_3]F_5C_6O$ (T_d = 198 °C) the decomposition temperature is decreased with increasing size of anion. The highest T_d observed is 393 °C for $[C_3(NEt_2)_3]TFSA$, due to large size and weak nucleophilic character of the TFSA anion.[12]

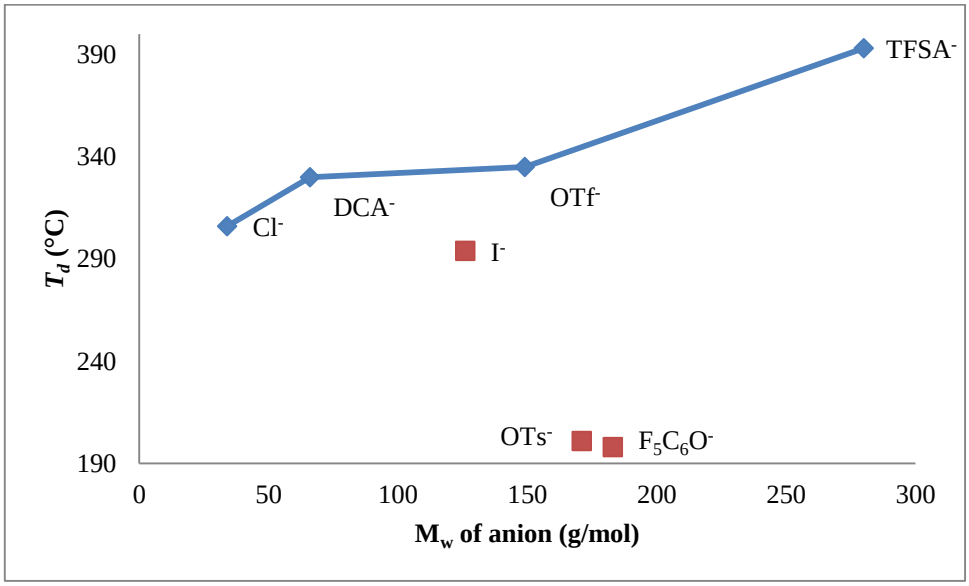

Figure 5.9-T_d (10 °C min^{-1}) *vs* molecular weight of anion for $[C_3(NEt_2)_3]X$

Similarly, in case of $[C_3(NBu_2)_3]^+$ cation as the size of anion increases from $[C_3(NBu_2)_3]DCA$ (T_d = 337 °C)[12], $[C_3(NBu_2)_3]B(CN)_4$ (T_d = 281 °C), $[C_3(NBu_2)_3]TFSA$ [12] and $[C_3(NBu_2)_3]FAP$ (T_d = 259 °C), the decomposition temperature is seen to decrease except for $[C_3(NBu_2)_3]TFSA$.

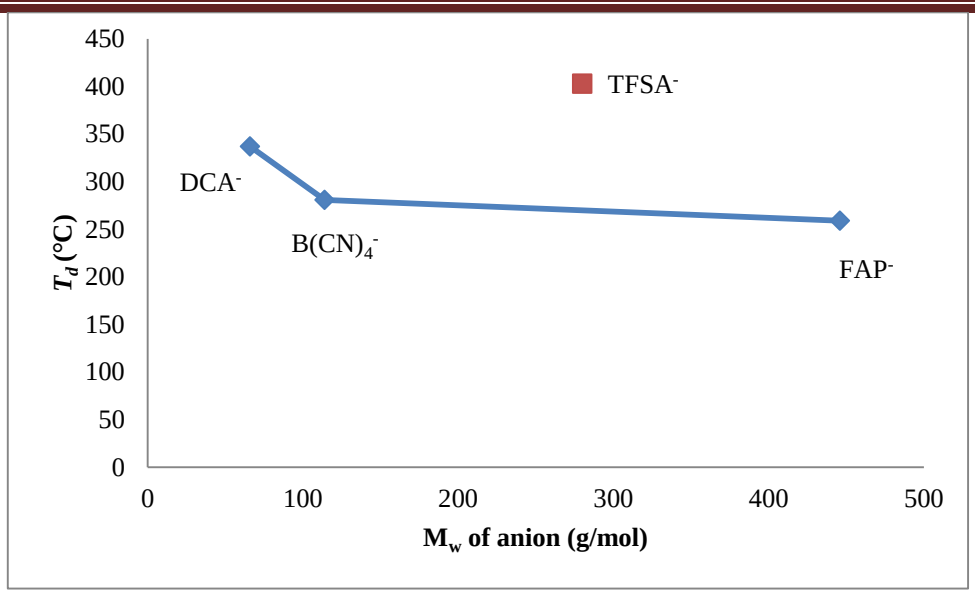

Figure 5.10-T_d (10 °C min^{-1}) *vs* molecular weight of anion for [$C_3(NBu_2)_3$]X

5.3 DSC

Differential scanning calorimetry (DSC) is a method for measuring the glass transition (T_g), solid-solid ($T_{s\text{-}s}$) or solid-liquid transition temperatures (T_m). DSC was carried out using a Perkin-Elmer DSC 8000 under a nitrogen or helium atmosphere. The samples were mechanically sealed in Al pans, heated up to 100 or 150 °C, followed by cooling to −100 °C. Three heating and cooling cycles were performed for each sample at a heating rate of 10 °C/min. Glass transition (T_g) and melting points (T_m) were determined from DSC curves (Appendix). The first cycle was ignored due to the melting of the sample and residue settling at the base of pan. From the second and third cycles, the T_g and/or T_m were determined. When reporting T_g, the change in slope was considered, while in the case of T_m, the onset temperatures were taken (fig. 5.11).[13] The DSC data is summarized in table 5.3.

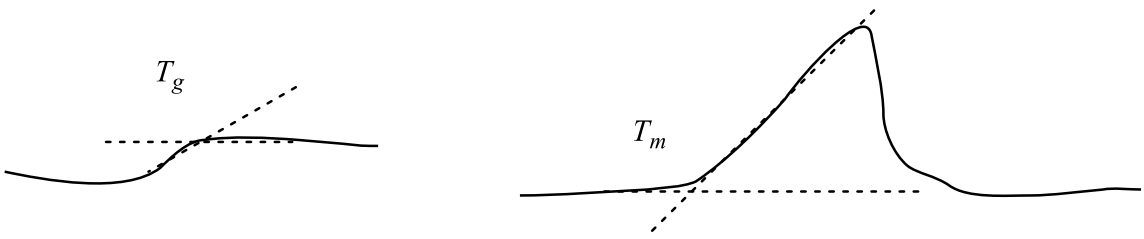

Figure 5.11-Glass transition (T_g) and melting temperatures (T_m).

Table 5.3-DSC data for ILs

	C_s Cations	Mol wt cation	T_g (°C)	T_{s-s} (°C)	ΔH (kJmol^{-1})	T_m (°C)	ΔH (kJmol^{-1})
1	$[C_3(NMe_2)_2(NEtH)]TFSA$	168.26	−71.7	---	---	---	---
2	$[C_3(NMe_2)_2(NEtMe]TFSA$	182.29	---	−6.0 32.2	4.5 6.2	63.2	46.5
3	$[C_3(NMe_2)_2(HN(CH_2CHCH_2))]TFSA$	180.27	−71.3	---	---	-53.7	0.5
4	$[C_3(NMe_2)_2(N(CH_2CHCH_2)Me)]TFSA$	194.30	---	---	---	14.8	109.7
5	$[C_3(NMe_2)_2(N(CH_2CHCH_2)Me)]DCA$	194.30	−61.8	---	---	---	---
6	$[C_3(NMe_2)_2(N(CH_2CH_2CH_3)H)]TFSA$	182.29	−71.5	---	---	---	---
7	$[C_3(NMe_2)_2(N(CH_2CH_2CH_3)Me)]TFSA$	196.31	---	---	---	19.7	105.9
8	$[C_3(NMe_2)_2(N(CH_2CH_2CH_3)Me)]DCA$	196.31	−73.6	---	---	---	---
9	$[C_3(NMe_2)_2(N(CH_2CH_2OCH_3)H)]TFSA$	198.29	−64.3	---	---	---	---
10	$[C_3(NMe_2)_2(N(CH_2CH_2OCH_3)Me)]TFSA$	212.31	−73.5	---	---	---	---
11	$[C_3(NMe_2)_2(N(CH_2CH_2OCH_3)Me)]DCA$	212.31	−69.3	---	---	29.1	236.1
12	$[C_3(NMe_2)_2(NBuH)]TFSA$	196.31	−73.2	---	---	---	---
13	$[C_3(NMe_2)_2(NBuMe)]TFSA$	210.34	−82.6	---	---	5.6	25.6
14	$[C_3(NMe_2)_2(NBuMe)]DCA$	210.34	−72.6	---	---	---	---
15	$[C_3(NMe_2)_2(NHexMe)]TFSA$	238.39	---	---	---	−13.7	16.0
16	$[C_3(NEt_2)_2(NHBu)]MeSO_4$	252.42	−77.1	---	---	---	---
17	$[C_3(NEt_2)_2(NHBu)]TFSA$	252.42	−85.7	---	---	---	---
18	$[C_3(NEt_2)_2(NHBu)]DCA$	252.42	−71.9	---	---	---	---
19	$[C_3(NEt_2)_2(NHBu)]BF_4$	252.42	−76.3	---	---	---	---
20	$[E_4Ala]MeSO_4$	268.37	−36.5	---	---	---	---
21	$[E_4Ala]TFSA$	268.37	−26.0	---	---	---	---
22	$[E_4Ser]TFSA$	284.37	−20.9	---	---	---	0.22
23	$[E_4Pro]MeSO_4$	294.41	−15.7	---	---	−7.3	0.8

24	$[E_4Pro]TFSA$	294.41	−40.9	---	---	---	---
25	$[E_4Val]MeSO_4$	296.43	−50.9	---	---	---	---
26	$[E_4Thr]MeSO_4$	298.40	---	---	---	40.4	---
27	$[E_4Thr]TFSA$	298.40	−15.8	---	---	---	0.8
28	$[E_4IIe]TFSA$	310.45	−37.2	---	---	---	---
29	$[E_8Lys]TFSA_2$	325.47	−48.3	---	---	---	---
30	$[E_4His]TFSA_2$	335.34	−17.6	---	---	---	0.7
31	$[E_4Tyr]TFSA$	360.47	0.3	---	---	---	---
	***C_{2v}*Cations**						
32	$[C_3(NMe_2)_2(NEt_2)]TFSA$	196.31	---	27.2	57.1	43.5	50.8
33	$[C_3(NMe_2)_2(N(CH_2CHCH_2)_2)]TFSA$	220.33	---	---	---	15.6	59.3
34	$[C_3(NMe_2)_2(NPr_2)]TFSA$	224.37	---	---	---	51.6	24.8
35	$[C_3(NMe_2)_2(N(CH_2CH_2OCH_3)_2)]TFSA$	256.35	−70.4	---	---	---	---
36	$[C_3(NMe_2)_2(NBu_2)]TFSA$	252.42	−76.1	---	---	36.3	22.9
37	$[C_3(NMe_2)_2(NHex_2)]TFSA$	308.52	−48.4	---	---	20.8	24.7
38	$[(Et_2N)_2C_3(NH_2)]MeSO_4$	196.31	−47.7	---	---	---	---
39	$[C_3(NEt_2)_2(NBu_2)]I$	308.55	---	---	---	75.1	150.5
40	$[C_3(NEt_2)_2(NHex_2)]I$	364.63	−45.6	---	---	---	---
41	$[C_3(NEt_2)_2(NHex_2)]OTf$	364.63	−68.9	---	---	---	---
	***C_{3h}*Cations**						
42	$[C_3(NEtMe_2)_3]TFSA$	210.34	---	1.7	23.9	7.3	5.9
43	$[C_3(NAllylMe_2)_3]TFSA$	246.37	−82.8	---	---	---	---
44	$[C_3(NAllylMe)_3]DCA$	246.37	−72.6	---	---	---	---
45	$[C_3(NMeCH_2CH_2OCH_3)_3]TFSA$	300.39	−65.3	---	---	---	---
46	$[C_3(NPhH)_3]TFSA$	312.39	---	---	---	16.7	0.5
	***D_{3h}* Cations**						
47	$[C_3(NEt_2)_3]I$	252.42	---	---	---	48.3	13.9
48	$[C_3(NEt_2)_3]OTf$	252.42	---	−0.3	1.1	77.5	5.7
				50.3	11.8		
49	$[C_3(NEt_2)_3][MeC_6H_4SO_3]$	252.42	−50.4	---	---	---	---
50	$[C_3(NEt_2)_3F_5C_6O$	252.42	−49.3	---	---	71	---

						(TGA)	
51	$[C_3(NBu_2)_3]B(CN)_4$	420.59	---	---	---	29.3	26.2
52	$[C_3(NBu_2)_3]FAP$	420.59	−72.6	---	---	---	---
	Open ring Cations						
53	$[(Me_2N)CCH_2C(NMe_2)]Cl_2$	214.35	---	---	---	201 (TGA)	---
54	$[(BuHN)CCH_2C(NHBu)]Cl_2$	326.56	---	---	---	49.5	0.6
55	$[(BuHN)CCH_2C(NHBu)]TFSA_2$	326.56	−43.8	---	---	---	---

In the case of $[C_3(NMe_2)_2(NMeEt)]TFSA$, $[C_3(NMe_2)_2(NEt_2)]TFSA$, $[C_3(NMeEt)_3]TFSA$, and $[C_3(NEt_2)_6]OTf$ multiple solid-solid transitions are seen. It is known that [emim]TFSA is a RTIL, which has two $TFSA^-$ conformers, where the CF_3 groups are located at *cis* and *trans* positions, with respect to S-N-S plane (fig. 5.12). These conformers are present in equilibrium with 1:1 ratio in RTILs. While, the *cis* conformer is found in crystals of $M(TFSA)_n$ (M = Li, K, Ca, Sr, Ba and Yb).[14] Thus, the multiple solid-solid transitions are thought to be due to these two conformers of TFSA anion.

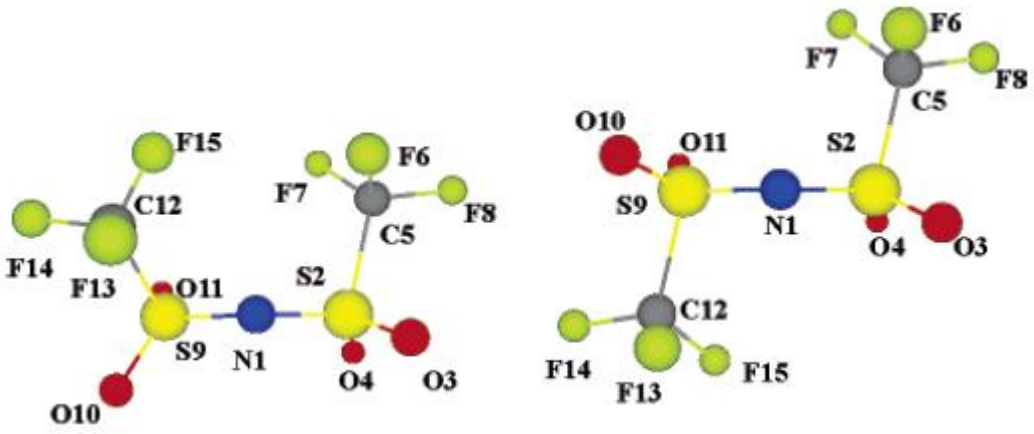

Figure 5.12-*cis* and *trans* conformers of TFSA anion.[15]

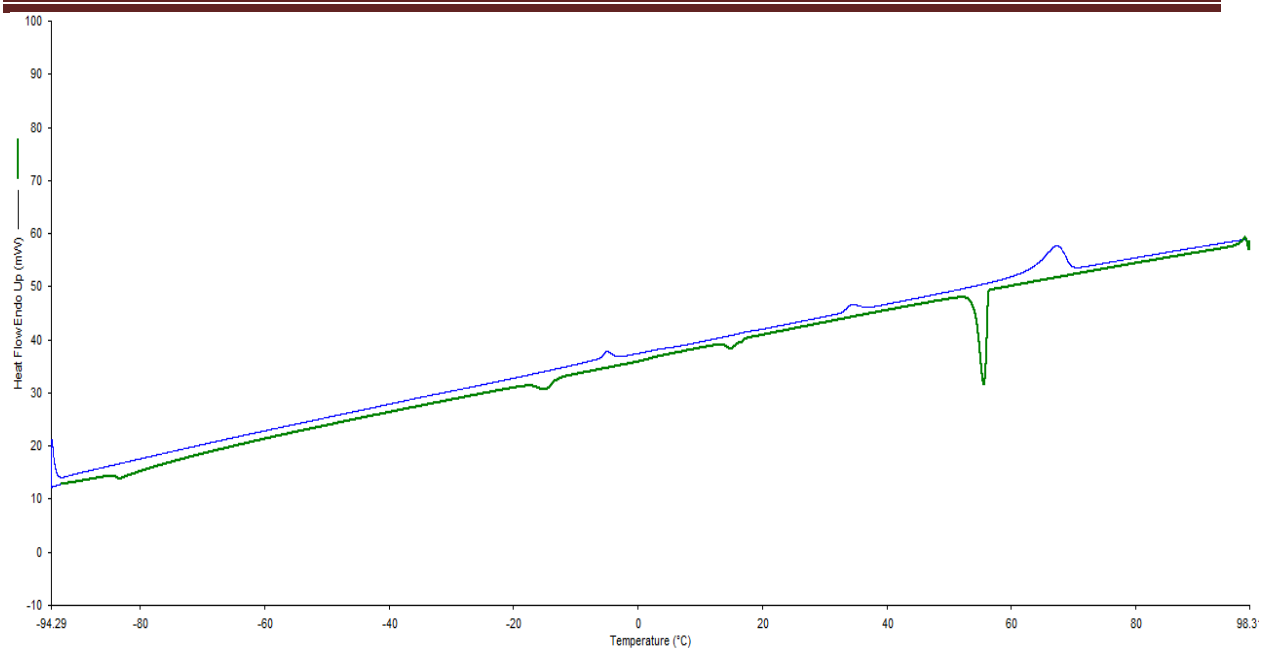

Figure 5.13-DSC curve for $[C_3(NMe_2)_2(NMeEt)]TFSA$

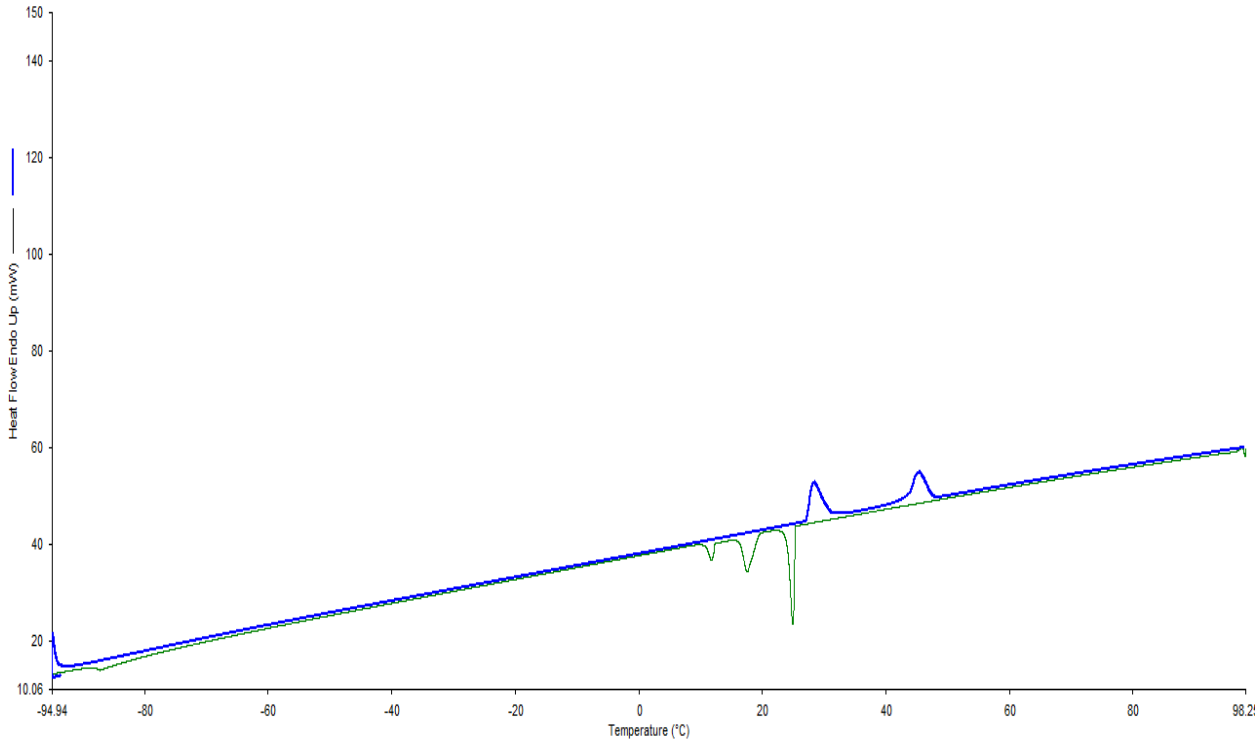

Figure 5.14–DSC curve for $[C_3(NMe_2)_2(NEt_2)]TFSA$

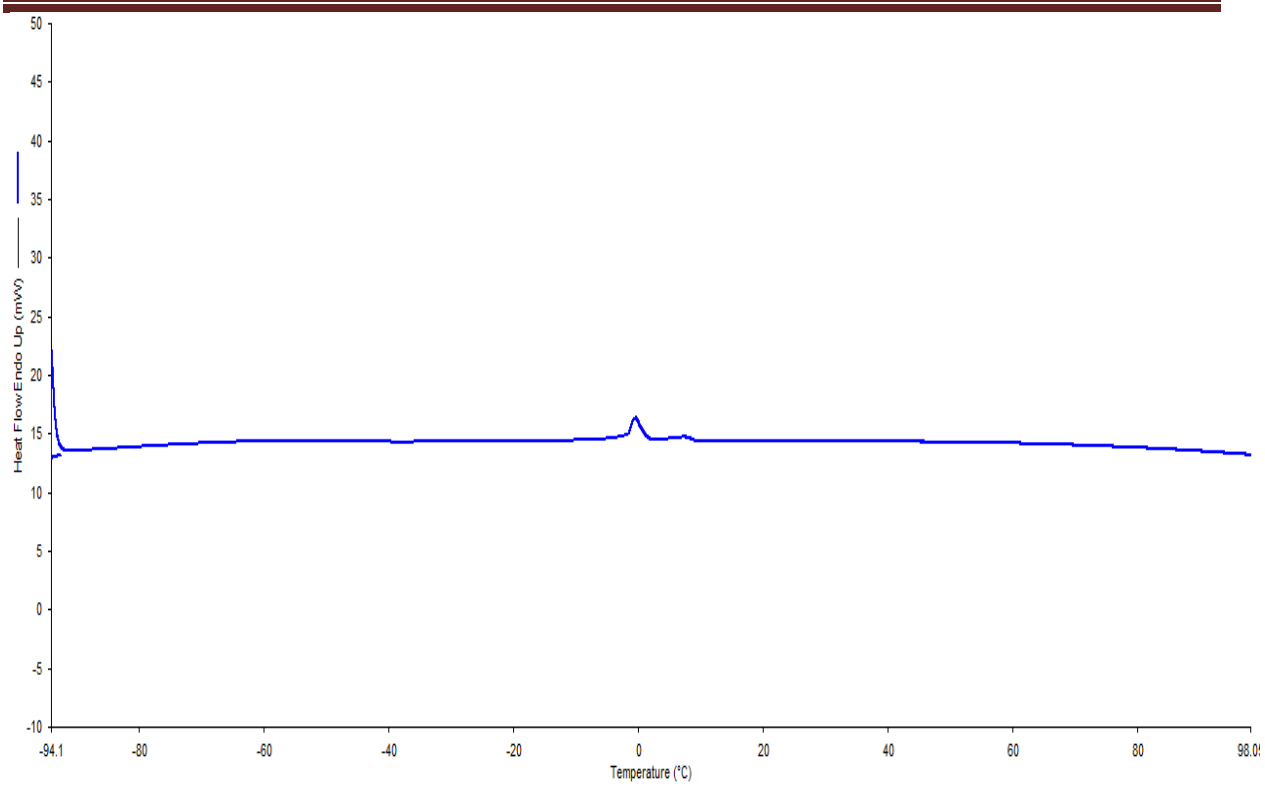

Figure 5.15–DSC curve for $[C_3(NMeEt)_3]TFSA$

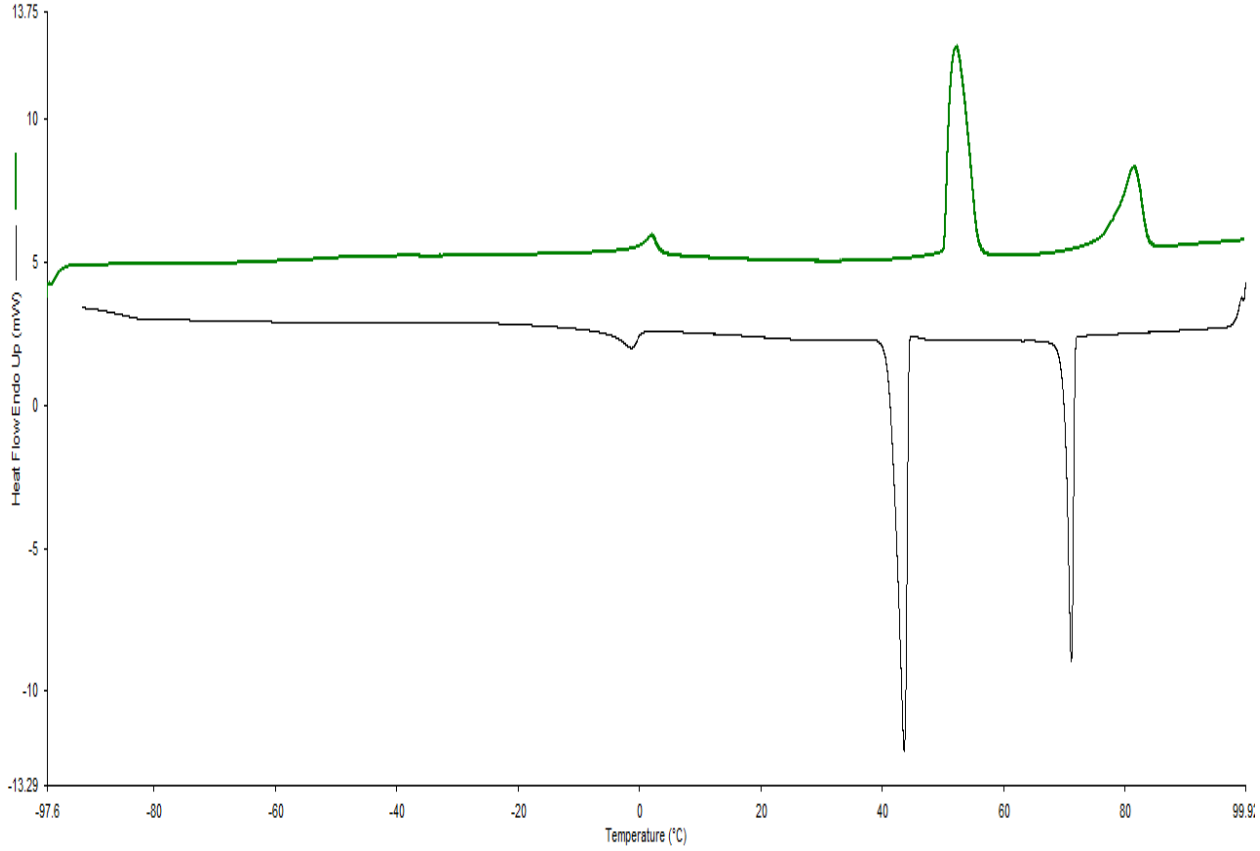

Figure 5.16–DSC curve for $[C_3(NEt_2)_3]$triflate.

In the DSC curve (fig. 5.13) of $[C_3(NMe_2)_2(NMeEt)]$TFSA, during the heating curve three endothermic transitions are observed. These transitions are seen at 6 °C, 32.2 °C and 62.3 °C for $T_{s\text{-}s}$ (solid to solid), $T_{s\text{-}s}$ (solid to solid) and $T_{s\text{-}l}$ (solid to liquid) respectively. These multiple solid-solid transitions, observed before melting, are either crystal-crystal polymorphism or more often plastic crystal phases.[5] On the cooling curve, we can see three exothermic peaks which are showing the crystallization is interrelated to the heating curve transitions. This sample fails to give a glass transition temperature (T_g) during the cooling cycle because it has already crystallized.

Usually, when a liquid is cooled to low temperatures, glass formation starts to occur. This is illustrated in the DSC curve of $[C_3(NMe_2)_2(NMe(CH_2CH_2OCH_3))]$DCA (fig below). Upon increasing the temperature from a glassy state to a rubbery state, changes in heat capacity occurs. The glass transition temperatures usually appear in the temperature range of −70 to −90 °C for most of the ILs. The glass transition temperature for $[C_3(NMe_2)_2(NMe(CH_2CH_2OCH_3))]$DCA appears at −69.3 °C. Further heating after the glass transition state, yields an exothermic peak around −20 °C, associated with crystallization followed by an endothermic peak at 29.1 °C, associated with melting.

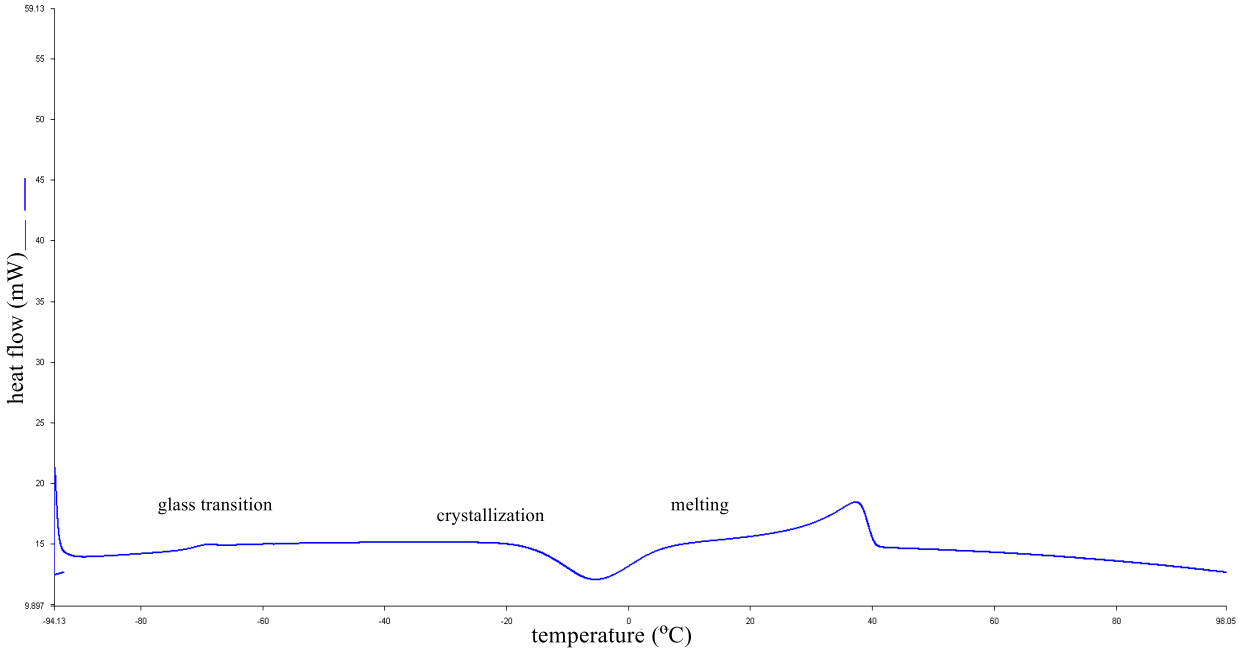

Figure 5.17-DSC curve for $[C_3(NMe_2)_2(NMe(CH_2CH_2OCH_3))]$DCA

The melting points of ionic solids are reduced by the disruption of crystal packing and reduction of crystal lattice energy.[5] The Coulombic attraction is usually given by;

$$E_c = \frac{M\, Z^- Z^+}{4\pi\varepsilon_o r}$$

Where Z^+ and Z^- are ion charges, M is the packing efficiency (Madelung constant), and r is the distance between the ions. Thus, melting points are reduced when the charges on the ions are ± 1, sizes of the ions are large ensuring large separation (r), and the packing efficiency (M) between the ions is reduced by lower symmetry.

The anion and cation size affects T_g and T_m. ILs usually have organic cations rather than inorganic cations. The Coulombic interactions are reduced among the ions of ILs due to large size and charge differences. The shape of the ion also controls the melting points. Reduction in the melting point is achieved by increasing the size of ion up to a certain point. Reduction in symmetry lowers the T_g which expands the range of the liquid state.

First, I will discuss the effect of reduced symmetry cations on DSC data. Among the C_s cations, $[C_3(NMe_2)_2(NMeR)]$TFSA (R = ethyl, allyl, $–CH_2CH_2OCH_3$, propyl, butyl and hexyl) the melting point should reduce with the increase in size of the cation. Except for allyl (M_w = 194.30 g/mol, T_m = 14.8 °C), the rest of the alkyl chains, ethyl (M_w = 182.29 g/mol, T_m = 63.2 °C), propyl (M_w = 196.31 g/mol, T_m = 19.7°C), butyl (M_w = 210.31 g/mol, T_m = 5.6 °C) and hexyl (M_w = 238.39 g/mol, T_m = −13.7 °C) follow a pattern of decreasing melting point with increasing molecular weight of the cation. The allyl chain is unsaturated which is responsible for lowering the melting point. While, the reduced flexibility in ether chain ($–CH_2CH_2OCH_3$),[16] causes the viscosity to increase and prevents the sample from crystallizing and only a T_g is observed at −73.5 °C.

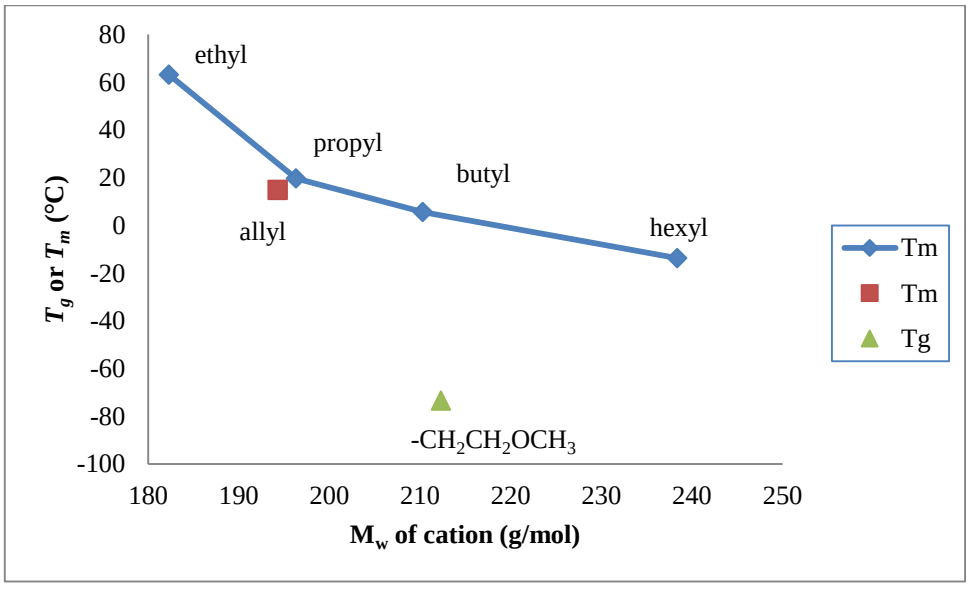

Figure 5.18–T_m or T_g vs molecular weight of cation $[C_3(NMe_2)_2(NMeR)]$TFSA

In contrast of the $[C_3(NMe_2)_2(NMeR)]$TFSA series with the $[C_3(NMe_2)_2(NMeR)]$DCA series (R = allyl, propyl, $-CH_2CH_2OCH_3$ and butyl), both melting points and glass transition temperatures are observed for TFSA salts instead of mainly glass transition temperatures for the DCA salts. This indicates that DCA salts are room temperature ILs (RTILs) that fail to crystallize. However for $[C_3(NMe_2)_2(NMe(CH_2CH_2OCH_3))]$DCA both T_g at −69.3 °C and a T_m at 29.1 °C are observed. While for $[C_3(NMe_2)_2(NMe(CH_2CH_2OCH_3))]$TFSA, only a T_g is observed at −73.5 °C. It was thought that larger TFSA anion is responsible for reducing the interactions between the inflexible ether alkyl chain on cation and an anion and results in lower glass transition temperature as compared to smaller DCA anion. Likewise, for $[C_3(NMe_2)_2(NMeBu)]$TFSA both T_g at −82.6 °C and a T_m at 5.6 °C are observed.

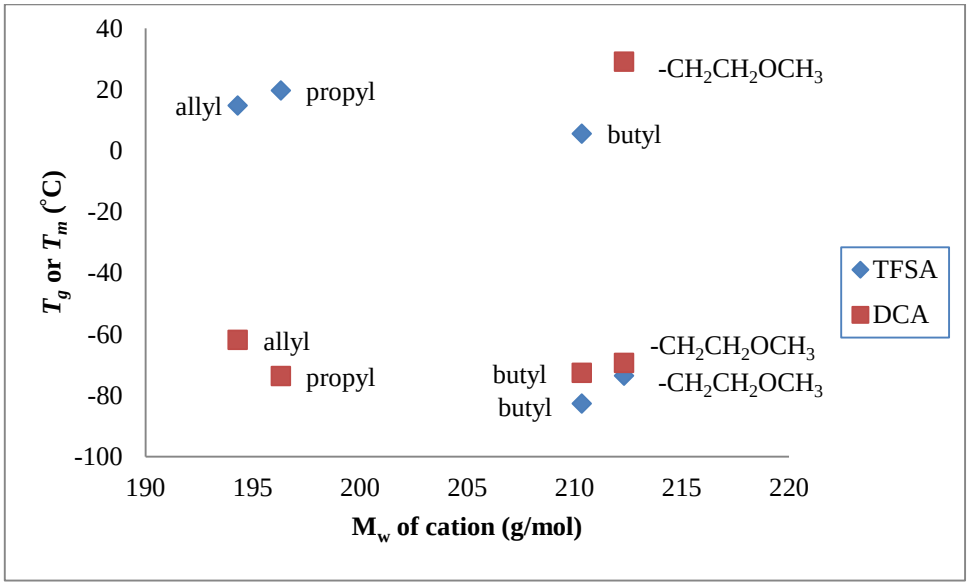

Figure 5.19–T_g or T_m *vs* molecular weight of cation $[C_3(NMe_2)_2NMeR]$X (X =TFSA and DCA).

For the protic ILs (PILs) of the C_s cations, $[C_3(NMe_2)_2(NHR)]$TFSA (R = ethyl, allyl, propyl, $CH_2CH_2OCH_3$, and butyl), hydrogen bonding between the NH group and the anion causes the viscosity to increase and rather than a T_m, usually a T_g transition is observed. The glass transition temperature for $[C_3(NMe_2)_2(NH(CH_2CH_2OCH_3))]$TFSA was observed at −64.3 °C, while for the rest of the series, lower T_g values ranging from −71.3 to −73.2 °C were observed. This is due to an additional NH---O hydrogen bonding in $[C_3(NMe_2)_2(NH(CH_2CH_2OCH_3))]$TFSA responsible for giving higher T_g.

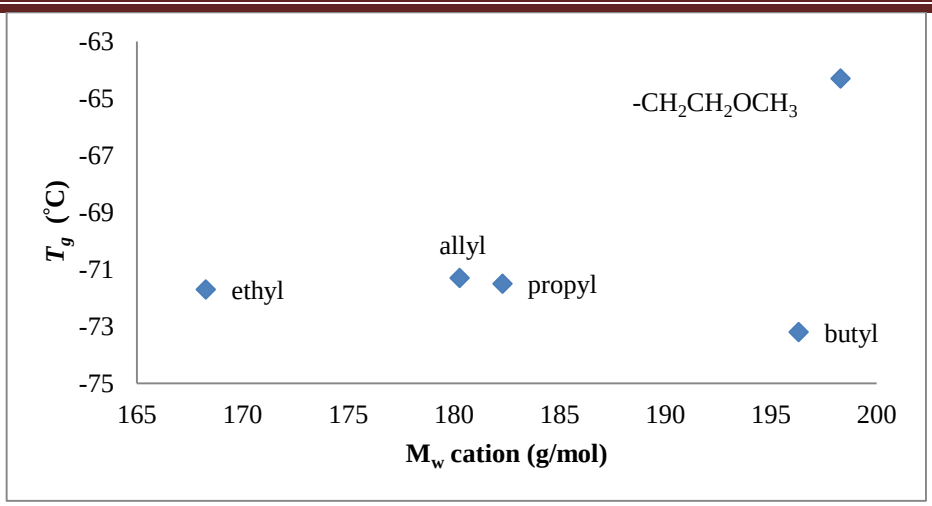

Figure 5.20–T_g *vs* molecular weight of cation [C3(NMe2)2(NRH)]TFSA

An increase in the size of the anion also reduces the melting point due to a reduction in Coulombic interactions. In [C3(NEt2)2(NBuH)]X (X = $MeSO_4^-$, BF_4^-, DCA^- and $TFSA^-$), thus, the glass transition temperature increases $TFSA^-$ (M_w = 280 g/mol, T_g =−85.7 °C) < $MeSO_4^-$ (M_w = 111 g/mol, T_g =−77.1 °C) < BF_4^- (M_w = 87 g/mol, T_g =−76.3 °C) < DCA^- (M_w = 66 g/mol, T_g =−71.9 °C) This anion dependence follows the decreasing molecular weight of the anion. As the size of the anion increases, the Coulombic attractions are reduced between the ions and this causes the viscosity to reduce.

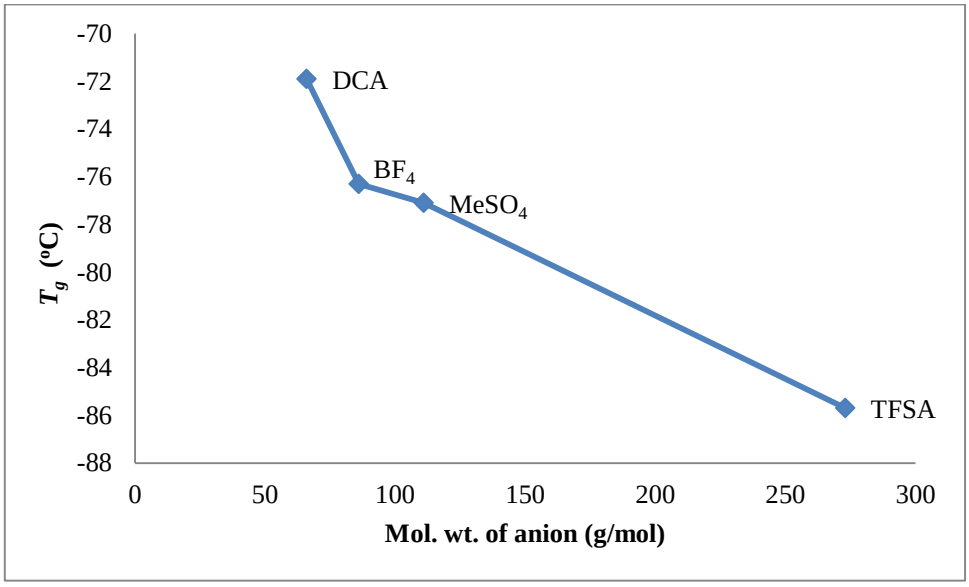

Figure 5.21–T_g *vs* molecular weight of anion for [C3(NEt2)2(NBuH)]X

A similar trend for a decrease of melting point with an increase of cation size was seen for the C_{2v} series [C3(NMe2)2(NR2)]TFSA. As we go from R = ethyl (T_m = 43.5 °C), R = allyl (T_m = 15.6 °C), R = -CH2CH2CH3 (T_m = 51.6 °C), R = -CH2CH2OCH3 (T_g = −70.4 °C), R = butyl

(T_m = 36.3 °C and T_g = −70.4 °C), and R = hexyl (T_m = 20.8 °C). The flexible alkyl chains contribute to the disruption of symmetry and increases vibrational modes of freedom. These hydrocarbon alkyl chains reduce melting points, which leads to glass formation with the inhibition of crystallization. However, $[C_3(NMe_2)_2(N(CH_2CHCH_2))_2)]$TFSA, and $[C_3(NMe_2)_2(N(CH_2CH_2OCH_3))_2)]$TFSA are showing a bit different behavior. In $[C_3(NMe_2)_2(N(CH_2CHCH_2))_2)]$TFSA, due to the presence of an unsaturated alkyl chain, there is a reduction of the melting point to 15.6 °C. While in $[C_3(NMe_2)_2(N(CH_2CH_2OCH_3))_2)]$TFSA, due to the reduced flexibility of ether alkyl chain results in high viscosity which does not allow the IL to give a melting point, but rather a glass transition temperature at −70.4 °C.

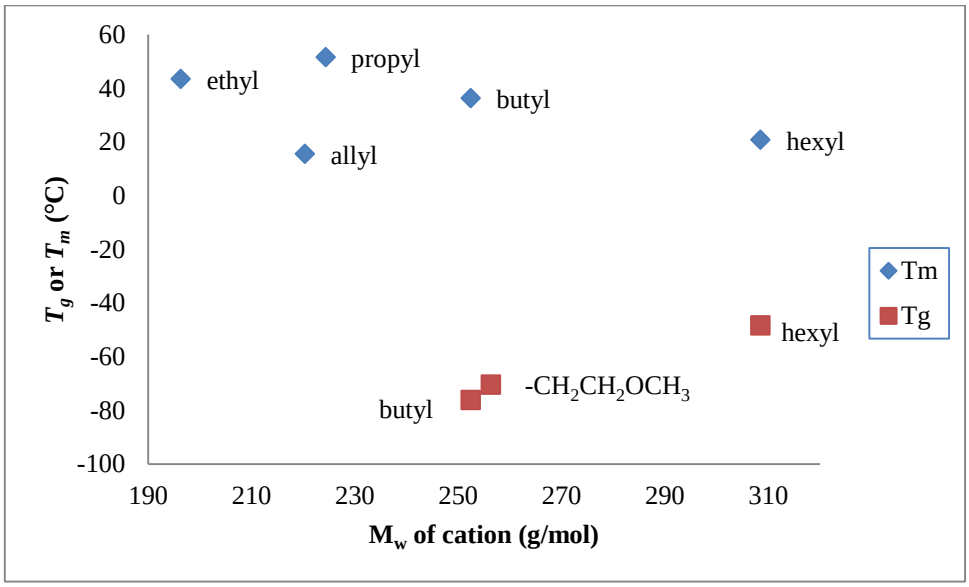

Figure 5.22–T_g or T_m *vs* molecular weight of cation, $[C_3(NMe_2)_2NR_2]$TFSA (R = ethyl, allyl, propyl, butyl, -$CH_2CH_2OCH_3$ and hexyl)

In the diprotic IL, $[C_3(NEt_2)_2NH_2]MeSO_4$ a further increase of hydrogen bonding (between –NH_2 and an anion) occurs. The glass transition temperature for $[C_3(NEt_2)_2NH_2]MeSO_4$ is observed at −47.7 °C.

With the increase in size of cation from $[C_3(NEt_2)_2NBu_2]I$ (T_m = 75.1 °C) to $[C_3(NEt_2)_2NHex_2]I$ (T_g = −45.6 °C), van der Waals forces increases due to longer hexyl chains in contrast to butyl chains. Increasing the alkyl chain length of the cation increases the conformational flexibility, which allows for more rotational degrees of freedom. This leads to the reduction of interaction between the cation and the anion and the tendency to give T_g increases in $[C_3(NEt_2)_2NHex_2]I$.

Now I will compare my C_{2v} cations with similar cations synthesized by Curnow's group. As the size of anion for C_{2v} cation, $[C_3(NEt_2)_2NBu_2]^+$ increases from DCA^- (66 g/mol)[12], I^- (126 g/mol) and $TFSA^-$ (280 g/mol),[12] the tendency to give glass transition temperature should increase. Except in $[C_3(NEt_2)_2NBu_2]I$ electrons of iodide anion are interacting strongly with the cation and gives a higher melting point at 75.1 °C rather than glass transition temperature. While, for $[C_3(NEt_2)_2NBu_2]TFSA$[12] and $[C_3(NEt_2)_2NBu_2]DCA$[12] glass transition temperatures are observed at −81 °C and −80 °C, respectively, due to weak nucleophilic behavior of TFSA and DCA anion.

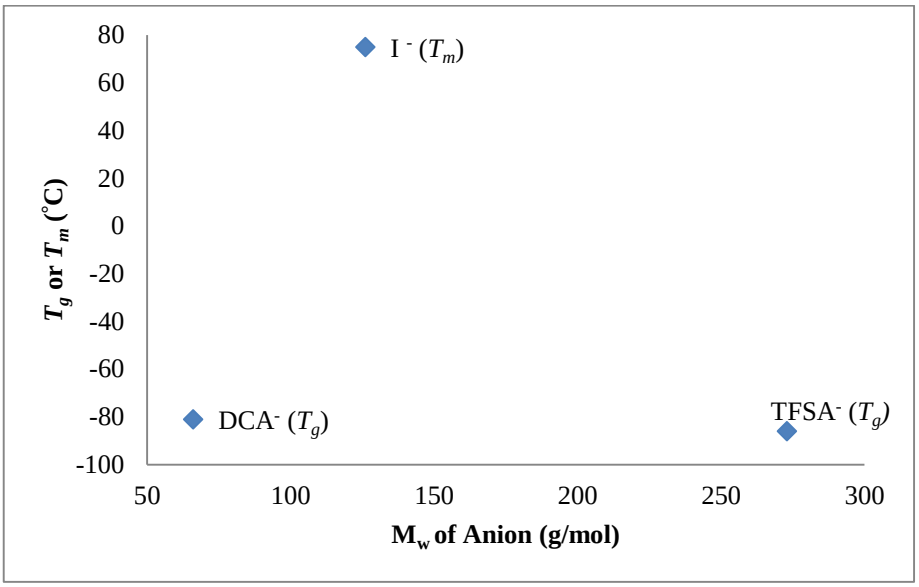

Figure 5.23–T_g or T_m *vs* molecular weight of anion for $[C_3(NEt_2)_2NBu_2]^+$.[16]

Similarly, as the size of anion increases for $[C_3(NEt_2)_2NHex_2]^+$ cation from DCA^- (66 g/mol)[12], I^- (126 g/mol), OTf^- (149 g/mol) and $TFSA^-$ (280 g/mol)[12]. The tendency to give low glass transition temperature increases, as seen for $[C_3(NEt_2)_2NHex_2]I$ (T_g = −45.6 °C), $[C_3(NEt_2)_2NHex_2]OTf$ (T_g = −68.9 °C), and $[C_3(NEt_2)_2NHex_2]TFSA$ (T_g = −81 °C). Except $[C_3(NEt_2)_2NHex_2]DCA$ have smallest DCA anion gives a low glass transition temperature at −80 °C due to weak nucleophilic character of DCA anion.

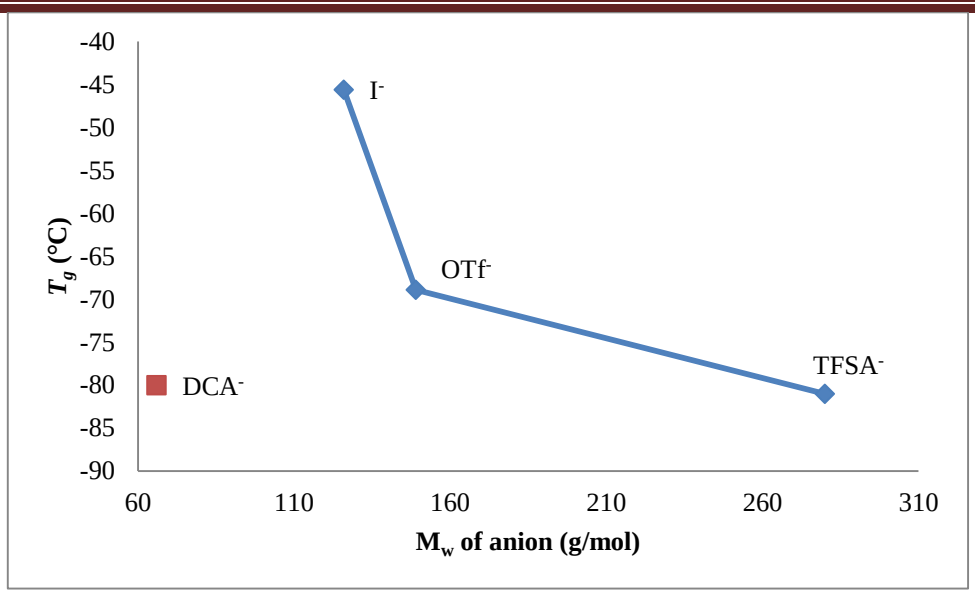

Figure 5.24–T_g *vs* molecular weight of anion for $[C_3(NEt_2)_2(NHex_2)]^+$ cation.[16]

In $[C_3(NPhH)_3]$TFSA (M_w = 312.39 g/mol), due to reduced flexibility of the phenyl rings and weak hydrogen bonding between the NH group and the anion, the melting point is increased to 16.7 °C as compared to other low molecular weight C_{3h} cations, $[C_3(NMeEt)_3]^+$ (M_w = 210 g/mol, T_m = 7.3 °C), $[C_3(NMeAllyl)_3]^+$ (M_w = 246 g/mol, T_g = −82.8 °C), and $[C_3(NMeEr)_3]^+$ (M_w cation = 300 g/mol, T_g = −65.3 °C).

So far, we have observed that initial lengthening of the alkyl chain leads to a reduction of the melting point by destabilization of Coulombic attractions, and the trend towards glass formation increases. Melting point reduction leads to an increase of the tendency for glass formation on cooling rather than crystallization. Further increase of alkyl chain length leads to an increase of van der Waals forces between the alkyl chains. This leads to high melting points due to increased structural ordering.

High symmetry increases the melting point by increasing packing efficiency. With the increase in size of anion among $[C_3(NEt_2)_3]^+$, from Cl^- (34 g/mol)[12] < DCA^- (66 g/mol)[12] < I^- (126 g/mol) < OTf^- (149 g/mol) < OTs^- (171 g/mol) < $F_5C_6O^-$ (183 g/mol) < $TFSA^-$ (280 g/mol)[12], the melting point should decrease and the tendency to give glass transition temperature should increase. This is obvious among $[C_3(NEt_2)_3]Cl$ (T_m = 92 °C),[12] $[C_3(NEt_2)_3]DCA$ (T_m = 10 °C),[12] $[C_3(NEt_2)_3]OTs$ (T_g = −50.4 °C), $[C_3(NEt_2)_3]F_5C_6O$ (T_g = −49 °C) and $[C_3(NEt_2)_3]TFSA$[12] (T_m = 19 °C and T_g = −86 °C). However, $[C_3(NEt_2)_3]I$ (T_m = 48 °C) and $[C_3(NEt_2)_3]OTf$ (T_m = 77.5 °C) are not following the regular decreasing pattern of melting point. Because the electrons of iodide are available to interact strongly with cation,

while in case of symmetric triflate anion increases the efficient packing with cation and results in higher T_m.

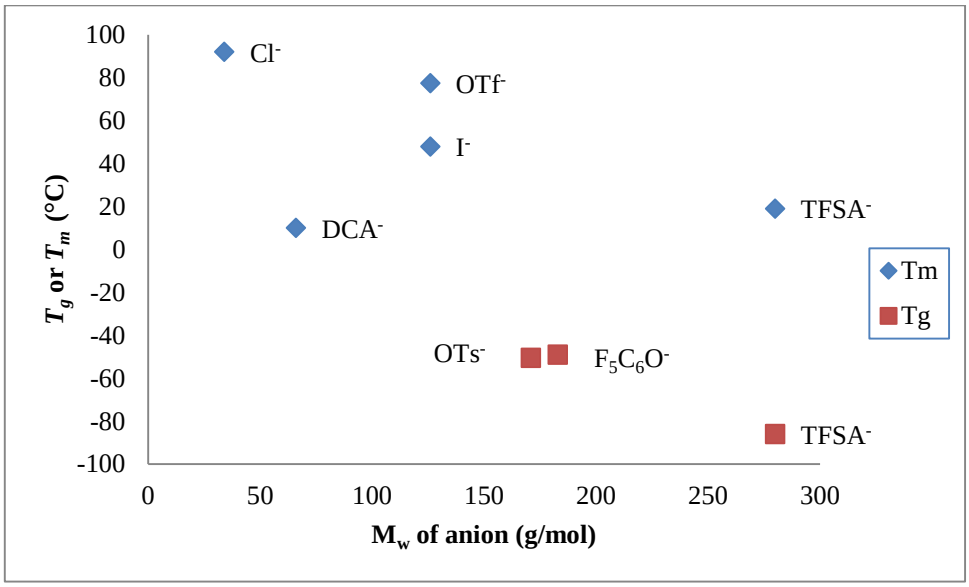

Figure 5.25–T_m or T_g *vs* molecular weight of anion for $[C_3(NEt_2)_3]^+$.

However, as the size of cation increases from $[C_3(NEt_2)_3]^+$ to $[C_3(NBu_2)_3]^+$ the van der Waals forces increase due to longer butyl chains. As the size of anion increases from $[C_3(NBu_2)_3]$DCA (T_m = 14 °C and T_g = −62 °C),[12] $[C_3(NBu_2)_3]B(CN)_4$ (T_m = 29.3 °C), $[C_3(NBu_2)_3]$TFSA (T_m = 3 °C and T_g = −74 °C)[12] and $[C_3(NBu_2)_3]$FAP (T_g = −72.9 °C), the T_m decreases and tendency to give T_g increases except $[C_3(NBu_2)_3]$DCA.

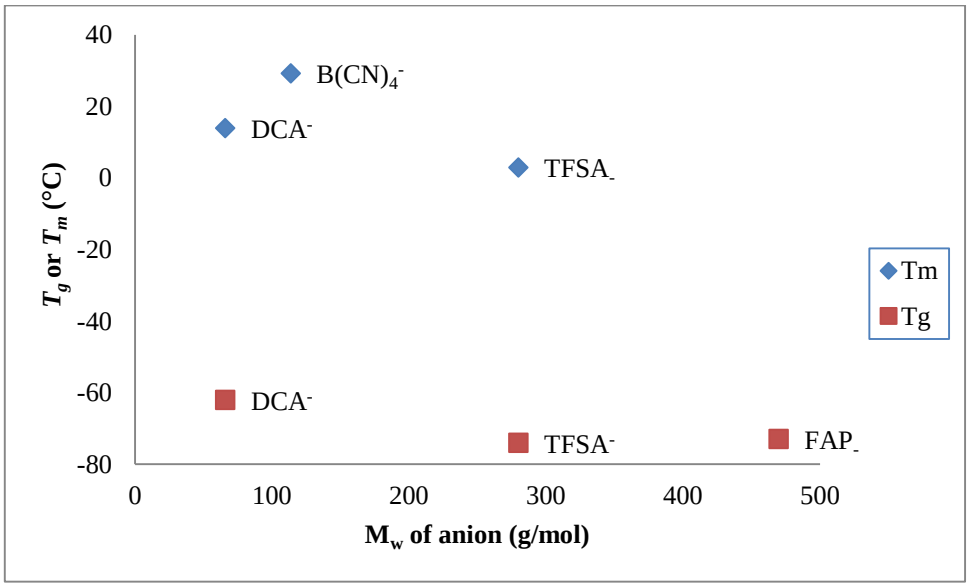

Figure 5.26–T_m or T_g *vs* molecular weight of anion for $[C_3(NBu_2)_3]^+$

Among the open ring cations, as the size of cation is increased from $[(Me_2N)_2CCH_2C(NMe_2)_2]^+$ to $[(BuHN)_2CCH_2C(NBuH)_2]^+$ the melting point is reduced. The latter cation has butyl chains which increases the conformational flexibility and causes the melting point to reduce from 201 °C ($[(Me_2N)_2CCH_2C(NMe_2)_2]Cl_2$) to 49.5 °C ($[(BuHN)_2CCH_2C(NBuH)_2]Cl_2$).

There is no strong correlation seen from the DSC data for tac-based AAILs with the size of cation. Except $[E_4Thr]MeSO_4$, glass transition temperatures were observed for tac-based AAILs. As the size of cation increases from $[E_4Ala]^+$ (268 g/mol) to $[E_4Tyr]^+$ (360 g/mol), there is a weak trend seen towards increasing glass transition temperature. For most of the AAILs, usually glass transition temperatures are observed. Due to the presence of hydrogen bonding between the cation of the AAIL and the zwitterion, the cation of the AAIL and the anion, or the zwitterion and anion, these samples were highly viscous. It was due to the viscous nature that samples failed to crystallize and gave only glass transition temperatures instead of melting points.

Table 5.4-DSC data of tac-based and imidazolium-based AAILs.

	***C_s* Cations**	**Total Mol. wt.**	***T_g*** **(°C)**	***T_m*** **(°C)**
1	$[E_4Ala]MeSO_4$	379.47	−36.5	---
2	$[E_4Pro]MeSO_4$	405.51	−15.7	−7.3
3	$[E_4Val]MeSO_4$	407.53	−50.9	---
4	$[E_4Thr]MeSO_4$	409.50	---	40.4
5	$[E_4Ala]TFSA$	548.52	−26.0	---
6	$[E_4Ser]TFSA$	564.52	−20.9	---
7	$[E_4Pro]TFSA$	574.56	−40.9	---
8	$[E_4Thr]TFSA$	578.55	−15.8	---
9	$[E_4IIe]TFSA$	590.60	−37.2	---
10	$[E_4His]TFSA_2$	895.64	−17.6	---
11	$[E_4Tyr]TFSA$	640.57	0.3	---
12	$[E_8Lys]TFSA_2$	1064.95	−48.3	---
	Imidazolium AAILs	**Total mol. wt.**	***T_g*** **(°C)[10]**	***T_m*** **(°C)**
13	[emim][Ala]	199.25	−57	
14	[emim][Ser]	215.25	−49	
15	[emim][Pro]	225.29	−48	
16	[emim][Val]	227.31	−52	
20	[emim][Thr]	229.28	−40	
17	[emim][IIe]	241.33	−52	
19	[emim][Lys]	256.35	−47	
19	[emim][His]	265.31	−24	
21	[emim][Tyr]	291.35	−23	

Now I will compare tac-based AAILs with imidazolium-based AAILs (table 5.4). Triaminocyclopropeniums gave higher glass transition temperatures (0 to −50 °C) than

imidazolium-based AAILs (−23 to −52 °C).[10] This was probably due to the increased hydrogen-bond interactions among triaminocyclopropeniums as compared to the less viscous nature of imidazolium. It was also thought that tac-based AAILs were obtained as a mixture of IL and zwitterion, which increased the hydrogen-bond interactions. The tac-based AAILs as TFSA salts have total molecular weight (380 to 1100 g/mol) higher than the imidazolium AAILs (200 to 300 g/mol). The delocalized charge on the cyclopropenium cation is responsible for giving the T_g almost in the same range to imidazolium ones. The presence of strong hydrogen bonding between the cation and methyl sulphate anion in $[E_4Thr]MeSO_4$ and $[E_4Pro]MeSO_4$ causes the melting point to increase to 40.4 °C and −7.3 °C respectively.

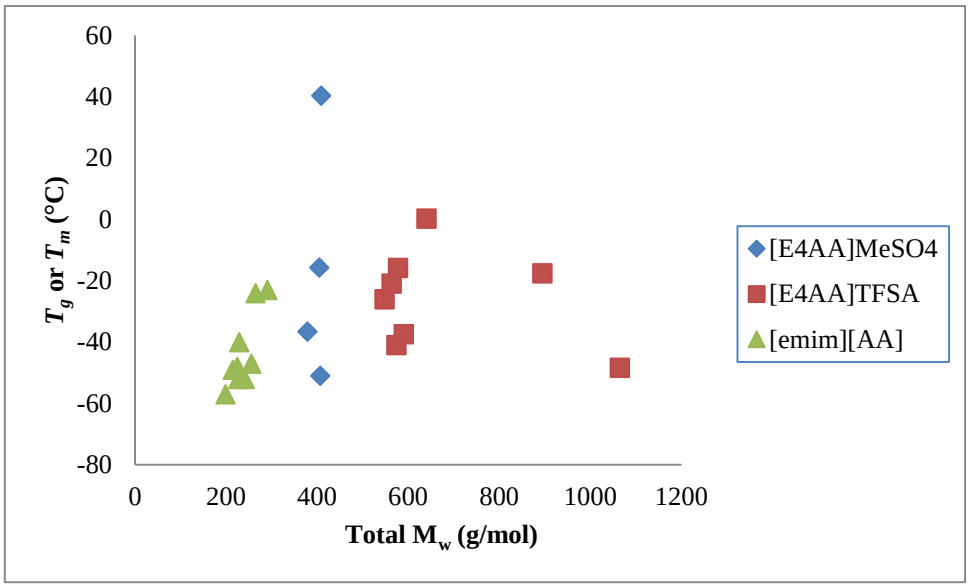

Figure 5.27–T_m or T_g *vs* total molecular weight of tac-based AAILs and [emim][AA]

In contrast of the DSC data for tac-based AAILs with cations derived directly from natural amino acids([Amino Acid]X, X = NO_3^-, BF_4^-, PF_6^-, CF_3COO^- , SO_4^{2-})[17] and ammonium-based ($[N_{2222}]$[Amino Acid][18] AAILs. The delocalization of charge in the tac-cation contributes to lowering of electrostatic interactions and thus only glass transition temperatures were observed instead of melting temperatures as found in other classes.[3]

Table 5.5–DSC data for Amino acid as cation and ammonium-based AAILs

	AAIL	T_m (°C)
	Amino Acid Cation[17]	
1	[Ala]NO_3	159
2	[Ala]BF_4	78
3	[Ala]PF_6	not observed
4	[Ala]CF_3COO	82
5	$[Ala]_2SO_4$	141
6	[Val]NO_3	134
7	[Ile]NO_3	105
8	[Thr]NO_3	not observed
9	[Pro]NO_3	not observed
10	[Pro]BF_4	76
11	[Pro]PF_6	not observed
12	[Pro]CF_3COO	78
13	$[Pro]_2SO_4$	92
	Ammonium-based[18]	
14	$[N_{2222}]$[Ser]	not observed
15	$[N_{2222}]$[Pro]	not observed
16	$[N_{2222}]$[Thr]	not observed
17	$[N_{2222}]$[Ile]	not observed
18	$[N_{2222}]$[Asn]	58
19	$[N_{2222}]$[Gln]	not observed
20	$[N_{2222}]$[Glu]	not observed
21	$[N_{2222}]$[Met]	not observed
22	$[N_{2222}]$[His]	54

There are many choices of anions available for ILs. In the present work, we have mainly used TFSA. TFSA contains weak electrostatic interactions due to electron-withdrawing and negative charge-delocalization effects of halogen and oxygen atoms.

For $[C_3(NMe_2)_2(NAllylH)]TFSA$ (T_g = −71.3 °C and T_m = −53.7 °C), $[C_3(NMe_2)_2(NMe(CH_2CH_2OCH_3))]DCA$ (T_g = −69.3 °C and T_m = 29.1 °C), $[C_3(NMe_2)_2(NMeBu)]TFSA$ (T_g = −82.6 °C and T_m = 5.6 °C), $[E_4Pro]TFSA$ (T_g = −15.7 °C and T_m = −7.3 °C), $[C_3(NMe_2)_2(NBu_2)]TFSA$ (T_g = −76.1 °C and T_m = 36.3 °C), $[C_3(NMe_2)_2(NHex_2)]TFSA$ (T_g = −48.4 °C and T_m = 20.8 °C), $[C_3(NMe_2)_2(NH_2)]TFSA$ (T_g = −59.5 °C and T_m = 94.2 °C), and $[C_3(NEt_2)_3]F_5C_6O$ (T_g = −49.3 °C and T_m = 71 °C), both melting points and glass transition temperatures are observed. Generally the glass transition is approximately 2/3 of the melting point.[19]

5.4 Viscosity

Knowledge of a material's viscosity is important in predicting the ease with which it may be handled, processed or used. The viscosity of a fluid arises from the internal friction of a fluid.[5] The viscosities of ILs at room temperature range from around 10 mPa s to > 1000 mPa s.[5] The viscosity of an ionic liquid is generally higher than molecular solvents. This does not limit the use of ionic liquids because viscosity decreases rapidly with temperature. The dynamic viscosity was measured on a Brookfield cone and plate viscometer; it measures viscosity between 1 and 1000 mPa s. The viscosities were measured under a dry nitrogen atmosphere, with a circulating water jacket for temperature control.

The dependence of the viscosities on shear rate was studied. The non-Newtonian behavior of ionic liquids can also be measured using cone and plate viscometer. The cone is turned through three different shear rates. While keeping the temperature constant, the sheer stress is measured. The viscosity remained constant showing Newtonian behavior. In other words, no non-Newtonian fluid was observed, under the shear rate tested.[20] For non-Newtonian ILs, the viscosity decreases at a certain point of applied shear stress, thus rheological behavior must be taken into account.[21]

The dynamic (absolute) viscosity (η) is tabulated in table 5.6. The ratio of dynamic or absolute (η) viscosity to density (ρ) is the kinematic (υ) viscosity;

$$\upsilon = \frac{\eta}{\rho}$$

Table 5.6-Viscosities of ILs in mPa s

	***C_s* Cations**	**Mol wt cation**	**20 °C**	**30 °C**	**40 °C**	**50 °C**	**60 °C**	**70 °C**	**80 °C**	**90 °C**
1	$[C_3(NMe_2)_2(NEtH)]TFSA$	168.26	143.5	79.7	47.8	31.9	21.7	15.5	12	9.09
						70 °C	**75 °C**	**80 °C**	**85 °C**	**90 °C**
2	$[C_3(NMe_2)_2(NEtMe]TFSA$	182.29	---	---	---	13.6	12	10.6	9.71	8.58
			20 °C	**30 °C**	**40 °C**	**50 °C**	**60 °C**	**70 °C**	**80 °C**	**90 °C**
3	$[C_3(NMe_2)_2(HN(CH_2CHCH_2))]TFSA$	180.27	153.2	84.8	51.3	33.3	22.5	16.1	12.1	9.35
4	$[C_3(NMe_2)_2(N(CH_2CHCH_2)Me)]TFSA$	194.30	69.0	43.5	28.6	19.7	14.3	10.9	8.38	6.69
5	$[C_3(NMe_2)_2(N(CH_2CH_2CH_3)H)]TFSA$	182.29	156.8	86.8	52.1	34.1	23.5	16.7	12.1	9.55
6	$[C_3(NMe_2)_2(N(CH_2CH_2CH_3)Me)]TFSA$	196.31	72.5	45.2	29.6	20.0	14.6	11.2	8.68	6.90
7	$[C_3(NMe_2)_2(N(CH_2CH_2CH_3)Me)]DCA$	196.31	107.3	61.3	38.2	25.1	17.5	12.8	10.1	8.02
8	$[C_3(NMe_2)_2(N(CH_2CH_2OCH_3)H)]TFSA$	198.29	214.5	112.4	62.8	37.6	26.6	18.7	13.3	10.2
9	$[C_3(NMe_2)_2(N(CH_2CH_2OCH_3)Me)]TFSA$	212.31	92.5	55.6	36.2	24.3	17.5	12.6	9.71	7.66
10	$[C_3(NMe_2)_2(N(CH_2CH_2OCH_3)Me)]DCA$	212.31	127.7	67.9	39.0	24.5	16.6	12.1	9.25	7.15
11	$[C_3(NMe_2)_2(NBuH)]TFSA$	196.31	170.6	91.9	57.2	36.8	25.3	18.0	13.6	10.3
12	$[C_3(NMe_2)_2(NBuMe)]TFSA$	210.34	76.1	47.4	31.1	21.9	15.4	12.2	9.3	7.41

13	$[C_3(NMe_2)_2(NBuMe)]DCA$	210..34	67.4	40.3	25.3	17.2	12.1	9.14	7.05	5.57
14	$[C_3(NMe_2)_2(NPeH)]TFSA$	210.24	201.3	110.3	65.9	42.3	28.0	19.8	14.6	10.7
15	$[C_3(NMe_2)_2(NPeMe)]TFSA$	224.37	112.9	67.4	43.1	28.6	20.8	15.4	11.5	8.89
16	$[C_3(NMe_2)_2(NHexMe)]TFSA$	238.39	94.0	56.4	36.4	24.7	18.0	13.4	10.3	8.07
17	$[C_3(NEt_2)_2(NHBu)]MeSO_4$	252.42	344.3	188.0	106.3	67.4	45	31.7	22.7	16.8
18	$[C_3(NEt_2)_2(NHBu)]TFSA$	252.42	175.7	96.0	54.5	36.5	25.5	18.4	13.8	10.8
19	$[C_3(NEt_2)_2(NHBu)]DCA$	252.42	251.3	126.2	75.6	47.0	31.6	23.0	17.0	12.9
20	$[C_3(NEt_2)_2(NHBu)]BF_4$	252.42	521.0	271.8	153.2	89.4	56.2	38.2	26.6	19.1
					65 °C	**70 °C**	**75 °C**	**80 °C**	**85 °C**	**65 °C**
21	$[E_4Ala]MeSO_4$	268.37			1006.0	741.7	561.9	437.3	362.7	348.9
				60 °C	**65 °C**	**70.1 °C**	**75 °C**	**80 °C**	**85 °C**	**90 °C**
22	$[E_4Ala]TFSA$	268.37		820.4	589.5	435.2	329.0	244.7	196.7	156.3
							75 °C	**79.9 °C**	**85 °C**	**90.1 °C**
23	$[E_4Pro]MeSO_4$	294.41					837.7	614.1	459.7	411.7
					60 °C	**64.9 °C**	**70.2 °C**	**75 °C**	**79.9 °C**	**84.9 °C**
24	$[E_4Pro]TFSA$	294.41			564.0	405.6	302.9	230.4	178.8	138.9
						70.4 °C	**75 °C**	**80 °C**	**84.9 °C**	**89.6 °C**
25	$[E_4Val]TFSA$	296.43				790.8	574.2	417.9	310.1	233.4

							75 °C	80.2 °C	84.8 °C	90 °C
26	$[E_4Thr]TFSA$	298.40					883.7	617.1	455.7	329.0
	C_{2v} Cations		**20 °C**	**30 °C**	**40 °C**	**50 °C**	**60 °C**	**70 °C**	**80 °C**	**90 °C**
27	$[C_3(NMe_2)_2(NEt_2)]TFSA$	196.31	---	---	---	25.1	18.2	13.5	10.5	8.17
28	$[C_3(NMe_2)_2(N(CH_2CHCH_2)_2)]TFSA$	220.33	95.5	58.4	37.6	24.7	17.7	12.9	10.1	7.71
29	$[C_3(NMe_2)_2(NPr_2)]TFSA$	224.37	---	---	---	28.9	19.8	14.7	11.0	8.63
30	$[C_3(NMe_2)_2(N(CH_2CH_2OCH_3)_2)]TFSA$	256.35	141.0	78.7	54.7	31.1	20.9	15.2	11.2	8.58
31	$[C_3(NMe_2)_2(NBu_2)]TFSA$	252.42	117.5	69	43.3	28.6	19.8	14.6	11.2	8.68
32	$[C_3(NMe_2)_2(NHex_2)]TFSA$	308.52	---	110.3	65.4	42.3	29.0	21.3	16.1	13.2
33	$[C_3(NEt_2)_2(NHex_2)]I$	364.63	---	---	544.6	283.0	122.6	75.1	36.4	24.9
34	$[C_3(NEt_2)_2(NHex_2)]OTf$	364.63	444.4	240.1	137.9	82.8	54.7	38.8	26.2	20.5
	C_{3h} Cations									
35	$[C_3(NEtMe_2)_3]TFSA$	210.34	72.5	45.8	31.3	22.0	16.2	12.2	9.45	7.46
36	$[C_3(NAllylMe_2)_3]TFSA$	246.37	76.1	45.4	29.4	20.6	14.3	11.0	8.33	6.54
37	$[C_3(NAllylMe)_3]DCA$	246.37	146.1	72	40.5	25.5	17.4	12.7	9.09	6.95
38	$[C_3(NMeCH_2CH_2OCH_3)_3]TFSA$	300.39	183.9	96	55.7	34.1	23.3	16.4	12.1	9.04
	D_{3h} Cations									
39	$[C_3(NEt_2)_3][MeC_6H_4SO_3]$	252.42	764.2	338.2	171.6	97.1	57.4	37.2	25.2	-
40	$[C_3(NBu_2)_3]B(CN)_4$	420.59	263.6	148.1	85.8	54.7	35.8	24.7	17.5	13.1
41	$[C_3(NBu_2)_3]FAP$	420.59	391.3	212.5	120.6	79.6	48.4	33.1	22.9	16.9

For all the synthesized triaminocyclopropenium ionic liquids, viscosity was measured in the temperature range from 20 to 90 °C. $[C_3(NMe_2)_2(NEtMe)]$TFSA, $[C_3(NMe_2)_2(NEt_2)]$TFSA and $[C_3(NMe_2)_2(NPr_2)]$TFSA were solids and their viscosities were measured above the melting point. In the case of highly viscous ILs, $[E_4Ala]MeSO_4$, [$[E_4Ala]$TFSA, $[E_4Pro]MeSO_4$, $[E_4Pro]$TFSA, $[E_4Val]$TFSA, $[E_4Thr]$TFSA, $[[C_3(NMe_2)_2(NHex_2)]$TFSA, and $[C_3(NEt_2)_2(NHex_2)]$I, the viscosity was measured by increasing the temperature until the viscosity was in the viscometer's range.

For $[C_3(NMe_2)_2(NMe(Pentyl))]$TFSA the viscosity measurements were done at 20 °C six times on the same sample to check the reproducibility of the results (table 5.7). Standard deviation and standard error were also measured. The standard error in the measurements was calculated as ≈ 1%, which agrees with the viscometer's manufacturer 1% error.

Table 5.7-Reproducibility in Viscosity Measurement

	Visocisty (20 °C) mPa.s	**Mean mPa.s**	**Standard Dev mPa.s**	**Standard Deviation**	**Standard Error**
1	111.4	111.5	2.8	111.5 ± 2.8 mPa.s	111.5 ± ≈1 mPa.s
2	113.4				
3	107.3				
4	109.3				
5	112.9				
6	114.8				

In the present study, the highest viscosity observed among achiral ILs was for $[C_3(NEt_2)_3]$I (544.6 mPa s at 40 °C), due to being a symmetric cation and also having a good packing efficiency of cation and spherical anion. It is important to note that highly viscous ILs are important in applications such as stationary phases for gas chromatography.[21] The viscosity and conductivity are correlated; a highly viscous IL tends to exhibit relatively low ionic conductivity.

The lowest viscosity observed in the present study is 67.4 mPa s at 20 °C for $[C_3(NMe_2)_2(NBuMe)]$DCA. Usually, the factors that affect viscosity are poorly understood but in this case, the dicyanamide anion is responsible for lowering of viscosity due to lowered interactions with the cation due to its small size.[22] The usual trend for increasing viscosity relative to the anion is DCA < TFSA, which follows the increasing molecular weight of anion. The introduction of a long butyl chain in $[C_3(NMe_2)_2(NBuMe)]$DCA disrupts the symmetry and also contributes to the lowering of viscosity.

The alkyl chains around the tac cation influence the symmetry and are responsible for varying the viscosity. The symmetry of the cation doesn't have a very large impact on viscosity; rather it is mainly the size of the cation that influences viscosity.

For protic ionic liquids, as the size of cation increases for TFSA salts from $[C_3(NMe_2)_2(NEtH)]^+$ (M_w = 168.26 g/mol, η = 143.5 mPa s at 20 °C), $[C_3(NMe_2)_2(NH(CH_2CHCH_2))]^+$ (M_w = 180.27 g/mol, η = 153.2 mPa s at 20 °C), $[C_3(NMe_2)_2(NPrH)]^+$ (M_w = 182.29 g/mol, η = 156.8 mPa s at 20 °C), $[C_3(NMe_2)_2(NH(CH_2CH_2OCH_3))]^+$ (M_w = 198.29 g/mol, η = 214.5 mPa s at 20 °C), $[C_3(NMe_2)_2(NBuH)]^+$ (M_w = 196.31 g/mol, η = 170.6 mPa s at 20 °C) and $[C_3(NMe_2)_2(NPeH)]^+$ (M_w = 210.24 g/mol, η = 201.3 mPa s at 20 °C), the viscosity usually increases. $[C_3(NMe_2)_2(NErH)]$TFSA does not follow the regular viscosity pattern and has a relatively higher viscosity is seen compared to the rest of the series (fig. 5.28). The introduction of an ether chain is known to increase the total free volume due to rotational flexibility and usually reduces the viscosity.[16]

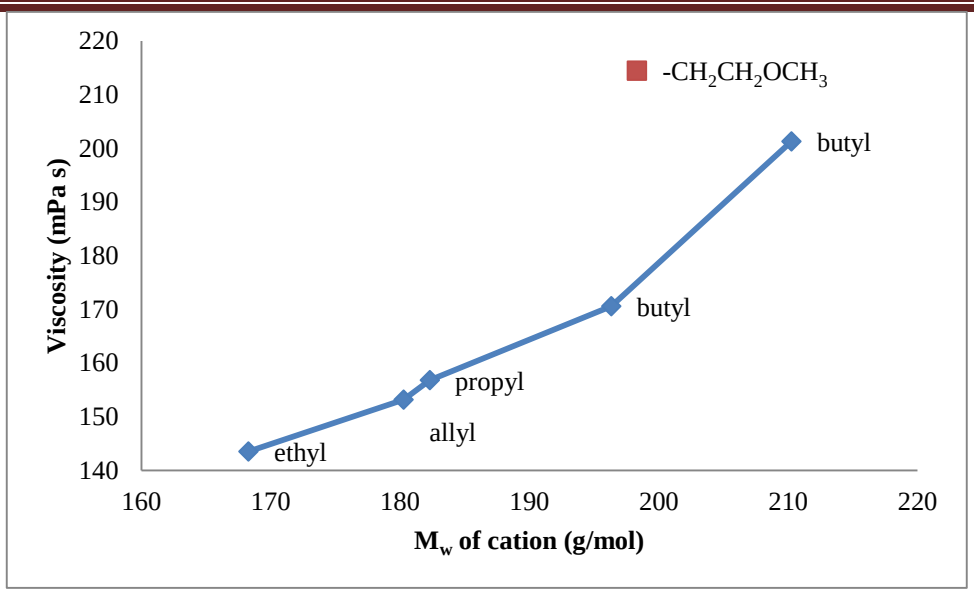

Figure 5.28-Viscosity data (at 20 °C) *vs* molecular weight of C_s protic cations $[C_3(NMe_2)_2NRH]TFSA$.

In $[C_3(NMe_2)_2(NErH)]^+$, the spacer length between the cationic core and the ether O atom is not short ($-CH_2CH_2OCH_3$). Secondly, there is intermolecular hydrogen bonding between the ether O and –NH groups. These factors are responsible for the high viscosity in $[C_3(NMe_2)_2(NErH)]^+$.[16]

A similar viscosity at 20 °C is seen for $[C_3(NMe_2)_2(NBuH)]TFSA$ (M_w = 196.31 g/mol, η = 170.6 mPa) and $[C_3(NEt_2)_2(NBuH)]TFSA$ (M_w = 252.42 g/mol, η = 175.5 mPa), even though they have different cation sizes. This is due to the ethyl chains around the cyclopropenium ring as in $[C_3(NEt_2)_2(NBuH)]TFSA$ have more rotational flexibility and are responsible for its relatively low viscosity of 175.7 mPa s at 20 °C: In the case of $[C_3(NMe_2)_2(NRH)]TFSA$ (R = ethyl, allyl, propyl, $-CH_2CH_2OCH_3$, butyl or pentyl), reduced rotational flexibility of methyl groups compared to ethyl groups of ring results in an increase of viscosity.

In the case of the $[C_3(NEt_2)_2(NBuH)]^+$ cation, the observed trend for the anion for increasing viscosity is $TFSA^-$ (M_w = 273 g/mol) < DCA^- (M_w = 66 g/mol) < $MeSO_4^-$ (M_w = 111 g/mol) < BF_4^- (M_w = 86 g/mol). Except for the DCA^- anion, the viscosity is increasing with the decreasing molecular weight of the anion. We need to take into consideration the hydrogen-bond interactions in this anion series. The DCA anion is of small size compared to the $MeSO_4^-$. While, more delocalization in DCA anion compared to BF_4^- lowers the viscosity of DCA salts. The DCA is a strong Lewis basic ligand compared to BF_4.

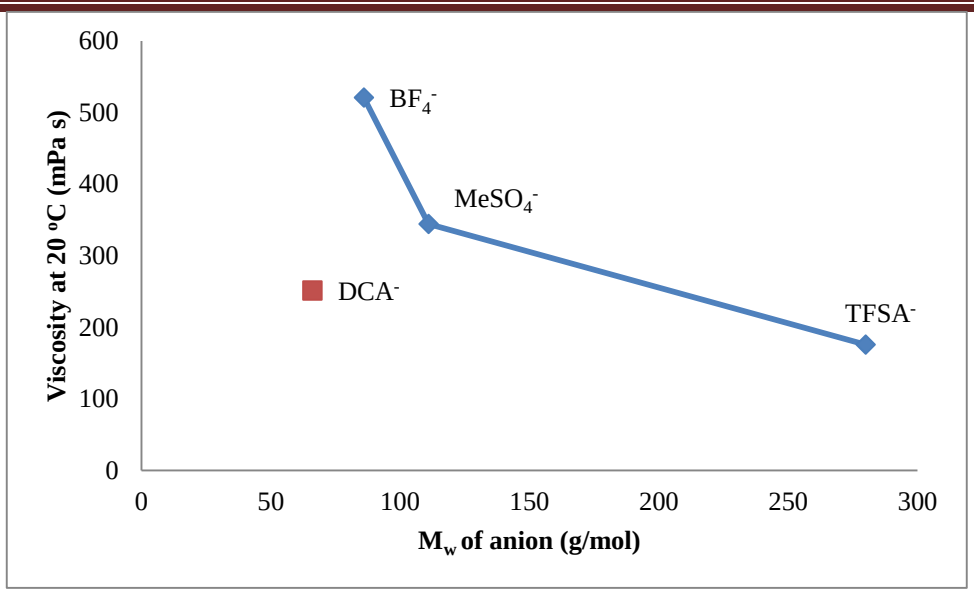

Figure 5.29–Viscosity *vs* molecular weight of anion for $[C_3(NEt_2)_2(NBuH)]^+$.

In the aprotic *Cs* cation series $[C_3(NMe_2)_2(NRMe))]$TFSA, for R = ethyl, allyl, propyl, butyl, -$CH_2CH_2OCH_3$, butyl, pentyl and hexyl, the viscosity should also increase as the molecular weight of cation increases. Except for $[C_3(NMe_2)_2(NEtMe)]$TFSA and $[C_3(NMe_2)_2(NHexMe)]$TFSA, the rest of the series follows the expected trend of increasing viscosity with an increase in the size of the cation. In $[C_3(NMe_2)_2(NEtMe)]$TFSA, it was thought that reduced rotational flexibility (due to ethyl chain) caused the viscosity to increase. $[C_3(NMe_2)_2(NHexMe)]$TFSA shows a marked decrease in viscosity possibly due to a greater disruption of symmetry because of the one long hexyl chain.

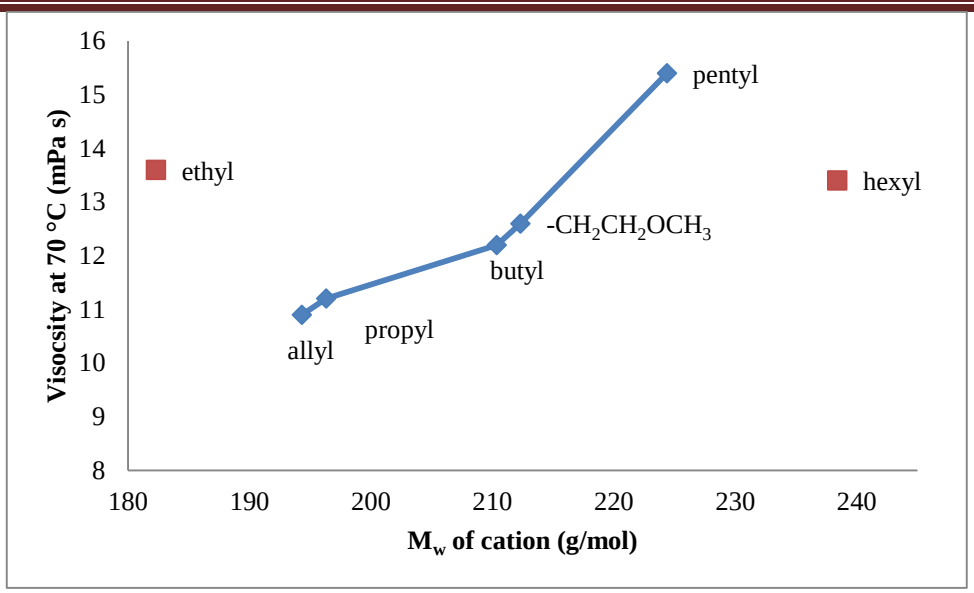

Figure 5.30–Viscosity (at 70 °C) *vs* molecular weight of [$C_3(NMe_2)_2(NRMe)$]TFSA (R = ethyl, allyl, propyl, -$CH_2CH_2OCH_3$, butyl, pentyl and hexyl)

In contrast to the viscosity of DCA salts are usually lower than the TFSA salts. The high chloride content (2.1%) in [$C_3(NMe_2)_2(NMe(CH_2CH_2CH_3))$]DCA caused the viscosity (107.5 mPa s at 20 °C) to increase as compared to [$C_3(NMe_2)_2(NMe(CH_2CH_2CH_3))$]TFSA (72.5 mPa s at 20 °C). While the inflexibility of ether alkyl chain and small size of anion causes the viscosity to increase in [$C_3(NMe_2)_2(N(CH_2CH_2OCH_3)Me)$]DCA (127.7 mPa s at 20 °C) compared to [$C_3(NMe_2)_2(N(CH_2CH_2OCH_3)Me)$]TFSA (92.5 mPa s at 20 °C).

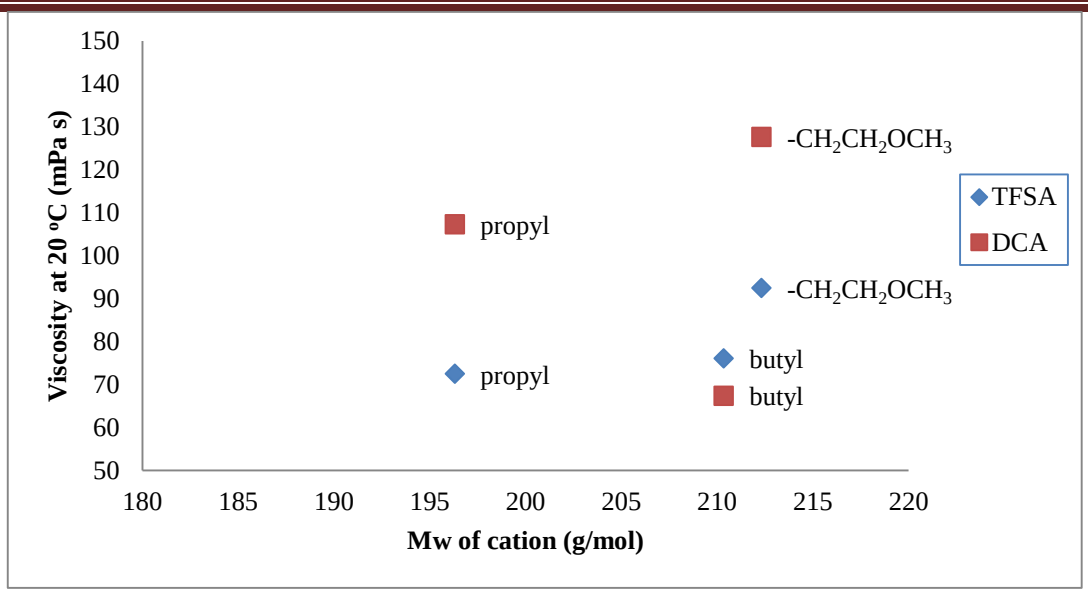

Figure 5.31–Viscosity (at 20 °C) *vs* molecular weight of $[C_3(NMe_2)_2(NRMe)]X$ (X = TFSA and DCA)

The amino acid ionic liquids (AAILs) $[E_4Ala]MeSO_4$ (η = 561.9 mPa s at 75 °C), $[E_4Ala]TFSA$ (η = 329 mPa s at 75 °C), $[E_4Pro]MeSO_4$ (η = 837.7 mPa s at 75 °C), $[E_4Pro]TFSA$ (η = 230.4 mPa s at 75 °C), $[E_4Val]TFSA$ (η = 574.2 mPa s at 75 °C), and $[E_4Thr]TFSA$ (η = 883.7 mPa s at 75 °C), have high viscosities relative to the other given in table 5.6. Their viscosities range from 200 to 890 mPa s at 75 °C. The viscosity of these AAILs was brought into the viscometer's range by increasing the temperature. High viscosities were observed due to the carboxylic acid and the mixture of IL/zwitterions, resulting from intermolecular hydrogen bonding. An attempt was not carried out to measure viscosities for the rest of the CILs due to their highly-viscous nature. The viscosity of $[E_4Ala]MeSO_4$ is 561.9 mPa s at 75 °C and $[E_4Pro]MeSO_4$ is 837.7 mPa s at 75 °C, due to the presence of methyl sulphate as anion showing relatively higher viscosities than the corresponding TFSA ones. With the increase in size of cation from $[E_4Ala]MeSO_4$ (268 g/ mol) to $[E_4Pro]MeSO_4$ (294 g/ mol), increase of viscosity from 561.9 mPa s to 837.7 mPa s at 75 °C is observed. The high chloride content in $[E_4Ala]MeSO_4$ (2.3%) and $[E_4Pro]MeSO_4$ (9.7%) is thought to be one of the other reasons for relatively high viscosities.

The viscosity of $[E_4Ala]MeSO_4$ (561.9 mPa s at 75 °C) is almost twice that of $[E_4Ala]TFSA$ (329 mPa s at 75 °C), while the viscosity of $[E_4Pro]MeSO_4$ (837.7 mPa s at 75 °C) is almost four times that of $[E_4Pro]TFSA$ (230.4 mPa s at 75 °C). The viscosity decreases with the increase in size of anion from methyl sulphate to TFSA, and the usual anion trend for increasing viscosity is $TFSA^-$

< $MeSO_4^-$. The TFSA anion may be more weakly associated with the cation because the negative charge is delocalized more widely over the two trifluoromethylsulfonyl groups than the corresponding methyl sulfate anion. With the increase in size of cation from [E_4Ala]TFSA (M_w = 268.37 g/mol and η = 329 mPa s at 75 °C), [E_4Pro]TFSA (M_w = 294.41 g/mol and η = 230.4 mPa s at 75 °C), [E_4Val]TFSA (M_w = 296.43 g/mol and η = 574.2 mPa s at 75 °C), and [E_4Thr]TFSA (M_w = 298.40 g/mol and η = 883.7 mPa s at 75 °C), the viscosity should increase. Except [E_4Pro]TFSA, the viscosity follows the regular increasing pattern. It was thought that the lack of –NH proton in [E_4Pro]TFSA is responsible for lowering the hydrogen-bond interactions and thus a low viscosity of 230.4 mPa s is observed at 75 °C.

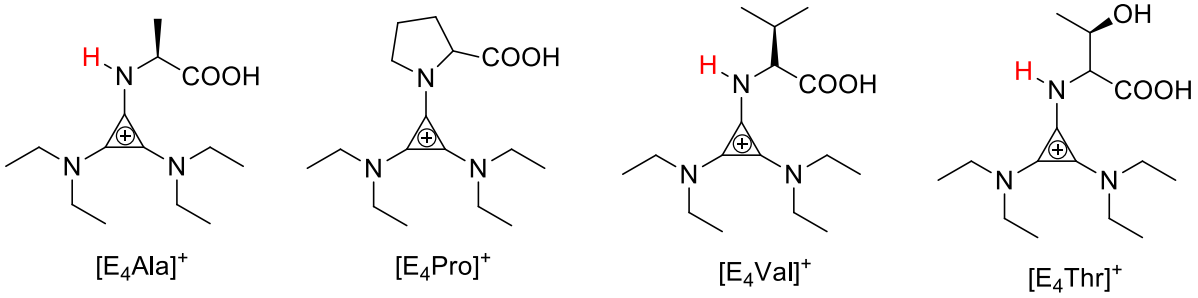

Figure 5.32-Structures of amino acid ionic liquids.

In contrast to tac-based AAILs (amino acid is anchored to cationic part); other classes, such as imidazolium, phosphonium and ammonium (amino acid in the anionic part) ionic liquids, the viscosities for tac-based AAILs range from 200 to 880 mPa s at 75 °C. In tac-based AAILs, hydrogen bonding is possible between the cation and the anion and/or between cations, which results in an increase in viscosities.

The viscosity of [emim][Gly] is 490 mPa s at 25 °C, which is the lowest reported for the 20 AAILs ([emim][amino acids]).[10] We can conclude that viscosities of our tac-based AAILs are higher in comparison to [emim][amino acids] because of IL/zwitterions mixtures which increase the hydrogen bond interactions. Another factor responsible for the increase in viscosity of our tac-based AAILs is the larger size as compared to [emim][amino acids]. Woo and coworkers have shown, with the help of a computational study, the existence of hydrogen bonding between counterions in [emim][amino acid] ILs.[23]

Table 5.8-Viscosities of other classes of ILs.

	Ionic Liquids	Viscosity at 25 °C (mPa s)[10]
1	[emim][Gly]	490
2	$[P_{4444}][Ala]$	340
3	$[P_{4444}][Val]$	420
4	$[P_{4444}][Pro]$	850
5	$[P_{4444}][Thr]$	970
6	$[P_{4441}][Ala]$	6930
7	$[P_{4448}][Ala]$	377
8	$[P_{44412}][Ala]$	619
9	$[P_{8888}][Ala]$	1620
10	$[P_{8888}][Val]$	1480
11	$[P_{8888}][Pro]$	670
12	$[P_{4443a}][Ala]$	758
13	$[P_{4443a}][Val]$	888
14	$[P_{4443a}][Pro]$	1772
15	$[N_{1111}][Ala]$	solid
16	$[N_{1111}][Val]$	solid
17	$[N_{2222}][Ala]$	81
18	$[N_{4444}][Val]$	660

In the case of phosphonium and ammonium-based AAILs, the hydrogen bonding interactions are usually only possible between anions and results in medium to higher viscosities (from 80 to 6900 mPa s at 25 °C).[10]

Now we will compare the viscosities of tac-based AAILs with another class of AAILs having amino acids as the cationic part, [Ala]X, [Pro]X, [Val]X and [Thr]X (X = NO_3^-, BF_4^-, PF_6^-, CF_3COO^-, SO_4^{2-}). The [Amino Acid]X, AAILs are usually solids with high melting points (78-186 °C) due to strong hydrogen bond interactions and smaller size compared to the delocalized electron charge density of the tac-cation. Because [Amino acid]X have high melting solids, no viscosity data was reported.[17]

For the C_{3h} cations $[C_3(NAllylMe_2)_3]$TFSA and $[C_3(NAllylMe_2)_3]$DCA, the viscosity is 76.1 mPa s and 146.1 mPa s, respectively, at 20 °C. The high viscosity observed in $[C_3(NAllylMe_2)_3]$DCA was thought to be due to π-π interactions between the cation's allyl chain and the DCA anion. With the DCA anion, lower viscosities are usually observed compared to the TFSA anion.

Now I will compare the D_{3h} cations already synthesized by Curnow group with my cations.[12] For $[C_3(NBu_2)_3]$FAP (M_w of anion = 445 g/mol, η = 391 mPa s), a higher viscosity at 20 °C is observed as compared to other small-sized anions: $[C_3(NBu_2)_3]$DCA (M_w of anion = 66 g/mol, η = 293 mPa s), $[C_3(NBu_2)_3]B(CN)_4$ (M_w of anion = 114 g/mol, η = 263 mPa s) and $[C_3(NBu_2)_3]$TFSA (M_w of anion = 280 g/mol, η = 230 mPa s). These ILs with less coordinating anions, $B(CN)_4$ and FAP, were synthesized to study the effect on viscosity. In comparison to imidazolium-based ILs, $[C_6mim]B(CN)_4$ (65 mPa s at 20 °C) and $[C_6mim]$FAP (74 mPa s at 20 °C), the viscosity of tac-based ILs are higher.[24] Possibly due to the large molecular weight of the cation in $[C_3(NBu_2)_3]^+$ (420 g mol^{-1}) as compared to $[C_6mim]^+$ (167 g mol^{-1}).

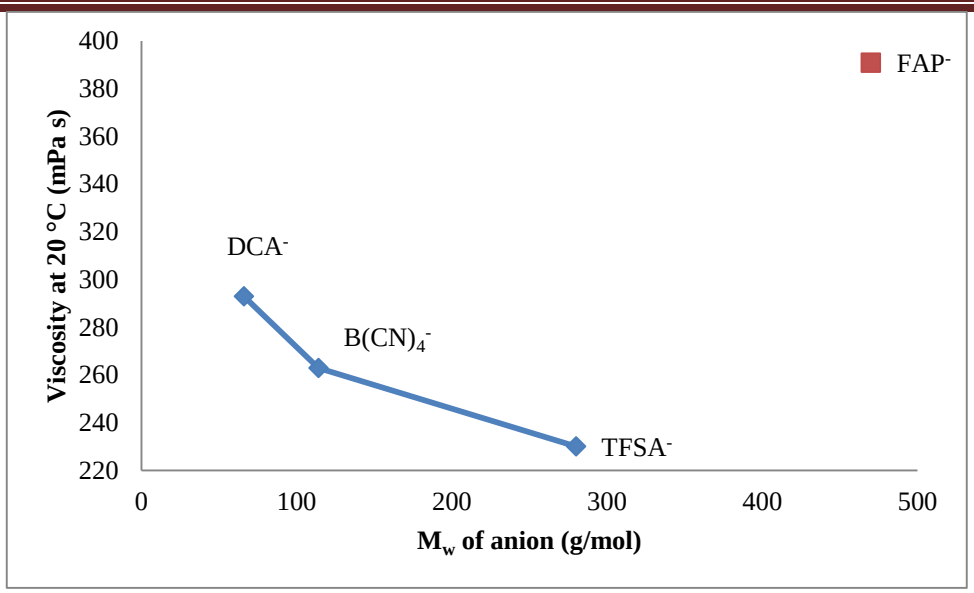

Figure 5.33–Viscosity (at 20 °C) *vs* molecular weight of anion for $[C_3(NBu_2)_3]^+$.

Now I will compare the viscosity of my tac-based ILs with imidazolium-type ionic liquids. The low viscosity obtained in the present work was 69 mPa s at 20 °C for $[C_3(NMe_2)_2(NMe(CH_2CHCH_2)]$TFSA ($M_w$ = 194 g/ mol). At 20 °C, a viscosity of 96 mPa s is observed for $[C_8mim]$TFSA (M_w = 195 g/ mol).[25] As the size of both the cations is similar, the viscosity of $[C_3(NMe_2)_2(NMe(CH_2CHCH_2)]$TFSA is less in comparison to a similarly-sized imidazolium IL. Thus, for comparable-sized cations, tac ILs have lower viscosities than imidazolium-type ILs due to less hydrogen bonding. But if we compare the viscosities of other classes having small sized cations (ammonium[21, 26], phosphonium[27] or guanidinium[20]) with the tac cation, the other classes reach lower viscosities.

A typical plot of viscosity of all the ILs versus temperature is shown in fig. 5.34.

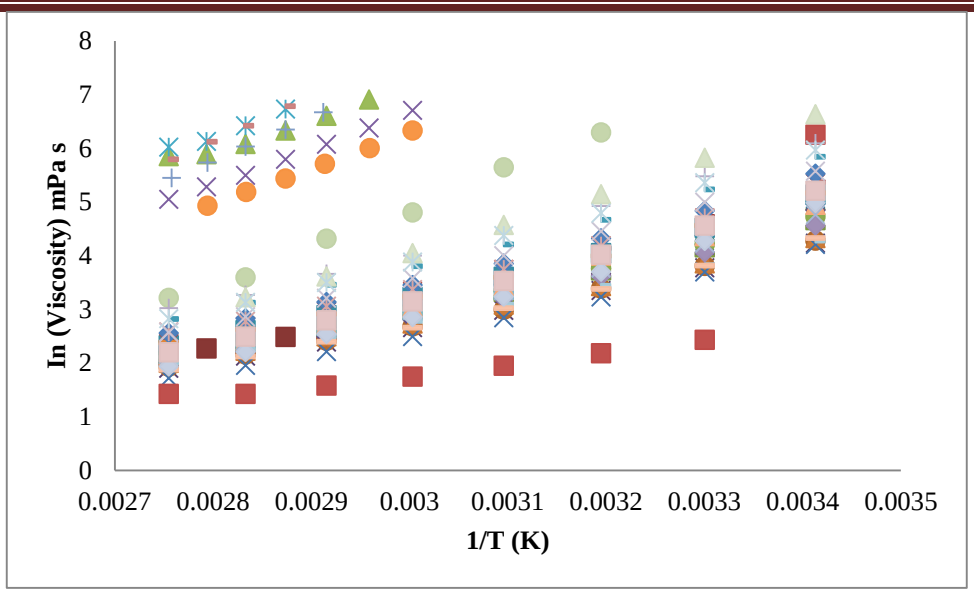

Figure 5.34– Arrhenius plot for temperature-dependent viscosity data for ILs.

The Arrhenius equation is;

$$\eta = A \exp\left[\frac{-E_a}{R\,T}\right]$$

Where η is viscosity, A is pre-exponential factor, E_a is activation energy, R is the universal gas constant and T is the temperature. The above equation can also be written as;

$$In(\eta) = In(A) + \frac{-E_a}{R}\left(\frac{1}{T}\right)$$

The values for A and E_a are calculated for all the ILs by using the above equation and is tabulated in table 5.8. The E_a for viscosity data ranged from 23 to 60 kJ/mol.

The viscosities of the ionic liquids decrease in a nonlinear fashion, as expected, with temperature. The viscosity of ILs often obeys Arrhenius behavior above room-temperature. But as the temperature of these ILs reaches glass transition temperature, it displays deviation from this behavior. [28]This gives rise to non-Arrhenius behavior in the low temperature region, which is consistent with glass forming liquids.[28] This glass transition temperature is associated with an extraordinary slowdown of the relaxation and transport mechanisms.

The η of a liquid follows Vogel-Fulcher-Tammann (VFT) law on lowering of temperature.[29] The VFT parameters are found by a least square fitting and show that VFT is more accurate that Arrhenius. The VFT equation is;

$$\eta = \eta_0 \exp\left[\frac{B}{T - T_o}\right]$$

Where, η_o (mPa s), B (K), and T_o (K) are best fitting parameters. Where $D = B/T_o$ and D is the fragility of the liquid. A D value of less than 10 means the liquid is fragile, while a D value nearer to 100 means the liquid is strong. Thus, all the triaminocyclopropenium ILs are fragile liquids. In the Arrhenius equation, the ideal glass transition state occurs at 0 K, while for the VFT equation, this occurs at T_o.[30] If B is replaced by the product DT_o the above equation;[31]

$$\eta = \eta_0 \exp\left[\frac{DT_o}{T - T_o}\right]$$

The value of D denotes fragility and quantify the deviation from Arrhenius behavior.

The standard deviation is calculated by using the following formula;

$$S.D. = \sqrt{\frac{1}{N}\frac{\sum_{i=1}^{N}(x_{observed} - x_{calculated})^2}{}}$$

The Arrhenius equation gives a higher standard deviation than the VFT equation, as seen from table 5.9.

Table 5.9-Arrhenius and VFT fitting parameters for viscosity data for ILs

	C_s Cations	η_o (mPa s)	B (K)	T_o (K)	D	*S.D. (mPa s)	$A \times 10^{-3}$ (mPa s)	E_a (kJ/mol)	*S.D. (mPa s)
1	$[C_3(NMe_2)_2(NEtH)]$TFSA	0.121	779	183	4.3	0.3	0.089	35	6.3
2	$[C_3(NMe_2)_2(NEtMe]$TFSA	0.162	777	168	4.6	0.06	3.61	23	0.09
3	$[C_3(NMe_2)_2(HN(CH_2CHCH_2))]$TFSA	0.096	841	179	4.7	0.2	0.073	35	6.4
4	$[C_3(NMe_2)_2(N(CH_2CHCH_2)Me)]$TFSA	0.082	883	162	5.5	0.2	0.362	29	1.9
5	$[C_3(NMe_2)_2(N(CH_2CH_2CH_3)H)]$TFSA	0.082	892	175	5.1	0.3	0.073	35	6.4
6	$[C_3(NMe_2)_2(N(CH_2CH_2CH_3)Me)]$TFSA	0.119	772	173	4.5	0.3	0.349	30	2.3
7	$[C_3(NMe_2)_2(N(CH_2CH_2CH_3)Me)]$DCA	0.185	642	192	3.3	0.4	0.140	33	4.7
8	$[C_3(NMe_2)_2(N(CH_2CH_2OCH_3)H)]$TFSA	0.129	745	193	3.9	1.2	0.028	38	11.2
9	$[C_3(NMe_2)_2(N(CH_2CH_2OCH_3)Me)]$TFSA	0.065	964	160	6.0	0.2	0.213	31	2.8
10	$[C_3(NMe_2)_2(N(CH_2CH_2OCH_3)Me)]$DCA	0.172	596	203	2.9	0.7	0.038	36	7.1
11	$[C_3(NMe_2)_2(NBuH)]$TFSA	0.106	848	178	4.8	0.9	0.085	35	7.6
12	$[C_3(NMe_2)_2(NBuMe)]$TFSA	0.118	805	169	4.8	0.2	0.426	29	2.4
13	$[C_3(NMe_2)_2(NBuMe)]$DCA	0.102	728	181	4.0	0.3	0.155	31	2.5
14	$[C_3(NMe_2)_2(NPeH)]$TFSA	0.045	1100	162	6.8	0.3	0.05	37	7.4

15	$[C_3(NMe_2)_2(NPeMe)]TFSA$	0.076	965	161	5.9	0.3	0.220	32	3.6
16	$[C_3(NMe_2)_2(NHexMe)]TFSA$	0.115	814	171	4.7	0.1	0.283	31	3.3
17	$[C_3(NEt_2)_2(NHBu)]MeSO_4$	0.083	1030	169	6.1	1.4	0.054	38	13.6
18	$[C_3(NEt_2)_2(NHBu)]TFSA$	0.246	625	198	3.2	0.9	0.092	35	9.4
19	$[C_3(NEt_2)_2(NHBu)]DCA$	0.227	672	197	3.4	1.3	0.055	37	14.6
20	$[C_3(NEt_2)_2(NHBu)]BF_4$	0.029	1342	156	8.6	2.2	0.017	42	17.7
	C_{2v} Cations								
21	$[C_3(NMe_2)_2(NEt_2)]TFSA$	0.047	1157	139	8.33	0.1	0.962	27	0.2
22	$[C_3(NMe_2)_2(N(CH_2CHCH_2)_2)]TFSA$	0.039	1182	140	8.4	0.5	0.197	32	2.66
22	$[C_3(NMe_2)_2(NPr_2)]TFSA$	0.174	662	194	3.4	0.1	0.504	29	0.5
24	$[C_3(NMe_2)_2(N(CH_2CH_2OCH_3)_2)]TFSA$	0.093	819	182	4.5	2.2	0.059	36	4.1
25	$[C_3(NMe_2)_2(NBu_2)]TFSA$	0.168	684	190	3.6	0.4	0.150	33	4.1
26	$[C_3(NMe_2)_2(NHex_2)]TFSA$	0.963	337	234	1.4	0.3	0.257	32	4.5
27	$[C_3(NEt_2)_2(NHex_2)]I$	0.0003	2557	136	18.9	13.5	0.058×10^{-3}	60	10.6
28	$[C_3(NEt_2)_2(NHex_2)]OTf$	0.076	1104	165	6.7	2.3	0.044	39	16.5
	C_{3h} Cations								
29	$[C_3(NEtMe_2)_3]TFSA$	0.057	1076	142	7.6	0.2	0.559	29	1.8
30	$[C_3(NAllylMe_2)_3]TFSA$	0.084	849	168	5.1	0.3	0.233	31	2.6
31	$[C_3(NAllylMe)_3]DCA$	0.154	608	204	2.9	0.6	0.028	38	9.4
32	$[C_3(NMeCH_2CH_2OCH_3)_3]TFSA$	0.09	793	188	4.2	0.3	0.031	45	9.2
	D_{3h} Cations								

33	$[C_3(NEt_2)_3][MeC_6H_4SO_3]$	0.051	1047	184	5.7	1.2	0.0014	49	35.8
34	$[C_3(NBu_2)_3]B(CN)_4$	0.023	1373	146	9.4	0.9	0.041	38	7.5
35	$[C_3(NBu_2)_3]FAP$	0.013	1650	133	12.7	1.8	0.030	40	10.8

*Standad Deviation=S.D.

T_g is always greater than T_o because the sample freezes before the thermodynamic equilibrium is reached for the ideal glass transition state. The D value of the viscosity data for tac-based ILs ranged from 0.1 to 23 and T_o range from 131 to 307 K.

5.5 Fragility

Fragility is an important liquid-state property that measures the thermal sensitivity of a liquid. 'Strong' liquids have directional bonds compared to 'fragile' liquids. In 'fragile' liquids there is a large increase in heat capacity at T_g.[32] The fragile liquids have a glassy structure which collapses under temperature variations, while strong liquids show resistance to temperature variations.[33]

A fragility plot was made for samples where viscosity and calorimetric glass transition temperatures were obtained. The viscosity data is scaled in an Arrhenius plot using the calorimetric glass transition temperature, T_g, to scale the temperature. The T_o was not used due to unreliable results obtained from the VFT equation (from viscosity, ionic conductivity and molar conductivity data). The diagonal line on the fragility plot represents the strong behavior. The SiO_2 have directional bonds and shows string behavior.

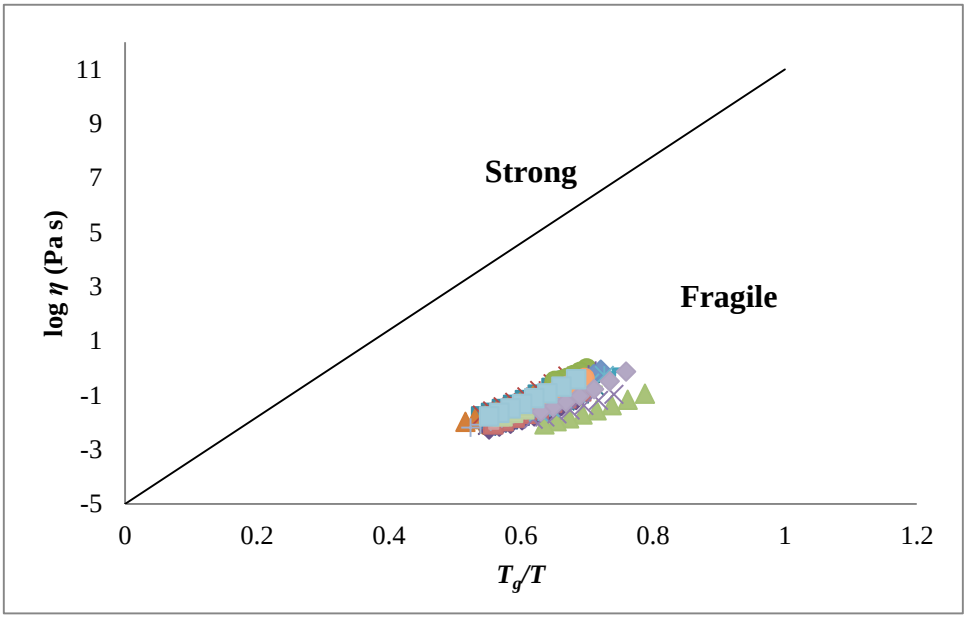

Figure 5.35-T_g scaled of Arrhenius plot for viscosity data.

From the fragility plot, it is seen that all the triaminocyclopropenium-type ILs show fragile behavior and all occur in the similar region. These results are similar to tac-type ILs previously synthesized by Curnow group.[12]

5.6 Conductivity

The measurement of conductivity is extensively used in many industries and is a good indicator of the presence or absence of conductive ions. The conductivity (σ) is related to the ion mobility and the number of charge carriers. It is expressed by the following equation;

$$\sigma = \sum n_i q_i \, u_i$$

where n_i, q_i and u_i are the number of charge carriers, the charge of each species, and the mobility of each species, respectively.[34] Ionic liquids are conductive because they are composed of cations and anions.

The ionic conductivity measurements of ILs were carried out using a Schott LF4100+ probe conductivity meter with a cell constant of 1 cm^{-1} under an inert N_2 atmosphere in the range of 20 to 90 °C. The sample (1.5 to 2 mL) was placed in a cell with a circulating water jacket for temperature regulation. The values were recorded at 10 °C intervals.

The conductivity (σ) of the IL can be obtained using the following equation;

$$\sigma = \frac{l}{AR}$$

Where l is the distance between the two electrodes in a cell, A is the area of the electrodes, and R is the resistance, while, $\frac{l}{A}$ is referred to as a cell constant and is determined by measuring the conductivity of dilute aqueous KCl solution.[28]

The conductivity of synthesized triaminocyclopropenium salts is comparable to the traditional ionic liquids and non-aqueous solvents. A less viscous sample gives a high conductivity. The conductivity in the present thesis ranged from 0.0137 mS cm^{-1} at 20 °C for $[C_3(NEt_2)_2(NHex_2)]I$ to 4.38 mS cm^{-1} at 20 °C for $[C_3(NMe_2)_2(NMeBu)]DCA$. The large ions have lower conductivity compared to small ions due to the difficulty in their mobility. The tendency to form ion pair or

aggregate lowers the conductivity as well, which is explained later with the discussions on ionicity.

Table 5.10-Conductivities of ILs in mS cm^{-1}

	***C_s* Cations**	**20 °C**	**30 °C**	**40 °C**	**50 °C**	**60 °C**	**70 °C**	**80 °C**	**90 °C**
1	$[C_3(NMe_2)_2(NEtH)]$TFSA	1.37	2.29	3.59	5.22	7.17	9.46	12.07	14.99
2	$[C_3(NMe_2)_2(HN(CH_2CHCH_2))]$TFSA	1.20	2.02	3.18	4.64	6.42	8.51	10.91	13.52
3	$[C_3(NMe_2)_2(N(CH_2CHCH_2)Me)]$TFSA	2.96	4.47	6.49	8.83	11.52	14.54	17.84	21.80
4	$[C_3(NMe_2)_2(N(CH_2CHCH_2)Me)]$DCA	4.10	6.85	10.54	15.37	21.0	27.4	34.5	42.1
5	$[C_3(NMe_2)_2(N(CH_2CH_2CH_3)H)]$TFSA	1.08	1.85	2.88	4.22	5.90	7.92	10.20	12.80
6	$[C_3(NMe_2)_2(N(CH_2CH_2CH_3)Me)]$TFSA	2.71	4.17	6.07	8.30	10.83	13.76	16.95	20.6
7	$[C_3(NMe_2)_2(N(CH_2CH_2CH_3)Me)]$DCA	3.17	5.42	8.44	12.38	16.90	22.50	28.30	35.0
8	$[C_3(NMe_2)_2(N(CH_2CH_2OCH_3)H)]$TFSA	0.813	1.46	2.45	3.71	5.28	7.17	9.35	11.83
9	$[C_3(NMe_2)_2(N(CH_2CH_2OCH_3)Me)]$TFSA	1.98	3.20	4.74	6.73	8.98	11.50	14.41	17.45
10	$[C_3(NMe_2)_2(N(CH_2CH_2OCH_3)Me)]$DCA	2.42	4.33	6.96	10.47	14.57	19.32	25.00	31.00
11	$[C_3(NMe_2)_2(NBuH)]$TFSA	0.89	1.56	2.48	3.69	5.15	6.93	8.96	11.32
12	$[C_3(NMe_2)_2(NBuMe)]$TFSA	2.36	3.61	5.23	7.23	9.46	12.01	14.85	17.94
13	$[C_3(NMe_2)_2(NBuMe)]$DCA	4.38	7.13	10.69	15.09	20.5	26.3	32.7	39.6
14	$[C_3(NMe_2)_2(NPeH)]$TFSA	0.64	1.10	1.76	2.65	3.77	5.16	6.77	8.50
15	$[C_3(NMe_2)_2(NHexMe)]$TFSA	1.31	2.17	3.34	4.83	6.63	8.73	11.09	13.74
16	$[C_3(NEt_2)_2(NHBu)]$TFSA	0.69	1.14	1.75	2.55	3.52	4.70	6.07	7.64
17	$[C_3(NEt_2)_2(NHBu)]$DCA	1.28	2.16	3.43	5.13	7.30	9.98	13.20	16.97

18	$[C_3(NEt_2)_2(NHBu)]BF_4$	0.318	0.595	1.02	1.66	2.54	3.66	5.10	6.82
	***C_{2v}*Cations**								
19	$[C_3(NMe_2)_2(NEt_2)]$TFSA	---	---	---	5.15	7.13	9.43	12.21	15.40
20	$[C_3(NMe_2)_2(N(CH_2CHCH_2)_2)]$TFSA	2.07	3.26	4.80	6.67	8.85	11.30	14.07	17.06
21	$[C_3(NMe_2)_2(NPr_2)]$TFSA	---	---	3.44	5.09	7.01	9.20	11.64	14.53
22	$[C_3(NMe_2)_2(N(CH_2CH_2OCH_3)_2)]$TFSA	1.06	1.83	2.88	4.21	5.82	7.7	9.87	12.28
23	$[C_3(NMe_2)_2(NBu_2)]$TFSA	1.23	2.03	3.12	4.50	6.16	8.10	10.29	12.80
24	$[C_3(NMe_2)_2(NHex_2)]$TFSA	0.29	0.53	0.89	1.41	2.12	3.03	4.15	5.52
25	$[C_3(NEt_2)_2(NHex_2)]$I	0.0137	0.0386	0.0948	0.206	0.396	0.711	1.192	1.885
26	$[C_3(NEt_2)_2(NHex_2)]$OTf	0.0936	0.186	0.344	0.586	0.946	1.44	2.09	2.95
	***C_{3h}* Cations**								
27	$[C_3(NEtMe_2)_3]$TFSA	2.42	3.62	5.19	7.05	9.18	11.57	14.26	17.19
28	$[C_3(NAllylMe_2)_3]$TFSA	1.83	2.87	4.25	5.99	7.99	10.24	12.77	15.54
29	$[C_3(NAllylMe)_3]$DCA	2.21	3.83	6.14	9.17	12.81	16.97	22.0	27.4
30	$[C_3(NMeCH_2CH_2OCH_3)_3]$TFSA	0.703	1.26	2.12	3.21	4.55	6.15	7.96	10.11
	***D_{3h}* Cations**								
31	$[C_3(NEt_2)_3][MeC_6H_4SO_3]$	0.089	0.217	0.446	0.828	1.394	2.180	3.220	4.51
32	$[C_3(NBu_2)_3]B(CN)_4$	0.423	0.746	1.227	1.881	2.72	3.77	5.02	6.46
33	$[C_3(NBu_2)_3]$FAP	0.145	0.278	0.493	0.809	1.256	1.85	2.59	3.54

For the protic C_s cations $[C_3(NMe_2)_2(NRH)]TFSA$, the conductivity decreases with the increase in size of alkyl chain length for R = ethyl, allyl, propyl, butyl, $-CH_2CH_2OCH_3$ and pentyl. With an increase in the size of the cation, the mobility is lowered and thus conductivity decreases. Interestingly, the conductivity for $[C_3(NEt_2)_2(NBuH)]TFSA$ (M_w cation = 252.42 g/mol, σ = 0.69 mS cm^{-1} at 20 °C) is lower than $[C_3(NMe_2)_2(NBuH)]TFSA$ (M_w cation = 196.31 g/mol, σ = 0.89 mS cm^{-1} at 20 °C). This is due to the smaller size of the latter cation.

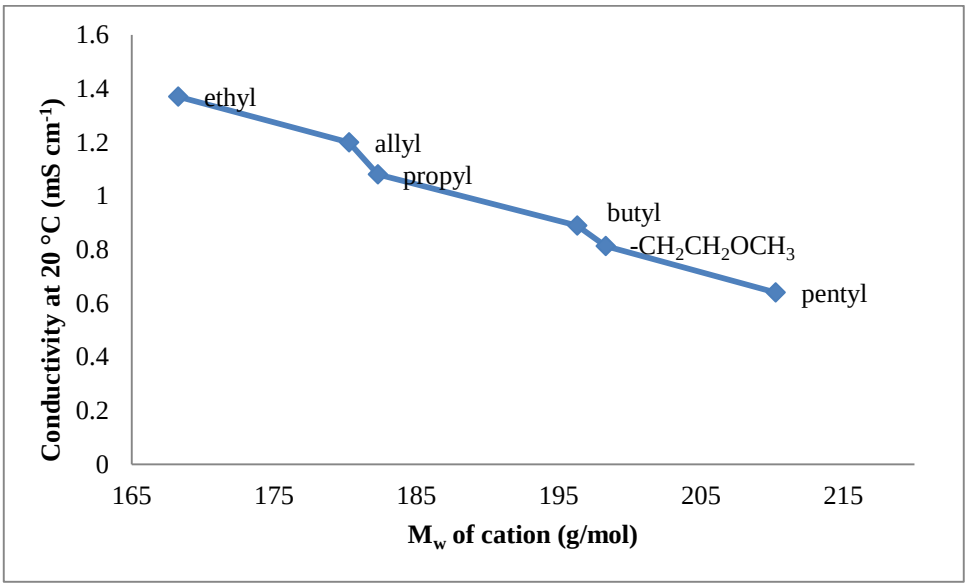

Figure 5.36–Conductivity (at 20 °C) *vs* molecular weight for protic $[C_3(NMe_2)_2(NRH)]TFSA$ cations.

Similarly, in case of the aprotic C_s cation series $[C_3(NMe_2)_2(NRMe)]TFSA$, for R = allyl, propyl, $-CH_2CH_2OCH_3$, butyl and hexyl, the conductivity decreases with the increasing size of the alkyl chain. Interestingly conductivities observed for ILs with DCA anions were higher than the TFSA ones due to the greater mobility of the smaller DCA anion. Apart from $[C_3(NMe_2)_2(NMeBu)]DCA$ (M_w cation =210.34 g/mol, σ = 4.38 mS cm^{-1} at 20 °C), the conductivities for $[C_3(NMe_2)_2(NMe(CH_2CHCH_2))]DCA$ (M_w cation =194.30 g/mol, σ = 4.1 mS cm^{-1} at 20 °C), $[C_3(NMe_2)_2(NMe(CH_2CH_2CH_3))]DCA$ (M_w cation =196.31 g/mol, σ = 3.17 mS cm^{-1} at 20 °C) and $[C_3(NMe_2)_2(NMe(CH_2CH_2OCH_3))]DCA$ (M_w cation =212.31 g/mol, σ = 2.42 mS cm^{-1} at 20 °C) decrease with increasing size of the cation. The highest conductivity observed in this work is 4.38 mS/cm for $[C_3(NMe_2)_2(NMeBu)]DCA$ at 20 °C. The small size of the DCA

anion and low viscosity (67.4 mPa s at 20 °C) makes the ion mobility facile and results in the high conductivity.

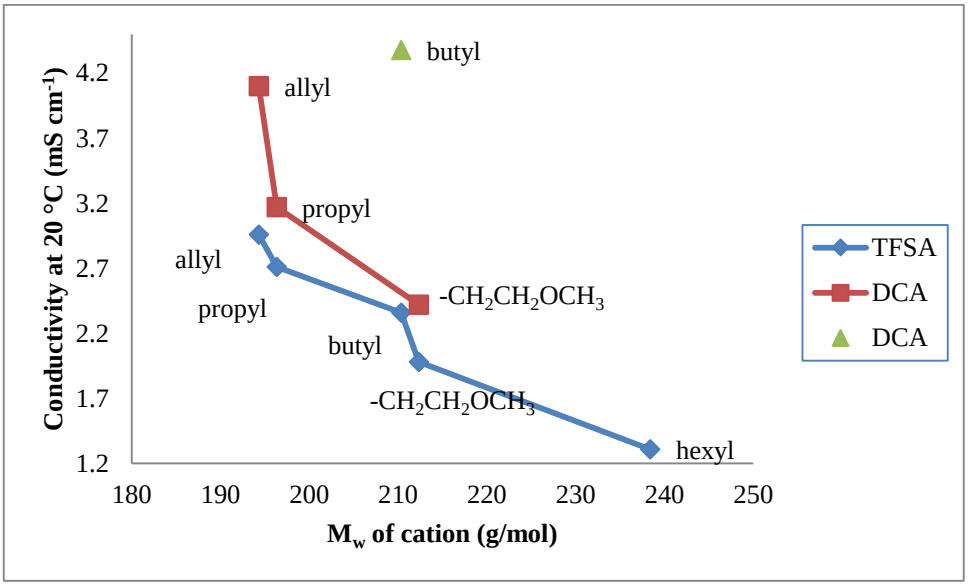

Figure 5.37–Conductivity (at 20 °C) *vs* molecular weight of C_s cations, [$C_3(NMe_2)_2(NMeR)$]X (X = TFSA and DCA).

Among the C_{2v} cation series [$C_3(NMe_2)_2(NR_2)$]TFSA, the conductivity decreases with the increasing size of the cation, R = ethyl > propyl > butyl > -$CH_2CH_2OCH_3$ > hexyl. However, the allyl chain being unsaturated increasing size the conductivity to 6.67 mS cm^{-1} at 50 °C for [$C_3(NMe_2)_2(N(CH_2CHCH_2)_2)$]TFSA, which is the maximum conductivity observed among [$C_3(NMe_2)_2(NR_2)$]TFSA.

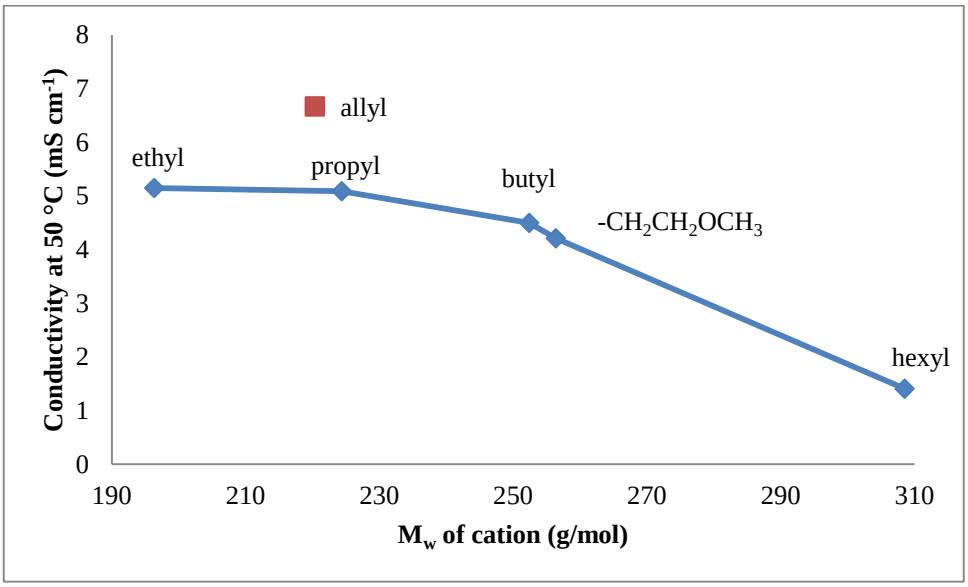

Figure 5.38–Conductivity (at 50 °C) *vs* molecular weight of cation [$C_3(NMe_2)_2NR_2$]TFSA.

The conductivity of the C_{3h} cation series [$C_3(NMeR)_3$]TFSA, decreases with an increasing size of the cation R = ethyl > allyl > -$CH_2CH_2OCH_3$. Again, the conductivity for [$C_3(NMeAllyl)_3$]DCA was higher than [$C_3(NMeAllyl)_3$]TFSA.

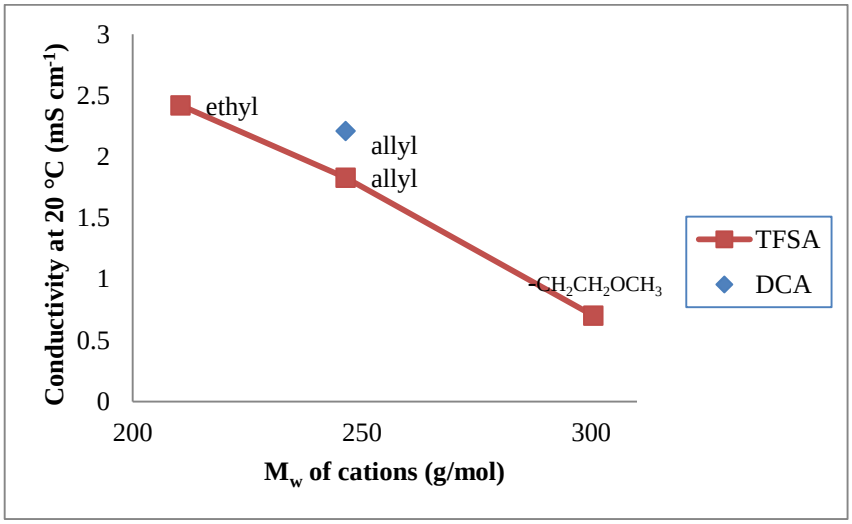

Figure 5.39– Conductivity (at 20 °C) *vs* molecular weight for the C_{3h} cation series [$C_3(NMeR)_3$]X (X = TFSA and DCA).

The anion size is also responsible for the variation of conductivity. With an increase in the size of the anion, the conductivity decreases due to lowered mobility. As the size of anion increases among the C_s cation series [$C_3(NEt_2)_2(NBuH]^+$ from DCA (M_w = 66 g/mol, σ = 1.28 at 20 °C) to BF_4 (M_w = 86 g/mol, σ = 0.318 at 20 °C) to TFSA (M_w = 280 g/mol, σ = 0.69 at 20 °C), the conductivity should decrease. However, [$C_3(NEt_2)_2(NBuH]BF_4$ shows lower conductivity than [$C_3(NEt_2)_2(NBuH]$TFSA and does not follow the decreasing conductivity pattern with increasing size of anion. This may be due to strong hydrogen bonding between NH-F in [$C_3(NEt_2)_2(NBuH]BF_4$.

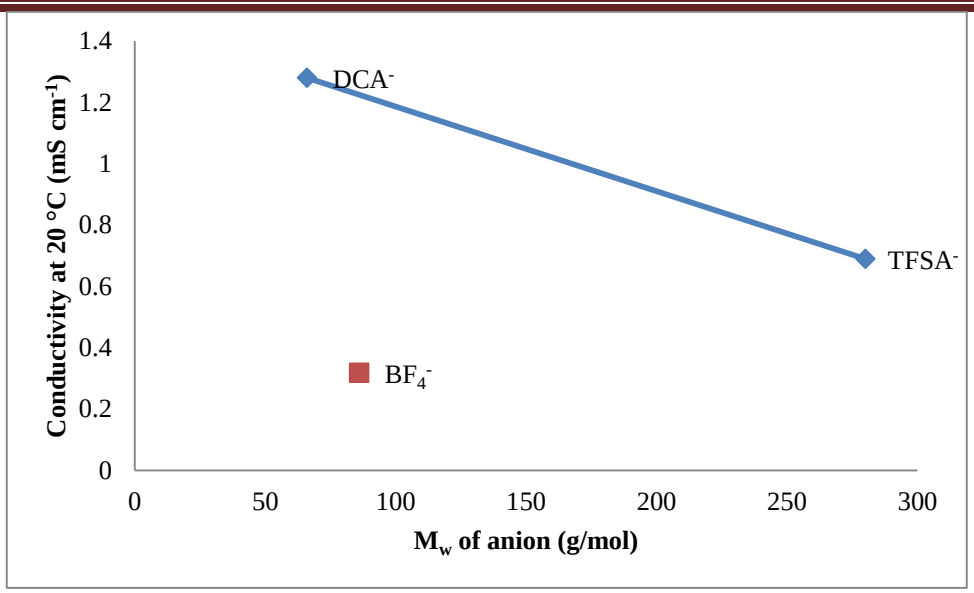

Figure 5.40–Conductivity (at 20 °C) *vs* molecular weight of cation $[C_3(NEt_2)_2(NBuH)]X$ (X = DCA, BF_4 and TFSA).

On comparison of identical cations, as the size of anion increases from $[C_3(NEt_2)_2(NHex_2)]DCA$[12], $[C_3(NEt_2)_2(NHex_2)]I$ and $[C_3(NEt_2)_2(NHex_2)]OTf$, the conductivity varies 1.03, 0.0137 and 0.0936 mS cm^{-1} at 20 °C, respectively. The iodide ion forms strong van der Waals interactions with the hexyl chain on the cation in $[C_3(NEt_2)_2(NHex_2)]I$ and results in lower conductivity than $[C_3(NEt_2)_2(NHex_2)]OTf$.

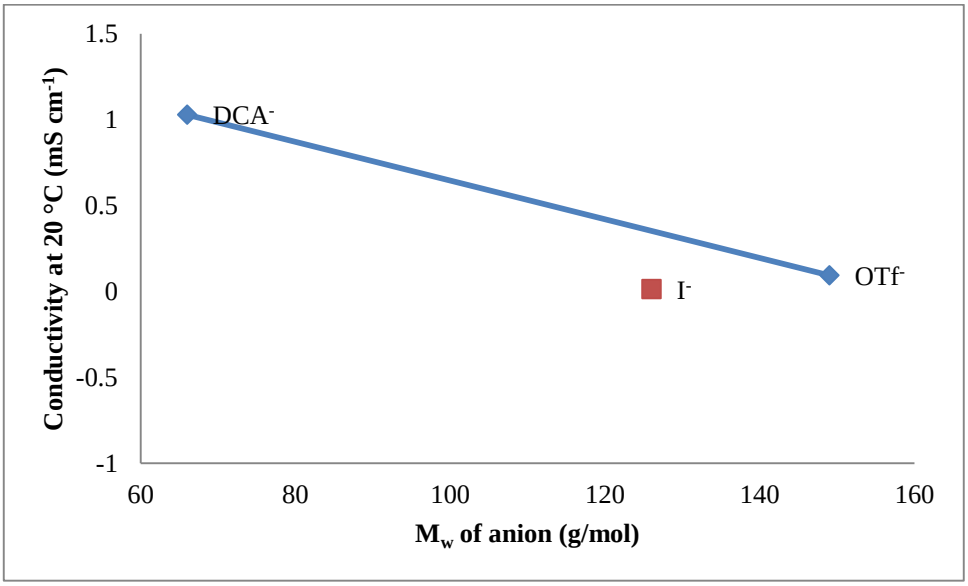

Figure 5.41–Conductivity data (at 20 °C) *vs* molecular weight of cation $[C_3(NEt_2)_2(NHex_2)]X$ (X = DCA, I and OTf).

Now I will compare my D_{3h} cation ILs with those already synthesized by the Curnow group.[12] For the $[C_3(NBu_2)_3]^+$ ILs, conductivity decreases with an increase in size of the anion: DCA (M_w = 66 g/mol)[12] > $B(CN)_4$ (M_w = 114 g/mol) > > FAP (M_w = 445 g/mol). Conductivities ranged from 0.423 mS/cm to 0.089 mS/cm at 20 °C. However, for $[C_3(NBu_2)_3]$TFSA (M_w of anion = 280 g/mol) higher conductivity, 0.428 mS cm^{-1} at 20 °C is observed than $[C_3(NBu_2)_3]B(CN)_4$ (0.423 mS cm^{-1} at 20 °C).

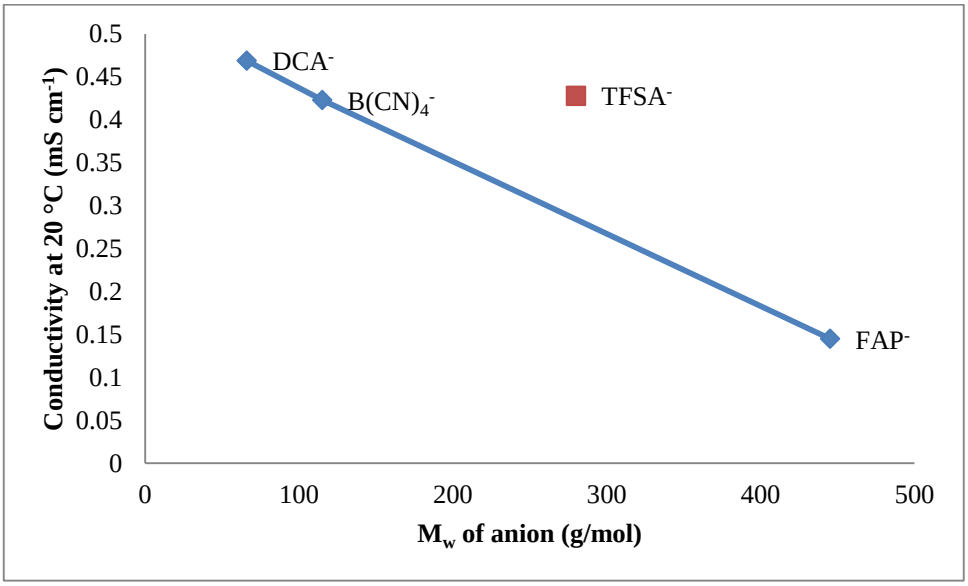

Figure 5.42–Conductivity (at 20 °C) *vs* molecular weight for D_{3h} cations, $[C_3(NBu_2)_3]X$ (X = DCA, $B(CN)_4$, TFSA and FAP).

For the $[C_3(NEt_2)_3]^+$ cation series, the anion trend for increasing molecular weight is DCA^- > $TFSA^-$, $[C_3(NEt_2)_3]$OTs (0.089 mS cm^{-1} at 20 °C) is less conductive than $[C_3(NEt_2)_3]$TFSA(1.387 mS cm^{-1} at 20 °C) and fails to follow the regular trend.

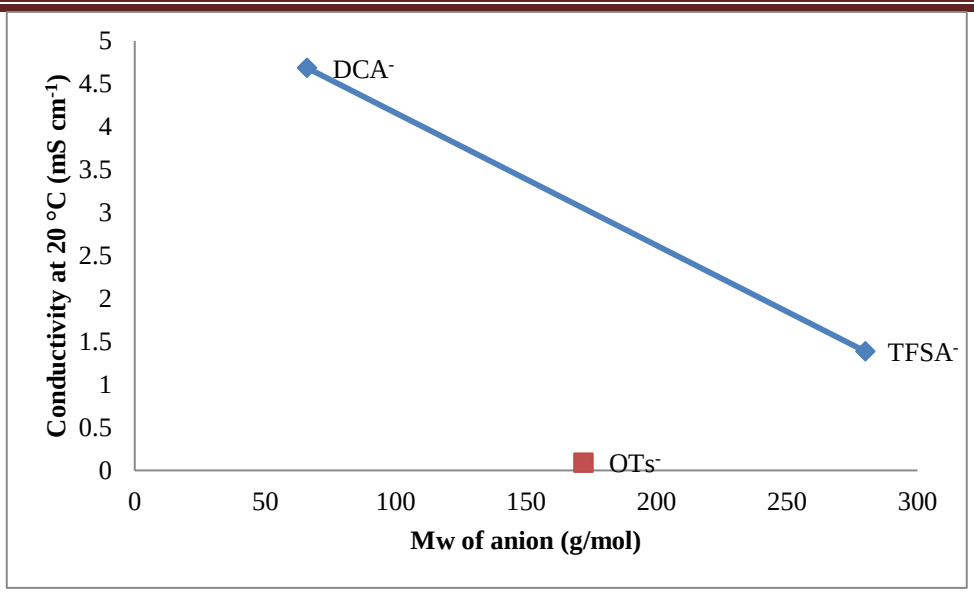

Figure 5.43–Conductivity data (at 20 °C) *vs* molecular weight of cation [$C_3(NEt_2)_3$]X (X = DCA, OTs and TFSA).

The conductivity for [$C_3(NMe_2)(NMe(CH_2CHCH_2)$]TFSA is 2.96 mS cm^{-1} at 20 °C. This is the highest conductivity obtained using TFSA as the anion in the present study. This is significantly larger than [C_8mim]TFSA (195 g/mol) for which the conductivity is 1.9 mS cm^{-1}, although the cation size are very similar.[25] Thus, we can say that our triaminocyclopropeniums have conductivities much higher than similarly-sized imidazolium-type ILs due to less hydrogen bonding.

Fig.5.44 illustrates the temperature dependency of conductivity for [$C_3(NMe_2)_2NH(CH_2CHCH_2)$]TFSA from 20 to 90 °C. An increase in temperature results in an increase of mobility via a reduction in the viscosity.

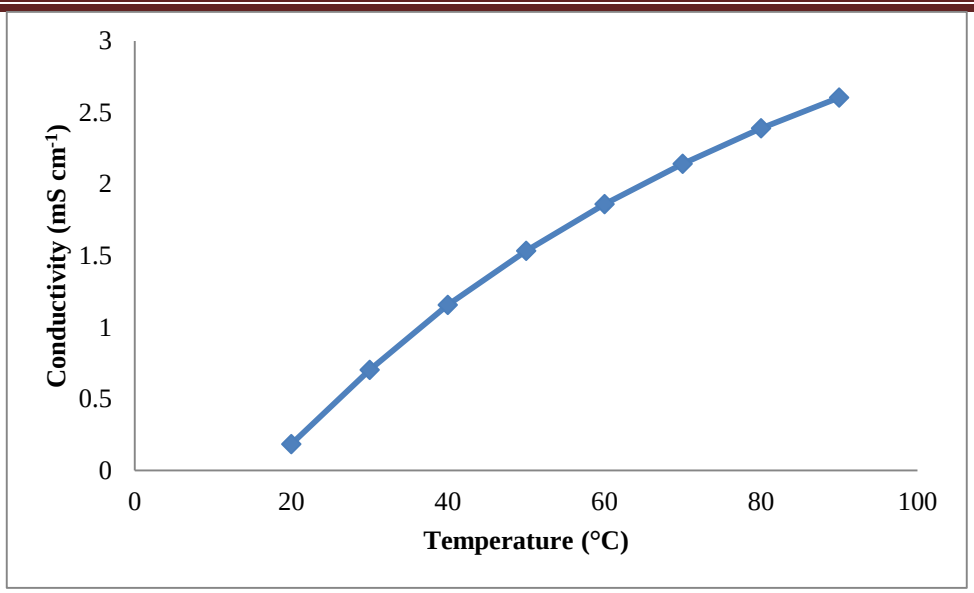

Figure 5.44-Temperature dependencies of conductivity for [C3(NMe2)2NH(CH2CHCH2)]TFSA.

The Arrhenius equation is;

$$\sigma = A \exp\left[\frac{-E_a}{R\,T}\right]$$

Where σ is conductivity, A is pre-exponential factor, E_a is activation energy, R is the Universal gas constant and T is the temperature. The above equation can also be written as;

$$In(\sigma) = In(A) + \frac{-E_a}{R}\left(\frac{1}{T}\right)$$

The values for A and E_a were calculated for all the ILs. The E_a values for conductivity have a good correlation with viscosity values and range from 25 to 62 kJ/mol. The Arrhenius activation energy is lower for conductivity compared to viscosity .[31]

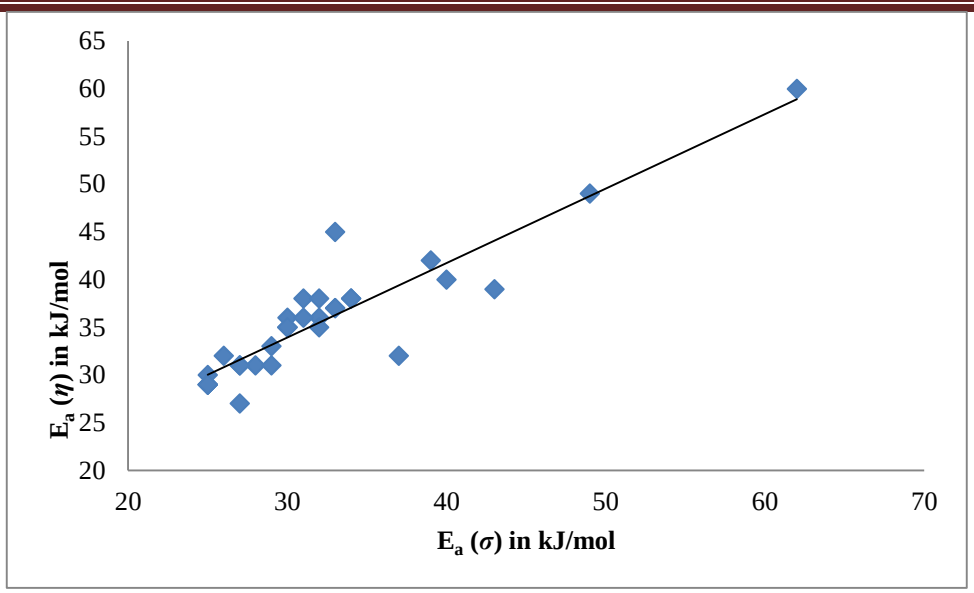

Figure 5.45–Correlation between E_a for conductivity versus viscosity.

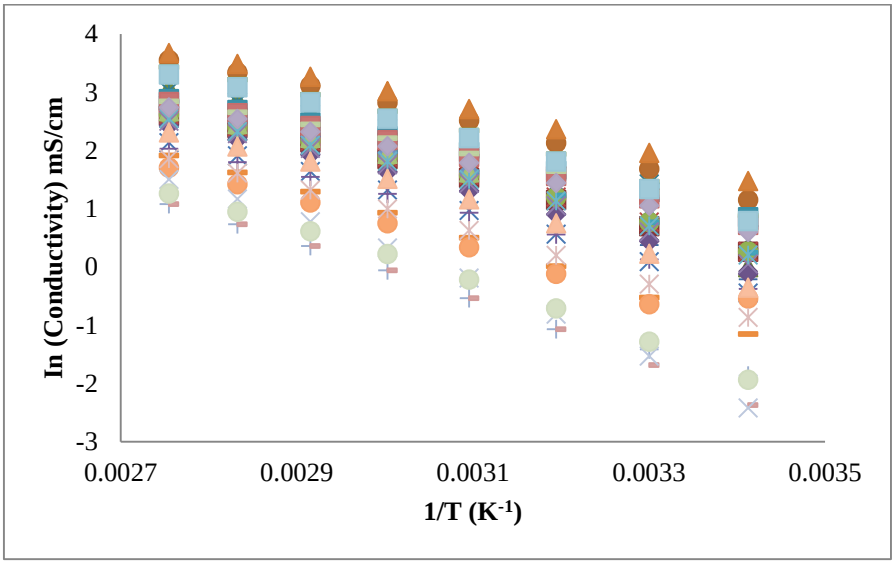

Figure 5.46–Arrhenius plot for temperature-dependent conductivity data for ILs.

As with the viscosity data, ILs deviate from Arrhenius-like behavior for the conductivity data by giving a higher standard deviation than is found using the VFT equation (table 5.11).

Table 5.11-Arrhenius And VFT fitting parameters for conductivity data for ILs

	C_s Cations	**σ_o (mS cm^{-1})**	**B (K)**	**T_o (K)**	**D**	***S.D. (mS cm^{-1})**	**$A \times 10^5$ (mS cm^{-1})**	**E_a (kJ/mol)**	***S.D. (mS cm^{-1})**
1	$[C_3(NMe_2)_2(NEtH)]TFSA$	497	603	191	3.2	0.01	3.4	30	0.6
2	$[C_3(NMe_2)_2(HN(CH_2CHCH_2))]TFSA$	887	806	170	4.7	0.1	2.9	30	0.5
3	$[C_3(NMe_2)_2(N(CH_2CHCH_2)Me)]TFSA$	557	597	179	3.3	0.1	0.9	25	0.6
4	$[C_3(NMe_2)_2(N(CH_2CHCH_2)Me)]DCA$	1038	530	197	2.7	0.1	7.6	29	2.0
5	$[C_3(NMe_2)_2(N(CH_2CH_2CH_3)H)]TFSA$	596	686	184	3.7	0.01	4.0	31	0.5
6	$[C_3(NMe_2)_2(N(CH_2CH_2CH_3)Me)]TFSA$	485	568	184	3.1	0.05	0.9	25	0.7
7	$[C_3(NMe_2)_2(N(CH_2CH_2CH_3)Me)]DCA$	925	541	198	2.7	0.1	8.3	30	1.7
8	$[C_3(NMe_2)_2(N(CH_2CH_2OCH_3)H)]TFSA$	441	594	199	2.9	0.01	8.9	34	0.6
9	$[C_3(NMe_2)_2(N(CH_2CH_2OCH_3)Me)]TFSA$	402	535	192	2.8	0.03	1.6	27	0.7
10	$[C_3(NMe_2)_2(N(CH_2CH_2OCH_3)Me)]DCA$	816	522	203	2.6	0.1	13.5	32	1.6
11	$[C_3(NMe_2)_2(NBuH)]TFSA$	452	634	191	3.3	0.02	4.7	32	0.5
12	$[C_3(NMe_2)_2(NBuMe)]TFSA$	459	589	181	3.2	0.02	0.9	25	0.6
13	$[C_3(NMe_2)_2(NBuMe)]DCA$	864	516	196	2.6	0.1	4.1	28	1.8
14	$[C_3(NMe_2)_2(NPeH)]TFSA$	582	774	179	4.3	0.04	4.7	33	0.9
15	$[C_3(NMe_2)_2(NHexMe)]TFSA$	484	626	187	3.3	0.01	2.6	29	0.6

16	$[C_3(NEt_2)_2(NHBu)]TFSA$	473	785	173	4.5	0.004	1.8	30	0.3
17	$[C_3(NEt_2)_2(NHBu)]DCA$	1968	944	164	5.7	0.01	8.8	33	0.6
18	$[C_3(NEt_2)_2(NHBu)]BF_4$	1746	1090	167	6.5	0.02	27.3	39	0.3
	C_{2v} Cations								
19	$[C_3(NMe_2)_2(NEt_2)]TFSA$	1339	908	160	5.7	0.01	1.1	27	0.1
20	$[C_3(NMe_2)_2(N(CH_2CHCH_2)_2)]TFSA$	420	565	188	3.0	0.01	1.2	26	0.6
21	$[C_3(NMe_2)_2(NPr_2)]TFSA$	490	616	188	3.3	0.04	0.7	25	0.2
22	$[C_3(NMe_2)_2(N(CH_2CH_2OCH_3)_2)]TFSA$	370	570	196	2.9	0.01	3.5	31	0.5
23	$[C_3(NMe_2)_2(NBu_2)]TFSA$	464	637	186	3.4	0.01	2.4	29	0.5
24	$[C_3(NMe_2)_2(NHex_2)]TFSA$	1224	1070	165	6.5	0.01	1.3	37	0.2
25	$[C_3(NEt_2)_2(NHex_2)]I$	5235	1448	181	8.0	0.001	17837	62	2.3
26	$[C_3(NEt_2)_2(NHex_2)]OTf$	2347	1371	158	8.7	0.003	58.2	43	0.1
	C_{3h} Cations								
27	$[C_3(NEtMe_2)_3]TFSA$	469	622	175	3.5	0.02	0.6	25	0.5
28	$[C_3(NAllylMe_2)_3]TFSA$	434	594	185	3.2	0.03	1.3	27	0.6
29	$[C_3(NAllylMe)_3]DCA$	920	588	196	3.0	0.05	10.7	32	1.3
30	$[C_3(NMeCH_2CH_2OCH_3)_3]TFSA$	338	569	201	2.8	0.02	7.2	33	0.5
	D_{3h} Cations								
31	$[C_3(NEt_2)_3][MeC_6H_4SO_3]$	849	855	200	4.2	0.01	627.7	49	0.3

32	$[C_3(NBu_2)_3]B(CN)_4$	584	834	178	4.7	0.01	6.1	34	0.3
33	$[C_3(NBu_2)_3]FAP$	1114	1126	167	6.7	0.01	23.7	40	0.1

*Standad Deviation=S.D.

The considerable restrictions suffered by the slowdown of relaxation and transport processes are governed by the Vogel-Fulcher-Tammann (VFT) equation. The VFT equation is used to fit the conductivity data. In the table 5.10, the VFT fit parameters are summarized. These allow precise interpolation of conductivity data in the given temperature range and even good extrapolation beyond the limits as well. The VFT equation for conductivity (σ) is;

$$\sigma = \sigma_o \exp\left[\frac{-B}{T - T_o}\right]$$

where σ_o(mPa s), B (K) and T_o (K) are constants/best fitting/adjustable parameters. Fitting the data to the VFT equation gives us the fragility parameter (D), and the VFT temperature T_o,[35] where $D = B/T_o$. The T_o and B parameters change with the cationic and anionic characters which agrees well with the literature.[11] As the size of anion increases from $[C_3(NMe_2)_2(NMeR)]$DCA to $[C_3(NMe_2)_2(NMeR)]$TFSA, $[C_3(NBu_2)_3]B(CN)_4$ to $[C_3(NBu_2)_3]$FAP and $[C_3(NEt_2)_2(NHex_2)]$I to $[C_3(NEt_2)_2(NHex_2)]$OTf, the value for B increases while T_o decreases, which in turn increases D.

There is no strong trend for the fragility index (D), as was seen for the viscosity data. The value of D for conductivity data is lower and ranged from 2.6-8.7 as compared to the viscosity data (D = 0.1-23).[36]

The ideal glass transition temperature, T_o,obtained from viscosity and conductivity data will generally not yield the same T_o because the temperature-dependent conductivity data takes into account the ion association in contrast to temperature-dependent viscosity.[37] There is no strong correlation seen for T_o for viscosity and conductivity data (fig). T_o for the conductivity data ranged from 158 K for $[C_3(NEt_2)_2(NHex_2)]$OTf to 203 K for $[C_3(NMe_2)_2(NMe(CH_2CH_2OCH_3)]$DCA. While, T_o for the viscosity data ranged from 131 K for $[E_4Val]$TFSA to 328 K for $[E_4Pro]MeSO_4$. T_o values of our ionic liquids differ from each other at large explained by assuming large ion association.

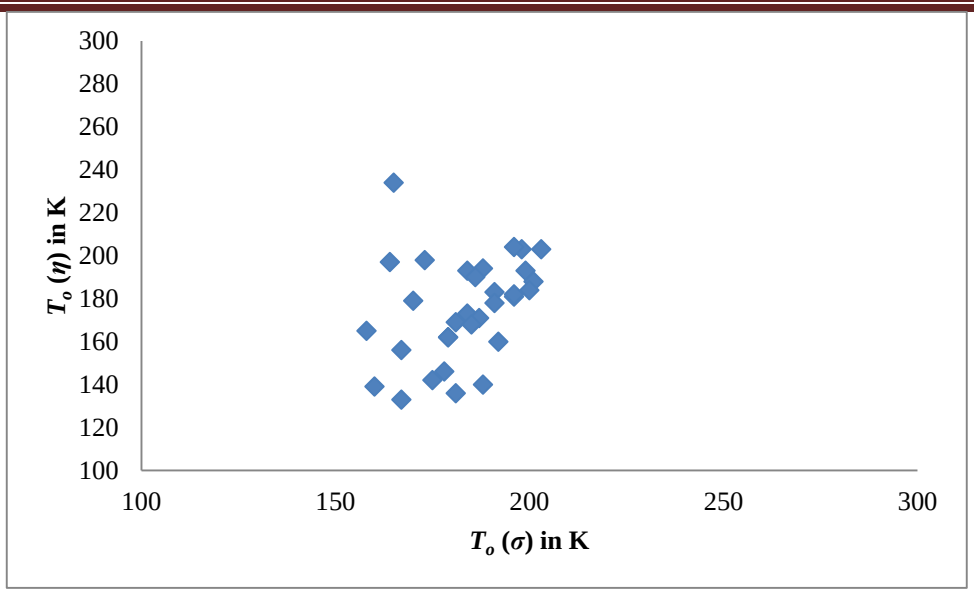

Figure 5.47–Correlation between T_o for conductivity versus viscosity.

Now I will explain the unusual Arrhenius and VFT fitting parameters obtained from conductivity data. Among the protic ILs, the presence of hydrogen bonding in $[C_3(NEt_2)_2(NHBu)]DCA$ and $[C_3(NEt_2)_2(NHBu)]BF_4$ causes the σ_o to increase to 1968 and 1746 mS cm^{-1} respectively. $[C_3(NEt_2)_2(NHBu)]BF_4$ (A = 27.3×10^5 mS cm^{-1}) is less conductive than $[C_3(NEt_2)_2(NHBu)]DCA$ (A = 8.8×10^5 mS cm^{-1}) and causes the value of A to increase.

The vaue of σ_o for the least conductive samples, $[C_3(NEt_2)_2(NHex_2)]I$ and $[C_3(NEt_2)_2(NHex_2)]OTf$ is 5235 and 2347 mS cm^{-1} respectively due to the presence of long hexyl chains, which causes the van der Waals force to increase. These van der Waals force also causes the value of A to increases in $[C_3(NEt_2)_2(NHex_2)]I$ (A = 17837×10^5 mS cm^{-1}) and $[C_3(NEt_2)_2(NHex_2)]OTf$ (A = 58.2×10^5 mS cm^{-1}). Similarly, the value of A for $[C_3(NEt_2)_3][MeC_6H_4SO_3]$ (A = 626.7×10^5 mS cm^{-1}) and $[C_3(NBu_2)_3]FAP$ (A = 23.7×10^5 mS cm^{-1}) is high again due to van der Waals forces.

5.7 Density

Density is a fundamental property of all materials, and decreases with increasing temperature. The determination of density is a well-established tool for product monitoring and quality control. The density was measured using an Anton Paar DMA 5000 density meter. A U-shaped glass tube of known volume is filled with a liquid sample and the change in the natural frequency is detected with a Piezo element, which is a function of the mass of the sample in the tube.

The reported densities of traditional ILs usually range between 1.12 to 2.4 g mL^{-1}.[5] The density of the triaminocyclopropenium type CILs at 20 °C in the present study range from 0.928 g mL^{-1} for $[C_3(NBu_2)_3]B(CN)_4$ to 1.401 g mL^{-1} for $[C_3(NMe_2)_2(NEtH)]TFSA$. For most of the ILs, the densities are comparable to organic solvents. The densities of tac-based ILs previously synthesized by the Curnow group were low and ranged from 0.89-1.30 g mL^{-1}.[12]

The density usually decreases linearly with the temperature, as can be seen in table 5.12.[38]

Table 5.12-Densities of ILs in g mL^{-1}

	***C_s* Cations**	**20 °C**	**30 °C**	**40 °C**	**50 °C**	**60 °C**	**70 °C**	**80 °C**	**90 °C**
1	$[C_3(NMe_2)_2(NEtH)]TFSA$	1.401	1.391	1.382	1.373	1.363	1.354	1.343	1.335
2	$[C_3(NMe_2)_2(HN(CH_2CHCH_2))]TFSA$	1.393	1.384	1.374	1.365	1.356	1.346	1.337	1.328
3	$[C_3(NMe_2)_2(N(CH_2CHCH_2)Me)]TFSA$	1.372	1.362	1.353	1.343	1.334	1.325	1.316	1.307
4	$[C_3(NMe_2)_2(N(CH_2CH_2CH_3)H)]TFSA$	1.373	1.364	1.354	1.345	1.336	1.327	1.317	1.308
5	$[C_3(NMe_2)_2(N(CH_2CH_2CH_3)Me)]TFSA$	1.356	1.346	1.337	1.328	1.319	1.309	1.301	1.292
6	$[C_3(NMe_2)_2(N(CH_2CH_2CH_3)Me)]DCA$	1.045	1.039	1.032	1.025	1.019	1.013	1.007	1.001
7	$[C_3(NMe_2)_2(N(CH_2CH_2OCH_3)H)]TFSA$	1.392	1.383	1.373	1.363	1.354	1.345	1.336	1.327
8	$[C_3(NMe_2)_2(N(CH_2CH_2OCH_3)Me)]TFSA$	1.378	1.368	1.356	1.349	1.339	1.330	1.321	1.312
9	$[C_3(NMe_2)_2(N(CH_2CH_2OCH_3)Me)]DCA$	1.077	1.069	1.061	1.053	1.045	1.038	1.031	1.026
10	$[C_3(NMe_2)_2(NBuH)]TFSA$	1.347	1.337	1.328	1.319	1.310	1.301	1.292	1.283
11	$[C_3(NMe_2)_2(NBuMe)]TFSA$	1.331	1.321	1.313	1.303	1.294	1.285	1.276	1.266
12	$[C_3(NMe_2)_2(NBuMe)]DCA$	1.032	1.026	1.020	1.014	1.007	1.002	0.995	0.989
13	$[C_3(NMe_2)_2(NPeH)]TFSA$	1.318	1.309	1.300	1.291	1.282	1.274	1.265	1.256
14	$[C_3(NMe_2)_2(NHexMe)]TFSA$	1.292	1.283	1.274	1.266	1.256	1.248	1.239	1.231
15	$[C_3(NEt_2)_2(NHBu)]TFSA$	1.266	1.257	1.249	1.240	1.232	1.223	1.214	1.206
16	$[C_3(NEt_2)_2(NHBu)]DCA$	0.995	0.989	0.983	0.977	0.971	0.965	0.959	0.953

17	$[C_3(NEt_2)_2(NHBu)]BF_4$	1.079	1.072	1.062	1.059	1.052	1.045	1.039	1.032
	C_{2v} Cations	**20 °C**	**30 °C**	**40 °C**	**50 °C**	**60 °C**	**70 °C**	**80 °C**	**90 °C**
18	$[C_3(NMe_2)_2(N(CH_2CHCH_2)_2)]TFSA$	1.343	1.332	1.323	1.314	1.305	1.296	1.287	1.278
19	$[C_3(NMe_2)_2(NPr_2)]TFSA$	---	---	---	1.287	1.279	1.271	1.262	1.254
20	$[C_3(NMe_2)_2(N(CH_2CH_2OCH_3)_2)]TFSA$	1.355	1.346	1.336	1.327	1.318	1.309	1.299	1.290
21	$[C_3(NMe_2)_2(NBu_2)]TFSA$	1.272	1.261	1.253	1.244	1.236	1.228	1.219	1.210
22	$[C_3(NMe_2)_2(NHex_2)]TFSA$	1.209	1.200	1.192	1.184	1.176	1.168	1.159	1.151
23	$[C_3(NEt_2)_2(NHex_2)]I$	1.130	1.123	1.17	1.09	1.102	1.096	1.095	1.083
24	$[C_3(NEt_2)_2(NHex_2)]OTf$	1.077	1.070	1.063	1.056	1.049	1.042	1.035	1.029
	C_{3h} Cations								
25	$[C_3(NEtMe_2)_3]TFSA$	1.333	1.324	1.315	1.306	1.297	1.288	1.279	1.270
26	$[C_3(NAllylMe_2)_3]TFSA$	1.315	1.306	1.297	1.288	1.279	1.270	1.261	1.252
27	$[C_3(NAllylMe)_3]DCA$	1.044	1.037	1.030	1.024	1.018	1.012	1.006	0.999
28	$[C_3(NMeCH_2CH_2OCH_3)_3]TFSA$	1.329	1.321	1.311	1.302	1.293	1.284	1.275	1.266
	D_{3h} Cations								
29	$[C_3(NEt_2)_3][MeC_6H_4SO_3]$	1.103	1.097	1.090	1.084	1.077	1.071	1.065	1.058
30	$[C_3(NBu_2)_3]B(CN)_4$	0.928	0.922	0.915	0.909	0.896	0.890	0.883	---
31	$[C_3(NBu_2)_3]FAP$	1.246	1.237	1.229	1.220	1.211	1.202	1.193	1.184

First, the effect of the cation on the density will be considered. With an increase in alkyl chain length around the cation, the van der Waals forces start to increase which dilutes the ionic charges and decreases the strong electrostatic interactions. The increase of weak van der Waals forces results in a decrease in density. The symmetry of the cation did not play much of a role in determining the density (fig. 5.48). However, the DCA salts have lower density than TFSA salts due to the lower atomic weights of atoms.

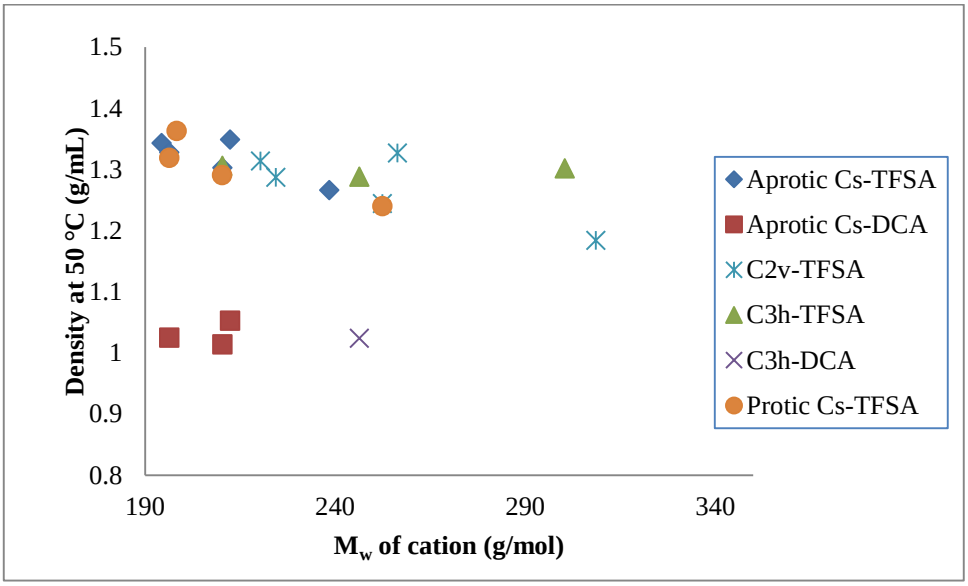

Figure 5.48–Molecular weight of cation versus density at 50 °C for the protic *Cs* ([C3(NMe2)2(NHR)]TFSA), aprotic *Cs* ([C3(NMe2)2(NMeR)]X), *C2v* ([C3(NMe2)2(NR2)]TFSA), and *C3h* ([C3(NRMe)3]X) type ILs.

If we consider the protic cations, the density at 20 °C for the smallest cation $[C_3(NMe_2)_2(NEtH)]$TFSA is 1.401 g/mL, which is the highest density observed in this thesis. As the cation size increases for the series $[C_3(NMe_2)_2(NHR)]$TFSA (R = ethyl, allyl, propyl, butyl and hexyl) to $[C_3(NEt_2)_2(NHBu)]$TFSA, the density decreases. However, $[C_3(NMe_2)_2(NH(CH_2CH_2OCH_3))]$TFSA is showing an anomalously high.

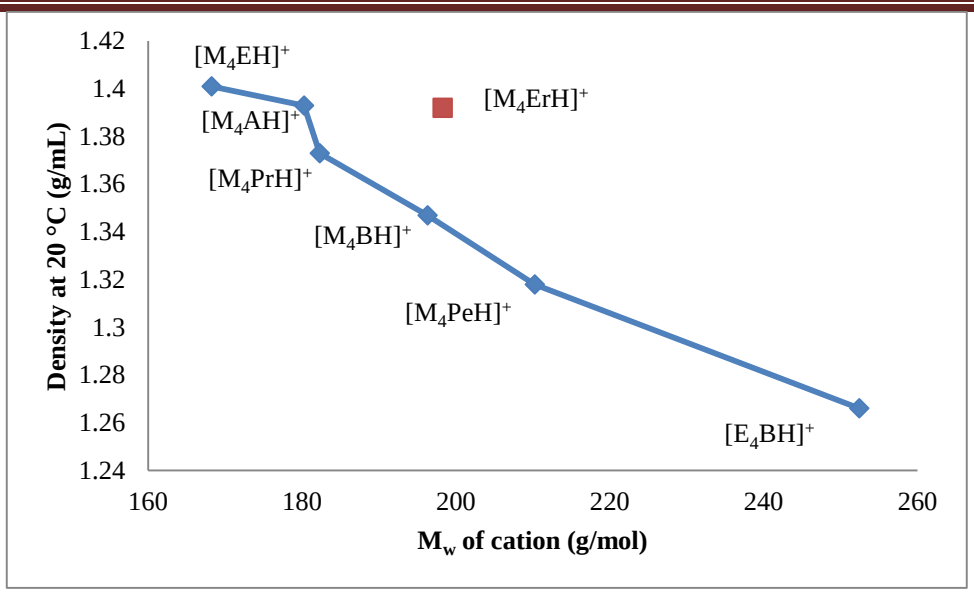

Figure 5.49–Density (at 20 °C) *vs* molecular weight of the protic cation for the [C3(NMe2)2(NRH)]TFSA and [C3(NEt2)2(NBuH)]TFSA salts.

Similarly, apart from $[C_3(NMe_2)_2(NMe(CH_2CH_2OCH_3))]$TFSA ($M_w$ = 212.31 g/mol, ρ = 1.378 g/mL) as the size of cation increases from $[C_3(NMe_2)_2(NMe(CH_2CHCH_2))]$TFSA ($M_w$ = 194.30 g/mol, ρ = 1.372 g/mL), $[C_3(NMe_2)_2(NMe(CH_2CH_2CH_3))]$TFSA ($M_w$ = 196.31 g/mol, ρ = 1.356 g/mL), $[C_3(NMe_2)_2(NMeBu)]$TFSA (M_w = 210.34 g/mol, ρ = 1.331 g/mL) and $[C_3(NMe_2)_2(NMeHex)]$TFSA (M_w = 238.39 g/mol, ρ = 1.292 g/mL), the density decreases. Interestingly, the densities observed for DCA salts were lower than TFSA salts. The density observed for $[C_3(NMe_2)_2(NMe(CH_2CH_2OCH_3))]$DCA ($M_w$ = 212.31 g/mol, ρ = 1.077 g/mL) is again high relative to other DCA salts of similar molecular weight.

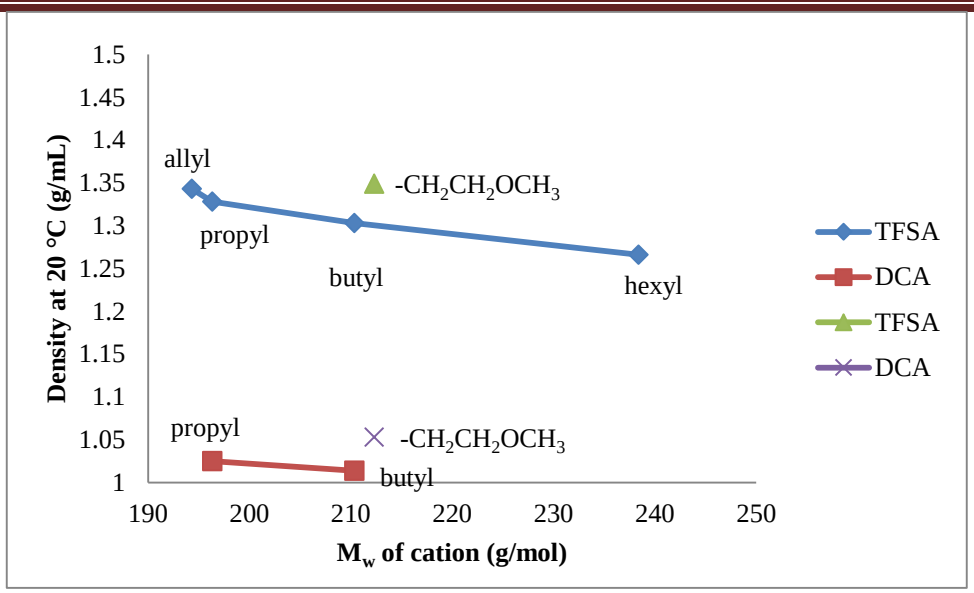

Figure 5.50–Comparison of density at 20 °C *vs* molecular weight of protic cation *Cs*, [C3(NMe2)2(NRMe)]X (X = TFSA and DCA).

Similarly, for C_{2v} cations, the highest density was observed for $[C_3(NMe_2)_2(N(CH_2CH_2OCH_3)_2)]$TFSA (1.327 g mL^{-1} at 50 °C). As the alkyl chain length increases for the $[C_3(NMe_2)_2(NR_2)_2]$TFSA, series from allyl (1.314 g/mL at 50 °C), propyl (1.287 g/mL at 50 °C), butyl (1.244 g/mL at 50 °C) and hexyl (1.184 g/mL at 50 °C), the density decreases.

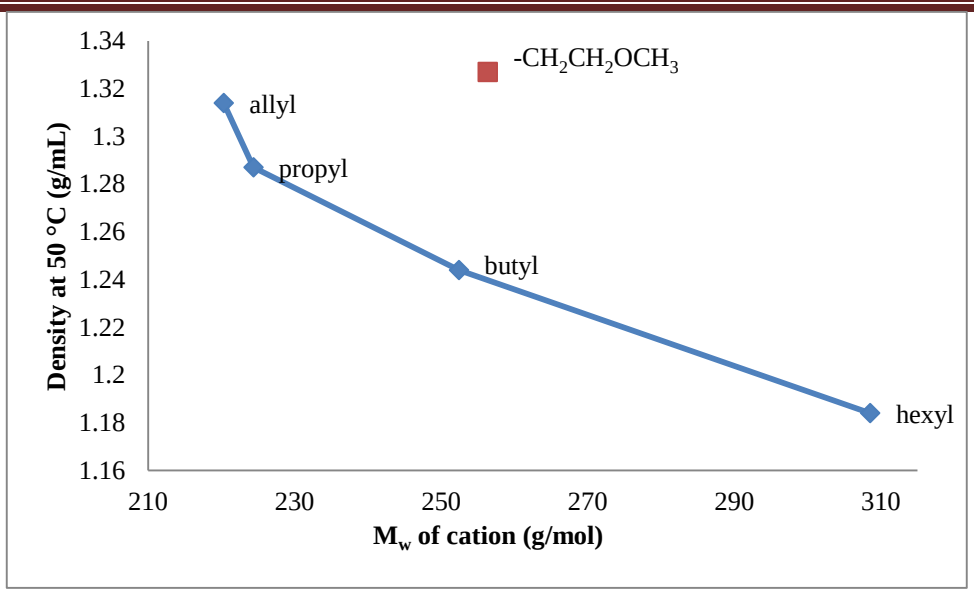

Figure 5.51–Density at 50 °C *vs* molecular weight of the C_{2v} cation in $[C_3(NMe_2)_2(NR_2)]$TFSA.

Among C_{3h} cations, the density for $[C_3(NMe(CH_2CH_2OCH_3))_3]$TFSA is increased due to the ether functionality in the side chain (fig). Again the density for $[C_3(NMeAllyl_2)_3]$DCA (1.044 g mL^{-1}) is lower than $[C_3(NMeAllyl_2)_3]$TFSA (1.315 g mL^{-1}).

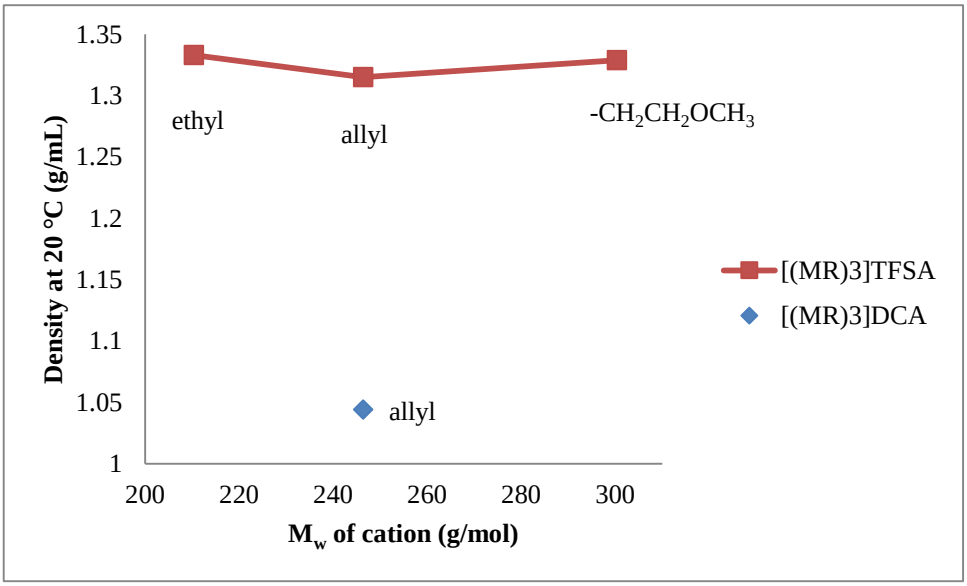

Figure 5.52–Density at 20 °C *vs* molecular weight of cation for $[C_3(NRMe)_3]$X (X = TFSA and DCA).

Now I will discuss the high density observed in the ether alkyl chain containing ILs.

The main purpose for introducing the ether linkage in the side chain was to study the effect on physicochemical properties. Due to less rotational flexibility around the MOE ($-CH_2CH_2OCH_3$) ether linkage compared to EOM ($-CH_2OCH_2CH_3$) and EOE ($-CH_2CH_2OCH_2CH_3$) ether linkages (as shown in fig. 5.53), an increase in the density results.[16] Oxygen makes two bonds compared with carbon which make four bonds and thus there is more rotational flexibility around oxygen.

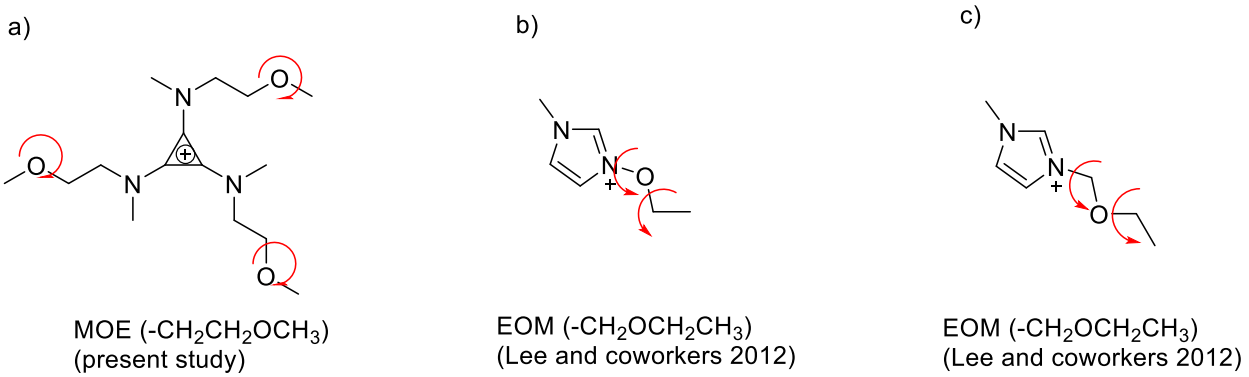

Figure 5.53–a) Structure of $[C_3(NMeCH_2CH_2OCH_3)_3]$TFSA showing rotational flexibility around the ether linkage of MOE b) Rotational flexibility around EOM and EOE.[16]

The molar volume is calculated by dividing their molecular weights with their density at 20 °C, as shown in table 5.13.

Table 5.13-Molar volume and molar concentration of ILs at 20 °C.

	C_s Cations	Mol. wt. (g/mol)	Density at 20 °C (g mL^{-1})	Molar Volume (mL mol^{-1})	Molar Concentration at 20 °C (10^{-3} mol mL^{-1})
1	$[C_3(NMe_2)_2(NEtH)]TFSA$	448.41	1.401	320.06	3.12
2	$[C_3(NMe_2)_2(HN(CH_2CHCH_2))]TFSA$	460.42	1.393	330.52	3.03
3	$[C_3(NMe_2)_2(N(CH_2CHCH_2)Me)]TFSA$	474.44	1.372	345.80	2.89
4	$[C_3(NMe_2)_2(N(CH_2CH_2CH_3)H)]TFSA$	462.43	1.373	336.80	2.97
5	$[C_3(NMe_2)_2(N(CH_2CH_2CH_3)Me)]TFSA$	476.46	1.356	351.37	2.85
6	$[C_3(NMe_2)_2(N(CH_2CH_2CH_3)Me)]DCA$	262.35	1.045	251.05	3.98
7	$[C_3(NMe_2)_2(N(CH_2CH_2OCH_3)H)]TFSA$	478.43	1.392	343.70	2.91
8	$[C_3(NMe_2)_2(N(CH_2CH_2OCH_3)Me)]TFSA$	492.46	1.378	357.37	2.79
9	$[C_3(NMe_2)_2(N(CH_2CH_2OCH_3)Me)]DCA$	278.35	1.077	258.45	3.87
10	$[C_3(NMe_2)_2(NBuH)]TFSA$	476.46	1.347	353.72	2.83
11	$[C_3(NMe_2)_2(NBuMe)]TFSA$	490.49	1.331	368.51	2.71
12	$[C_3(NMe_2)_2(NBuMe)]DCA$	276.38	1.032	267.81	3.73
13	$[C_3(NMe_2)_2(NPeH)]TFSA$	490.49	1.318	372.15	2.69
14	$[C_3(NMe_2)_2(NHexMe)]TFSA$	518.54	1.292	401.35	2.49
15	$[C_3(NEt_2)_2(NHBu)]TFSA$	532.56	1.266	420.66	2.38
16	$[C_3(NEt_2)_2(NHBu)]DCA$	318.46	0.995	320.06	3.12
17	$[C_3(NEt_2)_2(NHBu)]BF_4$	339.22	1.079	314.38	3.18
	C_{2v} Cations				
18	$[C_3(NMe_2)_2(N(CH_2CHCH_2)_2)]TFSA$	500.48	1.343	372.66	2.68
19	$[C_3(NMe_2)_2(NPr_2)]TFSA$	504.51	---	---	---
20	$[C_3(NMe_2)_2(N(CH_2CH_2OCH_3)_2)]TFSA$	536.51	1.355	395.95	2.53
21	$[C_3(NMe_2)_2(NBu_2)]TFSA$	532.56	1.272	418.68	2.39
22	$[C_3(NMe_2)_2(NHex_2)]TFSA$	588.67	1.209	486.91	2.05
23	$[C_3(NEt_2)_2(NHex_2)]I$	491.54	1.13	434.99	2.30
24	$[C_3(NEt_2)_2(NHex_2)]OTf$	513.7	1.077	476.97	2.09
	C_{3h} Cations				
25	$[C_3(NEtMe_2)_3]TFSA$	490.49	1.333	367.96	2.72
26	$[C_3(NAllylMe_2)_3]TFSA$	526.52	1.315	400.39	2.50
27	$[C_3(NAllylMe)_3]DCA$	312.41	1.044	299.24	3.34
28	$[C_3(NMeCH_2CH_2OCH_3)_3]TFSA$	580.56	1.329	436.84	2.29
	D_{3h} Cations				
29	$[C_3(NEt_2)_3][MeC_6H_4SO_3]$	423.61	1.103	384.05	2.60

30	$[C_3(NBu_2)_3]B(CN)_4$	517.48	0.928	557.63	1.80
31	$[C_3(NBu_2)_3]FAP$	847.6	1.246	680.26	1.47

According to the hole theory, the molar volume is the bulk volume of a liquid is inherent volume plus the total volume of holes between molecules. If there is rotational flexibility around an ether linkage, the molar volume increases and the density decreases.[16] However, the density increases from $[C_3(NMe_2)_2(NH(CH_2CH_2OCH_3))]$TFSA, $[C_3(NMe_2)_2(NMe(CH_2CH_2OCH_3))]$X (X = TFSA and DCA), $[C_3(NMe_2)_2(N(CH_2CH_2OCH_3)_2)]$TFSA and $[C_3(NMeCH_2CH_2OCH_3)_3]$TFSA, compared to rest of the protic C_s, aprotic C_s, C_{2v} and C_{3h} cations, respectively, due to less holes between the molecules in these ILs.

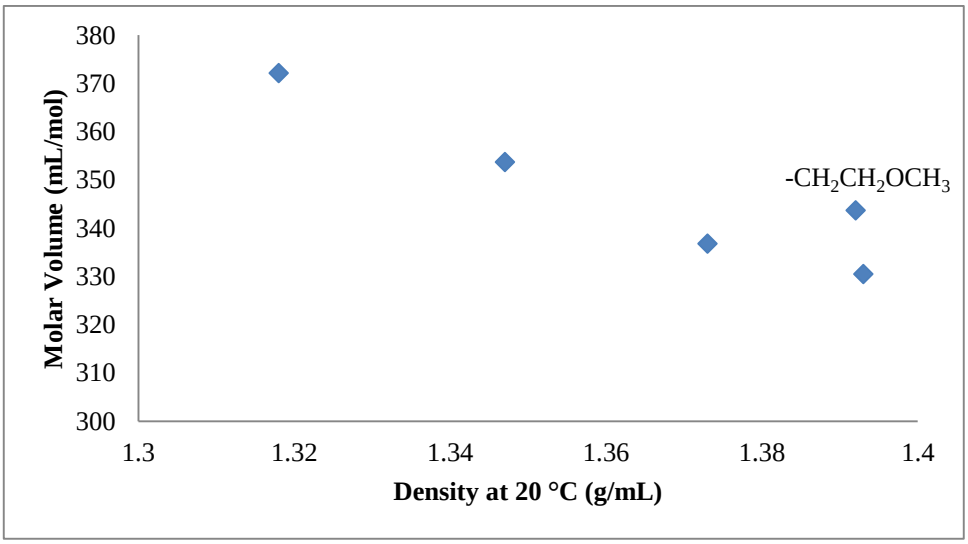

Figure 5.54–Comparison of molar volume and density at 20 °C for protic C_s cation, $[C_3(NMe_2)_2(NRH)]$TFSA.

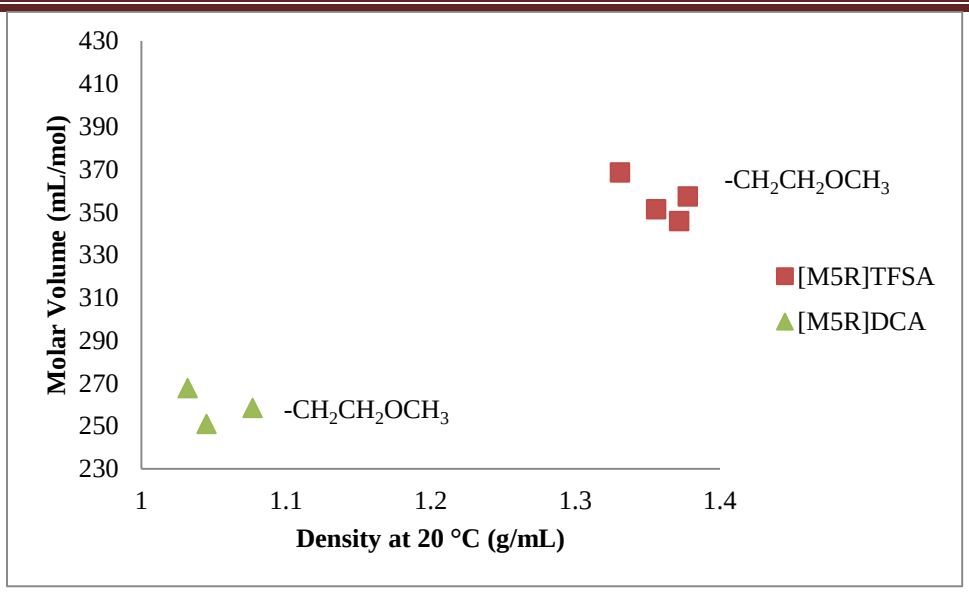

Figure 5.55–Comparison of molar volume and density at 20 °C for aprotic C_s cation, $[C_3(NMe_2)_2(NRMe)]X$ (X = TFSA and DCA).

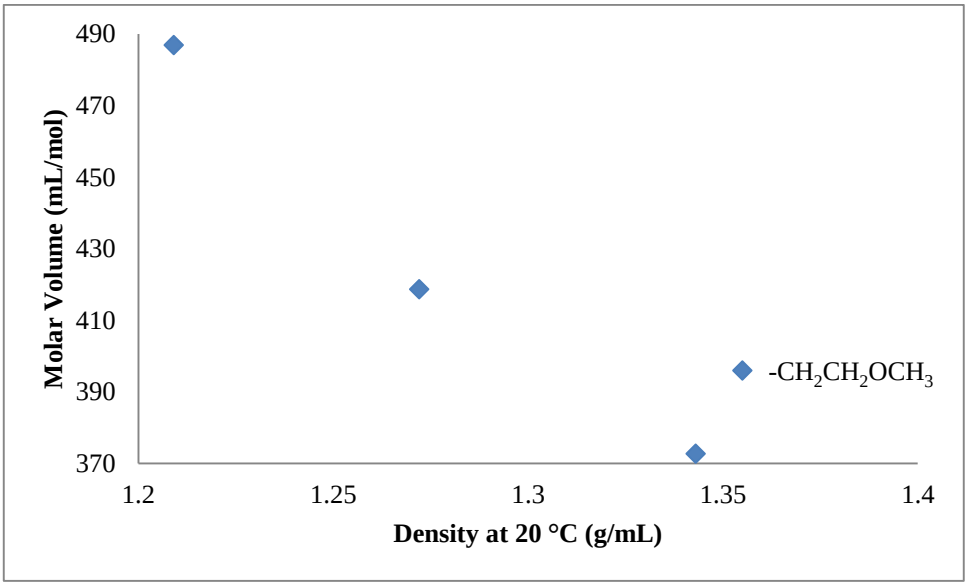

Figure 5.56–Comparison of molar volume and density at 20 °C for C_{2v} cation, $[C_3(NMe_2)_2(NR_2)]TFSA$.

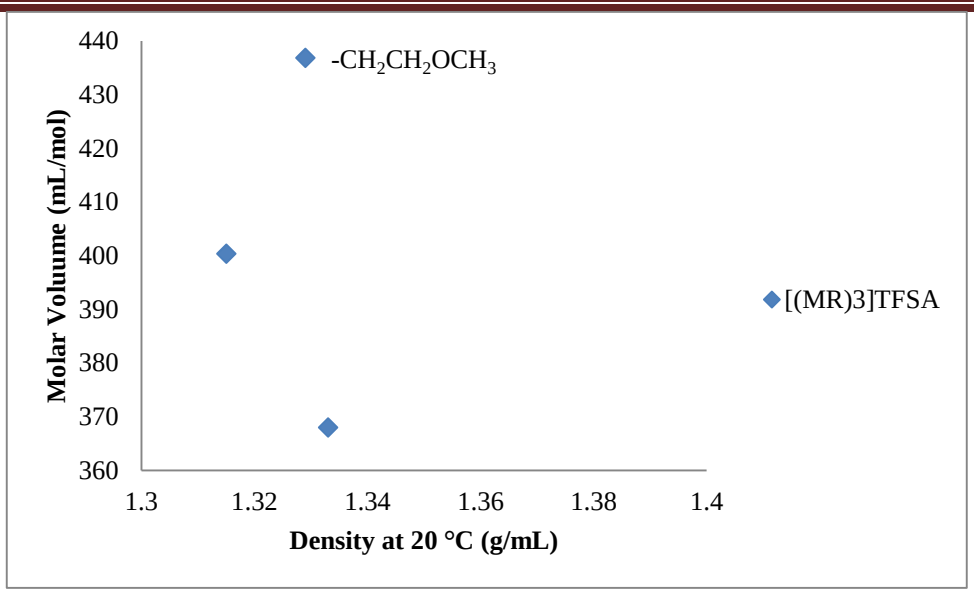

Figure 5.57–Comparison of molar volume and density at 20 °C for C_{3h} cation, [C3(NMeR)3]TFSA.

There was no symmetry dependency of molar volume for protic C_s, aprotic C_s, C_{2v} and C_{3h} cations was seen for TFSA salts and all lie in the same range (1 to 1.4 mL/mol). However, the molar volume for DCA salts were lower compared to the TFSA salts.

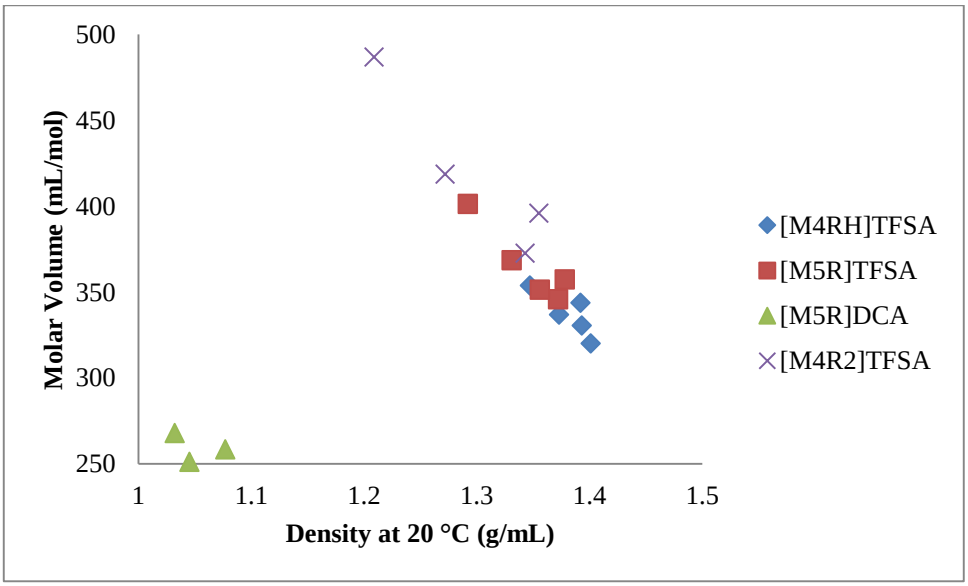

Figure 5.58–Comparison of molar volume and density at 20 °C for protic C_s, aprotic C_s, C_{2v} and C_{3h} cations.

The molar concentrations are calculated by taking the reciprocal of the molar volume. With a decrease in the molecular weight, an increase in the molar concentration is obtained. The molar concentration ranged from 1.47 to 3.98 mol mL^{-1} for the ILs in this study at 20 °C. The decrease in density with the increasing molecular weight causes the molar volume to increase and causes the salt concentration to decrease.[11]

So far we have considered the effect of cation size on the density. The anion size is another major factor responsible for affecting density; this usually follows the molecular weight of anions.[39] For the $[C_3(NEt_2)_2(NBuH)]^+$ cation, the anion trend for increasing density is DCA^- (M_w = 66 g/mol) < BF_4^- (M_w = 87 g/mol) <$TFSA^-$ (M_w = 280 g/mol). Thus, with the increase in size of anion the density is increased.

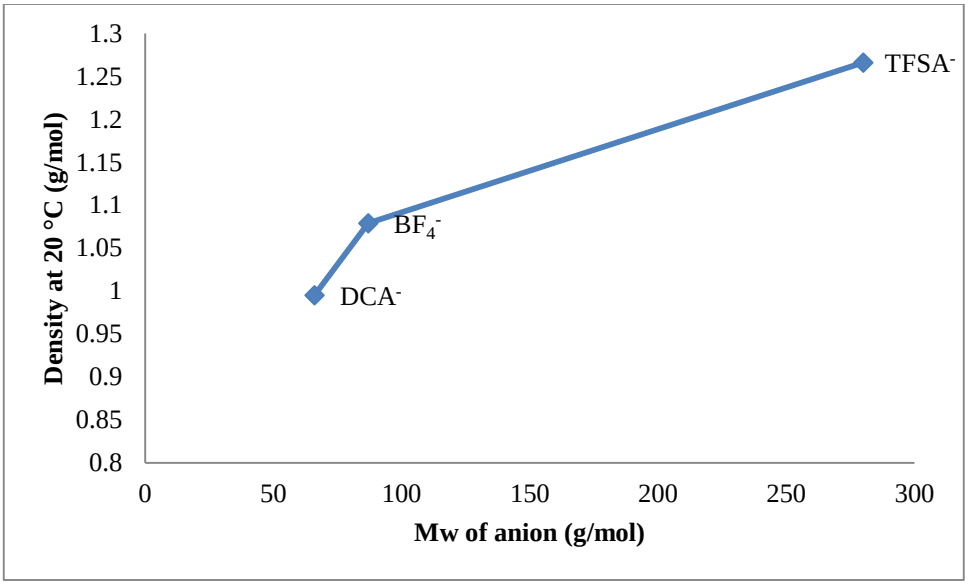

Figure 5.59–Comparison of density at 20 °C *vs* molecular weight of anion for $[C_3(NEt_2)_2(NBuH)]X$.

Now I will compare $[C_3(NEt_2)_2(NHex_2)]^+$ with similar cations already synthesized by the Curnow group.[12] For $[C_3(NEt_2)_2(NHex_2)]^+$, the anion trend for increasing density is DCA^- (M_w = 66 g/mol)[12] < OTf^- (M_w = 149 g/mol) < $TFSA^-$ (M_w = 280 g/mol)[12], which follows increasing molecular weight of anion. However, a higher density is observed for $[C_3(NEt_2)_2(NHex_2)]I$ (M_w of anion = 126 g/mol) than $[C_3(NEt_2)_2(NHex_2)]OTf$ (M_w = 149 g/mol), due to delocalized electron charge density in the triflate anion.

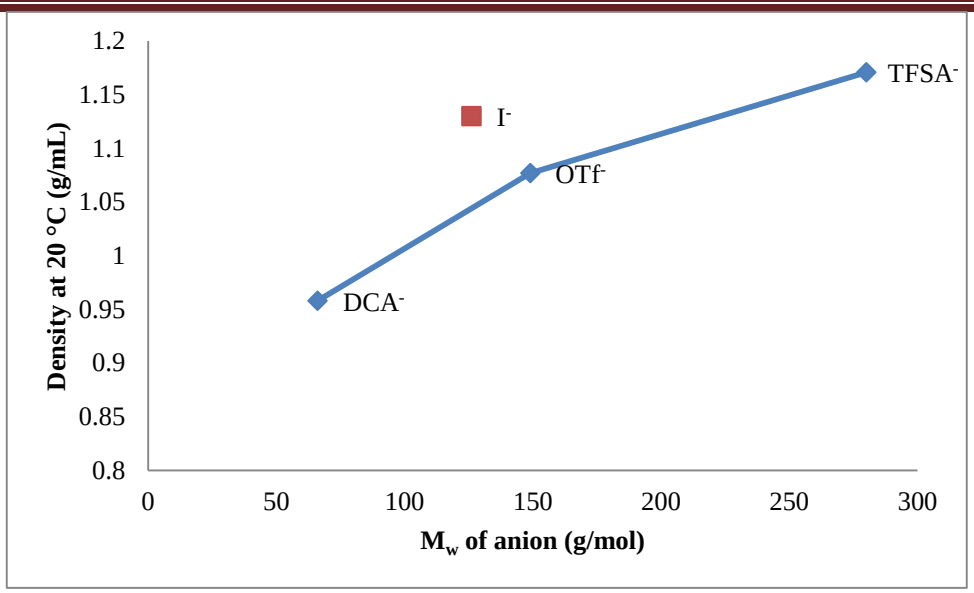

Figure 5.60–Comparison of density at 20 °C *vs* molecular weight of anion for $[C_3(NEt_2)_2(NHex_2)]X$.

Similarly, for the D_{3h} cation $[C_3(NEt_2)_3]^+$, the density increases with an increase in size of the anion from DCA^-,[12] OTs^- and $TFSA^-$.[12]

For $[C_3(NBu_2)_3]B(CN)_4$ (M_w = 114 g/mol) a lower density is observed than $C_3(NBu_2)_3]DCA$[12] (M_w = 66 g/mol). While for the rest of series the density increases with the increase in size of anion from DCA^-, $TFSA^-$ and FAP^-. The densities observed for $[C_3(NEt_2)_3]^+$ are higher than $[C_3(NBu_2)_3]^+$, due to the dilution of electron charge density of the later cation because of long butyl chains.

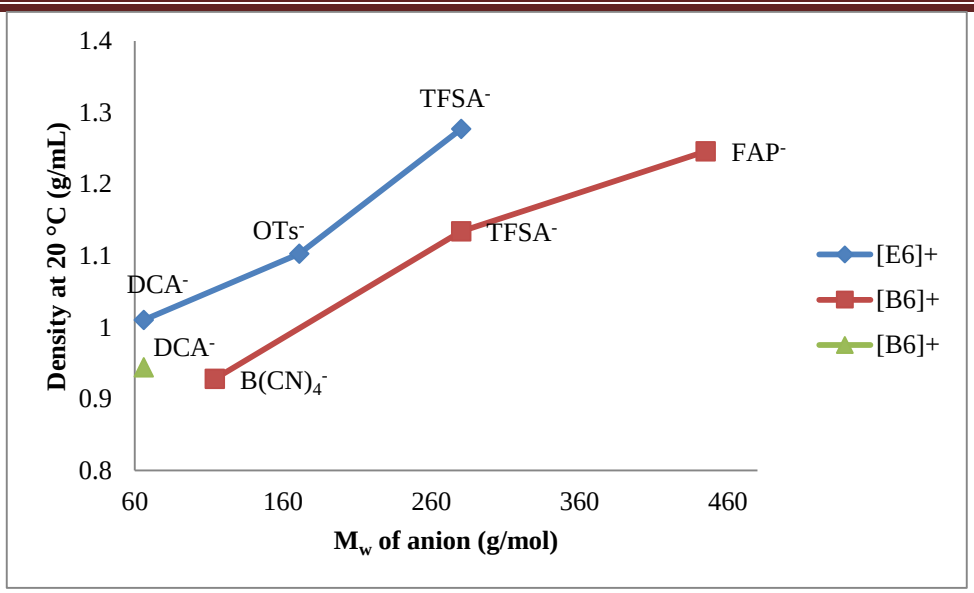

Figure 5.61–Comparison of density at 20 °C *vs* molecular weight of anion for $[C_3(NEt_2)_3]X$ and $[C_3(NBu_2)_3]X$.

Compared to other traditional classes of ILs, the densities of our triaminocyclopropenims are higher.[11, 38-40] This is due to the large molecular weight and delocalized charge of the triaminocyclopropenium cation. If the density of 1.372 g mL^{-1} for $[C_3(NMe_2)_2(NMe(CH_2CHCH_2))]$TFSA (194.30 g/mol) and 1.29 g mL^{-1} for $[C_8mim]$TFSA (195 g/mol) at 20 °C, are compared, we can clearly see that both are similarly sized but the density of $[C_8mim]$TFSA is lower than $[C_3(NMe_2)_2(NMe(CH_2CHCH_2))]$TFSA. It was thought that the cations are closer in than $[C_3(NMe_2)_2(NMe(CH_2CHCH_2))]$TFSA which results in less holes and causes the density to increase.

Generally, density (ρ) can be expressed as;

$$\rho = a - bT$$

Where a is the density at 0 K (g mL^{-1}), b is the co-efficient of volume expansion (g mL^{-1} K^{-1}), and T is the temperature (K). Density varies linearly with increasing temperature as shown in fig.5.62. The linear best fit parameters for density are shown in table 5.14.

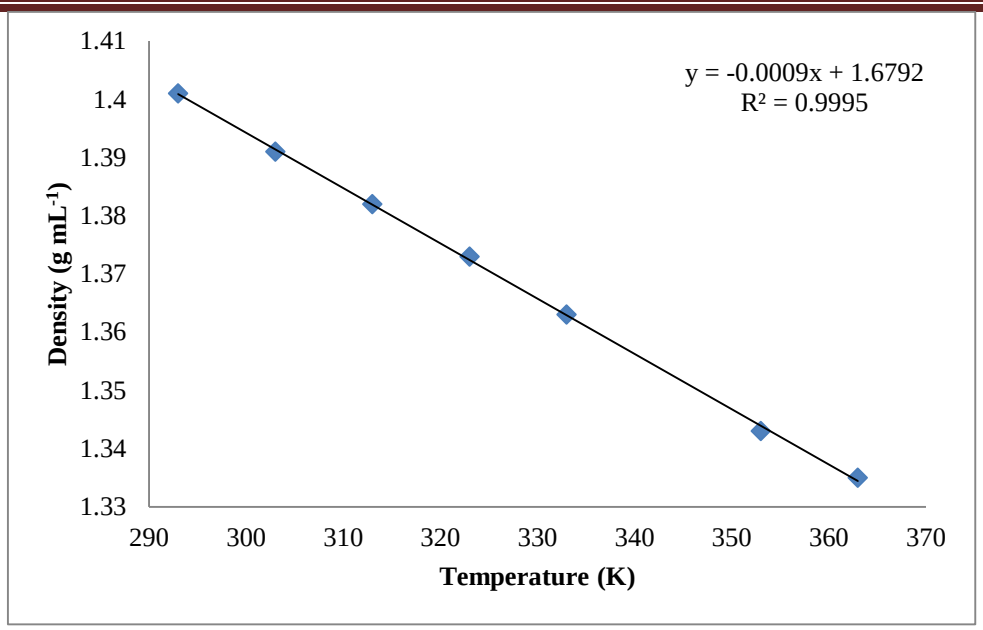

Figure 5.62–Linear plot for density dependence on temperature for $[C_3(NMe_2)_2NHEt]TFSA$.

Table 5.14–Fitting parameters for temperature dependence of density, $\rho = a - bT$

	C_s Cations	$-bx10^{-4}$ (g mL^{-1} K^{-1})	a (g mL^{-1})
1	$[C_3(NMe_2)_2(NEtH)]TFSA$	9.227	1.6786
2	$[C_3(NMe_2)_2(HN(CH_2CHCH_2))]TFSA$	9.304	1.6661
3	$[C_3(NMe_2)_2(N(CH_2CHCH_2)Me)]TFSA$	9.257	1.6428
4	$[C_3(NMe_2)_2(N(CH_2CH_2CH_3)H)]TFSA$	9.304	1.6451
5	$[C_3(NMe_2)_2(N(CH_2CH_2CH_3)Me)]TFSA$	9.083	1.6226
6	$[C_3(NMe_2)_2(N(CH_2CH_2CH_3)Me)]DCA$	6.315	1.2300
7	$[C_3(NMe_2)_2(N(CH_2CH_2OCH_3)H)]TFSA$	9.315	1.6649
8	$[C_3(NMe_2)_2(N(CH_2CH_2OCH_3)Me)]TFSA$	9.341	1.6506
9	$[C_3(NMe_2)_2(N(CH_2CH_2OCH_3)Me)]DCA$	7.714	1.3026
10	$[C_3(NMe_2)_2(NBuH)]TFSA$	9.083	1.6126
11	$[C_3(NMe_2)_2(NBuMe)]TFSA$	9.210	1.6005
12	$[C_3(NMe_2)_2(NBuMe)]DCA$	6.181	1.21125
13	$[C_3(NMe_2)_2(NPeH)]TFSA$	8.837	1.5762
14	$[C_3(NMe_2)_2(NHexMe)]TFSA$	8.750	1.5481
15	$[C_3(NEt_2)_2(NHBu)]TFSA$	8.583	1.5174
16	$[C_3(NEt_2)_2(NHBu)]DCA$	6.000	1.1708
17	$[C_3(NEt_2)_2(NHBu)]BF_4$	6.565	1.2705
	C_{2v} Cations		
18	$[C_3(NMe_2)_2(N(CH_2CHCH_2)_2)]TFSA$	9.167	1.6104
19	$[C_3(NMe_2)_2(NPr_2)]TFSA$	8.300	1.5553
20	$[C_3(NMe_2)_2(N(CH_2CH_2OCH_3)_2)]TFSA$	9.304	1.6271
21	$[C_3(NMe_2)_2(NBu_2)]TFSA$	8.681	1.5243
22	$[C_3(NMe_2)_2(NHex_2)]TFSA$	8.246	1.4497
23	$[C_3(NEt_2)_2(NHex_2)]I$	7.953	1.3763
24	$[C_3(NEt_2)_2(NHex_2)]OTf$	6.906	1.2795
	C_{3h} Cations		
25	$[C_3(NEtMe_2)_3]TFSA$	9.000	1.5967
26	$[C_3(NAllylMe_2)_3]TFSA$	9.000	1.5787
27	$[C_3(NAllylMe)_3]DCA$	6.319	1.2282
28	$[C_3(NMeCH_2CH_2OCH_3)_3]TFSA$	9.058	1.5948
	D_{3h} Cations		
29	$[C_3(NEt_2)_3][MeC_6H_4SO_3]$	6.417	1.2911
30	$[C_3(NBu_2)_3]B(CN)_4$	7.729	1.1576
31	$[C_3(NBu_2)_3]FAP$	8.859	1.5058

5.8 Molar Conductivity

In order to compare ionic conductivity of the ILs, we have to consider that every IL has a different ion concentration (*n*). Thus molar conductivity is helpful in estimating the contribution of ion mobility (μ) for ionic conductivity. The molar concentration of these ionic liquids is also dependent on the anion, thus molar conductivity was calculated. The molar conductivity Λ is obtained by using the following equation;

$$\Lambda = \sigma \frac{M}{\rho}$$

where M (g/mol), ρ (g/mL) and σ (mS cm^{-1}) are molecular weight, density, and ionic conductivity of the ionic liquids.

Table 5.15-Molar Conductivities in S cm^2 mol^{-1}

	***C_s* Cations**	**20 °C**	**30 °C**	**40 °C**	**50 °C**	**60 °C**	**70 °C**	**80 °C**	**90 °C**
1	$[C_3(NMe_2)_2(NEtH)]TFSA$	0.439	0.738	1.165	1.705	2.359	3.133	4.030	4.490
2	$[C_3(NMe_2)_2(HN(CH_2CHCH_2))]TFSA$	0.429	0.672	1.065	1.565	2.179	2.911	3.757	4.687
3	$[C_3(NMe_2)_2(N(CH_2CHCH_2)Me)]TFSA$	1.024	1.511	2.208	3.027	3.976	5.052	6.242	7.679
4	$[C_3(NMe_2)_2(N(CH_2CH_2CH_3)H)]TFSA$	0.364	0.627	0.984	1.451	2.042	2.759	3.581	4.525
5	$[C_3(NMe_2)_2(N(CH_2CH_2CH_3)Me)]TFSA$	0.952	1.476	2.163	2.978	3.912	5.008	6.207	7.597
6	$[C_3(NMe_2)_2(N(CH_2CH_2CH_3)Me)]DCA$	0.796	1.369	2.146	3.169	4.351	5.827	7.373	9.173
7	$[C_3(NMe_2)_2(N(CH_2CH_2OCH_3)H)]TFSA$	0.279	0.505	0.853	1.302	1.866	2.533	3.348	4.265
8	$[C_3(NMe_2)_2(N(CH_2CH_2OCH_3)Me)]TFSA$	0.708	1.152	1.721	2.457	3.303	4.258	5.372	6.549
9	$[C_3(NMe_2)_2(N(CH_2CH_2OCH_3)Me)]DCA$	0.625	1.127	1.826	2.768	3.881	5.181	6.749	8.410
10	$[C_3(NMe_2)_2(NBuH)]TFSA$	0.314	0.556	0.889	1.333	1.873	2.537	3.304	4.204
11	$[C_3(NMe_2)_2(NBuMe)]TFSA$	0.869	1.340	1.954	2.722	3.586	4.584	5.708	6.951
12	$[C_3(NMe_2)_2(NBuMe)]DCA$	1.173	1.921	2.897	4.113	5.626	7.254	9.083	11.066
13	$[C_3(NMe_2)_2(NPeH)]TFSA$	0.238	0.412	0.664	1.007	1.442	1.987	2.625	3.319
14	$[C_3(NMe_2)_2(NHexMe)]TFSA$	0.526	0.877	1.359	1.978	2.737	3.627	4.641	5.787
15	$[C_3(NEt_2)_2(NHBu)]TFSA$	0.290	0.483	0.746	1.095	1.521	2.047	2.663	3.374
16	$[C_3(NEt_2)_2(NHBu)]DCA$	0.409	0.696	1.111	1.672	2.394	3.294	4.383	5.671
17	$[C_3(NEt_2)_2(NHBu)]BF_4$	0.099	0.188	0.326	0.531	0.819	1.188	1.665	2.241

	C_{2v} Cations								
18	$[C_3(NMe_2)_2(N(CH_2CHCH_2)_2)]TFSA$	0.771	1.225	1.816	2.540	3.394	4.364	5.471	6.681
19	$[C_3(NMe_2)_2(NPr_2)]TFSA$	---	---	---	1.995	2.765	3.653	4.653	5.846
20	$[C_3(NMe_2)_2(N(CH_2CH_2OCH_3)_2)]TFSA$	0.419	0.729	1.156	1.701	2.368	3.154	4.075	5.105
21	$[C_3(NMe_2)_2(NBu_2)]TFSA$	0.515	0.857	1.326	1.926	2.654	3.513	4.496	5.634
22	$[C_3(NMe_2)_2(NHex_2)]TFSA$	0.141	0.259	0.439	0.701	1.061	1.527	2.107	2.823
23	$[C_3(NEt_2)_2(NHex_2)]I$	0.006	0.017	0.145	0.264	0.422	0.646	0928	1.339
24	$[C_3(NEt_2)_2(NHex_2)]OTf$	0.045	0.089	0.166	0.285	0.463	0.709	1.037	1.473
	C_{3h} Cations								
25	$[C_3(NEtMe_2)_3]TFSA$	0.890	1.341	1.936	2.648	3.472	4.406	5.469	6.639
26	$[C_3(NAllylMe_2)_3]TFSA$	0.733	1.157	1.725	2.449	3.289	4.245	5.332	6.535
27	$[C_3(NAllylMe)_3]DCA$	0.661	1.154	1.862	2.798	3.931	5.239	6.832	8.569
28	$[C_3(NMeCH_2CH_2OCH_3)_3]TFSA$	0.307	0.554	0.939	1.431	2.043	2.781	3.625	4.636
	D_{3h} Cations								
29	$[C_3(NEt_2)_3][MeC_6H_4SO_3]$	0.034	0.084	0.173	0.324	0.548	0.862	1.280	1.806
30	$[C_3(NBu_2)_3]B(CN)_4$	0.236	0.419	0.694	1.071	1.571	2.192	2.942	---
31	$[C_3(NBu_2)_3]FAP$	0.099	0.190	0.340	0.562	0.879	1.305	1.840	2.534

With an increase in the size of the cation and the anion, the molar conductivity decreases. The molar conductivity is calculated from ionic conductivity and molar concentration and follows the same pattern as for ionic conductivity.

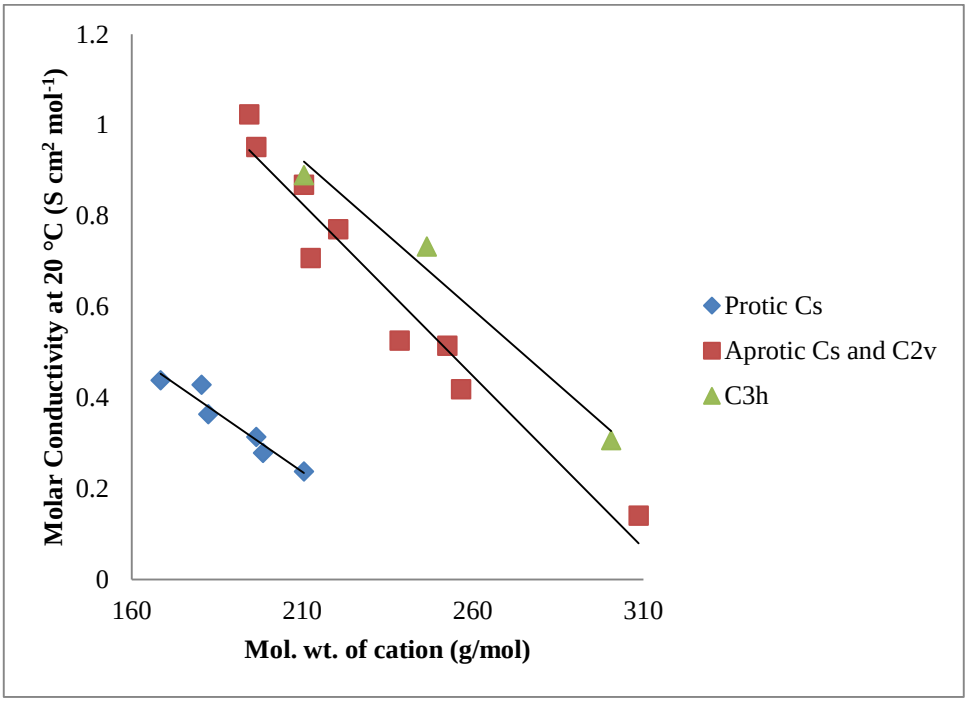

Figure 5.63-Graphical representation of molar conductivity *vs* Mol. wt. for cations.

The molar conductivity for the ionic liquids depends on temperature as shown in figure. The VFT equation is well fitted for the temperature dependencies for molar conductivity, just like viscosity and ionic conductivity;

$$\Lambda = \Lambda_0 \, exp\left[\frac{-B}{T - T_0}\right]$$

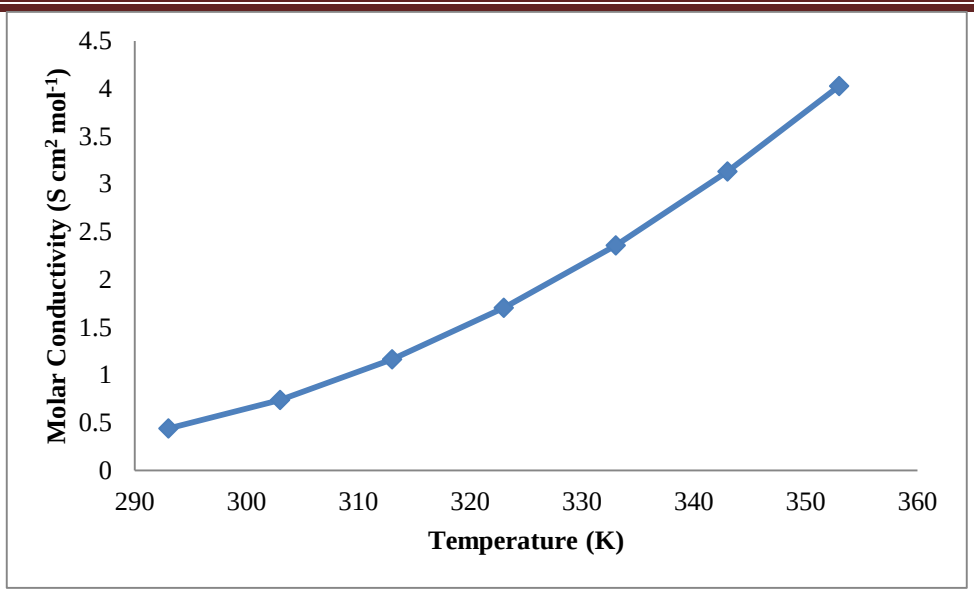

Figure 5.64–Arrhenius plot for molar conductivities for [$C_3NMe_2)_2$(NEtH)]TFSA.

Where Λ_0 (S cm^2 mol^{-1}), *B* (K) and T_o (K) are the fitting parameters. These are summarized in table 5.16.

Table 5.16-VFT fit parameters for molar conductivity of ionic liquids.

	C_s Cations	**Λ_o (S cm^2 mol^{-1})**	**B (K)**	**T_o (K)**	**D**	**S.D. (S cm^2 mol^{-1})**
1	$[C_3(NMe_2)_2(HN(CH_2CH_3))]TFSA$	497	603	191	3.2	0.01
2	$[C_3(NMe_2)_2(HN(CH_2CHCH_2))]TFSA$	371	856	167	5.1	0.03
3	$[C_3(NMe_2)_2(N(CH_2CHCH_2)Me)]TFSA$	306	729	165	4.4	0.03
4	$[C_3(NMe_2)_2(N(CH_2CH_2CH_3)H)]TFSA$	251	729	182	4.0	0.003
5	$[C_3(NMe_2)_2(N(CH_2CH_2CH_3)Me)]TFSA$	211	608	181	3.4	0.02
6	$[C_3(NMe_2)_2(N(CH_2CH_2CH_3)Me)]DCA$	275	569	196	2.9	0.02
7	$[C_3(NMe_2)_2(N(CH_2CH_2OCH_3)H)]TFSA$	183	627	197	3.2	0.01
8	$[C_3(NMe_2)_2(N(CH_2CH_2OCH_3)Me)]TFSA$	174	568	190	2.9	0.01
9	$[C_3(NMe_2)_2(N(CH_2CH_2OCH_3)Me)]DCA$	251	548	202	2.7	0.02
10	$[C_3(NMe_2)_2(NBuH)]TFSA$	196	670	189	3.5	0.01
11	$[C_3(NMe_2)_2(NBuMe)]TFSA$	214	635	178	3.5	0.01
12	$[C_3(NMe_2)_2(NBuMe)]DCA$	278	548	193	2.8	0.03
13	$[C_3(NMe_2)_2(NPeH)]TFSA$	270	817	177	4.6	0.01
14	$[C_3(NMe_2)_2(NHexMe)]TFSA$	240	665	185	3.6	0.004
15	$[C_3(NEt_2)_2(NHBu)]TFSA$	254	834	170	4.9	0.001
16	$[C_3(NEt_2)_2(NHBu)]DCA$	788	993	162	6.1	0.002
17	$[C_3(NEt_2)_2(NHBu)]BF_4$	678	1131	165	6.9	0.004
	C_{2v}Cations					

18	$[C_3(NMe_2)_2(N(CH_2CHCH_2)_2)]$TFSA	193	602	184	3.3	0.004
19	$[C_3(NMe_2)_2(NPr_2)]$TFSA	491	616	188	3.3	0.03
20	$[C_3(NMe_2)_2(N(CH_2CH_2OCH_3)_2)]$TFSA	180	606	193	3.1	0.01
21	$[C_3(NMe_2)_2(NBu_2)]$TFSA	240	675	183	3.7	0.01
22	$[C_3(NMe_2)_2(NHex_2)]$TFSA	767	1125	162	6.9	0.003
23	$[C_3(NEt_2)_2(NHex_2)]$I	31	341	254	1.3	0.04
24	$[C_3(NEt_2)_2(NHex_2)]$OTf	1422	1425	156	9.1	0.001
	***C_{3h}* Cations**					
25	$[C_3(NEtMe_2)_3]$TFSA	219	670	171	3.9	0.01
26	$[C_3(NAllylMe_2)_3]$TFSA	218	637	181	3.5	0.01
27	$[C_3(NAllylMe)_3]$DCA	327	616	194	3.2	0.01
28	$[C_3(NMeCH_2CH_2OCH_3)_3]$TFSA	180	602	199	3.0	0.01
	***D_{3h}* Cations**					
29	$[C_3(NEt_2)_3][MeC_6H_4SO_3]$	386	883	199	4.4	0.001
30	$[C_3(NBu_2)_3]B(CN)_4$	324	813	181	4.5	0.3
31	$[C_3(NBu_2)_3]$FAP	994	1186	165	7.2	0.003

The T_o and B parameters of molar conductivity change with the cationic and anionic structures. The value of D ranged from 1 to 9 and the value of T_o ranged from 162 to 254 K, which are similar to the values obtained from ionic conductivity data. With the increase in the size of the cation and the anion, the value of B increases while T_o decreases and the fragility index (D) increases.

5.9 Ionicity

The "ionicity" (ionicity = unity)[36] of the ionic liquids is the property which is responsible for their characteristic low vapor pressure.[41] It is defined as a degree to which a liquid is comprised

of charged particles and behave as a collection of completely free ions.[36] If the ions forming ionic liquids remain in ion-pairs, the liquids would have a high vapor pressure and a poor conductivity.

There are different techniques to assess the ionicity of ionic liquids, including the Walden plot, the Nernst-Einstein equation (molar conductivity ratios obtained from measured diffusivities) and potentiometric titration (direct measurement).[36] In 1906, Walden concluded that for strong electrolyte solutions, the molar conductivity (Λ) is inversely proportional to viscosity (η) and directly proportional to the fluidity ($\phi = \eta^{-1}$). Recently, it has been shown that Walden's rule is applicable to ILs for examining the ion-pairing problem. In Walden's rule, viscosity and conductivity of the electrolyte is correlated. Later, Angell correlated ionic conductivity to viscosity using the following approach;

$$\Lambda\, \eta^{\alpha} = C$$

Angell plotted log Λ versus log η, by using a reference of dilute aqueous KCl solution with a unity slope. KCl displays an ideal behavior because there is no association between the ions. Dilute aqueous KCl solution is used as a standard electrolyte because of its similar values for the cation's and anion's molar conductivities.[37]

$$log\, \Lambda = log\, C + \alpha\, log\, 1/\eta$$

Where Λ is the molar conductivity in $Scm^2\ mol^{-1}$, η is the viscosity in P^{-1}, C is a temperature-dependent constant or Walden product and α is the slope of the line, reflecting decoupling of ions. The Walden product is inversely proportional to the ion size and directly proportional to viscosity and molar conductivity.

Table 5.17-Walden product, deviation form ideal line (ΔW) and slope (α).

	C_s Cations	Walden Product		ΔW at 20 °C	α
		20 °C	60 °C		
1	$[C_3(NMe_2)_2(HN(CH_2CH_2CH_3)]TFSA$	0.63	0.51	0.41	0.88
2	$[C_3(NMe_2)_2(HN(CH_2CHCH_2))]TFSA$	0.66	0.49	0.17	0.86
3	$[C_3(NMe_2)_2(N(CH_2CHCH_2)Me)]TFSA$	0.71	0.57	0.11	0.86
4	$[C_3(NMe_2)_2(N(CH_2CH_2CH_3)H)]TFSA$	0.57	0.48	0.17	0.89
5	$[C_3(NMe_2)_2(N(CH_2CH_2CH_3)Me)]TFSA$	0.69	0.57	0.11	0.88
6	$[C_3(NMe_2)_2(N(CH_2CH_2CH_3)Me)]DCA$	0.85	0.76	0.05	0.94
7	$[C_3(NMe_2)_2(N(CH_2CH_2OCH_3)H)]TFSA$	0.59	0.49	0.16	0.89
8	$[C_3(NMe_2)_2(N(CH_2CH_2OCH_3)Me)]TFSA$	0.65	0.58	0.13	0.89
9	$[C_3(NMe_2)_2(N(CH_2CH_2OCH_3)Me)]DCA$	0.79	0.64	0.07	0.89
10	$[C_3(NMe_2)_2(NBuH)]TFSA$	0.54	0.47	0.19	0.93
11	$[C_3(NMe_2)_2(NBuMe)]TFSA$	0.66	0.55	0.13	0.89
12	$[C_3(NMe_2)_2(NBuMe)]DCA$	0.79	0.68	0.07	0.90
13	$[C_3(NMe_2)_2(NPeH)]TFSA$	0.50	0.40	0.21	0.89
14	$[C_3(NMe_2)_2(NHexMe)]TFSA$	0.49	0.49	0.22	0.98
15	$[C_3(NEt_2)_2(NHBu)]TFSA$	0.51	0.39	0.21	0.88
16	$[C_3(NEt_2)_2(NHBu)]DCA$	1.03	0.76	0.01	0.89
17	$[C_3(NEt_2)_2(NHBu)]BF_4$	0.52	0.46	0.20	0.94
	C_{2v}Cations				
18	$[C_3(NMe_2)_2(N(CH_2CHCH_2)_2)]TFSA$	0.74	0.60	0.1	0.85
19	$[C_3(NMe_2)_2(NPr_2)]TFSA$	---	0.55	0.17(at 50 °C)	0.88
20	$[C_3(NMe_2)_2(N(CH_2CH_2OCH_3)_2)]TFSA$	0.59	0.49	0.16	0.88
21	$[C_3(NMe_2)_2(NBu_2)]TFSA$	0.61	0.53	0.15	0.91
22	$[C_3(NMe_2)_2(NHex_2)]TFSA$	---	0.31	0.38 (at 30 °C)	1.12
23	$[C_3(NEt_2)_2(NHex_2)]I$	---	0.52	0.01 (at 40 °C)	0.69

24	$[C_3(NEt_2)_2(NHex_2)]OTf$	0.19	0.25	0.45	1.12
	***C_{3h}* Cations**				
25	$[C_3(NEtMe_2)_3]TFSA$	0.65	0.56	0.15	0.89
26	$[C_3(NAllylMe_2)_3]TFSA$	0.56	0.47	0.18	0.89
27	$[C_3(NAllylMe)_3]DCA$	0.97	0.68	0.01	0.85
28	$[C_3(NMeCH_2CH_2OCH_3)_3]TFSA$	0.56	0.48	0.18	0.90
	***D_{3h}* Cations**				
29	$[C_3(NEt_2)_3][MeC_6H_4SO_3]$	0.26	0.31	0.41	1.07
30	$[C_3(NBu_2)_3]B(CN)_4$	0.62	0.56	0.15	0.69
31	$[C_3(NBu_2)_3]FAP$	0.39	0.43	0.29	1.03

Due to the partial association of ions within ionic liquids, they lie below the KCl ideal line. Ion-pairing results in the formation of neutral species which do not carry charge. While aggregates being charged and cannot move and thus decreases the conductivity without largely affecting viscosity. The decrease of ionicity results in deviation from the Nernst-Einstein Equation, which means that the distance from the ideal line increases. Any deviation from the ideal line is thought to indicate the lack of complete proton transfer (in protic ionic liquids)[34] or formation of neutral clusters or aggregates that cannot conduct (in aprotic ionic liquids).[42] Angell calculated such deviations by measuring the vertical distance to the KCl ideal line and denoted them as ΔW. The value for ΔW in the present study for triaminocyclopropenium ionic liquids ranged from 0.01 to 0.4.

Ionic liquids can be classified as nonionic (molecular), poor ILs, good ILs, and superionic. Those ionic liquids that lie near diagonal line are "good ionic liquids", below the diagonal line are "subionic" and above the diagonal line are "superionic". All the synthesized ionic liquids in the present study were "good ionic liquids" and are present just below the KCl standard line with a slope around 1.[41] This does not mean that they have no interest as solvents or reaction media.[43] Due to ion-pair association, their conductivity is lower than an ideal IL, which leads to lower viscosity and higher vapor pressure.[44] Generally speaking, they lie between a true IL and molecular solvents.[43]

For $[C_3(NMe_2)_2(NHex_2)]$TFSA, $[C_3(NEt_2)_2(NHex_2)_2]$OTf, $[C_3(NEt_2)_3][MeC_6H_4SO_3]$ and $[C_3(NBu_2)_3]$FAP, the slope is greater than 1 and the data lie above the ideal Walden KCl line. While for small tac-cations the slope is around 0.8. Those ILs lying above the ideal line are superionic as suggested by Angell.

With an increase in the size of the cation, the deviation from the ideal KCl line increases due to an increase in ion-pairing and lowered mobility. An increase in the size of the cation forces ions apart and prevents the small anion to interact with as many cations and so increases the electrostatic interaction with only one cation. The low ionicity suggested by the large ΔW values of the ionic liquids is due to high viscosity and lower conductivity. These tac cations have reasonably good ionicity combined with a large molecular weight compared to other ionic liquids. It suggests that these tac cations would have low vapor pressures. No symmetry dependency for ΔW values was seen.

With an increase of temperature, the ion-pairing increases and this affects the slope of the Walden plot causing a departure from ideal behavior.[45]

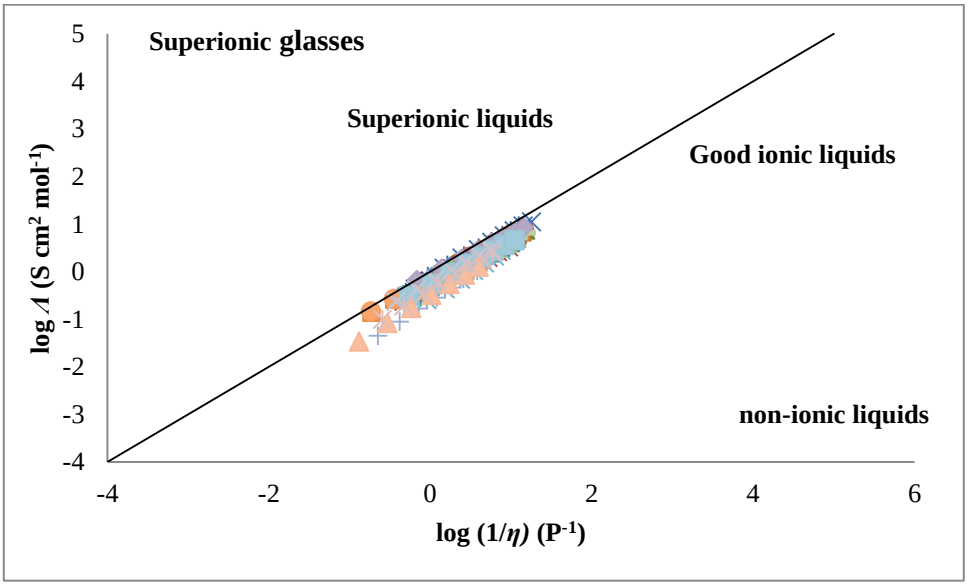

Figure 5.65-Walden plot

The Walden plot in fig. 5.65 shows all the ionic liquids presented in this thesis within a temperature range of 20 to 90 °C. The anion series for the triaminocyclopropenium, from least to most deviation from the reference KCl line is, DCA < TFSA < BF_4 < I < OTf.

Among the protic ionic liquids, the deviation in $[C_3(NMe_2)_2(HN(CH_2CH_3)]$TFSA is 0.41 at 20 °C, which is the largest seen among the other large protic ILs. It was thought that being a very small cation, it may have stronger hydrogen bonding with the anion.

Compared with other classes of ILs, the ionicity of triaminocyclopropeniums is very similar and all lie below the ideal line.[44] The linear behavior in the Walden plot shows that IL conductivity and viscosity are strongly coupled.[28]

The Walden plot described above is an unmodified form. Macfarlane used the modified Walden plot;

$$\Lambda = \boldsymbol{constant}\ \boldsymbol{\eta^{-1}} \left(\frac{\mathbf{1}}{\boldsymbol{r^{+}}} + \frac{\mathbf{1}}{\boldsymbol{r^{-}}}\right)$$

Where, r^+ and r^- are the cation and anion sizes respectively. Ion size has an influence on the Walden plot, which affects the "ideal" or "associated" behavior. Macfarlane constructed a Walden plot by plotting log molar conductivity *vs.* log $\eta^{-1}\left(\frac{1}{r^+} + \frac{1}{r^-}\right)$. This modified form reduced the effect on ΔW due to ion sizes.[44]

5.10 Specific Rotation

All the synthesized CILs were made from (*S*)-amino acids. (*R*)- and (*S*)-enantiomers both have identical NMR spectra, identical IR spectra, and identical physical properties except for optical rotation. Fortunately, if a plane-polarized light is passed through the solution of the specific configuration enantiomer, it rotates light in one direction, either right or left. But if the solution is a racemic mixture, light passes unrotated. Rotation of light to the right gives a positive value, while the rotation of light towards the left gives a negative value. The optical rotation α, is determined by polarimetry. The specific rotation $[\alpha]_D^{20}$ is determined using the following formula;

$$[\alpha]_D^{20} = \frac{\alpha}{c \times l}$$

Where α is the optical rotation, *c* is the concentration of solution in g/dm^3 and *l* is the path length of cell in dm. Usually, optical rotations are measured at 20 °C in ethanol or chloroform, and the light used is from a sodium lamp (*D* indicates that the λ = 589 nm).

Table 5.18-Optical rotation of AAILs

	C_s Cations	Mol wt of cation	$[\alpha]_D^{20}$
1	$[E_4Ala]MeSO_4$	268.37	−26.5° (c 3.4, EtOH)
2	$[E_4Ala]TFSA$	268.37	−31.2° (c 2.0, EtOH)
3	$[E_4Pro]MeSO_4$	294.41	−88.3° (c 0.6, H_2O)
4	$[E_4Pro]TFSA$	294.41	−42.5° (c 2.2, EtOH)
5	$[E_4Val]MeSO_4$	296.43	−0.6° (c 1.7, H_2O)
6	$[E_4Val]TFSA$	296.43	−16.5° (c 1.3, EtOH)
7	$[E_4Thr]MeSO_4$	298.40	−5.5° (c 2.7, H_2O)
8	$[E_4Thr]TFSA$	298.40	−18.1° (c 8.2, EtOH)
9	$[E_4Arg]TFSA_2$	353.48	+9.7° (c 1.9, CH_3CN)
10	$[E_4His]TFSA_2$	334.44	−1.4° (c 1.9, CH_3CN)
11	$[E_4Met]TFSA$	328.49	−28.6° (c 2.2, CH_3CN)
12	$[E_4Leu]TFSA$	310.45	−36.4°(c 1.4, CH_3CN)
13	$[E_4IIe]TFSA$	310.45	−20.9°(c 2.0, CH_3CN)
14	$[E_4Try]TFSA$	383.51	−29.9° (c 1.0, CH_3CN)
15	$[E_4Tyr]TFSA$	360.47	−11.5°(c 1.0, CH_3CN)
16	$[E_4Phe]TFSA$	344.47	−14.3°(c 1.5, CH_3CN)
17	$[E_4Ser]TFSA$	284.37	−6.9° (c 2.0, CH_3CN)
18	$[E_8Gln]TFSA_2$	325.42	−20.3°(c 1.5, CH_3CN)
19	$[E_8Lys]TFSA_2$	325.47	−4.3° (c 2.3, CH_3CN)

All the synthesized CILs gave either a positive (+) (*dextrorotatory enatiomers*) or a negative (−) (*laevorotatory enantiomers*) rotation, indicating chiral compounds. An (*S*)-CIL is equally as likely to be (+) or (−). Apart from $[E_4Arg]TFSA_2$, all other (*S*)-configuration CILs reported here show a negative optical rotation.

The amount of rotation depends on the nature of the four groups attached to the chiral carbon. The rotation generally increases with the increasing differences between the polarizabilities among the groups –COOH, -NH, alkyl (polar or non-polar alkyl side chains) and H functionalities are attached to the amino acid chiral carbon. They have different polarizabilities and are responsible for the optical rotation.[46] The $[\alpha]_D^{20}$ was measured in an aqueous medium for methyl sulphate based hydrophilic CILs and in ethanol or acetonitrile for the TFSA-based hydrophobic CILs. The solvent effect on the optical rotation reflects the interaction between the solute and the solvent. Thus, solute is capable of changing a chiral molecule's conformation in different solvents and thus comparison in different solvents cannot be made.[47]

The $[\alpha]_D^{20}$ value for CILs cannot be compared with the free amino acid because of the conformational changes in the structure of the amino acid result in a variation of the $[\alpha]_D^{20}$ values.[48]

5.11 ***pKa***

The *p*H of a solution only tells the acidity of the solution and this may vary with concentration. As we dilute an acid solution, acidity falls and *p*H increases. Thus, in order for better understanding of how strong or weak the acid is, we determine the strength of acid relative to water. Considering the following reaction;

$$AH + H_2O \rightleftharpoons A^- + H_3O^+$$

The equilibrium constant, K_{eq} for the above reaction is;

$$K_{eq} = \frac{[A^-][H_3O^+]}{[AH][H_2O]}$$

The concentration of water is constant thus the above equation becomes;

$$K_a = \frac{[A^-][H_3O^+]}{[AH]}$$

K_a, is the acidity constant. Thus in logarithmic form;

$$pK_a = -\log K_a$$

Thus, *p*Ka is the *p*H where the acid is exactly half dissociated. At *p*H above *p*Ka, the acid exists largely as A^-, while at *p*H below the *p*Ka, it exists largely as AH.

For all the synthesized CILs, *p*Ka was determined by acid-base titration with the help of a calibrated *p*H meter. For CILs having methyl sulphate as the anion, a known amount (0.01-0.1 g) was added to a 10 mL measuring flask and the volume was madeup with *Milli*-Q water. For TFSA salts, a known amount of CIL (0.01-0.1g) was dissolved in 1-2 mL of acetone and then the volume of 10 mL measuring flask was makeup with *Milli*-Q water. A standard 0.001M solution of NaOH was used to titrate against the 10 mL solution of CIL. The *p*Ka was calculated as *p*H at half equivalence point.

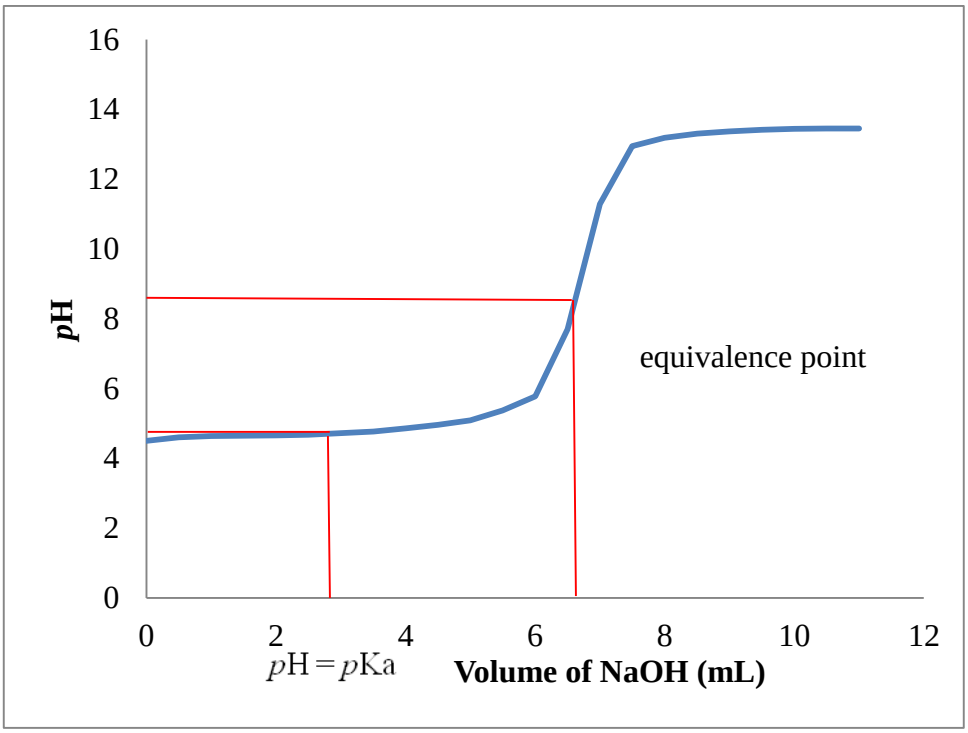

Figure 5.66-Titration curve for [E$_4$Ala]TFSA

The titration curve for a weak acid vs strong base at the start of curve usually shows a relatively rapid rise in *p*H and eventually slows down due to the presence of buffer solution containing weak acid and production of conjugate base. However, since my AAILs were a mixture of AAIL (weak acid) and zwitterion (conjugate base), the titration curves started from the buffer region (fig. 5.67).

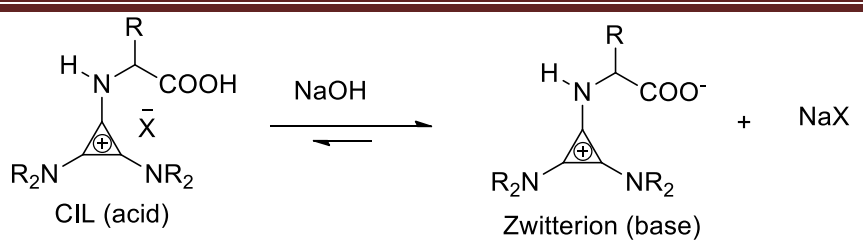

Figure 5.67-Equilibrium between IL and zwitterion by reaction with NaOH.

The *p*Ka of the AAILs ranged from 3.0 to 4.8 which is similar to other carboxylic acids.

For [E_4His]TFSA, the titration curve showed two half equivalence points (fig. 5.68). pKa_1 = 3.0 for the –COOH group while pKa_2 = 6.3 for the –NH group of the imidazole ring of histidine moiety.

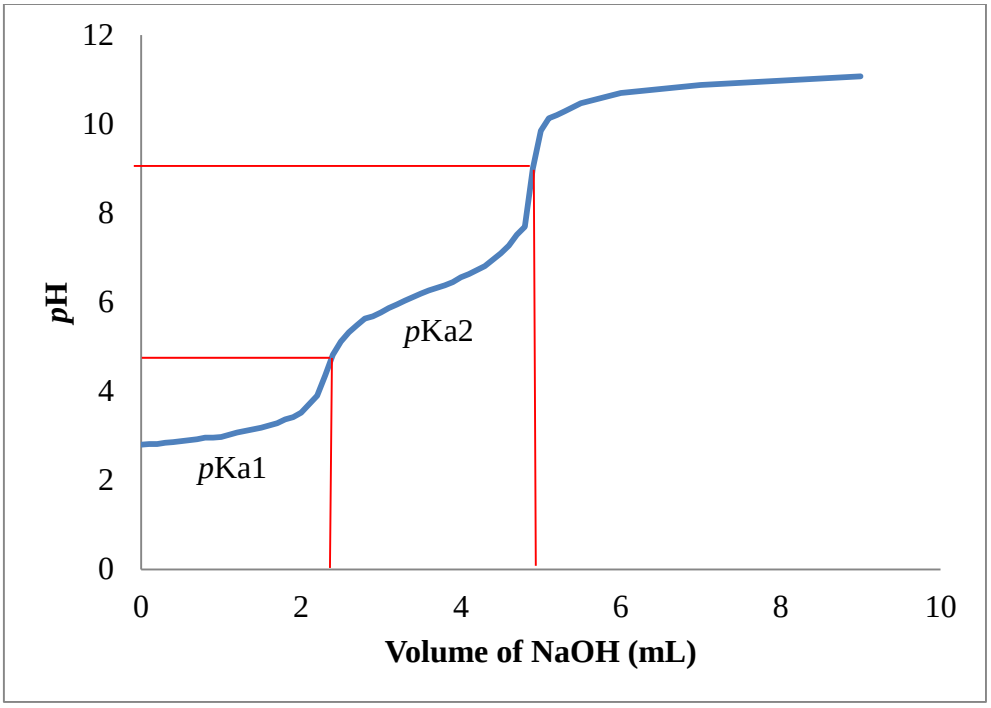

Figure 5.68–Titration curve for [E_4His]$TFSA_2$

The *pKa* values obtained for chiral cations with methyl sulphate (hydrophilic) as the anion were lower compared to the TFSA (hydrophobic) ones. This was thought to be due to the amount of acetone added to increase the solubility of the hydrophobic AAILs (TFSA ones).

*p*Ka values are tabulated in table 5.18. There is a marked increase in the pKa_1 values of AAILs compared to the protonated amino acids. This suggests weaker acidic behavior in the AAILs

compared with the amino acids. This is because the amino acid have an ammonium group two bonds from the carboxylic acid, whereas the AAILs have a delocalized positive charge three bonds from the carboxylic acid. Thus, AAILs behave as carboxylic acids.

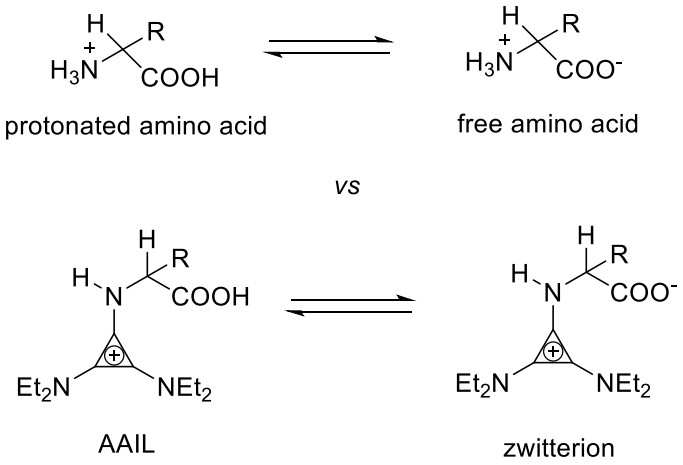

Figure 5.69–Comparison of equilibrium between amino acid (free and protonated form) and AAIL (IL and zwitterion form).

Table 5.19-Comparison of *p*Ka (±0.1) of AAIL and free amino acid.

	C_s Cations	*p*Ka$_1$ -COOH of CIL	*p*Ka$_2$ -NH_3^+ of CIL	*Free Amino Acid*	*p*Ka$_1$ -COOH of protonated Amino acid	*Δp*Ka
1	$[E_4Ala]MeSO_4$	3.2	---	Alanine (Ala)	2.3	0.8
2	$[E_4Ala]TFSA$	3.2	---	Alanine (Ala)	2.3	0.9
3	$[E_4Pro]MeSO_4$	2.9	---	Proline (Pro)	1.9	0.9
4	$[E_4Pro]TFSA$	4.4	---	Proline (Pro)	1.9	2.5
5	$[E_4Val]MeSO_4$	3.6	---	Valine (Val)	2.3	1.2
6	$[E_4Val]TFSA$	2.9	---	Valine (Val)	2.3	0.7
7	$[E_4Thr]MeSO_4$	3.9	---	Threonine (Thr)	2.1	1.9
8	$[E_4Thr]TFSA$	4.8	---	Threonine (Thr)	2.1	2.7
9	$[E_4Arg]TFSA$	3.5	---	Arginine (Arg)	2.2	1.3
10	$[E_4Asp]TFSA$	3.2	---	Aspartic acid (Asp)	2.0	1.2
11	$[E_4His]TFSA$	3.0	6.3	Histidine (His)	1.8	1.2
12	$[E_4Met]TFSA$	3.0	---	Methionine (Met)	2.3	0.7
13	$[E_4Leu]TFSA$	3.4	---	Leucine (Leu)	2.4	1.1
14	$[E_4IIe]TFSA$	3.5	---	Isoleucine (IIe)	2.4	1.1
15	$[E_4Try]TFSA$	3.6	---	Tryptophan (Try)	2.8	0.8
16	$[E_4Tyr]TFSA$	3.3	---	Tyrosine (Tyr)	2.2	1.1
17	$[E_4Phe]TFSA$	3.4	---	Phenylalanine (Phe)	1.8	1.5
18	$[E_4Ser]TFSA$	3.9	---	Serine (Ser)	2.2	1.7
19	$[E_8Gln]TFSA_2$	3.4	---	Glutamine (Gln)	2.2	1.2
20	$[E_8Lys]TFSA_2$	3.9	---	Lysine (Lys)	2.2	1.7

The *p*ka values for all the AAILs with hydrophobic TFSA anions were determined in 20% acetone-water to increase the solubility in water. In order to see the error in these *p*Ka values due

to the addition of acetone, *p*Ka values of acetic acid and benzoic acid were calculated. For acetic acid the *p*Ka values were determined in water (*p*Ka = 4.3), 10% acetone-water (*p*Ka = 4.5) and 20% acetone-water (*p*Ka = 4.5). The *p*Ka literature value for acetic acid is 4.76.[49] For water soluble-acetic acid the addition of acetone increased the *p*Ka value by 4.6%.

While, in case of hydrophobic benzoic acid, the *p*Ka values were determined in 30% acetone-water (*p*Ka = 3.9) and 40% acetone-water (*p*Ka = 4.2). It was again seen that with the increase in amount of acetone the *p*Ka values increased by 7.6% for hydrophobic benzoic acid.

5.12 Solubility/Miscibility Studies

Solubility/miscibility study gives a practical understanding about the polarity of ILs. This is important for the utilization of them in organic reactions. If the sample was solid, solubility studies were carried out and, if the sample was liquid, miscibility studies were carried out. In the case of solid samples, 0.1 g of the sample was taken and 1.5 mL of the dry solvent was added. If the solid dissolved, then it was considered soluble. If it formed a separate layer, then it was immiscible and, if it remained as a solid, then it was considered insoluble. For liquid samples, 0.5 mL of the sample was taken and 0.05 mL of dry solvent was added stepwise four times, followed by 0.1 mL three times, 0.25 mL twice, 0.5 mL twice, followed by 1 mL and 1.5 mL once. If the mixture was homogeneous, they are miscible and, if remained as separate layers, they are immiscible.

A broad range of solvents was selected to give a better understanding about the polarity of the triaminocyclopropenium based ILs. The solvents used were water, methanol, diethyl ether, toluene and hexane, from polar protic to non-polar solvents.

In table 5.20, N stands for not miscible or not soluble, while M stands for completely miscible or completely soluble. For most of the samples, a number is written to indicate miscibility percentage. For example the miscibility of ether, toluene and hexane in $[C_3(NMe_2)_2(NEtH)]$TFSA is M $\geq$ 50% IL. This means that 50% of IL and 50% of organic solvent are miscible. Upon further addition of organic solvent beyond 50%, separate layers form.

Table 5.20-Miscibility and solubility studies

	C_s Cations	Mol wt cation	H_2O	MeOH	Et_2O	Toluene	Hexane
1	$[C_3(NMe_2)_2(NEtH)]$TFSA	168.26	N	M	M ≥ 50% IL	M ≥ 50% IL	N
2	$[C_3(NMe_2)_2(NEtMe]$TFSA	182.29	N	M	N	N	N
3	$[C_3(NMe_2)_2(HN(CH_2CHCH_2))]$TFSA	180.27	N	M	M ≥ 50% IL	M ≥ 40% IL	N
4	$[C_3(NMe_2)_2(N(CH_2CHCH_2)Me)]$TFSA	194.30	N	M	M ≥ 50% IL	M ≥ 50% IL	N
5	$[C_3(NMe_2)_2(N(CH_2CHCH_2)Me)]$DCA	194.30	M	M	M ≥ 50% IL	M ≥ 50% IL	N
6	$[C_3(NMe_2)_2(N(CH_2CH_2CH_3)H)]$TFSA	182.29	N	M	M ≥ 40% IL	M ≥ 50% IL	N
7	$[C_3(NMe_2)_2(N(CH_2CH_2CH_3)Me)]$TFSA	196.31	N	M	M ≥ 50% IL	M ≥ 50% IL	N
8	$[C_3(NMe_2)_2(N(CH_2CH_2CH_3)Me)]$DCA	196.31	M	M	N	M ≥ 83% IL	N
9	$[C_3(NMe_2)_2(N(CH_2CH_2OCH_3)H)]$TFSA	198.29	N	M	M ≥ 40% IL	M ≥ 40% IL	N
10	$[C_3(NMe_2)_2(N(CH_2CH_2OCH_3)Me)]$TFSA	212.31	N	M	M ≥ 50% IL	M ≥ 50% IL	N
11	$[C_3(NMe_2)_2(N(CH_2CH_2OCH_3)Me)]$DCA	212.31	M	M	N	M ≥ 50% IL	N
12	$[C_3(NMe_2)_2(NBuH)]$TFSA	196.31	N	M	M ≥ 33% IL	M ≥ 50% IL	N
13	$[C_3(NMe_2)_2(NBuMe)]$TFSA	210.34	N	M	M ≥ 40% IL	M ≥ 50% IL	N
14	$[C_3(NMe_2)_2(NBuMe)]$DCA	210.34	M	M	N	M ≥ 50% IL	N
15	$[C_3(NMe_2)_2(NPeH)]$TFSA	210.34	N	M	M ≥ 33% IL	M ≥ 50% IL	N
16	$[C_3(NMe_2)_2(NPeMe)]$TFSA	224.37	N	M	M ≥ 40% IL	M ≥ 40% IL	N

17	$[C_3(NMe_2)_2(NHexMe)]TFSA$	238.39	N	M	M ≥ 25% IL	M ≥ 40% IL	N
18	$[C_3(NEt_2)_2(NHBu)]MeSO_4$	252.42	M	M	M ≥ 33% IL	M ≥ 40% IL	N
19	$[C_3(NEt_2)_2(NHBu)]TFSA$	252.42	N	M	M ≥ 50% IL	M ≥ 40% IL	N
20	$[C_3(NEt_2)_2(NHBu)]DCA$	252.42	N	M	N	M ≥ 33% IL	N
21	$[C_3(NEt_2)_2(NHBu)]BF_4$	252.42	N	M	N	M	N

		Mol wt cation	**H_2O**	**CH_3CN**	**CH_2Cl_2**	**$CHCl_3$**	**Et_2O**	**Toluene**	**Hexane**
22	$[E_4Ala]MeSO_4$	268.37	M	M	M	M	N	N	N
23	$[E_4Ala]TFSA$	268.37	N	M	M	M ≥ 50% IL	N	N	N
24	$[E_4Pro]MeSO_4$	294.41	M	M	M	M	N	N	N
25	$[E_4Pro]TFSA$	294.41	N	M	M	M	N	N	N
26	$[E_4Val]MeSO_4$	296.43	M	M	M	M	N	N	N
27	$[E_4Val]TFSA$	296.43	N	M	M	M	N	N	N
28	$[E_4Thr]MeSO_4$	298.40	M	M	M	M	N	N	N
29	$[E_4Thr]TFSA$	298.40	N	M	M	M	N	N	N
30	$[E_4Arg]TFSA$	353.48	N	M	N	N	N	N	N
31	$[E_4Asp]TFSA$	312.38	N	M	N	N	N	N	N
32	$[E_4His]TFSA$	334.44	N	M	N	N	N	N	N
33	$[E_4Met]TFSA$	328.49	M	M	M	M	N	N	N
34	$[E_4Leu]TFSA$	310.45	N	M	M	M	N	N	N

35	$[E_4IIe]TFSA$	310.45	N	M	M	M	N	N	N
36	$[E_4Try]TFSA$	383.51	N	M	M	N	N	N	N
37	$[E_4Tyr]TFSA$	360.47	N	M	M	N	N	N	N
38	$[E_4Phe]TFSA$	344.47	N	M	M	M	N	N	N
39	$[E_4Ser]TFSA$	284.37	N	M	M	N	N	N	N
40	$[E_8Gln]TFSA_2$	325.42	N	M	M	N	N	N	N
41	$[E_8Lys]TFSA_2$	325.47	N	M	M	M	N	N	N

	C_{2v}Cations	**Mol wt cation**	**H_2O**	**MeOH**	**Et_2O**	**Toluene**	**Hexane**
42	$[C_3(NMe_2)_2(NEt_2)]TFSA$	196.31	N	M	immiscible layer	N	N
43	$[C_3(NMe_2)_2(N(CH_2CHCH_2)_2)]TFSA$	220.33	N	M	M ≥ 40% IL	M ≥ 40% IL	N
44	$[C_3(NMe_2)_2(NPr_2)]TFSA$	224.37	N	M	M ≥ 71% IL	immiscible layer	N
45	$[C_3(NMe_2)_2(N(CH_2CH_2OCH_3)_2)]TFSA$	256.35	N	M	M ≥ 40% IL	M ≥ 40% IL	N
46	$[C_3(NMe_2)_2(NBu_2)]TFSA$	252.42	N	M	M ≥ 33% IL	M ≥ 50% IL	N
47	$[C_3(NMe_2)_2(NHex_2)]TFSA$	308.52	N	M	M	M ≥ 40% IL	N
48	$[(Et_2N)_2C_3(NH_2)]MeSO_4$	196.31	Not stable	M	N	N	N
49	$[(Et_2N)_2C_3(NH_2)]TFSA$	196.31	Not stable	M	immiscible layer	immiscible layer	N
50	$[C_3(NEt_2)_2(NBu_2)]I$	308.55	N	M	N	immiscible layer	N

51	$[C_3(NEt_2)_2(NHex_2)]I$	364.63	N	M	M ≥ 33% IL	M	N
52	$[C_3(NEt_2)_2(NHex_2)]OTf$	364.63	N	M	M	M	N

***C_{3h}* Cations**		**Mol wt cation**	**H_2O**	**MeOH**	**Et_2O**	**Toluene**	**Hexane**
53	$[C_3(NEtMe_2)_3]TFSA$	210.34	N	M	M ≥ 50% IL	M ≥ 40% IL	N
54	$[C_3(NAllylMe_2)_3]TFSA$	246.37	N	M	M ≥ 33% IL	M ≥ 40% IL	N
55	$[C_3(NAllylMe)_3]DCA$	246.37	N	M	N	M ≥ 56% IL	N
56	$[C_3(NMeCH_2CH_2OCH_3)_3]TFSA$	300.39	N	M	M ≥ 40% IL	M ≥ 40% IL	N

***D_{3h}* Cations**		**Mol wt cation**	**H_2O**	**MeOH**	**Et_2O**	**Toluene**	**Hexane**
57	$[C_3(NEt_2)_3]I$	252.42	N	M	N	N	N
58	$[C_3(NEt_2)_3]OTf$	252.42	M	M	M ≥ 25% IL	N	N
59	$[C_3(NEt_2)_3][MeC_6H_4SO_3]$	252.42	M	M	M ≥ 50% IL	N	N

		Mol wt cation	**H_2O**	**MeOH**	**CH_2Cl_2**	**$CHCl_3$**	**Et_2O**	**Toluene**	**Hexane**
60	$[E_6]F_5C_6O$	252	N	M	M	M	immiscible layer	immiscible layer	N

		Mol wt cation	**H_2O**	**MeOH**	**Et_2O**	**Toluene**	**Hexane**
61	$[C_3(NBu_2)_3]B(CN)_4$	420.59	N	M	M	M ≥ 50% IL	N
62	$[C_3(NBu_2)_3]FAP$	420.59	N	M	M	M ≥ 50% IL	N

Open ring Cations

63	$[(Me_2N)CCH_2C(NMe_2)]Cl_2$	214.35	M	M	N	N	N
64	$[(BuHN)_2CCH_2C(NHBu)_2]Cl_2$	326.56	M	M	N	N	N
65	$[(BuHN)_2CCH_2C(NHBu)_2]TFSA_2$	326.56	N	M	N	N	N

From the miscibility/solubility data, it is seen that the size of cation and anion are the two main factors responsible for affecting the polarity of the IL. The anions utilized were Cl^-, $MeSO_4^-$, DCA^-, OTf^-, $MeC_6H_4SO_3^-$, I^-, BF_4^-, $F_5C_6O^-$, $TFSA^-$, $B(CN)_4^-$ and FAP^-. The small size and hydrogen bonding interactions of the anions Cl^-, DCA^-, $MeSO_4^-$, OTf^-, and $MeC_6H_4SO_3^-$ with the solvent increase the solubility of the IL in polar protic solvents. In the case of bigger anions, (I^-, BF_4^-, $F_5C_6O^-$, $TFSA^-$, $B(CN)_4^-$ and FAP^-), the hydrophobic character increases which increases the solubility in non-polar solvents.

The size of the cation is another important factor affecting the solubility/miscibility studies. The anion trend discussed above can further be affected by the size of the cation. For small size cations the IL tends to be more hydrophilic even though the size of anion is larger (lipophilic). In case of $[C_3(NMe_2)_2(N(CH_2CHCH_2)Me)]DCA$, $[C_3(NMe_2)_2(N(CH_2CH_2CH_3)Me)]DCA$, $[C_3(NMe_2)_2(N(CH_2CH_2OCH_3)Me)]DCA$ and $[C_3(NMe_2)_2NBuMe]DCA$, all were completely soluble in water due to the small cation size. As the size of cation is increased to $[C_3(NEt_2)_2(NHBu)]DCA$ and $[C_3(NMeAllyl)_3]DCA$, the solubility in water is decreased. In other words, with the increase of cation size, the longer alkyl chains quantitatively increase the van der Waal forces, which dilute the ionic charge character and increase the hydrophobic character.

With an increase of the alkyl chain length of the protic C_s cation, $[C_3(NMe_2)_2(NHR)]TFSA$ from ethyl (M ≥ 50% IL in diethyl ether), allyl (M ≥ 50% IL in diethyl ether), propyl (M ≥ 40% IL in diethyl ether), $-CH_2CH_2OCH_3$ (M ≥ 40% IL in diethyl ether), butyl (M ≥ 33% IL in diethyl ether) and pentyl (M ≥ 33% IL in diethyl ether) the miscibility of the IL decreases in diethyl ether. However, the miscibility of $[C_3(NMe_2)_2(NHR)]TFSA$ in toluene does not vary with chain length from elthyl to pentyl (M ≥ 50% IL in toluene), almost remains the same. Except $[C_3(NMe_2)_2(NH(CH_2CHCH_2))]TFSA$ and $[C_3(NMe_2)_2(NH(CH_2CH_2OCH_3))]TFSA$ which are miscible ≥ 40% in toluene.

The presence of a small cation in $[C_3(NMe_2)_2(NMeEt)]TFSA$ makes it completely insoluble in diethyl ether and toluene. The miscibility of diethyl ether in the aprotic C_s cation series, $[C_3(NMe_2)_2(NRMe)]TFSA$ decreases as the alkyl chain length increases from allyl (M ≥ 50% IL), propyl (M ≥ 50% IL), $-CH_2CH_2OCH_3$ (M ≥ 50% IL), butyl (M ≥ 40% IL), pentyl (M ≥ 40% IL) and hexyl (M ≥ 25% IL). Swapping the anion from TFSA to DCA in

$[C_3(NMe_2)_2(NMe(CH_2CH_2CH_3))]DCA$, $[C_3(NMe_2)_2(NMe(CH_2CH_2OCH_3))]DCA$ and $[C_3(NMe_2)_2(NMeBu)]DCA$ makes them completely immiscible/insoluble with diethyl ether. While miscibility of $[C_3(NMe_2)_2(N(CH_2CHCH_2)Me)]DCA$ is ≥ 50% in diethyl ether due to the presence of the allyl chain. Similarly, the solubility/miscibility of toluene in $[C_3(NMe_2)_2(NMeR)]TFSA$ decreased with the increasing alkyl chain length from allyl (M ≥ 50% IL), propyl (M ≥ 50% IL), $-CH_2CH_2OCH_3$ (M ≥ 50% IL), butyl (M ≥ 50% IL), pentyl (M ≥ 40% IL) and hexyl (M ≥ 40% IL). The solubility/miscibility of DCA salts $[C_3(NMe_2)_2(NMe(CH_2CHCH_2))]DCA$, $[C_3(NMe_2)_2(NMe(CH_2CH_2OCH_3))]DCA$ and $[C_3(NMe_2)_2(NMeBu)]DCA$ almost remains ≥ 50% in toluene. However, a high miscibility observed is for $[C_3(NMe_2)_2(NMe(CH_2CH_2CH_3))]DCA$ (M ≥ 83%) in toluene. The solubility of $[C_3(NMe_2)_2(NMe(CH_2CH_2CH_3))]DCA$, $[C_3(NMe_2)_2(NMe(CH_2CH_2OCH_3))]DCA$ and $[C_3(NMe_2)_2(NMeBu)]DCA$ in aromatic toluene is greater as compared with diethyl ether due to π-π interactions. However, the polarity of both the solvents (toluene and diethyl ether) is similar.

$[C_3(NEt_2)_2(NBuH)]DCA$ and $[C_3(NEt_2)_2(NBuH)]BF_4$ are completely immiscible in diethyl ether due to the small anion. Upon further increasing the size of the anion from $[C_3(NEt_2)_2(NBuH)]MeSO_4$ to $[C_3(NEt_2)_2(NBuH)]TFSA$, the miscibility increases to ≥ 33% and ≥ 50% in diethyl ether, respectively. Similarly, the miscibility of $[C_3(NEt_2)_2(NBuH)]X$ increases in toluene with an increase in the size of the anion from $[C_3(NEt_2)_2(NBuH)]DCA$ (M ≥ 33% IL) to $[C_3(NEt_2)_2(NBuH)]MeSO_4$ (M ≥ 40% IL) to $[C_3(NEt_2)_2(NBuH)]TFSA$ (M ≥ 40% IL). However, $[C_3(NEt_2)_2(NBuH)]BF_4$ is completely miscibile with toluene.

The *Cs* cations, $[C_3(NMe_2)_2NHR]TFSA$ (R = ethyl, allyl, propyl, butyl, $-CH_2CH_2OCH_3$ and pentyl), $[C_3(NMe_2)_2NMeR]TFSA$ R = ethyl, allyl, propyl, butyl, $-CH_2CH_2OCH_3$ and pentyl), $[C_3(NEt_2)_2NBuH]TFSA$ and $[C_3(NEt_2)_2NBuH]BF_4$ were immiscible/insoluble in water in all proportions due to the presence of the hydrophobic TFSA anion. Whereas, $[C_3(NEt_2)_2NBuH]MeSO_4$ was completely miscible in water due to the presence of the hydrophilic methyl sulphate anion as well as the NH group.

For the AAILs, methyl sulphate salts were soluble in water, whereas the TFSA salts were not. The different functional groups on the side chain of the amino acids greatly influenced the solubility/miscibility in CH_2Cl_2 and $CHCl_3$. The miscibilities/solubilities of AAILs were intermediate between polar protic and halogenated solvents. Miscibility studies in methanol and ethanol were avoided due to tendency to form esters. $[E_4Ala]MeSO_4$, $[E_4Pro]MeSO_4$,

$[E_4Val]MeSO_4$ and $[E_4Thr]MeSO_4$ are completely soluble/miscible with water in all proportions. While, the AAILs as TFSA salts were completely immiscible/insoluble in water. All AAILs are immiscible/insoluble in diethyl ether, toluene and hexane. All AAILs are completely miscible/soluble in acetonitrile. The miscibility/solubility varied in dichloromethane and chloroform, dependent upon different functionalities on the side chains. Except for $[E_4Arg]TFSA$, $[E_4Asp]TFSA$ and $[E_4His]TFSA$, all AAILs were completely miscible/soluble in CH_2Cl_2. Except for $[E_4Arg]TFSA$, $[E_4Asp]TFSA$, $[E_4His]TFSA$, $[E_4Try]TFSA$, $[E_4Tyr]TFSA$, $[E_4Ser]TFSA$ and $[E_4Gln]TFSA$, the rest of AAILs were completely soluble/miscible in $CHCl_3$. The reduced number of miscible ILs in $CHCl_3$ *vs* CH_2Cl_2 is due to the lower polarity of $CHCl_3$.

$[C_3(NMe_2)_2(N(CH_2CH_3)_2)]TFSA$ has the smallest cation among the C_{2v} symmetry salts and formed an immiscible layer with diethyl ether and completely insoluble in toluene. Similar miscibility ($M \geq 40\%$ IL) is seen for $[(C_3(NMe_2)_2(N(CH_2CHCH_2)_2]TFSA$ and $[(C_3(NMe_2)_2(N(CH_2CH_2OCH_3)_2]TFSA$ in diethyl ether and toluene. The miscibility of diethyl ether in $[(C_3(NMe_2)_2(NPr_2)]TFSA$ is $M \geq 71\%$ IL but it formed an immiscible layer with toluene. While the miscibility of $[(C_3(NMe_2)_2(NBu_2)]TFSA$ in toluene ($M \geq 50\%$ IL) is more as compared to diethyl ether ($M \geq 33\%$ IL). $[(C_3(NMe_2)_2(NHex_2)]TFSA$ is completely miscible in diethyl ether. None of the $[C_3(NMe_2)_2(NR_2)]TFSA$ (ethyl, allyl, propyl, butyl, - $CH_2CH_2OCH_3$ and hexyl) was miscible/soluble in water.

The solubility/miscibility of $[(Et_2N)_2C_3(NH_2)]MeSO_4$ and $[(Et_2N)_2C_3(NH_2)]TFSA$ in water was not determined because both are not stable in water. $[(Et_2N)_2C_3(NH_2)]MeSO_4$ was miscible in neither diethyl ether nor toluene. However, upon exchanging the anion to TFSA, $[(Et_2N)_2C_3(NH_2)]TFSA$ formed an immiscible layer with diethyl ether and toluene.

As the size of cation is increased from $[C_3(NEt_2)_2(NBu_2)]I$ (not soluble) to $[C_3(NEt_2)_2(NHex_2)]I$ ($M \geq 33\%$ IL) the miscibility/solubility in diethyl ether increases. Similarly, $[C_3(NEt_2)_2(NBu_2)]I$ forms an immiscible layer in toluene whereas $[C_3(NEt_2)_2(NHex_2)]I$ is completely miscible with toluene. Increasing the size of the anion from $[C_3(NEt_2)_2(NHex_2)]I$ ($M \geq 33\%$ IL) to $[C_3(NEt_2)_2(NHex_2)]OTf$ (completely miscible) increases the miscibility in diethyl ether. $[C_3(NEt_2)_2(NHex_2)]OTf$ is completely miscible in toluene, as $[C_3(NEt_2)_2(NHex_2)]I$, due to long hexyl chains. None of $[C_3(NEt_2)_2(NBu_2)]I$, $[C_3(NEt_2)_2(NHex_2)]I$ and $[C_3(NEt_2)_2(NHex_2)]OTf$ are miscible or soluble in water.

Among the *C3h* cations, with as increase in the size of the cation from $[C_3(NEtMe_2)_3]$TFSA (M ≥ 50%) to $[C_3(NAllylMe_2)_3]$TFSA (M ≥ 33%) to $[C_3(NErMe_2)_3]$TFSA (M ≥ 40%), the miscibility in diethyl ether decreases, whereas the miscibility in toluene remains constant at ≥ 40%. In contrast to $[C_3(NAllylMe_2)_3]$TFSA, the DCA salt is not miscible in diethyl ether but is miscible in toluene to ≥ 56%. None of the *C3h* symmetry cation salts are miscible in water.

In the *D3h* cation $[C_3(NEt_2)_3]^+$, as the size of the anion increases from I^- (not miscible) to OTf^- (M ≥ 25%) to OTs^- (M ≥ 50%), the miscibility/solubility increases in Et_2O. $[C_3(NEt_2)_3]F_5C_6O$ forms an immiscible layer with diethyl ether and toluene. None of $[C_3(NEt_2)_3]I$, $[C_3(NEt_2)_3]OTf$ or $[C_3(NEt_2)_3]OTs$ is miscible or soluble in toluene. $[C_3(NEt_2)_3]I$ and $[C_3(NEt_2)_3]F_5C_6O$ are not soluble in water, whereas $[C_3(NEt_2)_3]OTf$ and $[C_3(NEt_2)_3]OTs$ are completely miscible in water.

With an increase in the size of the cation from $[C_3(NEt_2)_3]^+$ to $[C_3(NBu_2)_3]^+$, the miscibility/solubility in the diethyl ether/toluene is increased due to longer alkyl chains. $[C_3(NBu_2)_3]B(CN)_4$ and $[C_3(NBu_2)_3]FAP$ are completely miscible in diethyl ether, although no more than 50% of these ILs are miscible in toluene. $[C_3(NBu_2)_3]B(CN)_4$ and $[C_3(NBu_2)_3]FAP$ are completely insoluble/immiscible in water.

In the open ring compounds, as the size of the cation increases from $[(Me_2N)_2CCH_2C(NMe_2)_2]Cl_2$ to $[(BuHN)_2CCH_2C(NHBu)_2]Cl_2$ not much difference in solubility/miscibility is seen. This may be because the latter is a protic IL. Both are miscible/soluble in water but insoluble/immiscible in toluene and diethyl ether. However, with the increase in size of the anion from Cl^- to $TFSA^-$ in $[(BuHN)_2CCH_2C(NHBu)_2]TFSA_2$ the hydrophobic character is increased. All open ring salts, $[(Me_2N)_2CCH_2C(NMe_2)_2]Cl_2$, $[(BuHN)_2CCH_2C(NHBu)_2]Cl_2$ and $[(BuHN)_2CCH_2C(NHBu)_2]TFSA_2$ are soluble in methanol, whereas none of them are miscible/soluble in diethyl ether, toluene and hexane.

All of the ILs I studied, $[C_3(NMe_2)_2(NHR)]$TFSA, $[C_3(NMe_2)_2(NMeR)]X$ (X = TFSA and DCA), [C3(NEt2)2(NHBu)]X (X = $MeSO_4$, TFSA, DCA and BF_4), [E_4Amino Acid]X (X = TFSA and $MeSO_4$), $[C_3(NMe_2)_2(NR_2)]$TFSA, $[C_3(NEt_2)_2NR_2)]X$ (X = MeSO4, TFSA, I and OTf), $[C_3(NMeR)_3]X$ (TFSA and DCA), $[C_3(NEt_2)_3]X$ (X = I, OTf, OTs and F_5C_6O) and $[C_3(NBu_2)_3]X$ (X = $B(CN)_4$ and FAP) are immiscible/insoluble in hexane . Except for the AAILs, all the ILs are completely soluble/miscible in methanol.

5.13 X-Ray Crystallography

The crystal data and X-ray experimental details for three fully-refined structures are discussed in this thesis. Throughout the text, selected bond lengths and angles are discussed while the remaining distances and angles, as well as the coordinates, anisotropic displacement parameters and hydrogen atom coordinates are in the appendix.

X-ray diffraction data for single crystals of $[C_3(NHC_6H_5)_3]$TFSA, $[C_3(NEt_2)_3]FeCl_4$ and $[HC_3(NMe_2)_4]Cl.CHCl_3$ were collected. Table 5.20 gives the crystal data and structure refinement parameters for all X-ray structures. Data collection was performed and the unit cell was initially processed using the CrysAlisPro software package (Version 1.171.35.19). Empirical absorption corrections were applied using the SCALE3 ABSPACK scaling algorithm. The hydrogens of the nitrogen atoms were found in the difference map and their positions were refined with $U_{iso}(H) = 1.2U_{eq}$ (N) at a fixed distance of 0.86 Å. All other H atoms were introduced in calculated positions as riding atoms at calculated positions and $U_{iso}(H) = 1.2U_{eq}(C)$. All non-hydrogen atoms were refined anisotropically. Disordered atoms with the same connectivity were refined with the same thermal parameters (EADP) in $[C_3(NHC_6H_5)_3]$TFSA. The ratio of the disordered elements were allowed to refine before being fixed at 50:50

Single crystals were grown from the neat liquid. A suitable crystal was selected and mounted in a nylon loop in perfluoronated oil on a SuperNova, Dual, Cu at zero, Atlas diffractometer. The crystal was kept at 282.67(10) K during data collection. Using Olex2[50], the structure was solved with the XS[51] structure solution program using Direct Methods and refined with the XL[51] refinement package using Least Squares minimisation.

5.13.1 Crystal Structure of $[C_3(NHPh)_3]$TFSA

The asymmetric unit of $[C_3(NHC_6H_5)_3]$TFSA consists of half a cation disordered over two positions in a 50:50 ratio, and half an anion. The cyclopropenium ring C-C bonds are short with bond lengths in the range 1.368(5) to 1.392(5) Å, compared to the C-C bond distance of 1.363 Å in benzene. This shortening in the C-C ring bonds is due to "bent" bonds. The exocyclic C–N bonds lie in the range of 1.319(4) to 1.335(4) Å, which is intermediate between a C-N (1.47 Å) and a C=N bond (1.29 Å) due to π donation. The delocalization of the lone pair of electrons of the nitrogen atoms into the cyclopropenium rings accounts for the shortening of the exocyclic C-N bond. The sp hybridization of the ring carbon atoms is also partly responsible for the shortening of the exocylic C-N bonds. In $[C_3(NHC_6H_5)_3]$TFSA, the αC-N bond between the nitrogen atom and the benzyl ring is shorter (1.417(11) to 1.433(7) Å) than aniline C-N bond (1.431 Å) due to extension of delocalized cyclopropenium ring onto the nitrogen atoms. The

benzene ring C-C bond lengths ranged from 1.258(15) to 1.537(16) Å due to the distorted structure.

Table 5.21-Crystal data and structure refinement details

Identification code	RY1a	RYU13a	RYU14a
Empirical formula	$C_{46}H_{36}F_{12}N_8O_8S_4$	$C_{13}H_{27}Cl_7N_4$	$C_{15}H_{30}Cl_4FeN_3$
Formula weight	1185.07	487.53	450.07
Temperature/K	282.67(10)	120.02(10)	120.02(10)
Crystal system	monoclinic	monoclinic	orthorhombic
Space group	C2/c	C2/c	$P2_12_12_1$
a/Å	12.4325(5)	19.1426(4)	9.1118(3)
b/Å	15.5058(6)	9.7345(2)	14.4278(4)
c/Å	16.9596(7)	13.1140(3)	16.9451(7)
α/°	90.00	90	90
β/°	131.587(2)	108.805(2)	90
γ/°	90.00	90	90
Volume/$Å^3$	2445.34(17)	2313.27(9)	2227.67(13)
Z	2	4	4
$\rho_{calc}mg/mm^3$	1.609	1.400	1.342
m/mm^{-1}	2.767	7.878	9.848
F(000)	1208.0	1008.0	940.0
Crystal size/mm^3	0.2712 × 0.2421 × 0.1804	0.2566 × 0.2213 × 0.0659	0.2732 × 0.1612 × 0.0174
Radiation	Cu Kα (λ = 1.5418)	Cu Kα (λ = 1.5418)	Cu Kα (λ = 1.5418)
2Θ range for data collection	9.14 to 136.98°	9.762 to 147.894°	8.048 to 147.73°
Index ranges	$-14 \le h \le 9$, $-12 \le k \le 18$, $-19 \le l \le 20$	$-23 \le h \le 23$, $-12 \le k \le 11$, $-16 \le l \le 16$	$-10 \le h \le 11$, $-17 \le k \le 17$, $-20 \le l \le 18$
Reflections collected	5746	17410	12072
Independent reflections	2176 [R_{int} = 0.0349, R_{sigma} = 0.0312]	2335 [R_{int} = 0.0380, R_{sigma} = 0.0163]	4181 [R_{int} = 0.0480, R_{sigma} = 0.0502]
Data/restraints/parameters	2176/3/240	2335/0/114	4181/0/215
Goodness-of-fit on F^2	1.046	1.078	1.080
Final R indexes [I>=2σ (I)]	R_1 = 0.0379, wR_2 = 0.0963	R_1 = 0.0402, wR_2 = 0.1006	R_1 = 0.0384, wR_2 = 0.0916
Final R indexes [all data]	R_1 = 0.0424, wR_2 = 0.1012	R_1 = 0.0429, wR_2 = 0.1031	R_1 = 0.0483, wR_2 = 0.0984
Largest diff. peak/hole / e $Å^{-3}$	0.27/-0.39	0.58/-0.57	0.56/-0.37
Flack parameter			0.200(7)

The nitrogens are positioned evenly with the two exocyclic C-C-N angles for each nitrogen being approximately equal. The internal angles are close to 60° while the exocyclic C-N bonds are close to 150°. Thus, the nitrogen atoms are close to planar due to their sp^2 hybridization; the sum of angles around each nitrogen ranged from 355.6 to 359.9°.

One molecule of $[C_3(NHC_6H_5)_3]$TFSA is shown with the disorder in the cation removed. The TFSA is present in the *trans* configuration, which is its lowest energy conformation.[52]

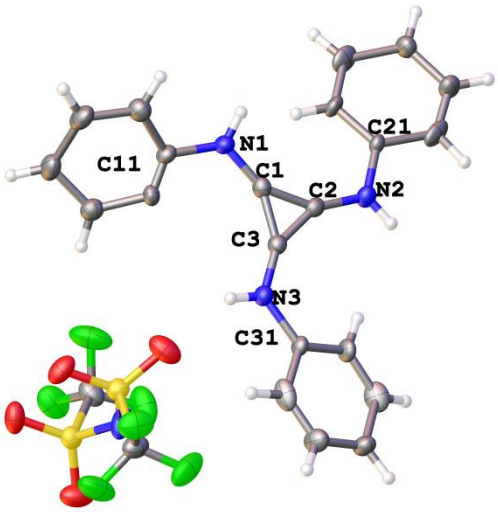

Figure 5.70-One molecule of $[C_3(NHC_6H_5)_3]$TFSA by OLEX-2

5.13.2 Crystal Structure of $[C_3(NEt_2)_3]FeCl_4$

In $[C_3(NEt_2)_3]FeCl_4$, the C-C and exocyclic C-N bond lengths ranged from 1.377(4) to 1.391(5) Å and 1.326(4) to 1.336(4) Å, respectively. These bond lengths are essentially the same as those found in $[C_3(N^iPr_2)_2(NMe_2)]ClO_4$ (ring C-C = 1.373 Å and exocyclic C-N = 1.330 Å) and $[C_3(NC_5H_{10})_3]^+$ (ring C-C = 1.381 Å and exocyclic C-N = 1.333 Å).[53] The bond length of N to α-C is again short and ranged from 1.460(4) to 1.473(4) Å due to back donation of electron charge density from the nitrogen to the ring. Almost similar ring C-C and exocyclic C-N bond lengths were found for $[C_3(NHPh)_3]$TFSA and $[C_3(NEt_2)_3]FeCl_4$.

The C_3N_3 core and nitrogen substituents are planar to maximize the π-donation into the C_3 ring.[53] The substituents on N(3) and N(14) show some deviation with one substituent bent onto one side while the other substituent is bent onto the other side of the ring. While, the substituents on N(1) are both bent onto same side of the ring. This is thought to be due to possible rotation about the exocyclic C-N bond. Thus, the torsion angle at N(14) is C8-N14-C6-C4 = 6.4(8)° and C7-N14-

C6-C2 = −3.5(8)°, while at at N(3) is C11-N3-C2-C6 = 2.0(8)° and C9-N3-C2-C4 = −6.0(8)°. However, the dihedral angle at N(1), C18-N1-C4-C2 = 2.5(8)° and C5-N1-C4-C6 = 10.2(8)° is larger than at N(14) and N(3). Again the range of sum of angles around each nitrogen is 359.3 to 359.7°.

The asymmetric unit of $[C_3(NEt_2)_3]FeCl_4$ consists of one cation and one anion.

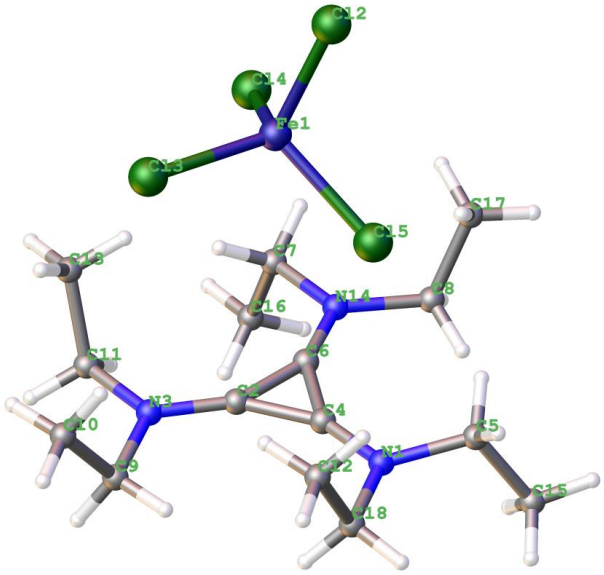

Asymmetric unit of $[C_3(NEt_2)_3]FeCl_4$ with atomic numbering scheme by OLEX-2

5.13.3 Crystal Structure of $[C_3(NMe_2)_4]Cl$

$[HC_3(NMe_2)_4]Cl.2CH_3Cl$ consists of an allylium unit, with two Me_2N groups at each of the external carbons connected through the nitrogen atom. The C2-C3-C2 bond angle is 126.5° showing the presence of unsaturated bonds due to an allyl unit similar to $[C_3H(NH^tBu)_4]^+$.[54] The sum of angles around the central C(3) which carries a single hydrogen is close to 360° (126.5°+116.7°+116.7°) and has a trigonal coordination. The outer carbons C(2) are also trigonal. Similarly, the sum of angle around C(2), N(4) and N(5) is 359.9, 356.3 and 359.7°, respectively. The dihedral angle for N5-C2-C3-C2 and N4-C2-N5-C1 are 30.9° and 31.7° respectively. In the same way the dihedral angle for H3-C3-C2-N4 and H3-C3-C2-N5 is 29.2° and 30.9°, respectively. The C-C bond lengths are 1.405 Å showing allyl character similar to $[C_3H(NH^tBu)_4]^+$.[54] The C-N bond lengths of the amidinium system range from 1.353 to 1.358(3) Å, similar to those found in $[C_3H(NH^tBu)_4]^+$ (C-N = 1.36 Å average).[54]

The electron delocalization is extended over the seven atoms N_2CCCN_2 and the C-C and C-N bond lengths are all shorter than normal single bonds. The C2-N4 bond length is 1.358(3)Å in

CN_2 core is longer than C2-N5 bond length 1.3532 Å.[55] These are also short due to back-bonding from the nitrogen atoms which reduces the positive charge on the electropositive carbon atoms. The dihedral angle for C3-C2-N5-C6 and C3-C2-N4-C9 is 23.5° and 17.7°, respectively. The asymmetric unit consist of one cation, one anion and two chloroform molecules.

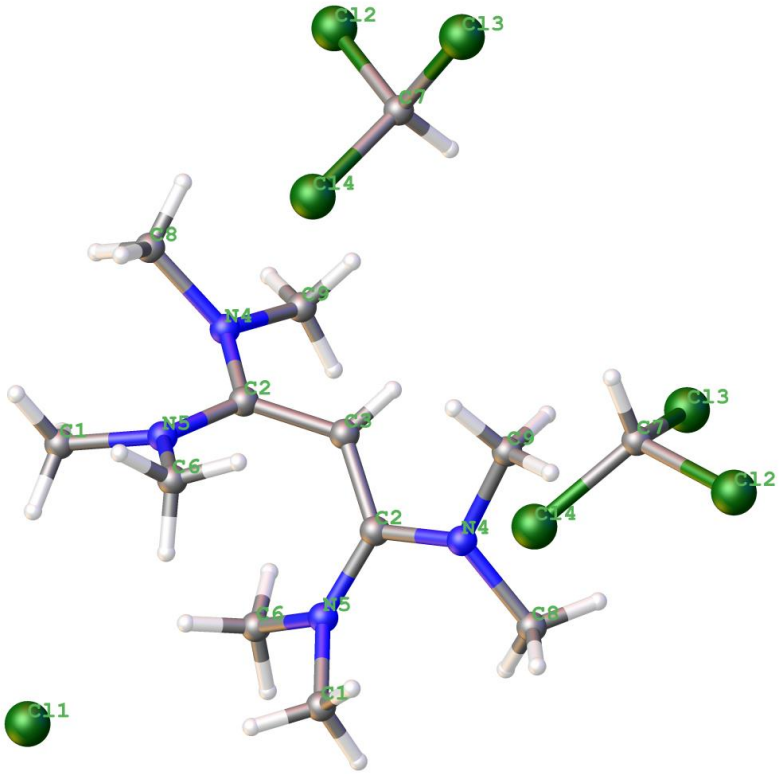

Figure 5.74-One molecule of $[C_3(NMe_2)_4]Cl$ by OLEX-2 with labelled atoms.

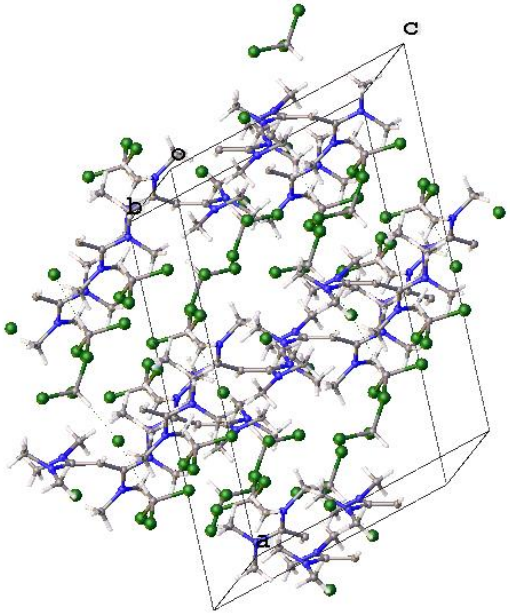

Figure 5.75-Unit cell of [$C_3(NMe_2)_4$]Cl by OLEX-2

In [$C_3(NMe_2)_4$]Cl.2CH_3Cl a chloride-chloroform cluster formed. Previously, chloride-chloroform clusters with weak hydrogen and chloride bondings are fully characterized by x-ray diffraction.[56] In the present work a weak C-H.....Cl^- bonding in [$Cl^-(CHCl_3)_2$] cluster anion was observed where the Cl^- ion is involved in the hydrogen bonding with the two chloroform molecules forming chloride cluster bridges.

Conclusions

The chloride and water content in ILs have a large impact on their physicochemical properties. High chloride content increases viscosity and decreases conductivity. Whereas, high water content decreases viscosity and increases conductivity. ILs with anions DCA and $MeSO_4$ have high chloride and high water content compared to TFSA ones.

The thermal stabilities of the triaminocyclopropenium salts ranged for 1 °C min^{-1} from 132 ([E_8Gln]$TFSA_2$) to 296 °C ([$C_3(NEt_2)_2$(NBuH)]TFSA and [$C_3(NEt_2)_2(NBu_2)$]I), while for 10 °C min^{-1} they ranged from 161 ([E_4Ser]TFSA) to 366 °C ([$C_3(NEtMe)_3$]TFSA). Thermal stabilities compare very well with other classes of ILs. The thermal stabilities in the present thesis are around 300 °C at 10 °C min^{-1}, this range is less than previously large tac-based ILs (over 400 °C) synthesized by Curnow group.

DSC results for the triaminocyclopropenium salts gave glass transition temperatures, solid-solid transitions and melting points. For most of the room temperature triaminocyclopropenium ILs glass transition temperatures were obtained, ranging from −85.7 °C ($[C_3(NEt_2)_2(NBuH)]$TFSA) to 0.32 °C ($[E_4Tyr]$TFSA). The melting points for the tac ILs ranged from −53.7 °C ($[C_3(NMe_2)_2(N(CH_2CHCH_2)Me)]$TFSA) to 94.2 °C ($[C_3(NEt_2)_2(NH_2)]$TFSA). Some of the tac-based ILs showed multiple solid-solid transitions before melting. The glass transition temperatures observed for my small size tac cations are higher compared to large size tac cations (−89 to −6 °C) synthesized by Curnow group.

The viscosity of triaminocyclopropeniums ranged from 67.4 mPa s ($[C_3(NMe_2)_2(NBuMe)]$DCA) at 20 °C to 884.7 mPa s ([E4Thr]TFSA) at 75 °C. Even though the viscosity observed for $[C_3(NMe_2)_2(NBuMe)]$DCA is still higher than previously low viscous $[C_3(NEt_2)_3]$DCA (64.2 mPa s) IL. The size of the cation and the anion had large effect on viscosities. For the AAILs viscosity increase was due to increased hydrogen bonding interactions. The viscosity data was fitted to Arrhenius and VFT equations.

A fragility plot was made for the ILs where viscosity and calorimetric glass transition temperatures were obtained. All the triaminocyclopropenium ILs were classified as “fragile” liquids and were found in the same region on plot like previously synthesized tac cations.

The ionic conductivity for the triaminocyclopropenium ILs at 20 °C ranged from 137 μS cm^{-1} ($[C_3(NEt_2)_2(NHex_2)]$I) to 4.38 mS cm^{-1} ($[C_3(NMe_2)_2(NBuMe)]$DCA). Molar conductivity was also calculated to estimate the contribution of ion mobility towards ionic conductivity. Both the cation and anion sizes affect conductivity. The high conductivity observed in present thesis for $[C_3(NMe_2)_2(NMeBu)]$DCA is still low than previously synthesized $[C_3(NEt_2)_3]$DCA (4.67 mS cm^{-1} at 20 °C). Like visocisty data, the conductivity data was also fitted for Arrhenius and VFT equations.

The density for tac-type ILs ranged at 20 °C from 0.928 ($[C_3(NBu_2)_3]B(CN)_4$) to 1.401 g mL^{-1} ($[C_3(NMe_2)_2(NEtH)]$TFSA). The density observed for ($[C_3(NMe_2)_2(NEtH)]$TFSA is high compared to previously synthesized $[C_3(NEt_2)_3]$TFSA (1.277 g mL^{-1} at 20 °C). Density increased with the increase in cation size and vice versa. Molar volume and molar concentrations were calculated at 20 °C. The fitting parameters for linear best-fit of the density were also calculated.

The ionicity for all the triaminocyclopropenium ILs were calculated with the help of a Walden plot. All triaminocyclopropenium ILs were classified as 'good ionic liquids' because they fell just below the KCl standard line.

For the AAILs, optical rotation and *p*Ka values were calculated. The *p*Ka values ranged from 2.97 to 4.79. These *p*Ka values are higher than protonated amino acids but are similar to other carboxylic acids.

The solubility and miscibility studies of triaminocyclopropenium ILs were studied in a range of different solvents (water, methanol, acetonitrile, dichloromethane, chloroform, diethyl ether, toluene and hexane). ILs with small anions are hydrophilic compared to large hydrophobic anions. None of the IL is miscible/soluble in hexane.

Finally, crystal structures of $[C_3(NPhH)_3]$TFSA, $[C_3(NEt_2)_3]FeCl_4$ and $[HC_3(NMe_2)_4]Cl.2CH_3Cl$ were reported. The $[C_3(NPhH)_3]$TFSA and $[C_3(NEt_2)_3]FeCl_4$ structures are compared well with already reported structures. Similarly, the bond lengths and the bond angles of $[HC_3(NMe_2)_4]Cl.2CH_3Cl$ compared well with $[HC_3(NH^tBu)_4]^+$.

References

1. Bratovcic, A.; Odobasic, A., *Determination of Fluoride and Chloride Contents in Drinking Water by Ion Selective Electrode*. 2011.
2. Dietrich, A. *Am. Lab.* **1994,** *36*.
3. Endres, F.; Abbot, A. P.; Macfarane, D. R., *Electrodeposition from Ionic Liquids*. WILEY-VCH: 2008; p 47.
4. Navarro, P.; Larriba, M.; Rojo, E.; García, J. n.; Rodríguez, F. *J. Chem. Eng. Data* **2013,** *58*, 2187.
5. Holbrey, J. D.; Rogers, R. D., *Ionic Liquid in Synthesis*. Wiley-VCH: 2008; p 57.
6. Ngo, H. L.; LeCompte, K.; Hargens, L.; McEwen, A. B. *Thermochim. Acta* **2000,** *357-358*, 97.
7. MacFarlane, D. R.; Pringle, J. M.; Johansson, K. M.; Forsyth, S. A.; Forsyth, M. *Chem. Commun.* **2006**, 1905.
8. Wooster, T. J.; Johanson, K. M.; Fraser, K. J.; MacFarlane, D. R.; Scott, J. L. *Green Chem.* **2006,** *8*, 691.

9. Greaves, T. L.; Drummond, C. J. *Chem Rev.* **2008,** *108*, 206.
10. Kagimoto, J.; Ohno, H., Ionic Liquids Derived from Natural Resources. In *Ionic Liquids UnCOILed: Critical Expert Overviews*, First Edition ed.; Plechkova, N. V.; Seddon, K. R., Eds. John Wiley & Sons, Inc.: 2013.
11. Tokuda, H.; Hayamizu, K.; Ishii, K.; Susan, M. A. B. H.; Watanabe, M. *J. Phys. Chem. B* **2005,** *109*, 6103.
12. Walst, K. J. Synthesis and Characterization of Triaminocyclopropenium as a New Class of Ionic Liquids. PhD Thesis, University of Canterbury, Christchurch, 2013.
13. Leng, Y., *Materials Charaterization Introduction to Microscopic and Spectroscopic Methods*. John Wiley & Sons (Asia) Pte Ltd: Hong Kong, 2008; p 301.
14. Fujii, K.; Nonaka, T.; Akimoto, Y.; Umebayashi, Y.; Ishiguro, S.-i. *Ananlytical Sci.* **2008,** *24*, 1377.
15. Fujii, K.; Fujimori, T.; Takamuku, T.; Kanzaki, R.; Umebayashi, Y.; Ishiguro, S.-i. *The Journal of Physical Chemistry B* **2006,** *110*, 8179.
16. Chen, Z. J.; Xue, T.; Lee, J.-M. *RSC Advances* **2012,** *2*, 10564.
17. Tao, G.-h.; He, L.; Sun, N.; Kou, Y. *Chem. Communications (Cambridge, England)* **2005,** (28), 3562.
18. Rahman, M. B. A.; Jumbri, K.; Basri, M.; Abdulmalek, E.; Sirat, K.; Salleh, A. B. *Molecules* **2010,** *15*, 2388.
19. Belieres, J.-P.; Angell, C. A. *J. Phys. Chem. B* **2007,** *111*, 4926.
20. Kunkel, H.; Maas, G. *Eur. J. Org. Chem.* **2007**, 3746.
21. Kulkarni, P. S.; Branco, L. C.; Crespo, J. G.; Nunes, M. C.; Raymundo, A.; Afonso, C. A. M. *Chem. Eur.J.* **2007,** *13*, 8478.
22. MacFarlane, D. R.; Forsyth, S. A.; Golding, J.; Deacon, G. B. *Green Chemistry* **2002,** *4*, 444.
23. Sirjoosingh, A.; Alavi, S.; Woo, T. K. *J. Phys. Chem. B* **2009,** *113*, 8103.
24. Brennecke, J. F.; Rogers, R. D.; Seddon, K. R., *Ionic Liquids VI Just Not Solvents Anymore*. ACS: 2007; p 320.
25. Fitchett, B. D.; Knepp, T. N.; Conboy, J. C. *J. Electrochem. Soc.* **2004,** *151* (7), E219.
26. Sun, J.; Forsyth, M.; MacFarlane, D. R. *J. Phys. Chem. B* **1998,** *102*, 8858.
27. Tsunashima, K.; Sugiya, M. *Electrochem. Commun.* **2007,** *9*, 2353.
28. Wasserscheid, P.; Welton, T., *Ionic Liquids in Synthesis*. Wiley VCH: 2008; p 141.

29. Trachenko, K. *J. Non-Cryst. Solids* **2008,** *354*, 3903.
30. Ediger, M. D.; Angell, C. A.; Nagel, S. R. *J. Phys. Chem.* **1996,** *100*, 13200.
31. Angell, C. A., *Molten Salts and Ionic Liquids Never the Twain?* John Wiley & Sons: USA, 2010.
32. Angell, C. A. *J. Non-Cryst. Sol.* **1991,** *131-133*, 13.
33. Capelo, S. B. n.; Méndez-Morales; Carrete, J.; Lago, E. L. p.; Vila, J.; Cabeza, O.; Rodríguez, J. R.; Turmine, M.; Varela, L. M. *J. Phys. Chem. B* **2012,** *116*, 11302.
34. Wu, T.-Y.; Hao, L.; Kuo, C.-W.; Lin, Y.-C.; Su, S.-G.; Kuo, P.-L.; Sun, I.-W. *Int. J. Electrochem. Sci.* **2012**, 2047.
35. Evenson, Z.; Raedersdorf, S.; Gallino, I.; Busch, R. *Scripta Mater.* **2010,** *63*, 573.
36. Ueno, K.; Zhao, Z.; Watanabe, M.; Angell, C. A. *J. Phys. Chem. B* **2012,** *116*, 63.
37. Schreiner, C.; Zugmann, S.; Hartl, R.; Gores, H. J. *J. Chem. Eng. Data* **2010,** *55*, 1784.
38. Tokuda, H.; Ishii, K.; Susan, M. A. B. H.; Tsuzuki, S.; Hayamizu, K.; Watanabe, M. *J. Phys. Chem. B* **2006,** *110*, 2833.
39. Tokuda, H.; Hayamizu, K.; Ishii, K.; Susan, M. A. B. H.; Watanabe, M. *J. Phys. Chem. B* **2004,** *108*, 16593.
40. Tokuda, H.; Tsuzuki, S.; Susan, M. A. B. H.; Hayamizu, K.; Watanabe, M. *J.Phys.Chem. B* **2006,** *110*, 19593.
41. Angell, C. A.; Byrne, N.; Belieres, J.-P. *Acc. Chem. Res.* **2007,** *40*, 1228.
42. Stoimenovski, J.; Izgorodina, E. I.; MacFarlane, D. R. *Phys. Chem. Chem. Phys.* **2010,** *12*, 10341.
43. Fraser, K. J.; Izgorodina, E. I.; Forsyth, M.; Scott, J. L.; MacFarlane, D. R. *Chem. Commun.* **2007**, 3817.
44. MacFarlane, D. R.; Forsyth, M.; Izgorodina, E. I.; Abbott, A. P.; Annat, G.; Fraser, K. *Phys. Chem. Chem. Phys.* **2009,** *11*, 4962.
45. Xu, W.; Cooper, E. I.; Angell, C. A. *J. Phys. Chem. B* **2003,** *107*, 6170.
46. March, J., *Advanced Organic Chemistry*. 3rd ed.; Wiley: New York, 1985.
47. Kumata, Y.; Furukawa, J.; Fueno, T. *Bull. Chem. Soc. Jpn.* **1970,** *43*, 3920.
48. Allen, C. R.; Richard, P. L.; Ward, A. J.; Water, L. G. A. v. d.; Masters, A. F.; Maschmeyer, T. *Tetr. Lett.* **2006,** *47*, 7367.
49. http://en.wikipedia.org/wiki/Acetic_acid.

50. Dolomanov, O. V.; Bourhis, L. J.; Gildea, R. J.; Howard, J. A. K.; Puschmann, H. *J. Appl. Cryst.* **2009,** *42*, 339.

51. Sheldrick, G. M. *Acta. Cryst.* **2008,** *A64*, 112.

52. Holbrey, J. D.; Reichert, W. M. *Dalton Trans.* **2004**, 2267.

53. Butchard, J. R.; Curnow, O. J.; Pipal, R. J.; Robinson, W. T.; Shang, R. *J. Phys. Org. Chem.* **2008,** *21*, 127.

54. Taylor, M. J.; Surman, P. W. J.; Clark, G. R. *J. Chem. Soc., Chem. Commun.* **1994**, 2517.

55. Clark, G. R.; Rickard, C. E. F.; Surman, P. W. J.; Taylor, M. J. *J. Chem. Soc., Faraday T rans.* **1997,** *93* (15), 2503.

56. Guschin, P. V.; Starova, G. L.; Haukka, M.; Kuznetsov, M. L.; Eremenko, I. L.; Kukushkin, V. Y. *Crystal Growth & Design* **2010,** *10* (11), 4839.

Applications

Applications

The discovery of a new IL is relatively easy, but the work required to determine its usefulness is quite substantial. The interesting properties of ILs such as recyclability, non-volatility, and non-flammability make these solvents promising candidates to replace the traditional volatile organic solvents used in industry. However, in order to increase the chances of large-scale commercial applications, their toxicity and biodegradation properties also need to be determined. There is not much evidence that ILs derived from natural resources have low toxicity. This chapter will highlight the preliminary investigation of applications related to ILs detailed in this thesis.

Applications of CILs

Enantiopure CILs show a high degree of organization which makes them more attractive than organic solvents for applications in chiral discrimination, including asymmetric synthesis. Here, some preliminary investigations of optically-active tac-based CILs in chiral discrimination and asymmetric synthesis will be discussed.

6.1 Chiral Discrimination

6.1.1 Diastereomeric interactions with racemic Mosher's salt

The enantiomeric forms of a compound frequently have different physiological properties. One form of the enantiomeric pair may be pharmalogically beneficial while other can have harmful effects. Thus, pharmaceutical industries need to determine effective methods for the determination of enantiomeric excesses (ee).[1] The techniques usually utilized are High Performance Liquid Chromatograpy (HPLC), Gas Chromatography (GC), Capillary Electrophoresis (CE), Circular Dichromism (CD), NMR and MS.

The use of various chiral selectors (cyclodextrins, molecular micelles, antibodies, and crown ethers) is limited because of their low solubility, difficult synthesis, and high cost. CILs have been recently used as chiral shift reagents (CSR) or chiral solvating agents.[2] When enantiomers are dissolved in optically active CILs, diastereomeric complexes are formed which have different physical and chemical properties and are easily accessed by NMR after dissolving them in a deuterated solvent.[3] The good performance and easy accessibility of NMR spectroscopy makes the determination of ee easy.[4]

In recent years, CILs with a chiral cation or chiral anion, or both, have been used as chiral solvents.[5-6] Zwitterions incorporating imidazolium and sulfonate or sulfamate groups have also been reported.[7]

order to investigate the effect of a mixture of CIL and its zwitterion, a study was performed as chiral solvating agents and the results are described herein.

6.1.2 Experimental

(*S*)-(+)-α-Methoxy-α-trifluoromethylphenylacetic acid, (*R*)-(−)-α-methoxy-α-trifluoromethylphenylacetic acid, sodium hydroxide, d_8-DMSO, $CDCl_3$, and 18-crown-6 were obtained from Sigma Aldrich and were used without further purification. ^1H and ^{19}F NMR spectra were recorded on an Agilent MR400 NMR Spectrometer (running at $J_{3.2}$ Software) at 400 and 375 MHz respectively.[4] The proton spectra were calibrated to TMS.

6.1.3 NMR experiment with Mosher's acid salt

The CIL (5 mg) was added to a mixture of the sodium salt of Mosher's acid (15 mg, 1.6 mmol) and 18-crown-6 (6.4 mg, 2.45 mmol).[8] This mixture was dissolved in 0.5 mL of 25% DMSO-d_6-$CDCl_3$, sonicated for 30 minutes at room temperature in a vial, then transferred to an NMR tube and the spectrum was recorded.

6.1.4 Results and Discussions

In the current study, the usefulness of AAILs (tac-based) was evaluated for enantioselective and separation techniques. 18-Crown-6 was added to increase the solubility via complexation of sodium with crown ether (fig 6.1).[5,9] The diastereomeric interaction between the chiral cation and Mosher's acid anion results in an upfield/downfield shifting and/or splitting of the CF_3 signal in ^{19}F NMR spectra and –OMe in the ^1H NMR spectra. This indicates that the substrate has been dissolved in a chiral environment. Clavier modified the NMR experiments by using potassium salts instead of sodium salts due to the bulky nature of the former ion which decreases the tightness of the anion pair binding and results in increased diastereomeric interactions by solubilization and dissociation.[9,5,10]

In the present study, a mixture of CIL and zwitterions are used as a chiral selector reagent for an enantioenriched salt of Mosher's acid (fig 6.1).

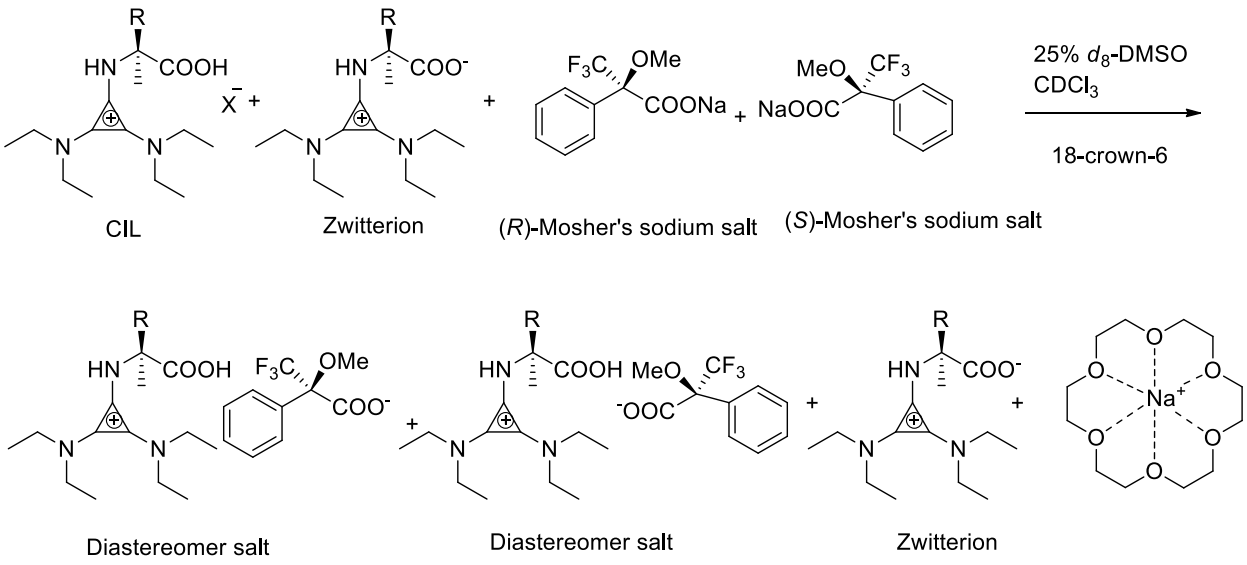

Figure 6.1-Proposed reaction scheme.

The CILs employed in this study have methyl sulphate and TFSA as anions. The latter soft anion has a delocalized charge through the O-S-N-S-O core, and the inductive effects of the highly electronegative fluorine atoms cause a decrease in Coulombic interactions between the cation and the anion in comparison to the more localized charge of methyl sulphate.[4,11] Thus, the large anions are weakly nucleophilic due to delocalized charge and increases the peak splitting in ^{19}F NMR.[12,13] It is noticed that in the cases of $[E_4Ala]MeSO_4$ (no splitting of peak) and $[E_4Val]MeSO_4$ (0.083 ppm), upon swapping the anion to TFSA, the peak splitting increased to 0.054 ppm and 0.134 ppm in ^{19}F NMR respectively, indicating the presence of stronger diastereomeric interactions when using TFSA as the anion.

The interaction between the CIL's cation and Mosher's acid anion causes a downfield or upfield shift of the hydrogen or fluorine atom signal in the ^{1}H or ^{19}F NMR spectrum, respectively.[4,13,14] The interaction also causes the signal to split illustrating the strength of the diastereomeric interaction.[5] The interaction between counterions is usually via hydrogen bonding. The chemical shifts in $[E_4Ala]MeSO_4$ (OMe and CF_3 peaks), $[E_4Pro]MeSO_4$ (OMe peak), $[E_4Pro]TFSA$ (OMe peak), $[E_4Thr]MeSO_4$ (OMe peak), $[E_4Thr]TFSA$ (OMe and CF_3 peaks), $[E_4His]TFSA_2$ (OMe and CF_3 peaks), $[E_4Met]TFSA$ (OMe and CF_3 peaks), $[E_4Ser]TFSA$ (OMe and CF_3 peaks), $[E_4Try]TFSA$ (OMe and CF_3 peaks), $[E_4Tyr]TFSA$ (OMe and CF_3 peaks), $[E_4Gln]TFSA$ (OMe and CF_3 peaks) and $[E_8Lys]TFSA_2$ (OMe peak) ranged from 2.5 to 4 ppm (δ) in their ^{1}H NMR spectra and −65 to −74 ppm (δ) in the ^{19}F NMR spectra in comparison to 4.794 ppm (δ) in the ^{1}H NMR spectrum and −65.279 ppm (δ) in the ^{19}F NMR spectrum of the sodium salt of Mosher's acid (table 6.1).

Table 6.1-Chemical shifts of diastereomeric complexes between CIL and Mosher's carboxylate.

Entry	Salt	δ (^{1}H) ppm				Av. δ ppm	Δδ* ppm	δ (^{19}F) ppm				Av. δ ppm	Δδ* ppm
		(R)	*(S)*	Peak	Splitting			*(R)*	*(S)*	Peak	Splitting		
1	Mosher's acid	4.794	4.794	0		4.794	---	−65.279	−65.279	0		−65.279	---
2	[E_4Ala]$MeSO_4$	2.461	2.461	0		2.461	2.333	−70.515	−70.515	0		−70.515	5.236
3	[E_4Ala]TFSA	3.438	3.458	0.020		3.448	1.346	−70.429	−70.483	0.054		−70.456	5.177
4	[E_4Pro]$MeSO_4$	3.480	3.480	0		3.480	1.314	−70.921	−70.961	0.040		−70.941	5.662
5	[E_4Pro]TFSA	3.480	3.480	0		3.480	1.314	−71.015	−70.979	0.036		−70.997	5.718
6	[E_4Val]$MeSO_4$	3.419	3.439	0.020		3.429	1.365	−70.711	−70.628	0.083		−70.669	5.391
7	[E_4Val]TFSA	3.490	3.510	0.020		3.500	1.294	−70.849	−70.715	0.134		−70.782	5.503
8	[E_4Thr]$MeSO_4$	3.450	3.450	0		3.450	1.344	−71.310	−71.279	0.031		−71.295	6.016
9	[E_4Thr]TFSA	3.471	3.471	0		3.471	1.323	−71.113	−71.113	0		−71.113	5.834
10	[E_4Leu]TFSA	3.537	3.525	0.012		3.531	1.263	−71.026	−71.010	0.016		−71.018	5.739
11	[E_4His]$TFSA_2$	4.077	4.077	0		4.077	0.717	−65.743	−65.743	0		−65.743	0.464
12	[E_4Met]TFSA	3.605	3.605	0		3.605	1.189	−69.668	−69.668	0		−69.668	4.389
13	[E_4Phe]TFSA	3.560	3.580	0.020		3.570	1.224	−71.319	−71.272	0.047		−71.296	6.017
14	[E_4IIe]TFSA	3.517	3.540	0.023		3.529	1.266	−71.196	−71.117	0.079		−71.157	5.878
15	[E_4Ser]TFSA	3.450	3.450	0		3.450	1.344	−71.160	−71.160	0		−71.160	5.881
16	[E_4Arg]$TFSA_2$	3.455	3.443	0.012		3.449	1.345	−64.877	−64.961	0.084		−64.919	0.360
17	[E_4Try]TFSA	3.481	3.481	0		3.481	1.313	−73.840	−73.840	0		−73.840	8.561
18	[E_4Tyr]TFSA	3.480	3.480	0		3.480	1.314	−66.166	−66.166	0		−66.166	0.887
19	[E_4Gln]TFSA	3.520	3.520	0		3.520	1.274	−71.623	−71.623	0		−71.623	6.344
20	[E_4Asn]TFSA	3.147	3.161	0.014		3.154	1.640	−66.025	−66.065	0.040		−66.0545	0.766
21	[E_8Lys]$TFSA_2$	3.524	3.524	0		3.524	1.270	−71.279	−71.340	0.161		−71.309	6.031

* Δδ is calculated by difference of chemical shift between average peak and Mosher's acid salt peak.

Low polarity solvents ($CDCl_3$ or C_6D_6) have a low dielectric[15] constant which makes the ion-pair interactions between the CIL's cation and Mosher's acid anion strong.[16] On the other hand, in strongly

polar solvents (d_6-DMSO, d_3-methanol and d_6-acetone), no chiral recognition has been observed previously by Warner and coworkers due to strong interactions between the solvent and CIL, which mask or impair interactions between the CIL and Mosher's salt and so diminishes the splitting of the peak.[15] In other words, with the increasing polarity of the solvent, the hydrogen bonding interactions are reduced between the host and guest molecules.[7] A deuterated solvent mixture of 25% d_8-DMSO in $CDCl_3$, and 18-crown-6 is employed in this study to increase the solubility of Mosher's acid salt. The d_8-DMSO is thought to be responsible for diminishing the peak splitting by increasing the interactions between the CIL and solvent as seen in $[E_4Ala]MeSO_4$ (OMe and CF_3 peaks), $[E_4Pro]MeSO_4$ (OMe peak), [E4Pro]TFSA (OMe peak), $[E_4Thr]MeSO_4$ (OMe peak), [E4Thr]TFSA (OMe and CF_3 peaks), $[E_4His]TFSA_2$ (OMe and CF_3 peaks), [E4Met]TFSA (OMe and CF_3 peaks), [E4Ser]TFSA (OMe and CF_3 peaks), [E4Try]TFSA (OMe and CF_3 peaks), [E4Tyr]TFSA (OMe and CF_3 peaks), [E4Gln]TFSA (OMe and CF_3 peaks) and $[E_8Lys]TFSA_2$ (OMe peak) in table 6.1.

Wasserscheid has shown that the concentration of the CIL in CD_2Cl_2 and the amount of water added plays a part in hydrogen bonding interactions and has a strong impact on the extent of signal splitting.[5] The same group later verified that the concentration dependence of chiral induction is based on the ion-pair interactions between the cation and anion of the ionic liquid.[17] In the present study, the concentration of CIL was not varied and was kept at 1%. Using less than 1% of CIL gave no splitting of the peak.

The presence of a positive charge is important for the chiral discrimination of Mosher's acid anion involving ion-pair interactions.[15,18] The dications $[E_8Lys]TFSA_2$ (**6.1**) (0.161 ppm) and $[E_4Arg]TFSA_2$ (**6.2**) (0.084 ppm) gave the highest diastereomeric interactions as seen by highest highest peak splitting in ^{19}F NMR in comparison to all other CILs (0.022-0.134 ppm in ^{19}F NMR) due to the presence of a greater positive charge.

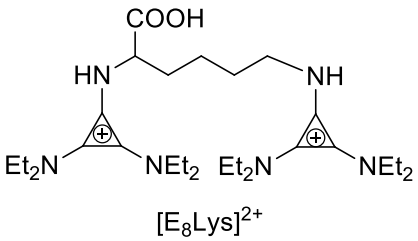

6.1

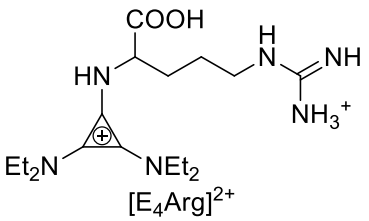

6.2

The structure of the cation plays an important part in chiral recognition abilities.[15] Ion-pair, hydrogen bonding, π-π stacking (inherently multi-point), dipole stacking, and steric interactions are thought to be responsible for chiral discrimination.[14]

An increase in the number of aromatic rings increases enantiomeric discrimination due to the ring current anisotropy. [E_4Phe]TFSA (table 6.1, entry 13) (**6.3**), which has one benzyl ring, shows a peak splitting of 0.02 ppm in the ^{1}H NMR and 0.047 ppm in the ^{19}F NMR due to ring current anisotropy in comparison to [E_4Ala]$MeSO_4$. But this splitting was very similar to the 0.02 ppm in the ^{1}H NMR and 0.054 ppm in the ^{19}F NMR of [E_4Ala]TFSA. This trend agrees with the weak nucleophilic character of TFSA rather than the aromatic ring effects. Similarly, in $[E_4Tyr]^+$ (table 6.1, entry 18) (**6.4**), $[E_4Try]^+$ (table 6.1, entry 17) (**6.5**), and $[E_4His]^{2+}$ (table 6.1, entry 11) (**6.6**), having aromatic rings, peak splitting was not seen, but an upfield/downfield shifting of peaks in the NMR spectrum was observed as indicated by Δδ which shows weaker interactions. It was thought that *d_8*-DMSO could be interacting with these CILs and suppressing the interactions.

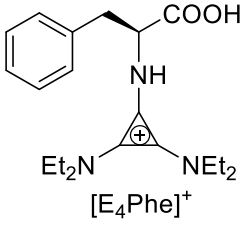

6.3

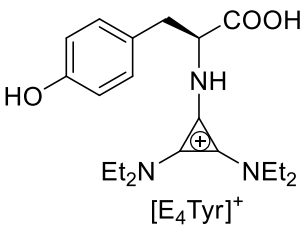

6.4

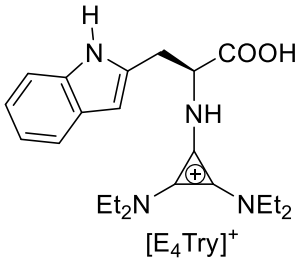

6.5

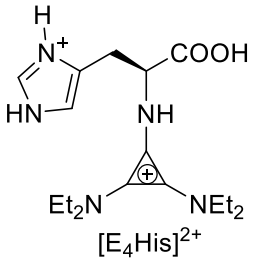

6.6

Longer alkyl chains offer hydrophobic interactions with Mosher's salt which are important for chiral recognition.[15] With an increase of the alkyl chain length from [E_4Ala]TFSA (**6.7**), through [E_4Val]TFSA (**6.8**) and [E_4Leu]TFSA (**6.9**), to [E_4Ile]TFSA (**6.10**), there is no regular increase seen in the peak splitting pattern. The peak splitting in [E_4Ala]TFSA is 0.054 ppm. Upon substituting two hydrogen atoms of the methyl group in [E_4Ala]TFSA with methyl groups gives [E_4Val]TFSA and increases the peak splitting to 0.134 ppm. [E_4Val]TFSA showed the greatest peak splitting among [E_4Ala]TFSA, [E_4Leu]TFSA and [E_4Ile]TFSA. When two hydrogen atoms of the methyl group in [E_4Ala]TFSA are substituted with methyl and ethyl groups to give [E_4Ile]TFSA. The peak splitting observed in [E_4Ile]TFSA is 0.079 ppm which is reduced from [E_4Val]TFSA (peak splitting = 0.134 ppm). Thus, two shorter methyl groups in [E_4Val]TFSA offered higher steric interactions which are

more beneficial for chiral recognition than methyl and ethyl groups in [E4Ile]TFSA.[15] When the one hydrogen atom of the methyl group in [E4Ala]TFSA is replaced by an isopropyl group, to give [E4Leu]TFSA, it results in the slowest peak splitting of 0.016 ppm.

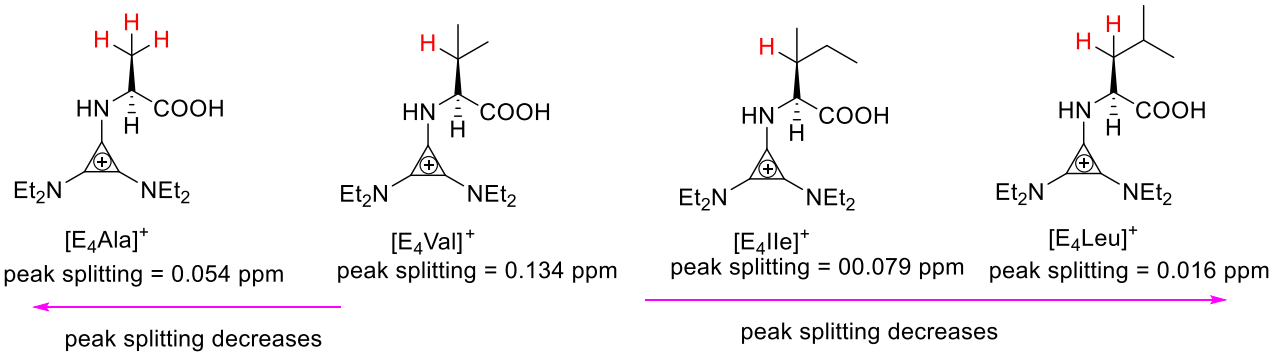

6.7 **6.8** **6.9** **6.10**

Clavier explained that alkyl chain length has a minimal effect on the diastereomeric interaction but that the introduction of a polar group (hydroxyl) increases the peak splitting of the signal considerably.[9] Unfortunately, in [E4Thr]MeSO4 (**6.11**) having one hydroxyl group gave a splitting of 0.031 ppm in ^{19}F NMR which was lower compared to the non-polar chains (0.040 ppm in [E4Pro]MeSO4 and 0.083 ppm in [E4Val]MeSO4).

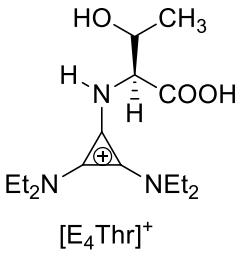

6.11

One of the interesting features seen in table 6.1 was that if the splitting was seen in ^{1}H NMR, we always see the splitting in ^{19}F NMR, as seen in the case of [E4Ala]TFSA, [E4Val]MeSO4, [E4Val]TFSA, [E4Leu]TFSA, [E4Phe]TFSA, [E4IIe]TFSA, [E4Arg]TFSA2, [E4Asn]TFSA and [E8Lys]TFSA2. However, if the splitting is seen in ^{19}F NMR, it does not mean it will also be seen in ^{1}H NMR, as seen in the case of [E4Pro]MeSO4, [E4Pro]TFSA and [E4Thr]MeSO4. Thus, ^{19}F NMR seems to be more sensitive to the determination of diastereomeric interactions.

There was no correlation seen with Δδ, which is the difference of the chemical shift between average peak of the two enantiomers and Mosher's acid peak. The Δδ indicates that there is some interaction after the formation of diastereomeric complexes but no clear trend was found. Shifts ranged from 0.7 to 2.0 ppm in the ^{1}H NMR and 0.3 to 8.5 ppm in the ^{19}F NMR. The smallest Δδ was found for $[E_4His]TFSA_2$ (0.717 in ^{1}H NMR and 0.464 in ^{19}F NMR) and was thought to be due to the imidazole ring preventing the diastereomeric interactions due to its bulkiness. The highest Δδ was found for $[E_4Ala]MeSO_4$ is 2.33 ppm in ^{1}H NMR and for $[E_4Gln]TFSA$ is 6.344 ppm in ^{19}F NMR was not understood because.

These CILs can also be utilized to determine the ee values by using enantioenriched mixtures of Mosher's acid of sodium salt approximately (*R*/*S*) = 3:1. The ratios of enantiomers was easily calculated by integrating the –OMe or $–CF_3$ signal peak (fig 6.2).

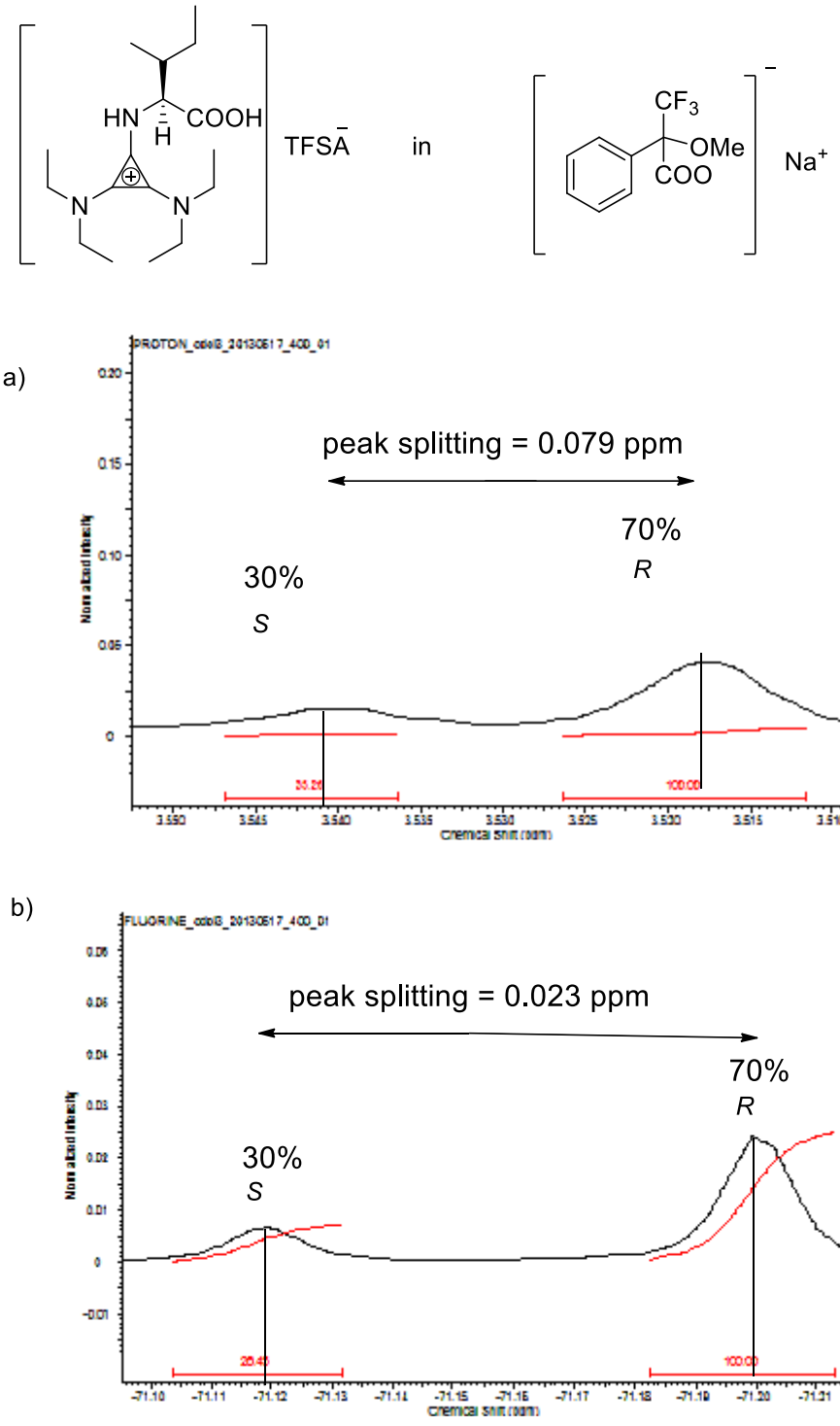

Figure 6.2–a) ^{1}H NMR (400 MHz) and b) ^{19}F NMR of enantioenriched sodium salt of Mosher's acid in 18-crown-6 in the presence of [E$_4$IIe]TFSA.

In conclusion, a novel class of tac-type AAILs was successfully shown to be an efficient chiral shift reagent for Mosher's carboxylate. The high solubility and enantiomeric-recognition ability of the CIL

make it possible to induce diastereomeric interactions for the determination of enantiomeric purity of the sodium salt of Mosher's acid.[2] Unfortunately, no direct trend was seen with Δδ. This NMR chiral discrimination study indicated that these AAILs could provide a highly-efficient chiral environment useful for asymmetric synthesis.

6.2 The Aldol Reaction

6.2.1 Introduction

The aldol reaction is a method to prepare β-hydroxy carbonyls or 1,3-diol units (found in the skeleton of many natural products) from a ketone and an aldehyde (fig 6.3) or two aldehydes. In nature, this reaction is used for the building of carbohydrate molecules with the help of aldolase. In 2000, three decades after utilizing proline as a catalyst in an aldol reaction, it was found that other α-amino acids are also able to catalyze the asymmetric reaction.[19]

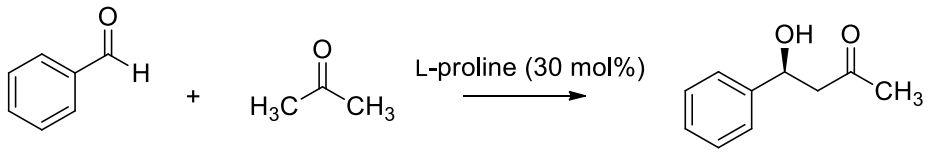

Figure 6.3-Aldol reaction.

Unlike aldolases that catalyze the reaction in an aqueous medium, the aldol reaction is catalyzed by the organocatalysts in a CIL. CILs are considered as 'microaldolases', and are used as a solvent and as a catalyst for inducing chirality in the aldol reaction. There are two advantages associated with CILs; (i) tunable miscibility and; (ii) reaction taking place in the homogeneous phase.

The structure of aldolase and organocatalysts are similar but they have some differences as well. The organocatalyst performs the reaction in organic solvents or in solvent-free conditions, while aldolase reactions run in an aqueous medium. The enzyme retains a high catalytic activity, up to thousands of cycles, whereas most of the organocatalysts lose their activity during reaction workup.

The first example of the use of a CIL in an aldol reaction was reported by Howarth *et al*. in 1997, after which a large number of CILs bearing chiral cations, anions or both have been reported by other groups.[20] The experimental observations and data show that CILs allow the direct asymmetric aldol reaction via the enamine pathway (fig 6.4), while the dehydration side products might be explained by an aldimine-Mannich catalytic cycle.[21]

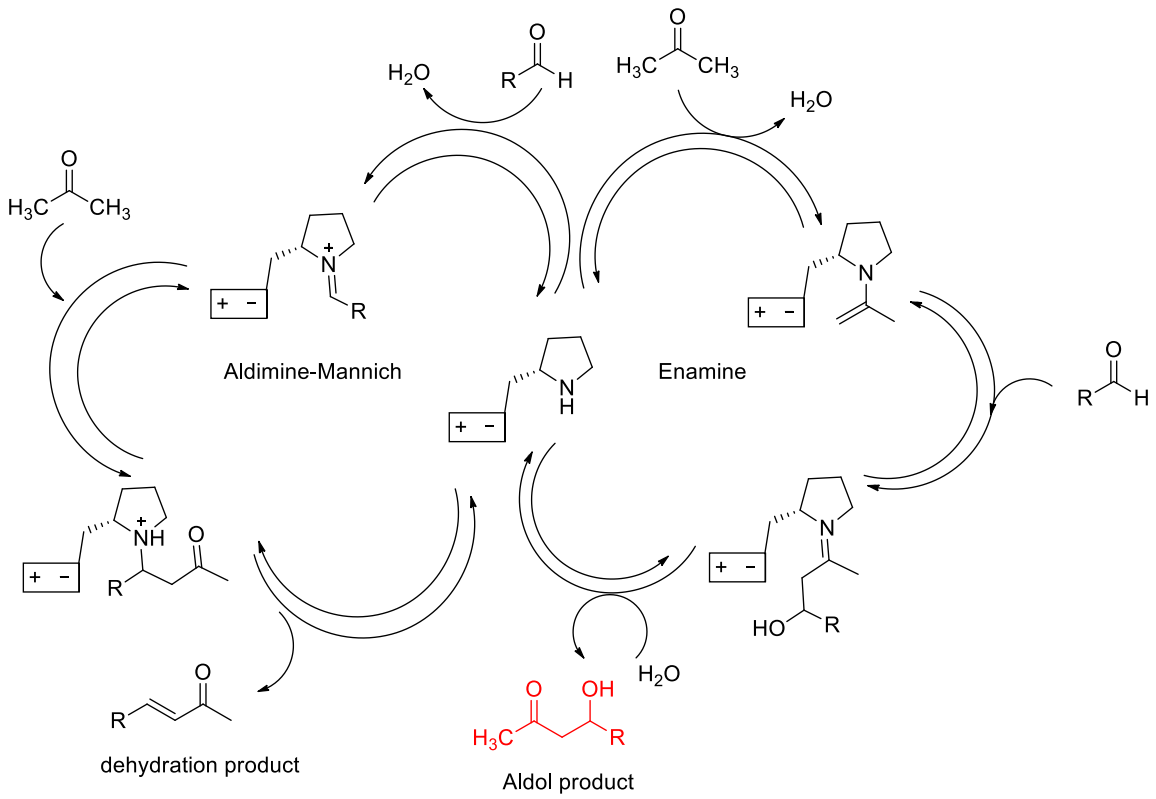

Figure 6.4-Propsed mechanism for a CIL-catalyzed aldol reaction.[21]

6.2.2 Experimental

All organic compounds were purchased from commercial suppliers and were used without further purification. CILs were dried *in vacuo* at 60 °C for 48 hours before the reaction. Specific optical rotations were measured on a Perkin Elmer Polarimeter 341 in $CHCl_3$. Silica gel 60 (230-400 mesh) was used for column chromatography.

6.2.2.1 General Procedure for the L-proline catalyzed aldol reaction

Benzaldehyde (4 mL, 39 mmol) and acetone (78 mL, 27 eq.) was introduced in a round bottom flask containing the L-proline (1.35 g, 30 mol%) and dried CIL (10 g, 27 mmol). The reaction mixture was vigorously stirred at room temperature for 25 h and then filtered to recover L-proline and acetone was then removed *in vacuo*. The aldol product and the remaining starting compounds were extracted with Et_2O (3 × 10 mL) while leaving behind the CIL. The combined organic extracts were evaporated *in vacuo.* The pure aldol addition product was obtained as a yellow oil after purification by flash silica gel column chromatography, eluting with *n*-hexane:EtOAc = 2:1.

6.2.2.2 General Procedure for the CIL-catalyzed aldol reaction

Benzaldehyde (4 mL, 39 mmol) and acetone (78 mL, 27 eq.) was introduced into a round bottom flask containing a dried CIL (10 g, 26 mmol). The reaction mixture was vigorously stirred at room temperature for 25 h and then acetone was removed *in vacuo*. The aldol product and the remaining starting compounds were extracted with Et_2O (3× 10 mL) while leaving behind the CIL. The combined organic extracts were evaporated *in vacuo.* The pure aldol addition product was obtained as a yellow oil after purification by flash silica gel column chromatography, eluting with *n*-hexane:EtOAc = 2:1.

6.2.3 Results and Discussions

First, we will discuss the aldol reaction between benzaldehyde and a ketone using L-proline as a catalyst in the presence of a CIL as a co-solvent. A CIL alone cannot promote the aldol reaction (as will be discussed in the next section), so addition of L-proline preceded the reaction and catalyses formation of the desired aldol products. These results are summarized in table 6.3. When the reaction is performed in the presence of L-proline as a catalyst without CIL, it gave moderate yields (41%) and good *ee* (61%) (table 6.3, entry 1). However, when $[E_4Ala]MeSO_4$, $[E_4Pro]MeSO_4$ or $[E_4Val]MeSO_4$ were used as chiral solvents in the presence of L-proline, it gave *ee* as 42%, 64% and 64%, respectively. The yields obtained with all the three chiral solvents were decreased in comparison to the reaction without the CIL (41%) (table 6.2, entry 1), and ranged from 13-34%. It agrees with the results obtained from Bica and coworkers.[22] Upon swapping L-proline with D-proline, in the presence of $[E_4Ala]MeSO_4$ as a co-solvent, a decrease in yield (13%) and *ee* (42%) was also obtained (table 6.2, entry 3).

Table 6.2-Results of aldol reaction when CIL as a co-solvent

Entry	Catalyst	Reaction Time (hrs)	Co-solvent (CIL)	Physical State of	*ee* %	Yield %	TON (Turn Over Number)
1	L-proline	25	none	---	61	41	1.4
2	L-proline	25	$[E_4Ala]MeSO_4$	Viscous	47	30	1
3	D-proline	25	$[E_4Ala]MeSO_4$	Viscous	42	13	0.4
4	L-proline	25	$[E_4Pro]MeSO_4$	Viscous	64	20	0.7
5	L-proline	25	$[E_4Val]MeSO_4$	Solid	64	34	1.1

[a]The ee was determined by polarimetry.[23]

The investigations in this study were done only on hydrophilic CILs having the methyl sulphate anion due to its easy recycling from the product mixture. However, swapping the anion from hydrophilic methyl sulphate to hydrophobic bis(trifluoromethanesulfonyl)amide might have increased the selectivity due to a weaker ion-pair interaction.[24,25]

Earlier studies have shown that water molecules can be mechanistically involved in the aldol reaction. Previously, Pericas and coworkers showed the reaction performed with a water-swollen gel enhanced the aldo reaction rate and selectivities.[26] The CILs employed in this study are all hydrophilic and, due to their viscous nature, could hold a large water content. In the present study, water was not added to the system which may have been responsible for lowering the rate of reaction. However, these significantly water-soluble CILs may allow the reaction to be performed in water.

The catalyst loading (30 mol%) was kept high to reduce the reaction time (25 h), but it resulted in lower selectivity.[22,27] The reaction was performed at room temperature to increase selectivity and avoid side product formation, but, unfortunately, there was not much change in observed ee. A slightly higher yield was reported by Zhou, along with decreased *ee*, when the reaction was performed at 40 °C.[28]

The catalyst performance or activity is expressed in terms of TON (Turn Over Number) and TOF (Turn Over Frequency) values, which vary immensely depending upon the nature of cation and anion.[29] The TON values in the current study ranged from 0.4 to 1.4, which are very small in comparison to the ones reported earlier (TONs up to 17-96).[25, 30,31] The high catalyst loading may be responsible for the poor TONs.[32]

However, from previously-reported data, the acidic proton of proline is essential for catalysis.[33] In this study, the reaction is performed without the addition of the acidic additive. Although, the CILs utilized in the present study are weakly acidic (pka = 2.9-3.55). Scientists have observed that strong acids like TFA (pka = 0.23) are strong enough to protonate the counterion of the catalyst and can lead to anion metathesis and destruction of the catalyst, resulting in poor yields and selectivities.[34] However, weak acids such as acetic acid and water favor the formation of the aldol product. The acidic additives may promote the rate of reaction by the enamine catalytic cycle and retard the general base-mediated condensation pathway.[24]

The *ee* seems to increase with increasing alkyl chain length.[22] The *ee* of aldol product obtained by $[E_4Ala]MeSO_4$, $[E_4Pro]MeSO_4$ and $[E_4Val]MeSO_4$ is 47%, 64% and 64% respectively and agrees with increasing alkyl chain size.

Blackmond and coworkers showed that the presence of water is important for the enamine mechanism of the proline-catalyzed aldol reaction *via* the inhibition of iminium ion formation (fig. 6.4).[35] The off-cycle processes with respect to the generally-accepted enamine-driven catalytic cycle reduced the catalyst concentration and resulted in lower yield and lower selectivities than expected (fig 6.5).

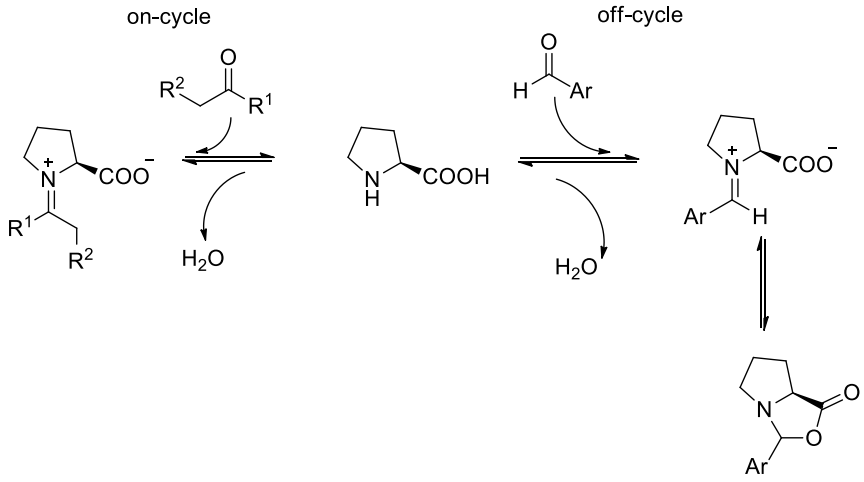

Figure 6.5-Off-cycle and on-cycle route.[35]

The tunable solubility of the CILs allows for easy separation and recycling of the catalyst. The biphasic property of the CILs made it possible to recover them after the completion of the reaction. The aldol product is easily separated from the product mixture by repeated extraction with diethyl ether, leaving behind the CIL. The CIL is dissolved in water and repeated washings with diethyl ether leaves the pure CIL in the aqueous layer. The recycled CIL was not used again in an aldol reaction, but its color remained the same. Based on environmental considerations, these hydrophilic CILs may be of interest due to their ease of recycling.

When an aldol reaction is performed in the presence of a CIL as a catalyst and solvent without the addition of L-proline, a marked decrease in yield (2-8%) and *ee* (12-33%) is found in comparison to aldol reaction when L-proline was used as a catalyst (61% yield and 41% ee) (Table 6.4). This may be due to an inability of the acidic proton to follow the enamine pathway (fig 6.1) in $[E_4Pro]MeSO_4$ (**6.8**). While steric hindrance in $[E_4Ala]MeSO_4$ (**6.7**) and $[E_4Val]MeSO_4$ (**6.9**) are thought to be responsible for the low activity of their reaction.

Table 6.3-Results of aldol reaction when a CIL is catalyst and solvent

Entry	Catalyst	Physical State	Reaction time (hrs)	*ee* %	Yield %
1	L-proline	---	25	61	41
2	$[E_4Ala]MeSO_4$	Visocus	25	12	8
3	$[E_4Pro]MeSO_4$	Visocus	25	9	2
4	$[E_4Val]MeSO_4$	Solid	25	33	2

[a]The ee was determined by polarimetry.[23]

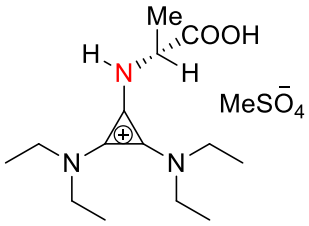

6.12

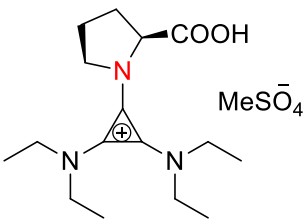

6.13

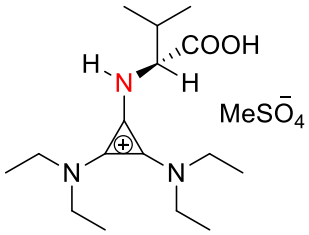

6.14

In conclusion, AAILs containing L-alanine, L-proline and L-valine units catalyzed the aldol reaction between benzaldehyde and acetone. When the reaction was carried out in the presence of L-proline in the CIL at 25 °C, the aldol product was generated in good but reduced yields and *ee*. However, in the absence of L-proline <30 % ee and <10 % yield was obtained. The CILs were easily recycled but were not used in the reaction again.

6.3 Diels-Alder Reaction

The Diels-Alder reaction is one of the methods used to construct carbon-carbon six-membered rings with four stereogenic centers.[36] It is a useful reaction in organic chemistry and requires very little energy to create a cyclohexene ring upon cycloaddition between a conjugated diene and a substituted alkene (dieneophile).

The Diels-Alder reaction is a pericyclic reaction. For example, four carbon atoms of cyclopentadiene and two carbon atoms of methyl acrylate combine to form a six-membered carbon ring (fig 6.6). Placing a carbonyl group (electron-withdrawing group) on the dienophile facilitates the reaction. However, cyclopentadiene is reactive both as a dienophile and diene and converts to dicyclopentadiene (Diels-Alder adducts). In the product, two π-bonds (bond breaking) are reduced to single bonds and two more σ-bonds (bond forming) are formed. Thus, this exchange of two weak π-bonds for two strong σ-bonds is the major driving force in this reaction.

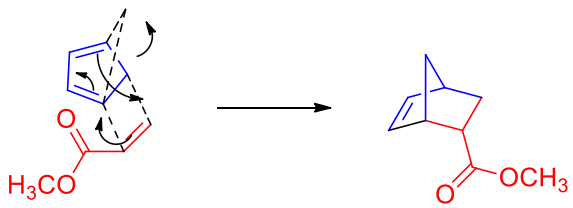

endo-

Figure 6.6-Mechanism of Diels-Alder reaction.

Usually, the reaction is not selective and gives a mixture of isomers.[37] Scientists have developed an interest in this reaction for targeting one product and for increasing the rate of reaction (and the selectivity). The use of ILs lead to a reverse of selectivity in comparison to organic solvents in the Diels-Alder reaction.[38,29] The reaction between cyclopentadiene and methyl acrylate favors the *exo* product in organic solvents.[38] The polarity of the solvent and Lewis acidity of catalyst increases the selectivity and rate of reaction.[39,40] The hydrogen-bonding interaction between electron lone pairs on the dieneophile and acid hydrogen atoms of the solvent increases the rate of reaction.[40] Polar solvents increase the reaction rate and selectivity compared to non-polar solvents, due to enhanced hydrogen bonding.[41]

ILs are polar, have no vapor pressure and give high selectivity and easy product separation in the Diels-Alder reaction. However, the reaction in water is faster than in RTILs. Unfortunately, despite the strong charge of ILs, their solvation effects are weaker as compared to that of water.[42]

Jaeger and Tucker, in 1989, performed the Diels-Alder reaction in ethylammonium nitrate for the first time.[43] When amino acid-derived CILs [ProR]NO_3 (**6.15**), [AlaR]NO_3 (**6.16**) and [ProR]Sac (**6.17**) were used as catalysts or "fully green" solvents in an asymmetric Diels-Alder reaction, it resulted in the enhancement of yields, enantiomeric excesses and diastereoselectivities.[44] The recycling of catalysts was done several times without the loss of activity or enantioselectivity.

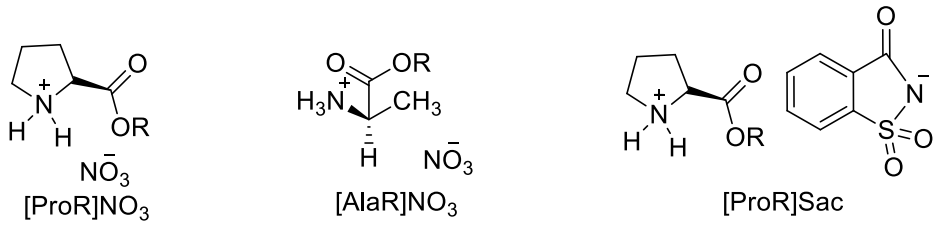

6.15 **6.16** **6.17**

6.3.1 Experimental

The cyclopentadiene was freshly cracked from its dimer and methyl acrylate was purchased from Merck. Here, we perform the reaction of cyclopentadiene with methyl acrylate (fig 6.7), which forms

mixture of *exo* and *endo* products in the presence of CILs derived from amino acids. The CIL has the ability to act as a hydrogen-bond donor (cation effect) and hydrogen-bond acceptor (anion effect).

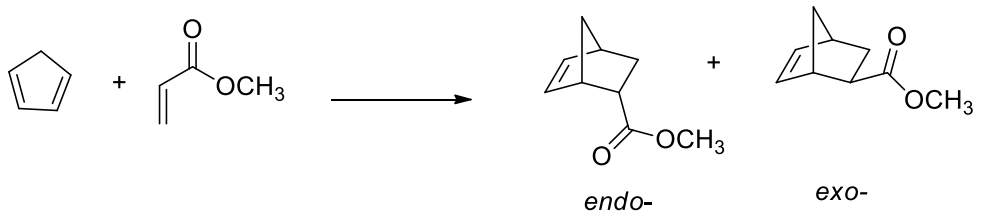

Figure.6.7-Diels-Alder reaction between methyl acrylate and cyclopentadiene.

6.3.2 Procedure

In a typical Diels-Alder reaction, freshly cracked cyclopentadiene (0.35 mL, 8 mmol) and methyl acrylate (0.5 mL, 12 mmol) is added to 1 g of CIL and stirred with a magnetic stirrer on a water bath at 25 °C (for viscous CILs, the reaction is performed at a higher temperature) for 24 hours under an inert atmosphere. The products are extracted with diethyl ether (10 × 2 mL) and analyzed by GC after adding decane as an internal standard. The % conversion and *endo/exo* selectivities are determined. The *exo*-product (approximately 8.2 min) appears before the *endo*-product (approximately 8.3 min) on the GC, in agreement with the literature (fig 6.8).[45]

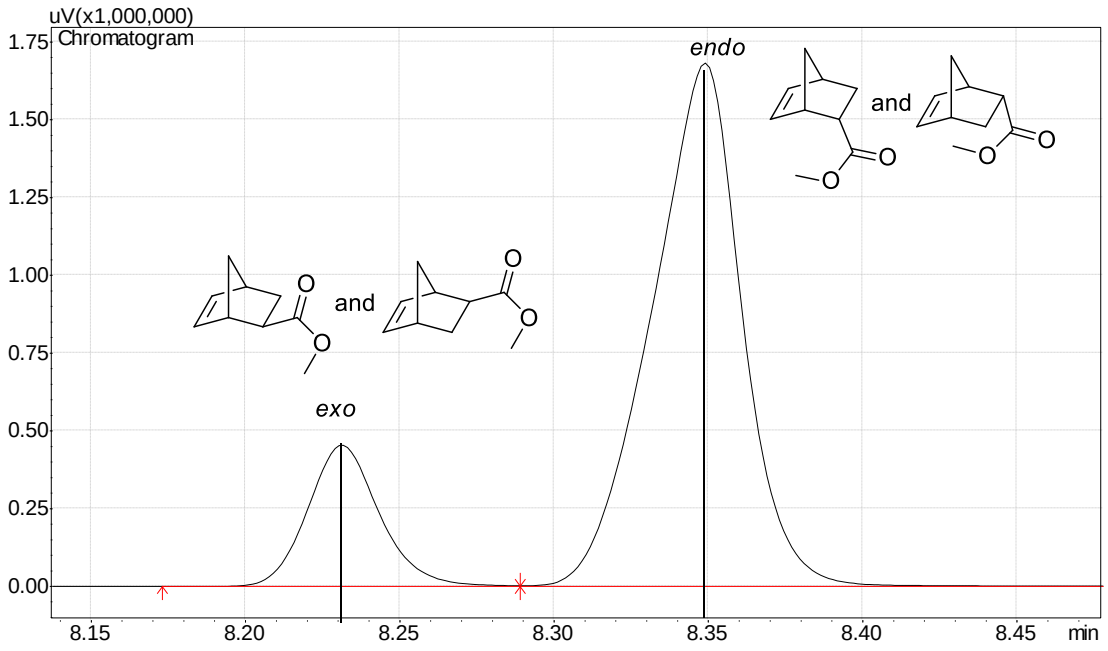

Figure 6.8-GC spectrum showing *exo*- and *endo*- product peaks of Aldol reaction when the reaction was carried out in [E_4Arg]TFSA_2.

6.3.3 Results and Discussions

The Diels-Alder reaction has been extensively studied in molecular solvents and these studies suggests that hydrogen-bond donation of the solvent is necessary to effect both the kinetic and stereochemical behavior. My results are summarized in table 6.4.

Table 6.4-Results of Diels-Alder reaction between methyl acrylate and cyclopentadiene.

CIL	Amino acid structure	^{1}H NMR of NH peak	Chloride Content (ppm)	Physical State	*T* (°C)	%Conversion[a]	*endo*/*exo*[b]	*endo*%	exo%
No CIL[46]	----		----	----	25	96	3.85	76	20
[E_4Ala] $MeSO_4$	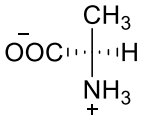	8.36	2289	very Viscous liquid (biphasic)	25	95	3.14	72	23
[E_4Ala] TFSA	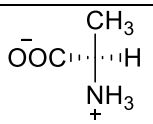	6.99	435	liquid	25	98	4.31	80	18
[E4Pro] $MeSO_4$	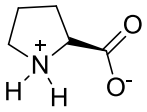	-	31212	very Viscous liquid (biphasic)	25	96	3.24	73	23
[E_4Pro] TFSA	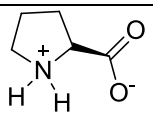	-	174	viscous liquid	25	95	3.89	75	19
[E_4Val] $MeSO_4$	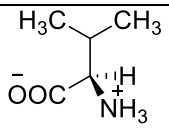	8.44	41370	solid (biphasic)	75	99	2.79	73	26
[E_4Val] TFSA	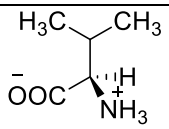	7.13	186	viscous liquid	25	98	4.23	80	18

[E_4Thr]	$MeSO_4$	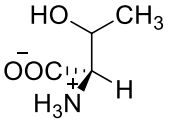	8.04	3229	solid (biphasic)	47.7	98	3.17	75	24
[E_4Thr]	TFSA	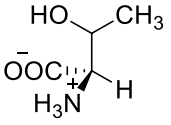	6.75	38	viscous liquid	25	99	4.34	80	19
[E_4Leu]	TFSA	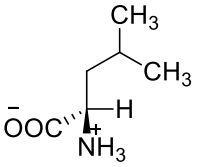	6.92	93	viscous liquid	25	98	4.43	80	18
[E_4His]	$TFSA_2$	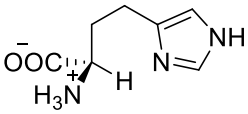	8.74	161	viscous liquid	25	99	5.96	84	14
[E_4Met]TFSA		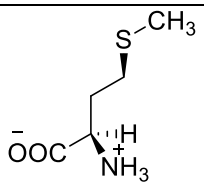	-	968	viscous liquid	25	99	3.73	78	21
[E_4Phe]TFSA		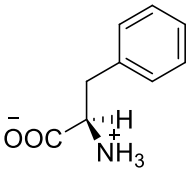	6.66	112	viscous liquid	25	98	5.11	82	16
[E_4Ile]	TFSA	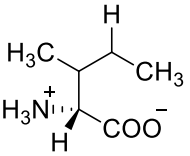	6.64	109	viscous liquid	25	95	4.74	78	16
[E_4Ser]	TFSA	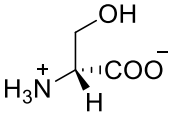	8.41	100	viscous liquid	25	98	5.01	82	16

[E_4Arg] $TFSA_2$	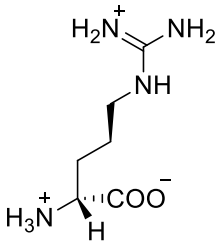	-	475	solid	55	99	4.64	81	18
[E_4Try]TFSA	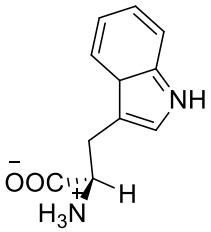	-	11	viscous liquid	55	99	3.58	77	22
[E_4Tyr]TFSA	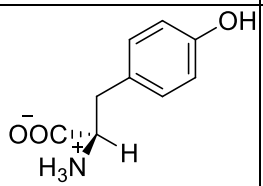	-	474	solid	25	98	5.73	84	15
[E_8Gln] $TFSA_2$	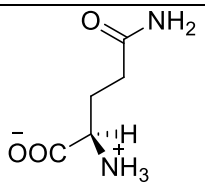	-	36	viscous liquid	25	96	5.52	81	15
[E_4Asn] TFSA	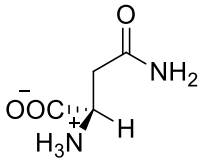	8.04	43	solid	55	85	4.17	69	17
[E_8Lys] $TFSA_2$	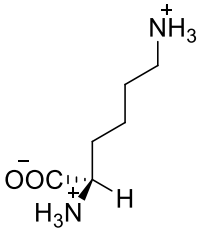	6.41	182	viscous liquid	25	98	4.63	80	17

a) Calculated from methyl acrylate conversion by Gas Chromatography b) from Gas Chromatography

From the results detailed in table 6.4 the following observations can be made;

1. The CILs with $MeSO_4^-$ as the anion have strong ion-pair interactions, so the cation interaction with the carbonyl oxygen of the methyl acrylate during intermediate formation is weak and this decreases the selectivity (fig 6.9).[45] Increasing hydrogen-bond donor ability of the CIL increases reactivity and selectivity. This was seen in the case of $[E_4Ala]^+$, $[E_4Pro]^+$, $[E_4Val]^+$ and $[E_4Thr]^+$ with the $MeSO_4^-$ anion. In the ^1H NMR, the chemical shift of the NH of the amino acid moiety attached to the tac cation also shows the strength of the ion pair (table 6.4). The selectivity of the $MeSO_4^-$ CILs ranged from 2.79-3.24 which is less than when the reaction is performed without the CIL (*endo/exo* 3.85).

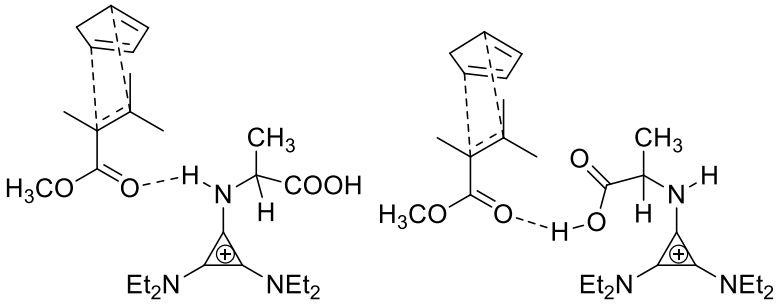

Figure 6.9-The proposed hydrogen bond interaction of tac cation (Lewis acid) with carbonyl oxygen of methyl acrylate during the formation of transition state (TS).[47]

The greatest selectivity is observed in CILs with the strongest hydrogen-bond donor cation coupled to a weak hydrogen-bond acceptor anion (inert ions).[29]

2. CILs with $MeSO_4^-$ as the anions usually have a high chloride content which can disrupt hydrogen bonding and result in decreased *endo/exo* ratios.[37] Usually, the presence of hydrogen-bond interaction leads to increased selectivities. It was also noted that, if the system was biphasic, then the reaction did not occur in the CIL phase, but in monophasic systems, residual chloride had more effect.[29] Thus, smaller hydrogen-bond interactions between the counterions of the CIL leads to higher selectivities.

3. It has been observed previously that water (up to 1 mole percent) increases *endo* selectivity over *exo* by enhancing the hydrophobic effects and surface area for the reaction.[48] However, our CILs with $MeSO_4^-$ (more water content than TFSA ones) as an anion gave less *endo* selectivity than with TFSA. Possibly, ion-pair interactions were dominant while the TFSA type gave greater *endo* selectivity due to a weaker ion-pair interaction.[37]

4. With an increase of temperature, the *endo/exo* selectivity decreases as it disrupts the hydrogen bonding. $[E_4Val]^+$, $[E_4Arg]^{2+}$, $[E_4Try]^+$ and $[E_4Asp]^+$ were highly viscous or solid and could not dissolve the reactants, so heat was required to reduce the viscosity. With the increased viscosity, high vibrational and low translational energies are favored and thus increased viscosities retard the bond making.[49] In other words at higher viscosity the reactants encountering is limited therefore resulting in a lowering of reaction rate, due to limited encountering of pair formation in TS.

5. It is known that the *endo/exo* selectivity decreases with the increase of viscosity of solvent. As the CIL's visocity increases, the reactants cannot see each other, and the rate of reaction is slowed down.[49] Significant enhancements in selectivity were observed when the mixture was homogenous (CILs with TFSA as an anion). When the reaction mixture was biphasic (CILs with $MeSO_4^-$ as an anion), the reactants could not interact effectively with the chiral environment.

6. The most important factor was seen when the cation had –OH or –NH hydrogen-bond donor capabilities.[45] This was seen in the case of histidine, phenylalanine, serine, tyrosine and glutamine. They have functionalized (hydroxyl, carbonyl, imidazole, phenol or benzyl groups) cations having strong hydrogen-bond donor moieties and anions having the ability to delocalize charge (TFSA), leading to a greater interaction between the cation of the ionic liquid and the TS (fig 6.9). The ability of the cation to act as a hydrogen-bond donor increased the *endo* selectivity which ranged from 5.01 to 5.96, which was similar to molecular solvents. AAILs formed hydrogen bonds with the carbonyl oxygen of methyl acrylate and had a dramatic effect on the rates and selectivity of the Diels-Alder reaction (fig 6.9). However, in the case of asparagine, tryptophan and arginine, an increase in temperature disrupted the hydrogen bonding and is responsible for lowering of selectivities (*endo/exo*) to 4.64, 3.58 and 4.17 respectively.

7. The highest selectivity of 5.96 was obtained in $[E_4His]TFSA_2$ which was shown to be the most polar dication among all synthesized CILs due to two N-H hydrogen-bond donor groups. As mentioned earlier, these hydrogen-bond donor groups are able to stabilize the TS by the formation of hydrogen bonds.

8. In the case of lysine, isoleucine, leucine, methionine, threonine, and valine, long alkyl chain substituents on the cation can lead to lower selectivities of 3.73-4.74 due to steric

interactions between the transition state and the cation,[50] leading to less interaction of the CIL's cation with methyl acrylate and decreasing the selectivities.

9. Among all the amino acids, proline is a secondary amine and, when coupled with tac cation, gives [E_4Pro]$MeSO_4$ and [E_4Pro]TFSA where there is no –NH hydrogen-bond donor ability. This causes a lowering of selectivity to 3.24 and 3.89 respectively. Indicating that the NH group in the other CILs is important to stereochemical induction.

The selectivities obtained from the Diels-Alder reaction between cycopentadiene and methyl acrylate catalyzed by AAILs ranged from 2.79-5.96 which are better with those previously reported in AAILs (3.1-3.9).[44a] All the reactions were run on an 8 mmol scale using 1 g of CIL at 25 °C. Since both methyl acrylate and cyclopentadiene were mostly soluble in CIL, the reaction was performed without the need of a co-solvent. Also, without the addition of a Lewis acid, it still gave excellent product yields.

These CILs were recycled after the reaction and were not used in the reaction again. However, they can be used as a reaction media for the Diels-Alder reaction. The cation of the CILs proved to be very important in obtaining selectivity. Unfortunately, due to the lack of a chiral column, no enantiomeric excesses were determined.

The use of CILs as solvents in asymmetric synthesis is not necessarily an environmentally-friendly alternative, but does have considerable enhancements on reaction reactivity and selectivity. The interactions within the counterions of CILs formed ordered three-dimensional networks which affected the solute and transition states and thus the products. The ability of CILs to affect reaction rate is very complex and more factors must be considered to explain their effect on reactivity and selectivity of reaction.

6.4 Applications of Metal ILs (MILs)

ILs can be used for recovery of metals from waste waters, in mining, nuclear fuel and waste reprocessing, and immobilizing transition metal catalysts.[51] Most of the metals discharged by industrial wastes into waste water pollute the environment and their removal is needed to protect animals and humans. Most of the metals are essential (Fe, Zn, or Cu) for humans while some are extremely toxic (Cd). Previously, the coupling of metals with the ILs has helped to remove metals from the waste waters. ILs can serve as complexing agents for metals with either the cation or the anion.

In the present study, we synthesized MILs by coupling metal chlorides with $[C_3(NEt_2)_3]Cl$ (fig 6.10). Most of the metal halides can be dissolved in chloride-rich ILs and form ILs with chloro-containing metallate species. This is the basic principle for the formation of chlorometallate ILs.

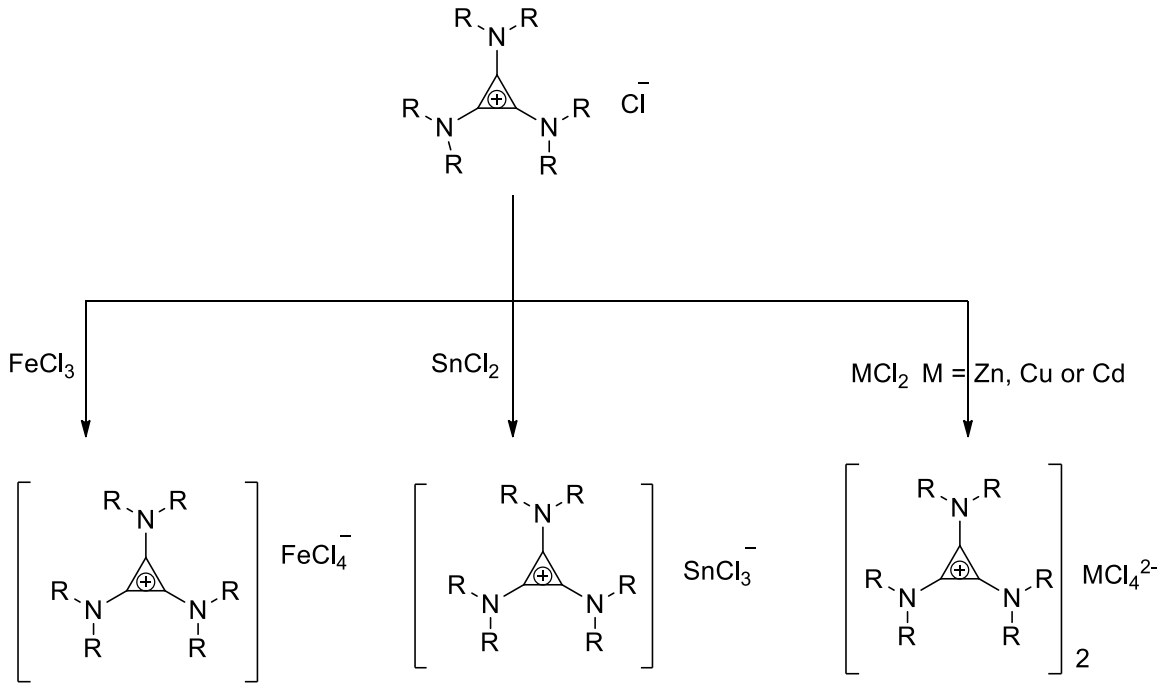

Figure 6.10-Reaction scheme for MILs.

These tac-based ILs based on complexation with metals, could be used to remove toxic metals from waste water. They could also be useful as catalysts in an organic synthesis.

6.4.1.1 Properties of MILs

In order to explore the physical properties of these MILs, thermal, magnetic, and miscibility/solubility studies were carried out. These properties are useful for a good understanding for further applications.

6.4.1.1 Thermal Properties

Thermogravimetric analyses (TGA) and differential scanning calorimetry (DSC) experiments were carried out for the MILs under a nitrogen atmosphere.

The example below (fig 6.11) shows the DSC curve for $[(C_3(NEt_2)_3]FeCl_4$. Three different transitions are seen when the sample is heated from −100 to 200 °C due to different structural changes. The first endothermic transition occurs at −4.4 °C, which is a solid-solid transition with an enthalpy change of

4.86 kJ/mol. Then, at 50.1 °C, another endothermic solid to solid transition is observed with an enthalpy change of 3.36 kJ/mol. Finally, at 148 °C, the sample melts with an enthalpy of fusion of 8.04 kJ/mol. The fairly large enthalpy change of fusion corresponds to a major structural change.[52]

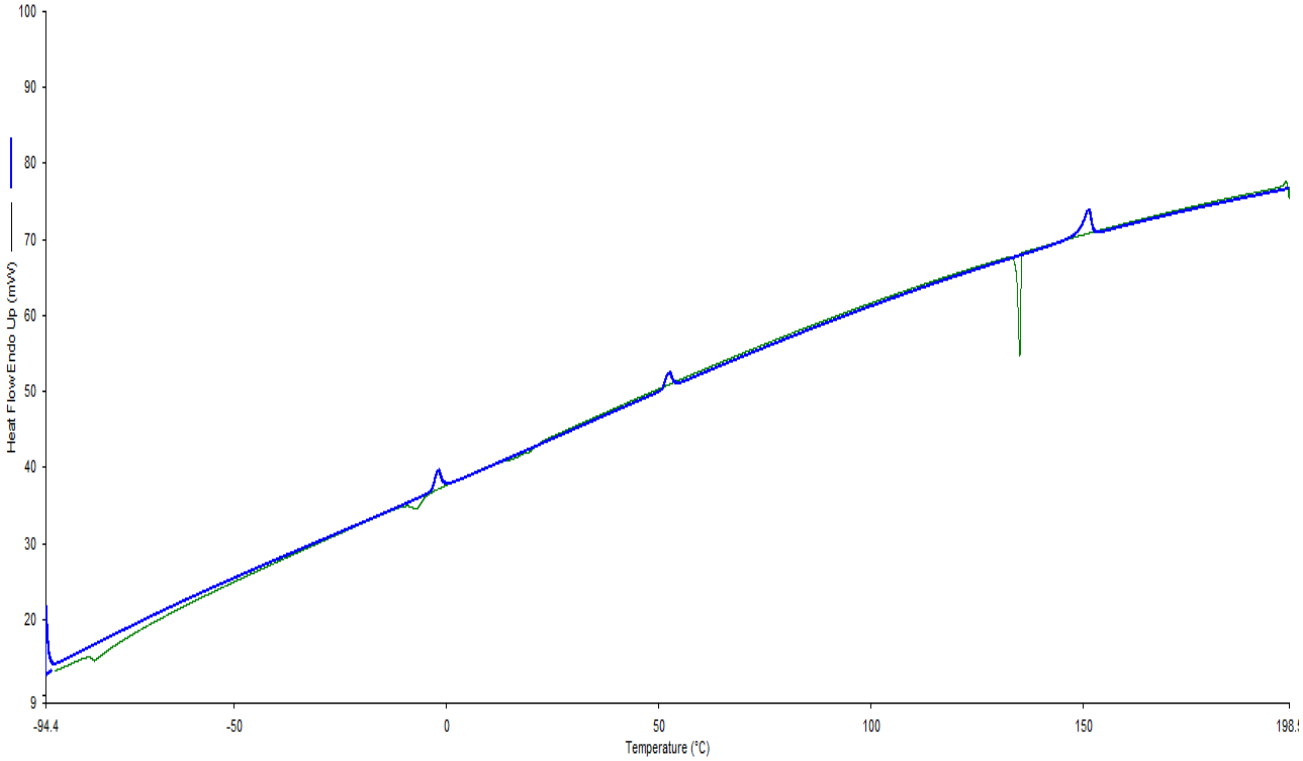

Figure 6.11-DSC curve for $[(C_3(NEt_2)_3]FeCl_4$

The DSC results are summarized for all the metal salts in table 6.5. The short ethyl chains on the $[C_3(NEt_2)_3]^+$ and symmetric metal chloride results in a close packing and make them solids. Except for $[(C_3(NEt_2)_3]FeCl_4$ (with a melting point of 148 °C) all other salts have melting points below 100 °C.

Table 6.5-DSC results

Entry	IL	M_w of cation (g/mol)	M_w of anion (g/mol)	Geometry of anion	T_g (°C)	T_m (°C)	ΔH (kJ/mol)
1	$[(C_3(NEt_2)_3]BF_4$[53]	252.43	86.77	tetrahedral	---	24.0	20.0
2	$[(C_3(NEt_2)_3]ClO_4$[53]	252.43	99.41	tetrahedral	−65.0	39.0	23.0
3	$[(C_3(NEt_2)_3]FeCl_4$	252.43	197.66	tetrahedral	---	148.7 (solid-liquid)	8.0
					---	50.1 (solid-solid)	3.3
					---	−4.4 (solid-solid)	4.9
4	$[(C_3(NEt_2)_3]_2CuCl_4$	252.43	205.36	distorted tetrahedral	---	26.5	35.8
5	$[(C_3(NEt_2)_3]_2ZnCl_4$	252.43	207.19	tetrahedral	---	80.9	40.4
6	$[(C_3(NEt_2)_3]SnCl_3$	252.43	225.07	trigonal pyramidal	---	58.2	1.5
7	$[(C_3(NBu_2)_3]BF_4$[53]	420.75	86.77	tetrahedral	−53.0	29.0	19.0
8	$[(C_3(NBu_2)_3]FeCl_4$	420.75	197.66	tetrahedral	−65.9	8.8	0.2
9	$[(C_3(NBu_2)_3]_2CuCl_4$	420.75	205.36	distorted tetrahedral	−54.1	---	---
10	$[(C_3(NBu_2)_3]_2ZnCl_4$	420.75	207.19	tetrahedral	−34.3	---	---
11	$[(C_3(NBu_2)_3]SnCl_3$	420.75	225.07	trigonal pyramidal	−31.6	---	---

* T_g = glass transition temperature, T_m = melting point, ΔH = enthalpy change

The geometry of the anion is considered to correlate well with the melting point trend in table 6.5. There is a tetrahedral geometry for BF_4^-, ClO_4^-, $FeCl_4^-$, and $ZnCl_4^{2-}$. However, $CuCl_4^{2-}$ has a distorted tetrahedral geometry and $SnCl_3^-$ has a trigonal pyramidal shape. BF_4^- and ClO_4^- were compared with these metal chlorides due to their similar geometries.

Among the $[C_3(NEt_2)_3]^+$ series, $[C_3(NEt_2)_3]BF_4$ had the lowest melting point of 24 °C. It was thought to be due to the smaller size of the fluorine atom, which holds its electrons tightly and interacts less with the cation. With the increase in size of anion from $BF_4^- < ClO_4^- < FeCl_4^-$, the melting point increases. In the case of $[C_3(NEt_2)_3]FeCl_4$, the highest melting point of 148 °C is seen, probably due to symmetry packing and the tetrahedral shape of the anion. It was also thought that since the chlorine atom has a bigger size than fluoride ion, its electrons are interacting strongly with the cation causing strong van der Waals interactions. In $[C_3(NEt_2)_3]_2CuCl_4$, the size of the anion is increased as compared to $[C_3(NEt_2)_3]FeCl_4$ but the melting point is reduced to 26.5 °C, due to the distorted tetrahedral shape of $CuCl_4^{2-}$ which causes poor packing. The $CuCl_4^{2-}$ and $ZnCl_4^{2-}$ are same sized dianions, the later dianion results in a high melting point of 80.9 °C due to tetrahedral geometry. In $[C_3(NEt_2)_3]SnCl_3$, the trigonal pyramidal shape of the anion, causes poor packing between the counterions resulting in a decrease of melting point of 58.2 °C, although the size of anion is largest among all other metal chloride anions.

As the size of cation is increased to $[C_3(NBu_2)_3]^+$ from $[C_3(NEt_2)_3]^+$, van der Waals forces increases significantly due to the longer butyl chains. However, there is a marked depression of melting points on going to the $[C_3(NBu_2)_3]^+$ series from $[C_3(NEt_2)_3]^+$ series, this is likely due to the increased conformational flexibility of the butyl chains. The effect of anion is not clear in regard to melting points among $[C_3(NBu_2)_3]^+$ series. There is not much difference between the melting point of $[C_3(NEt_2)_3]BF_4$ (24 °C) and $[C_3(NBu_2)_3]BF_4$ (29 °C). Due to the high electronegativity of the fluorine atom hold its electrons tightly in BF_4^- and is interacting less with $[C_3(NEt_2)_3]^+$ and $[C_3(NBu_2)_3]^+$. However, there is a marked depression in the melting point from $[C_3(NEt_2)_3]FeCl_4$ (148.7 °C) to $[C_3(NBu_2)_3]FeCl_4$ (8.8 °C).

Among the $[(C_3(NBu_2)_3]^+$ series, glass transition temperatures in the range from -65.9 to -31.6 °C are observed rather than melting points. Mostly, glass transition temperatures are seen during the heating cycle because they fail to crystallize during the cooling cycle due to an increase of viscosity. With an increase in the size of anion from $FeCl_4^-$, $CuCl_4^{2-}$, $ZnCl_4^{2-}$ and $SnCl_3^-$, the glass transition temperature increases: -65.9 °C, -54.1 °C, -34.3 °C and -31.6 °C respectively.

The TGA results indicate excellent thermal stabilities for all of these MILs. All the samples were run at both 1 °C/min and 10 °C/min (table 6.6).

Table 6.6-TGA results showing onset decomposition temperatures

Entry	IL	M_w of anion (g/mol)	T_d(1) 1 °C/min	T_d(10) 10 °C/min
1	$[(C_3(NEt_2)_3]BF_4$[53]	86.77	344	372
2	$[(C_3(NEt_2)_3]ClO_4$[53]	99.41	241	274
3	$[(C_3(NEt_2)_3]FeCl_4$	197.66	260	320
4	$[(C_3(NEt_2)_3]_2CuCl_4$	205.36	146	182
			261[a]	293[a]
5	$[(C_3(NEt_2)_3]_2ZnCl_4$	207.19	280	314
6	$[(C_3(NEt_2)_3]SnCl_3$	225.07	277	305
7	$[(C_3(NBu_2)_3]BF_4$[53]	86.77	330	388
8	$[(C_3(NBu_2)_3]FeCl_4$	197.66	244	306
9	$[(C_3(NBu_2)_3]_2CuCl_4$	205.36	163	199
			256[a]	298[a]
10	$[(C_3(NBu_2)_3]_2ZnCl_4$	207.19	146	188
			293[a]	318[a]
11	$[(C_3(NBu_2)_3]SnCl_3$	225.07	144	223
			290 [a]	350[a]

[a]second decomposition temperature

For the $[(C_3(NEt_2)_3]^+$ series, the onset/second decomposition temperatures for the MILs ranged from 293-320 °C (10 °C/min) and 260-280 °C (1 °C/min), while for the $[(C_3(NBu_2)_3]^+$ series, onset/ second decomposition temperatures for MILs ranged from 298-306 °C (10 °C/min) and 244-293 °C (1 °C/min)

(table 6.6). For $[(C_3(NEt_2)_3]_2CuCl_4$, $[(C_3(NBu_2)_3]_2CuCl_4$, $[(C_3(NBu_2)_3]_2ZnCl_4$, and $[(C_3(NBu_2)_3]SnCl_3$, two-stage decomposition was observed. Thus, the second-decomposition temperature is considered.

It is known that the cation and anion both affect the decomposition temperatures. With an increase of steric protection of the cyclopropenium ring (due to alkyl chains), the decomposition temperature usually increases.[53]

Xiaoqing and coworkers explained that the thermal decomposition of magnetic CILs, (*R*)-(+)-β-(1-methylimidazole)-propionate tetrachloroferrate(III) and (*R*)-(+)-β-(pyridinium)-propionate tetrachloroferrate(III)[54] was due to partial decomposition of tetrachloroferrate and the volatile organic solvent taking place with the evolution of CO_2, followed by decomposition of the organic part with the evolution of HCl. The strong hydrogen-bond interaction between the chiral cation and tetrachloroferrate(II) anion in Metal CIL (MCIL) (**6.19**) improved the thermal stability as compared to the analogous CIL (**6.18**).[54]

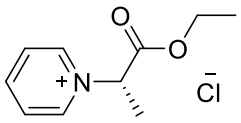

CIL
Decomposition temperature = 175 °C

6.18

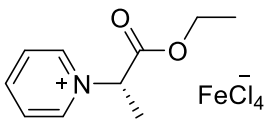

MCIL
Decomposition temperature = 284 °C

6.19

One important thing needs to be mentioned here: that for $[(C_3(NEt_2)_3]_2CuCl_4$, $[(C_3(NBu_2)_3]_2CuCl_4$, $[(C_3(NBu_2)_3]_2ZnCl_4$ and $[(C_3(NBu_2)_3]SnCl_3$, two-step processes temperatures were observed, while in all other MILs, only a one-step decomposition process was observed. The first decomposition temperatures in $[(C_3(NEt_2)_3]_2CuCl_4$ ($T_d(1)$ = 146 ° C and $T_d(10)$ = 182 °C) (fig 6.12), $[(C_3(NBu_2)_3]_2CuCl_4$ ($T_d(1)$ = 163 ° C and $T_d(10)$ = 199 °C) (fig 6.13), $[(C_3(NBu_2)_3]_2ZnCl_4$ ($T_d(1)$ = 146 ° C and $T_d(10)$ = 188 °C) (fig 6.14), and $[(C_3(NBu_2)_3]SnCl_3$ ($T_d(1)$ = 144 ° C and $T_d(10)$ = 223 °C) (fig 6.15) are very low compared to the rest of the MILs.

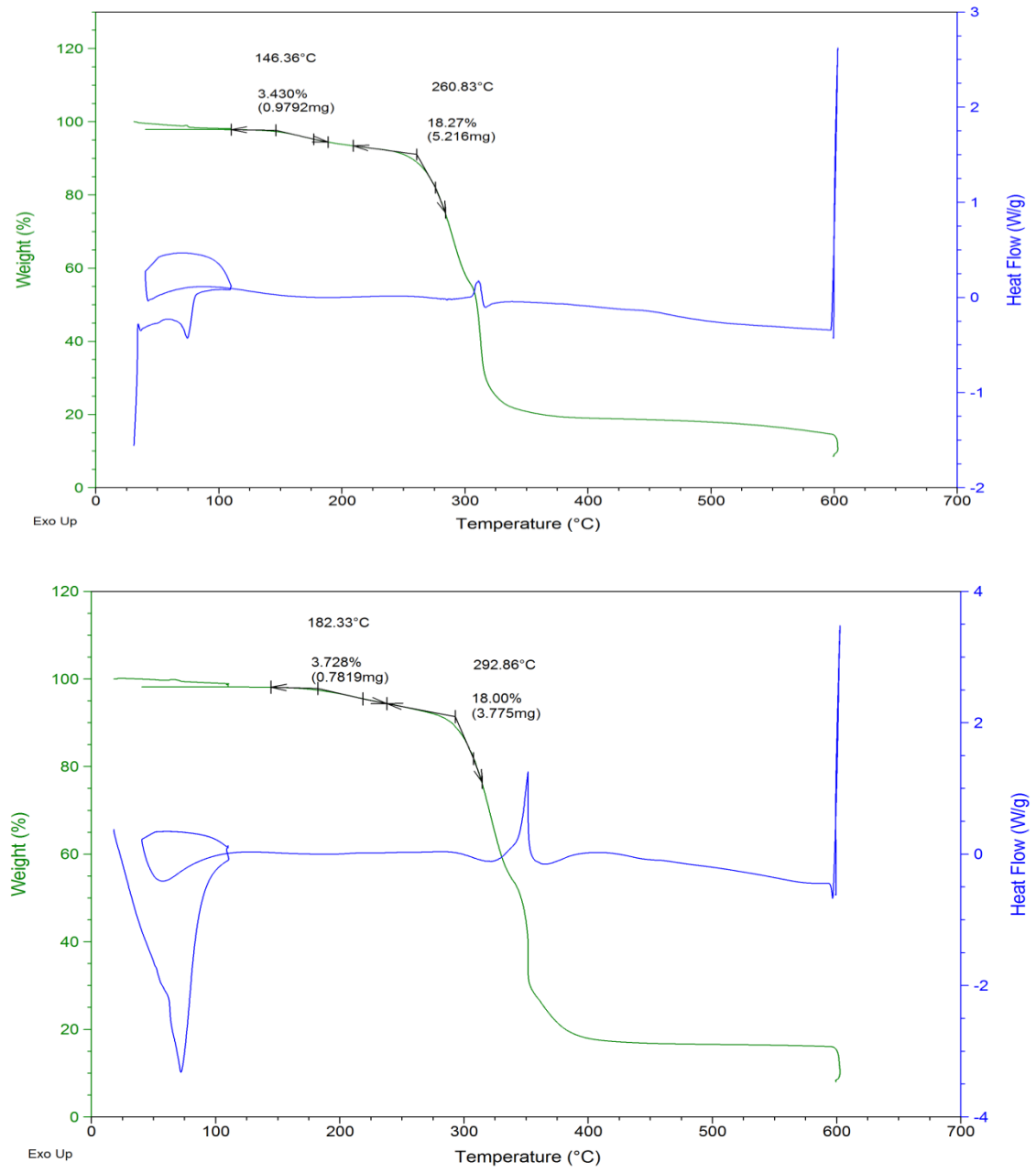

Figure 6.12-TGA curve for $[C_3(NEt_2)_3]_2CuCl_4$ showing two-step decomposition for 1 °C/min (top) and 10 °C/min (bottom).

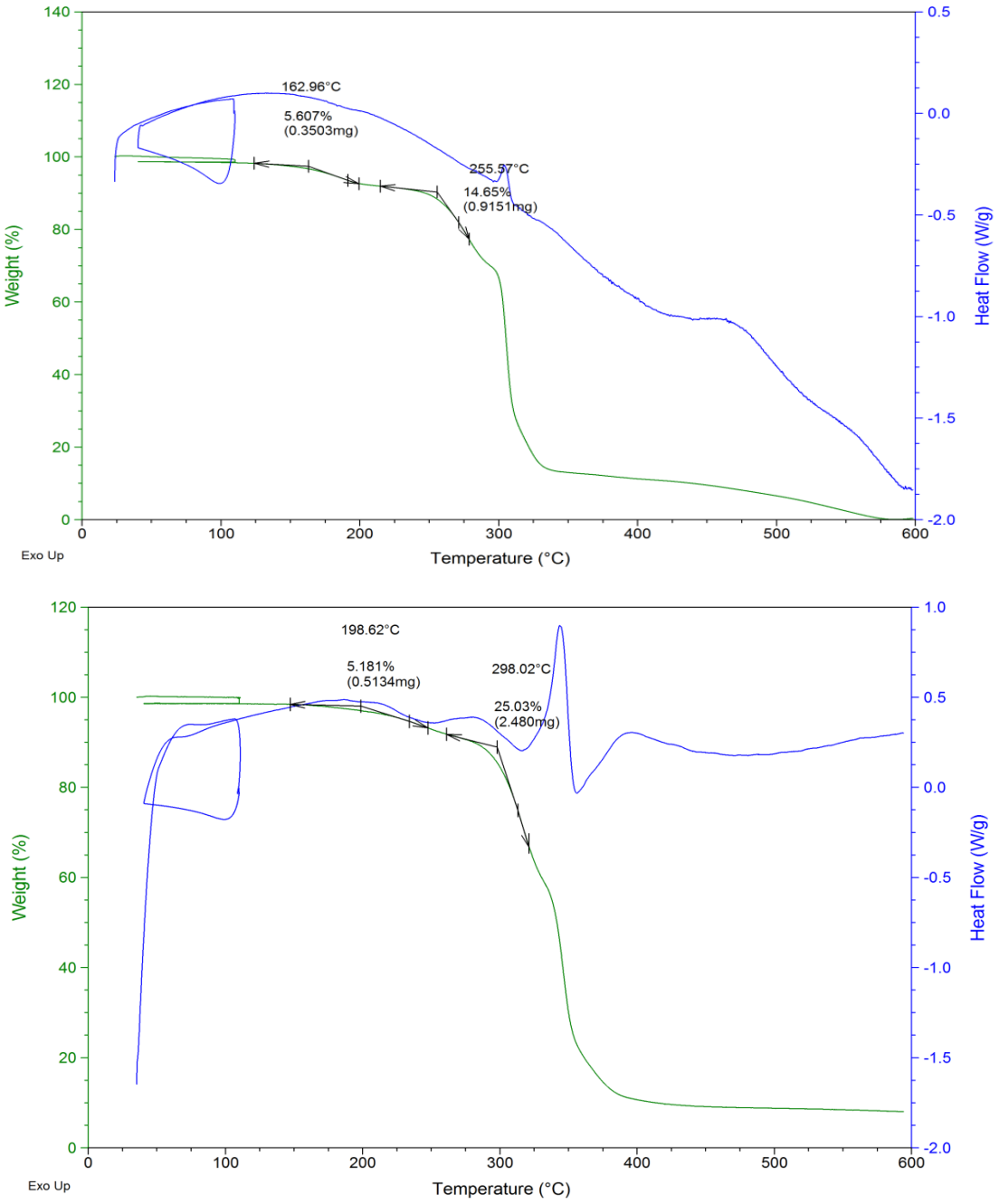

Figure 6.13-TGA curve for $[C_3(NBu_2)_3]_2CuCl_4$ showing two-step decomposition for 1 °C/min (top) and 10 °C/min (bottom).

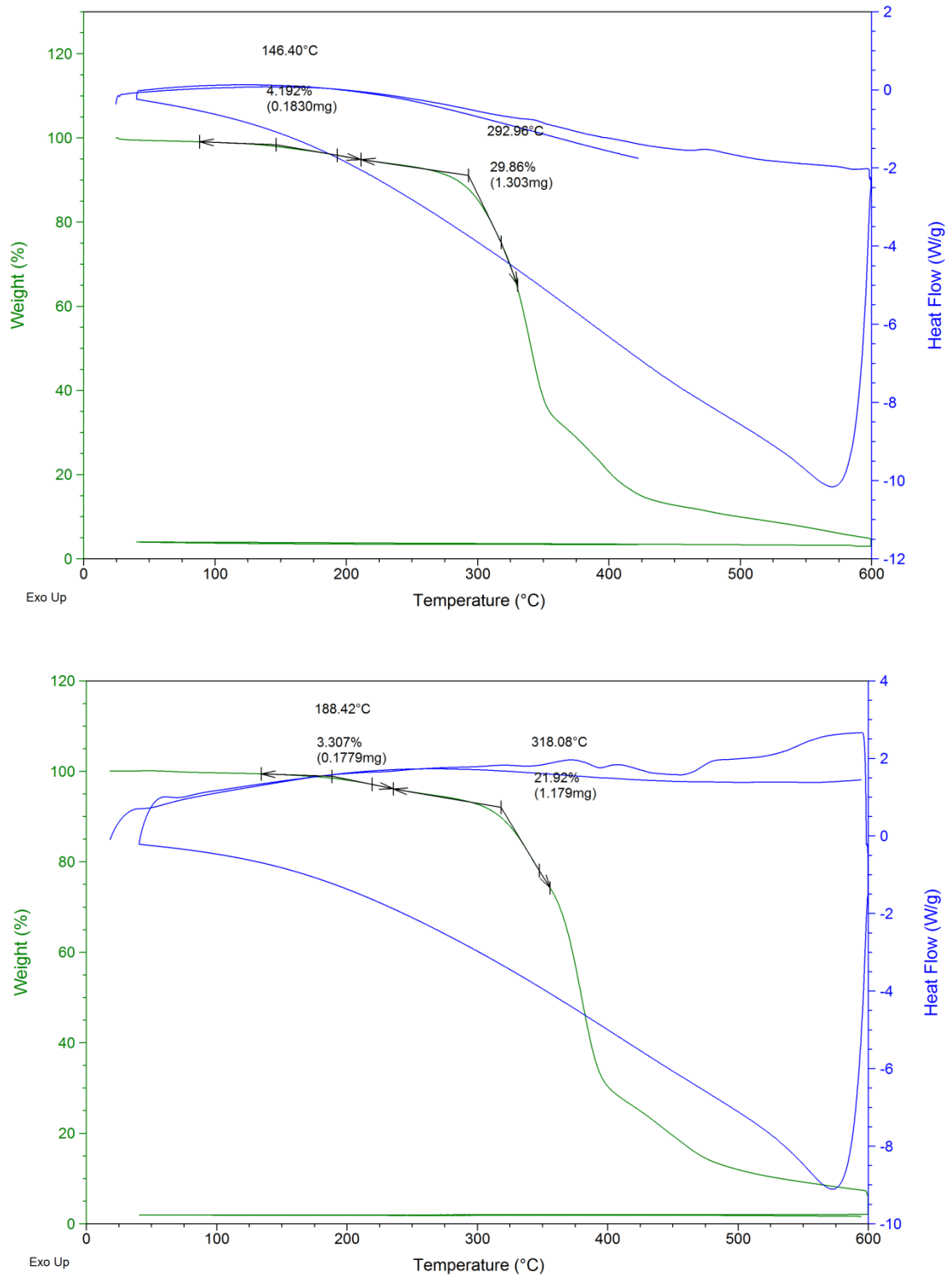

Figure 6.14-TGA curve for $[C_3(NBu_2)_3]_2ZnCl_4$ showing two-step decomposition for 1 °C/min (top) and 10 °C/min (bottom).

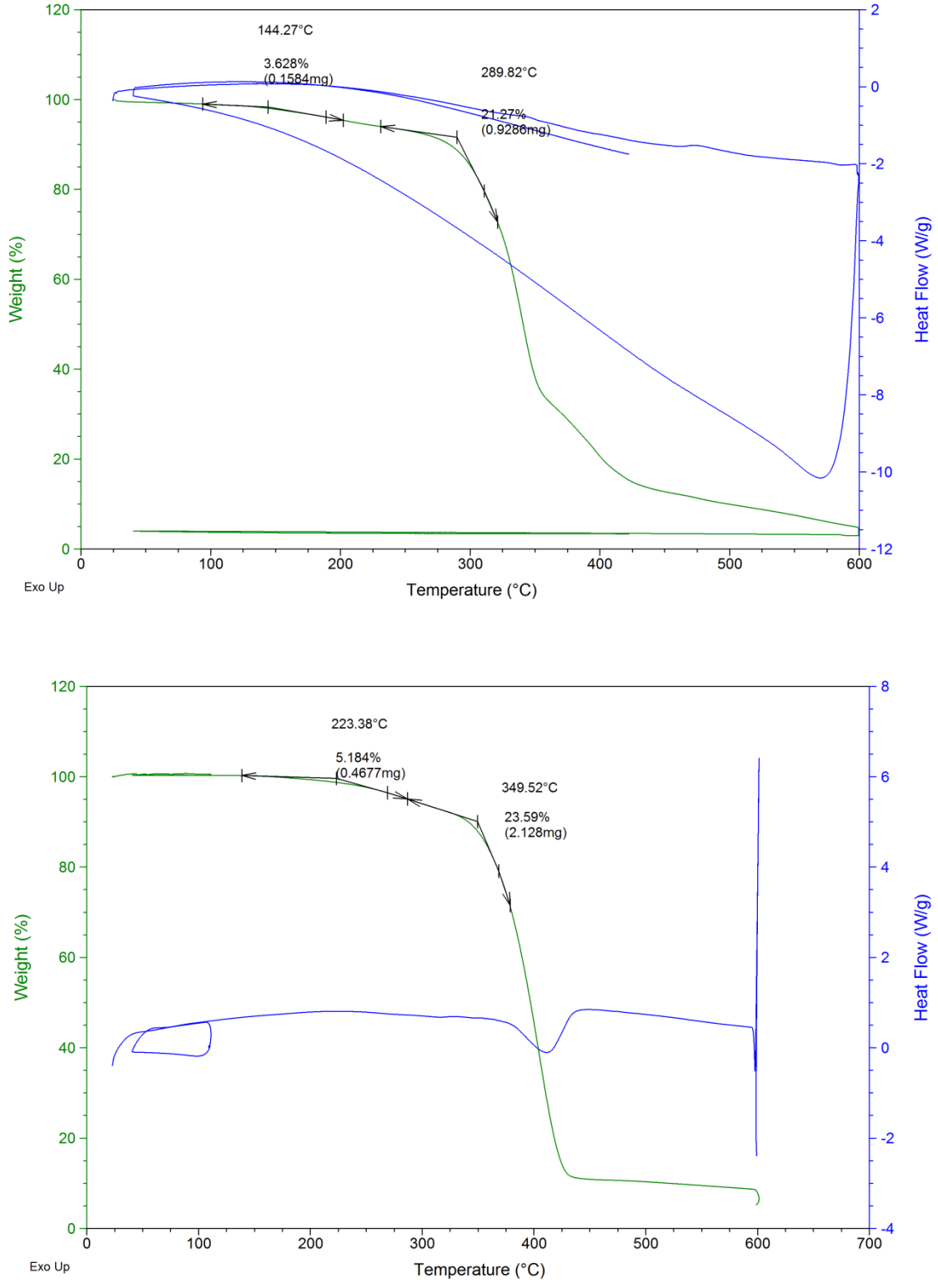

Figure 6.15-TGA curve for $[C_3(NBu_2)_3]SnCl_3$ showing two-step decomposition for 1 °C/min (top) and 10 °C/min (bottom).

Eringathodi and coworkers described two-step decompositions for ILs with tetrachlorocuprate(II) and tetrachlorozincate(II). According to their work, tetrachlorocuprate(II) and tetrachlorozincate(II) exhibit a weight loss in the temperature ranges of 85-145 and 195-260 °C (fig 6.16). A weight loss near 85-145 °C was attributed to the loss of water molecules (fig 6.16). While the second decay around 195-260 °C indicated the commencement of decomposition of the IL (fig 6.16).[55]

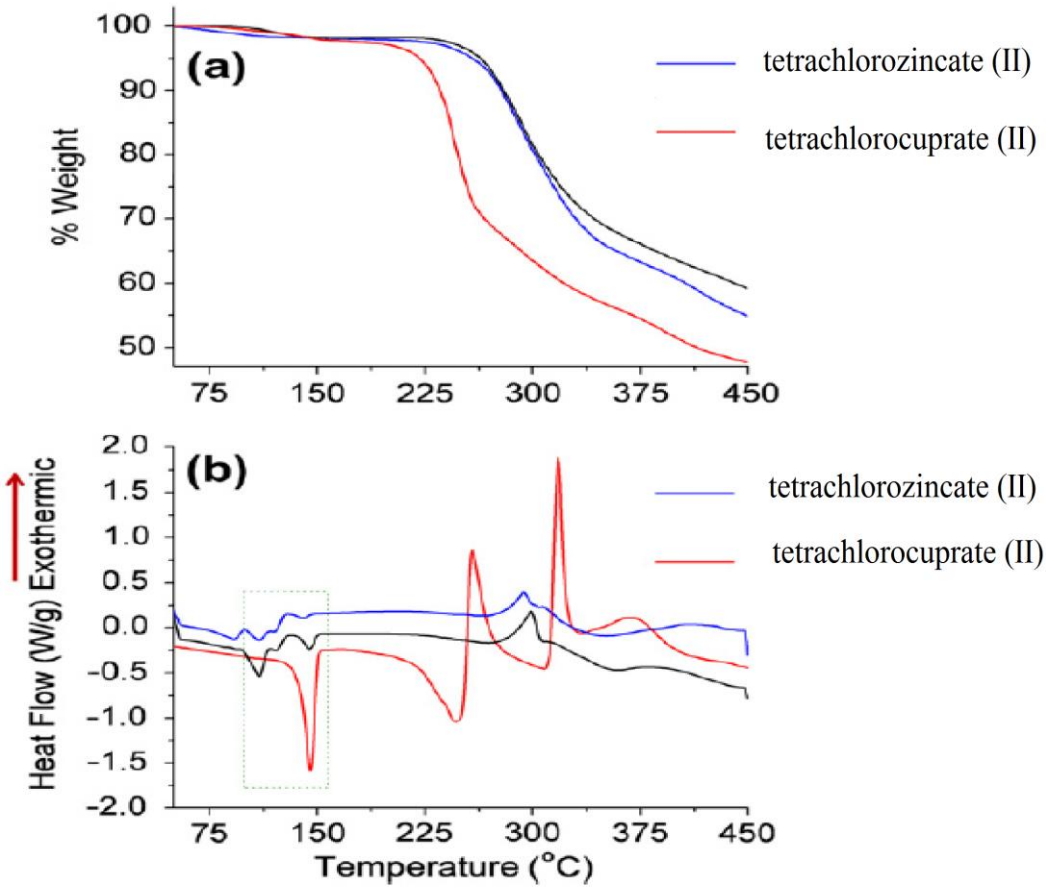

Figure 6.16-a) TGA and b) DSC plots for Pyridinium tetrachlorocuprate(II) and pyridinium tetrachlorozincate(II).[55]

Rissanen and coworkers verified the residue of the first decomposition of tetrachlorocuprate(II) by powder diffraction to be a mixture of copper(I) halide and elemental carbon. While in the second stage (300-600 °C), the carbon is oxidized leaving behind the copper halide in the pan.[56] In the present study, after every TGA run, the platinum pans seemed to change in their color (blacken) due to the deposition of the residual metal chloride.

Thus, we have also reported the second decomposition temperatures for $[(C_3(NEt_2)_3]_2CuCl_4$ (T_d(1) = 261 ° C and T_d(10) = 293 °C) (fig 6.14), $[(C_3(NBu_2)_3]_2CuCl_4$ (T_d(1) = 256° C and T_d(10) = 298 °C) (fig 6.15), $[(C_3(NBu_2)_3]_2ZnCl_4$ (T_d(1) = 293° C and T_d(10) = 318 °C) (fig 6.16), and $[(C_3(NBu_2)_3]SnCl_3$ (T_d(1) = 290° C and T_d(10) = 350 °C) (fig 6.17). Due to the viscous nature of $[(C_3(NBu_2)_3]_2CuCl_4$, $[(C_3(NBu_2)_3]_2ZnCl_4$ and $[(C_3(NBu_2)_3]SnCl_3$, they have a tendency to hold water, which was thought to be responsible for two step-decomposition.

6.4.1.2 Magnetic Properties of $[C_3(NEt_2)_3]FeCl_4$ and $[C_3(NBu_2)_3]FeCl_4$

Among all the synthesized MILs, $[C_3(NEt_2)_3]FeCl_4$ and $[C_3(NBu_2)_3]FeCl_4$ exhibit paramagnetic behavior at room temperature. The molar magnetic susceptibility (χ_M) of these magnetic ILs was measured with a magnetic susceptibility balance. The χ_M of $[C_3(NEt_2)_3]FeCl_4$ and $[C_3(NBu_2)_3]FeCl_4$ were obtained (0.0148 and 0.0118 emu mol^{-1} respectively), which agreed well with the literature values for Fe(III).[57] The effective magnetic moment (μ_{eff}) values for $[C_3(NEt_2)_3]FeCl_4$ and $[C_3(NBu_2)_3]FeCl_4$ were 5.89 and 5.25μ_B respectively.[58] The magnetic moment is useful because it relates to the number of unpaired electrons. It agrees well with the expected value for thr paramagetic S = 5/2 high-spin electronic state of Fe(III) (spin-only value is 5.92μ_B).

Table 6.7-Magnetic Properties

IL	M_w (g/mol)	χ_M (emu mol^{-1})	χ_T (emu mol^{-1})	μ_{eff} (μ_B)
$[C_3(NEt_2)_3]FeCl_4$	459.05	0.0148	4.34	5.89
$[C_3(NBu_2)_3]FeCl_4$	589.19	0.0118	3.46	5.25

* M_w = molecular weight, χ_M = molar magnetic susceptibility, χ_T = molar magnetic susceptibility measured at 300 K, μ_{eff} = effective magnetic moment.

Among both magnetic ILs, $[C_3(NEt_2)_3]FeCl_4$ responded well to an applied magnetic field in its solid state. Their crystals were placed on a paper and they were easily attracted to an external strong magnetic field, such as a neodymium iron boride magnet ($Nd_2Fe_{14}B$) (fig 6.17).

Figure 6.17-Response towards a $Nd_2Fe_{14}B$ magnet of crystals of $[C_3(NEt_2)_3]FeCl_4$.

6.4.1.3 Miscibility and Solubility Studies

The miscibility and solubility parameters were determined for all the MILs. The solvents used were water, methanol, CH_2Cl_2, $CHCl_3$, diethyl ether, toluene and hexane (ranging from polar protic to nonpolar solvents) (table 6.8).

Table 6.8-Miscibility and Solubility results

Entry	IL	Physical state	T_m (°C)	H_2O	MeOH	CH_2Cl_2	$CHCl_3$	Et_2O	Toluene	Hexane
1	$[C_3(NEt_2)_3]BF_4$[53]	Solid	24	N	M	M	M	N	M ≥ 50%	N
2	$[C_3(NEt_2)_3]ClO_4$[53]	Solid	39	partially soluble	M	M	M	N	M	N
3	$[C_3(NEt_2)_3]FeCl_4$	Solid	148.7	partially soluble	M	M	M	N	Immiscible liquid	N
4	$[C_3(NEt_2)_3]_2CuCl_4$	Solid	26.5	M	M	M	M	N	N	N
5	$[C_3(NEt_2)_3]_2ZnCl_4$	Solid	80.9	M	M	M	M	N	N	N
6	$[C_3(NEt_2)_3]SnCl_3$	Solid	58.2	N	N	Immiscible liquid	Immiscible liquid	N	N	N
7	$[C_3(NBu_2)_3]BF_4$[53]	Solid	29	N	M	M	M	partially soluble	M	partially soluble
8	$[C_3(NBu_2)_3]FeCl_4$	Viscous Liquid	8.8	N	M	M	M	N	N	N
9	$[C_3(NBu_2)_3]_2CuCl_4$	Viscous Liquid	---	N	M	M	M	M	M	N
10	$[C_3(NBu_2)_3]_2ZnCl_4$	Viscous Liquid	---	N	M	M	M	N	N	N
11	$[C_3(NBu_2)_3]SnCl_3$	Viscous Liquid	---	N	M	M	M	N	N	N

M = totally soluble or miscible, N = Not soluble or immiscible.

The size of the cation and anion influences the solubility and miscibility. With an increase of the alkyl chain length from ethyl to butyl, the van der Waals forces increase, this decreases the solubility in water. Thus, for the $[C_3(NBu_2)_3]^+$ series, as the size of cation is increased compared to the $[C_3(NEt_2)_3]^+$ series, its water solubility is decreased at all the measured solvent ratios.

With an increase in size of the anion (BF_4^- < ClO_4^- < $FeCl_4^-$ < $ZnCl_4^{2-}$ < $CuCl_4^{2-}$ < $SnCl_3^-$) in the $[C_3(NEt_2)_3]^+$ series, the solubility in toluene decreases. $[C_3(NEt_2)_3]BF_4$ is soluble in a 1:1 ratio with toluene, but with an increase in toluene, it separates as an immiscible liquid. $[C_3(NEt_2)_3]FeCl_4$ also forms an immiscible liquid upon addition of toluene probably due to its larger size and tetrahedral shape (symmetric) of the anion.

The small size and high electronegative character of the fluorine atom results in holding its electrons tightly and therefore unable to interact with water, thus making the BF_4^- anion hydrophobic. $[C_3(NEt_2)_3]FeCl_4$ is partially soluble in water. Whereas, in the case of $[C_3(NEt_2)_3]_2ZnCl_4$ and $[C_3(NEt_2)_3]_2CuCl_4$, due to a greater magnitude of charge on the anion, they are completely soluble in water. In $[C_3(NEt_2)_3]SnCl_3$, the trigonal pyramidal shape and the large size of the anion makes it completely hydrophobic. The trigonal pyramidal geometry of anion in $[C_3(NEt_2)_3]SnCl_3$ results in the formation of immiscible liquid layer with CH_2Cl_2 and $CHCl_3$.

Among the $[C_3(NBu_2)_3]^+$ series, the van der Waals forces are increased which makes them hydrophobic and none of these MILs are miscible with water. Except for $[C_3(NBu_2)_3]_2CuCl_4$, all other MILs for $[C_3(NBu_2)_3]^+$ cation were immiscible with diethyl ether and toluene. Possibly, the distorted tetrahedral shape of the anion in $[C_3(NBu_2)_3]_2CuCl_4$ causes to be miscible in toluene and diethyl ether. In contrast to $[C_3(NBu_2)_3]MCl_x$ with $[C_3(NBu_2)_3]BF_4$, the smaller size of the fluoride atoms in BF_4^- decreases its nucleophilicity and increases its solubility in non-polar solvents (diethyl ether, toluene and hexane).

None of the MILs were soluble or miscible with hexane. Except for $[C_3(NEt_2)_3]SnCl_3$, all MILs were soluble/miscible in methanol, CH_2Cl_2 and $CHCl_3$.

Conclusions

The applications of ILs have been studied. 22 CILs form diastereomeric salts with the enantioenriched sodium salt of Mosher's acid. Their chiral discrimination abilities were screened using ^1H and ^{19}F NMR spectroscopy. Intermolecular interactions including ion-pairing, hydrogen bonding, π-π stacking, hydrophobic and steric interactions were found to affect chiral discrimination. These observations indicate that the tac-class of CILs derived from amino acids has the potential to act as chiral shift reagents.

The aldol reaction between benzaldehyde and acetone was performed in the presence of a CIL as a co-solvent (in the presence of L-proline as catalyst) and as a catalyst. Good enantioselectivities were

obtained when a CIL was used as a co-solvent and catalyst. Unfortunately, poor selectivities were obtained when a CIL was used as a catalyst and solvent because the CIL alone could not catalyze the reaction.

The Diels-Alder reaction was successfully performed using the tac-based CILs. Excellent *endo/exo* ratios were obtained. The reaction proceeds at room temperature (for some viscous CILs, higher temperatures were required) without a catalyst in the presence of a CIL. Thus, they proved to be an effective media for the Diels-Alder reaction.

The tac-based IL chlorides were successfully complexed with metal halides. Thermal studies, magnetic properties, and miscibility studies of these MILs gave a better understanding about the properties of these materials.

References

1. Tran, C. D.; Oliveira, D.; Yu, S. *Anal. Chem.* **2006,** *78*, 1349.
2. Bwambok, D. K.; Marwani, H. M.; Fernand, V. E.; Fakayode, S. O.; Lowry, M.; Negulescun, I.; Strongin, R. M.; Warner, I. M. *Chirality* **2008,** *20* (2), 151.
3. Tulashie, S.; lorenz, H.; Seidel-Morgenstern, A., Potential of chiral solvents for chiral dischrimination in crystallization processes. In *14th International Workshop on Industrial Crystallization*, Lewis, A. E.; Oslen, C., Eds. IOS Publisher: Amsterdam, 2007; pp 259.
4. Altava, B.; Barbosa, D. S.; Burguete, M. I.; Escorihuela, J.; Luis, S. V. *Tetrahedron: Asymmetry* **2009,** *20*, 999.
5. Wasserscheid, P.; Bösmanna, A.; Bolmb, C. *Chem. Commun.* **2002**, 200.
6. Winkel, A.; Wilhelm, R. *Eur. J. Org. Chem.* **2010,** *30*, 5817.
7. Tabassum, S.; Gilani, M. A.; Wilhelm, R. *Tetrahedron Asymmetry* **2011,** *22*, 1632.
8. Jurcık, V.; Wilhelm, R. *Tetrahedron: Asymmetry* **2006,** *17*, 801.
9. Clavier, H.; Boulanger, L.; Audic, N.; Toupet, L.; Mauduit, M.; Jean-Claud *Chem. Commun.* **2004**, 1224.
10. Bonanni, M.; Soldaini, G.; Faggi, C.; Goti, A.; Cardona, F. *Synlett* **2009,** (5), 747.
11. Kumar, V.; Olsen, C. P. C. E.; Schaffer, S. J. C.; Parmarb, V. S.; Malhotraa, S. V. *Tetrahedron Asymmetry* **2008,** *19*, 664.

12. Kumar, V.; Olsen, C. E.; Schaffer, S. J. C.; Parmar, V. S.; Malhotra, S. V. *Org. Lett.* **2007,** *7* (20), 3905.

13. Jurcík, V.; Gilani, M.; Wilhelm, R. *Eur. J. Org. Chem.* **2006**, 5103.

14. Levillain, J.; Dubant, G.; Abrunhosa, I.; Gulea, M.; Gaumont, A.-C. *Chem. Commun.* **2003**, 2914.

15. Li, M.; Gardella, J.; Bwambok, D. K.; El-Zahab, B.; Rooy, S. d.; Cole, M.; Lowry, M.; Warner, I. M. *J. Comb. Chem.* **2009,** *11*, 1105.

16. Parker, D. *Chem. Rev.* **1991,** *91*, 1441.

17. Schulz, P. S.; Muller, N.; Bosmann, A.; Wasserscheid, P. *Angew. Chem. Int. Ed.* **2007,** *46*, 1293.

18. Rizvi, S. A. A.; Shamsi, S. A. *J. Anal. Chem.* **2006,** *78* (19), 7061.

19. Corodova, A.; Zou, W.; Dziedzic, P.; Ibrahem, I.; Reyes, E.; Xu, Y. *Chem. Eur. J.* **2006,** *12*, 5283.

20. Howarth, J.; HanIon, K.; Fayne, D.; McCormac, P. *Tetrahedron Lett.* **1997,** *38* (17), 3097.

21. (a) Nakadai, M.; Saito, S.; Yamamoto, H. *Tetrahedron* **2002,** *58*, 8167; (b) Wang, W.; Mei, Y.; Li, H.; Wang, J. *J. Org. Chem.* **2007,** *7*, 601.

22. Vasiloiu, M.; Rainer, D.; Gaertner, P.; Reichel, C.; Schroder, C.; Bica, K. *Catal. Today* **2013,** *200*, 80.

23. (a) List, B.; Lerner, R. A.; Barbas, C. F. *J. Am. Chem. Soc.* **2000,** *122*, 2395; (b) Loh, T.-P.; Feng, L.-C.; Yanga, H.-Y.; Yang, J.-Y. *Tetrahedron Lett.* **2002,** *43* (48), 8741.

24. Luo, S.; Mi, X.; Zhang, L.; Liu, S.; Xu, H.; Cheng, J.-P. *Tetrahedron* **2007,** *63*, 1923.

25. Lombardo, M.; Pasi, F.; Easwar, S.; Trombini, C. *Adv. Synth. Catal.* **2007,** *349*, 2061.

26. Font, D.; Sayalero, S.; Bastero, A.; Jimeno, C.; Pericas, M. A. *Org. Lett.* **2008,** *10* (2), 337.

27. Lombardo, M.; Easwar, S.; Pasi, F.; Trombini, C. *Adv. Synth. Catal.* **2009,** *351*, 276.

28. Zhou, L.; Wang, L. *Chem. Lett.* **2007,** *36* (5), 628.

29. Freemantle, M., *An Introduction to Ionic Liquids*. Royal Society of Chemistry: 2010.

30. Hayashi, Y.; Gotoh, H.; Hayashi, T.; Shoji, M. *Angew. Chem. Int. Ed.* **2005,** *44*, 4212.

31. Hayashi, Y.; Aratake, S.; Itoh, T.; Okano, T.; Shoji, M.; Sumiya, T. *Chem. Commun.* **2007**, 957.

32. Miao, W.; Chan, T. H. *Adv Synth Catal* **2006,** *348*, 1711.

33. Sakthivel, K.; Notz, W.; Bui, T.; Barbas, C. F. *J. Am. Chem. Soc.* **2001,** *123*, 5260.

34. Gauchot, V.; Schmitzer, A. R. *Journal Organic Chemistry* **2012,** *77*, 4917.

35. Zotova, N.; Franzke, A.; Armstrong, A.; Blckmond, D. G. *J. Am. Chem. Soc.* **2007,** *129*, 15100.

36. March, J., *Advanced Organic Chemistry*. 3rd ed.; Wiley: New York, 1985.

37. Vidis, A.; Ohlin, C. A.; Laurenczy, G.; Kusters, E.; Sedelmeier, G.; Dyson, P. J. *Adv. Synth. Catal.* **2005,** *347*, 266.

38. Dyson, P. J.; Geldbach, T. J., *Metal Catalyzed Reactions in Ionic Liquids*. Springer: 2005; Vol. 29.

39. Garrigues, B.; Gonzaga, F.; Roberts, H.; Dubac, J. *J. Org. Chem.* **1997,** *62*, 4880.

40. Pindur, U.; Lutz, G.; Otto, C. *Chem. Rev.* **1993,** *93*, 741.

41. Cativiela, C.; Garcia, J. I.; Mayoral, J. A.; Royo, A. J.; Salvatella, L.; Assfeld, X.; Ruiz-Lopez, M. F. *J. Phys. Org. Chem.* **1992,** *5*, 230.

42. Tiwari, S.; Kumar, A. *Angew. Chem. Int. Ed.* **2006,** *45*, 4824.

43. Jaeger, D. A.; Tucker, C. E. *Tetrahedron Lett.* **1989,** *30*.

44. (a) Tao, G.-h.; He, L.; Liu, W.-s.; Xu, L.; Xiong, W.; Yuan, T. W. a. *Green Chemistry* **2006,** *8*, 639; (b) Zheng, X.; Qian, Y.; Wang, Y. *Catal. Commun.* **2010,** *11*, 567; (c) Doherty, S.; Goodrich, P.; Hardacre, C.; Knight, J. G.; Nguyen, M. T.; Parvulescu, V. I.; Paun, C. *Adv. Synth. Catal.* **2007,** *349*, 951.

45. Aggarwal, A.; Lancaster, N. L.; Sethi, A. R.; Welton, T. *Green Chemistry* **2002,** *4*, 517.

46. Berson, J. A.; Hamlet, Z.; Mueller, W. A. *J. Am. Chem. Soc.* **1962,** *84*, 297.

47. Schreiner, P. R.; Wittkopp, A. *Org. Lett.*, **2002,** *4*, 217.

48. Kumar, A.; Phalgune, U.; Pawar, S. S. *J. Phy. Org. Chem.* **2000,** *13*, 555.

49. Kumar, A.; Deshpande, S. S. *J. Org. Chem.* **2003,** *68*, 5411.

50. Janus, E.; Bittner, B. *Catal. Lett.* **2010,** *134*, 147.

51. Cocalia, V. A.; Visser, A. E.; Rogers, R. D.; Holbrey, J. D., *Ionic Liquids in Synthesis*. WILEY-VCH Verlags GmbH & Co. KGaA: Weinheim, 2008; Vol. 2.

52. Neve, F.; Francescangeli, O.; Crispini, A. *Inorg. Chim. Acta* **2002,** *338*, 51.

53. Walst, K. J. Synthesis and Characterization of Triaminocyclopropenium as a New Class of Ionic Liquids. PhD Thesis, University of Canterbury, Christchurch, 2013.

54. Liwei, Q.; Xiaoling, H.; Ping, G.; Xiaoqing, G. *Applied Mechanics and Materials* **2012,** *161*, 128.

55. Bisht, K. K.; Kathalikkattil, A. C.; Eringathodi, S. *J. Mol. Struct.* **2012,** *1013*, 102.

56. Busi, S.; Lahtinen, M.; Valkonen, J.; Rissanen, K. *J. Mol. Struct.* **2006,** *794*, 277.

57. Li, M.; Rooy, S. L. D.; Bwambok, D. K.; El-Zahab, B.; DiTusab, J. F.; Warner, I. M. *Chem. Commun.* **2009,** *45*, 6922.

58. Sesto, R. E. D.; McCleskey, T. M.; Burrell, A. K.; Baker, G. A.; Thompson, J. D.; Scott, B. L.; Wilkes, J. S.; Williams, P. *Chem. Commun.* **2007**, 447.

Appendix

Table 7.1 Fractional Atomic Coordinates ($\times 10^4$) and Equivalent Isotropic Displacement Parameters ($Å^2 \times 10^3$) for $[C_3(NEt_2)_3]FeCl_4$ U_{eq} is defined as 1/3 of of the trace of the orthogonalised U_{IJ} tensor.

Atom	*x*	*y*	*z*	U(eq)
Fe1	9236.9(6)	5196.3(4)	6195.9(4)	25.32(13)
Cl2	10704.1(10)	5633.6(6)	7158.0(6)	32.77(19)
Cl3	8448.6(11)	3780.7(6)	6425.0(8)	43.8(3)
Cl4	7348.7(10)	6133.6(6)	6132.6(8)	44.2(3)
Cl5	10482.9(13)	5276.7(9)	5092.3(6)	48.3(3)
N1	9697(3)	4789(2)	3051.2(19)	24.5(6)
C2	7060(4)	4640(2)	3660(2)	22.3(7)
N3	6176(3)	3940.4(19)	3860(2)	25.4(6)
C4	8377(3)	4947(2)	3357(2)	21.5(7)
C5	10771(4)	5544(2)	2983(2)	26.3(7)
C6	7331(4)	5578(2)	3620(2)	22.6(7)
C7	5462(4)	6653(2)	4057(2)	28.3(8)
C8	7831(4)	7224(2)	3472(2)	26.8(8)
C9	6572(4)	2980(2)	3677(2)	29.1(8)
C10	6770(5)	2387(3)	4399(3)	39.4(10)
C11	4735(4)	4139(2)	4196(2)	27.6(8)
C12	10688(4)	3347(2)	3639(3)	37.3(9)
C13	4779(4)	4333(3)	5081(3)	34.4(8)
N14	6923(3)	6443.7(18)	3744(2)	24.5(6)
C15	10901(5)	5902(3)	2151(3)	39.1(9)
C16	4315(4)	6724(2)	3416(3)	34.8(9)
C17	8660(5)	7671(3)	4149(3)	43.6(11)
C18	10194(4)	3843(2)	2897(2)	29.7(8)

Table 7.2-Anisotropic Displacement Parameters ($Å^2×10^3$) for $[C_3(NEt_2)_3]FeCl_4$. The Anisotropic displacement factor exponent takes the form: $-2\pi^2[h^2a^{*2}U_{11}+2hka^*b^*U_{12}+\ldots]$.

Atom	U_{11}	U_{22}	U_{33}	U_{12}	U_{13}	U_{23}
Fe1	22.6(2)	25.1(2)	28.3(3)	1.3(2)	-2.3(2)	-0.9(2)
Cl2	32.7(4)	37.2(4)	28.4(5)	-5.0(4)	-6.5(4)	2.6(4)
Cl3	35.9(5)	27.1(4)	68.5(8)	-4.5(3)	-6.6(5)	2.1(5)
Cl4	28.9(4)	34.8(4)	69.0(8)	7.8(3)	-8.1(5)	-4.3(5)
Cl5	56.0(6)	62.3(6)	26.5(5)	10.4(5)	6.6(4)	0.7(5)
N1	19.5(13)	25.9(12)	28.1(16)	-0.9(11)	4.1(11)	1.1(14)
C2	19.2(15)	26.8(15)	21.0(19)	2.8(11)	-1.3(13)	1.6(14)
N3	17.9(12)	26.0(13)	32.5(18)	-4.4(10)	1.1(12)	2.7(14)
C4	18.1(14)	22.1(14)	24.2(18)	-0.8(12)	1.4(12)	-0.5(13)
C5	17.8(14)	31.0(15)	30(2)	-2.8(13)	3.1(15)	2.7(15)
C6	19.5(15)	30.6(14)	17.6(18)	-1.0(12)	-0.6(13)	2.0(14)
C7	23.8(17)	26.3(14)	35(2)	2.3(13)	3.3(15)	-1.8(15)
C8	27.1(17)	24.2(14)	29(2)	-2.3(13)	3.1(15)	1.9(15)
C9	32.2(18)	28.2(15)	27(2)	-7.7(14)	1.6(15)	1.5(16)
C10	50(2)	32.3(18)	36(3)	6.6(17)	4(2)	8.7(18)
C11	19.7(16)	30.7(15)	32(2)	-4.5(13)	3.8(14)	1.3(16)
C12	31.1(19)	32.0(16)	49(3)	4.2(16)	-12(2)	2.5(18)
C13	30.9(18)	40.5(18)	32(2)	-1.8(15)	6.4(16)	1.4(19)
N14	21.3(13)	22.1(11)	30.2(19)	-3.1(10)	1.8(12)	1.0(13)
C15	40(2)	45(2)	33(2)	-1.0(17)	8.4(18)	15.9(19)
C16	22.8(17)	31.2(16)	50(3)	5.0(15)	0.0(18)	-6.2(17)
C17	43(2)	46(2)	41(3)	-15.0(18)	0(2)	-8(2)
C18	24.5(16)	29.4(16)	35(2)	0.9(13)	6.0(15)	-3.3(17)

Table 7.3- Bond Lengths for $[C_3(NEt_2)_3]FeCl_4$.

Atom	Atom	Length/Å	Atom	Atom	Length/Å
Fe1	Cl2	2.2003(11)	N3	C11	1.459(4)
Fe1	Cl3	2.1995(10)	C4	C6	1.391(5)
Fe1	Cl4	2.1909(10)	C5	C15	1.507(5)
Fe1	Cl5	2.1905(12)	C6	N14	1.320(4)
N1	C4	1.329(4)	C7	N14	1.465(4)
N1	C5	1.469(4)	C7	C16	1.511(5)
N1	C18	1.461(4)	C8	N14	1.472(4)
C2	N3	1.336(4)	C8	C17	1.516(6)
C2	C4	1.377(5)	C9	C10	1.504(5)
C2	C6	1.377(4)	C11	C13	1.526(6)
N3	C9	1.465(4)	C12	C18	1.515(6)

Table 7.4- Bond Angles for $[C_3(NEt_2)_3]FeCl_4$

Atom	Atom	Atom	Angle/°	Atom	Atom	Atom	Angle/°
Cl3	Fe1	Cl2	109.51(5)	C2	C4	N1	151.4(3)
Cl4	Fe1	Cl2	109.65(5)	C6	C4	N1	148.9(3)
Cl4	Fe1	Cl3	108.99(4)	C6	C4	C2	59.6(2)
Cl5	Fe1	Cl2	107.60(5)	C15	C5	N1	112.4(3)
Cl5	Fe1	Cl3	111.65(5)	C4	C6	C2	59.7(2)
Cl5	Fe1	Cl4	109.41(5)	N14	C6	C2	150.6(3)
C5	N1	C4	120.4(3)	N14	C6	C4	149.7(3)
C18	N1	C4	120.7(3)	C16	C7	N14	112.5(3)
C18	N1	C5	118.1(3)	C17	C8	N14	111.6(3)
C4	C2	N3	149.6(3)	C10	C9	N3	113.3(3)
C6	C2	N3	149.7(3)	C13	C11	N3	113.3(3)
C6	C2	C4	60.7(2)	C7	N14	C6	120.6(3)
C9	N3	C2	120.8(3)	C8	N14	C6	121.0(3)
C11	N3	C2	119.6(3)	C8	N14	C7	117.8(3)
C11	N3	C9	119.4(3)	C12	C18	N1	112.6(3)

Table 7.5-Hydrogen Atom Coordinates (Å×10^4) and Isotropic Displacement Parameters (Å^2×10^3) for [C$_3$(NEt$_2$)$_3$]FeCl$_4$

Atom	*x*	*y*	*z*	U(eq)
H5a	10482(4)	6048(2)	3328(2)	31.5(9)
H5b	11723(4)	5322(2)	3157(2)	31.5(9)
H7a	5178(4)	6171(2)	4426(2)	33.9(10)
H7b	5500(4)	7234(2)	4344(2)	33.9(10)
H8a	8527(4)	7004(2)	3081(2)	32.2(9)
H8b	7208(4)	7684(2)	3222(2)	32.2(9)
H9a	5812(4)	2711(2)	3348(2)	34.9(10)
H9b	7478(4)	2978(2)	3376(2)	34.9(10)
H10a	7030(40)	1769(6)	4243(3)	59.2(15)
H10b	7530(30)	2643(13)	4723(10)	59.2(15)
H10c	5869(12)	2370(19)	4693(10)	59.2(15)
H11a	4320(4)	4672(2)	3928(2)	33.1(9)
H11b	4092(4)	3615(2)	4100(2)	33.1(9)
H12a	11070(30)	2747(9)	3502(3)	56.0(14)
H12b	11440(30)	3703(11)	3894(10)	56.0(14)
H12c	9869(9)	3280(20)	3990(9)	56.0(14)
H13a	5450(30)	4833(14)	5185(3)	51.5(13)
H13b	3815(8)	4500(20)	5261(4)	51.5(13)
H13c	5100(30)	3788(7)	5356(3)	51.5(13)
H15a	11270(30)	5419(7)	1814(4)	58.7(14)
H15b	9953(8)	6100(20)	1967(7)	58.7(14)
H15c	11570(30)	6418(15)	2140(4)	58.7(14)
H16a	4565(19)	7220(14)	3063(11)	52.2(13)
H16b	4280(20)	6152(8)	3127(12)	52.2(13)
H16c	3374(7)	6840(20)	3649(3)	52.2(13)
H17a	9250(30)	8168(17)	3950(4)	65.3(16)
H17b	7973(5)	7910(20)	4527(11)	65.3(16)
H17c	9280(30)	7217(7)	4398(14)	65.3(16)
H18a	9400(4)	3496(2)	2656(2)	35.6(10)
H18b	11002(4)	3861(2)	2524(2)	35.6(10)

Table 7.6-Fractional Atomic Coordinates ($\times 10^4$) and Equivalent Isotropic Displacement Parameters ($Å^2 \times 10^3$) for $[HC_3(NMe_2)_4]Cl$. U_{eq} is defined as 1/3 of of the trace of the orthogonalised U_{IJ} tensor.

Atom	*x*	*y*	*z*	U(eq)
Cl1	5000	1348.2(7)	2500	24.71(17)
Cl2	6970.8(3)	10730.0(7)	4916.8(5)	45.36(19)
Cl3	7313.5(4)	11476.9(8)	3005.3(6)	53.7(2)
Cl4	6875.9(4)	8682.4(8)	3283.2(7)	58.0(2)
C1	5843.5(12)	4361(2)	4398.1(17)	30.9(5)
C2	5400.9(11)	6567(2)	3468.7(15)	23.8(4)
C3	5000	7216(3)	2500	24.8(6)
N4	5482.3(12)	7198.6(19)	4423.2(14)	35.7(5)
N5	5735.3(9)	5334.4(17)	3511.4(13)	24.4(4)
C6	5951.2(11)	4802(2)	2620.6(17)	29.7(4)
C7	6754.8(12)	10426(3)	3526(2)	37.9(5)
C8	6186.9(18)	7150(3)	5306.1(18)	55.2(8)
C9	4993(2)	8324(2)	4470(2)	55.4(9)

Table 7.7-Anisotropic Displacement Parameters ($Å^2×10^3$) for $[HC_3(NMe_2)_4]Cl$. The Anisotropic displacement factor exponent takes the form: $-2\pi^2[h^2a^{*2}U_{11}+2hka^*b^*U_{12}+\ldots]$.

Atom	U_{11}	U_{22}	U_{33}	U_{23}	U_{13}	U_{12}
Cl1	21.1(3)	23.8(3)	27.0(3)	0	4.6(2)	0
Cl2	41.0(3)	54.2(4)	41.5(3)	-3.0(3)	14.1(3)	-9.0(3)
Cl3	42.0(3)	70.9(5)	49.3(4)	22.6(3)	16.2(3)	1.7(3)
Cl4	54.2(4)	52.2(4)	71.4(5)	-14.9(3)	25.4(4)	0.5(3)
C1	27.3(10)	33.7(11)	28.6(10)	10.0(8)	4.5(8)	1.8(8)
C2	32.9(10)	20.6(9)	18.8(9)	-1.4(7)	9.7(8)	-7.6(7)
C3	38.8(15)	16.8(14)	20.3(12)	0	11.4(11)	0
N4	63.7(13)	25.2(9)	18.7(8)	-4.4(7)	14.0(8)	-11.9(9)
N5	24.9(8)	26.6(9)	21.1(8)	3.6(6)	6.7(6)	-1.9(6)
C6	24.6(9)	34.6(12)	30.6(10)	1.1(8)	10.2(8)	3.6(8)
C7	23.7(10)	47.8(14)	40.0(12)	3(1)	7.2(9)	4.1(9)
C8	83(2)	51.8(16)	19.8(10)	1.1(10)	0.6(11)	-38.9(15)
C9	126(3)	20.9(11)	36.0(13)	-2.3(9)	49.1(16)	0.6(14)

Table 7.8-Bond Lengths for $[HC_3(NMe_2)_4]Cl$

Atom	Atom	Length/Å	Atom	Atom	Length/Å
Cl2	C7	1.760(3)	C2	N5	1.352(3)
Cl3	C7	1.768(3)	C3	$C2^1$	1.405(2)
Cl4	C7	1.756(3)	N4	C8	1.468(3)
C1	N5	1.462(2)	N4	C9	1.455(4)
C2	C3	1.405(2)	N5	C6	1.454(3)
C2	N4	1.358(2)			

Table 7.9-Bond Angles for $[HC_3(NMe_2)_4]Cl$

Atom	Atom	Atom	Angle/°	Atom	Atom	Atom	Angle/°
N4	C2	C3	119.78(19)	C2	N5	C1	123.50(17)
N5	C2	C3	123.35(18)	C2	N5	C6	122.41(16)
N5	C2	N4	116.85(18)	C6	N5	C1	113.80(17)
C2	C3	$C2^1$	126.5(3)	Cl2	C7	Cl3	109.50(14)
C2	N4	C8	121.0(2)	Cl4	C7	Cl2	110.47(14)
C2	N4	C9	119.7(2)	Cl4	C7	Cl3	110.93(13)
C9	N4	C8	115.5(2)				

Table 7.10-Hydrogen Atom Coordinates ($Å\times10^4$) and Isotropic Displacement Parameters ($Å^2\times10^3$) for $[HC_3(NMe_2)_4]Cl$

Atom	*x*	*y*	*z*	U(eq)
H1A	6359	4306	4804	46
H1B	5668	3471	4113	46
H1C	5574	4666	4860	46
H6A	6439	4423	2892	45
H6B	5946	5534	2127	45
H6C	5611	4099	2254	45
H7	6237	10670	3168	46
H8A	6116	6705	5919	83
H8B	6363	8068	5498	83
H8C	6542	6646	5078	83
H9A	5167	9159	4246	83
H9B	4987	8425	5196	83
H9C	4504	8130	4001	83
H3	5000	8110(40)	2500	28(9)

Table 7.11-Fractional Atomic Coordinates ($\times 10^4$) and Equivalent Isotropic Displacement Parameters ($Å^2 \times 10^3$) for $[C_3(NPhH)_3]TFSA$. U_{eq} is defined as 1/3 of of the trace of the orthogonalised U_{IJ} tensor.

Atom	*x*	*y*	*z*	U(eq)
C1B	9509(4)	7128(3)	7344(3)	22.4(7)
C2	9508(4)	6241(3)	7395(3)	23.7(7)
C1A	9221(4)	6684(3)	6962(3)	23.0(7)
N1A	7800(3)	6648(2)	6176(2)	26.3(6)
C11A	6865(5)	7376(4)	5694(3)	21.2(13)
C12A	5407(10)	7271(7)	4734(7)	36.2(19)
C13A	4520(16)	7891(6)	4235(11)	34.8(14)
C14A	4933(7)	8700(10)	4671(5)	31.8(15)
C15A	6436(12)	8809(6)	5766(12)	36.1(18)
C16A	7297(7)	8172(3)	6150(5)	26.8(13)
N1B	8781(3)	7866(2)	6940(2)	27.0(6)
C11B	7287(6)	7888(3)	6005(4)	21.2(13)
C12B	6522(13)	8729(6)	5632(12)	36.2(19)
C13B	5196(8)	8790(11)	4849(6)	34.8(14)
C14B	4444(16)	8070(6)	4229(11)	31.8(15)
C15B	5208(10)	7230(7)	4485(7)	36.1(18)
C16B	6574(6)	7190(4)	5374(4)	26.8(13)
N2	8796(3)	5505.4(19)	7078(3)	26.7(7)
C21	9492(11)	4696(6)	7355(7)	24.0(11)
C22	8872(19)	3998(9)	7466(12)	33.0(18)
C23	9508(6)	3189(3)	7696(4)	40.5(10)
C24	9283(6)	3080(3)	7188(4)	40.5(10)
C25	8711(19)	3778(9)	7273(12)	33.0(18)
C26	9305(10)	4579(6)	7516(7)	24.0(11)
S1	5335.6(5)	5428.4(3)	6858.2(3)	27.51(16)
O1	5323.9(16)	4508.9(9)	6844.0(11)	39.5(4)
O2	6487.7(16)	5855.9(11)	7036.0(13)	48.6(4)
N4	5000	5868.4(15)	7500	39.2(6)
C4	3756(2)	5736.7(14)	5518.7(17)	36.3(5)
F1	3891.1(14)	5426.4(9)	4858.1(10)	50.5(4)
F2	2583.2(13)	5411.1(11)	5260.9(11)	63.6(5)
F3	3619.9(17)	6577.1(9)	5409.7(12)	60.1(4)

Table 7.12-Anisotropic Displacement Parameters ($Å^2×10^3$) for[$C_3(NPhH)_3$]TFSA. The Anisotropic displacement factor exponent takes the form: $-2\pi^2[h^2a^{*2}U_{11}+...+2hka×b×U_{12}]$

Atom	U_{11}	U_{22}	U_{33}	U_{23}	U_{13}	U_{12}
C1B	23.7(17)	21.1(18)	23(2)	-3.2(17)	15.7(18)	-2.8(15)
C2	24.8(17)	21.6(19)	23.1(19)	2.8(17)	15.2(17)	3.8(15)
C1A	25(2)	20(2)	26(2)	-1(2)	17.6(19)	-0.3(17)
N1A	25.2(15)	20.2(15)	31.4(16)	-0.4(13)	17.9(14)	-0.2(12)
C11A	24.1(18)	14(3)	23(2)	-3(3)	14.9(17)	-1.1(18)
C12A	55(3)	30(3)	39(4)	-21(2)	38(2)	-19(2)
C13A	30(3)	29(3)	33(2)	-10(2)	16(2)	-3(3)
C14A	25(2)	26(3)	35(3)	2(3)	15.6(18)	4(2)
C15A	51(3)	36(3)	32(3)	-17(2)	32(2)	-12(2)
C16A	29.1(17)	16(3)	31(2)	-8(2)	17.6(15)	-6.2(18)
N1B	26.7(15)	21.8(16)	26.3(15)	-2.0(13)	15.0(13)	-0.6(13)
C11B	24.1(18)	14(3)	23(2)	-3(3)	14.9(17)	-1.1(18)
C12B	55(3)	30(3)	39(4)	-21(2)	38(2)	-19(2)
C13B	30(3)	29(3)	33(2)	-10(2)	16(2)	-3(3)
C14B	25(2)	26(3)	35(3)	2(3)	15.6(18)	4(2)
C15B	51(3)	36(3)	32(3)	-17(2)	32(2)	-12(2)
C16B	29.1(17)	16(3)	31(2)	-8(2)	17.6(15)	-6.2(18)
N2	22.2(14)	22.3(16)	32.5(17)	-0.6(12)	16.8(13)	-2.2(12)
C21	24(2)	19(2)	28(3)	0.9(18)	16.6(13)	-2.9(16)
C22	29(3)	31(6)	32(5)	3(3)	18(4)	3(4)
C23	35.6(18)	23.8(16)	45(3)	1(2)	19(3)	-4.0(13)
C24	35.6(18)	23.8(16)	45(3)	1(2)	19(3)	-4.0(13)
C25	29(3)	31(6)	32(5)	3(3)	18(4)	3(4)
C26	24(2)	19(2)	28(3)	0.9(18)	16.6(13)	-2.9(16)
S1	28.5(3)	28.8(3)	25.1(3)	-0.74(17)	17.8(2)	1.45(17)
O1	53.2(9)	28.4(8)	34.0(8)	2.7(6)	27.8(7)	11.4(6)
O2	37.0(8)	68.4(11)	43.7(9)	-11.8(8)	28.2(7)	-14.6(8)
N4	68.6(17)	24.5(12)	44.9(15)	0	46.2(14)	0
C4	36.6(10)	41.7(12)	36.8(11)	10.5(9)	26.9(9)	9.8(9)
F1	51.1(8)	70.5(10)	28.7(7)	3.8(6)	26.0(6)	11.5(6)
F2	28.0(6)	101.8(13)	47.9(9)	18.3(8)	19.7(6)	1.6(7)
F3	87.2(10)	49.0(8)	61.6(9)	28.4(7)	56.8(9)	30.0(8)

Table 7.13-Bond Lengths for $[C_3(NPhH)_3]TFSA$

Atom	Atom	Length/Å	Atom	Atom	Length/Å
C1B	C2	1.378(5)	C12B	C13B	1.258(15)
C1B	C1A[1]	1.374(5)	C13B	C14B	1.387(8)
C1B	N1B	1.332(5)	C14B	C15B	1.496(14)
C2	C1A[1]	1.368(5)	C15B	C16B	1.327(9)
C2	N2	1.320(5)	N2	C21	1.417(11)
C1A	C1B[1]	1.374(5)	C21	C22	1.41(2)
C1A	C2[1]	1.368(5)	C22	C23	1.395(16)
C1A	N1A	1.332(5)	C23	C24[1]	1.391(6)
N1A	C11A	1.425(6)	C24	C25	1.354(15)
C11A	C12A	1.430(8)	C25	C26	1.362(16)
C11A	C16A	1.363(6)	S1	O1	1.4259(14)
C12A	C13A	1.272(14)	S1	O2	1.4172(15)
C13A	C14A	1.371(8)	S1	N4	1.5579(11)
C14A	C15A	1.537(16)	S1	C4	1.823(2)
C15A	C16A	1.273(11)	N4	S1[2]	1.5578(11)
N1B	C11B	1.433(7)	C4	F1	1.329(2)
C11B	C12B	1.486(11)	C4	F2	1.314(2)
C11B	C16B	1.358(6)	C4	F3	1.311(3)

Table7.14-Bond Angles for $[C_3(NPhH)_3]TFSA$

Atom	Atom	Atom	Angle/°	Atom	Atom	Atom	Angle/°
C1A[1]	C1B	C2	59.6(3)	C13B	C14B	C15B	120.2(16)
C1A	C1B	C2[1]	53.4(4)	C16B	C15B	C14B	117.3(11)
C1A[1]	C1B	N1A	124.5(3)	C15B	C16B	C11B	122.1(8)
N1B	C1B	C2	149.5(4)	C2	N2	C21	122.3(4)
N1B	C1B	C1A[1]	150.9(3)	C21	N2	C1A	135.9(4)
C1A[1]	C2	C1B	60.1(3)	C22	C21	N2	117.1(9)
N2	C2	C1B	149.9(4)	C26[1]	C21	N2	122.0(8)
N2	C2	C1A[1]	150.0(4)	C26[1]	C21	C22	120.8(12)
C2[1]	C1A	C1B[1]	60.3(3)	C23	C22	C21	117.9(14)
N1A	C1A	C1B[1]	152.3(4)	C22	C23	C24[1]	120.5(10)
N1A	C1A	C2[1]	147.1(4)	C24[1]	C24	C25	115.7(8)
C1A	N1A	C11A	125.1(4)	C24	C25	C26	123.0(15)
N1A	C11A	C12A	119.8(7)	O1	S1	N4	116.44(10)
C16A	C11A	N1A	121.8(4)	O1	S1	C4	104.52(10)
C16A	C11A	C12A	118.3(7)	O2	S1	O1	117.95(10)
C13A	C12A	C11A	123.7(12)	O2	S1	N4	110.37(9)
C12A	C13A	C14A	119.0(17)	O2	S1	C4	104.07(10)
C13A	C14A	C15A	118.2(15)	N4	S1	C4	100.91(7)
C16A	C15A	C14A	117.9(11)	S1[2]	N4	S1	128.06(16)
C15A	C16A	C11A	122.1(9)	F1	C4	S1	108.74(13)
C1B	N1B	C11B	121.8(3)	F2	C4	S1	110.70(14)
N1B	C11B	C12B	119.0(7)	F2	C4	F1	108.29(19)
C16B	C11B	N1B	122.8(4)	F3	C4	S1	111.58(16)
C16B	C11B	C12B	117.8(8)	F3	C4	F1	108.53(17)
C13B	C12B	C11B	122.3(12)	F3	C4	F2	108.92(17)
C12B	C13B	C14B	119.4(17)				

Table 7.15-Hydrogen Bonds for $[C_3(NPhH)_3]TFSA$

D	H	A	d(D-H)/Å	d(H-A)/Å	d(D-A)/Å	D-H-A/°
N1B	H1B	$O1^1$	0.837(19)	2.56(3)	3.256(3)	142(4)
N1B	H1B	$O1^2$	0.837(19)	2.27(3)	2.989(3)	144(4)
N2	H2	O2	0.838(19)	2.08(3)	2.875(3)	158(4)

Table 7.16-Hydrogen Atom Coordinates (Å×10^4) and Isotropic Displacement Parameters (Å^2×10^3) for $[C_3(NPhH)_3]TFSA$

Atom	*x*	*y*	*z*	U(eq)
H1A	7430(40)	6156(16)	5960(30)	32
H12A	5089	6717	4458	43
H13A	3607	7797	3585	42
H14A	4320	9169	4314	38
H15A	6708	9324	6136	43
H16A	8251	8252	6761	32
H1B	9240(40)	8330(17)	7190(30)	32
H12B	7042	9229	5989	43
H13B	4725	9314	4688	42
H14B	3463	8109	3652	38
H15B	4745	6756	4040	43
H16B	7058	6666	5570	32
H2	7990(30)	5560(30)	6900(30)	32
H22	8064	4077	7389	40
H23	9121	2717	7773	49
H24	8716	2630	6727	49
H25	7875	3707	7160	40
H26	9021	5054	7675	29